A Study on Forces, Tool Wear and Surface finish in Orthogonal Machining of Aluminum 6061 T6 alloy and AISI 1020 Steel with HSS and Uncoated Carbide tool inserts under different gaseous cutting environments

by

Vishnu Vardhan Chandrasekaran

A dissertation submitted to the Graduate Faculty of
Auburn University
in partial fulfillment of the
requirements for the Degree of
Doctor of Philosophy

Auburn, Alabama
December 14, 2013

Keywords: Orthogonal machining, gaseous metal working fluids, tool wear, Surface finish, metal cutting mechanics, LS DYNA

Approved by

Lewis N. Payton, Chair, Associate Research Professor, Mechanical Engineering
Robert L. Jackson, Associate Professor, Mechanical Engineering
Dan Marghitu, Professor, Mechanical Engineering
Robert E. Thomas, Professor Emeritus, Industrial and Systems Engineering

Abstract

The current study is a statistically designed Orthogonal tube turning experiment to evaluate different cutting environments that can be used in machining aluminum 6061 T6 alloy and AISI 1020 Steel alloy. Two different tool material types, solid uncoated carbide and High Speed Steel (HSS) inserts were used along with different levels of uncut chip thickness in a classic orthogonal tube turning experiment. Three different rake angles of 0°, 7° and 15° using customized tool holders were designed and made to hold the inserts which had identical cutting angles. The cutting fluids used in this study are Nitrogen, Liquid Nitrogen and Cold Compressed "shop" air the performance of which were compared to the results obtained from dry machining. The force data (cutting force and the thrust force) were collected using a Kistler force dynamometer and processed using LabVIEW software. The tools are subjected to 1 minute of cutting at two different feed rates of 0.002”/rev. and 0.004”/rev at a constant depth of cut of 0.125” and at a constant speed. The tool inserts after 1 minute of cutting are studied for tool wear using a Keyence 3- D microscope. The surface finish of the work piece surface (average surface roughness) after one minute of cutting is examined under a contact type profilometer.

The force data was used to calculate the different cutting parameters using classic orthogonal expressions as derived by Merchant and Payton and variation

trend was validated against the literature. The ratio of the force along the shear plane to the force normal to the shear plane was studied and was found to be varying only with the cutting geometry (feed in this case) while remaining statistically unaffected by, tool rake angle and environment, suggesting that it is a material constant. Payton's corrected Merchant's force diagram (MFD) is revisited to obtain expressions to calculate the shear stress and shear strain. The mechanisms of dislocation movement are applied on the activation plane to obtain expression for activation energy. A finite element model to simulate the cutting process was used, results of which shows that, the cutting force values and shear strain were within 10% variation from the experimental value while the thrust force predicted by the model largely varied.

Acknowledgments

In the first place, I would like to show my gratitude to my parents Mrs. C. Sujine and Mr. S. Chandrasekaran for rendering a constant support, encouraging and inspiring me throughout my life to always achieve greater heights.

I take this opportunity to thank my mentor and my advisor Dr. Lewis Payton, for rendering tremendous support, not only in completing my dissertation but throughout my course, academically and morally, without whom, completion of my course work and the dissertation would not have been possible.

I would also like to thank my committee members, Dr. Robert Jackson, Dr. Dan Marghitu and Dr. Robert Thomas for their guidance in this dissertation. A special thanks to Dr. Michael Bozack for helping with the Microscope.

I would also like to thank my colleagues, Justin Evans, Chase Wortman and Wesley Hunko for their support and guidance with my work.

I would take this opportunity to show my gratitude to my parents for rendering a constant support, encouraging and inspiring me throughout my life. A special thanks to all my relatives and friends far and near for motivating me to achieve more.

Table of Contents

List of Tables

List of Figures

List of Symbols

F_c Cutting Force; Force component acting in direction of motion of tool.

F_t Thrust Force; Force component acting in direction normal to shear plane

R Resultant force

F Frictional Force upon Chip

N Normal Force upon Chip

μ Friction Co efficient

F_s Shear Force on the Plane

F_n Normal Force on the Plane

t Uncut Chip Thickness (also referred to as Feed Rate)

t_c Cut Chip Thickness

t/t_c Chip Thickness Ratio

A_s Area of the Shear Plane

τ_s Shear Stress on the Shear Plane

γ Shear strain

σ Normal Stress

γ' Shear strain rate

α Rake Angle

β Friction Angle

φ Shear Plane Angle

ψ Shear Front Angle

V Cutting Velocity

Vc Chip Velocity

Vs Shear Velocity

k Boltzmann's Constant

T Temperature

G Shear modulus

b Burgers vector

R Universal gas constant

Q Activation Energy

λ Angle between resultant and F_s

χ Angle between resultant and F_n

ζ Angle between shear force (Payton) & vertical

Introduction

Fred W. Taylor [1] in his article “On the art of cutting metals”, observes that the major reason for the failure of any cutting tool is the wear or dullness caused by rubbing of the chip on the tool lip which in turn produces heat that causes the tool to soften and wear off. The heat generated to cause the softening of the tool material is attributed to the following main events that occur during the cutting process,

- The pressure created when the chip slides over the tool
- The speed with which the chip slides along the tool face
- The co-efficient of friction between the chip and the tool surface.

From the above it is evident that the best way to increase the longevity of the cutting tool is somehow to control the temperature that causes the tool to soften and ultimately fail due to wear. The best solution that immediately crosses one’s mind is the application of relatively cooler substances (coolants/lubricants - Modern convention is to refer to coolants/lubricants as metal working fluids) on the tool to reduce the temperature while cutting.

Using metal working fluids (MWFs) for tribological reasons has been shown to be potentially dangerous to humans. The National Institute for Occupational Safety and Health (NIOSH)’s report of 2007 documents that of the

35 workers sampled (between March 8th and 12th, 2004), 6 workers were diagnosed with bronchitis and 3 with pneumonia while 2 other workers reported skin allergies when they were constantly exposed to Metal working fluids (MWFs) while employed at COL-FIN specialty steel, Pennsylvania. According to the plant's Material Safety Data Sheet (MSDS) one of the MWF used consisted of 85% petroleum distillates/paraffins and 15% proprietary additives while the other MWF was a soluble oil/MWF mix with 3% aqueous triethanolamine as the active ingredient. The investigators found from the samples of aerosol and stored MWF collected at the facility that the aerosol levels exceeded the NIOSH REL of 0.5 mg/m^3 with a maximum of 2.3 mg/m^3 and also had high levels of endotoxins [2].

The National Institute for Occupational Safety and Health (NIOSH), acting for the U.S. Department of Labor, classifies metal cutting fluids as follows (March, 1998):

1. Straight oil (neat oil) MWFs are severely solvent-refined petroleum oils (lubricant-base oils) or other animal, marine, vegetable, or synthetic oils used singly or in combination and with or without additives. Straight oils are not designed to be diluted with water.

2. Soluble oil (emulsifiable oil) MWFs are combinations of 30% to 85%severely refined lubricant-base oils and emulsifiers that may include other performance additives. Soluble oils are diluted with water at ratios of 1part concentrate to 5B40 parts water.

3. Semi-synthetic MWFs contain a lower amount of severely refined lubricant-base oil in the concentrate (5% to 30%), a higher proportion of emulsifiers, and 30% to 50% water. The transparent concentrate is diluted with 10 to 40 parts water.

4. Synthetic MWFs contain no petroleum oils and may be water-soluble or water dispersible. The synthetic concentrate is diluted with 10 to 40 parts water.

Identified MWF Hazards

Each MWF class consists of a wide variety of chemicals used in different combinations and the risk these chemicals pose to workers may vary because of different manufacturing processes, various degrees of refining, recycling, improperly reclaimed chemicals, different degrees of chemical purity, and potential chemical reactions between components.

Contamination may occur from (1) process chemicals and ancillary lubricants inadvertently introduced, (2) contaminants, metals, and alloys from parts being machined, (3) water and cleaning agents used for routine housekeeping, and (4) contaminants from other environmental sources at the worksite. In addition, bacterial and fungal contaminants may metabolize and degrade the MWFs to hazardous end products as well as produce endotoxins.

Water-based MWFs are excellent nutritional sources for many kinds of bacteria and fungi. The predominant microbial species routinely recovered from MWFs are virtually identical to those routinely recovered from natural water

systems. Anaerobic bacteria, specifically the sulfate reducers, may produce hydrogen sulfide and other disagreeable and toxic gases. Research suggests that microorganisms and/or their products such as endotoxins may cause some of the respiratory health effects seen in exposed workers. However, this research has not determined the specific role that the contaminating microorganisms play in causing MWF associated respiratory effects.

Substantial evidence indicates that some MWFs are associated with an increased risk of larynx, rectum, pancreas, skin, scrotum, and bladder cancer. Because the time between initial exposure to a carcinogen and the appearance of most types of cancer is often 20 or more years, these studies most likely reflect the cancer risk associated with exposure conditions in the mid-1970s and earlier. It should be noted that the studies results were not highly consistent with respect to the specific types of cancer which were associated with MWF. In addition, the specific MWF constituent(s) or contaminant(s) responsible for the various cancers remain to be determined. The inconsistencies in the results, and the inability to identify the responsible MWF constituent(s) or contaminant are a likely result of the diverse nature of the MWF mixtures studied, and the absence of detailed exposure information.

NIOSH recommends in a published criteria document, Occupational Exposure to Metalworking Fluids, that airborne exposures to MWF aerosol be limited to 0.4 mg/m^3 for thoracic particulate mass as a Time Weighted Average (TWA) for up to 10 hours per day during a 40-hour week. The 0.4 mg/m^3 concentration corresponds to approximately 0.5 mg/m^3 for total particulate mass

in most workplaces. The OSHA PEL for oil mist is 5 mg/m^3 as an 8-hour TWA and typical bacterial counts are 10^5 to10^7 CFU/mL fluid. [2].

Also Sreejith, P, S., and Ngoi, B, K, A., (2000) in their study on dry machining document that in a typical manufacturing plant around 16% -20 % of the cost to make a product is associated with coolants and lubricants used for the process (involving various metal cutting and forming process)[3]. This paves way for exploring additional alternatives that improves the efficiency of the metal cutting process and as well increase the tool life but at the same time does not expose the workers handling it to a potentially hazardous environment.

There are not many recent studies showing the benefits of MWF to the orthogonal machining process and no studies on file that show any change in the forces of cutting at all. Above mentioned facts substantiate the need for exploring alternative metal working fluids, which do not pose a hazard to workers and as well be economical while improving the cutting process.

Scope and Objectives

The goal of this dissertation is to conduct orthogonal tube turning experiments to study gaseous metal working fluids while machining Al 6061 T6 and 1020 alloy steel using High Speed Steel (HSS) and Uncoated carbide (UC) cutting tools. Such alternate gaseous fluids will not only avoid the exposure of operators to carcinogenic environments but also should help in improving the efficiency of cutting process by increasing the tool life and reducing the forces involved in machining.

The primary objectives of this study include:

- Set up an orthogonal tube turning set up which is statistically repeatable, sensitive and is able to achieve atleast 90% statistical confidence with 4 replicates.
- Establish a Statistical Design of experiments (DOE) with different factor levels under observation, such as tool rake angle, feed, cutting environment and position of coolant supply.
- Conduct experiments based on the DOE to determine the following :
    - Observe the Cutting force and thrust force while machining using force dynamometer and LabVIEW.
    - Calculate the Chip thickness ratio and shear plane angle.

        - Measure the tool wear using 3-D optical microscope.
        - Measure the surface roughness of the finished work surface using a profilometer.
    - Statistically analyze the effects of various factor level combinations under observation on the forces, tool wear and surface finish.

Secondary objectives of this research include:

- Determine the effect of coolant supply pressure on cutting forces.
- Determine the hardness of the work piece to check if the coolants used altered the material properties using Rockwell hardness tester.
- Compare the experimental data with simulated results (for two different cases) using a previously developed simulation model (at Auburn University) in LS DYNA.
- Revisit the dislocation theory to predict the activation energy across the activation plane (Merchant's shear plane)

Literature review

Tool makers have historically sought to make even better cutting tools, from ancient butchery/warfare to modern manufacturing. Onset of the industrial revolution during the late 18th century paved path to new and modernized techniques to process metals than the old conventional hand production methods. The first well documented study found in the literature of metal cutting starts in middle of 19th century.

In the earliest documented reference, Cocquilhat (1851) [4] centered his studies upon the cutting with a drill of a rotating work piece. From these fundamental studies, he was able to extend his basic observations of the metal cutting process to more worldly interests. With the knowledge of work required per unit volume of material removed and assumptions of wages and working days, he then made some calculations on the costs of digging tunnels, cutting marble and trench digging.

The first experiments in which the influence of tool geometry was studied were reported by Joessel (1865) [5]. Forces were obtained in lathe cutting and drilling by measuring the torque required to turn the machine while cutting, care being taken to subtract the torque required to overcome the friction of the machine. The effects of depth of cut, speed and rake angle were studied.

References to “cutting fluids” are also found in his work (linseed oil, quicklime and nitric acid to name a few), although no explanation of their benefit was attempted.

The first attempts to study chip formation are those of Time (1877) [6] and Tresca (1878) [7] . Time was the first to correctly model the process ahead of the tool as one of shear, although he may be criticized for his viewpoint that the chip formation took place by fracturing of the metal on successive shear planes rather than by plastic deformation. This is understandable though since the plastic deformation of metals in operations other than cutting was only beginning to be investigated at the time.

Mallock (1881) [8] produced a set of drawings of polished and etched chips in 1881, which rival modern photomicrographs in quality. He deduced that the cutting process was one of shear along a sharply defined shear plane with friction occurring along the tool face. With Time, he thought of fracture as occurring on the successive shear planes and described the chip as a “metallic slate.” Mallock observed that the friction between the chip and the tool decreased when a “cutting fluid” was applied. His drawings clearly show that when cutting copper, the use of soap and water as a cutting fluid increased the shear plane angle, which is most easily described as a line from the tip of the tool to the back of the undeformed chip, Figure 1. He was also the first to attempt to categorize the bluntness of the leading edge of the tool (the cutting edge) as a factor.

Haussner (1892) [9] was successful in building the first instrument, which could directly measure the forces involved in metal cutting. In this planning dynamometer, the work was restrained by a stiff spring. Deflections of the spring were magnified and a record was drawn by the dynamometer of the force against the distance of the cut. Although he was successful only in measuring the force horizontally along the cut, this was a major advance. He also noted the earliest comments on what appears to be the built up edge in stating, "with ductile materials, after cutting starts, chips welded to the tool and were very hard to separate". He may also have been the first to deduce the presence of a normal stress along the shear plane, concluding that the elements were not "freely sheared but is under a normal pressure".

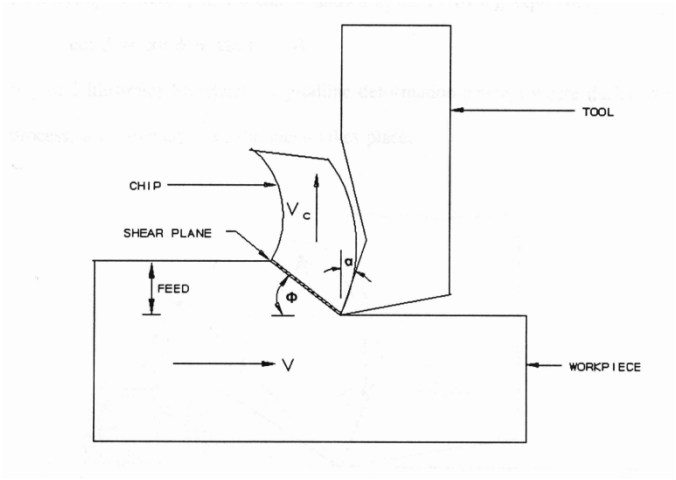

Figure 1: Shear Plane Angle and Tool Rake Angle

Zvorkin (1893) [10] published an extensive review of "planing" in 1893 using his new hydraulic dynamometer. He concurred with Haussner that the resultant force was not necessarily in the cutting direction. Assuming that the

force in the direction of the cutting velocity would be a minimum led him to conclude the first attempt to predict the shear plane angle of Figure 1. In terms of the tool rake angle α and friction angle β

$$\phi = 45 + \alpha/2 - \beta/2 - \beta'/2 \qquad 1$$

where Φ corresponds to the shear plane angle, β is the friction angle on the chip and β' is a friction angle for the shear plane itself. This is the first of many formulations of the functional relationship amongst the various angles detailed shortly in an attempt to formulate a predictive relationship based upon the observed geometries at the tool interface. This equation will appear again in the literature review of modern theory, with β' equal to zero:

$$\phi = 45 + \alpha/2 - \beta/2 \qquad 2$$

Equation 2 was derived independently in 1896, in the German engineering handbook "Ingenieur und Maschininenmechanick" (1896)[11] . The basis of derivation in that case was that the shear plane would be the plane of maximum shear stress. The German handbook marks the beginning of the ongoing search for a predictive approach to the shear plane angle that eludes engineers to the current day. It carefully compared equations 1 and 2 at great length, offering reasons for the disagreement. Those equations continued in the literature after the turn of the 20th century. Lindner (1907) [12] followed by Ernst and Merchant in 1941 [13], obtained equation 1, while Piispanen (1937) [14] , and Merchant (1945) [15] , obtained equation 2. The development of the many versions of this

predictive equation will be detailed at great length in the Shear Zone Section, since the nature of the material action within this zone will be one of the objectives of this experiment.

Force analysis would continue to improve to the current day dynamometers and began to be joined with photographic studies in the "Roaring Twenties" when Coker and Chakko (1925) [16] carried out experiments in 1925, and Coker [17] in 1922 carried out a series of photoelastic experiments on the action of cutting tools. They were able to show in their photographs that there were zones of approximately radial compression and tension ahead of and behind a line going forward from the tool point, which corresponds to the plane defined by the angle Φ in Figure 1. Coker's photographs were not taken during cutting however, but during a stoppage of the tool. Ishi (1929) [18] and Schwerd (1935) [19] were the first to study the cutting process while cutting was actually in progress. Photographs were also taken through a microscope by Boston (1930) [20], which presented detailed appearance of the metal cutting process. Their photographs were instrumental in the thought processes of the metal cutting investigators of the 1940's and continue to be highly regarded today by photographic experts in the metal cutting field.

It was also at this time that one of the first experiments examining hardness was conducted in 1926 by Herbert [21] . He showed that the chip material was harder than the work material and demonstrated that metal cutting involved intense strain hardening which could only come about through the mechanisms of plastic flow.

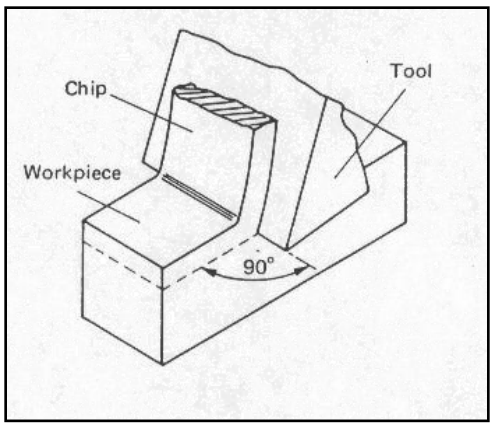

Figure 2: Orthogonal Machining Cut [22]

Orthogonal cutting such as depicted in Figure 2 is seldom used in practice, although it remains the simplest model for scientific analysis. This perpendicular, overlapping cut is only observed in the laboratory and extensively used for research purposes. Nearly all of the practical cutting processes are oblique, where the leading tool edge is inclined to the relative velocity vector between the tool and work. Even in today's computer age, modeling such a difficult geometry remains a daunting task. Thus, it is necessary to consider how the mechanics of the orthogonal cutting can be extended and altered to describe oblique cutting.

Dr. Merchant's work in 1944 [22] presented a simplified 2-D model of the conventional oblique machining process called the orthogonal machining process which considers only two axes at a time which is also one of the widely used research model as it involves less complicated computations, easier to analyze and moreover is found to be in good agreement when extended to a 3-D model. Merchant's orthogonal machining model is of two types 1) orthogonal plate

turning at moderate and high speeds, 2) orthogonal tube turning at moderate speeds and is generally characterized by the following [23, 24]:

- The cutting edge is sharp and there is no contact with the work piece on the clearance face.
- The plane of the cutting edge is perpendicular to the direction of motion.
- The tool moves at a constant velocity and depth of cut generating the chip.
- The cutting edge on the tool is wider than the thickness of the work piece machined.

The work describes a geometrical model of the force system commonly referred to as Merchant's force diagram / merchant's circle is shown in figure 3. Fc is the cutting force acting along the horizontal axis at the tool tip and the work piece interface due to the motion of the work piece against the tool which is also accompanied by the thrust force Ft acting in the vertical axis perpendicular to the Fc at the same instance.

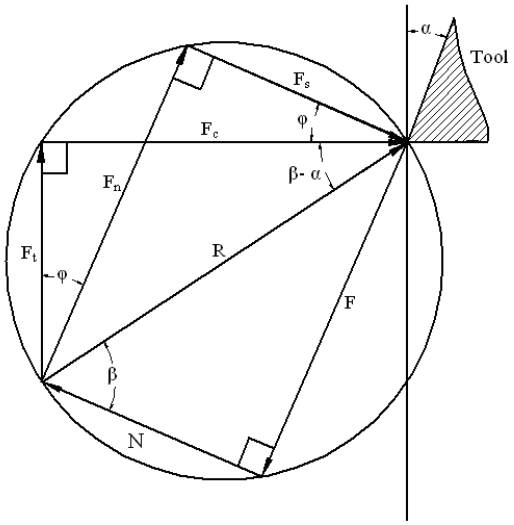

Figure 3: Merchant's 1945 force diagram (MFD) [25].

There are three different chip types mentioned in the literature as first defined by Ernst. They are: Type 1: Discontinuous or Segmented chip, Type 2: Continuous and Smooth chip and Type 3: Continuous chip with built up edge (BUE) of the chip material between the tool and chip [25].

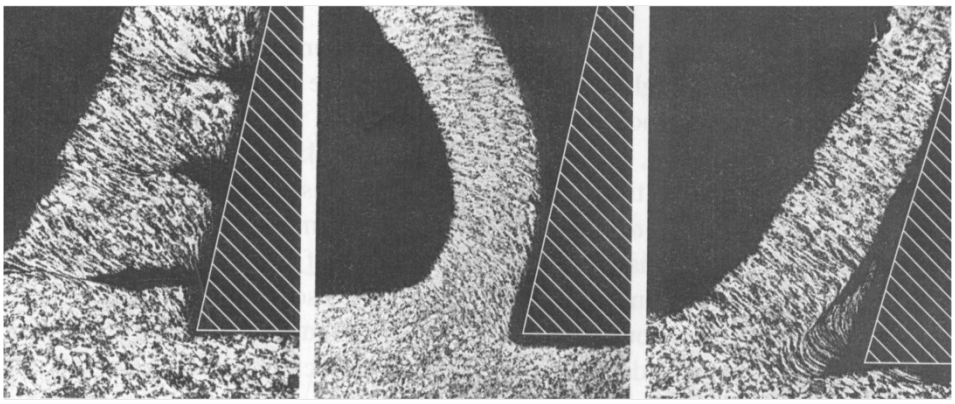

Figure 4: Type 1, 2 and 3 chips in that order.

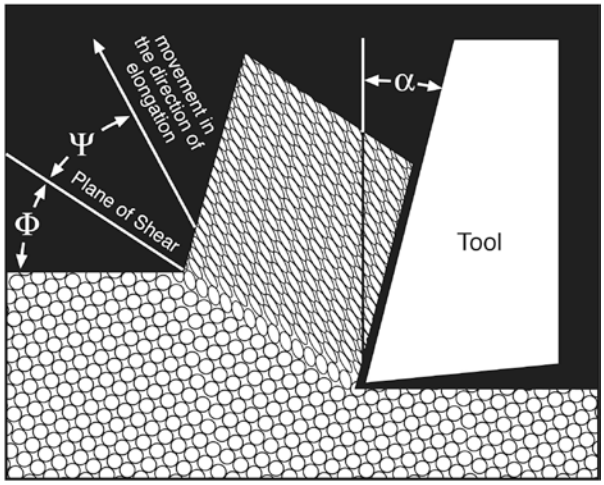

Figure 5: Merchant's observation of chip formation (Merchant, 1945) [22]

Merchant's model represented the shear zone as a single plane, or thin-zone model. The angle of inclination of the shear plane to the cutting direction

was defined by the angle Φ. Merchant observed that the crystal structure of the material was elongated by the shear process and called direction of crystal elongation the direction ψ.

Merchant did not develop the plastic deformation aspect of his observations. Both Merchant and Piispanen used a “deck of cards” concept to visualize the shear zone process, where the shear mechanism during chip formation can be illustrated by the incremental displacement of cards in a stack (Figure 6). Each card moves forward a small amount in respect to the next card in the stack as the cutting process occurs. Merchant (1945) [22] proposed that the shear process elongated the crystalline structure of the metal, and that the direction of elongation was in a different direction than the shear plane.

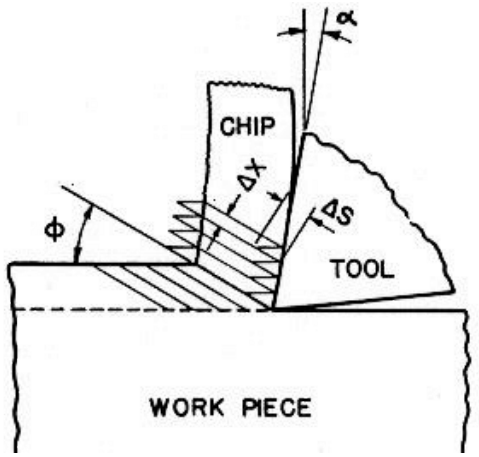

Figure 6: Merchant's Stack of Cards Model (Merchant, 1945)[15]

The thickness of each card element was ΔX, and each element in the model was displaced through distance ΔS with respect to its adjacent neighbor.

Therefore, the shear strain, γ, could be expressed as $\gamma = \Delta S / \Delta X$. From the geometry of his stack of cards, Merchant thus developed the following equation:

$$\gamma = \frac{\cos\alpha}{\sin\phi \times \cos(\phi - \alpha)} \qquad 3$$

Ernst and Merchant would eventually observe (Ernst and Merchant, 1941) [13] that the angle between the resultant force R and the shear plane was thus given by:

$$\phi = 45 + \frac{\alpha}{2} - \frac{\beta}{2} \qquad 4$$

Equation 4 was the first of many modern attempts to derive a functional angle relationship f(α,β) of some type. It has come to be referred to as the Ernst and Merchant solution (Eggleston et al, 1959) [26] . Although independently derived, this is again the result Zvorkin published in 1893[10] .

Lee and Shaffer (1951) [27] examined the geometry by considering that a part of the chip would behave as an ideal plastic solid. Using Mohr diagrams they developed the following relationship amongst the angles of the Merchant model:

$$\phi = 45 + \alpha - \beta \qquad 5$$

Thus both equation 4 and 5 suggest a strong interaction between the frictional angle and the tool rake angle in determining the shear plane angle. This has not proven to be a very satisfactory observation. Eggleston et al (1959) [26] noted in his detailed review of the observations of the angle relationships that neither the Ernst nor Merchant formulation, based upon the minimum energy

criterion, or the ideal plastic-solid solution of Lee and Shaffer, nor the mathematical derivations of Hill are in agreement with all the experimental observations.

The cutting action in any metal cutting operation involves two surfaces with distinct characteristics to come in contact (tool surface and the work piece surface) leading to friction between them. This generates heat which further accelerates the physical and chemical processes associated with tool wear. In metal cutting the type of friction occurring at the tool-chip interface is mainly solid friction. Solid friction can be defined as the resistance to movement of one solid body over another. In metal cutting the movement may involve sliding or seizure at the tool-chip interface.

Traditionally, it has been assumed that coulombic friction controls the interface forces at low loads and that as the load grows to the point where the real area of contact is equal to the apparent area of contact, friction becomes independent of pressure and takes on the value of k, which is the shear flow stress of the weaker material (Bowden et al, 1964) [28]. In metal cutting, k is not a simple value. It is modified by the hydrostatic pressure, high strain rates, large strains and high temperatures at high cutting speeds so that the final value is lower than the k determined from uniaxial tension tests (Ling et al, 1987)[29] . A recent analysis of friction in metal working processes based on slip line field studies has been presented by Kopalinsky et al (1991) [30] . The frictional processes in metal cutting are complex because of the existence of very high normal loads. Friction under high normal loads has been discussed in detail by Thomsen (1969) [31]. An

increase in the normal load across the contacting surfaces produces an increase in the real area of contact. Relative motion between the surfaces produces shearing of welded asperities and some subsurface plastic flow.

The frictional force F is given by the equation $F=A_rS$ where S is the shear strength of the asperities of the softer material, but is not linearly related to the normal force N. In Region II of Figure 7, it has been shown that at very high normal loads the real area of contact approaches the apparent area of contact A_a. With this condition Ar has reached its maximum value ($A_r/A_a=1$) and conditions of sticking friction are said to exist [103].

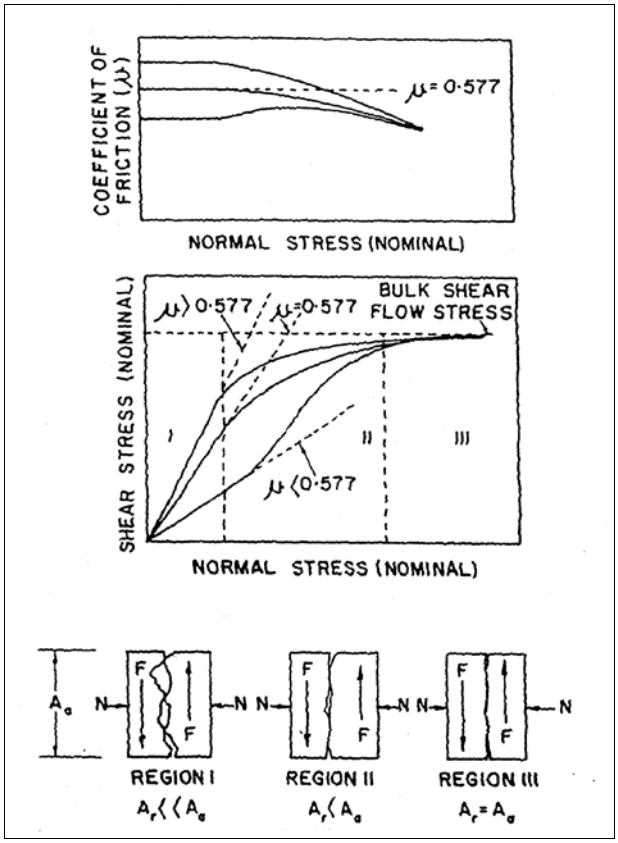

Figure 7: A schematic representation of dry friction for pressures in the metal cutting range showing that for light pressures the coefficient of friction is independent of pressure and Amontons' law applies. (As the pressure increases in clean surfaces sub-surface flow takes place when F=At and p=0.577 and F remains constant at large pressures unless t is altered by

phenomena such as work hardening. p decreases with increase of pressure if t remains constant) (Thomsen, 1969) [31].

Relative motion between the surfaces produces gross subsurface flow and the coefficient of friction reaches its limiting value of 0.577 if it is assumed that the Von Mises flow rule applies. Then the frictional force F is independent of the normal force N and the coefficient of friction decreases with a further increase in normal load. Friction in metal cutting occurs at the flank and the rake faces of the tool. There is ample evidence in the literature supporting the existence of sticking friction at the flank face of the tool (Hitomi et al, 1962 and Trigger et al, 1952) [32, 33]. Ham et al (1961) [34] also showed that adhesion at the flank face could be prevented by the application of a lubricant and an increase in tool clearance angle.

$$\phi = \mathrm{F}(\beta, \alpha) \qquad 6$$

The severely work hardened chip which is formed by a shear process in the primary shear zone flows up the tool rake face under the action of large normal and shear stresses (Ham et al 1961)[34]. Assumption that the frictional condition in this region controls the geometry of the metal cutting process has led to the representation of the frictional behaviour by a single parameter β, the mean angle of friction on the tool face. β is related to the mean normal and frictional forces by the expression tan β = F/N or tan β = μ where μ is the coefficient of friction on the tool rake face. A large proportion of previous theoretical work concerning the mechanics of metal cutting has dealt with the effect of the mean angle of friction β and the tool rake angle α on the shear angle.

The most extensive work on the influence of cutting conditions on tool chip interface friction appears to be that of Zorev (1966) [35]. Under dry machining the mean coefficient of friction increases with increase in cutting speed. For certain ferrous materials, the mean coefficient of friction is shown to reach a maximum and then decrease continuously with further increase in cutting speed. For certain non-ferrous materials the mean coefficient of friction continues to increase but tends to become constant at high cutting speeds. Typical results produced by Zorev are shown in Figure 8 (a) and (b). Zorev (1966) [35] attributed the observations to the generation of surface contaminant oxide films that lower adhesion at the interface when machining at extremely low cutting speeds and to the existence of conditions of seizure at high cutting speeds. The increased coefficient of friction produces a decrease in the shear angle and increase in cutting forces. An increase in tool rake angle produces an increase in the mean coefficient of friction (Zorev, 1966 and Eggleston et al, 1959) [26, 35]. An increase in the tool rake angle produces little change in the conditions of strain, strain rate and temperature at the tool-chip interface and hence little change in the shear flow stress of the chip material. However, by comparison an increase in the tool rake angle causes a large decrease in the normal stress. The coefficient of friction is low at low feeds due to the formation of a built-up edge, which in turn increases the effective rake angle.

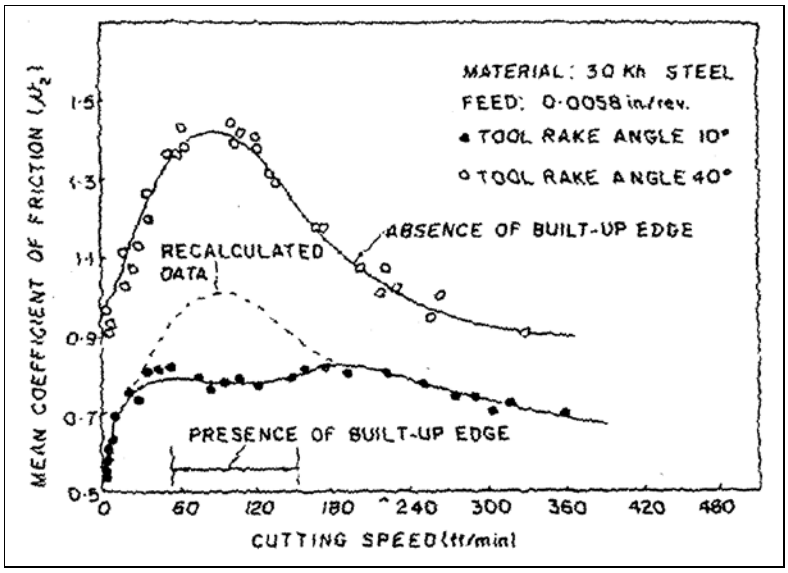

(a) Effect of Cutting Speed on Mean Coefficient of Friction, μ on tool rake face (Zorev, 1966)[35].

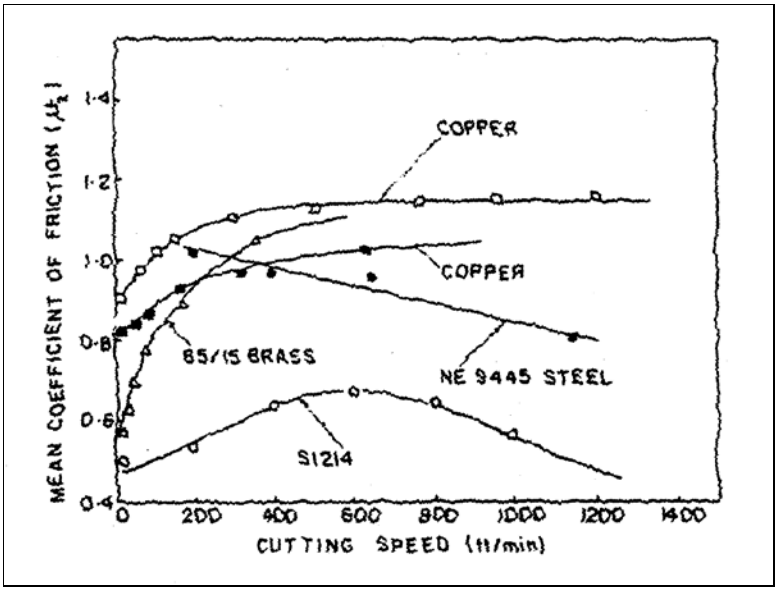

(b) Effect of Cutting Speed on mean coefficient of friction (Zorev, 1966)

Figure 8: Zorev's observations (a) and (b) [35]

Lubrication is achieved either through application of an external fluid or through the presence of inclusions of a lubricating nature in the work piece. These inclusions are known as free cutting additives. The most common method of application is by flooding the cutting point with a lubricant fluid. A general view is that lubricating action occurs at the tool-chip interface through the formation of a film, which tends to restrict metal-to-metal contact. However some confusion still exists concerning the true lubricating action of the cutting fluids. While Trent (1965) [36] has provided metallographic evidence to show that the lubricant cannot penetrate the whole of the contact area, Williams et al (1970) [37] claim that cutting lubricants reduce frictional forces through reduction of the tool-chip contact length. Childs (1972) [38] has shown that while sticking friction conditions may prevail very close to the cutting edge of the tool in well-lubricated cutting, the elastically stressed portion of the contact area that exists during unlubricated cutting is eliminated by lubrication. There is ample evidence to show that at high cutting speeds where conditions of seizure prevail at the tool-chip interface externally applied lubricants become ineffective, as the atomic contact at the interface is inaccessible to external lubricants (Mullick et al, 1966) [39]. Therefore, the most viable method is in-situ lubrication of the interface from either the workpiece or the tool. One method of achieving in-situ lubrication of the tool-chip interface is by inclusion engineering of the workpiece with glassy phase inclusions which remain viscous under the prevailing strain, strain rate, pressure and temperature at the tool-chip interface.

Even though, the complete metal cutting literature (vast) has not been covered, efforts have been taken to introduce the basic theory of metal cutting with some of the notable models that best describe the process. Also with the understanding of role of friction in metal cutting, it is now necessary to explore the efforts taken (in the literature) to minimize it in order to avoid/reduce tool wear.

Use of coolants in metal cutting has been first documented by Fred W. Taylor in the famous keynote address delivered by him in the New York meeting of ASME in December 1906, stating that in 1883, along with his teammates he found that using a heavy stream of water (Supersaturated with carbonate of soda to prevent rusting) on the chip at the point of removal from a steel forging permitted an increase in cutting speed and hence an increase in work done from 30 to 40%. Up to this point in the history of metal cutting even though use of small quantities of water in machining has been reported in several instances but was not used with an objective of cooling, but to obtain a finish that the historians (machinist) claim to be a water finish.

In the same address, it was reported that, in the year 1894-95, a heavy stream of water was used on the tool nose while cutting wrought iron and steel increased the cutting speed by 33%. This was a major breakthrough in terms of using water as a coolant because, up till then tool makers warned not use water on tools. Also in 1906, the same team observed that flooding of water during machining of cast iron improved the cutting speed and thereby the work done by 16% [1].

Since then a lot of different types of coolants starting with water to different synthetic/non-synthetic based fluids, oil based fluids, organic/ mineral oils etc., have been used in the metal cutting process with a primary objective of increasing the tool life. On the down side it led to some serious concerns including the difficulty involved in separating the coolant from the chip, handling and disposal of the coolant itself to name a few. The industry started paying attention only when severe health hazards were encountered by the workers who were exposed to these coolants and when the safety organizations started making the rules on handling and use of coolants more stringent.

This scenario gave rise to exploration of other alternative fluids that were easy, safe and more user friendly and at the same time served the primary objective of increasing the tool life and the efficiency of the process itself.

Niebusch, R, B., and Strieder, E, H., in 1950 conducted experiments using metal cutting fluids in machining and grinding operations. Their study was based off the “rule of thumb”, ‘gallons of cutting fluid per minute = maximum horsepower required for cut’. They concluded that adequate supply of coolant on the cutting tool (wheel in case of grinding) only will result in improvement in efficiency of the process, improving the tool life by 100% and also resulted in better surface finish, greater accuracy, elimination or reduction in stem and smoke and hence the operator complaints [40].

Rowe, G, W., and Smart, E, F., (1963) reported the role of oxygen in dry machining of mild steel, stating that, oxygen in particular is effective in reducing

the cutting forces and improving the surface finish. The experiments were carried out at different speed ranging from 20 feet per minute to 350 feet per minute at constant tool rake angle of 18 degrees and clearance angle of 6 degrees with varying feeds ranging from 0.001 inch per rev to 0.005 inch per rev. the results showed that when using oxygen, the cutting forces were low compared to air cutting and nitrogen atmosphere with later producing higher cutting force values. They concluded that there is a marked change in the chip formation criteria when using oxygen as built up edge is avoided in this case where as it was observed in dry machining and vacuum chamber machining. Further, a thin coating of MoS2 over the tool face eliminated the formation of built up edge even in vacuum machining until the coating wore out [41].

Williams, J, E., Smart, E, F., and Milner, D, R., (1970) conducted experiments to assess the effect of carbon tetrachloride (CCl_4 spray cooling) in machining operations of different materials. Their study revealed some important results such as, CCl_4 had a very little effect when machining brittle materials like grey cast iron and magnesium, but in pure metals and single phase alloys, the cutting forces were observed to be lower (one fifth to one half of cutting forces observed in air cutting) when machining under 100 feet per minute (cutting speed) and increased thereafter as the softening of chip due to heating is reduced. The effect was higher at rake angles of 6 degrees when compared to a 35 degree tool as the tool chip contact area decreased with decrease in tool face force. However in machining two phase alloy elements a similar trend was observed but formation of built up edge was absent when machining under low cutting speeds [37].

Childs, T, H, C.,(1972) analyzed the effect of Carbon tetrachloride in machining of high permeability iron with a 30 degree rake angle high speed steel tool. The feed and cutting speed was maintained at 10^{-2} inch/pass and inch/ minute respectively and the cutting fluid was flooded over the cutting zone continuously. The results indicated that the horizontal force (cutting force) reduced by half and so was the coefficients of friction when the cutting environment was changed from dry (air) machining to CCl4 environment. The study also notes that the same difference in the cutting force was observed by Shaw in his experiments carried out with CCl_4 at higher cutting speeds of 6 inch/ minute with mild steel. It is also important to note that the changes in the chip shape which was more curlier and hence a large shear plane angle in the lubricated condition than the dry machining [38].

Zhao, Z., and Hong, S, Y., (1992) carried out experiments to determine the ability of cutting tool materials to work in cryogenic cutting conditions. Even though a metal cutting experiment was not conducted, the researchers were careful enough to subject the six different tool materials to different material testing techniques which were similar to the ones the tools would experience in metal cutting operations. Another important feature that the researchers observed was that, all the materials including 1010 steel, 1070 steel, E52100 steel, Ti-6Al-4V Titanium alloy, A390 cast aluminum showed an increase in hardness and strength (both tensile, yield) while conducting material strength analysis at low cryogenic temperatures. At the end of their study they concluded that the carbide

tool material possessed good rupture strength, hardness and impact strength and would be more suitable to be used in cryogenic conditions [42].

Zhao, Z., and Hong, S, Y., (1992) studied the response of five commonly machined materials in cryogenic cutting environment by conducting standard mechanical testing procedures in a range of temperatures varying from 100 degree Celsius to -196 degrees Celsius. The results showed that low temperatures were ideal to machining conditions for 1010 low carbon steel materials whereas use of cryogens impaired the tool wear in 1070 high carbon steel and E52100 high alloy steels. When analyzing A390, it showed a trend to resist abrasive wear and in case of Ti-6AI-4V reduced the affinity between the titanium and tool material [43].

It is important to note that both the studies carried out by Zhao, Z., and Hong, S, Y., were not doing exactly machining experiments but subjecting both the tool material and the work material separately to various mechanical testing procedures (tensile testing, impact testing, hardness testing, micro structural analysis etc.,) that resembles to the cutting conditions. This becomes important as it gives us an idea of how materials would behave in cryogenic environments.

There are several studies carried out to determine the position of coolant supply in a metal cutting operation wherein it was concluded that high pressure jet cooling was significantly better than the flood cooling procedures. On such study was carried out by Kovacevic, R., Cherukuthota, C., and Masurkiewicz, M., in 1994 in which Milling of Stainless steel AISI 304 and Titanium Ti-6AI-4V were considered under two different coolant(water) supply conditions including flood

cooling, supply through a hole in the rake face of the tool and through an external nozzle. The experiments were carried out at constant feed and speeds and tool geometry which indicated that the use of high pressure jet cooling was significantly better than the flood cooling technique. There was a drastic reduction in cutting forces when using high pressure coolant along with an improved surface finish and at some instances it was similar to a ground surface finish. Intense shearing of chips in case of flood cooling is absent in case of high pressure jet cooling which was evident from the SEM micrographs of the chips. Formation of built up edge in machining of titanium was completely eliminated in case of high pressure cooling and when the coolant was supplied through a hole in the rake face, it reduced the tool chip contact area by curling the chip up and in case of external nozzle supplying coolant, the high pressure jet fragmented the chips and hence causing a reduce tool chip contact area and thereby decreasing the tool wear and increasing the tool life significantly [44]

Kim, S, W., Lee, D, W., Kang, M, C., and Kim, J, S., (2001) conducted studies to determine the effect of compressed cold air system in machining of difficult to cut metals such as hardened steel, die steel (HRc 42) nickel based alloys etc., Two different tool materials including high speed steel and coated carbide tools were used in this investigation which was conducted on a vertical milling machine with cutting speed set at 90 and 210 m/min. Tool wear (Flank) was measured using a CCD camera and a tool makers microscope. The results showed that when machining Die steel the tool life improved two folds when using compressed air than dry environment and went up 3.5 times when

comparing compressed air with flood coolant, former being more efficient. The authors also note that the compressed air environment did not create any significant improvements in machining Inconnel 718 (HRc 43) at a speed of 210 m/min when compared to flood of dry environments and they attribute such an observation to that the severe thermal friction taking place when machining at such high speeds and the inability of the coolant to infiltrate the tool chip interface [45].

Hong, Shane, Y., Ding, Yucheng., and Jeong, Woo-cheol., in 2001 studied the behavior of friction and the cutting force while machining Ti-6Al-4V under cryogenic cutting conditions. For this study the authors developed a new system for Liquid nitrogen delivery consisting of two nozzles, one on the rake face of the tool very much close to the tool chip interface in the cutting zone itself by placing the supply nozzle under the chip breaker present in the tool insert. The primary nozzle cools two regions of the tool including the rake face and the flank face and the second nozzle is placed on the clearance face of the tool and both the nozzles supply liquid nitrogen at variable flow rates which is monitored by a cryogenic turbine flow meter. The flow rate was maintained at 0.625 l/min on the rake face, 0.53 l/min on the flank face and 0.814 l/min for the clearance face and a cutting speeds ranging between 1 m/s to 2.5 m/s along with depth of cut and feed maintained at 0.05 inches and 0.01 inches respectively. The authors conclude that the use of liquid nitrogen helps in reduction of feed force, co efficient of friction between the tool and chip, but cutting force increased due to the cooling of the work material making it harder to cut [46].

Dhar, N, R., and Chattopadhyay, A, B., (2001) carried out experiments to determine the beneficial effects of cryogenic cooling when machining AISI 1060 steel. The experiments were carried out with carbide inserts at cutting speeds of 110 m/min with feed rate at .20mm/rev and depth of cut maintained at 2mm. The tool wear was monitored at regular intervals and measured using an inverted metallurgical microscope (Olympus model MG) fitted with a micrometer capable of measuring accurately upto 1 micron change. Surface finish was observed with a contact type stylus profilometer (Talysurf: model Surtonic 3P, Rank Taylor Hobson) and the cutting inserts were evaluated at the end of machining under scanning electron microscope (model: JSM 5800, JEOL, Japan). The results show that the cryogenic cooling yielded better surface finish reduced tool wear and thereby prolonged the tool life when compared with wet machining and dry machining conditions [47].

The same authors in the year 2002 carried out similar experiments on different tool materials including E4340C and AISI1040 steels with different cutting parameters. The cutting speed was varied between 60 and 150 m/min with the feed rate range being between 0.12 mm/rev to 0.24 mm/rev and depths of cut of 1.5 mm and 2 mm. The authors conclude that the use of cryogens for cooling machining operations especially in the current experiments reduced the temperature values of up to 34% and also contributed to a significant decrease in flank wear of the tool [48].

Dahlman, Patrik., and Escursell, Marcel., in 2003 employed the technique of high pressure jet-assisted cooling to machine decarburized steel. The cutting

speeds were varied between 300 and 650 m/min with feed rate variation in the range of 0.2 to 0.7 mm/rev. The authors first examined the wear and surface finish closely using a Scaning Electron Microscope and then used a microscope fitted with a digital camera and imaging software to measure wear. Surface roughness was measured by a rubber-replica method in which a mixture of rubber and reactive was applied to the surface and allowed to polymerize after which it was examined under a Wyko optical reflecting equipment. The high pressure jet-assisted cooling system made a major contribution in improving the surface finish of the work piece by about 80% even though a drastic reduction in tool wear is observed, it is important to note that tool is sensitive to thermal cracking with the above environment [49].

Cakir , O., Kiyak, M., and Altan, E., in 2004 investigated the effects of cutting fluids to provide quantitative results about the cutting force, thrust force and the surface roughness. A 5% emulsion type cutting fluid was used as liquid coolant and compressed oxygen, nitrogen and carbon dioxide gas stored in cylinders at their normal temperatures were used. They used tubes ending with nozzles and fitted with suitable pressure regulators to direct the gases and the coolant at the cutting edge of the tool. The response curve of the mean cutting force and the thrust force showed that all gaseous and flood coolant is different from the dry cutting and also increases with increase in feed. Later Cakir analyzed the response of the shear plane angle under varying depth of cut. This showed an appreciable increase in the shear angle in the gaseous and flood coolant environment leading to smaller shear area and reduced cutting forces as compared

to dry cutting environment. Although the effect of feed was obvious on the surface roughness of the machined parts the investigation concluded that the dry machining produced the highest value of roughness then wet machining [50].

Stanford, M., and Lister, P. M., in the year 2004 published their work, in which a relationship between cutting environment and tool wear was established. In their experiments, they used En32 steel with the cutting parameters of 200 m/min to 600 m/min speeds, 0.1mm/rev feed and 1.5 mm depth of cut. The tool parameters were zero rake angle and 0.8mm cutting nose radii for both coated and uncoated carbide inserts. The cutting duration was varied between 20 seconds and 80 seconds wherein different cutting environments like semi synthetic flood coolant, atmospheric air without coolant (dry), air blast at 0.2MPa and nitrogen blast at 0.2 MPa. From the above experiments the inferred that nitrogen rich environments, reduce the flank wear upto 55% in both coated and uncoated tools and also concluded that nitrogen rich environments have a potential in high speed cutting and high temperature scenarios [51]. The authors also note the important work carried out by Trent and Wright in 2000 wherein they conclude that the coolant cannot prevent the heat generation while machining as it has no access to the primary deformation zone in the cutting process which brings us the next question of the effect of the position of coolant supply.

M'Saoubi, R., Chandrasekaran, H., in 2004 investigated the effect of tool micro-geometry and temperature on coated tools. During their investigation they found that machining parameters chosen has an effect on temperature. An increase in cutting speed or feed resulted in the increase in the temperature. It was

noted that the maximum temperature moved closer to the tip of the tool as cutting speed increased and away as the feed increased. The material hardness as well had an effect on the temperature. This may be explained by the fact that harder the materials, smaller will be the plastic deformation zone and the size of tool chip contact length[52].

Salgam, H., Yaldiz, S., Unsarcar, F., in 2005 investigated the effect of tool geometry on the cutting forces and tool temperature. During machining large amount of energy is converted into heat energy considerably on the shear plane, rake face and clearance face. In orthogonal machining, the cutting is assumed to be uniform along the cutting edge; hence it is a two dimensional plane strain deformation. The cutting forces are exerted only in the direction of velocity and uncut chip. Rake angle determines the tool/chip contact area. They found that with the increase in the rake angle from 0^o up to 20^o has a positive effect on the tool by increasing the shear plane angle causing the reduction in the force system. But increasing beyond a point affects the tool's performance and accelerates tool wear. Smaller positive rake angles leaves a better finish but excessive positive angle weakens the tool causing tool breakage. The optimal rake angle was obtained as 12^o [53].

Dhar, N. R., Kamruzzaman, M., and Ahmed, M., 2006,[54] studied the effect of minimum quantity lubrication (MQL) on tool wear and surface finish in machining 4340 steel. The turning experiment was carried out on a solid piece of the fore mentioned grade steel using a carbide insert under different cutting environments like dry, wet (flood) and MQL. The cutting fluid used was a

combination of air at 7 bar and 60 ml/h lubricant while the cutting parameters were maintained at 1.5 mm depth of cut, 110 m/min speed and 0.16 mm/rev feed. Tool wear and surface finish was measured using a metallurgical microscope (Carl Zesis, 351396, Germany)fitted with a micrometer (atleast 1 micron), a scanning electron microscope (Hitachi, S-2600N, Japan) and a contact stylus type profilometer (surtronic 3+ roughness checker, UK). In all, the MQL demonstrated minimum flank wear (both principal and auxiliary) and at the same time improved the surface finish of the work piece which primarily was attributed to the reduced tool wear and damage of the tool tip.

Su, Y., He, N., Li, L., and Li, X. L., 2006, conducted high speed milling experiments on Ti -6Al-4V to determine the effects of different cutting environments on tool wear during the process. A coated carbide tool was used to perform the down milling operation at 400 m/min cutting speed, 0.1 mm/rev feed and depth of cuts at 5 mm axial and 1 mm radial. Different cutting environments like dry, flood, nitrogen, nitrogen oil mist (UNILUB 2032 cutting oil, Blaster 2000 lubricant) compressed cold nitrogen and oil mist (-10 °C) were investigated with the tool nozzle positioned at entry and exit of the tool. Different wear phenomena occurred during the machining process like flank wear, notch wear and nose wear were observed and measured using a toolmakers microscope. The results showed that Cold compressed nitrogen gas oil mist environment resulted in 2.93 times improved tool life than dry cutting and nitrogen gas oil mist improved the tool life by 1.93 times. The coated carbide tools predominantly

showed diffusion wear under the environments investigated and flood coolant showed the maximum.[55]

Dhar, N. R., and Kamruzzaman, M.,[56] in 2007 reported from their experiments the cutting temperature, tool wear surface roughness and dimensional deviation in machining 4037 steel under cryogenic environments. The turning operation was carried out using a -6 ° rake angle coated carbide insert under dry, wet and cryogenic cooling using liquid nitrogen. The cutting parameters used in this study were 1.5 mm depth of cut, with speeds varied between 165 to 264 m/min and feed variation of 0.1 to 0.2 mm/rev. The authors conclude that the cryogenic machining environment provided better surface finish, less dimensional deviation, low tool wear and low interface temperatures (measured using work tool thermocouple) compared to that of flood coolant which had similar results as that of dry machining.

Su, Y., He, N., Li, L., Iqbal, A., Xiao, M. H., Xu, S., and Qiu, B. G., 2007, [57] conducted experiments using refrigerated cooling air while turning difficult to cut material Inconel 718 (HRc 41) with coated carbide insert. Three different environments including dry, cooling air (-20° C) and a combination of cooling air (-20° C) and Minimum quantity lubrication (30 mL/h of UNILUB 2032 cutting oil) at 0.5 mm depth of cut, 0.1 mm/rev feed and a cutting speed of 76 m/min. Tool wear and surface finish was measured using a tool makers microscope and Mahr Perthometer M1 respectively. The results showed that the third case provided a 124% improvement in tool life and the second case 78% improvement in tool life over the dry scenario. The authors also make an interesting observation

of the chip curl formed during the different cutting environments, which shows that the conventional long tubular chips changed its profile when cooling air was used to a short continuous tubular chips.

The same paper also reports the results of high speed milling experiment carried out on AISI D2 steel (62 HRc) at cutting speed of 175 m/min with feed at0.08 mm/rev and depth of cut axially at 4 mm and 0.4 mm radially under the same set of environments. The results showed that the cooling air environment improved the tool life by 130% slightly better than the combination environment and a considerable change in chip morphology from a tight curl during dry machining to a flat due to reduced cutting region temperatures.

Kalyankumar, K. V. B. S., Choudry, S.K., in 2007 investigated the effects of cryogenic cooling on tool wear and high frequency dynamic cutting forces generated during high speed machining of stainless steel. They observed from their experiments that the cutting force decreased with increase in cutting speed since the co-efficient of friction at the tool chip interface decreases and the shear plane angle increases, decreasing the area of shearing. They also found that the increase in feed and depth of cut increased the cutting force. Due to the increase in depth of cut and feed, the material removal rate also increases eventually the rate of plastic deformation and hence the cutting force increases. With the increase in cutting speed, higher cutting temperature and shortened contact area were observed. As a result the temperature concentration moved towards the tip of the tool resulting in the reduction of tool strength and increased tool wear. They concluded that the cutting force and tool wear was considerably less using

the cryogenic environment compared to a dry environment wherein tool wear (Flank) was measured using a tool room microscope [58].

Sreejith, P. S., 2008,[59] published the results of the study on effects of different lubricating environments in machining Aluminum 6061. The turning experiment was conducted using a 15° rake angle, diamond coated carbide tool insert at a speed of 400 m/min, depth of cut at 1 mm and feed rate of 0.15 mm/rev. Surface roughness was measured using a Hommelwerke T1000 profilometer and the tool wear was measured using a toolmakers microscope. The environments used were dry, flooded and Minimum quantity lubrication which was applied at 50mL/h and 100 mL/h using a commercial oil BP Microtrend 231L. The results showed that the cutting forces were low for flood cooling which was attributed to the lower adhesion of the tool and hence lower friction forces. The author also concludes that application of coolant does not necessarily reduce tool wear as it was observed that MQL conditions showed low tool wear and also as it produced comparative results as flood coolant suggesting that MQL could be economically a viable solution.

Stanford, M., Lister, P.M., Morgan, C., Kibble, K.A., in 2008 studied the effects of cutting forces and tool wear under different cutting conditions. The behavior of the responses were derived by using a 4% dilution semi synthetic flood coolant, compressed air (20% oxygen at 0.27 MPa), Nitrogen gas (6% oxygen at 0.27 MPa) and liquid nitrogen and eventually compared against dry cutting. Plain carbon steel with UTS of 217 MPa was machined on a CNC turning center with a constant depth of cut of 1.2 mm and a feed rate of 0.1inch/rev under

different cutting environments. Tool wear was measured optically using a Vickers optical tool makers microscope and tool chip contact length, crater wear position etc., were determined using an Zeiss EVO50 Scanning Electron microscope. A Coordinate measuring Machine with Renishaw TP 200 touch trigger system and a stylus probe was used in to determine the chip thickness which the authors claim to be more repeatable when compared to other conventional (Micrometer) and optical methods (microscopy and SEM). Results show that the cutting force and the thrust force decreases with the use of flood coolant and liquid nitrogen as compared to the other gaseous environments and dry machining. Also the use of flood coolants showed a significant increase in the shear plane angle as compared to dry and gaseous environment cutting. It was observed that compressed air and nitrogen environment produced significantly thicker chips which can be confirmed by smaller shear angle and longer shear plane. Stanford et al further discusses the behavior of the crater wear and flank wear and concludes that although all the environments show significant wear, the dry cutting environment produces the highest level of wear. According to their experiments the best performing environment with considerably less wear is produced when flood coolant is used and lowest density of work piece adherence at the crater face and the flank edge is achieved. It is also explained that the use of nitrogen environment would assist in the reduction of notch wear reducing oxidation and providing better finish of the machined component [60].

Yalçın, B., Özgür, A. E., and Koru, M., 2009,[61] conducted experiments to study the performance of air cooling in milling of 1050 steel with a High speed

steel cutting insert. The cutting parameters were maintained at 2.5 mm depth of cut, feed rate of 0.4 mm/rev and speed of 20 m/min under dry, fluid cooling, and air cooling at 0° C directed towards the cutting edge. The results showed that work material adhesion to the tool under dry cutting environments, but air cooling reduced adhesion and as well formation of built up edge (SEM photographs). The authors also conclude that air cooling will avoid corrosion, chemical reaction which would accompany the fluid cooling technique.

Payton, L. N., and Sripathi, P., 2010,[24] conducted orthogonal tube turning experiments on aluminum 6061 T6 alloy with a high speed steel tool under 4 different cutting environments including nitrogen, cold compressed air, kool mist and dry (zero coolants of any sort used). The experiment was carried at five different feeds (0.001” to 0.005” at increments of 0.001”) and four different rake angles (0°, -10°, 15° and 30°) with a constant depth of cut of 0.125” and speed at 640 RPM. The cutting forces and the thrust forces documented shows an increase with increase in feed but decreased with increase in rake angles. Cold compressed air environment recorded marginally low cutting force and thrust force values closely followed by nitrogen environment, with spray coolant (kool mist) in the third position. The tool wear was recorded in terms of surface roughness of the affected area of the tool measured using a confocal non-contact type profilometer. The results showed that the tool wear was least when the cutting was performed under nitrogen cutting environments. The author also provides a summary table of the variation of forces with different parameters

involved in the cutting process collected from previous literature in the following table.

Parameter	Change	Cutting Force	Thrust Force	Chip Thickness	Wear	Shear Angle
Feed, **t**	↑	↑	↑	↑	↑	↑
Rake Angle α (0-20)	↑	↓	↓	↓	↓	↑
Negative Rake Angle ($\alpha < 0$)	↑	↑	↑	↑	↑	↓
Cutting Speed, **v**	↑	↓	↓	↓	↑	↓
Width of Cut, **w**	↑	↑	↑	↑	↑	↓
Compressed Air	**ON**	↑	↑	↑	↓	↑
Metal Working Fluid (MWF)	**ON**	↓	↓	↓	↓	↑
Contact Length	↑	↑	↑	↑	↑	↑

Table 1: Parametric responses to changes in cutting conditions during orthogonal tube turning experiments.

Tool wear (life) plays a crucial role in determining the efficiency of the machining process in terms of dimensional accuracy, surface finish which rule the quality of parts produced in any industry. It is a very important phenomena that has been carefully studied over the past whenever evaluating a machining technique. A well experienced operator or a machinist can easily identify a tool that wears out while machining by just observing the noise of vibration from the machine. The most basic method to determine tool life is to record the time the tool was used before it broke during a machining process. Other common method used in carrying out such studies in the past is optical techniques specially using microscopes (tool makers / metallurgical microscopes / Scanning Electron Microscope). With advent in technologies and development of new tools like profilometer has really taken this study to the next level. Apart from the optical

methods and profilometry there are several other methods that are used in line (during the cutting process) as well offline (after the cutting process) to monitor tool wear and surface finish which are documented in the following pages. (Note: Some of the measuring strategies used by researchers have been discussed in the previous pages while discussing the effects of coolants in machining).

Before getting into the detailed literature available about tool wear it is necessary to introduce the standards established by international societies. The American Society of Mechanical Engineers (ASME) in its publication titles “Tool life testing with single- point turning tools” discusses about various scenarios that a tool could be deemed worn or failed. The common criteria for wear evaluation of high speed steel tools and sintered carbide tools are [62]:

- The average width of the flank wear in zone B is 0.3 mm for being regularly worn and a maximum width of 0.6 mm when not regularly worn.
- The depth of crater KT varies from a minimum of 0.14 mm for a feed rate of 0.25 mm/rev and to a maximum of 0.25 mm for a feed rate of 0.63 mm/rev. also in general it is given by the equation.,

$$KT = 0.06 + 0.3\,f \qquad (7)$$

f feed rate in mm/rev.

- Wear in minor flank is often hard to directly measure and hence, surface roughness values of the finished surface of the work piece can be used to ascertain the tool wear/life indirectly. The range of Ra values used in this case vary from 0.4-0.8-1.6-3.2-6.3-12.5 μm.

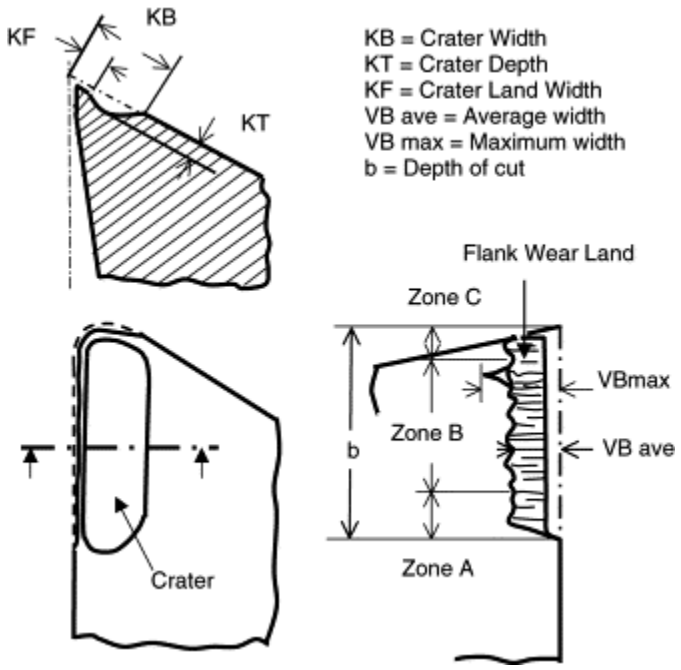

Figure 9: Schematic representation parameters considered for tool wear evaluation. [63]

Lim, G, H., in 1995 during his study to determine the tool wear, used the vibration analysis procedure. The author also cites the ISO standards for tool failure (for single point cutting tools) criterion which is divided into 3 categories as follows (i) catastrophic failure (ii) maximum flank wear of 0.3 mm for regular wear and (iii) maximum flank wear of 0.6mm in case of irregular flank wear. The natural frequency of the tool holder along with the insert was studied by conducting a dynamic analysis. An accelerometer was connected to the shank of the tool on to the side to monitor the feeding direction (axial in this case) and the signals from the accelerometer are amplified and transformed (FFT) and plotted. It was observed that the amplitude of vibration during the cutting process produced two peaks in which the second peak serves to be a warning before the tool fails. The author concludes that the initial peak in vibration as a system

characteristic attributed to the mass of the work piece which decreases as the cut progresses and the second peak (which was lower than the first one) due to increase in friction which is a result of tool wear [64].

Routio, Mauri., and Saynatjoki, Matti., (1995) [65] conducted experiments to study tool wear and failure during the drilling process of stainless steel using online tool wear measurement techniques. In the method the examiners measured and analyzed the current output (in the form of voltage) from the spindle motor (spindle power) with the aid of a data recorder and as well the axial feed force and torque on the spindle using the dynamometer. The measurement values remained almost constant for the entire period of the tool life which makes this technique not appropriate to monitor tool wear but can be utilized to notify the operator when a tool breaks during machining so that further damage to the work piece and unnecessary rejection is avoided.

Lee, J, H., and Lee, J, S., in 1999 applied the concepts of neural networks to predict the tool wear (flank wear) for a turning process. The authors considered force ratios (Feed force, tangential force and radial force) and force increments (initial to final) obtained from force signals to predict the flank wear as force ratios are a function of tool wear. As there are several other factors like cutting condition variation, tool geometry variation and material property variation influencing the force signals, a multi-layer perceptron model which utilizes an error-back-propagation algorithm with a nonlinear sigmoid function was used. Force increments when used as an input to the algorithm yielded marginally more error percentage when compared to the force ratio inputs and among the force

ratio inputs, the one that incorporates all the three components reduced the error percentage significantly.[66]

Gekode, Haron, O., and Subramanian, S, V., in 2002 studied the tribological phenomenon of tool chip interface and tool wear mechanisms while machining AISI 1045 and AISI 1020 steels using tungsten carbide inserts. In this study the authors evaluated the chips for diffusion of tool material (tungsten and cobalt in this case) which is extremely low in the order of Parts per million (ppm). A well established technique to handle such low concentrations and a very high sensitivity is the Inductively Coupled Plasma Mass Spectrometry technique (ICP-MS) was used by the authors with a detection limit of 0.1ppm and 4-7% standard deviation. Also the atomically dissolved tungsten was measured by first dissolving the chips in sub boiling nitric acid and the total tungsten (atomically dissolved tungsten in matrix and as tungsten carbide) by dissolving separately in a aqua regia plus hydrofluoric acid mixture. The difference in the above measurements led to the dissolution wear (measurement) and the mechanical wear in the form of crater depth was measured using a Mitutoyo surftest 211 series 178 [67].

Kim, Jeon-ha., Moon, Deok-kyu., Lee, Deuk-woo., Kim, Jeong-suk., Kang, Myung-chang., and Kim, Kwang ho., in 2002 initially used an optical microscope (Olympus 50X- 500X) to measure the tool wear but later used a Charge Coupled Device (CCD) camera (Pulnix 200X, Neocom 200X) with a exclusive jig on the same optical microscope in order to minimize the error during wear measurement on the milling cutters. In the CCD method, a new program

called image pro plus was used to exclude the subjective views of the measurer and an additional light source was introduced in order to minimize the error. Also the jig was designed in such a way that the base of the end mill as well the side of the end mill could be analyzed without manhandling it (as is the case with the conventional optical microscope used initially) [68].

Otto, T., Kurik, L., Papstel, J., (2003) used a CCD camera (1/3" and 680, 000 pixels) equipped with changeable standard lenses and adapter to measure tool wear. The measuring system was capable of making angular measurements, area measurements, maximum and minimum measurement in both vertical and horizontal directions and as well the perimeter from a black and white image processed by the camera which was subjected to digital noise filtering. This set up also had the capability of measuring the 3-d wear area by measuring from two different angular positions with respect to the optical axis (similar to the modern sophisticated 3-d microscopes). The authors conclude that coupling of CCD image analysis along with the indirect measurement of vibration accelerations and noise analysis will give additional information of cutting tools condition, surface /contact areas, average wear and chip movement so that the machining process could be optimized accordingly [69].

There are several tool wear prediction models (based on forces and cutting conditions in machining) available in the literature which primarily considers the force values obtained during the cutting process and predicts the tool wear which is ideally a function of forces involved in machining. Oraby and Hayhurst model (1991), Korean, Ulsoy and Danni model (1986) , Choudhury and Rath model

(1999)[70], Choudhury and Kishore model (2000) [71], Zhao, Barber and Zou model (2002) Oraby and Hayhurst model (2004) [72] , Astakhov model (2004) [73] to name a few [74] . Since the current study focuses only on practical tool wear measuring, the details of the above model are not explored much.

Optical measuring techniques were utilized to quantify the finished surfaces and most of them in the literature correspond to offline measurement modes. Pavel, Radu., Marinescu, Ioan., Deis, Mick., and Pillar,Jim., in 2005 [75] used a Mommelwerke T1000 Profilometer to measure the surface roughness of the cut surface and a Wyco machine was used to analyze the surface topography (3-D surface) and texture. Kishawy, H, A., Dumitrescu, M., Ng, E.-G., and Elbestawi, M, A.,(2005) in their efforts to measure the average surface roughness of the finished surface on a high speed machined aluminum alloy, utilized a Zeiss Handysurf E-30A profilometer [76]. Tamizharasan, T., Selvaraj, T ., and Noorul Haq, K., in 2005 used a VERSAMET 3, optical Microscope with a magnification range of 50X to 1000X and a MITUTOYA surface tester with a measuring range of 0.3 microns to 10 microns to evaluate the finished surface from a hard turning process [77]. A MITUTOYA's surftest surface finish measuring instrument was used by Anthony Xavier, M., and Adithan, M.,(2009) in their study involving cutting fluids in turning of 304 Stainless steel [78]. Khidhir, Basim, A., and Mohamed, Bashir.,(2011) used a hand-held surface roughness tester TR200 instrument to study the machined surface of nickel based hastealloy-276 [79].

Materials, Instruments and Machines

Raw materials, tools, software, instruments and machines used in this study to collect force data and wear data are listed below:

- Raw Material
  - Aluminum 6061 T6 Tube. (3” OD, 0.125 wall thickness)
  - AISI 1020 Steel Tube. (3” OD, 0.125 wall thickness)
- Tool Material
  - High Speed Steel Tool Inserts (Arthur R.Warner Co.)
  - Uncoated Carbide Inserts (ISCAR)
- Machines
  - HAAS Three axis Mill (TM2)
  - HAAS Two axis Lathe (TL2)
  - South bend Lathe
- Gases and equipments
  - VORTEC cold air gun. (For cold compressed shop air).
  - Nitrogen (at room temperature) from Airgas.
  - Liquid Nitrogen (at -278 degree C) from Airgas.
- Instruments
  - KISTLER Three component Dynamometer (9257A)

- Kistler Charge Amplifier(Model 5004)
- National Instruments DAQ device (NI USB-6008)
- Daktak 150 Surface Profilometer
- Keyence VHX 1000E Microscope
- Fowler Digitrix II 0-1” Micrometer

♦ Softwares

- LabVIEW 8.2 data acquisition software.
- Minitab 15 Statistical analysis software.
- Daktak-vision software for surface profilometer

Aluminum 6061 T6 alloy was chosen as one of the raw materials for this study as it is one of the most commonly used materials in the aerospace industry. The other AISI 1020 steel which is low carbon grade steel was chosen to study the impact of gaseous coolants, as it was one of the easy to machine and largely consumed in the industry.

The chemical composition and the physical properties of the raw materials used in the research are given below

AISI 1020 STEEL	% C	%Mn	% Si	% S	% P	% Al	Iron remainder
	0.210	0.466	0.011	0.000	0.009	0.031	

ALUMINUM 6061 T6	% Fe	% Mn	% Si	%Mg	%Cr	%Zn	%Ti	% Cu	Aluminum reminder
	0.7	0.15	0.8	1.2	0.35	0.25	0.15	0.40	

Table 2: Chemical compositions of the raw material.

Material Property	Aluminum 6061 T6	AISI 1020 Steel
Yield Strength	42.70 KSI	81647 PSI
Tensile Strength	46.85 KSI	91641 PSI
% Elongation	13.225	17
Hardness	96.75 HRE	81 HRB

Table 3: Physical properties of the raw materials.

Two different tool types were used in this study including, High Speed Steel (HSS) and uncoated carbide. Unlike previous research carried out at Auburn University, which utilized a whole stick of HSS tools with rake angle ground into it, this study used tool inserts thereby significantly cost of the research. The inserts used, both HSS and uncoated carbide, do not have any form of chip breaker built into them and the rake angle is 0 degrees (three different rake angles 0°, 7° and 15° used in this study are obtained by using custom designed tool holder). The clearance angle is 20 degrees and the node radius is $1/16^{th}$" with a thickness of 0.125" and a size of 0.5" * 0.5".

HAAS TM2, 4 axis tool room mill was used to machine the custom designed tool holder and the modified tool post to be used on the 2 axis HAAS lathe for the orthogonal tube turning experiments.

Figure 10: HAAS TM2 MILL

The actual experiment was carried out on a 2 axis HAAS Tool room lathe (TL2) machine with a swing of 16” * 48”. The machine has 12 HP Spindle with the maximum spindle RPM of 2000 and maximum traverse feeds in x axis of 75”/ min. and 150”/min. on the Z axis.

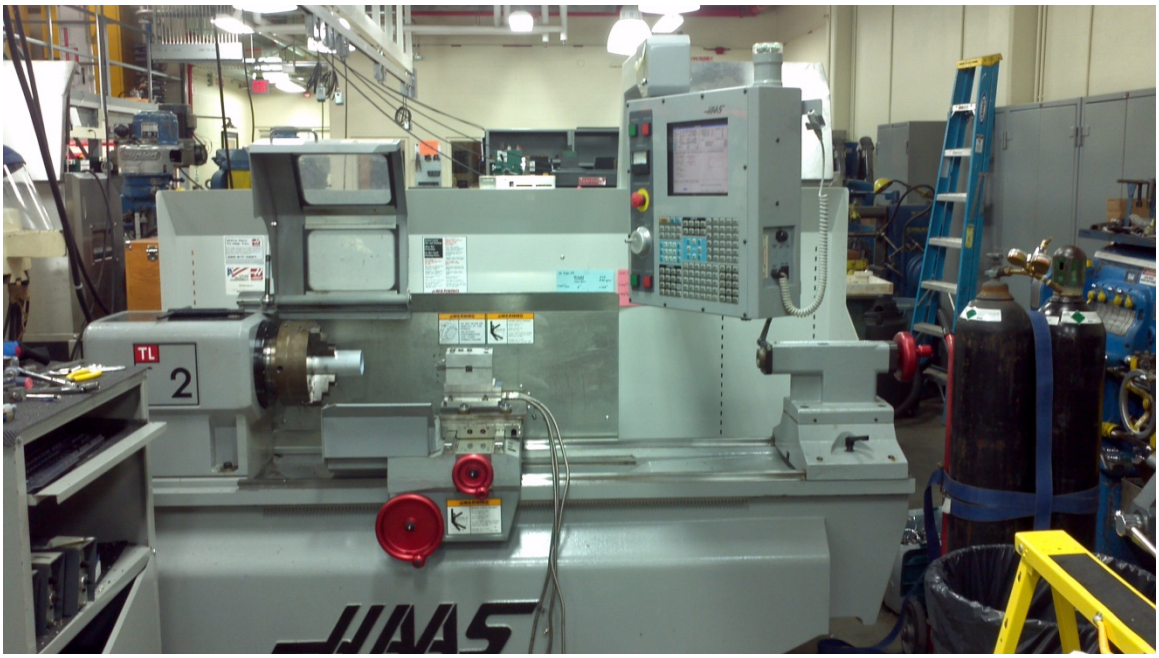

Figure 11: HAAS TL2 Lathe.

The manual all geared south bend lathe is used in preparing the samples by parting the saw cut edge of pipe sections of the raw material flat so that it sits on flush in the chuck during the experiment. Also after the experiment is complete a thin section of the work piece is parted on this same machine in order to perform the surface roughness study of the machined surface and as well for other observations like hardness tests.

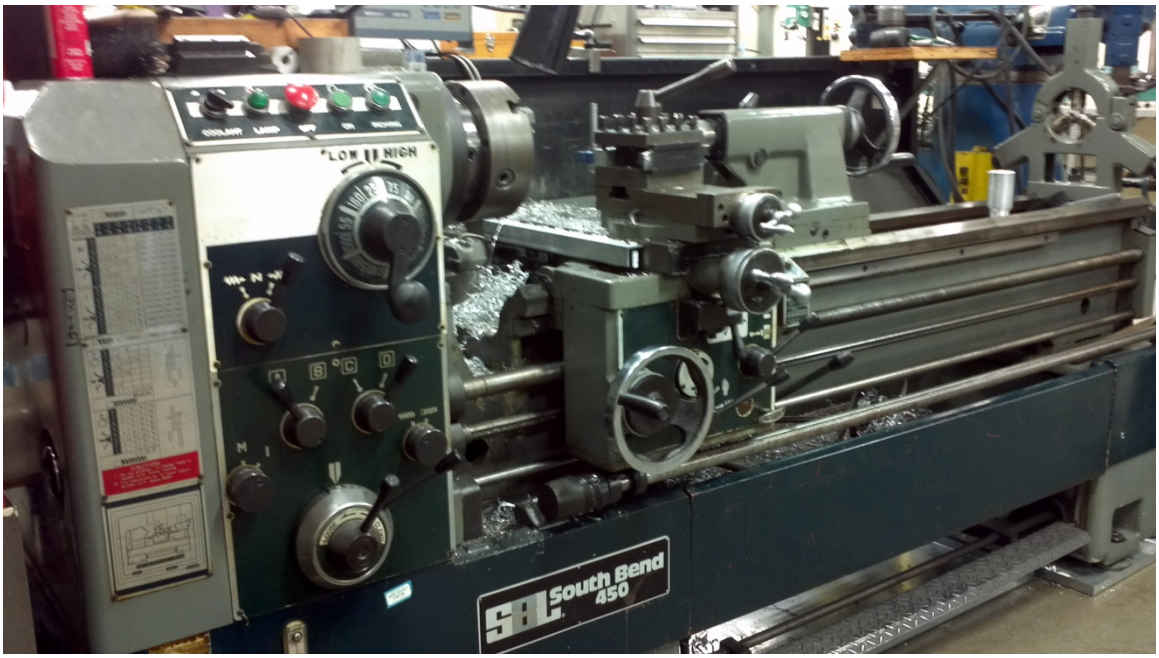

Figure 12: South Bend 450 all geared manual lathe.

The performances of three different cutting environments are compared against the dry machining environment for this study. The dry machining is carried out with no application of any form of cooling in order to aid the dissipation of heat generated during the cutting process.

The first environmental control used is the cold compressed shop air supplied at the point of cutting on the rake face of the tool through a Vortec Cold air gun. The compressed shop air is connected to the inlet of the cold air gun which then enters a cylindrical generator causing the air to rotate. The rotating air is forced through the inner walls of a hot tube present inside the air gun, reaching speeds of up to 1,000,000 rpm. A small portion of the rotating air escapes out through a needle valve present at the end of the hot tube as hot exhaust and the remaining cold air is forced back at the center of the tube where it interacts with

the slow incoming air stream generating a super cooled air which flows out through a outlet nozzle which is directed on the region of cutting. The air coming out of the outlet nozzle consistently reached temperatures of 0 ° +/- 1 ° Celsius.

Figure 13: Vortec Cold Air Gun.

Figure 14: Nitrogen cylinder with regulator.

The second environment used in this study is the nitrogen gas at room temperature. A suitable high pressure regulator was used to regulate a constant output pressure and also monitor the bottle pressure.

Cryogenic cooling is the third type of environment in this study wherein liquid nitrogen at a temperature of -278° C was used. A special cryogenic hose was used to deliver the liquid nitrogen from the bottle on to the cutting region.

Figure 15: Liquid nitrogen bottle

It is also important to mention the use of same nozzle delivering the different types of coolants used in this study. The nozzle has a 1/8” diameter opening through which the different coolants flow, thus maintaining a constant flow rate (as flow rate Q is proportional to velocity V and area A through which it flows; Q α VA) across all the environments making it suitable for a direct comparison of the existing scenarios.

Figure 16: Nozzle supplying the coolants at the point of cutting.

The instrument used in this study to collect force data is the KISTLER 3 component type-9257A Piezo electric dynamometer. Piezo- electric materials are the ones that exhibit a unique electro mechanical property, i.e., whenever the crystal is subjected to a tensile or compressive or shears stresses it exhibits a change in voltage. Many crystalline materials like quartz, barium titanate exhibit this phenomenon. The KISTLER 9257 A dynamometer works on the fore

mentioned principal and the type of Piezo-electric crystal used is Quartz which also is used in many other modern day piezo- electric dynamometers.

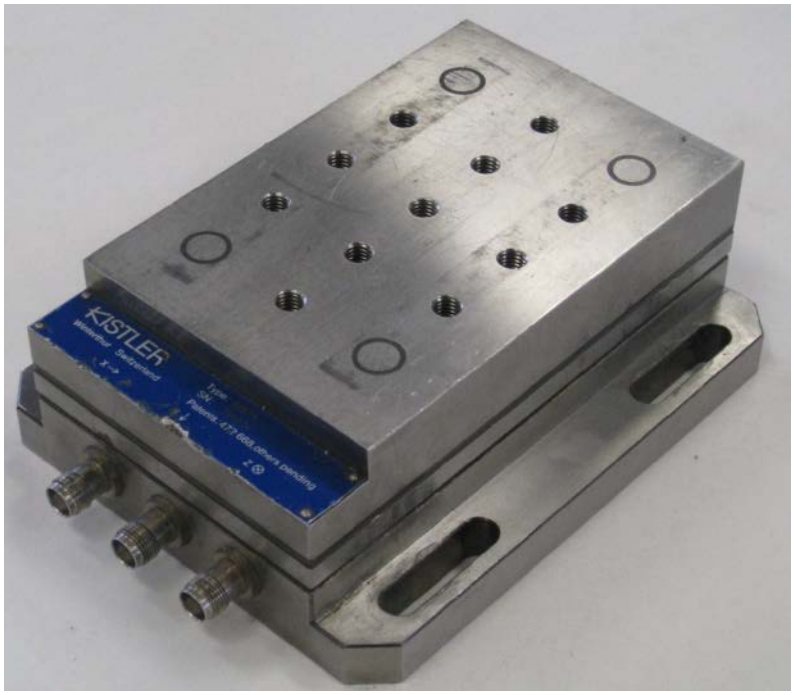

Figure 17: Kistler 3 component Dynamometer Type 9257A.

In this instrument [80], the platform on which the tool is mounted consists of 4 washers each consisting of 3 component force sensors oriented in the respective directions to measure the forces acting in the direction. The 3 component force sensors are nothing but three platelets cut out of a single crystal quartz which are carefully insulated and stacked in such a way to avoid any slipping due to shear. The 4 washers are mounted on the platform in such a way the forces and moment are balanced.

In milling experiments as the work piece is centrally mounted over the dynamometer and hence the forces act centrally over the dynamometer. The dynamometer is designed in such a way that where ever the force is applied over the dynamometer, it accurately measures it. In orthogonal tube turning experiments, the tool is eccentrically mounted (as shown in Figure 18) and hence the dynamometer will also be eccentrically loaded. In this situation, each of the 4 washers containing the 3 component force sensor will experience different loads but they are positioned in such a way that the forces and moments are balanced and the balanced change in voltage corresponding to the applied forces is outputted.

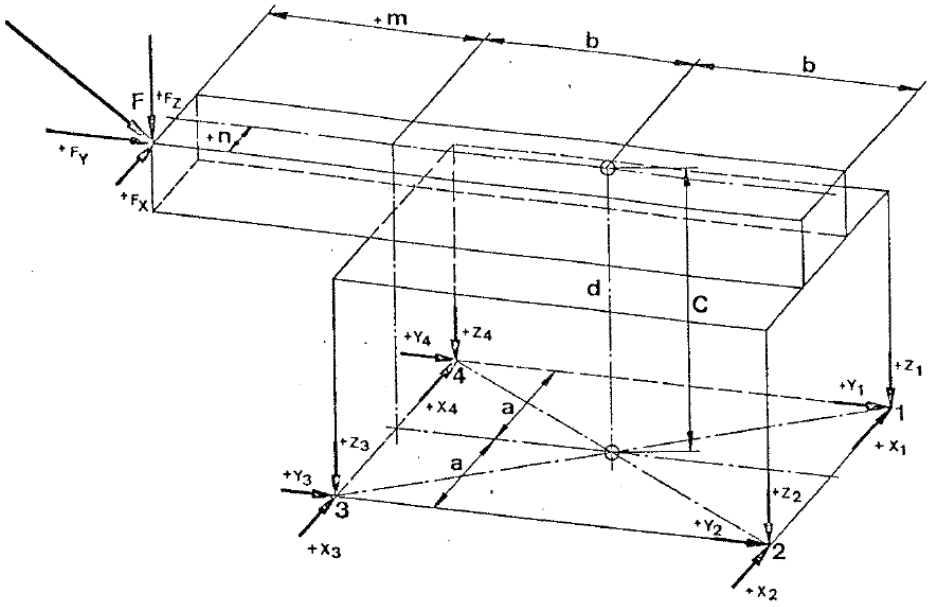

Figure 18:Schematics of Forces acting at various points in a dynamometer for an eccentric load [80].

When a force is applied anywhere on the platform, the force sensors experience strains which are recorded in the form of small voltage changes. It becomes difficult to measure the forces with these very small voltage signals and hence is send through a charge amplifier unit which in the current study is Kistler Model 5004.

Figure 19: Kistler Model 5004 Charge Amplifiers

Figure 20: DAQ Module, NI USB 6006.

The signals from the charge amplifier are send to a National Instruments', Data acquisition module NI USB 6008 which process the amplified voltage signals from the charge amplifier. LabVIEW 8.2 software is used to output the digital voltage signals in the form of plots involving the different force components versus time. The software is also capable of saving all the data points (forces) in the form of excel spread sheets which are used for further analysis. The LabVIEW program used in the current study to process the data is described in detail in the following chapters.

The chips obtained during the machining process are collected to measure the cut chip thickness in order to compute the chip thickness ratio which is extensively used to calculate different parameters governing the mechanics of metal cutting. A 0"-1" Fowler Digitrix II micrometer with a least count of 0.0001" and an accuracy of +/-0.00005 was used for the purpose.

Figure 21: Fowler Digitrix II 0-1" Micrometer.

A Rockwell hardness tester Model HR 150 A was used to test the incoming work piece raw material and as well also in testing the machined surface which was cut under different cutting environments. The C-scale was used to test the hardness of steel samples while the B-scale was used to test Aluminum samples. The instrument was calibrated before testing each batch with the calibration standard blocks provided by the instrument manufacturer.

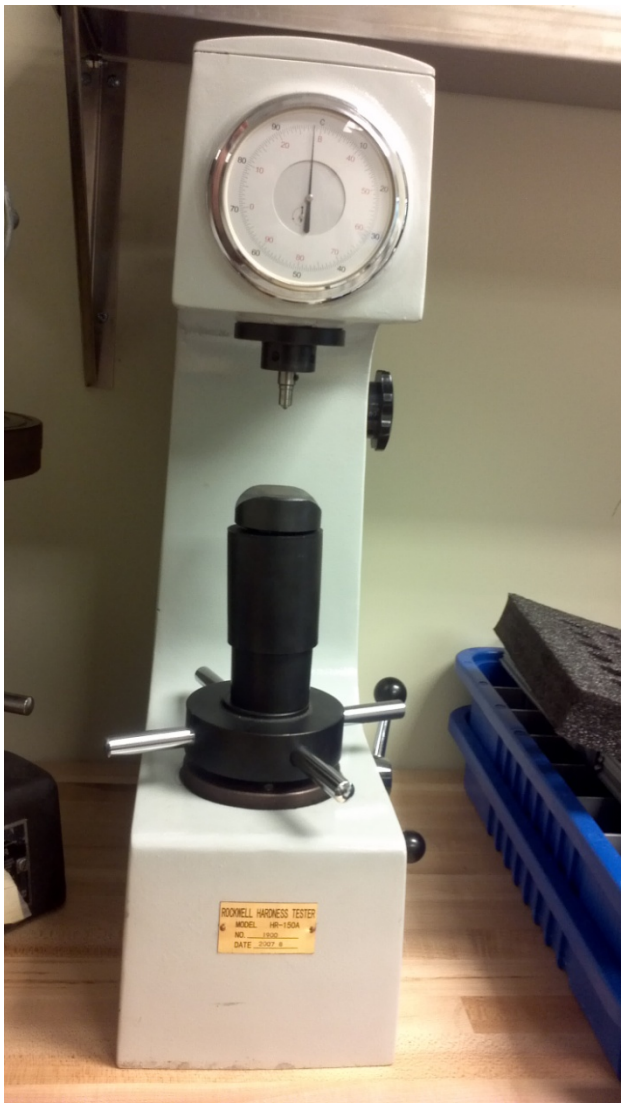

Figure 22: Model HR 150 A Rockwell Hardness tester.

A Dektak 150 contact type surface profilometer was used to obtain the surface roughness data from the work piece sample. The profilometer uses a 2.5 micron radius spherical tip with a resolution of 0.667 microns/sample and a constant downward force of 10.0 mg.

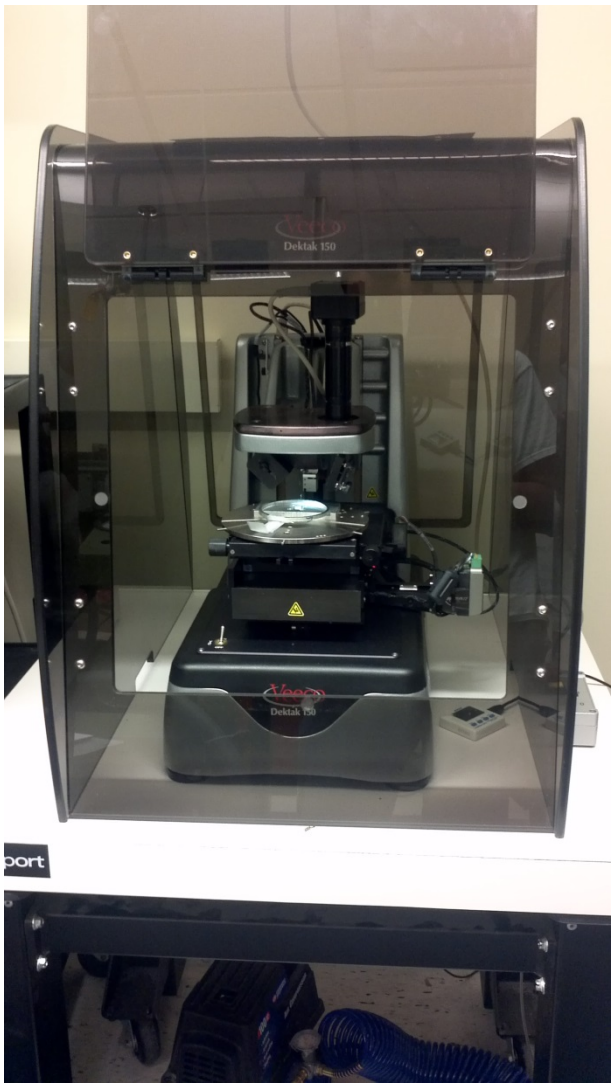

Figure 23: DEKTAK 150 Surface profilometer.

A Keyence VHX 1000 E model digital microscope with 3-d measurement capabilities was used to determine the volumetric tool wear on the tool inserts used in the cutting process. It is a 2 stage microscope with the 1 stage having a magnification range of 100x to 1000x and the second stage has a 500x to 5000x magnification range. The resolution of this microscope is +/-0.05 micron and a repeatability of +/-0.5 microns.

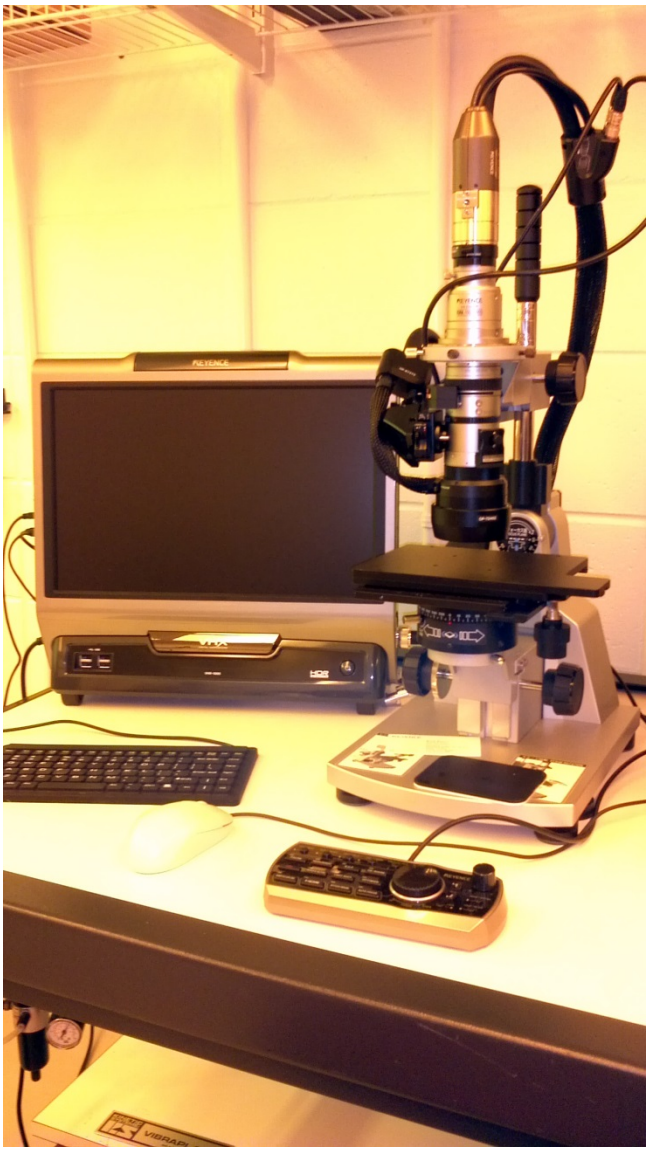

Figure 24: Keyence VHX 1000 E digital microscope

Construction and methodology of experiment

All the material removal operations out in the industry are carried out as an oblique machining process which involves 3 component force system. In the academia and research a simplified model involving only two force system called the “orthogonal machining” [22] is considered, the details of which is provided in the literature review chapter. Orthogonal tube turning process involving two of the force components, the cutting force and the thrust force was considered for the study to evaluate the gaseous fluids.

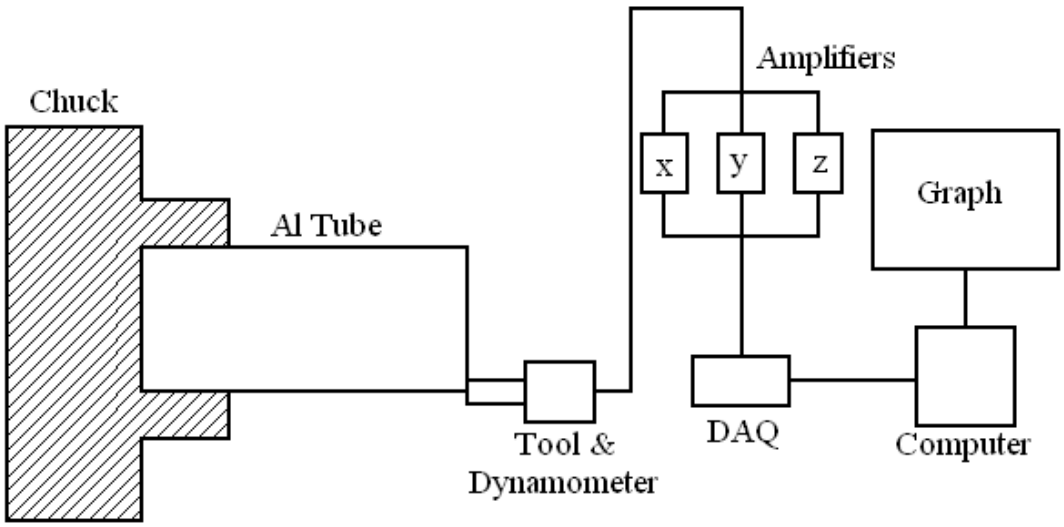

Figure 25: Schematic representation of orthogonal tube turning set up.

The basic layout of the orthogonal tube turning set up is depicted in figure 23. The work piece is held in the 3 jaw chuck flush against the chuck face and the tool is mounted on the modified tool post mounted on a dynamometer fastened to

the lathe carriage. The dynamometer is connected to the charge amplifiers which amplify the voltage signals and send it to a data acquisition device. The data is processed and the forces are plotted against time by the LabVIEW 8.2 software installed on a PC.

Before setting up the tube turning experiment, the conventional tool post on the HAAS lathe (TL2) was replaced with a modified tool post in order to accommodate for the dynamometer and as well hold the customized tool holders. A steel plate of 0.5” thickness formed the base over the carriage of the lathe with holes in the desired position to mount the dynamometer. The dynamometer was then mounted on the steel plate over which the modified tool post was mounted. The modified tool post contained two aluminum blocks with slots machined in them to seat the customized ¾” tool holders. The tool post was designed in such a way that it covered the entire dynamometer, in order to achieve the total load transfer from the tool to the instrument. The bottom part of the two-block modified tool holder is fastened down on to the dynamometer and the top part is adjustable to facilitate tool change. The top half of the block is clamped down using ¼-20 steel bolts and also in order to avoid any vibration in the tool, an additional set of 3, 3/8”-16 bolts are used.

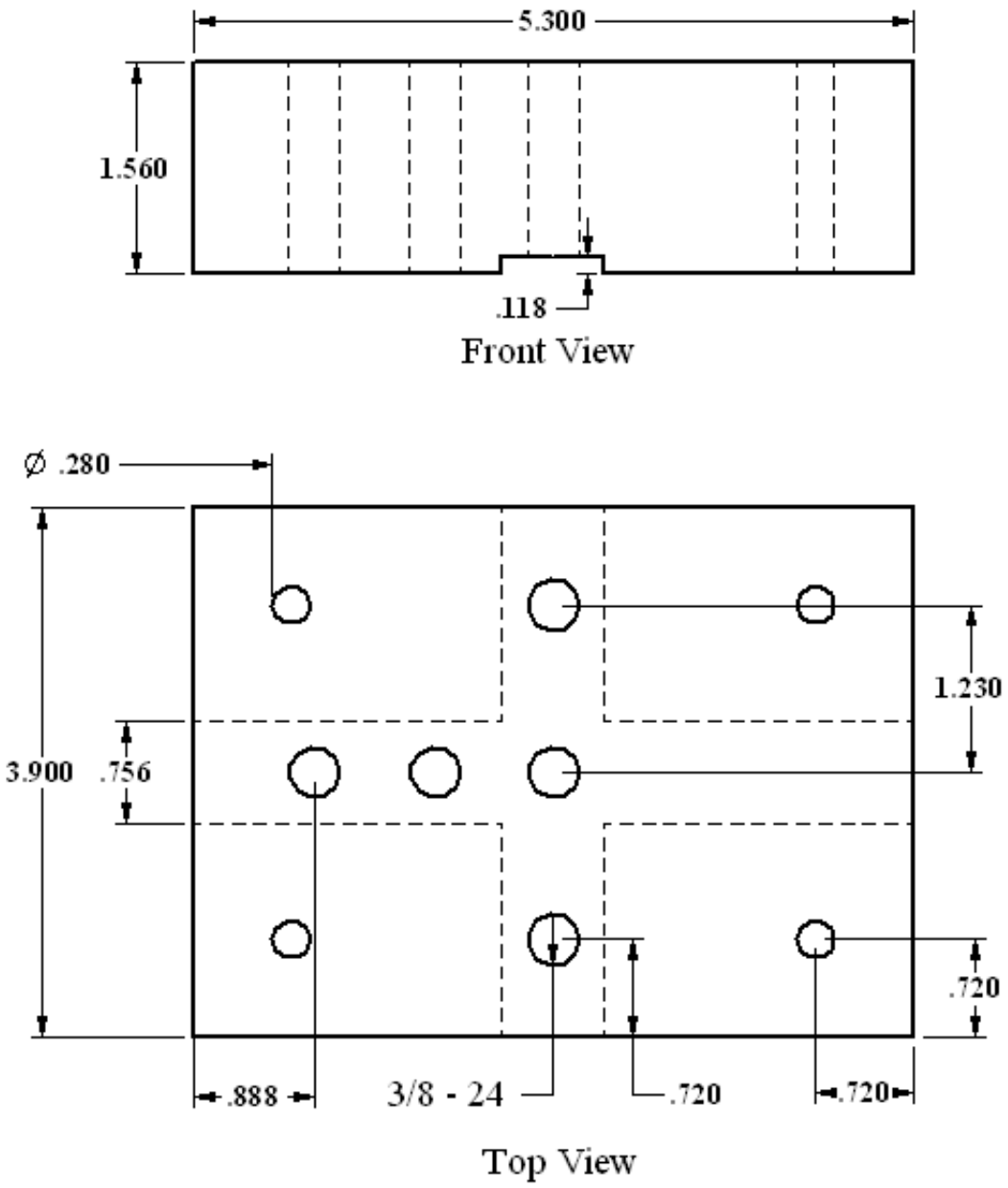

Figure 26: Top block of the modified tool holder.

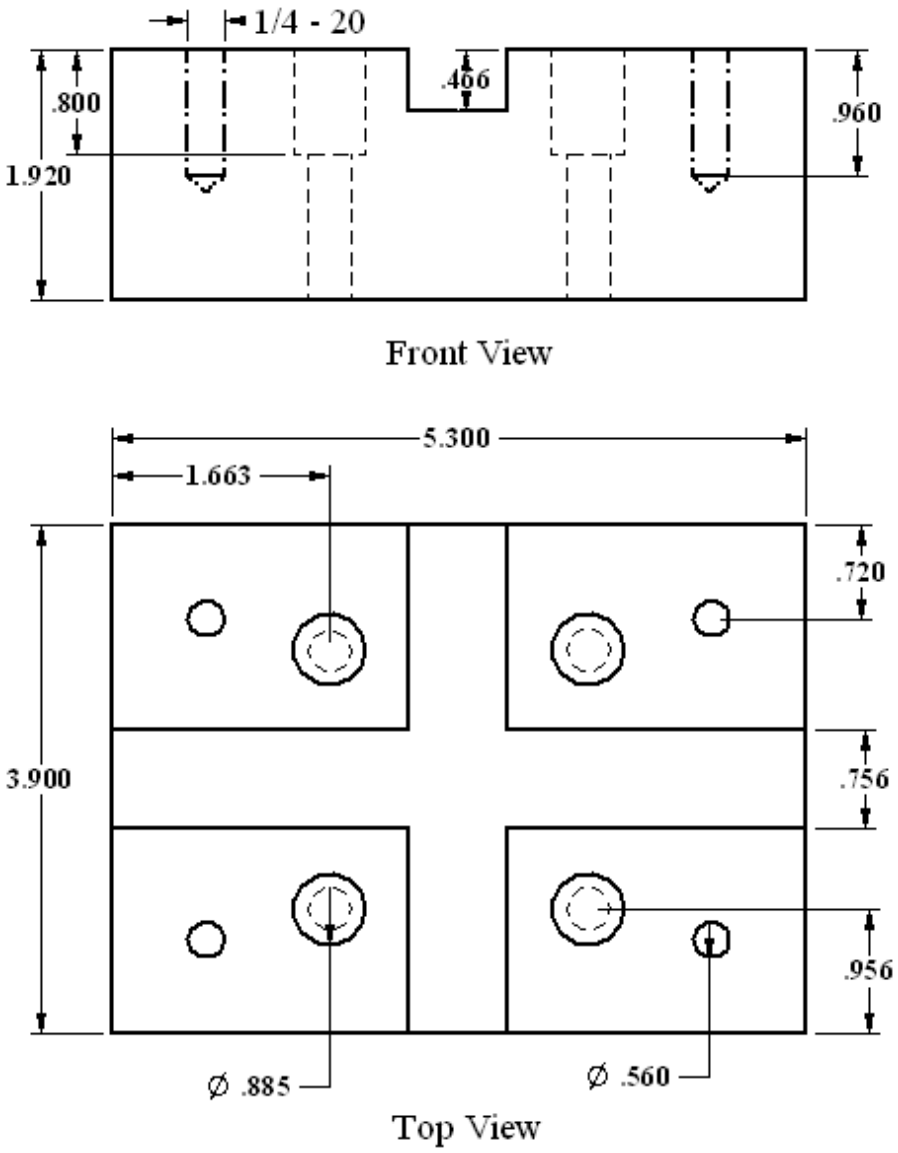

Figure 27: bottom block of the tool holder

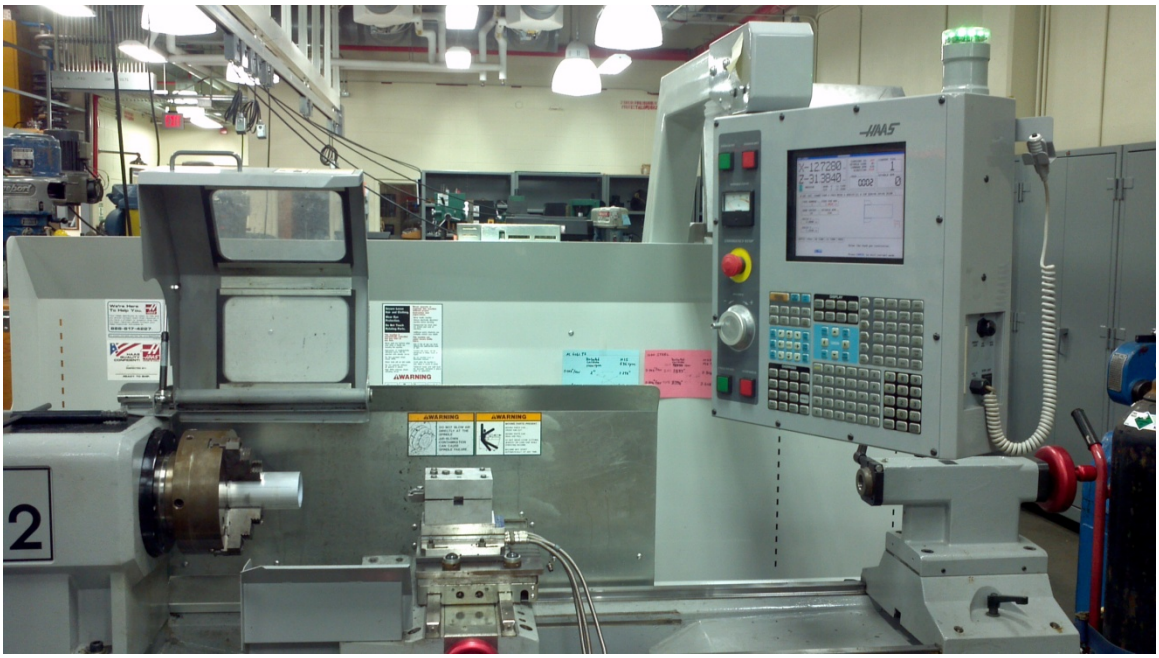

Figure 28: Dynamometer and modified tool post mounted on the HAAS lathe (TL2)

The dynamometer mounted on the lathe has three output terminals labeled X, Y and Z which is connected to three separate charge amplifiers (Kistler 5004) using steel shielded co-axial cables. The range is set up to long and the sensitivity and linearity of the charge amplifier are set to the values recommended by the manufacturer's calibration certificate (refer appendix 1) for the respective axis. The role of the charge amplifiers was to amplify the very low voltage signals from the dynamometer to a more sensible output range. An NI Data Acquisition Device (DAQ) with 12 Digital Input and Output (DIO) channels and a 32- bit counter is connected to a PC installed with LabVIEW 8.2 data acquisition software through a full speed USB interface. The input to the DAQ was provided by cables from the charge amplifiers supplying amplified voltage signals.

Figure 29: Data processing station containing charge amplifiers, DAQ, a PC with LabVIEW 8.2 software.

The LabVIEW 8.2 software is set up with a program that can output the thrust force and cutting force data from the voltage signals received by the DAQ. The software starts processing the signals by activation of a start button in the program which the operator triggers with a mouse click once the tube turning set

up is ready to start cutting. The signals are first received by the DAQ assistant block in the program where the sampling rate is set up, which then sends it to a signal filter block. The filtered signal is send to a wave form generator which outputs the plot of cutting force and thrust force versus time. The processed data from the wave generator is sent to a write to file block where the software stores all the data in a excel spread sheet.

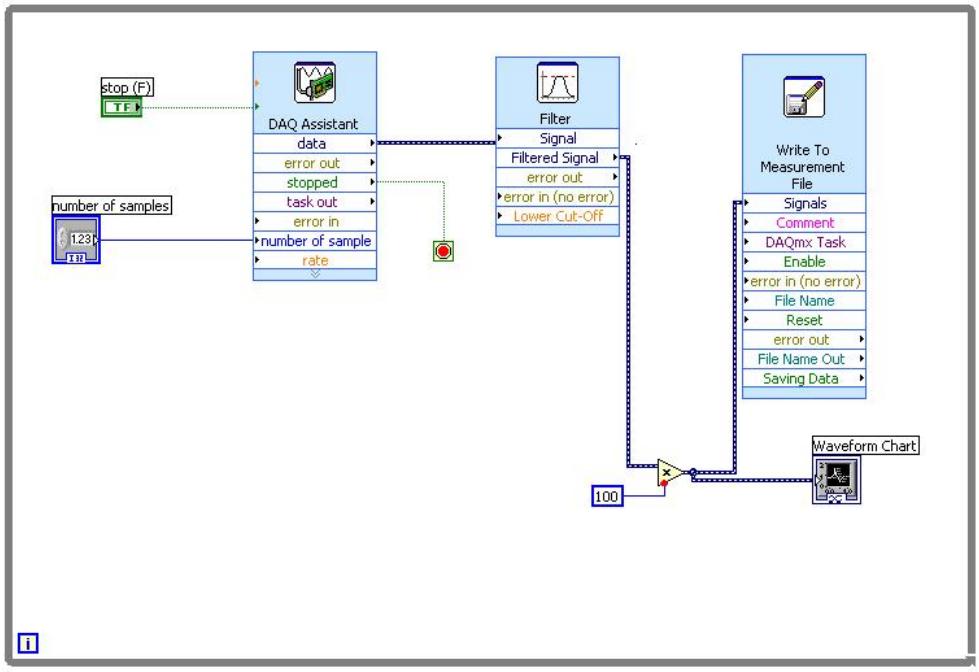

Figure 30: Block diagram of the data acquisition program in LabVIEW 8.2

The work pieces used in this study both, the Aluminum 6061 T6 and the AISI 1020 steel were purchased in forms of hollow pipe with a 3” outer diameter and a wall thickness of 0.125”. The pipes are all purchased from the same vendor in 20 feet long sections delivered from the same lot thereby ensuring same physical properties and chemical composition. The long pipes are cut into smaller lengths in order to avoid any oscillation/vibration of the work piece which would

affect the data collected as no steady or follower rest or tail stock is used to support longer sections. The length of pipe to cut was based off of the length of material removed during each run.

The HAAS lathe has few canned routines built into the controller to perform standard machining operations on a lathe like, turning, facing, threading, etc., one of which was to run the machine at a constant feed and RPM specified by the operator. The time period of cut has to be given in the form of the distance to cut in the respective axis as the programming module of the machine does not provide with an option to enter time. The length of cut is important because, every factor level combination in this current study has to be run for the same time so that a direct comparison of tool wear can be done. Distance to cut can be determined from the formula involving RPM, feed per revolution and time. For example, if the time of cut was to be 1 minute at a constant RPM of 600 and a feed of 0.002”/revolution, the length of cut can be computed as follows,

$$L=RPM*F\ (in/rev.)*T\ (minutes) \quad (8)$$

$$\text{i.e., } L=600*0.002*1=1.2”$$

For the different speeds, feeds and material tool combinations in the study, lengths of cut are calculated and 9”long pipe section was selected to be more rigid, safe and would lead to less wastage. The smaller sections of pipe were cut on a horizontal band saw and the mounted on a South Bend manual lathe to part off the saw cut edges to provide the work piece a flush seating on the chuck face of the HAAS lathe.

The tool holders used in the study to hold inserts were custom designed and machined at the Design and Manufacturing lab at Auburn University. The reason to use inserts over stick tools (as used by [24]) is approximately atleast 4 runs could be taken using a insert costing approximately $15 but whereas the stick tools can only be sued to take 2 runs and the cost for each tool blank was approximately $30. Moreover, in the case of stick tools, the rake angle was to be ground using a surface grinder for each tool and doing it for 384 tools would be tedious. But it has to be noted that rigidity provided by the stick tools should not be compromised while designing the tool holder for the inserts.

Three different ¾”* ¾ ” tool holders with various rake angles of 0°, 7° and 15° and a constant clearance angle of 20° were designed. The design was subjected to a static finite element analysis in solid works with an applied load of 5000N (maximum force observed for this study was less than 1000 N) and a factor of safety of 2. The deflection was measured for different tool materials which are given in table 4.

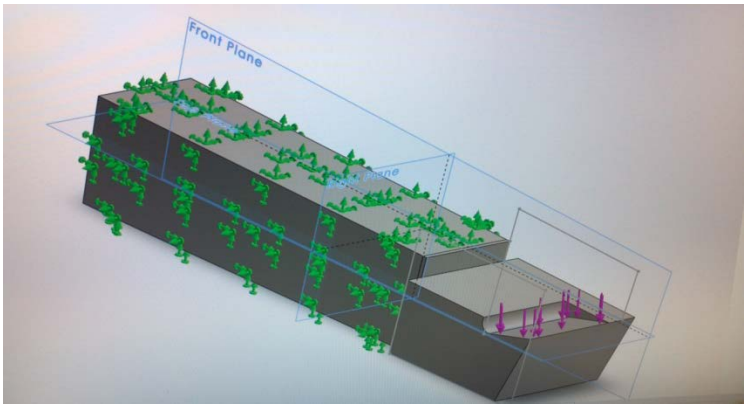

Figure 31: Solid works model of a 15° tool holder with loads applied for Finite Element Analysis.

S. no.	Material	Deflection (mm)
1	AISI 4130	0.3327
2	AISI 4340	0.3303
3	AISI 1020	0.3826
4	316 Stainless Steel	0.3942
5	Tool steel (H13)	0.3427

Table 4: Deflection values for different materials from Finite Element study

Based off of the deflection values, AISI 4140 steel was selected to machine the tool holder, which was programmed in Mastercam X6 and machined on a HAAS 3 axis Mill (TM2). The tool holder was secured in place using a clamping mechanism held on the tool shank with a1/4” -20 bolts which also facilitate insert changes.

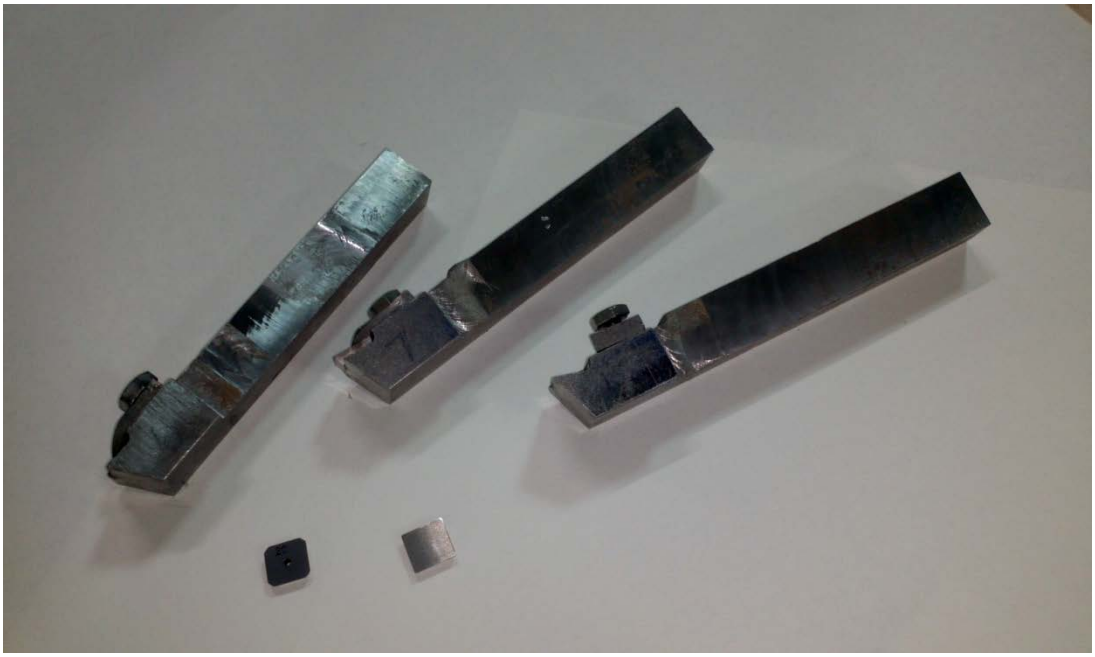

Figure 32: Three different tool holders with different rake angles machined in AISI 4140 Steel stock.

Once the work piece is loaded on the chuck and the tool in the tool post, the tool is paper touched off the edge of the pipe section to zero the x axis. The appropriate RPM and feed per revolution and the distance to cut for the run in progress are entered in to canned routine. The coolant supply is started and waited on till a steady flow is achieved, then the LabVIEW program is started up before triggering the canned routine program on the machine. As we have no chip breaker in the insert or the tool holder, the chips generated are long and continuous in all cases except for the AISI 1020 steel with uncoated carbide tool combination, where the chips were segmented while applying coolants. The long continuous chips are continuously being pulled using long handled hooks so as to keep it from strangling the rotating work piece. The program automatically stops after the prescribed distance, and then the LabVIEW software is stopped and then the coolant supply is cut off when in use. The long chips are then measured at at least 3 different locations using a micrometer and the average is taken to determine the cut chip thickness which is extensively used in calculating several cutting parameters. The tool insert is marked with a code to identify the run number and then stored for measurement of tool wear. The work piece is then loaded on to the South bend lathe to part off a thin section which was used to determine the surface finish in terms of surface roughness measurement taken using a surface profilometer.

First batch of runs were performed without any coolant supply and this becomes a very important set of observation as the performance of the tool and the cutting parameters under other cutting environments, have to be compared to a

benchmark which in this case would be dry machining. The second environment that was used in this study was cold compressed shop air. The compressed shop air at 75 psi was connected to the inlet of the cold air gun and the output from which was diverted on to the tool rake face using a nozzle of 0.125” diameter. The exiting air from the cold air gun was at a temperature of 32 degree Fahrenheit +/- 2° F while the inlet temperature was at 72° F (approximate room temperature). The second environment was set up using Nitrogen gas supplied in bottles from Airgas, was supplied to the same location on the tool using the same nozzle thereby maintaining the same flow rate. A special pressure regulator was used to monitor the pressure of the nitrogen bottle as well the outlet stream. The third environment used in the study was Liquid nitrogen supplied at -278° F. The liquid was directed on to the tool rake face using the same nozzle connected to the bottle via a stainless steel cryogenic hose, so as to ensure that the same flow rate has been maintained across all three cutting environments enabling a direct comparison to be made.

Figure 33: Example of a fully constructed orthogonal tube turning apparatus with liquid nitrogen cutting environment.

The surface finish of the machined samples were measured from using a contact type Daktak 150 surface profilometer. The samples are prepared by parting off a thin section of the work piece containing the machined surface on a South bend all geared manual lathe. The sample was then coded to identify the run number and taped to protect any surface damage due to handling. A special fixture was machined on a HAAS TM2 mill to be placed on the table of the surface profilometer to maintain a repetability and ease of sample handling. The profilometer was programed to do a standard scan over the radius of the sample using a 2.5 micron spherical tip. The software automatically calculated the surface roughness values Ra in microns.

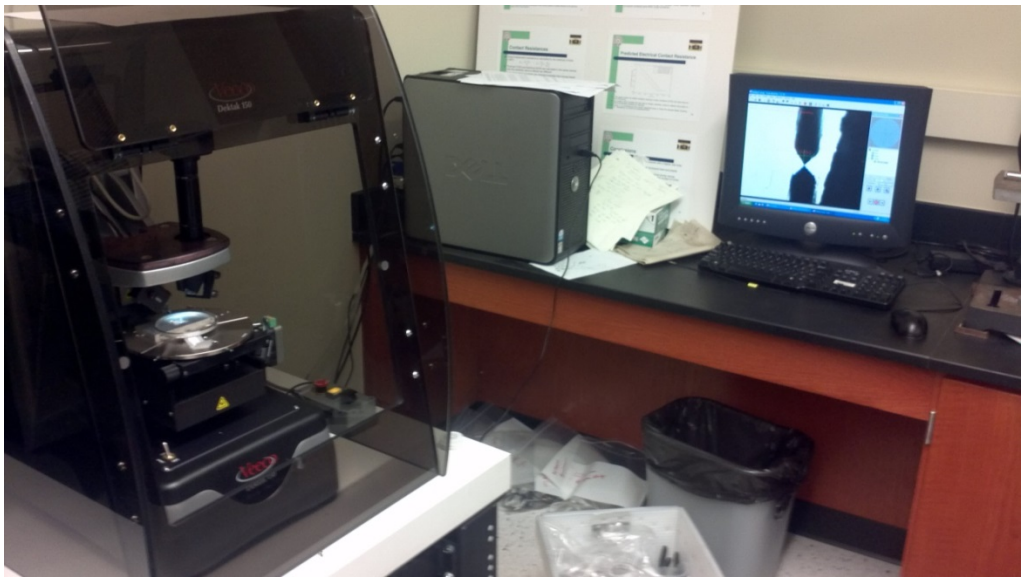

Figure 34: Surface profilometer with the computer screen in the background showing the scanning profile

Two types of tool wear parameters were measured using a Keyence VHX 1000 Digital microscope. The first type of wear characterization was a 2-d measure of the length and width of the wear area and the second type of characterization was the volume of the tool deformed plastically, in other words a measure of the volume of the crater formed on the rake face of the tool. The 2-d measure was taken at 100x magnification setting on the microscope. For measuring the volume of the tool deformation (crater) the microscope is set up into the depth up 3-d mode with a magnification setting of 300x. The magnification cannot be increased further as the sample area of interest gets out of the measuring range of the microscope. even at 300x magnification the entire volume of the deformed surface cannot be measured in a single shot and instead, a image stitching method is followed. In this method, the area of interest was focused separately as different small sections and a 3-d measure is taken at each

of these which are finally stitched up (put together) by the software accompanying the microscope. This particular microscope had a motorized z-axis movement which enabled it to shoot pictures of a 3-d profile at different depths (1 micron increment for a total of 150 micron height range setting was used in this study) and the inbuilt software outputs a 3-d profile. From the profile generated by the software, the volume of the area of interest was obtained.

Instrument Validation and Statistical Design of Experiments

Before statistically designing an experiment it is necessary to validate the capability of the instrument. In the current study, once the orthogonal tube turning experimental set up was constructed, the force collection system was tested for its statistical repeatability, statistical sensitivity and the statistical power. A random combination of tool and work piece was chosen along with a rake angle and feed for validating the instrument. All the statistical analysis in this study are performed using Minitab 15 statistical software.

First test carried out was to determine the repeatability of the feed in z axis on the lathe. As mentioned earlier, the time period of cut cannot be directly given to the lathe control and so the distance to cut based on the rpm, feed and duration of cut was calculated. For the validation purpose, the feed was at 0.002”/revolution, with a spindle rpm of 500 and the duration of cut at 1 minute. Using equation (8) we the length to be cut is determined to be 1 inch. A 0-2” dial indicator was set up on the lathe bed zeroed against the carriage. Once the corresponding parameters were set up on the lathe controller, the cycle was started, simultaneously triggering a stop watch manually. The stopwatch was stopped as the lathe carriage stopped at the predetermined cut distance and the time was noted down. The same procedure was repeated several times, and it was concluded that the timing on the stopwatch was at 60 seconds + 1 second on an

average. Similarly the x axis feed was tested and the timing was observed to be 60 seconds + 2seconds. The variation in the timing can be attributed to the fact that the stop watch is manually handled and the possibility in human eye to hand coordination.

Repeatability Analysis:

For the repeatability analysis, aluminum 6061 T6 work piece was chosen and the tool was High Speed steel. The rake angle was set up at 0 degrees while the feed was maintained at 0.002”/revolution with a spindle 636 rpm. Three different data sets were observed, with the second data set recorded the next day after the first was done, while the third was observed after a week from the day the second data set was collected. A set of four replicates were machined for each set and the cutting force and thrust force were recorded for duration of 1 minute of cutting. The mean and standard deviation of each of the force data for individual replicates are calculated and presented in the table 5.

SET 1				SET 2				SET 3			
Thrust Force Fy		Cutting Force Fz		Thrust Force Fy		Cutting Force Fz		Thrust Force Fy		Cutting Force Fz	
Mean	SD	Mean	SD	Mean	SD	Mean	SD	Mean	SD	Mean	SD
165.1068	6.4372	209.9344	6.7156	175.6599	11.404	216.7389	9.5698	178.82	11.0679	212.64	9.1327
178.0052	7.869	218.2937	7.9506	177.6808	9.9394	219.5274	7.6538	176.4451	6.5802	219.3411	7.4059
176.4845	8.112	216.4324	7.6801	164.7387	7.2363	210.0176	7.1887	175.4492	6.8551	213.342	6.3775
160.001	8.6781	206.4613	8.3264	163.3861	5.7064	209.0176	5.6464	179.7514	8.7382	216.8086	7.865

Table 5: Mean and Standard Deviation of Cutting force and thrust force data from repeatability analysis.

A 2 sample t-test is performed comparing two data sets at a time. The p-values of the tests are tabulated in table 6. The p-values of both the cutting force

and the thrust force are greater than 0.05 for all levels of combination suggesting that the setup yields highly repeatable data.

Combination	p-value		Remarks
	Thrust Force	Cutting Force	
Set1 Vs Set2	0.939	0.853	Repeatable
Set1 Vs Set3	0.233	0.598	Repeatable
Set3Vs Set2	0.279	0.724	Repeatable

Table 6: p-values for different data set combinations from a 2 sample t-test for repeatability analysis.

Sensitivity analysis:

Once the instrument is found to be repeatable, it now becomes necessary to prove that the setup is not reporting the same (false) results every time. Two of the parameters feed and rake angle was varied and the force data were recorded as presented in table 7.

SET 1		SET 2		SET 3		SET 4	
0 RAKE, 0.002"FEED		0 RAKE, 0.004"FEED		7 RAKE, 0.002"FEED		7 RAKE, 0.004"FEED	
Thrust Force Fy	Cutting Force Fz	Thrust Force Fy	Cutting Force Fz	Thrust Force Fy	Cutting Force Fz	Thrust Force Fy	Cutting Force Fz
178.82	212.64	233.3745	335.5765	144.1816	198.5818	197.652	323.2784
176.4451	219.3411	241.8935	339.2945	140.8573	199.7019	197.6554	324.414
175.4492	213.342	235.166	338.0937	142.4506	200.2728	190.1233	316.9521
179.7514	216.8086	248.1928	346.0426	141.7632	203.0096	190.6575	317.9177

Table 7: Mean values for cutting and thrust force observed with different rake angle and feed for sensitivity analysis.

A 2-sample t test was performed between data sets when one of the parameter was varied while keeping the other a constant. The work piece used for this sensitivity study was aluminum 6061 T6 and a High Speed Steel tool, with two different rake angels of 0° and 7° and feeds of 0.002”/revolution and 0.004”/revolution. For instance data set 1 was compared with set 2 in which case the rake angle was constant while the feed was changed, when comparing set 1 with 3, rake angle was changed maintaining a constant feed. The p-values form the t-test are presented in table 8, which shows that the p-value is always less than 0.05, thereby proving that the instrument is sensitive enough to record the changes in forces when contributing parameters are changed.

Combinations	p-value		Remarks
	Thrust Force	Cutting Force	
Set1 Vs Set 2	0	0	Sensitive
Set1 Vs Set 3	0	0.001	Sensitive
Set2 Vs Set4	0	0	Sensitive
Set3 Vs Set 4	0	0	Sensitive

Table 8: p-values for different data set combinations from a 2 sample t-test for sensitivity analysis.

Standard deviation of the instrument:

The entire force collection instrument has two parts of standard deviation, one coming from the dynamometer and the other one from the Ni USB 6008 Data acquisition module. The manufacturer recommends a standard deviation in their calibration certificate for the dynamometer to be +/-10 N. The NI Data acquisition module comes with a standard deviation of +/-1N, thereby making the cumulative

standard deviation of the entire force collection set up to be +/-11 N. Also from table 5, it is evident that all the standard deviation values observed for both the cutting force values and thrust force values are within the range of the instrument's standard deviation supporting the fact that the force collection instrument is accurate.

Power analysis:

In order to design a statistical experiment to study various effects of controllable factors, it is necessary to establish a sample size based of the statistical confidence limit. Sample size is dictated by how accurate the results must be, or how large a margin of error that can be tolerated. The larger the sample size, the more sure one can be that their averages truly reflect the population. For the current study, the confidence interval was set to be at 90% implying that the conclusions of this study will be at 90% confidence. Generally a statistical power is defined as the capability of the analysis to detect a difference which actually exists between two sets of data or the ability that the test will reject a false null hypothesis to avoid Type II error. A Type II error is the error of not rejecting a null hypothesis when it is not true and increases with decreases with increase in power.[81]

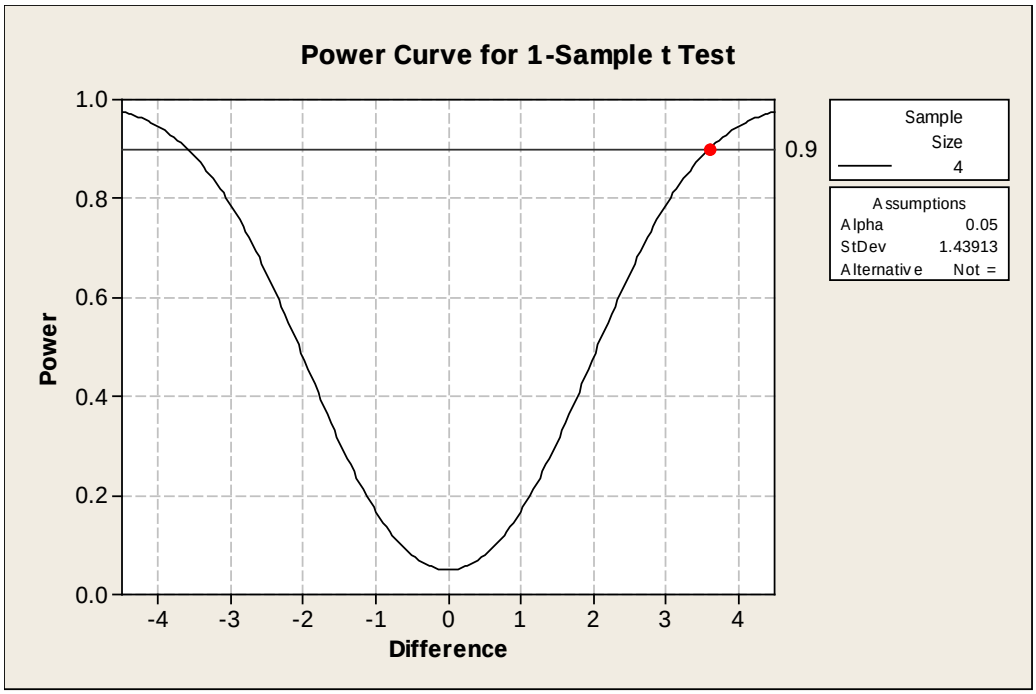

Figure 35: Power analysis curve for cutting force.

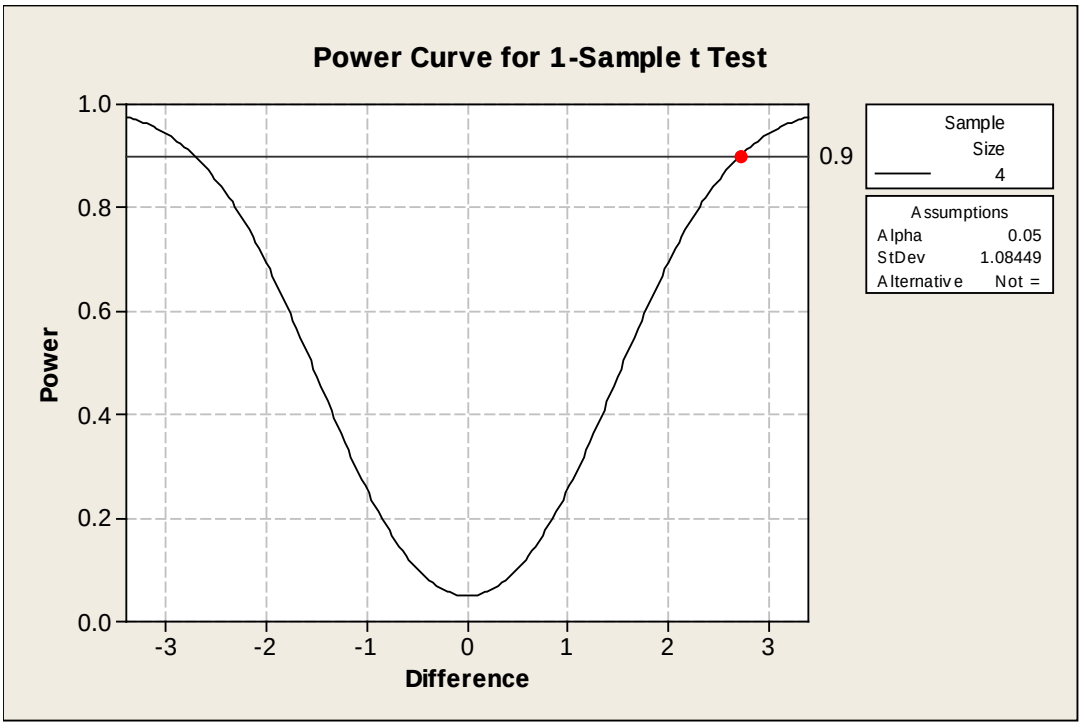

Figure 36: Power analysis curve for thrust force.

Using the previously collected force data from the repeatability analysis, a power analysis was set up in Minitab to determine the minimum number of samples necessary to achieve a statistical confidence of 90%. From the figures 32 and 33, it is evident that a sample size of 4 will yield a statistical confidence of 90% for both the cases of cutting force and as well the thrust force.

Statistical Design of Experiments (DOE):

In this study, the influences of 5 different controllable factors were chosen to study the performance of the cutting process. The time of cut for each factor level combination was maintained a constant which enables a direct comparison made on tool wear for a constant cutting duration. As mentioned in the earlier chapters, Aluminum 6061 T6 alloy and AISI 1020 alloy steel were chosen as the work materials (first factor) along with High Speed Steel Inserts and Uncoated carbide tool inserts as tool materials being the second controllable factor with both of at 2 factor levels. In order to evaluate the effect of tool geometry, rake angle (third factor) of the tool was considered, which according to the literature has a major contribution on the cutting forces and as well tool life. In industries, it is quiet common to see a 0° rake angle in use as it is considered to give superior tool life because of its rigidity[25] and also a nominal range of tool rake angle used in industry would be 0° -15° [81]. To get a good spread of the range used in industry 3 factor levels at 0°, 7° and 15° were chosen for in this case.

The fourth factor in this study was the feed per revolution or the uncut chip thickness which adds a significant contribution to tool forces and also the

chip thickness ratio which is pivotal in determining several important metal cutting parameters. Traditionally, lathe operators (machinist) consider, 0.001”/revolution to be a finer cut used for finish turning while, 0.005”/revolution a heavy cut used for roughing [81]. Preliminary tests were conducted to evaluate different feeds starting from 0.001”/revolution to 0.005”/revolution at 0.001”/revolution increments. The heavier cut 0.005”/revolution had a lot of chatter along with spindle load percentage of the machine exceeding 100% in most of the combinations and even produced smoke while machining steel with uncoated carbide inserts. Therefore, 0.004”/revolution was chosen to be a close enough representation of a heavier cut that would yield data without overloading the machine as well the force collection system. 0.002”/revolution was selected to represent a fine cutting or finish turning process that would yield better surface finishes.

The next factor level, 3 different cutting environments Cold Compressed Shop air, Nitrogen and Liquid Nitrogen were tested against the dry machining scenario thus making setting it 4 levels. The cutting environments were chosen based on the literature and from the results of experiments previously carried out at Design and Manufacturing Lab, Auburn University. Other than the above mentioned factors, factors like, ambient temperature, position of coolant supply, nose radius of the tool etc., were not considered in this study thus making the effect of such parameters as noise in the experiment.

With five controllable factors, of which 3 are at 2 levels, and one of it at 3 levels while the fifth one at 4 levels, the number of unique data runs lead to 96

runs. From the power analysis, we have a sample size of 4 in order to gain a 90% confidence, taking the overall run tally to 384 runs. The following table summarizes the different factors and the number of levels.

Factor	Levels	Description
Work material	2	Aluminum 6061 T6 alloy AISI 1020 Steel alloy
Tool Material	2	High Speed Steel Uncoated Carbide
Tool Rake Angle	3	0°, 7° and 15°
Uncut chip thickness or feed	2	0.002”/revolution 0.004”/revolution
Environment	4	Dry Cold Compressed Shop Air Nitrogen Liquid Nitrogen
Number of unique runs= 2*2*3*2*4=96 runs. @4 replicates for each unique run= 96*4= 384 runs.		

Table 9: Summary of factors and factor levels used in this study.

RPM values for different factor level combinations for the work geometry were calculated based on the surface speed values from the machinery’s hand book [82] a sample of which is provided in the appendix.

The tool wear and surface finish were not measured for all the runs, instead only measured for a set of unique runs which was 96. The reason to do so was because of the very small scale of standard deviation observed within the replicates of each unique runs, thereby reducing the time taken to collect the wear and surface roughness data. Also, the length of the wear area did not change across the samples measured and hence only width of the wear area is considered for further analysis. This is due to the fact that the depth of cut is constant in a

tube turning process and it corresponds to the tube thickness which in this particular study is 0.125".

The table below lists the standard deviation values for 3 sets using both the Microscope and as well the surface profilometer.

Instrument	Keyence 3-d Microscope		Dektak Surface profilometer		Hardness tester HR 150 A	
Data Set	Mean Width microns	Standard Deviation microns	Mean Ra microns	Standard Deviation microns	Mean HRB	Standard Deviation HRB
Set 1	641.3925	5.580259	0.0726	0.003318	85.5	1.4142
Set 2	730.8825	5.002382	6.63178	0.271559	53.75	2.47785
Set 3	439.5025	4.982485	0.173273	0.002363	53.25	1.767767

Table 10: Mean and standard deviation for different measuring instruments

Results and Discussions

Once the experiment was completed, force data for all the runs were saved as separate files in excel format for further analysis. The entire 384 runs were separated in to 4 different scenarios based of the different tool and work piece combination as follows:

- Scenario 1: Aluminum 6061 T6 alloy work piece cut with High Speed Steel tool.
- Scenario 2: Aluminum 6061 T6 alloy work piece cut with Uncoated Carbide tool.
- Scenario 3: AISI 1020 Steel alloy work piece cut with High Speed Steel tool.
- Scenario 4: AISI 1020 Steel alloy work piece cut with Uncoated Carbide tool.

The reason for separating the scenarios because, it would not be fair to directly compare the forces obtained from machining steel with the high speed steel tool to the forces obtained from machining the same steel with an uncoated carbide tool because of the vast difference in material properties of the tool materials. Cutting force Fc (N), thrust force Ft (N) and radial force Fr (N) were calculated for each run by averaging out the respective values for the duration of

cut which excluded the first 5 seconds and the last five seconds of cut which involved the unsteady force variations. As mentioned earlier, the radial force in this case was close to 0 N +/- 10 N, thereby validating the assumption of the orthogonal tube turning process.

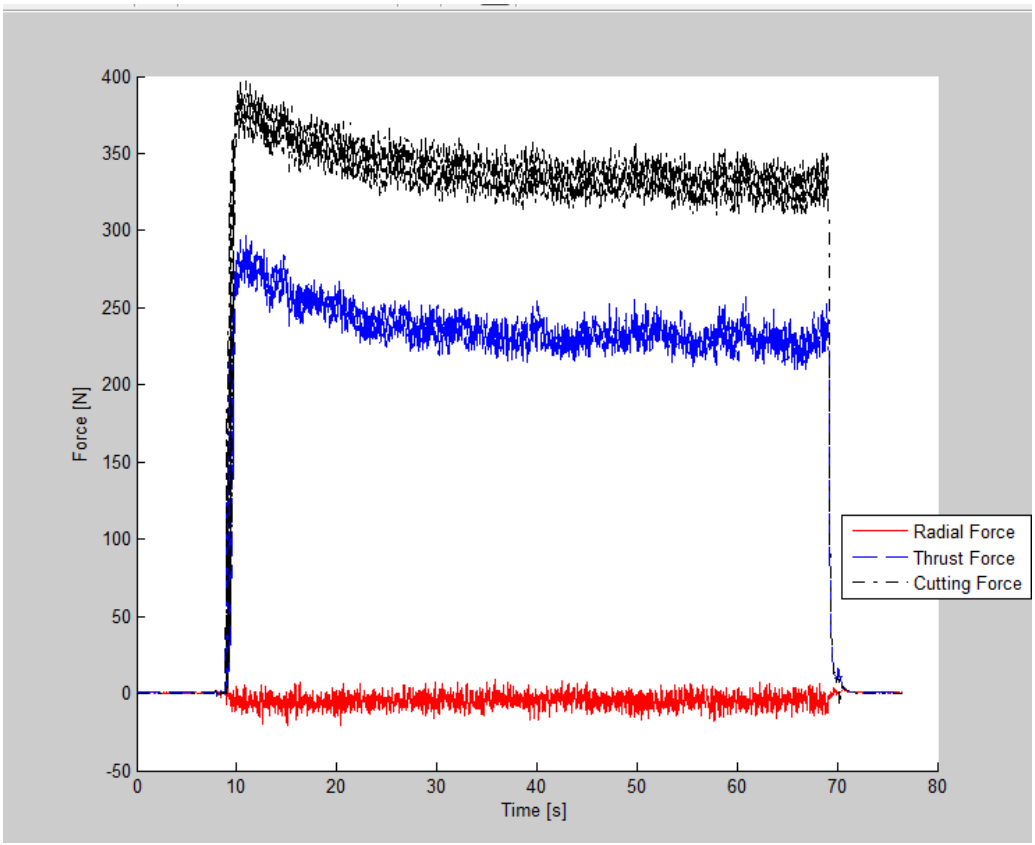

Figure 37: Plot showing different force components for one of the factor level runs.

Along with the forces, the cut chip thickness was measured using a micrometer and the values were recorded which was used in calculating several parameters involved in mechanics of cutting. The following table shows a sample of the raw data collected.

Run	Environment	Work Piece	Tool	Rake Angle	Feed in/rev	Radial force (Fr) N	Thrust force (Ft) N	Cutting force (Fc) N	Cut chip thickness (Tc) inches
1	Dry	Aluminum	HSS	0	0.002	-6.0151	198.82	232.64	0.010583
2	Dry	Aluminum	HSS	0	0.002	-4.5624	172.65	216.1996	0.0099
3	Dry	Aluminum	HSS	0	0.002	-0.6681	175.4492	213.342	0.01002
4	Dry	Aluminum	HSS	0	0.002	-0.6698	177.0113	214.6294	0.01057

Table 11: A sample of the raw force (in N) data and cut chip thickness in inches as measured.

Parameter	Symbol	Units	Equations
Chip Thickness Ratio	r_c	none	$r_c = \frac{t_1}{t_2}$
Friction Force	F	N	$F = F_c.\sin\alpha + F_t.\cos\alpha$
Normal Force	N	N	$N = F_c.\cos\alpha - F_t.\sin\alpha$
Friction Co-efficient	μ	none	$\mu = \frac{F}{N}$
Shear Force on Shear Plane, Merchant	(F_s) M	N	$(F_s)M = F_c.\cos\phi - F_t.\sin\phi$
Normal Force on Shear Plane, Merchant	(F_n) M	N	$(F_n)M = F_c.\sin\phi - F_t.\cos\phi$
Shear Plane Angle	φ	degree	$\phi = \arctan\left(\frac{r\cos\alpha}{1 - r\sin\alpha}\right)$
Area of Shear Plane	A_s	$inch^2$	$A_s = \frac{t_1.w}{\sin\phi}$
Shear Stress on Shear Plane	τ_s	MPa	$\tau_s = \frac{F_s}{A_s}$
Friction Angle	β	degree	$\beta = \arctan\left[\frac{F}{N}\right]$

Table 12: List of formulae used in calculating the cutting parameters.

Once all the raw data were collected several formulae listed in table 11 were used to calculate different cutting parameters based on Merchant's force circle as well Payton's correction to the basic Merchant's Force Diagram. A set of sample calculations for each parameter are provided in the appendix.

Along with the aforementioned parameters, several other direct measurements were taken from the tool as well as from the work piece. This included the average surface roughness value obtained from the work piece as a measure of surface finish, the width of tool wear area and the maximum depth of any deformation in the rake face of the inserts as a quantity to signify wear. Also, hardness values were recorded from the work piece samples in order to study the effect of coolants on the finished work piece property.

Table 13 lists a sample of the calculated parameters like shear plane angle, shear stress, forces along and normal to the shear plane, forces along and normal to the rake face of the tool etc., All the values for the entire data run are listed in appendix.

Run	Chip thickness ratio	Phi radians	Psi degrees	Friction Force (F)	Normal Force (N)	F/N Ratio
1	0.188982	0.18678	34.29832	198.82	232.64	0.854625
2	0.20202	0.199337	33.57881	172.65	216.1996	0.798568
3	0.199601	0.197012	33.71206	175.4492	213.342	0.822385
4	0.189215	0.187004	34.28546	177.0113	214.6294	0.82473

Fs (Merchant)	Fn (Merchant)	Fs/Fn (Merchant)	Fs (Payton)	Fn (Payton)	Fs/Fn (Payton)	Beta (degrees)
191.67381	238.56218	0.803454	23.91435	305.0883	0.078385	40.51803
177.7303	212.04299	0.838181	30.79422	274.9582	0.111996	38.60973
174.87271	213.81479	0.81787	26.79426	274.9169	0.097463	39.43336
177.97826	213.82825	0.832342	26.60001	276.9318	0.096053	39.51342

Shear Area, As	Shear Area, As P	Shear Stress, Ts Merchant (Mpa)	Shear Stress, Ts (Payton) (Mpa)	Shear Stress, Ts (Payton) corrected (Mpa)	χ	λ	Friction Co-efficient
0.001292	0.001796	229.8716	28.68013	20.63888	4.481966	85.51803	0.707173
0.001212	0.00168	227.2958	39.38212	28.40994	6.390269	83.60973	0.673867
0.001226	0.0017	221.0662	33.87209	24.42364	5.566643	84.43336	0.688242
0.001291	0.001794	213.7002	31.93889	22.98493	5.486576	84.51342	0.689639

Normal Stress σ (Merchant)	Shear Strain ϒ (Merchant)	Normal Stress σ (Payton)	Normal Stress σ (Payton) corrected	Shear Strain ϒ (Payton)	Resultant Force N	Resultant shear stress Payton MPA	Resultant shear stress Merchant MPA
184582.94	5.480482	236056.3	163076.6	2	306.0241	253.5446	367.0102
174952.96	5.15202	226863.2	157110.9	2	276.6772	245.045	353.8371
174383.51	5.209601	224217.3	155206.1	2	276.2195	241.7098	349.1842
165641.98	5.474215	214525.1	148208.4	2	278.2064	230.7808	334.045
161288.15	4.133065	209433.8	146826.1	2	408.7484	231.2235	329.8188

Table 13: Calculated cutting parameter values for a portion of runs.

A General Linear Model ANOVA was evaluated for each of the parameters under four different scenarios using on Minitab 15 statistical software. The ANOVA testing involved analysis of two different effects on the parameter considered, as listed below,

- Main Effects
    - Environment
    - Rake angle
    - Feed
- Interactions
    - Environment versus Rake angle
    - Environment Vs Feed
    - Rake angle versus feed
    - Environment versus rake angle versus feed

General Linear Model: Fy Thrust, Fz Cutting, ... versus Environment, Rake Angle

```
Factor       Type   Levels  Values
Environment  fixed       4  Cold Comp. Air, Dry, Liquid Nit., Nitrogen
Rake Angle   fixed       3  0, 7, 15
Feed in/rev  fixed       2  0.002, 0.004
```

Analysis of Variance for **Fz Cutting**, using Adjusted SS for Tests

Source	DF	Seq SS	Adj SS	Adj MS	F	P
Environment	3	6237	6237	2079	72.73	0.000
Rake Angle	2	31171	31171	15586	545.21	0.000
Feed in/rev	1	364563	364563	364563	12752.96	0.000
Environment*Rake Angle	6	1430	1430	238	8.34	0.000
Environment*Feed in/rev	3	464	464	155	5.41	0.002
Rake Angle*Feed in/rev	2	57	57	28	0.99	0.376
Environment*Rake Angle*Feed in/rev	6	453	453	75	2.64	0.023
Error	72	2058	2058	29		
Total	95	406432				

```
S = 5.34664   R-Sq = 99.49%   R-Sq(adj) = 99.33%
```

Unusual Observations for Fz Cutting

Obs	Fz Cutting	Fit	SE Fit	Residual	St Resid	
1	232.640	219.203	2.673	13.437	2.90	R
74	239.012	252.579	2.673	-13.567	-2.93	R
75	268.992	252.579	2.673	16.413	3.54	R
78	362.834	373.720	2.673	-10.886	-2.35	R
79	389.360	373.720	2.673	15.640	3.38	R

R denotes an observation with a large standardized residual.

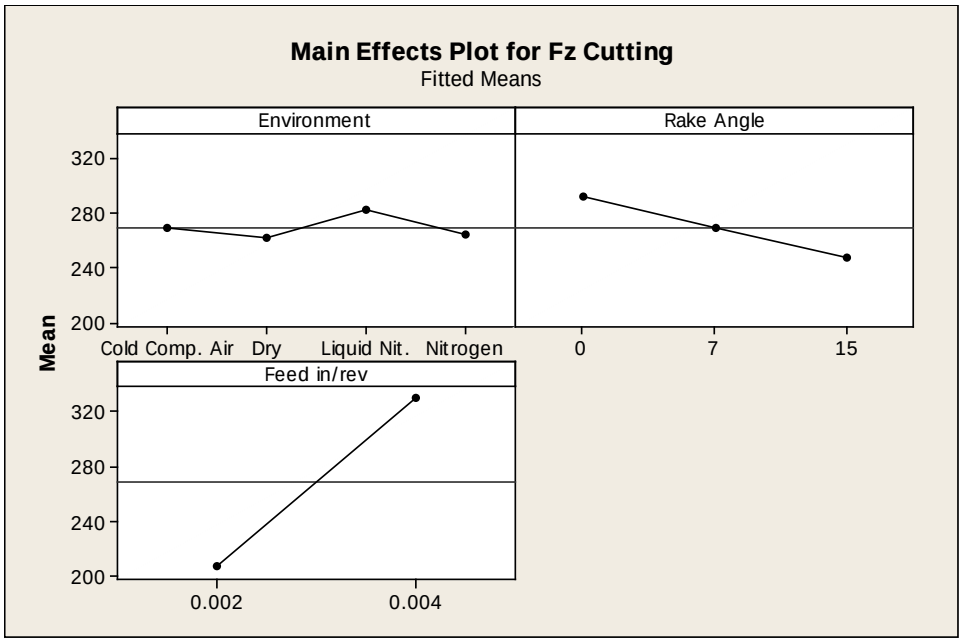

Figure 38: Main effects plot for cutting force in machining of Aluminum with High speed steel tool.

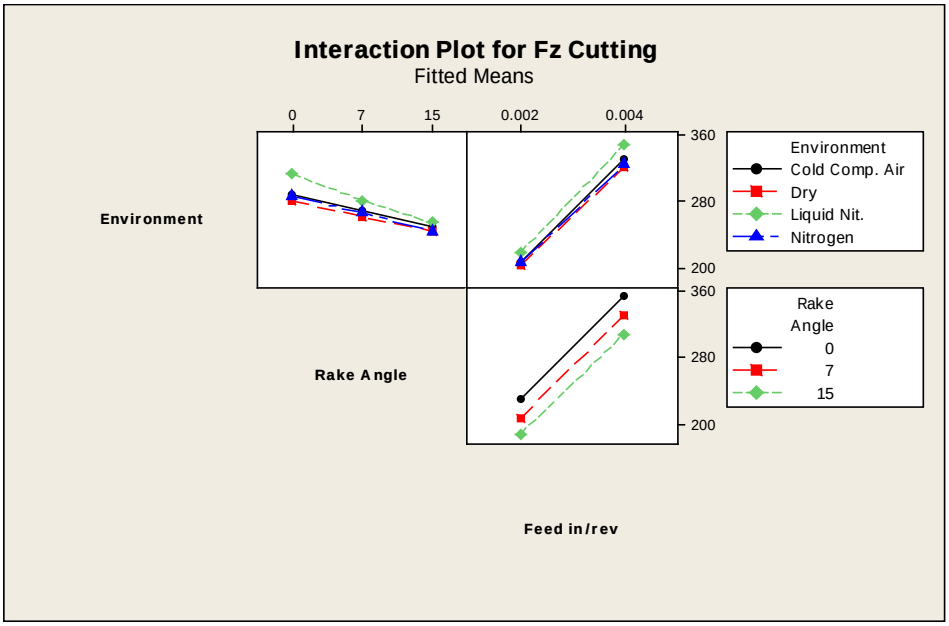

Figure 39: Interactions plot for cutting force in machining of Aluminum with High speed steel tool.

To draw conclusions as of which of the above influenced the parameter considered each time, the F-statistic and the p-value form the ANOVA were considered with the support of the trend from main effects and interactions plots.

An example of the ANOVA table is presented above with the main effects plot in figure 36 and interactions plot in figure 37.

From observing the ANOVA table and the main effects and interaction plots (refer appendix) the results are tabulated for four different scenarios separately. The results are tabled as whether the factor is statistically significant or insignificant, value of F-statistic, p-value, significance rank based of the values as follows,

0- Statistically Insignificant

1- First Significant factor contributing to the change.

2- Second Significant factor contributing to the change.

3- Third Significant factor contributing to the change.

4- Fourth Significant factor contributing to the change.

5- Fifth Significant factor contributing to the change.

6- Sixth Significant factor contributing to the change.

7- Seventh Significant factor contributing to the change.

The tool wear profile obtained using the Keyence microscope is presented in the following figure. The software is cable of determining the surface area, 3-d profile and volume of which only volume is taken in to account for this study. Figure 41 shows a typical profile output from a surface profilometer (Dektak 150 A) which was used to collect surface finish data in terms of average surface roughness Ra.

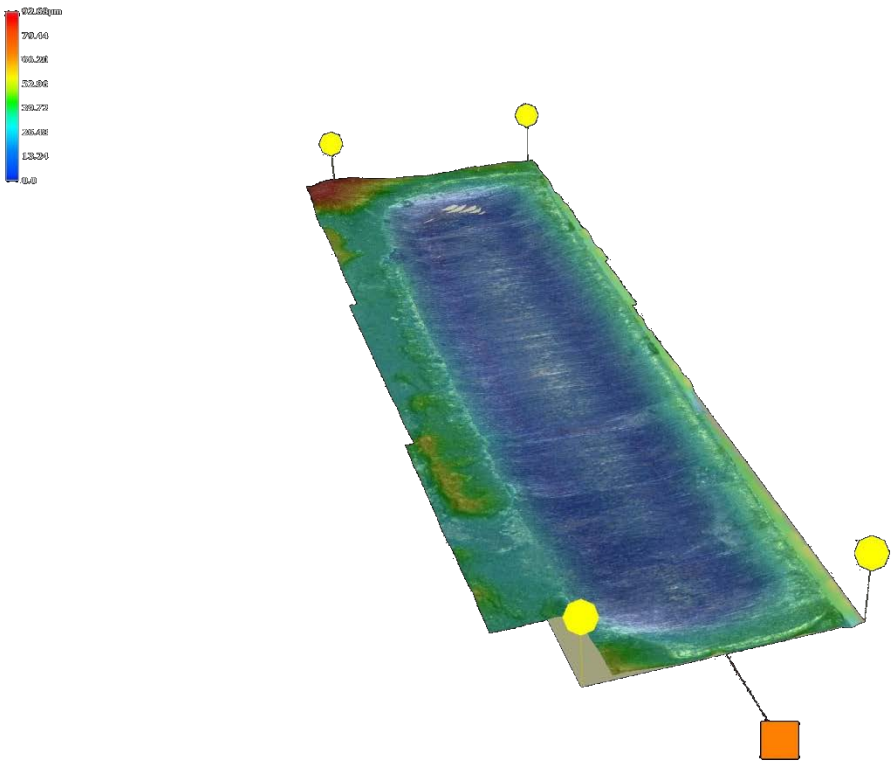

Figure 40 : A typical 3-d volume profile obtained on a Keyence VHX 1000 Digital microscope.

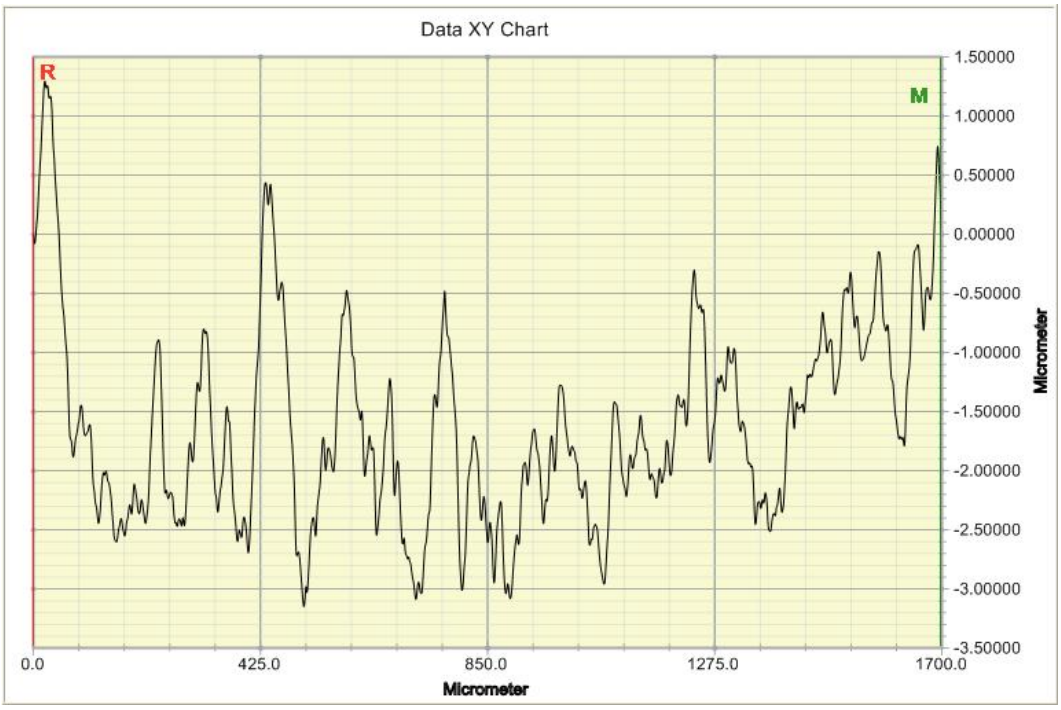

Figure 41: A typical Surface roughness profile output by a Dektak 150 surface profilometer.

Parameter		Main Effects			Interactions			
		Environment	Rake angle	Feed	Environment * Rake angle	Environment * Feed	Rake angle * Feed	Environment * rake angle * feed
Cutting force Fc N	F-statistic	72.73	545.21	12752.96	8.34	5.41	0.99	2.64
	p-value	0.000	0.000	0.000	0.000	0.002	0.376	0.023
	Significance	yes	yes	yes	yes	yes	no	no
	Rank	3	2	1	4	5	0	0
Thrust force Ft N	F-statistic	7.47	236.70	315.53	3.41	2.78	2.87	0.22
	p-value	0.000	0.000	0.000	0.005	0.047	0.063	0.970
	Significance	yes	yes	yes	yes	no	no	no
	Rank	3	2	1	4	0	0	0
Resultant force R N	F-statistic	22.64	325.95	2459.83	5.18	3.74	1.15	0.50
	p-value	0.000	0.000	0.000	0.000	0.015	0.323	0.809
	Significance	yes	yes	yes	yes	no	no	no
	Rank	3	2	1	4	0	0	0
Shear plane angle Merchant Φ	F-statistic	98.97	265.86	43.78	14.03	13.41	1.70	1.43
	p-value	0.000	0.000	0.000	0.000	0.000	0.189	0.216
	Significance	yes	yes	yes	yes	yes	no	no
	Rank	2	1	3	4	5	0	0
Shear plane angle Payton ψ	F-statistic	98.97	0.63	43.78	14.03	13.41	1.70	1.43
	p-value	0.000	0.536	0.000	0.000	0.000	0.189	0.216
	Significance	yes	no	yes	yes	yes	no	no
	Rank	1	0	2	3	4	0	0
Friction Force Merchant F N (M)	F-statistic	8.61	23.29	492.0	3.03	3.15	0.92	0.23
	p-value	0.000	0.000	0.000	0.011	0.030	0.403	0.964
	Significance	yes	yes	yes	no	no	no	no
	Rank	3	2	1	0	0	0	0
Normal Force Merchant N N (M)	F-statistic	76.42	2505.4	12759.08	10.05	3.61	27.88	2.05
	p-value	0.000	0.000	0.000	0.000	0.017	0.000	0.070
	Significance	yes	yes	yes	yes	no	yes	no
	Rank	3	2	1	5	0	4	0
F/N ratio (M)	F-statistic	0.61	207.70	184.42	2.55	4.45	0.87	0.54
	p-value	0.611	0.000	0.000	0.027	0.006	0.423	0.778
	Significance	no	yes	yes	No	yes	no	no
	Rank	0	1	2	0	3	0	0
Force along shear plane Fs N (M)	F-statistic	33.81	296.71	2972.06	6.09	10.55	0.16	0.83
	p-value	0.000	0.000	0.000	0.000	0.000	0.851	0.548
	Significance	yes	yes	yes	yes	yes	no	no
	Rank	3	2	1	5	4	0	0
Force normal to shear plane Fn N (M)	F-statistic	25.37	123.73	758.30	3.44	2.07	0.76	0.41
	p-value	0.000	0.000	0.000	0.005	0.112	0.471	0.869
	Significance	yes	yes	yes	yes	no	no	no
	Rank	3	2	1	4	0	0	0
Fs/Fn ratio (M)	F-statistic	47.46	0.39	21.94	5.25	2.12	0.70	0.89
	p-value	0.000	0.676	0.000	0.000	0.105	0.502	0.508
	Significance	yes	no	yes	yes	no	no	no
	Rank	1	0	2	3	0	0	0
Force along shear plane Fs N (P)	F-statistic	0.08	4.32	417.79	1.12	1.75	0.40	0.34
	p-value	0.973	0.017	0.000	0.358	0.164	0.670	0.915
	Significance	no	no	yes	no	no	no	no
	Rank	0	0	1	0	0	0	0
Force normal to shear plane Fn N (P)	F-statistic	20.49	290.78	2079.70	4.90	3.71	0.90	0.46
	p-value	0.000	0.000	0.000	0.000	0.015	0.410	0.833
	Significance	yes	yes	yes	yes	yes	no	no
	Rank	3	2	1	4	5	0	0

Fs/Fn ratio (P)	F-statistic	0.58	3.22	192.74	2.21	4.14	0.000	0.39
	p-value	0.629	0.046	0.0000	0.051	0.009	0.997	0.884
	Significance	no	no	yes	no	no	no	no
	Rank	0	0	1	0	0	0	0
Shear area As (M)	F-statistic	1.78	3.12	8.31	0.79	1.08	1.06	0.94
	p-value	0.158	0.05	0.005	0.578	0.365	0.352	0.471
	Significance	no	no	Yes	no	no	no	no
	Rank	0	0	1	0	0	0	0
Shear stress τs MPa (M)	F-statistic	59.20	49.22	53.00	1.97	7.27	0.23	2.39
	p-value	0.000	0.000	0.000	0.081	0.000	0.795	0.037
	Significance	yes	yes	yes	no	yes	no	no
	Rank	1	3	2	0	4	0	0
Shear area As (P) corrected	F-statistic	2254.92	10760.76	36717.10	206.05	432.36	76.63	60.28
	p-value	0.000	0.000	0.000	0.000	0.000	0.000	0.000
	Significance	yes	yes	yes	yes	yes	yes	yes
	Rank	3	2	1	5	4	6	7
Shear stress τs MPa (P)	F-statistic	19.87	21.22	68.09	3.70	10.07	0.12	0.54
	p-value	0.000	0.000	0.000	0.003	0.000	0.884	0.778
	Significance	yes	yes	yes	yes	yes	no	no
	Rank	3	2	1	5	4	0	0
Shear strain γ (M)	F-statistic	2.20	5.28	0.05	0.75	0.86	0.47	1.03
	p-value	0.095	0.007	0.817	0.614	0.465	0.625	0.412
	Significance	no	no	no	no	no	no	no
	Rank	0	0	0	0	0	0	0
Shear strain γ (P)	F-statistic	Depends only on Rake angle Shear strain decreases with increasing rake angle. **NA**						
	p-value							
	Significance							
	Rank							
Shear strain γ (P) corrected	F-statistic	2371.87	3216.39	1371.82	561.92	435.27	67.84	11.67
	p-value	0.000	0.000	0.000	0.000	0.000	0.000	0.000
	Significance	yes	yes	yes	yes	yes	yes	yes
	Rank	2	1	3	4	5	6	7
Friction Co-efficient μ	F-statistic	0.57	210.81	189.58	2.23	4.11	0.00	0.39
	p-value	0.635	0.000	0.000	0.05	0.009	0.997	0.883
	Significance	no	yes	yes	no	no	no	no
	Rank	0	1	2	0	0	0	0

Table 14: Scenario1- Aluminum 6061 T6 alloy cut with High Speed Steel tool.

The following inferences can be made from the table 14 for scenario 1 based of the values from ANOVA and the corresponding main effects and interactions plots given in appendix5.

- The cutting force decreased with increase in rake angle but increased when the feed was increased. Using liquid nitrogen significantly increased the cutting force values even higher to dry conditions. Though nitrogen and cold compressed air performed closer to dry environments, nitrogen was marginally better. Also, from the interaction plots, using a sharper

tool reduced the thrust force even at higher feeds while use of nitrogen with a sharper tool at lower feeds gave lower cutting force values.

- The thrust force decreased with increase in rake angle but increased when the feed was increased. Using liquid nitrogen significantly increased the cutting force values even higher to dry conditions. Though nitrogen and cold compressed air performed closer to dry environments, nitrogen was marginally better. Also, from the interaction plots, using a sharper tool reduced the thrust force even at higher feeds while use of nitrogen with a sharper tool at higher feeds gave lower thrust force values.

		Increasing rake angle α	Increasing feed f
Resultant force R		decrease	increase
Chip thickness ratio r		increase	increase
Friction force F		decrease	increase
Normal force N		decrease	increase
F/N ratio		increase	decrease
Shear plane angle	Merchant Φ	increase	increase
	Payton ψ	decrease	decrease
Force along shear plane Fs	Merchant	decrease	increase
	Payton	decrease	increase
Force normal to shear plane Fn	Merchant	decrease	increase
	Payton	decrease	increase
Fs/Fn ratio	Merchant	increase	increase
	Payton	Statistically insignificant	increase
Shear area As	Merchant	decrease	increase
	Payton	decrease	increase
	Vishnu	decrease	increase
Shear stress τ s	Merchant	increase	decrease
	Payton	increase	increase
Shear strain γ	Merchant	decrease	increase
	Payton	increase	no change
	Vishnu	increase	increase

Table 15: Variation of different parameters while increasing feed f and rake angle α for scenario 1

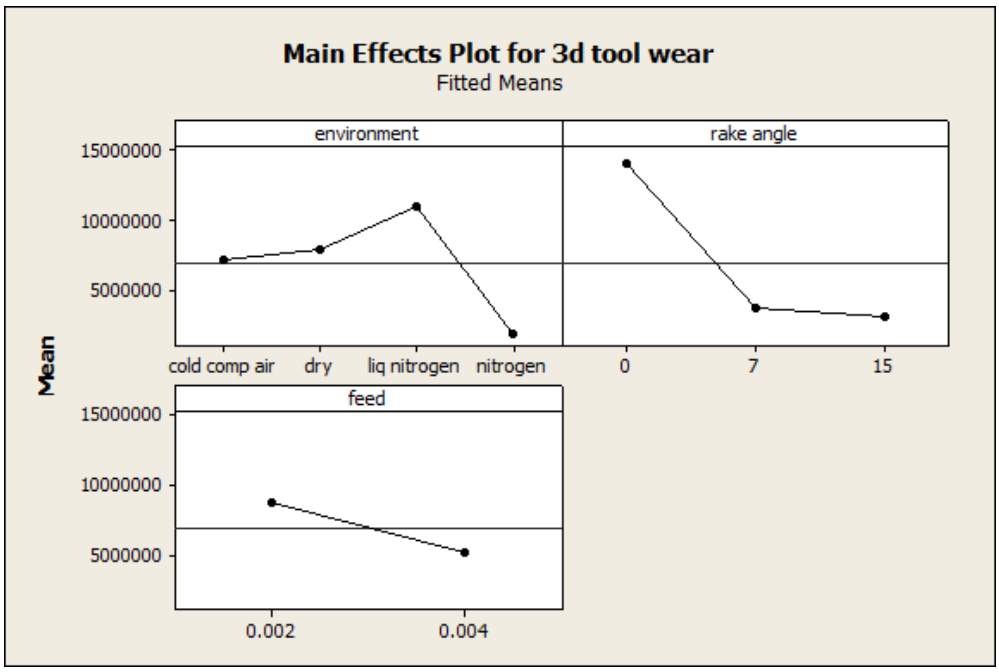

Figure 42: Main Effects plots for variation of volumetric tool wear. (Scenario 1)

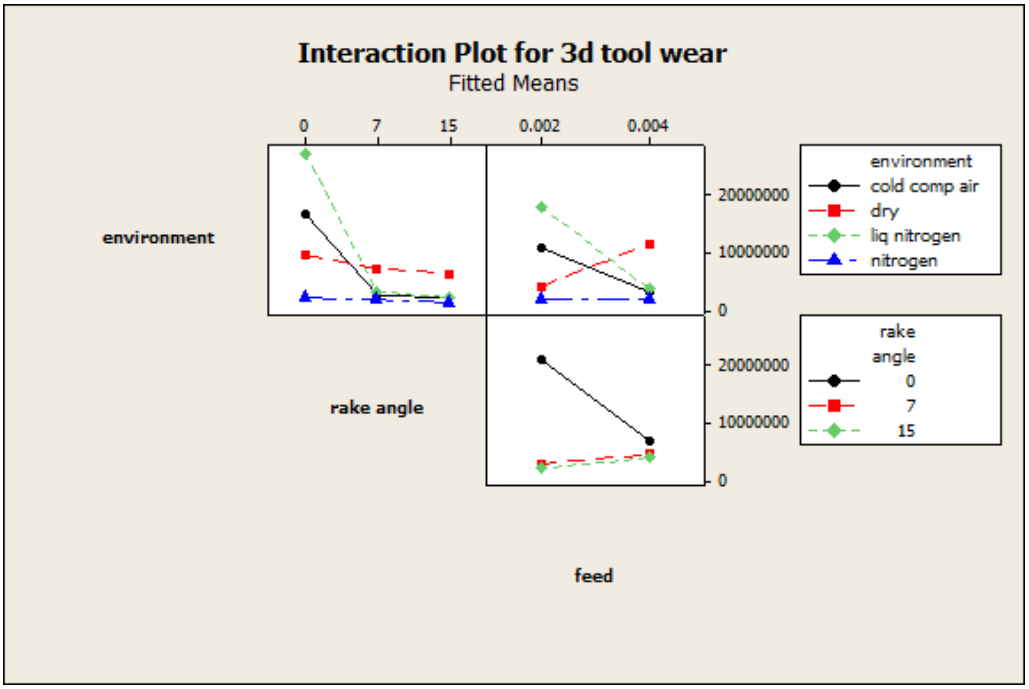

Figure 43: Interaction plots for variation of volumetric tool wear. (Scenario 1)

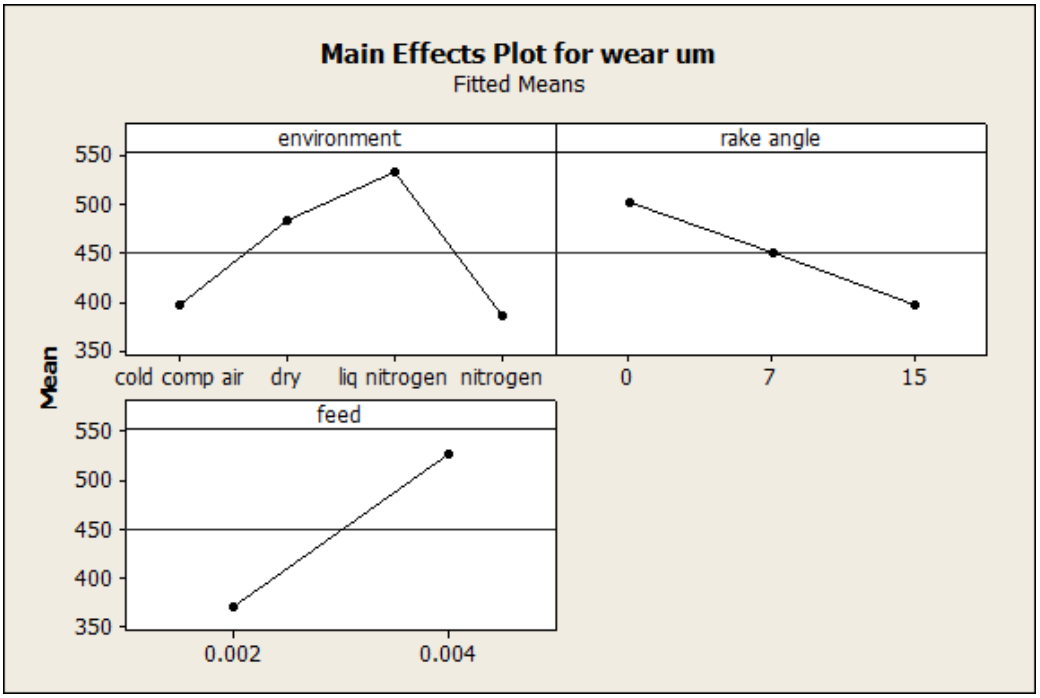

Figure 44: Main Effects plots for variation of volumetric tool wear. (Scenario 1)

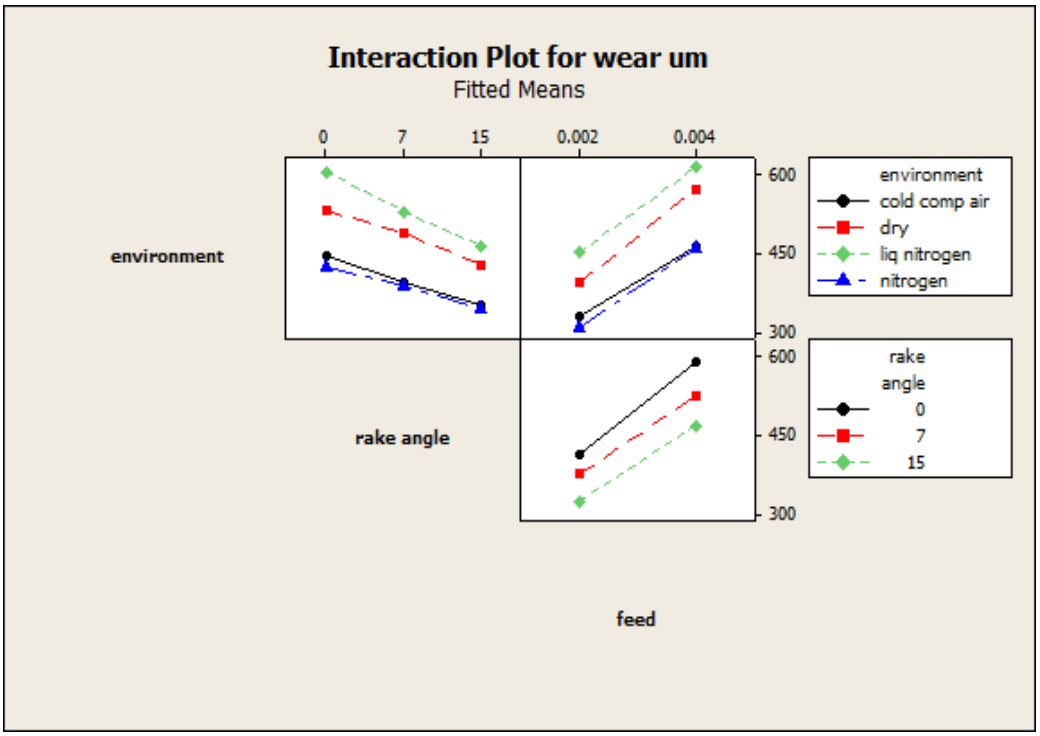

Figure 45: Interaction plots for variation of volumetric tool wear. (Scenario 1)

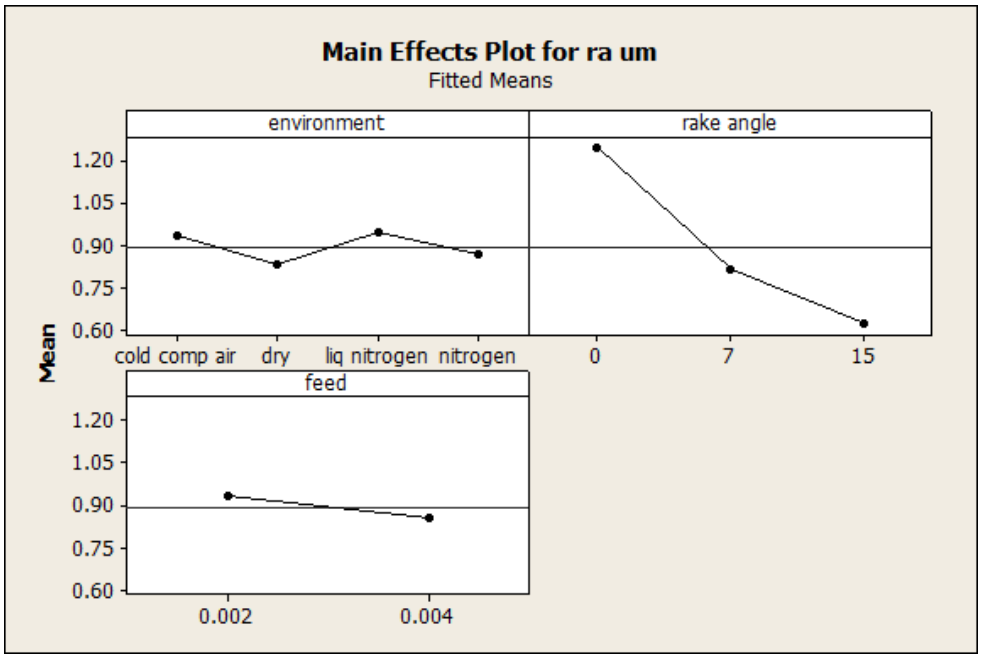

Figure 46: Main Effects plots for variation of volumetric tool wear. (Scenario 1)

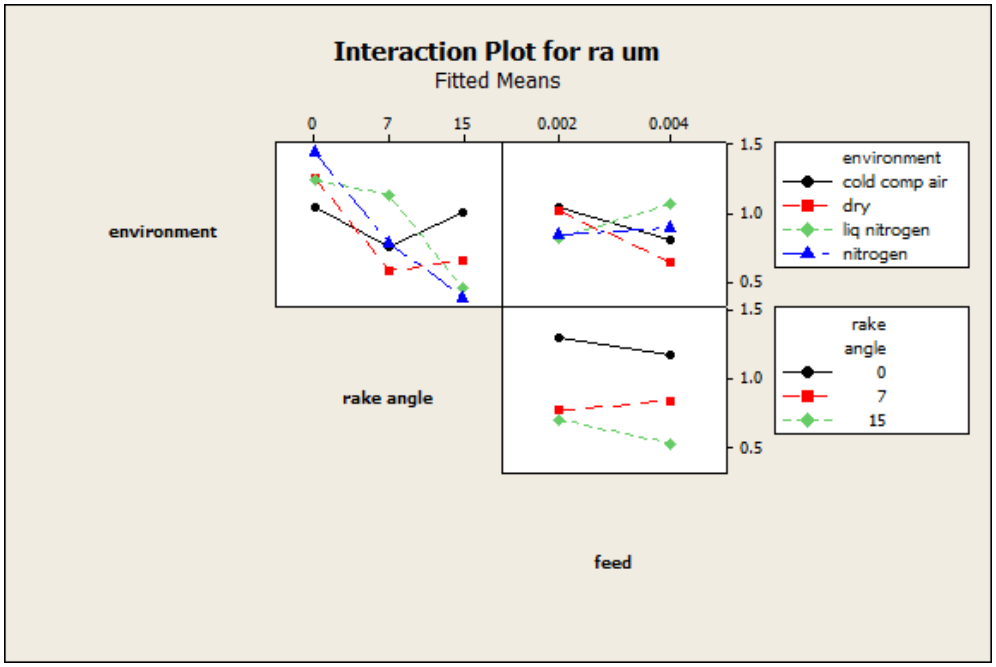

Figure 47: Interaction plots for variation of volumetric tool wear. (Scenario 1)

- The tool wear width decreased with increase in rake angle but increased when the feed was increased. Also, the width of tool wear was found to be minimal in case of nitrogen environment with cold compressed air very closely following behind, liquid nitrogen resulted in maximum.
- Volumetric tool wear decreased when feed was increased and to a large extent when rake angle changed from 0 – 7 degrees and a little when moving from 7 – 15 degrees.
- The surface finish (Ra) decreased with increase in rake angle and also when the feed was increased. Also, there was a mixed response observed when the environment was changed, with certain environment performing good at a particular tool rake angle and feed but was not consistent.

Parameter		Main Effects			Interactions			
		Environment	**Rake angel**	**Feed**	**Environment * Rake angle**	**Environment * Feed**	**Rake angle * Feed**	**Environment * rake angle * feed**
Cutting force Fc N	F-statistic	90.76	500.56	15402.97	2.81	3.44	9.17	1.35
	p-value	0.000	0.000	0.000	0.016	0.021	0.000	0.245
	Significance	yes	yes	yes	yes	yes	yes	no
	Rank	3	2	1	6	5	4	0
Thrust force Ft N	F-statistic	54.81	1092.17	1616.24	4.71	5.59	24.11	3.49
	p-value	0.000	0.000	0.000	0.000	0.002	0.000	0.004
	Significance	yes	yes	yes	yes	yes	yes	yes
	Rank	3	2	1	6	5	4	7
Resultant force R N	F-statistic	80.44	800.75	8147.43	3.88	4.34	11.61	2.32
	p-value	0.000	0.000	0.000	0.002	0.007	0.000	0.042
	Significance	yes	yes	yes	no	no	yes	no
	Rank	1	2	3	0	0	4	0
Shear plane angle Merchant Φ	F-statistic	55.64	127.90	10.34	26.59	4.07	3.09	2.09
	p-value	0.000	0.000	0.002	0.000	0.010	0.052	0.065
	Significance	yes	yes	yes	yes	yes	no	no
	Rank	2	1	4	3	5	0	0
Shear plane angle Payton ψ	F-statistic	55.64	6.30	10.34	26.59	4.07	3.09	2.09
	p-value	0.000	0.003	0.002	0.000	0.010	0.052	0.065
	Significance	yes	yes	yes	yes	yes	no	no
	Rank	1	4	3	2	5	0	0
Friction Force Merchant F N (M)	F-statistic	64.13	49.93	2614.05	3.46	5.63	5.76	3.31
	p-value	0.000	0.000	0.000	0.005	0.002	0.005	0.006
	Significance	yes	yes	yes	yes	yes	yes	no
	Rank	2	3	1	5	4	5	0
Normal Force Merchant N N (M)	F-statistic	77.60	2225.06	14247.98	4.18	3.57	51.36	1.43
	p-value	0.000	0.000	0.000	0.001	0.018	0.000	0.215
	Significance	yes	yes	yes	yes	yes	yes	no
	Rank	3	2	1	5	6	4	0
F/N ratio Merchant	F-statistic	11.28	1105.78	1247.42	0.84	4.98	10.19	3.12
	p-value	0.000	0.000	0.000	0.541	0.003	0.000	0.009
	Significance	yes	yes	yes	no	yes	yes	yes
	Rank	3	2	1	0	5	4	6
Force along shear plane Fs N (M)	F-statistic	47.34	191.26	2288.40	18.01	4.30	0.78	2.02
	p-value	0.000	0.000	0.000	0.000	0.008	0.462	0.074
	Significance	yes	yes	yes	yes	no	no	no
	Rank	3	2	1	4	0	0	0
Force normal to shear plane Fn N (M)	F-statistic	43.27	192.71	1514.25	7.16	3.88	5.06	3.04
	p-value	0.000	0.000	0.000	0.000	0.012	0.009	0.011
	Significance	yes	yes	yes	yes	no	no	no
	Rank	3	2	1	4	0	0	0
Fs/Fn ratio (M)	F-statistic	27.46	3.54	29.98	12.81	3.04	1.47	2.20
	p-value	0.000	0.034	0.000	0.000	0.034	0.237	0.052
	Significance	yes	no	yes	yes	no	no	no
	Rank	2	0	1	3	0	0	0
Force along shear plane Fs N (P)	F-statistic	2.38	104.46	5653.27	1.84	4.84	15.32	3.17
	p-value	0.077	0.000	0.000	0.102	0.004	0.000	0.008
	Significance	no	yes	yes	no	no	yes	no
	Rank	0	2	1	0	0	3	0
Force normal to shear plane	F-statistic	78.96	738.70	7080.78	4.06	4.82	10.05	2.57
	p-value	0.000	0.000	0.000	0.001	0.004	0.000	0.026
	Significance	yes	yes	yes	yes	yes	yes	no

Fn N (P)	Rank	3	2	1	6	5	4	0
Fs/Fn ratio (P)	F-statistic	13.51	1.49	1392.39	1.47	5.87	2.97	3.44
	p-value	0.000	0.233	0.000	0.200	0.001	0.057	0.005
	Significance	yes	no	yes	no	yes	no	no
	Rank	2	0	1	0	3	0	0
Shear area As (M)	F-statistic	0.42	1.87	14.38	1.09	0.72	0.96	1.05
	p-value	0.740	0.161	0.000	0.375	0.541	0.387	0.403
	Significance	no	no	yes	no	no	no	no
	Rank	0	0	1	0	0	0	0
Shear stress τs MPa (M)	F-statistic	18.50	12.24	24.19	2.60	2.05	1.30	1.71
	p-value	0.000	0.000	0.000	0.024	0.115	0.278	0.132
	Significance	yes	yes	yes	no	no	no	no
	Rank	2	3	1	0	0	0	0
Shear area As (P) corrected	F-statistic	0.41	2.36	13.64	1.08	0.71	0.98	1.05
	p-value	0.745	0.102	0.000	0.381	0.548	0.382	0.403
	Significance	no	no	yes	no	no	no	no
	Rank	0	0	1	0	0	0	0
Shear stress τs MPa (P)	F-statistic	23.56	12.33	147.20	9.99	0.84	2.01	1.49
	p-value	0.000	0.000	0.000	0.000	0.478	0.142	0.195
	Significance	yes	yes	yes	yes	no	no	no
	Rank	2	3	1	4	0	0	0
Shear strain γ (M)	F-statistic	0.48	3.67	0.03	1.12	1.10	1.09	1.07
	p-value	0.695	0.030	0.859	0.360	0.355	0.340	0.390
	Significance	no	no	no	no	no	no	no
	Rank							
Shear strain γ (P)	F-statistic	Depends only on Rake angle Shear strain decreases with increasing rake angle. **NA**						
	p-value							
	Significance							
	Rank							
Shear strain γ (P) corrected	F-statistic	877.29	840.39	124.51	409.44	33.54	26.66	8.85
	p-value	0.000	0.000	0.000	0.000	0.000	0.000	0.000
	Significance	yes	yes	yes	yes	yes	yes	yes
	Rank	1	2	4	3	5	6	7
Friction Co-efficient μ	F-statistic	13.42	1215.27	1393.41	1.44	5.77	3.02	3.42
	p-value	0.000	0.000	0.000	0.211	0.001	0.055	0.005
	Significance	yes	yes	yes	no	yes	no	no
	Rank	3	2	1	0	4	0	0

Table 16: Scenario 2 - Aluminum 6061 T6 alloy work piece cut with Uncoated Carbide tool

The following inferences can be made from the table 16 for scenario 2 based of the values from ANOVA and the corresponding main effects and interactions plots given in appendix5.

- The cutting force decreased with increase in rake angle but increased when the feed was increased. Also, from the interaction plots, using a sharper tool reduced the thrust force even at higher feeds while use of liquid nitrogen significantly increased the cutting force values and both

nitrogen and cold compressed air performed closely to dry environment conditions.

- The thrust force decreased with increase in rake angle but increased when the feed was increased. Also, from the interaction plots, using a sharper tool reduced the thrust force even at higher feeds. Using liquid nitrogen significantly increased the thrust force values even greater than dry environments and both nitrogen and cold compressed air performed closely to dry environment conditions.

		Increasing rake angle α	Increasing feed f
Resultant force R		decrease	increase
Chip thickness ratio r		increase	increase
Friction force F		decrease	increase
Normal force N		decrease	increase
F/N ratio		increase	decrease
Shear plane angle	Merchant Φ	increase	increase
	Payton ψ	decrease	decrease
Force along shear plane Fs	Merchant	decrease	increase
	Payton	decrease	increase
Force normal to shear plane Fn	Merchant	decrease	increase
	Payton	decrease	increase
Fs/Fn ratio	Merchant	decrease	increase
	Payton	Statistically insignificant	increase
Shear area As	Merchant	decrease	increase
	Payton	decrease	increase
	corrected	Statistically insignificant	increase
Shear stress τ s	Merchant	increase	decrease
	Payton	increase	increase
Shear strain γ	Merchant	decrease	increase
	Payton	increase	no change
	Vishnu	Increase	increase

Table 17: Variation of different parameters while increasing feed f and rake angle α for scenario 2

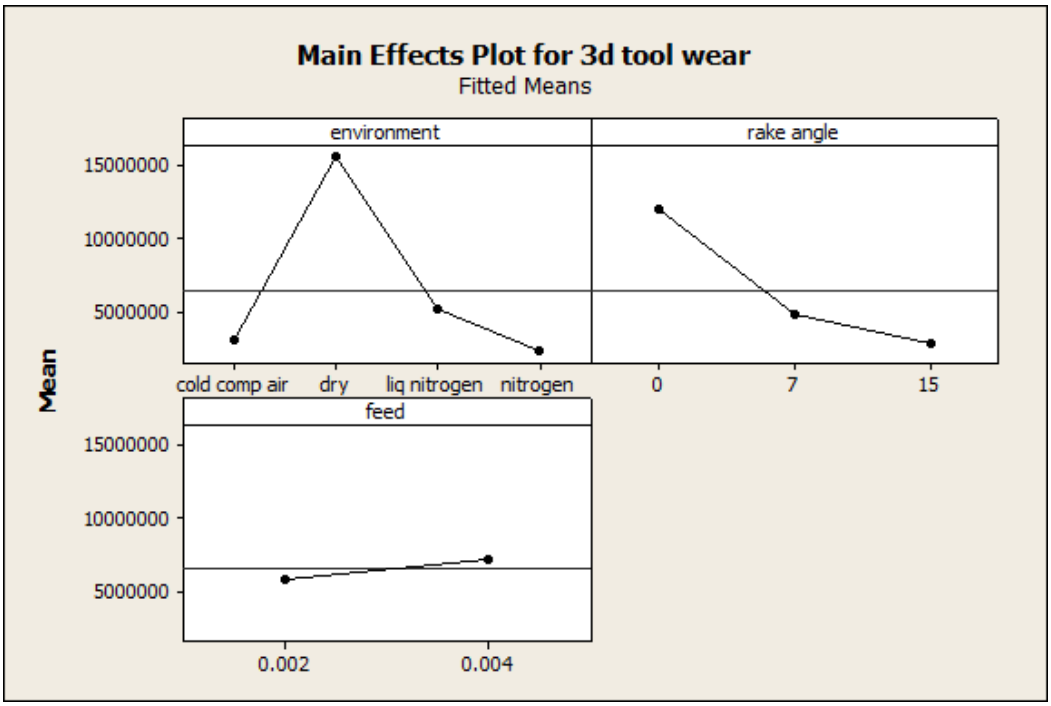

Figure 48: Main Effects plots for variation of volumetric tool wear. (Scenario 2)

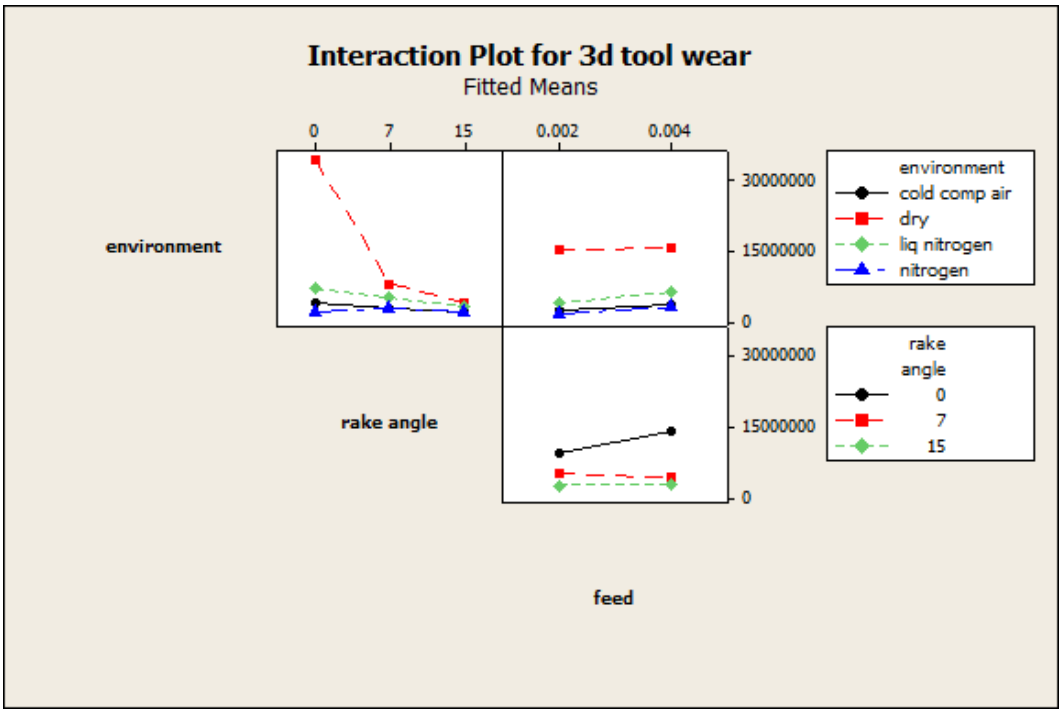

Figure 49: Interaction plots for variation of volumetric tool wear. (Scenario 2)

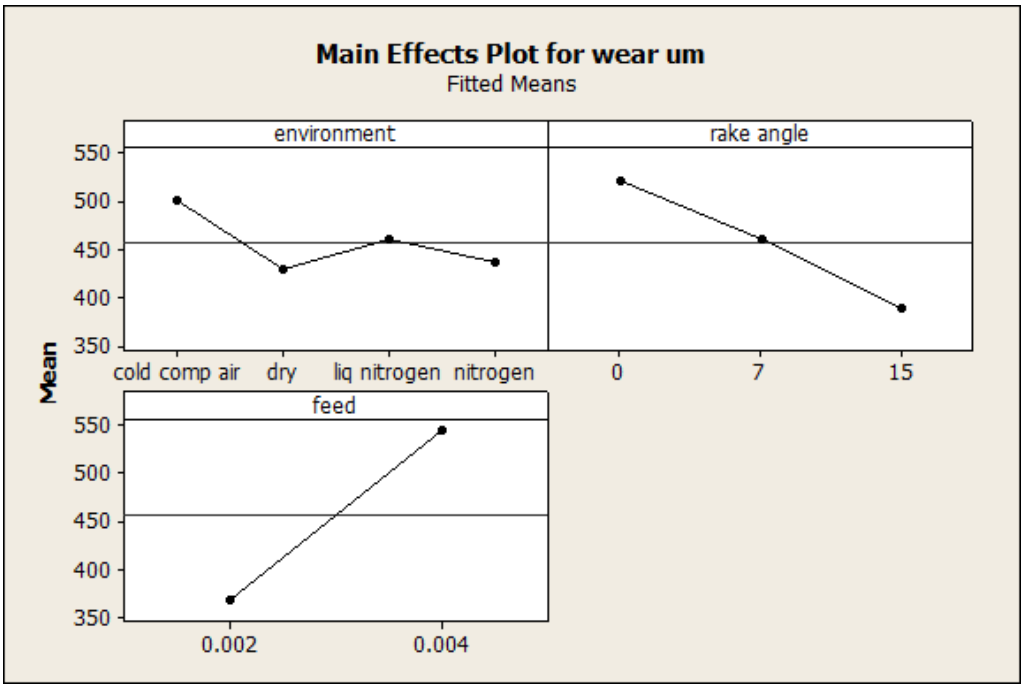

Figure 50: Main Effects plots for variation of volumetric tool wear. (Scenario 2)

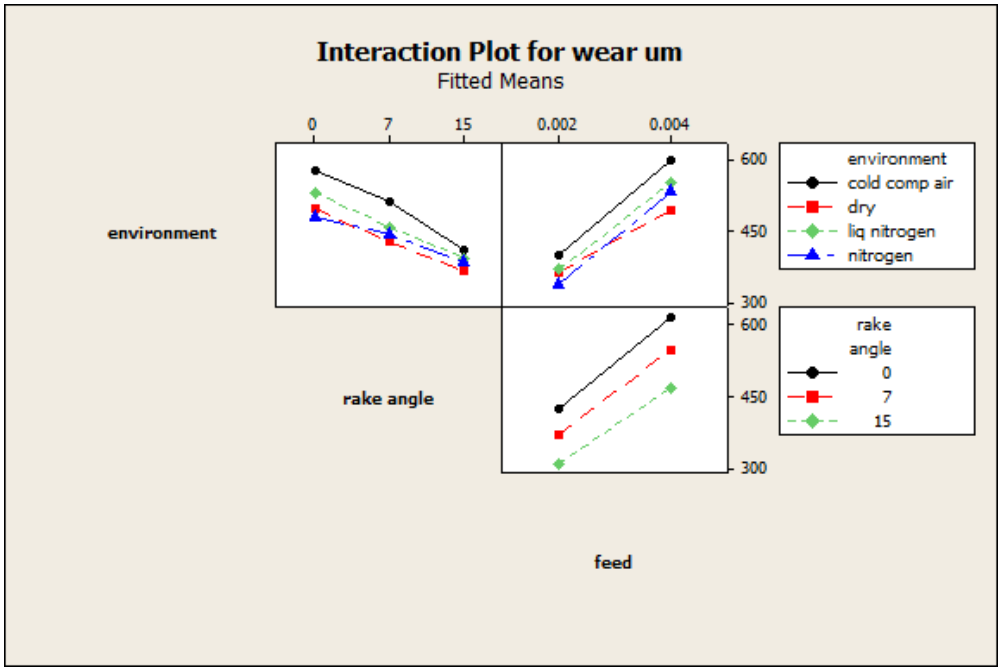

Figure 51: Interaction plots for variation of volumetric tool wear. (Scenario 2)

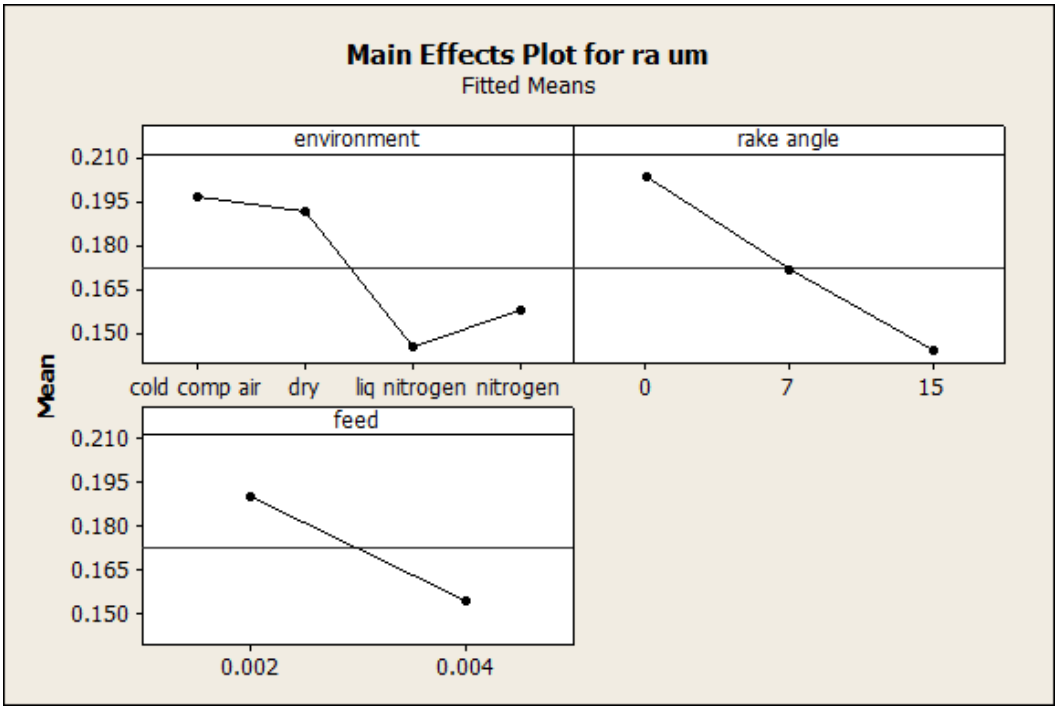

Figure 52: Main Effects plots for variation of surface finish. (Scenario 2)

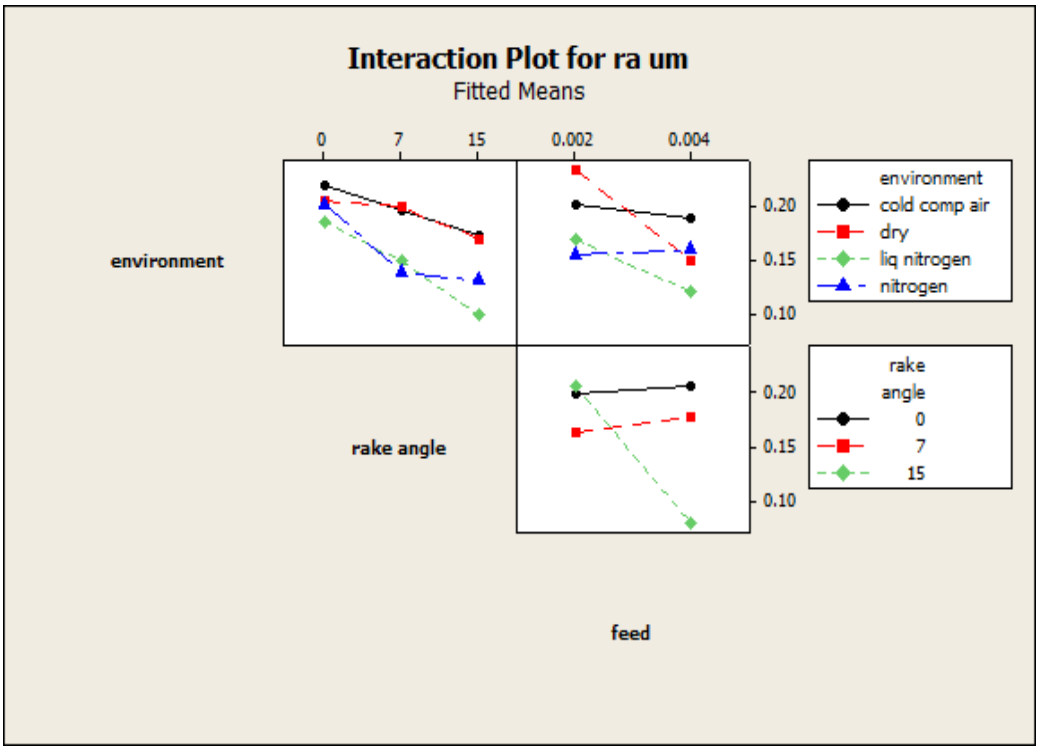

Figure 53: Interaction plots for variation of surface finish. (Scenario 2)

- The tool wear width decreased with increase in rake angle but increased when the feed was increased. Also, the width of tool wear was found to be minimal in case of nitrogen environment at lower feed rates.
- Volumetric tool wear increased when feed increased but rapidly decreased with decrease in rake angle from 0 -7 degrees and slowly between 7 and 15 degrees. Nitrogen resulted in minimum volumetric wear while cold compressed air and liquid nitrogen falling closely behind in that order.
- The surface finish (Ra) decreased with increase in rake angle and feed. Liquid nitrogen yielded better surface finishes with nitrogen closely behind.

Parameter		Main Effects			Interactions			
		Environment	Rake angel	Feed	Environment * Rake angle	Environment * Feed	Rake angle * Feed	Environment * rake angle * feed
Cutting force Fc N	F-statistic	237.68	453.78	17241.73	13.52	86.75	85.34	45.89
	p-value	0.000	0.000	0.000	0.000	0.000	0.000	0.000
	Significance	yes	yes	yes	yes	yes	yes	yes
	Rank	3	2	1	7	4	5	6
Thrust force Ft N	F-statistic	23.30	28.84	341.46	2.23	0.78	5.78	1.18
	p-value	0.000	0.000	0.000	0.050	0.509	0.005	0.325
	Significance	yes	Yes	yes	yes	no	yes	no
	Rank	3	2	1	5	0	4	0
Resultant force R N	F-statistic	110.78	179.48	4037.77	6.70	16.94	36.65	11.48
	p-value	0.000	0.000	0.000	0.000	0.000	0.000	0.000
	Significance	yes	yes	yes	yes	yes	yes	yes
	Rank	3	2	1	7	5	4	6
Shear plane angle Merchant Φ	F-statistic	2070.32	2494.03	18.64	139.67	72.33	43.91	41.03
	p-value	0.000	0.000	0.000	0.000	0.000	0.000	0.000
	Significance	yes	yes	yes	yes	yes	yes	yes
	Rank	2	1	7	3	4	5	6
Shear plane angle Payton ψ	F-statistic	2070.32	92.45	18.64	139.67	72.33	43.91	41.03
	p-value	0.000	0.000	0.000	0.000	0.000	0.000	0.000
	Significance	yes	yes	yes	yes	yes	yes	yes
	Rank	1	3	7	2	4	5	6
Friction Force Merchant F N (M)	F-statistic	25.87	0.53	443.14	2.16	0.88	1.15	1.13
	p-value	0.000	0.589	0.000	0.057	0.458	0.322	0.353
	Significance	yes	no	yes	no	no	no	no
	Rank	2	0	1	0	0	0	0
Normal Force Merchant N N (M)	F-statistic	187.41	2199.71	16347.50	15.85	100.24	295.84	53.10
	p-value	0.000	0.000	0.000	0.000	0.000	0.000	0.000
	Significance	yes	yes	yes	yes	yes	yes	yes
	Rank	4	2	1	7	5	3	6
F/N ratio Merchant	F-statistic	28.62	142.41	24.57	2.21	0.83	0.77	0.56
	p-value	0.000	0.000	0.000	0.052	0.480	0.469	0.762
	Significance	yes	yes	yes	no	no	no	no
	Rank	2	1	3	0	0	0	0
Force along shear plane Fs N (M)	F-statistic	296.66	540.13	4628.74	13.72	23.45	86.47	30.58
	p-value	0.000	0.000	0.000	0.000	0.000	0.000	0.000
	Significance	yes	yes	yes	yes	yes	yes	yes
	Rank	3	2	1	7	6	4	5
Force normal to shear plane Fn N (M)	F-statistic	10.74	12.81	643.16	3.88	2.29	3.35	1.46
	p-value	0.000	0.000	0.000	0.002	0.085	0.041	0.206
	Significance	yes	yes	yes	yes	no	no	no
	Rank	3	2	1	4	0	0	0
Fs/Fn ratio (M)	F-statistic	1.12	5.30	0.55	3.02	1.26	0.71	0.76
	p-value	0.345	0.007	0.463	0.011	0.295	0.497	0.606
	Significance	no	yes	no	no	no	no	no
	Rank	0	1	0	0	0	0	0
Force along shear plane Fs N (P)	F-statistic	6.77	11.28	12.07	1.37	0.73	0.80	0.72
	p-value	0.000	0.000	0.001	0.238	0.535	0.455	0.634
	Significance	yes	yes	yes	no	no	no	no
	Rank	3	2	1	0	0	0	0
Force normal to shear plane	F-statistic	50.33	63.72	1645.73	3.52	6.13	13.56	4.24
	p-value	0.000	0.000	0.000	0.004	0.001	0.000	0.001
	Significance	yes	yes	yes	no	yes	yes	yes

Fn N (P)	Rank	3	2	1	0	5	4	6
Fs/Fn ratio (P)	F-statistic	10.60	7.04	7.76	1.86	0.69	0.37	0.56
	p-value	0.000	0.002	0.007	0.1	0.564	0.691	0.761
	Significance	yes	yes	yes	no	no	no	no
	Rank	1	3	2	0	0	0	0
Shear area As (M)	F-statistic	2200.78	2022.72	12431.54	28.18	48.58	416.33	17.81
	p-value	0.000	0.000	0.000	0.000	0.000	0.000	0.000
	Significance	yes	yes	yes	yes	yes	yes	yes
	Rank	2	3	1	6	5	4	7
Shear stress τs MPa (M)	F-statistic	249.87	99.85	230.87	4.93	1.34	1.18	4.30
	p-value	0.000	0.000	0.000	0.000	0.270	0.313	0.000
	Significance	yes	yes	yes	yes	no	no	yes
	Rank	1	3	2	4	0	0	5
Shear area As (P) corrected	F-statistic	2446.52	2989.15	12736.92	43.40	53.92	582.15	19.87
	p-value	0.000	0.000	0.000	0.000	0.000	0.000	0.000
	Significance	yes	yes	yes	yes	yes	yes	yes
	Rank	3	2	1	6	5	4	7
Shear stress τs MPa (P)	F-statistic	60.09	2.28	49.31	1.05	2.14	1.28	0.95
	p-value	0.000	0.110	0.000	0.398	0.102	0.285	0.465
	Significance	yes	no	yes	no	no	no	no
	Rank	1	0	2	0	0	0	0
Shear strain γ (M)	F-statistic	3282.20	3258.43	0.03	49.85	180.29	53.0	30.81
	p-value	0.000	0.000	0.860	0.000	0.000	0.000	0.000
	Significance	yes	yes	no	yes	yes	yes	yes
	Rank	1	2	0	5	3	4	6
Shear strain γ (P)	F-statistic	Depends only on Rake angle Shear strain decreases with increasing rake angle. **NA**						
	p-value							
	Significance							
	Rank							
Shear strain γ (P) corrected	F-statistic	1139.32	991.17	22.69	138.15	60.38	21.12	55.74
	p-value	0.000	0.000	0.000	0.000	0.000	0.000	0.000
	Significance	yes	yes	yes	yes	yes	yes	yes
	Rank	1	2	6	3	4	7	5
Friction Co-efficient μ	F-statistic	14.46	77.64	12.37	2.12	0.77	0.60	0.54
	p-value	0.000	0.000	0.001	0.061	0.513	0.551	0.775
	Significance	yes	yes	yes	no	no	no	no
	Rank	2	1	3	0	0	0	0

Table 18: Scenario 3 - AISI 1020 Steel alloy work piece cut with High Speed Steel tool.

The following inferences can be made from the table 18 for scenario 3 based of the values from ANOVA and the corresponding main effects and interactions plots given in appendix5.

- The cutting force decreased with increase in rake angle but increased when the feed was increased. Also, from the interaction plots, using a sharper tool reduced the cutting force even at higher feeds. Using liquid nitrogen and cold compressed air (both performing equally) significantly

decreased the cutting force values. Nitrogen performed between dry environments the other two, inclining away from dry condition.

- The thrust force decreased with increase in rake angle but increased when the feed was increased. Also, from the interaction plots, using a sharper tool reduced the thrust force even at higher feeds. Using liquid nitrogen and cold compressed air (both performing equally) significantly decreased the thrust force values. Nitrogen performed between dry environments the other two, inclining away from dry condition.

		Increasing rake angle α	Increasing feed f
Resultant force R		decrease	increase
Chip thickness ratio r		increase	decrease
Friction force F		decrease	increase
Normal force N		decrease	increase
F/N ratio		increase	decrease
Shear plane angle	Merchant Φ	increase	decrease
	Payton ψ	decrease	increase
Force along shear plane Fs	Merchant	decrease	increase
	Payton	decrease	increase
Force normal to shear plane Fn	Merchant	decrease	increase
	Payton	decrease	increase
Fs/Fn ratio	Merchant	decrease	decrease
	Payton	decrease	decrease
Shear area As	Merchant	decrease	increase
	Payton	decrease	increase
	corrected	decrease	increase
Shear stress τ s	Merchant	increase	decrease
	Payton	decrease	decrease
Shear strain γ	Merchant	decrease	no change
	Payton	decrease	no change
	Vishnu	Increase	decrease

Table 19: Variation of different parameters while increasing feed f and rake angle α for scenario 3

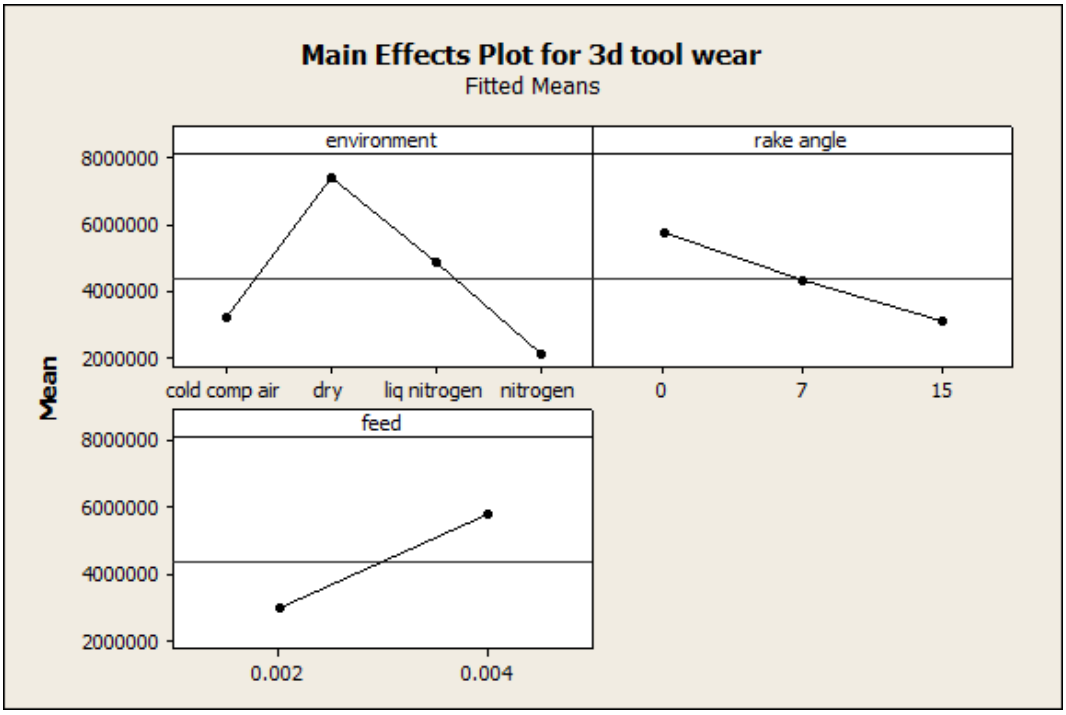

Figure 54: Main Effects plots for variation of volumetric tool wear. (Scenario 3)

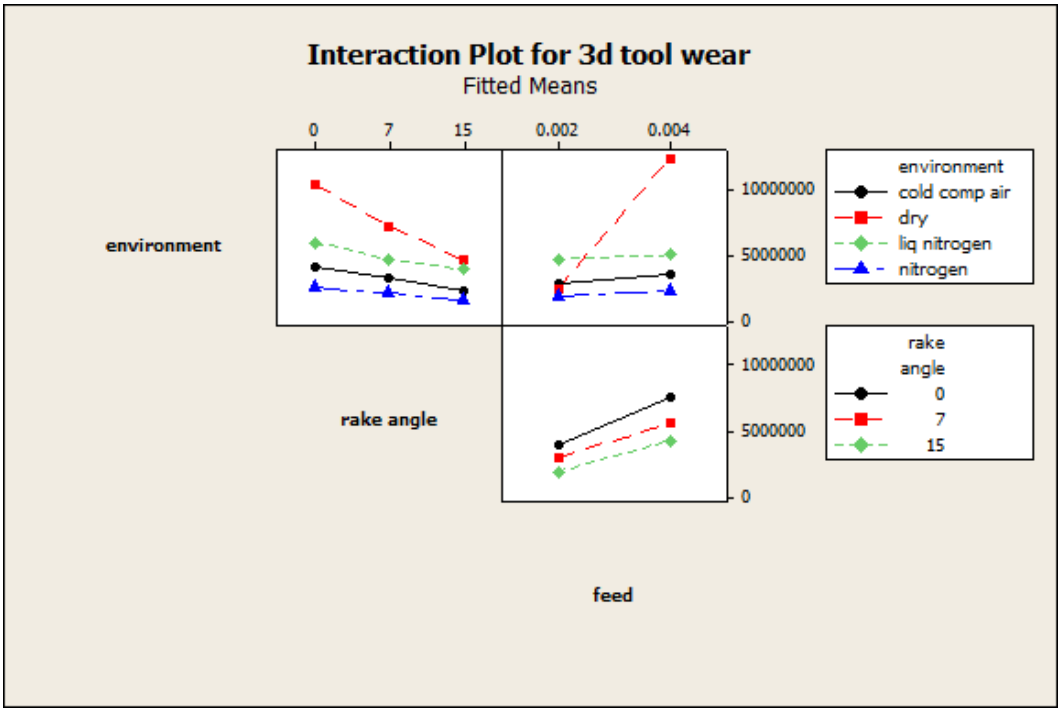

Figure 55: Interaction plots for variation of volumetric tool wear. (Scenario 3)

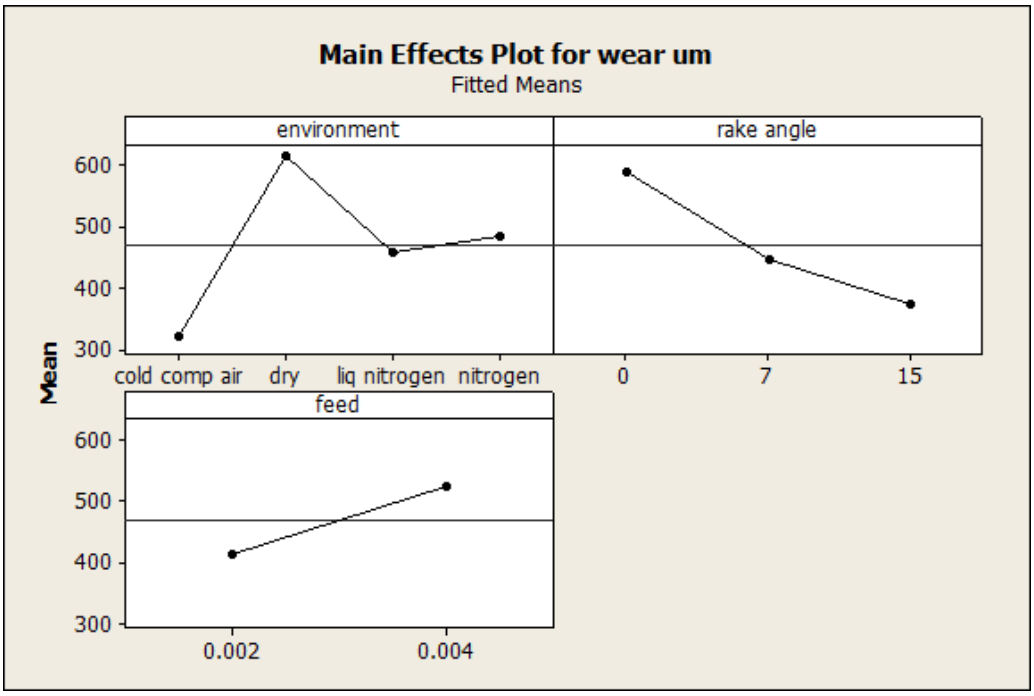

Figure 56**:** Main Effects plots for variation of tool wear width. (Scenario 3)

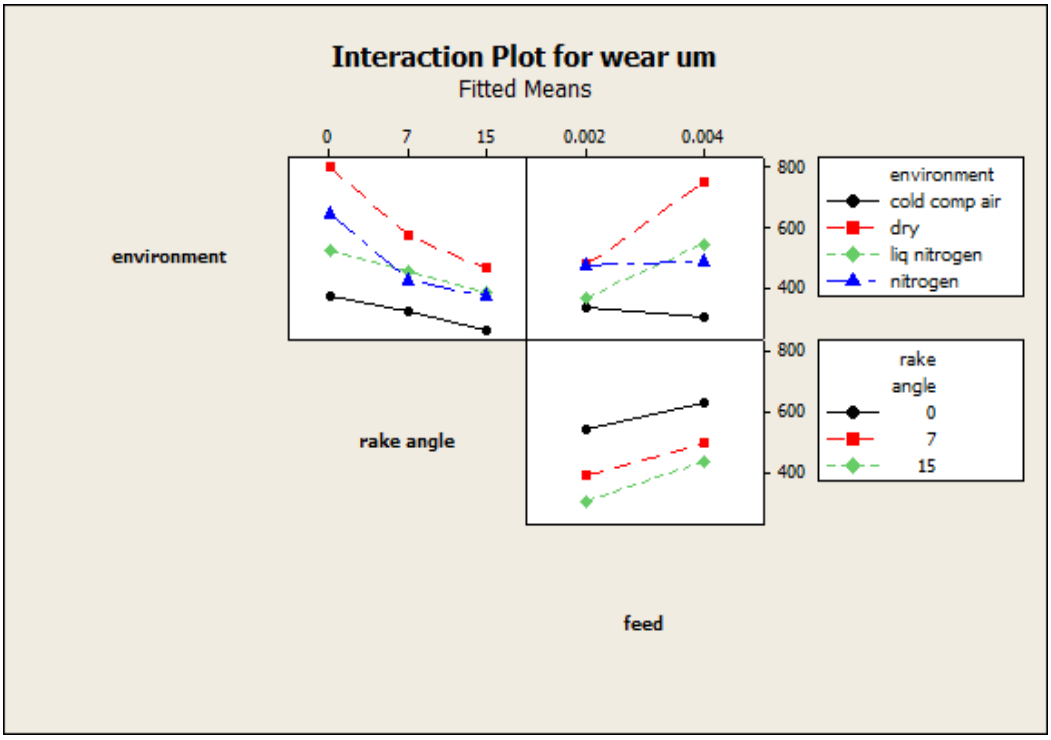

Figure 57: Interaction plots for variation of tool wear width. (Scenario 3)

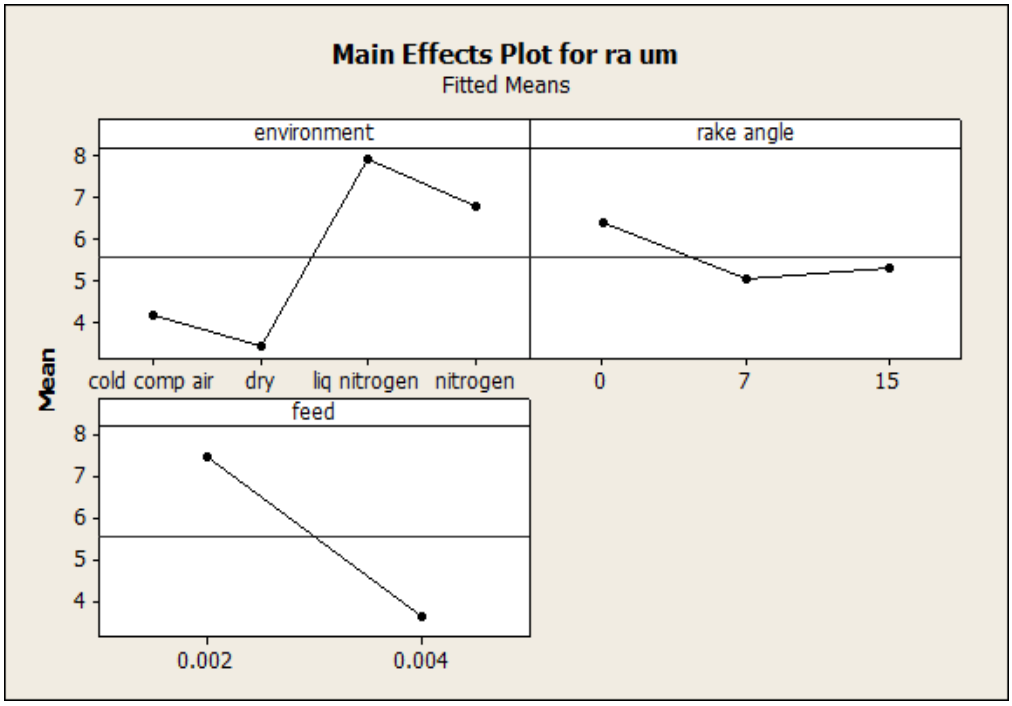

Figure 58: Main Effects plots for variation of surface finish. (Scenario 3)

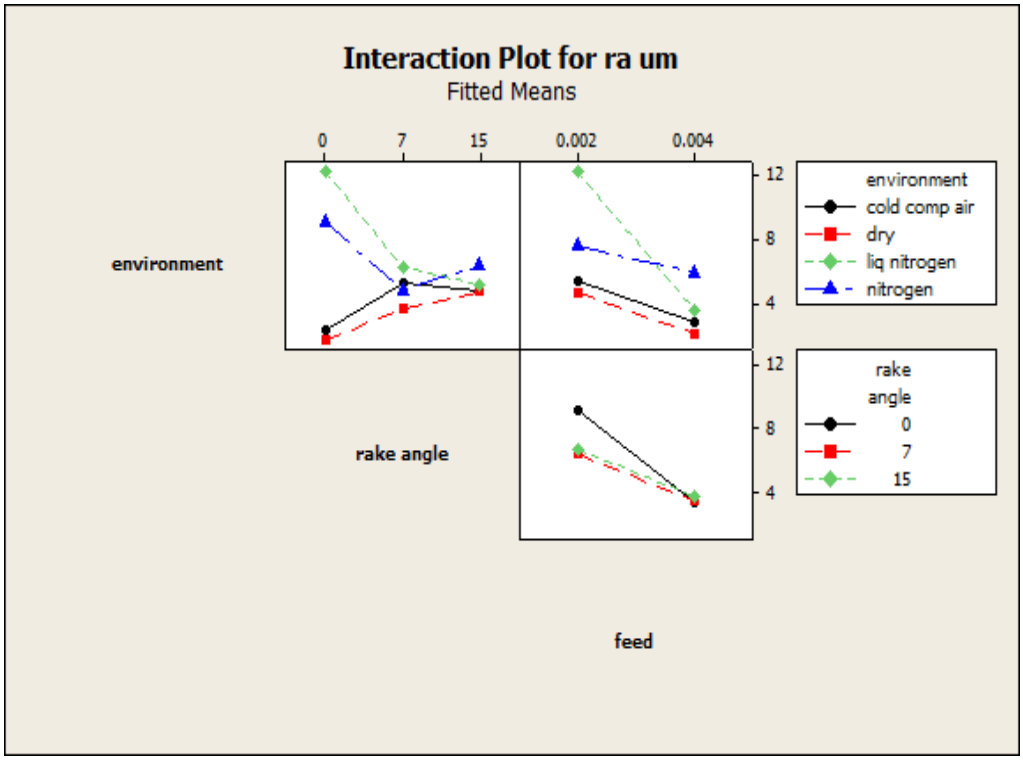

Figure 59: Interaction plots for variation of surface finish. (Scenario 3)

- The tool wear width decreased with increase in rake angle but increased when the feed was increased. Also, the width of tool wear was found to be minimal in case of cold compressed air environment, with liquid nitrogen falling behind, while nitrogen lay between liquid nitrogen and dry environments.
- Volumetric tool wear increased when feed was increased but decreased with increase in rake angle. Volumetric wear was found to be minimal under nitrogen environment closely followed by cold compressed air.
- The surface finish (Ra) decreased with increase in rake angle but increased when the feed was increased. Using cutting environments increased the surface roughness values, with cold compressed air yielding better results amongst the three environments, closer to the dry cutting conditions.

Parameter		Main Effects			Interactions			
		Environment	Rake angel	Feed	Environment * Rake angle	Environment * Feed	Rake angle * Feed	Environment * rake angle * feed
Cutting force Fc N	F-statistic	63.06	65.57	99.61	12.27	22.11	16.48	11.06
	p-value	0.000	0.000	0.000	0.000	0.000	0.000	0.000
	Significance	yes	yes	yes	yes	yes	yes	yes
	Rank	3	2	1	6	4	5	7
Thrust force Ft N	F-statistic	106.09	93.03	74.45	6.74	14.89	3.01	12.52
	p-value	0.000	0.000	0.000	0.000	0.000	0.056	0.000
	Significance	yes	yes	yes	yes	yes	no	yes
	Rank	1	2	3	6	4	0	5
Resultant force R N	F-statistic	92.96	92.30	1.44	8.29	16.35	6.77	12.55
	p-value	0.000	0.000	0.235	0.000	0.000	0.002	0.000
	Significance	yes	yes	no	yes	yes	no	yes
	Rank	1	2	7	5	3	6	4
Shear plane angle Merchant Φ	F-statistic	3786.38	3602.54	1296.98	2876.24	487.21	17.99	64.79
	p-value	0.000	0.000	0.000	0.000	0.000	0.000	0.000
	Significance	yes	yes	yes	yes	yes	yes	yes
	Rank	1	2	4	3	5	7	6
Shear plane angle Payton ψ	F-statistic	3786.38	1402.38	1296.98	2876.24	487.21	17.99	64.79
	p-value	0.000	0.000	0.000	0.000	0.000	0.000	0.000
	Significance	yes	yes	yes	yes	yes	yes	yes
	Rank	1	3	4	2	5	7	6
Friction Force Merchant F N (M)	F-statistic	110.06	35.08	61.87	6.91	15.77	2.22	11.67
	p-value	0.000	0.000	0.000	0.000	0.000	0.116	0.000
	Significance	yes	yes	yes	yes	yes	no	yes
	Rank	1	3	2	6	4	0	5
Normal Force Merchant N N (M)	F-statistic	44.72	164.26	144.47	15.83	22.47	10.82	11.88
	p-value	0.000	0.000	0.000	0.000	0.000	0.000	0.000
	Significance	yes	yes	yes	yes	yes	yes	yes
	Rank	3	1	2	5	4	7	6
F/N ratio Merchant	F-statistic	13.96	7.87	61.57	3.75	0.78	1.18	2.54
	p-value	0.000	0.001	0.000	0.003	0.507	0.312	0.028
	Significance	yes	yes	yes	yes	no	no	no
	Rank	2	3	1	4	0	0	0
Force along shear plane Fs N (M)	F-statistic	57.79	79.69	203.06	19.07	9.53	16.61	11.52
	p-value	0.000	0.000	0.000	0.000	0.000	0.000	0.000
	Significance	yes	yes	yes	yes	yes	yes	yes
	Rank	3	2	1	4	7	5	6
Force normal to shear plane Fn N (M)	F-statistic	93.41	80.38	30.05	6.69	19.15	3.93	12.21
	p-value	0.000	0.000	0.000	0.000	0.000	0.024	0.000
	Significance	yes	yes	yes	yes	yes	no	yes
	Rank	1	2	3	6	4	0	5
Fs/Fn ratio (M)	F-statistic	79.68	63.57	583.60	32.34	35.30	9.27	7.98
	p-value	0.000	0.000	0.000	0.000	0.000	0.000	0.000
	Significance	yes	yes	yes	yes	yes	yes	yes
	Rank	2	3	1	5	4	6	7
Force along shear plane Fs N (P)	F-statistic	61.38	18.95	492.38	9.94	2.34	3.65	4.94
	p-value	0.000	0.000	0.000	0.000	0.081	0.031	0.000
	Significance	yes	yes	yes	yes	no	no	yes
	Rank	2	3	1	4	0	0	5
Force normal to shear plane Fn N (P)	F-statistic	96.77	85.37	0.14	8.89	20.86	6.68	13.33
	p-value	0.000	0.000	0.711	0.000	0.000	0.002	0.000
	Significance	yes	yes	no	yes	yes	yes	yes
	Rank	1	2	0	5	3	6	4

Fs/Fn ratio (P)	F-statistic	88.97	27.23	491.10	13.33	9.24	0.71	5.15
	p-value	0.000	0.000	0.000	0.000	0.000	0.496	0.000
	Significance	yes	yes	yes	yes	yes	no	yes
	Rank	2	3	1	4	5	0	6
Shear area As (M)	F-statistic	1968.87	2251.21	30249.0	1173.82	307.47	298.67	62.75
	p-value	0.000	0.000	0.000	0.000	0.000	0.000	0.000
	Significance	yes	yes	yes	yes	yes	yes	yes
	Rank	3	2	1	4	5	6	7
Shear stress τs MPa (M)	F-statistic	42.70	0.59	152.53	32.94	46.76	5.90	7.22
	p-value	0.000	0.555	0.000	0.000	0.000	0.004	0.000
	Significance	yes	no	yes	yes	yes	yes	yes
	Rank	3	0	1	4	2	6	5
Shear area As (P) corrected	F-statistic	53.82	8.36	179.94	13.04	4.97	0.70	3.59
	p-value	0.000	0.001	0.000	0.000	0.003	0.501	0.004
	Significance	yes	yes	yes	yes	yes	no	yes
	Rank	2	4	1	3	5	0	6
Shear stress τs MPa (P)	F-statistic	54.75	8.48	189.00	12.99	5.09	0.75	3.83
	p-value	0.000	0.000	0.000	0.000	0.000	0.476	0.002
	Significance	yes	yes	yes	yes	yes	no	yes
	Rank	2	4	1	3	5	0	6
Shear strain γ (M)	F-statistic	1595.35	1858.97	2393.43	688.33	618.80	11.26	39.27
	p-value	0.000	0.000	0.000	0.000	0.000	0.000	0.000
	Significance	yes	yes	yes	yes	yes	yes	yes
	Rank	3	2	1	4	5	7	6
Shear strain γ (P)	F-statistic	Depends only on Rake angle. Shear strain decreases with increasing rake angle. **NA**						
	p-value							
	Significance							
	Rank							
Shear strain γ (P) corrected	F-statistic	2681.34	1585.52	365.58	2252.0	232.85	0.30	49.356
	p-value	0.000	0.000	0.000	0.000	0.000	0.742	0.000
	Significance	yes	yes	yes	yes	yes	no	yes
	Rank	1	3	4	2	5	0	6
Friction Co-efficient μ	F-statistic	89.85	42.62	493.94	13.65	7.72	0.38	5.09
	p-value	0.000	0.000	0.000	0.000	0.000	0.684	0.000
	Significance	yes	yes	yes	yes	yes	no	yes
	Rank	2	3	1	4	5	0	6

Table 20: Scenario 4 - AISI 1020 Steel alloy work piece cut with Uncoated Carbide tool.

The following inferences can be made from the table 20 for scenario 4 based of the values from ANOVA and the corresponding main effects and interactions plots given in appendix5.

- The cutting force decreased with increase in rake angle but increased when the feed was increased. Also, from the interaction plots, using a sharper tool reduced the cutting force even at higher feeds. Using liquid nitrogen and nitrogen (both performing equally) significantly decreased the cutting force values. Cold compressed air performed between dry

environments the other two, inclining away from dry condition. An interesting observation was made with cold compressed air performing better than any other environment for a 0° rake angle at lower feeds.

- The thrust force decreased with increase in rake angle but increased when the feed was increased. A significant drop in thrust force was observed the rake angle increased from 7° to 15°. Also, from the interaction plots, using a sharper tool reduced the thrust force even at higher feeds. Using liquid nitrogen significantly decreased the thrust force values. Nitrogen performed almost as same as the liquid nitrogen at 7° to 15° tool rake angles. Cold compressed air performed between dry environments the other two, inclining away from dry condition.

		Increasing rake angle α	Increasing feed f
Resultant force R		decrease	increase
Chip thickness ratio r		increase	increase
Friction force F		decrease	decrease
Normal force N		decrease	increase
F/N ratio		increase	decrease
Shear plane angle	Merchant Φ	increase	increase
	Payton ψ	increase	decrease
Force along shear plane Fs	Merchant	decrease	increase
	Payton	decrease	increase
Force normal to shear plane Fn	Merchant	decrease	decrease
	Payton	decrease	decrease
Fs/Fn ratio	Merchant	increase	increase
	Payton	increase	increase
Shear area As	Merchant	decrease	increase
	Payton	increase	increase
	corrected	decrease	increase
Shear stress τ s	Merchant	decrease	decrease
	Payton	increase	increase
Shear strain γ	Merchant	decrease	decrease
	Payton	increase	no change
	Vishnu	increase	increase

Table 21: Variation of different parameters while increasing feed f and rake angle α for scenario 4

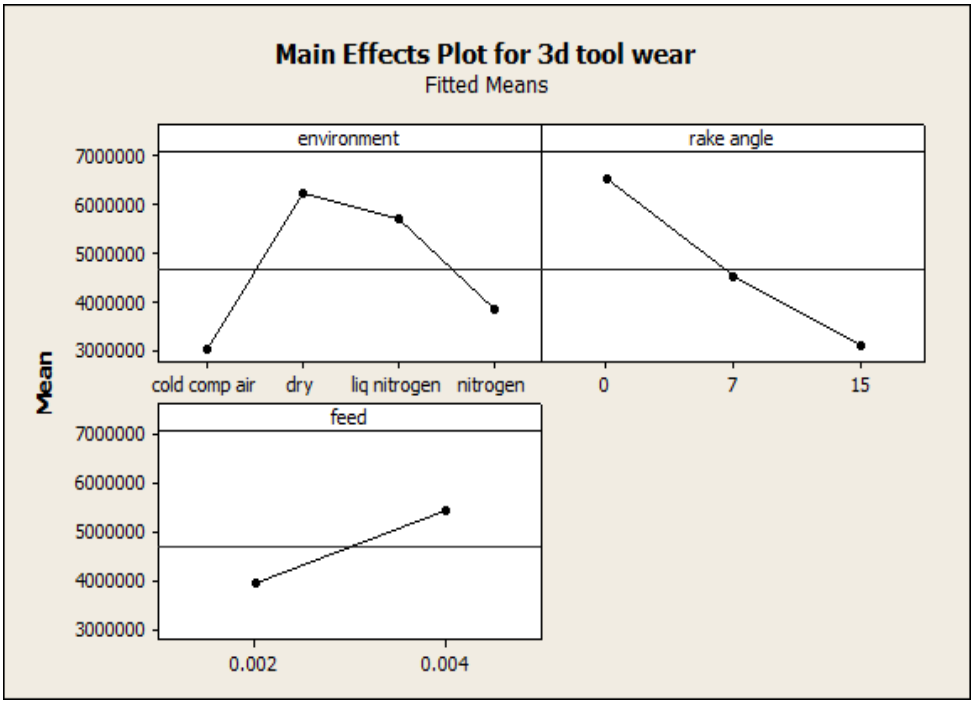

Figure 60: Main Effects plots for variation of volumetric tool wear. (Scenario 4)

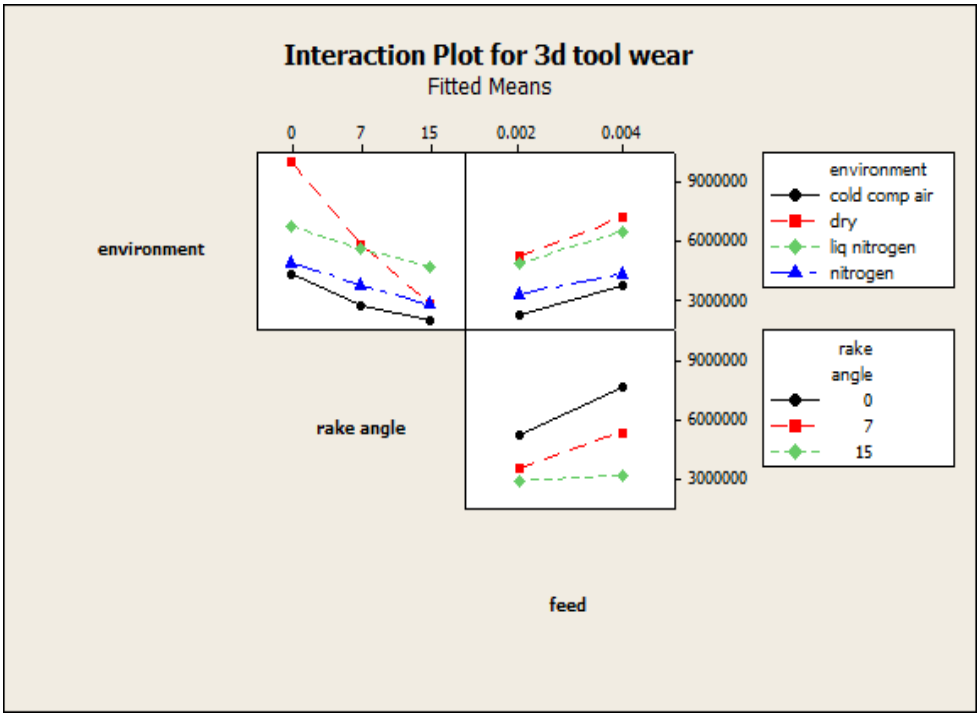

Figure 61: Interaction plots for variation of volumetric tool wear. (Scenario 4)

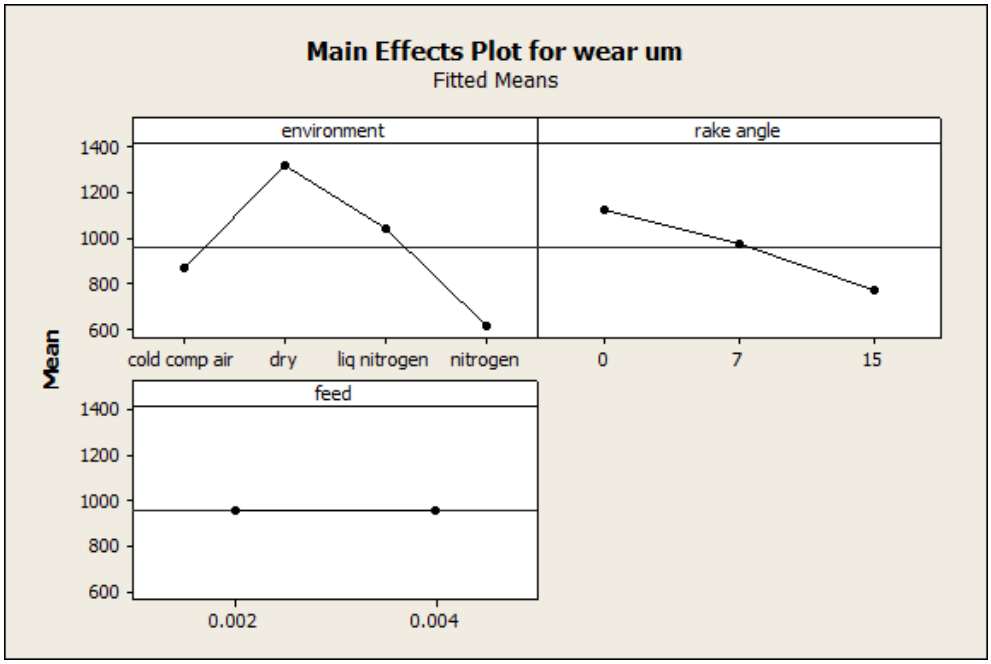

Figure 62: Main Effects plots for variation of tool wear width. (Scenario 4)

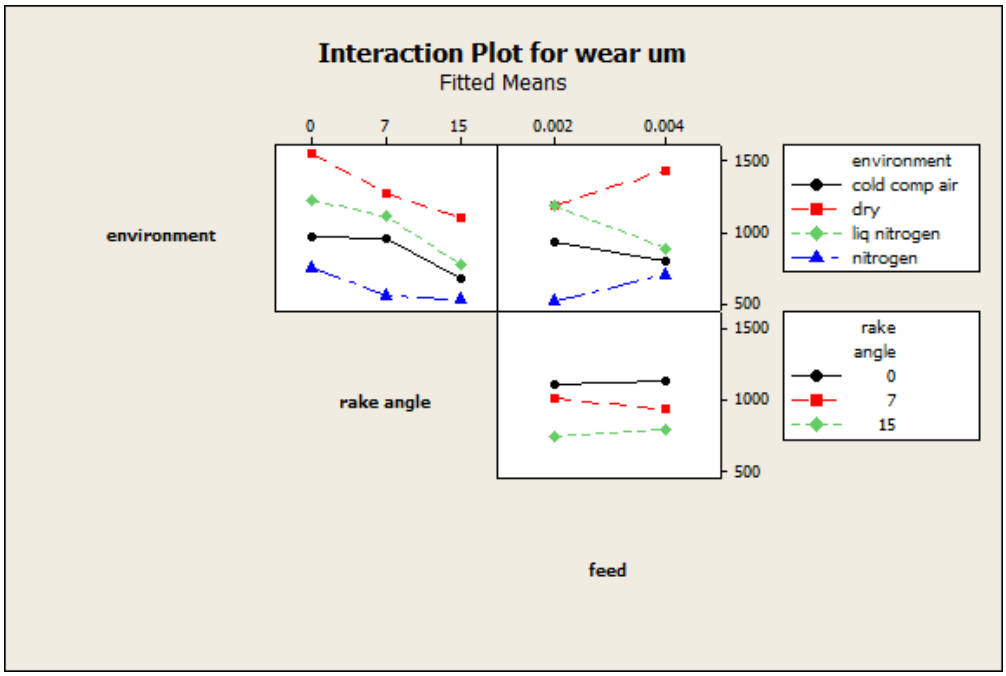

Figure 63: Interaction plots for variation of tool wear width. (scenario 4)

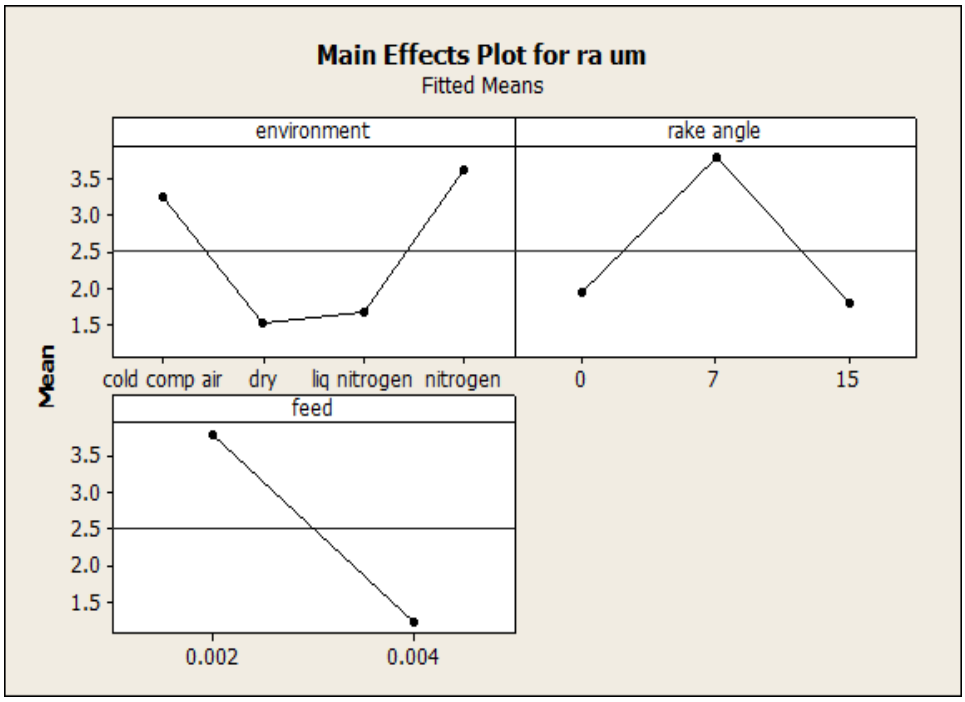

Figure 64: Main Effects plots for variation of Surface finish. (Scenario 4)

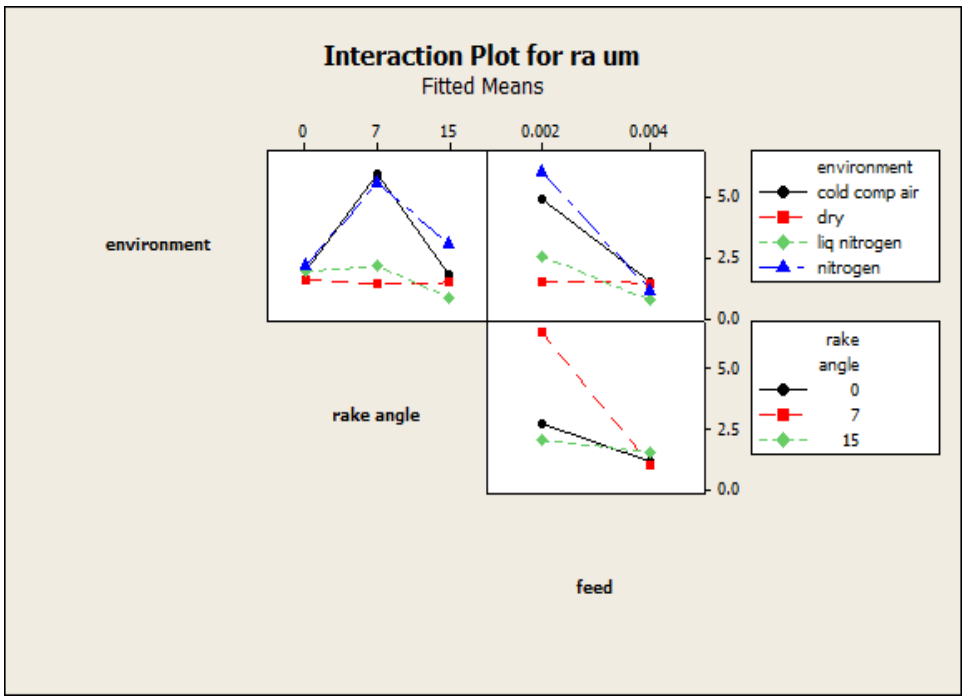

Figure 65: Interaction plots for variation of surface finish. (Scenario 4)

- The tool wear width decreased with increase in rake angle but remained constant when the feed was increased. Also, the width of tool wear was found to be minimal in case of nitrogen closely followed by cold compressed air environment, with liquid nitrogen very closely following behind, while dry environment resulted in maximum.
- Volumetric tool wear increased when rake angle decreased and decreased with increase in feed. Cold compressed air resulted in low volumetric wear closely followed by nitrogen while dry machining produced the maximum.
- The surface finish (Ra) showed a mixed response with change in environment and as well rake angle. When feed was reduced, surface finish also reduced to a low Ra value resulting in better finish.

Effect of variation of supply pressure

One of the environments was randomly chosen to study the effect of change in supply of coolant pressure. The environment chosen was liquid nitrogen while cutting aluminum 6061 work piece with an uncoated carbide insert at 15° rake angle at a feed of 0.002”/revolution. Three different pressure settings of 22 psi, 75 psi and 100 psi were used. Cutting force and thrust force was recorded for a sample size of 2 at each pressure range and the data was used in conducting a 2 sample T – test. Table 17 shows that there is no significant change in either cutting force or the thrust force for the different pressure ranges used.

Combinations	p - Value		Remarks
	Thrust force	cutting force	
22 psi vs. 75 psi	0.754	0.419	Insignificant
75 psi vs. 100 psi	0.514	0.307	Insignificant
22 psi vs. 100 psi	0.479	0.669	Insignificant

Table 22: T- test to determine the effect of change in coolant pressure at 95% confidence interval.

Variation of Fs/Fn Ratio:

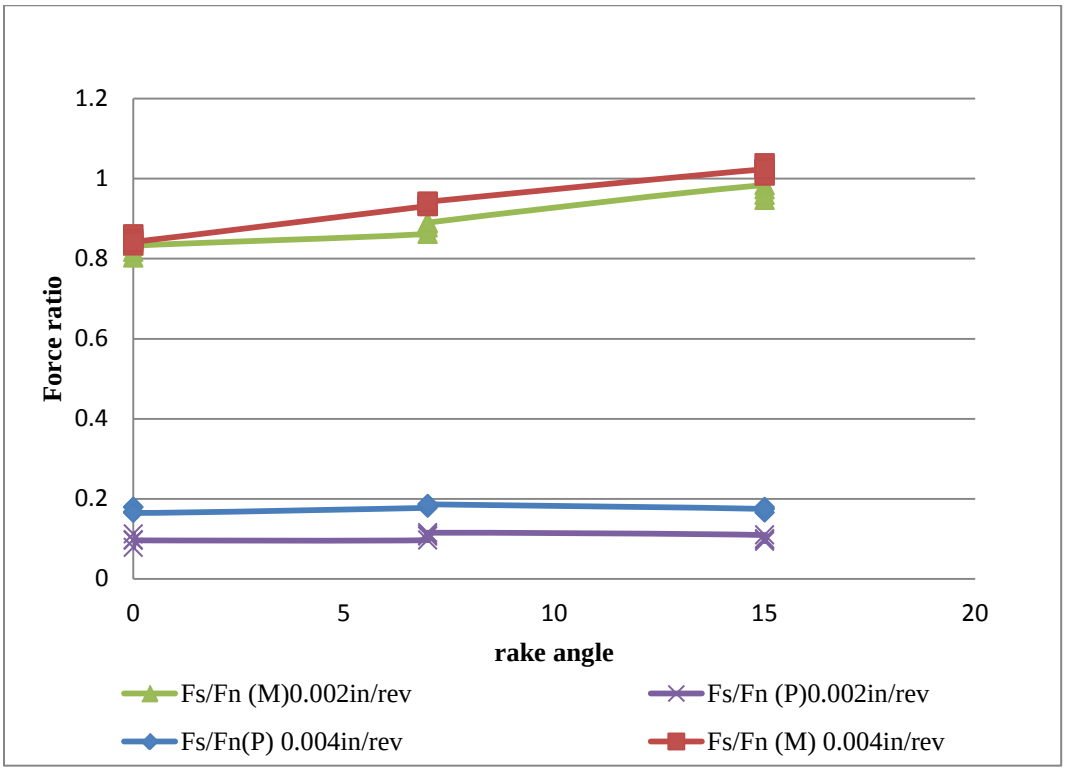

Figure 66: Variation of Fs/Fn versus rake angle for scenario 1

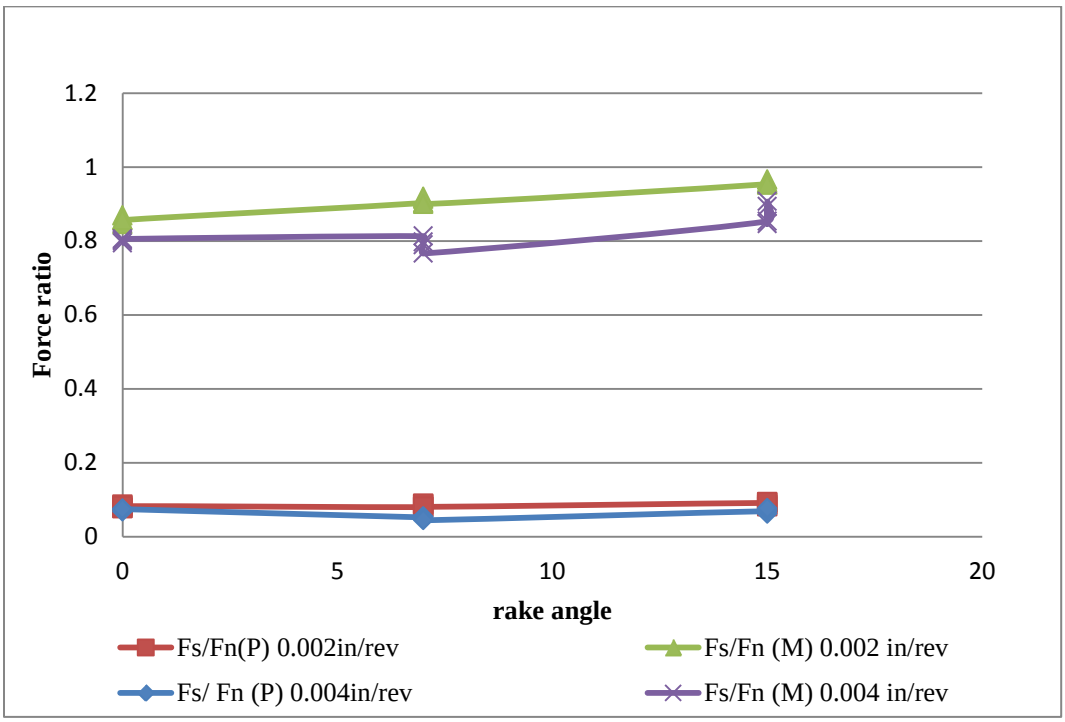

Figure 67: Variation of Fs/Fn versus rake angle for scenario 3

From the above plot, it is evident that the ratio of forces along (Fs) and normal (Fn) to shear plane as predicted by Payton (ψ) is almost a constant whereas the one predicted based on Merchants (Φ) equation varies with rake angle. Also form the results of the ANOVA table, it can be inferred that apart from the geometry of cutting (feed f) all other parameters like environment and rake angle (α) are insignificant. Therefore it can be concluded that the force ratio is a constant for a given material combination and feed. It also has to be noted that, Fs/Fn ratio is nothing but the ratio of Shear stress τs to normal stress σs along and perpendicular to the shear plane respectively.

Variation of hardness:

It becomes necessary to test the hardness of the work piece after it was machined with different cutting environments so as to determine if the cutting fluids changed any of the parent material properties. For a good cutting fluid it should not change the parent material properties while machining. Two random samples for each cutting tool material and work piece combination was selected for all four different cutting environments. Both the steel and aluminum samples were subjected to rockwell hardness test using 1/16" steel ball indenter at a load of 100kgf. The data were plotted, from which it was concluded that the hardness did not significantly change when the cutting environment was changed as compared to the dry machining. Thus the cutting fluid used aides the cutting process by reducing wear and cutting forces (in some cases) but does not alter the parent material properties.

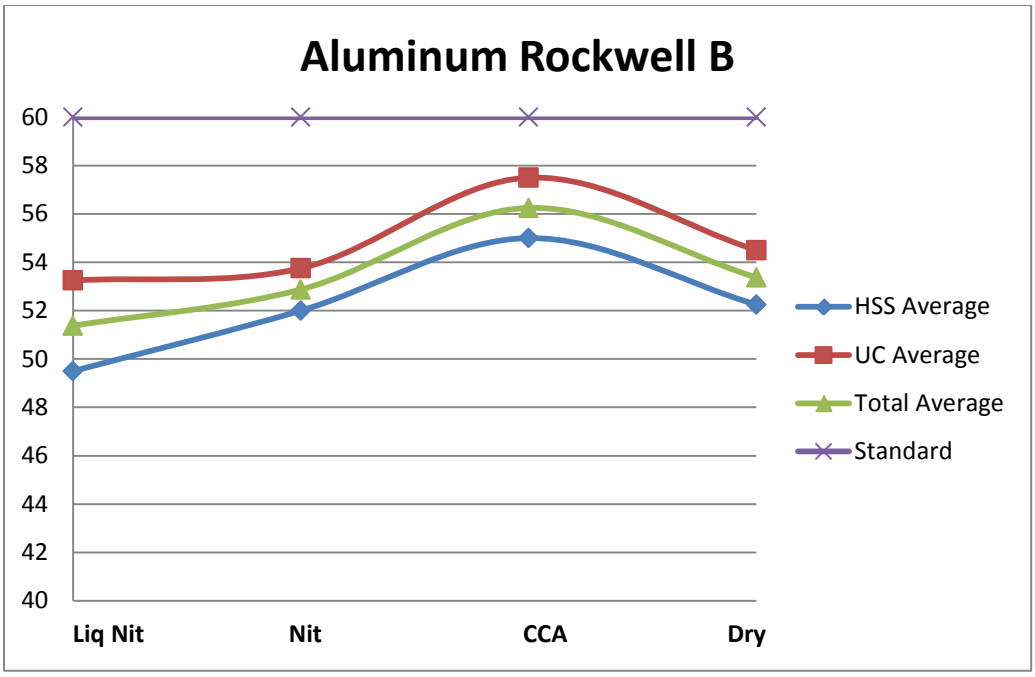

Figure 68: Variation of hardness values of Aluminum 6061 T6 subjected to cutting under different environments.

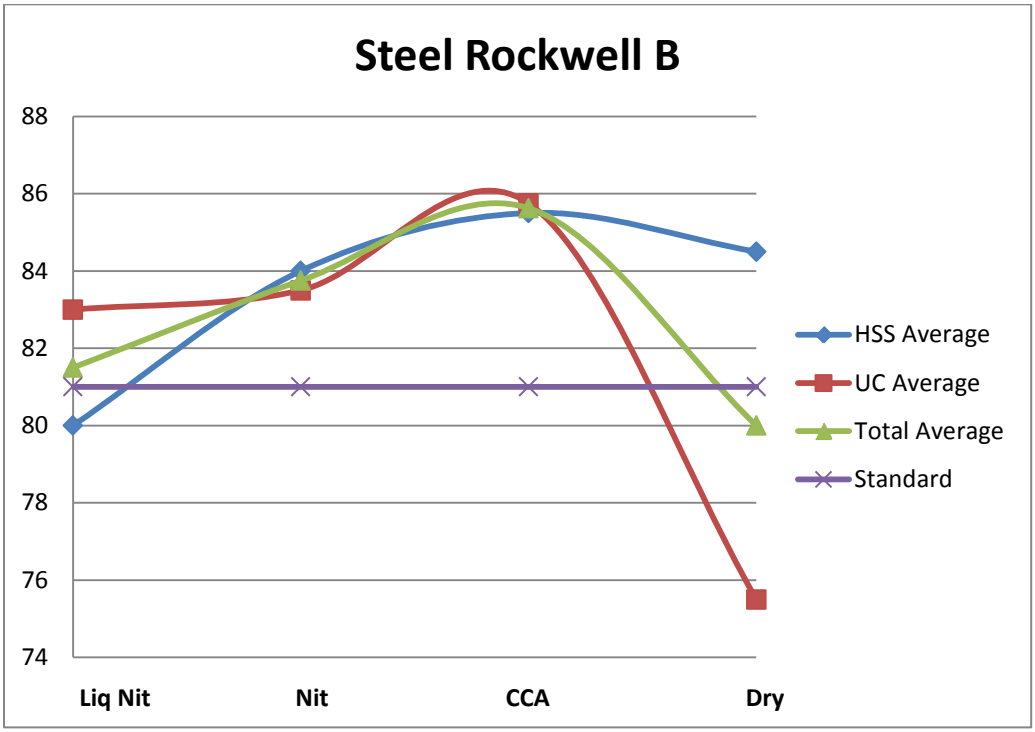

Figure 69: Variation of hardness values of AISI 1020 Steel subjected to cutting under different environments.

Material	Liq Nit	Nit	CCA	Dry Hardness
Steel	1.875 %	4.6875 %	7.03125 %	80
Aluminum	-3.74707 %	-0.93677 %	5.386417 %	53.375

Table 23: % variation of hardness values for different cutting environments based of dry machining hardness

From the the figures 68 and 69, it is evident that the the change in hardness of the work piece is not significant, this is further substantiated by table 22. The percentage change in hardness values when compared to dry machining is approximately close to 5%which is very minimal and would not even contribute to an increase of 1Rc.

Corrections to Payton's MFD

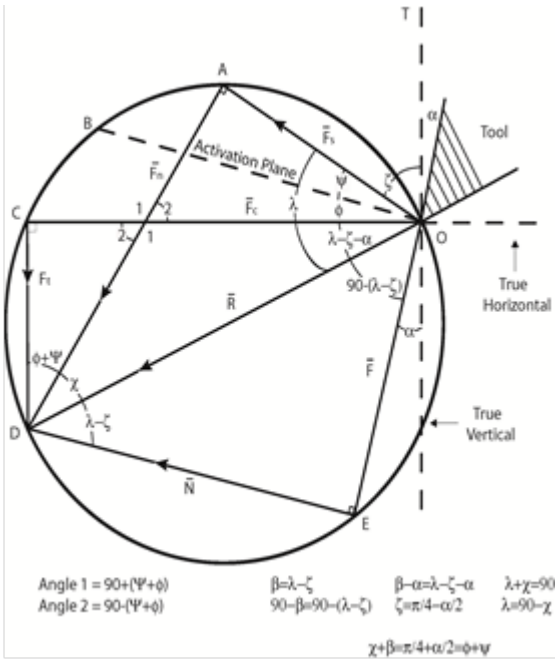

Figure 70: Payton's corrected Merchants Force Diagram (MFD).

Several equations have been used to calculate different metal cutting parameters as summarized in table 10. To calculate shear area, both Merchant and Payton used the same expression even though the angle of shear plane was different in their respective theories. On examining Payton's shear area closely, it was noted that the area of shear has to be calculated differently, as angle ψ (Payton's shear plane angle) is greater than angle Φ (Merchant's shear plane angle) which is described below.

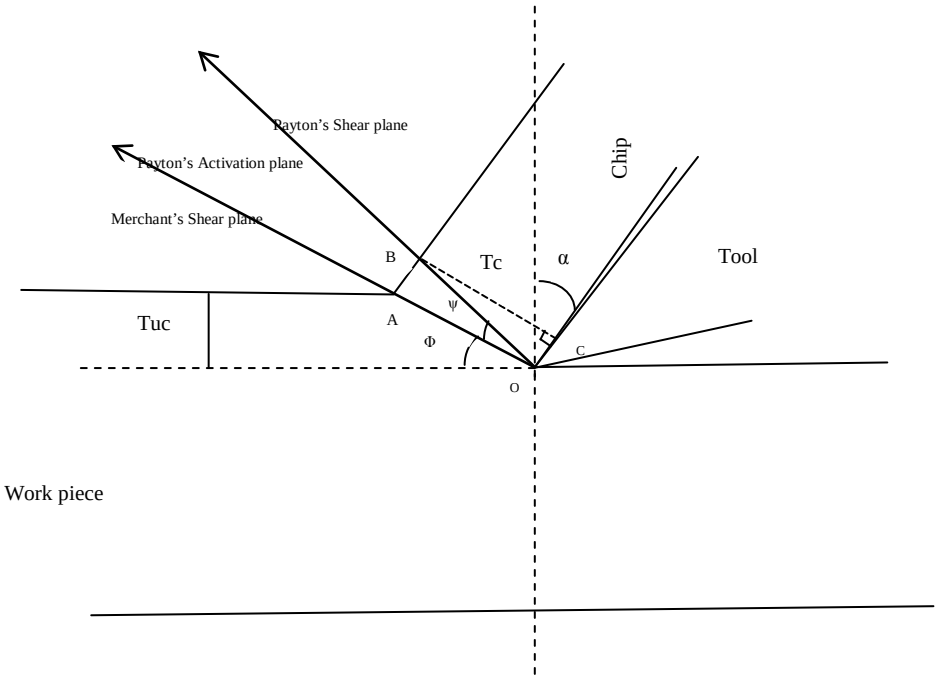

Figure 71: Depiction of Shear plane as defined by Merchant and Payton.

The model used by Payton in 2002 and later by Sripathi 2009, defines the shear area with the following equation

$$\boldsymbol{As = \frac{Tuc * w}{\sin \Phi}} \qquad 9$$

On examining the above equation closer, it was found that, the area depicted is actually the area of Merchant's shear plane which according to Payton is the activation plane (OA). In order to use the expression derived by Payton to calculate the force along the shear plane F_s p in computing Shear stress $\tau_{s\ p,}$ the area has to be calculated along Payton's shear plane (OB).

Considering the triangle OBC,

$$\boldsymbol{\sin (BOC) = \frac{BC}{OB}} \qquad 10$$

$$\boldsymbol{\sin ((90 - \Phi + \psi) + \alpha) = \frac{Tc}{OB}} \qquad 11$$

But,

$$(\mathbf{90} - \boldsymbol{\Phi} + \boldsymbol{\psi}) = \boldsymbol{\zeta} \quad (12)$$

And

$$\boldsymbol{\zeta} = \frac{\boldsymbol{\pi}}{\mathbf{4}} - \frac{\boldsymbol{\alpha}}{\mathbf{2}} \quad (13)$$

Substituting, equation 12 and 13 in 11,

$$\mathbf{Sin}\left(\left(\frac{\boldsymbol{\pi}}{\mathbf{4}} - \frac{\boldsymbol{\alpha}}{\mathbf{2}}\right) + \boldsymbol{\alpha}\right) = \frac{\boldsymbol{Tc}}{\boldsymbol{OB}} \quad (14)$$

i.e.,

$$\mathbf{Sin}\left(\frac{\boldsymbol{\pi}}{\mathbf{4}} + \frac{\boldsymbol{\alpha}}{\mathbf{2}}\right) = \frac{\boldsymbol{Tc}}{\boldsymbol{OB}} \quad (15)$$

Also,

$$\frac{\boldsymbol{\pi}}{\mathbf{4}} + \frac{\boldsymbol{\alpha}}{\mathbf{2}} = \Phi + \psi \quad (16)$$

Therefore,

$$\boldsymbol{OB} = \frac{\boldsymbol{Tc}}{\boldsymbol{Sin}\,(\boldsymbol{\Phi}+\boldsymbol{\psi})} \quad (17)$$

Corrected Shear area is calculated as

$$\boldsymbol{Asc} = \boldsymbol{OB} * \boldsymbol{w} \quad (18)$$

$$\boldsymbol{Asc} = \frac{\boldsymbol{Tc}*\boldsymbol{w}}{\boldsymbol{Sin}\,(\boldsymbol{\Phi}+\boldsymbol{\psi})} \quad (19)$$

And therefore, the corrected Payton's shear stress $\tau_{s\,pc}$ is given by

$$\boldsymbol{\tau s\ pc} = \frac{\mathbf{Fs\ p}}{\boldsymbol{Asc}} \quad (20)$$

$$\boldsymbol{\tau s\ pc} = \frac{\mathbf{Fs\ p}}{\boldsymbol{Tc}*\boldsymbol{w}} * \mathbf{Sin}\,(\boldsymbol{\Phi} + \boldsymbol{\psi}) \quad (21)$$

Equation 21 exactly predicts the shear stress along Payton's shear plane inclined at angle ψ. Also on taking a closer look at the velocity triangle proposed by Payton as depicted in figure 40, relations expressing ratio of different velocities (Vs, Vc and V) and cutting ratio (r= T/Tc) can be derived.

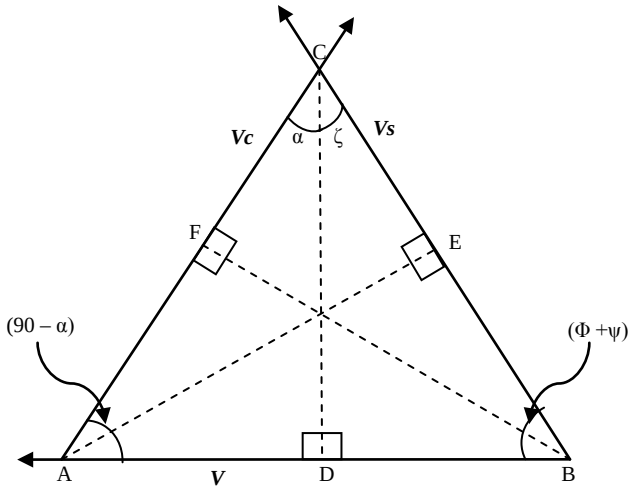

Figure 72: Velocity Triangle.

Cook presented three important velocities involved in chip formation as V, cutting velocity along the direction of cut, Vc the velocity with which the chip moves with relative to the tool and is parallel to the rake face of the tool and Vs the velocity of chip formation along the shear plane ignoring the secondary shear and chip curl.

Considering the triangle ABC, formed by the three velocity vectors, the vector sum of AB and AC must be equal to BC. From figure 39, the following angular relationships can be inferred.

Angle, ABC= Φ +ψ; angle ACB= α+ζ and angle CAB= 90- α

On further simplifying,

$$\Phi + \psi = \pi/4 + \alpha/2 \quad (22)$$

$$\alpha + \zeta = \pi/4 + \alpha/2 \quad (23)$$

Because of the isosceles nature of the triangle ABC, the sides AB and AC are equal implying that

$$V = Vc \quad (24)$$

Also,

$$V + Vc = Vs \quad (25)$$

i.e.,

$$Vs = 2V \quad (26)$$

Equation 26 shows that the shear velocity is twice the cutting velocity which can be used as boundary condition in predicting the chip flow.

Now consider the triangle ABC with AC as base and a perpendicular line from AC connecting the vertex B and the line BF representing the cut chip thickness Tc. From triangles BFA and BFC respectively,

$$\text{Sin}(90 - \alpha) = \text{Cos}\,\alpha = Tc/V \quad (27)$$

Also,

$$\text{Cos}(90 - \alpha) = \text{Sin}\,\alpha = Vc/V \quad (28)$$

Similarly when triangle ABC is considered with AB as base and CD as the perpendicular from AB to C, the uncut chip thickness T is represented by CD. From triangles, ADC and CDB respectively,

$$\text{Sin } \alpha = T/Vc \quad (29)$$

And $$\text{Cos } (\Phi + \psi) = \text{Cos } (\pi/4 + \alpha/2) = V/Vs \quad (30)$$

From equations 27 and 29,

$$Tc/T = (V/Vc) \text{ Tan } \alpha \quad (31)$$

Or, $$r = T/Tc = (Vc/V) \text{ Cot } \alpha \quad (32)$$

i.e., $$r = \text{Cot } \alpha \quad (33)$$

Consider the region AOB in Figure 40, with Payton's activation plane OA as the lower boundary and Payton's Shear plane OB as upper boundary.

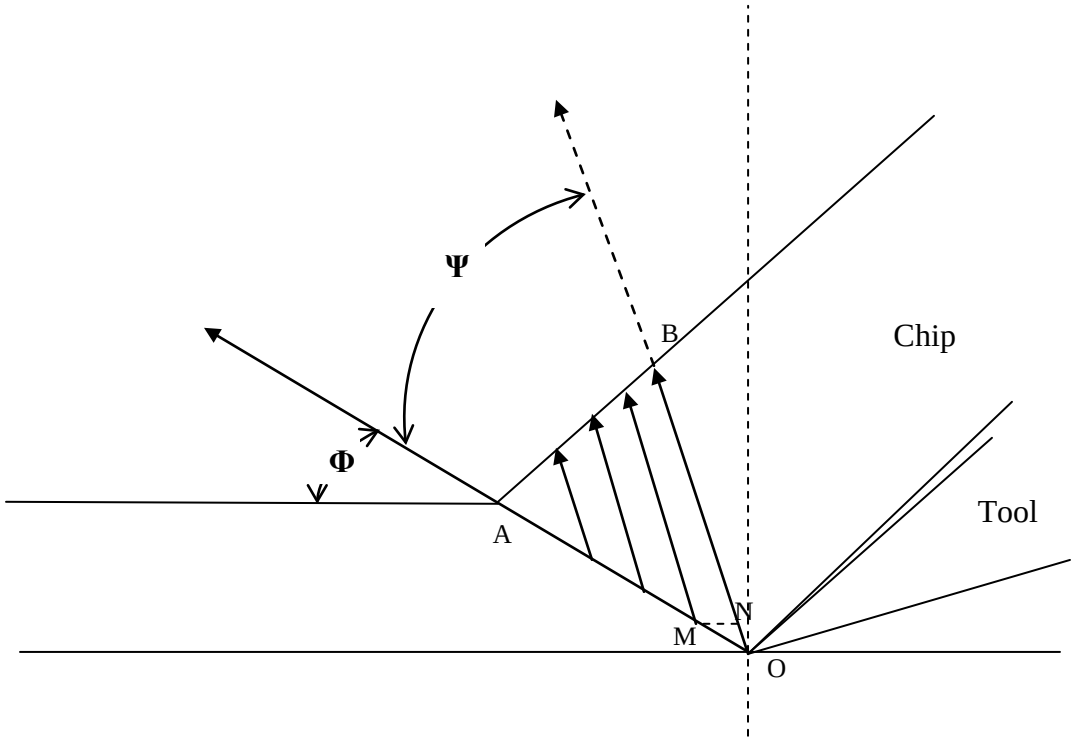

Figure 73: Enlarged portion of shear area OAB from figure 40.

Consider triangle OMN where the actual shearing takes place, the shear strain is expressed as follows

$$\gamma = \Delta S/\Delta Y = ON/MN \quad (34)$$

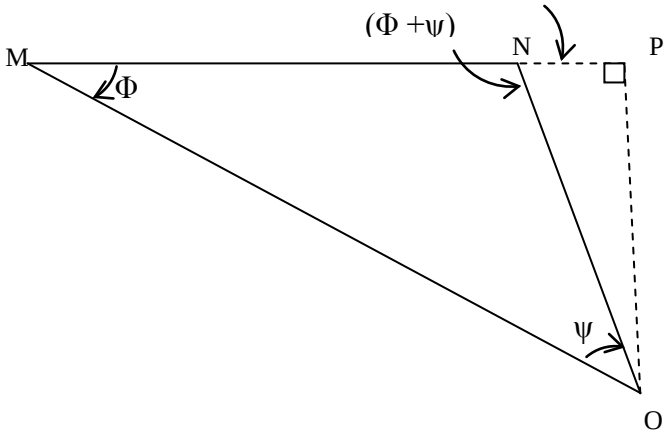

Figure 74: Shear triangle to calculate shear strain.

From Triangles OPN and OMP, following relations can be derived,

$$ON = OP/\ \mathrm{Sin}\ (\Phi + \psi) \quad (35)$$

$$NP = OP * \mathrm{Cot}\ (\Phi + \psi) \quad (36)$$

And $$PM = OP * \mathrm{Cot}\ (\Phi) \quad (37)$$

But, $$MN = PM - NP \quad (38)$$

$$ON = OP*[\{\mathrm{Cot}\ (\Phi)\} - \{\mathrm{Cot}\ (\Phi + \psi)\}] \quad (39)$$

Substituting Eqs. 34 and 38 in 33,

$$\boldsymbol{\gamma} = \frac{\mathbf{OP/\ Sin\ (\Phi + \psi)}}{\mathbf{OP} * [\{\mathbf{Cot}\ (\mathbf{\Phi})\} - \{\mathbf{Cot}\ (\mathbf{\Phi} + \boldsymbol{\psi})\}]} \quad (40)$$

On further simplifying, using trigonometric identities, it can be shown that

Shear strain $$\boldsymbol{\gamma} = \frac{\mathbf{Sin}\ (\mathbf{\Phi})}{\mathbf{Sin}\ (\boldsymbol{\psi})} \quad (41)$$

Also strain rate γ', as given by Shaw [83]

$$\gamma' = \gamma / \Delta t \quad (42)$$

here Δt is the time elapsed for the metal to travel a distance of ΔS with ΔY as the distance between two consecutive slip planes.

From equations, 34 and 42

$$\gamma' = \Delta S/(\Delta Y * \Delta t) \quad (43)$$

but, $\Delta S/ \Delta t = Vs$ (shear velocity) (44)

and $Vs = 2*V$ (45)

therefore,

$$\gamma' = 2*V/ \Delta Y \quad (46)$$

Finite Element Modeling

R. Komanduri 2001[84] in his work states that nearly US $300 billion is spent in conducting metal cutting research in United States alone. This cost includes only the labor and over heads and does account for the raw material, cutting tools or machine tools. Another interesting fact mentioned by Komanduri is that for the experiments conducted by Taylor his team has utilized 363636 Kg of work material in the form of cast iron and steel over a span of 26 years in which they conducted nearly 30000 – 50000 experiments. The fact that conducting metal cutting experiments involves a huge investment is evident; there rises a need for alternative techniques to perform analysis to optimize the metal cutting process.

Demonstration to use concepts involving the finite elements modeling and analysis (FEA) along with growth in the field of computer technology has to an extent reduced the need for conducting the metal cutting experiments. A lot of researchers have applied the FEA concept to model metal cutting simulations, not many have validated the simulated results against the real time experiments to make the model more dependable/reliable. There are several commercial FEA simulation softwares available in the market ABAQUS, LS-Dyna, AdvantEdge to mention a few with each of them having its own advantages and disadvantages.

The following list briefly summarizes some of the finite element modeling results from the past.

- Villumsen et.al, [85] used LS DYNA to simulate as orthogonal machining of Al 6082 and the results obtained were; F (thrust) was under estimated by 60% and F (cutting) was over estimated upto 104%.

- Komvopoulus and Erpenbeck [86] generated force values from simulation, that were off by upto 160 N on Fp and upto 130 N on Fn.

- Zhang and Bagchi [87] in their experiments obtained the feed force and the cutting force to be in good agreement with the experimental results, but were using a very high velocity values of upto 238 mm/s.

- Haung and Black [88] in their work reported that the cutting force obtained from the model was 9690 N whereas the experimental values were 1060 N.

- The force values obtained by Schermann et. al., [89]was found to be in close agreement with the experimental values, but a constant friction coefficient value was used even when the rake angle changed.

- Arrzola et.al.,[72] predicted the cutting forces in an orthogonal machining of AISI 4140 steel to be 126N using ABAQUS and 216 N using AdvantEdge whereas the experimental result showed that it was 189N.

- Svoboda et. al., [90] utilized two different material models to orthogonal metal cutting process in MSC.Marc finite element software and the force values obtained by him were varying upto 19.9% for cutting force and upto 8.9% for thrust force.

- Espinaso et.al., [91] used Smoothed particle hydrodynamic method to predict the cutting forces for a orthogonal machining of Al 6061 T6 alloy and reported that the cutting force variation was upto 10% and the thrust force upto 30%.

In this study, the Finite element model developed by Chandrasekaran 2011(unpublished) in LS-Dyna was used to simulate two random cases from the four different scenarios. The model used is a 2-d plane strain model set up for simulating the machining of

- (Case 1) Aluminum 6061 T6 alloy with High Speed Steel tool, rake angle 15 degrees, feed of 0.002”/revolution and cutting velocity of 500 SFPM under dry machining conditions.
- (Case 2) AISI 1020 Steel alloy with Uncoated carbide tool, rake angle 15 degrees, feed of 0.002”/revolution and a cutting velocity of 805 SFPM under dry machining conditions.

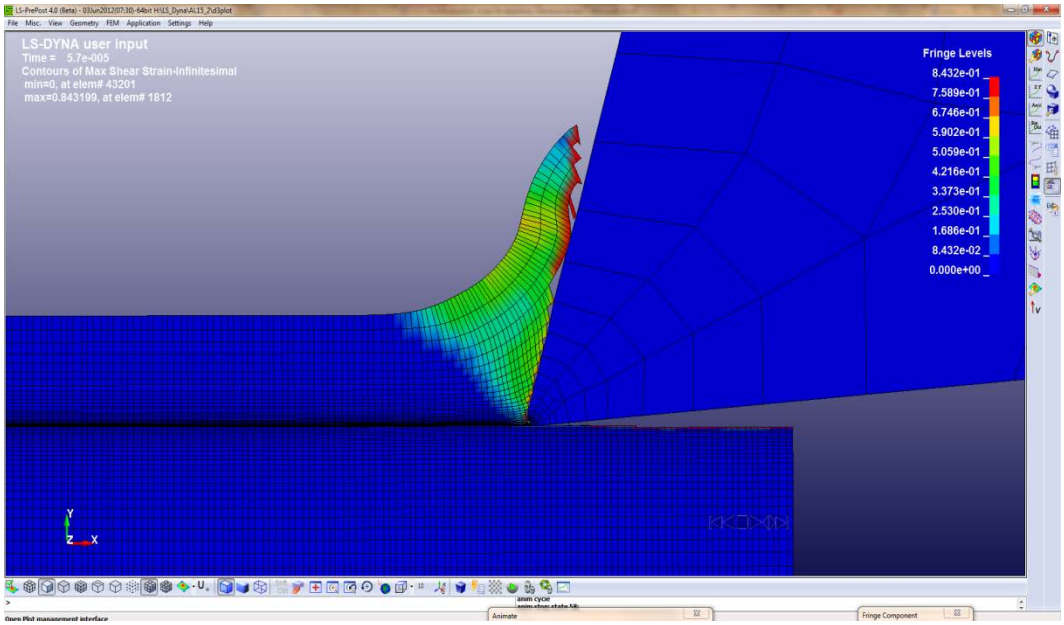

Figure 75: Finite element model depicting the cutting of Aluminum 6061 T6 alloy with HSS tool.

In the model, the entire cutting duration was not simulated as it would involve an infinitely long processing time and hence restricted to 2mm (approx. 0.080”) of cut length. The tool was modeled as a rigid body and no wear or tool deflection was considered in this case so as to reduce the complexity and run time. A 2-D solid, 4-node shell element was used to mesh the model, with a Variable density meshing technique so as to very finely mesh the area in the work piece undergoing deformation. A 2-D automatic single surface contact model was used to model the contact and a constant columbic friction was assumed between the cutting tool and the work piece. The Plastic kinematic hardening model available in LS-Dyna was used to model the work material which abides the following equation.

$$\sigma_y = \left[1 + \left(\frac{\dot{\varepsilon}}{C}\right)^{1/P}\right]\left(\sigma_0 + \beta E_p \varepsilon_p^{eff}\right) \quad (47)$$

The cutting forces, the thrust force and the chip thickness ratio were determined form the finite element model for both the cases and compared to the experimental values obtained in this study. Also, shear strain along the shear plane from the simulation is compared to the calculated (Merchant and Payton) values for the two selected cases.

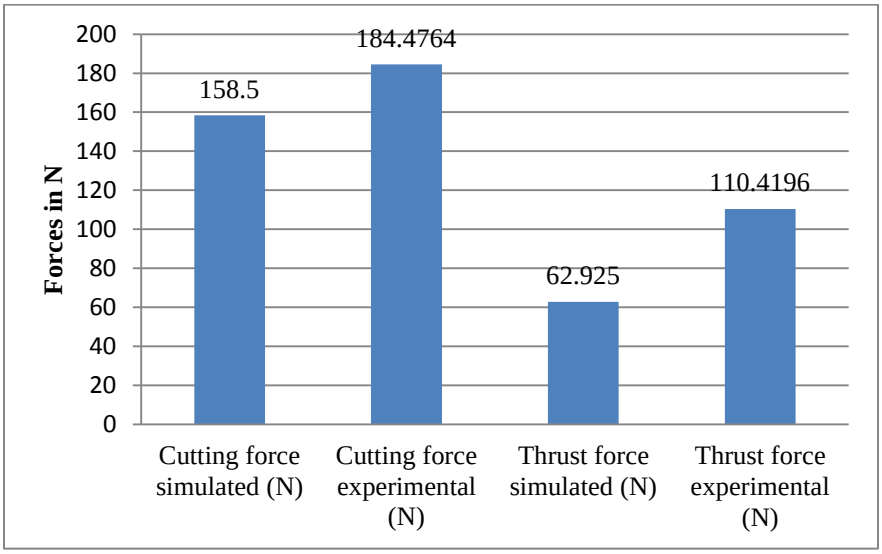

Figure 76: Comparison of cutting force and thrust force for Case 1versus experimental values.

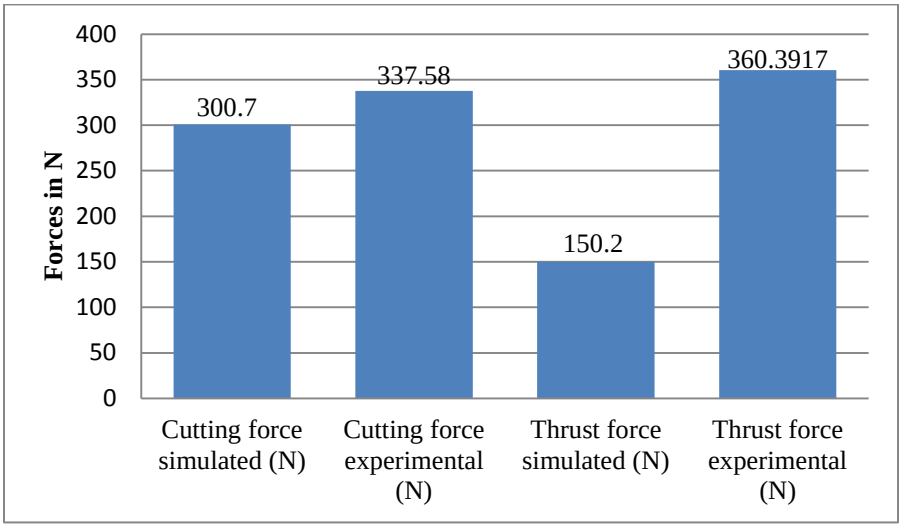

Figure 77: Comparison of cutting force and thrust force for Case 2 versus experimental values.

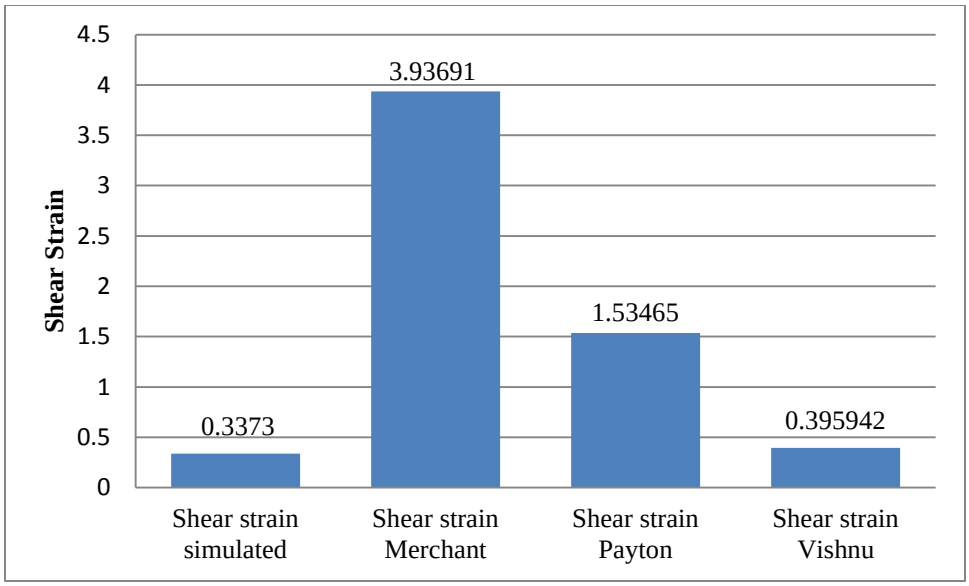

Figure 78: Comparison of shear strain along the shear plane simulated versus calculated (Merchant, Payton, Vishnu) for case 1.

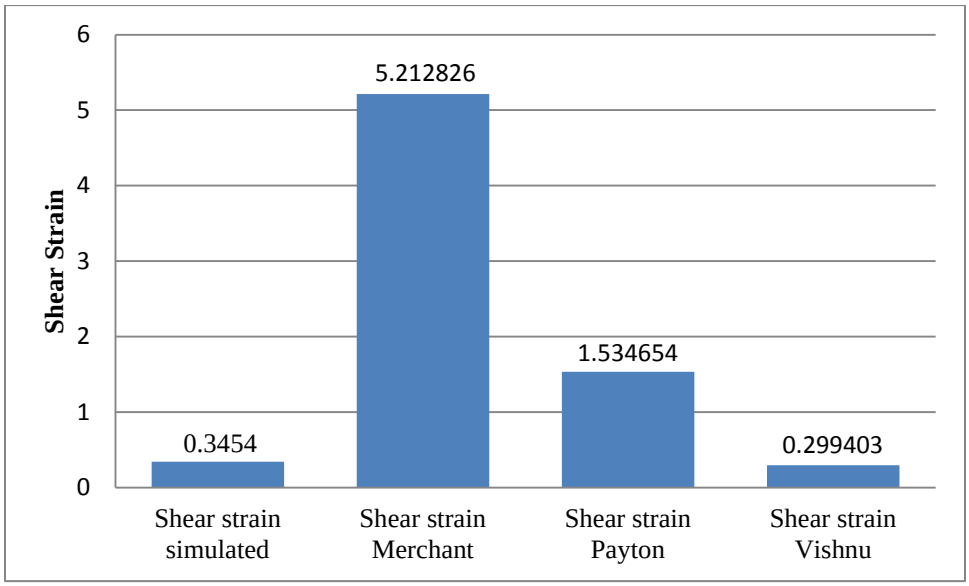

Figure 79: Comparison of shear strain along the shear plane simulated versus calculated (Merchant, Payton, Vishnu) for case 2.

Variation of force values (figures 45 and 46) while comparing both simulated and experimental values suggest that the simulation model

underestimates both the force values (thrust and cutting). The cutting force variation is within 10% of the experimental results whereas the thrust force is approximately two third of the experimental results. And the variation of thrust force by a factor of three is almost applicable to both the combinations considered in the present study.

The primary reason for such observation can be attributed to the limitations of modeling metal cutting problems using finite element analysis software of which a few are mentioned below.

- It was not possible to maintain the tool work piece contact, at the point of cutting at all times in the current model. The reason being that, in the current model the chip separation takes place based on the failure strain specified in the input. When the cutting edge of the tool approaches an element in the cutting zone, the plastic strain of the element in the work piece increases and reaches the failure strain even before the tool completely crosses over the length of that element leading to the deletion. This causes the force values to drop down at that instant but only for a very little time in which the tool reaches the next successive element. The frequency of occurrence of the above stated process is so high leading to a force output with high noise/vibration.

- The tool was modeled as a rigid body in the current model and does not have any impact due to the cutting process. But in actual case, the tool is deformable, and is subjected to wear. It is really hard to model such a

simulation incorporating the effects of tool as it would increase the computation time.

- Also using a better material model that precisely follows the material behavior along with the consideration of dynamic friction can improve the finite element model and provide better results.

- Shear strain predicted by the model closely compares with the shear strain calculated based on the shear strain expression (equation 41) shown in the previous chapter which is small value when compared to expression derived by Merchant and Payton in their studies.

Dislocation in Metal cutting

Dislocations have been a major field of study in material engineering and applied physics for over seventy years now, but metal cutting researchers have not typically addressed hardness, dislocation density or dislocation movement in their work with a few noted exceptions. Dieter (1986) [92] gives an excellent overview of dislocation theory in general as it applies to material. His integrated overview of the effects of cold rolling in his discussion of metallurgical structure will prove useful later in discussing the conclusions of this experiment.

Von Turkovich (1967)[93] discussed dislocation theory as it applied to shear stress in his 1967 paper. Although he was primarily concerned with high speed machining in this paper, he believed that shear stress computation in a Type 2 Chip was possible using the materials elastic constant G (T), the materials characteristic Burger's vector (b) and the dislocation density.

Ramalingham and Black (1971) [94] showed that the important variables involving dislocations are the "number and orientation of slip systems, certain characteristic dislocation parameters as the stacking fault energy, the interaction of dislocations with vacancies and solute atoms" in the scanning and transmitting electron microscopy studies of α brass. In their microscopic studies, they cut the material with diamond blades and studied the recrystallization at a molecular level.

Black [95] proposed a model in 1979 for the plastic deformation that occurs in metal cutting. He demonstrated that the magnitude of the flow stress and the onset of shear angle Φ correlated to the stacking fault energy of the material being cut. His resultant flow stress model predicts a catastrophic shear front, or shear plane, ahead of the tool, created by the annihilation and subsequent heat generation as the metastable cells in his model rearrange themselves. The model observes that dislocations sources originate near the tool tip, driving dislocations into the cell networks. There is a rapid build up of applied stress levels as the number of dislocations increases, causing a forest hardening effect at the tip of the tool (Cottrell (1964)).

Black's paper notes that more than one shear front would be crossing the material from the tool tip to the free surface at any one point in time, comparing this effect to waves at the seashore. Waves from the ocean will intersect a jetty on the beach at many different points along the length of the jetty, but always at the same angle. This is a good analogy to the deformation observed by Black and Huang in aluminum as they developed the "new stack of cards" model. Note that there are many cards sitting on the "onset of shear plane" at angle Φ. The onset angle ψ is dictated by other material properties. Black's theory predicted that as work-hardening increased, the resistance to the onset of shear will increase. This delay in the initiation of shear would translate into an increase in the onset shear plane angle. In a series of experiments in 1999 (Payton and Black, 2000) [25], direct observations over a full range of hardness in Copper 10101 alloy supported the Black Huang model conclusively over all other models.

Black and Krishnamurthy (unpublished) conducted a small experiment where they examined the relationships between hardness and shear stress in 6061-T6 aluminum. They noted that shear stress varied with the material hardness over the four samples. They were widely spaced, with varying hardness produced by annealing the as received aluminum. There results suggested that dislocations could possibly explain the differences that they had observed. In particular, when the aluminum was softened by heat-treating, the dislocation density was reduced as predicted by Cottrell and others. This reduces the amount of pinning in the material, allowing more mobility, which translates into a lower yield stress. This is also discussed in Dieter (1986). Thus we see that while dislocation discussion in the metal cutting literature has been sparse to date, it is on a par with the general overall metal cutting level of knowledge about the material being machined. It is now necessary to examine some important properties of other dislocation mechanisms, which might be incorporated into metal cutting models.

High strain rate deformation mechanisms for metals may be governed by either dislocation glide, mechanical twinning or phase transformations. These mechanisms heavily depend on the strain rate, which is given as:

$$\dot{\gamma} = \rho b v \qquad 48$$

where ρ, b, v are the density, length of burgers vector, and velocity of the dislocations respectively. The limiting strain rate is set up by the limiting velocity of the dislocation, which in turn is set as the velocity of propagation of elastic shear waves. The dislocation velocity tends toward saturation as the shear wave velocity is approached. This has been shown (Meyers, 1984) [96] to occur when

the stress approaches 10 GPa , which is close to the theoretical strength is steels. If we set the upper limit for the velocity of elastic waves in a metal to be the speed of sound waves in a metal ~5000 m/s, the upper limit of the dislocation density in a deformed metal as 10^{11} cm^{-2} and a burgers vector of 2×10^{-8} cm the strain rate obtained is of the order of 10^8 /s. This is too high compared to the typical strain rates encountered in metal cutting which range between 10^3 and 10^6/s. Dislocation glide mechanisms have been delineated (Meyers, 1984) into three governing mechanisms. These mechanisms are thermally activated dislocation motion, phonon drag and relativistic effects.

(1) Thermally Activated Dislocation Motion

The obstacles that oppose dislocation motion include solute atoms, vacancies, small-angle grain boundaries, vacancy clusters, inclusions, precipitates and other dislocations. The Peierls-Nabarro forces oppose the movement at the atomic level. A force has to be applied to overcome an energy barrier in order to move a dislocation from one equilibrium atomic position to the next. The smaller narrower barriers are called short-range obstacles, which, if strong, produce a rapidly varying glide stress. The larger wider barriers are called long-range obstacles for which the glide stress hardly varies with temperature and strain rate. The principal short-range barrier is the Peierls-Nabarro stress, which is important for BCC metals. For FCC and HCP metals, dislocation forests are the primary short-range barriers at lower temperatures. The different nature of these barriers is responsible for the major differences in temperature and strain rate sensitivity of the yield strength between FCC and BCC metals. Figure 38 shows measured yield

stresses at various fractions of the absolute melting point, T_m. The BCC metals are shown to exhibit a higher thermal sensitivity of the yield stress than FCC and HCP alloys. The activation energy required to overcome the short range barriers is expresses in terms of strain rate as (Meyers, 1994):

$$\Delta G = kT \ln \frac{\dot{\varepsilon}_o}{\dot{\varepsilon}} \qquad 49$$

where k is Boltzmann's constant, T is the temperature, $\dot{\varepsilon}_o$ is a constant and $\dot{\varepsilon}$ is the strain rate. This is the foundation for constitutive equations that are based on thermally assisted overcoming of obstacles.

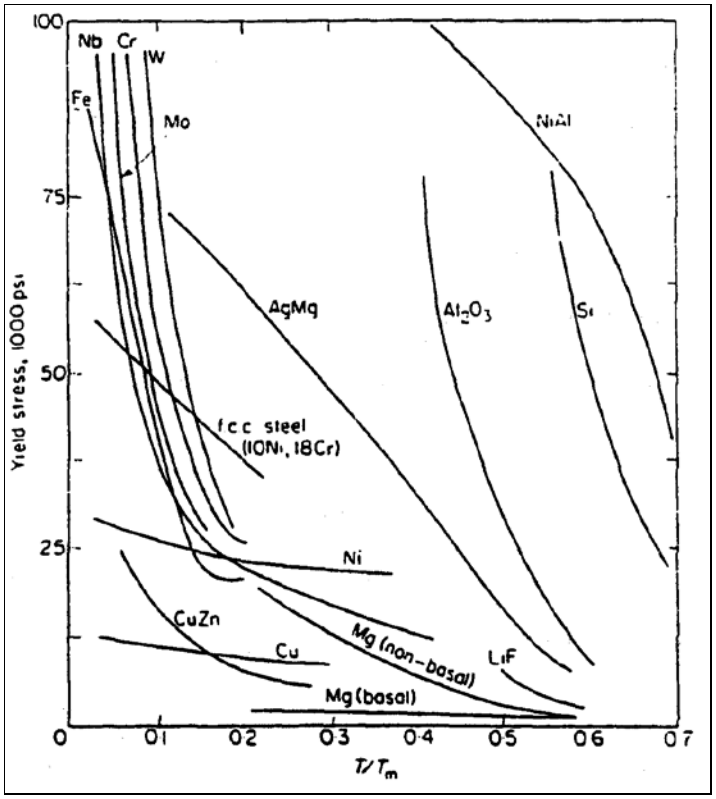

Figure 80: Yield stress at various temperatures (Cottrell, 1964)[97]

(2) Dislocation Drag Mechanisms

Out of the total energy expanded in plastic deformation, 90% is dissipated by forces opposing the applied stresses. Those forces can be expressed as a viscous behavior of the solid. To a first approximation, the solid is assumed to act as a Newtonian viscous material with respect to the dislocation. Then under external stress, the dislocation will accelerate until it reaches a steady-state velocity. The stress is expressed by Gilman (1969) [98]as:

$$\sigma = \frac{2B_c M_o}{\rho b^2}\dot{\varepsilon} \qquad 50$$

where B_c is the viscous damping coefficient, and M_o is an orientation factor (Meyers, 1984). Thus the flow stress is proportional to the strain rate when dislocation drag mechanisms are operative. Gillis et al (1969) [99]have expressed B_c as:

$$B_c = \frac{B_0}{1-\frac{v^2}{v_s^2}} \qquad 51$$

where B_o = viscosity at rest, v_s is shear wave velocity. This implies that viscous drag decreases as the velocity increases.

The drag mechanisms that are not thermally activated are the interaction of the dislocation with thermal vibrations (phonon drag) and with electrons (electron viscosity). In addition relaxation effects in the dislocation core are included (Meyers, 1994). For metals phonons cause drag at ambient and higher temperatures and electrons cause drag at low temperatures (< 100^0 K

(Parameswaran et al, 1971) [100]. The drag stress establishes a steady state velocity of about 0.5 the shear wave velocity.

(3) Relativistic Effects on Dislocation Motion

Relativistic effects start gaining importance when the dislocation velocity is in the range of 0.8 of the shear wave velocity (Eshelby, 1953 and Weertman et al, 1964) [101, 102]. Even though a supersonic dislocation was proposed by Eshelby (1953), supersonic dislocations have neither been observed experimentally nor predicted analytically.

When the applied stress is lower than the threshold stress σ_o (height of activation barrier), thermal activation controls the velocity of propagation. When the applied stress is higher than the short-range barrier height, drag (viscous and scattering) controls the resistance to dislocation motion. At higher velocities, in the range of 0.8 C_σ, relativistic effects start becoming important.

Above mentioned mechanisms are the usually seen in metal cutting as proposed by pioneers in the field of metal cutting. Payton [103] reports that, dislocations are continuously generated at the onset of shear plane and that its density keeps increasing in the flow area where the chip is still in the process of forming. Due to the fact that these large quantities of dislocations are chaotically generated along different orientations, they tend to tangle when moving in the respective directions and plane causing pile ups which tend to act as a potential barrier to the normal dislocation motion.

The phenomenon of dislocation generation and movement can be explained by considering the initial contact of the tool with work piece. At the instance when the tool first touches the work piece, let us say that the tool tip comes in contact with a small group of grains (work piece), the force from the motion of the tool acts upon the group at a particular angle which is mostly dependent on the tool rake angle and the geometry of cut.

Because of the angle of incidence of the resultant force, these grains are subjected to a moment, causing it to displace both linearly and rotationally. Depending upon the orientation of the grains it leads to an avalanche of grain displacements and generation of dislocations in different orientations. This effect cannot move further as the bulk of the work piece material opposes the displacements and dislocations beyond a certain point. But as the tool keeps moving further, a similar mechanism develops at every instant thus deforming the material continuously.

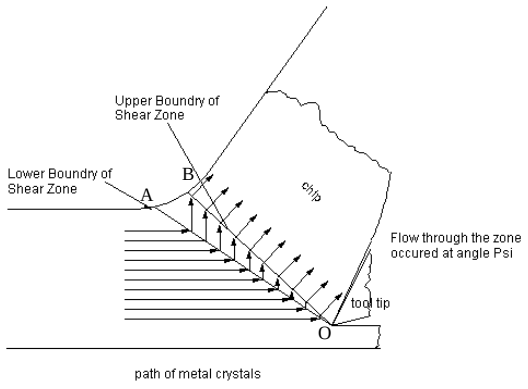

Figure 81: Deformation zone in metal cutting

On further close examination of the flow area, where all the primary deformation is taking place, it can be seen that, there three stages governing the mechanism of chip generation.

- Stage I: Barrier stopping the dislocation movement along the plane inclined at angle Φ, line OA.
- Stage II: An energy source continuously moving dislocations along the shear plane ψ.
- Stage III: An upper barrier to stop the continuously displacing dislocations along the shear plane, line OB.

But in order to continuously deform the material, a constant source of thermal activation is required for these dislocations to move further and even cross barriers. This thermal activation is provided by the resultant force acting on the work piece. During the stage I, the primary obstacles hindering the dislocation flow comes in the form of atomic defects (vacancies, inclusions, precipitates, etc.), grain boundaries and tangling dislocations (pile ups). Also there is a constant opposing force from the bulk of the undeformed work material which is far away from the area of deformation.

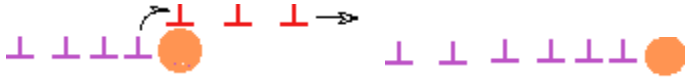

Figure 82: Pictorial representation of Dislocation climb and dislocation pile up [104]

The presence of an angle to the activation plane (OA) can be attributed to the fact that, the dislocation motion is inhibited by first dislocation pile ups, which

lock high strain energy within them, which are overcome by the energy from the trailing dislocations and also the primary source, the energy supplied by the tool motion. These energies add up together to cause dislocation climb over the pile ups easily but are not enough to overcome the forces exhibited by atomic imperfections and the bulk undeformed material itself. Such a shunted dislocation climb when viewed microscopically would represent steps, with the lower step closer to the source of initial dislocation generation (tool tip O) and the upper step at the farther end (A). These steps macroscopically represent the activation plane which is inclined at an angle of Φ.

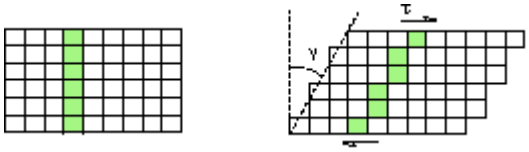

Figure 83: Example of dislocation motion (shaded region represents dislocations) leading to microscopic step formations [104]

Applying the same explanation to stage II, the difference being that, there is no opposing force exhibited by the bulk undeformed material in this region, leading to a continuous dislocation motion, pile up and dislocation climb, it can be suggested that the steps formed during dislocation climb leads to the growth of chip thickness. Also, due to the fan shaped region, the stresses at the narrow region start piling up and act on creating more and more dislocations in the direction of shear and pushing it towards the free surface or the region between A and B. this is supported by the fact that the dislocations climb upwards under compression and downward when in tension. Since the area below the shear plane is under compressive loading and the area above is in tension, it constantly pushes the dislocations outwards towards the back of chip.

Before getting any further, it becomes necessary to define the boundary conditions which cause the dislocation pile ups. For a dislocation to be mobile across a crystal structure it is necessary to have finite force acting on it. The critical shear strength (and the force) necessary to keep the dislocation in motion can be calculated using the method of Peierls and the calculated stress is referred to a Peierls stress or Peierls force. [105]

The Peierls force F is given by

$$\boldsymbol{F = \frac{2\mu b}{1-\nu} sin4\pi\alpha exp\left(-\frac{4\pi\zeta}{b}\right)} \quad 52$$

Here, μ is the rigidity, ν is the poison's ratio, 2ζ is the half width of the dislocation, b burger's vector and α is a constant based on the position of dislocation.

If the P is the critical shear stress necessary for the dislocation to be in motion then the force necessary to keep the dislocations in motion is

$$F=Pb \quad 53$$

The force above calculated can be compared with the force acting along the merchant's shear plane Fs (M) and the following two cases can be inferred

If F > Fs (M) the dislocations stop moving and results in pile up while if F, Fs (M), the dislocations are mobile. Since there is a constant dislocation generation, the stress on the dislocation trailing behind the pile up increases and once the stress τ* exceeds the critical stress P it initiates a climb over the barrier.

The stresses due to other dislocations is given by (Meyer's) [106]

$$\tau^* = n\,\tau \quad (54)$$

and

$$\boldsymbol{\tau = \frac{1}{b}\sum_{\substack{j=0 \\ i\neq j}}^{n} \left\{\frac{Gb^2}{2\pi(1-\nu)(xi-xj)}\right\}} \quad (55)$$

The rate at which the dislocation climb happens over a barrier (atomic inclusions or defects and dislocation pile ups)is given by Weertman [107]

$$\text{Rate of climb} = 2N_0 D\sigma^2 \int b^4/\mu kT \quad (56)$$

This activation plane OA causes the grains ahead of the plane to start shearing at an angle ψ as observed by Payton[103] in his study. This leads the discussion to a point where, if the activation energy along the activation plane is known that would represent the minimum energy to cause continuous shearing and thus forming the chip. In metal cutting, once the process reaches the steady state, which is within a few micro seconds, the strain rate (shear) remains a constant or in other words, a steady state strain rate. This can be compared to a steady state creep deformation (plastic) governed by dislocation mechanism. The steady state creep rate (έ) for a dislocation governed deformation is given by Mukherjee-Bird-Dorn [106] as

$$\boldsymbol{\acute{\varepsilon} = A\left(\frac{D*G*b}{k*T}\right)\left(\frac{\sigma}{G}\right)^5} \quad (57)$$

here A is a material constant, G the shear modulus, D diffusivity which is a function of activation energy Q and temperature T, b the grain geometry and k is the Boltzmann's constant. The same equation based of Orowan model [108]can be written relating the shear strain rate ($\acute{\gamma}$) and the shear stress (τ) as

$$\boldsymbol{\acute{\gamma} = A\left(\frac{D*G*b}{k*T}\right)\left(\frac{\tau}{G}\right)^3} \quad (58)$$

$$D = D_0 \exp(-Q/RT) \quad (59)$$

On simplifying and rearranging so as to relate activation energy (Qa) with temperature (T)

$$\left[\ln\left(\frac{1}{T}\right) - C\right] * RT = Qa \quad (60)$$

Here $$C = \ln\left[\frac{\dot{\gamma} * G^2 * k}{A * \tau^3 * b}\right] \quad (61)$$

The expression C shown is a constant value for a given material and cutting condition.

Substituting the maximum shear strain rate calculated along the plane OA $(\dot{\gamma})_\Phi$ and the corresponding shear stress $(\tau)_\Phi$ in equation 52, the constant C can be obtained. Using equation 51, activation energy along the plane OA can be calculated provided the temperature along the same is known. An expression to calculate temperature along plane OA is given by Shaw [83].

$$\theta s = \frac{R1q1(bt(\csc(\Phi)))}{C1\rho1(Vbt)} + \theta \quad (62)$$

Here, θs,θ are the temperatures along plane OA and ambient temperature respectively. R1q1 is the heat per unit area per unit time leaving the plane OA and C1ρ1 is the volume specific heat at mean temperature between θs and θ and V is the velocity of cutting.

Substituting, the temperature across the shear plane θs for T in equation 56**,**

Rate of climb of dislocations across the activation plane can be determined as follows

$$\text{Rate of climb} = \frac{\mathbf{2N0D\sigma2\int b4}}{\boldsymbol{\mu k\left(\frac{R1q1(bt(\csc(\Phi)))}{C1\rho1(Vbt)}+\theta\right)}} \qquad 63$$

Vacancies is one of the primary sources of obstacles leading to pile ups of dislocations, the rate of creation of vacancies (Nc) along a dislocation line is given by weertman [107],

$$Nc = V\exp(n\sigma b^3/kT) \qquad 64$$

This equation implies that, at higher temperatures, the number of vacancies are less thereby the probability of dislocation pile ups also reduce.

This is well supported by the fact that, the rate of climb (see equation 63) also decreases with increase in temperature, which can be observed once the cutting process reaches, a steady state. Also at this point, only less force is required to keep the dislocation in motion and hence lower activation energy is required along the shear plane. This can be supported to an extent by the fact that the cutting forces are higher at the beginning of a cut, but reduce and remain a constant once steady state is reached (refer figure 37).

The limiting boundary condition represented by the plane OB is along which the dislocation pile up density is high containing a high amounts of strain energy which is greater than the activation energy generated from the source, thereby ending the primary formation of the chip. This limiting boundary in stage III can be obtained by drawing a perpendicular line from the back of chip to the point O which represents the cut chip thickness. From the geometry of this line

OB, it can be shown that, it makes an angle of α (rake angle of the tool) with the horizontal.

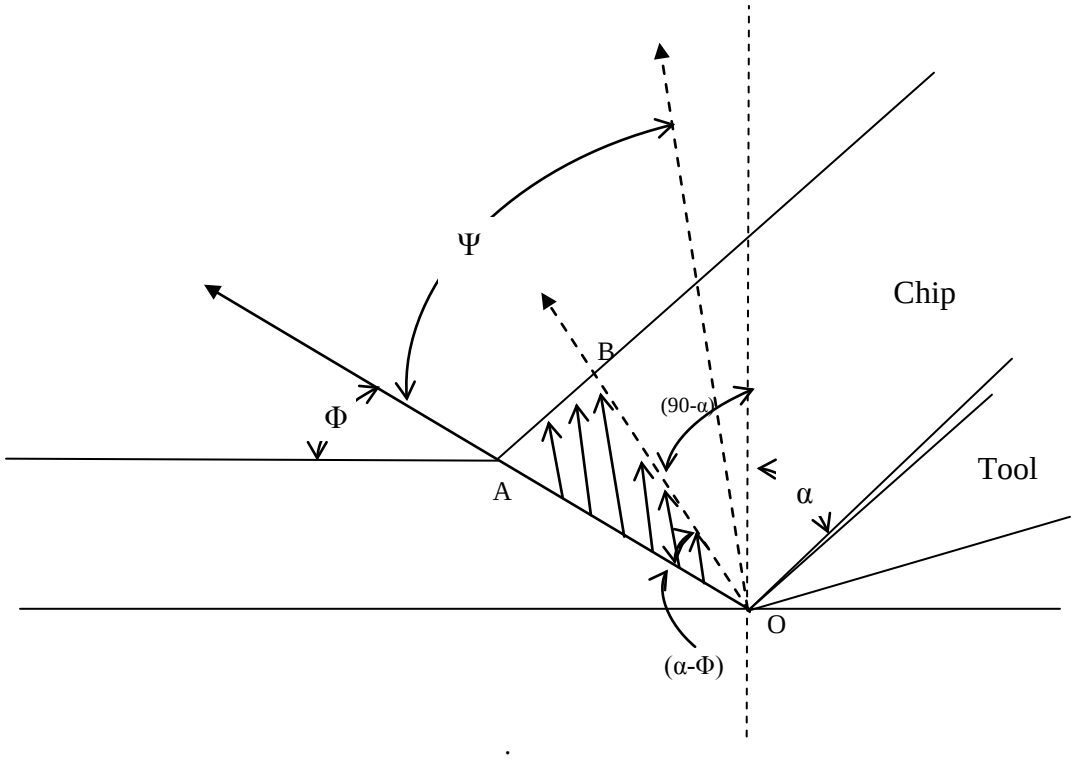

Figure 84: Depiction of the angular position of the primary plastic flow area OAB

Now it is clear that the flow zone in the cutting process were the chip is primarily formed depends upon the rake angle of the tool. If the tool is sharper, the deformation zone is wider and for a dull tool is very small. Also Payton in his dissertation concludes that as hardness of the material increases at constant tool rake angle, the angle of activation plane Φ increases. In such a case from the angular relationships shown in figure 62, it can be seen that the span of the flow zone decreases with increase in hardness.

Conclusions

A detailed investigation of the machining data collected, yielded several consequential results showing the variation of various critical parameters that are considered for improving the machining process. Most of the metal cutting parameters like, friction force, normal force, forces on shear plane, stresses, etc had a good agreement with the literature and so only the cutting force, thrust force, tool wear and surface finish variations are discussed in detail below.

In machining of aluminum 6061 T6 with HSS tool it was observed that, the environment had very less impact on the cutting and thrust force values. Use of nitrogen in the above scenario slightly decreased the forces while use of cold compressed air and liquid nitrogen resulted in higher values with the highest observed for liquid nitrogen environment. Tool wear was found to be minimal while using nitrogen while liquid nitrogen resulted in higher tool wear values. The environments did not have any significant impact on the surface finish

In machining of aluminum 6061 T6 with uncoated carbide tool it was observed that, the environment had very less impact on the cutting and thrust force values. Use of nitrogen in the above scenario slightly decreased the forces while use of cold compressed air and liquid nitrogen resulted in higher values with the highest observed for liquid nitrogen environment. Tool wear was found to be minimal while using nitrogen with cold compressed air and liquid nitrogen

following closely while dry resulted in higher tool wear values. Better surface finishes were observed while machining with Liquid nitrogen environment.

In machining of AISI 1020 alloy steel with HSS tool it was observed that, the environment had significant impact on the cutting and thrust force values. Use of liquid nitrogen and cold compressed air (both performing equally) in the above scenario decreased the forces while use of nitrogen resulted in slightly higher values with the highest observed for dry environment. Tool wear was found to be minimal while using nitrogen while dry machining resulted in higher tool wear values. The environments used did not help in producing better surface finishes.

In machining of AISI 1020 alloy steel with uncoated carbide tool it was observed that, the environment had significant impact on the cutting and thrust force values. Use of liquid nitrogen in the above scenario decreased the forces significantly with nitrogen performing almost closer to liquid nitrogen while use of cold compressed air resulted in slightly higher values with the highest observed for dry environment. Tool wear was found to be minimal while using cold compressed air followed by nitrogen while dry machining resulted in higher tool wear values. The environments used in this study did not significantly vary the surface finish.

Varying the coolant pressure was studied for one of the randomly chosen environment and cutting conditions and was found that it did not have any significant effect on the cutting force and thrust force values.

The coolant also did not have any significant impact on hardness of the material, implying that the extreme temperatures of liquid nitrogen did not contaminate the work piece.

An expression to calculate the activation energy along the activation plane has been proposed in this study based off of the dislocations mechanisms. Efforts have been taken to logically explain the movement of dislocations in the flow region (in chip formation).

The expressions for calculating shear stress and shear strain were re derived based on Payton's corrected MFD. The shear strain values calculated based on the new expression was lower than the ones predicted by both Merchant's and Payton's expressions and also closely compared to the simulated results.

A finite element model developed previously at Auburn University was used to simulate a couple of dry environment runs. The simulated cutting force was within 10% (lower) of the experimental values while the simulated thrust force was only 50%-60% of the experimental values. The variation was as expected because of several limitations involved in developing a suitable finite element model that can exactly replicate the real nature of the experiment.

Future Work

The primary objective of the current study focused on evaluating the performance of gaseous cutting fluids in metal cutting. There are few things that can be continued to work upon based off this study as follows

- Some of the parameters like coolant flow rate, tool nose radius, position of coolant supply can be varied for the optimal conditions in each of the scenarios considered in order to further improve the efficiency of the cutting process.
- A statistical study could be done to evaluate the effect of coolants on the same material with different hardness values.
- A thermal imaging system can be used to measure the temperature in the cutting zone so that, the equation proposed for activation energy in this study could be verified.
- Laser interferometry combined with image processing technique (widely used in crack propagation studies) could be applied in low speed orthogonal machining experiment with video graphic quick stop device to measure the strain along the activation plane and shear plane and as well to verify the upper boundary condition of the flow zone presented in this study.

- A new tool can be designed supply coolant internally into the tool instead of externally applying. This could be useful especially in case of liquid nitrogen which when applied externally cools the work piece, thereby negating the advantage of localized hot work phenomenon.
- A fully optimized cutting condition for each of the scenarios is determined after the aforementioned studies; a progressive tool wear study could be carried out to determine the tool life under that particular environment by subjecting the tool to continuous cuts for longer period of time.
- The finite element model used in this study could be improved upon so that the error percentage reduces, by using a different material model that best prescribes the behavior of the material considered and as well modeling the tool as not a rigid body, so that the effect of tool wear and secondary deformation of chip be considered.
- A combination of CFD and FE analysis model could be developed, to simulate the metal cutting process under the influence of cutting fluids.

Reference

[1] Taylor, F. W., 1905, "On the art of cutting Metals," Keynote address at the annual conference of ASME.

[2] Chandran Achutan, J. N., March 2007, "Health Hazard Evaluation Report 2003-0175-3033 COL-FIN Specialty Steel Fallston, Pennsylvania," DEPARTMENT OF HEALTH AND HUMAN SERVICES Centers for Disease Control and Prevention National Institute for Occupational Safety and Health http://www.cdc.gov/niosh/hhe/.

[3] Sreejith, P., S., Ngoi, B, K, A.,, 2000, "Dry machining: Machining of the future," Journal of Materials Processing Technology, 101, pp. 287-291.

[4] Cocquilhat, M., 1851, "Experiences sur la Resistance Utile Produites dans le Forage," Annales des Travaus Publics en Belgigque, 10, p. 199.

[5] Joessel, H., 1865, "Experiments on the Most Favorable Form of Tool in Workshops From the Point of View of Economy of Power," Annuaire de la Societe des Anciens Eleves des Ecoles Imperiales D'Arts et Meteiers.

[6] Time, I., 1877, "Memoire sur le Rabotage de Metaux,"St. Petersburg, Russia.

[7] Tresca, H., 1878, "On Further Applications of the Flow of Solids," Proceedings of the Institutionof Mechanical Engineers, p. 301.

[8] Mallock, A., 1881, "The Action of Cutting Tools," Proceedings of the Royal Society of London, 33, p. 127.

[9] Haussner, A., 1892, "Das Holben von Metallen,"Wien, p. 117.

[10] Zvorkin, N. N., 1893, "Rabota I Usilie Neobkhodimyya dlya Oteleniya Metallicheskikh Struzhek,"Moscow, Russia.

[11] Weibach, H., 1896, "Ingeniuer und Maschinenmechanik,"Berlin, IG.

[12] Lindner, G., 1907, "Book Review of Taylor's "On the Art of Cutting Metals"," Zeitschrift VDI, 51, p. 1070.

[13] Ernst, H., and Merchant, M. E., 1941, Chip formation, fiction and finish, The Cincinnati milling machine co., Cincinnati, Ohio,.

[14] Pissipanen, V., 1937, "Lastuntnuodostumiesn Terias," Teknillinen Aikakauslehti, 27, p. 315.

[15] Merchant, M. E., 1945, "Mechanics of the Metal Cutting Process-I. Orthogonal Cutting and a Type 2 Chip," Journal of Applied Physics, 16, pp. 267-317.

[16] Coker, E., and Chakko, K., 1925, "Report on the Action of Cutting Tools," Proceedings of the Institution of Mechanical Engineers, p. 357.

[17] Coker, E., 1922, "Experiments on the Action of Cutting Tools," Proceedings of the Institution of Mechanical Engineers, p. 567.

[18] Ishi, S., "Macroscopic Kinematographs Applied to Research in Metal Cutting," Proc. World Engineering Conference, p. 478.

[19] Schwerd, F., 1935, "Filmaufnahmen des Ablaufenden Spans bei Ueeblichen und bei SHer Hohen Schnittgeschwindigkeiten," Zeitschrift VID, 80, p. 233.

[20] Boston, O. W., 1930, "What Happens When Metal is Cut," Transactions of ASME, 52, p. 119.
[21] Herbert, E. G., 1926, "Work-Hardening Properties of Metals," Transactions of ASME, 48, p. 705.
[22] Merchant, M. E., 1944, "Basic Mechanics of the Metal Cutting Process," Journal of Applied Physics, 16, pp. 168-175.
[23] DeGarmo, E. P., Black, J. T., and Kohser, R. A., 1997, Materials and processes in manufacturing, Prentice Hall, Upper Saddle River, NJ.
[24] Payton, L. N., and Sripathi, P., 2010, "Effects of Alternative Metal Working Fluids Upon Tool Face Wear," ASME Conference Proceedings, 2010(44489), pp. 433-445.
[25] Payton L.N., June 2000, "Orthogonal Machining of copper using a virtual quick stop device," Master's thesis, Auburn University, USA.
[26] Eggleston, D. M., Herzog, R., and Thomsen, E. G., 1959, "Observations on the Angle Relationships in Metal Cutting," Journal of Engineering for Industry, pp. 263-279.
[27] Lee, E. H., and Shaffer, B. W., 1951, "The Theory of Plasticity Applied to a Problem of Machining," Journal of Applied Mechanics, 18(4), pp. 405-413.
[28] Bowden, F. P., and Tabor, D., 1964, Friction and Lubrication of Solids, Clarendon Press, Oxford.
[29] Ling, F. F., and Peterson, M. B., 1987, "Simple Model of Metal Working Friction Under Extreme Pressure," Approaches to Modeling Friction and Wear, F. F. Ling, and C. T. H. Pan, eds., Springer-Verlag.
[30] Kopalinsky, E. M., Li, X., and Oxley, P. L. B., 1991, Tribological Aspects in Manufacturing, ASME.
[31] Thomsen, E. G., 1969, Annals of the CIRP, 17, p. 187.
[32] Okushima, K., and Hitomi, K., 1961, "An Analysis of the Mechanism of Orthogonal Cutting and Its Application to Discontinous Chip Formation," ASME Journal of Engineering for Industry, pp. 545-556.
[33] Trigger, K. J., Zylstra, L. B., and Chao, B. T., 1952, Transactions of ASME, 74, p. 1017.
[34] Ham, I., Hitomi, K., and Thuering, G. L., 1961, Transactions of ASME, B83, p. 282.
[35] Zorev, N. N., 1966, Metal cutting mechanics, Pergamon Press, Oxford, New York,.
[36] Trent, E. M., Proc. Proceedings Conference Machinability, Iron and Steel Institute, pp. 11-18.
[37] Williams, J., E., Smart, E, F., and Milner, D, R., , 1970, "The metallurgy of machining Part 3: The effect of a lubricant and an Assesment of the current understanding of materials behaviour in machining," Metallurgia, 81, pp. 89- 93.
[38] Childs, T., H, C.,, 1972, "Rake face action of cutting lubricants: An analysis of, and Experiments on, The machining of iron lubricated by Carbon Tetrachloride," Proceedings of Institution of Mechanical Engineers 186 63/72, pp. 717- 727.
[39] Mullick, B. K., and Bhattachary, J., 1966, Journal of Instrument Engineers (India), 46, p. 183.

[40] Niebusch, R., B., Strieder, E, H.,, 1950, "Application of Cutting fluids to Machining Operations," Annual Meeting of ASME New York, pp. 203- 207.
[41] Rowe, G., W., Smart, E, F.,, 1963, "The importance of oxygen in dry machining of metal on lathe," British Journal of Applied Physics, 14, pp. 924 - 926.
[42] Zhao, Z., and Hong, S, Y., , 1992, "Cryogenic properties of some cutting tool materials," journal of materials engineering and performance, 1 (5), pp. 705- 714.
[43] Zhao, Z., and Hong, S, Y., , 1992, "Cooling stratergies for cryogenic machining from a materials view point," Journal of materials engineering and performance, 1 (5), pp. 669- 678.
[44] Kovacevic, R., Cherukuthota, C., and Masurkiewicz, M., , 1995, "High Pressure Water jet cooling/ lubrication to improve machining efficiencyin Milling," International Journal of Machine Tools & Manufacture, 35(10), pp. 1459- 1473.
[45] S.W. Kim, D. W. L., M.C. Kang, J.S. Kim, 2001, "Evaluation of machinability by cutting environments in high-speed milling of difficult-to-cut materials," Journal of Materials Processing Technology(111), pp. 256-260.
[46] Hong, S., Y., Ding, Yucheng., Jeong, Woo-cheol., , 2001, "Friction and cutting forces in cryogenic machining of Ti-6Al-4V," International Journal of Machine Tools & Manufacture, 41, pp. 2271- 2258.
[47] S. Paul, N. R. D., A. B. Chattopadhyay, 2001, "Beneficial effects of cryogenic cooling over dry and wet machining on tool wear and surface finish in turning AISI 1060 steel," Journal of Materials Processing Technology(116), pp. 44-48.
[48] N.R. Dhar, S. P., A.B. Chattopadhyay, 2002, "The influence of cryogenic cooling on tool wear, dimensional accuracy and surface finish in turning AISI 1040 and E4340C steels," Wear(246), pp. 932-942.
[49] Dahlman, P., and Escursell, Marcel., , 2003, "High pressure jet-assisted cooling: a new possibility for near net shape turning of decarburized steel.," International Journal of Machine Tools & Manufacture.
[50] Cakir , O., Kiyak, M., and Altan, E., , 2004, "Comparison of Gases applications to wet and dry cuttings in turning," Journal of Materials Processing Technology, 153-154, pp. 35-41.
[51] Stanford, M., and Lister, P. M., 2004, "Investigation into the relationship between tool-wear and cutting environments when turning EN32 steel," Industrial Lubrication and Tribology, 56(2), pp. 114-121.
[52] M'Saoubi, R., Chandrasekaran, H.,, 2004, "Investigation of the Effects of Tool Micro-geometry and Coating on Tool Temperature during Orthogonal Turning of Quenched and Tempered Steel," International Journal of Machine Tools & Manufacture, 44(2), pp. 213-224.
[53] Salgam, H., Yaldiz, S., Unsarcar, F.,, 2005, "The Effect of Tool Geometry and Cutting Speed on Main Cutting Force and Tool Tip Temperature," Thesis-Mechanical Engineering department, Technical Science College, Selcuk University, Konya, Turkey.

[54] Dhar, N. R., Kamruzzaman, M., and Ahmed, M., 2006, "Effect of minimum quantity lubrication (MQL) on tool wear and surface roughness in turning AISI-4340 steel," Journal of Materials Processing Technology, 172(2), pp. 299-304.
[55] Su, Y., He, N., Li, L., and Li, X. L., 2006, "An experimental investigation of effects of cooling/lubrication conditions on tool wear in high-speed end milling of Ti-6Al-4V," Wear, 261(7-8), pp. 760-766.
[56] Dhar, N. R., and Kamruzzaman, M., 2007, "Cutting temperature, tool wear, surface roughness and dimensional deviation in turning AISI-4037 steel under cryogenic condition," International Journal of Machine Tools and Manufacture, 47(5), pp. 754-759.
[57] Su, Y., He, N., Li, L., Iqbal, A., Xiao, M. H., Xu, S., and Qiu, B. G., 2007, "Refrigerated cooling air cutting of difficult-to-cut materials," International Journal of Machine Tools and Manufacture, 47(6), pp. 927-933.
[58] Kalyankumar, K. V. B. S., Choudry, S.K., , 2007, "Investigation of Tool Wear and Cutting Force in Cryogenic Machining using Design of Experiments," Journal of Materials Processing Technology, 203, pp. 95-101.
[59] Sreejith, P. S., 2008, "Machining of 6061 aluminium alloy with MQL, dry and flooded lubricant conditions," Materials Letters, 62(2), pp. 276-278.
[60] Stanford, M., Lister, P.M., Morgan, C., Kibble, K.A., , 2009, "Investigation into the use of Gaseous and Liquid Nitrogen as a Cutting Fluid when Turning BS 970-80A15 (En32b) Plain Carbon Steel using WC-Co uncoated tooling," Journal of Materials Processing Technology, 209(2), pp. 961-997.
[61] Yalçın, B., Özgür, A. E., and Koru, M., 2009, "The effects of various cooling strategies on surface roughness and tool wear during soft materials milling," Materials & Design, 30(3), pp. 896-899.
[62] ASME, 1986, "Tool life testing with single-point turning tools ANSI/ASME B94.55M 1985.," The American Socitey of Mechanical Engineers.
[63] Yang, L. J., 2004, "Wear coefficient of tungsten carbide against hot-work tool steel disc with two different pin settings," Wear, 257(5–6), pp. 481-495.
[64] Lim, G. H., 1995, "Tool-Wear Monitoring in Machine Turning," Journal of Materials Processing Technology, 51(1-4), pp. 25-36.
[65] Mauri Routio*, M. S., 1995, "Tool wear and failure in the drilling of stainless steel," Journal of Materials Processing Technology(52), pp. 35-43.
[66] J.H. Lee, S. J. L., 1999, "One-step-ahead prediction of flank wear using cutting force," International Journal of Machine Tools and Manufacture(39), pp. 1747-1760.
[67] Gekonde, H. O., and Subramanian, S. V., 2002, "Tribology of tool–chip interface and tool wear mechanisms," Surface and Coatings Technology, 149(2–3), pp. 151-160.
[68] Jeon-ha Kim, D.-k. M., Deuk-woo Lee, Jeong-suk Kim, Myung-chang Kang, Kwang ho Kim, 2002, "Tool wear measuring technique on the machine using CCD and exclusive jig," Journal of Materials Processing Technology(130-131), pp. 668-674.
[69] Otto T, K. L., Papstel J. , 2003, "A digital Measuring Module for tool wear estimation," Book- DAAAM International Scientific Book, pp. 435-444.

[70] S. K. Choudhury, S. R., 2000, "In-process tool wear estimation in milling using cutting force model," Journal of Materials Processing Technology(99), pp. 113-119.
[71] S.K. Choudhury, K. K. K., 2000, "Tool wear measurement in turning using force ratio," International Journal of Machine Tools and Manufacture(40), pp. 899-909.
[72] Oraby, S. E., and Hayhurst, D. R., 2004, "Tool life determination based on the measurement of wear and tool force ratio variation," International Journal of Machine Tools and Manufacture, 44(12-13), pp. 1261-1269.
[73] Astakhov, V. P., 2004, "The assessment of cutting tool wear," International Journal of Machine Tools and Manufacture, 44(6), pp. 637-647.
[74] H. Zhao, G. C. B., Q.Zou, 2002, "A study of flank wear in orthogonal cutting with internal cooling," Wear(253), pp. 957-962.
[75] Pavel, R., Marinescu, I., Deis, M., and Pillar, J., 2005, "Effect of tool wear on surface finish for a case of continuous and interrupted hard turning," Journal of Materials Processing Technology, 170(1-2), pp. 341-349.
[76] Kishawy, H. A., Dumitrescu, M., Ng, E. G., and Elbestawi, M. A., 2005, "Effect of coolant strategy on tool performance, chip morphology and surface quality during high-speed machining of A356 aluminum alloy," International Journal of Machine Tools and Manufacture, 45(2), pp. 219-227.
[77] Tamizharasan, T., Selvaraj, T., and Noorul Haq, A., 2005, "Analysis of tool wear and surface finish in hard turning," The International Journal of Advanced Manufacturing Technology, 28(7-8), pp. 671-679.
[78] Anthony Xavier, M., and Adithan, M .,, 2009, "Determinig the influence of cutting fluidson tool wear and surface roughness during turning of AISI 304 austeniticstainless steel," Journal of Materials Processing Technology, 209, pp. 900-909.
[79] Khidhir, B. A., and Mohamed, B., 2011, "Analyzing the effect of cutting parameters on surface roughness and tool wear when machining nickel based hastelloy – 276," IOP Conference Series: Materials Science and Engineering, 17, p. 012043.
[80] Kistler, "" 3-Component measuring Platform, Type 9257A" Operating Manual," Edition 5/87.
[81] Sripathi, P. S., 2009, "Investigations into the effects of tool geometry and metal working fluids on tool forces and tool wear during orthogonal tube turning of Aluminum 6061 alloy.," Master's Thesis Report, Auburn University.
[82] Oberg, E., Jones, Franklin D., Horton, Holbrook L., and Ryffel, Henry H.,, 2008, "Machinery's Handbook," 28.
[83] Shaw, M. C., 2005, Metal Cutting Principles, Oxford, New york.
[84] E. Kuram, B. O., E. Demirbas, and E. Şık, 2010, "Effects of the Cutting Fluid Types and Cutting Parameters on Surface Roughness and Thrust Force," Proceedings of the World Congress on Engineering 2010, II.
[85] M'Saoubi, R., and Chandrasekaran, H., 2005, "Innovative Methods for the Investigation of Tool-Chip Adhesion and Layer Formation during Machining," CIRP Annals - Manufacturing Technology, 54(1), pp. 59-62.

[86] A. Hamdan, M. F., K.A. Abou-El-Hossein, M. Hamdi1, "PERFORMANCE EVALUATION OF DIFFERENT TYPES OF CUTTING FLUID IN THE MACHINING OF AISI 01 HARDENED STEEL USING PULSED JET MINIMAL QUANTITY LUBRICATION SYSTEM," Invited paper.
[87] Kardekar, A. D., 2005, "MODELING AND OPTIMIZATION OF MACHINING PERFORMANCE MEASURES IN FACE MILLING OF AUTOMOTIVE ALUMINUM ALLOY A380 UNDER DIFFERENT LUBRICATION/COOLING CONDITIONS FOR SUSTAINABLE MANUFACTURING," Thesis-University of Kentucky.
[88] Huang, J. M., and Black, J. T., 1996, "An Evaluation of Chip Separation Criteria for the FEM Simulation of Machining," Journal of Engineering for Industry.
[89] Jawaid, A., Sharif, S., and Koksal, S., 2000, "Evaluation of wear mechanisms of coated carbide tools when face milling titanium alloy," Journal of Materials Processing Technology, 99(1–3), pp. 266-274.
[90] List, G., Nouari, M., Géhin, D., Gomez, S., Manaud, J. P., Le Petitcorps, Y., and Girot, F., 2005, "Wear behaviour of cemented carbide tools in dry machining of aluminium alloy," Wear, 259(7–12), pp. 1177-1189.
[91] Trent, E. M., 1988, "Metal cutting and the tribology of seizure: I seizure in metal cutting," Wear, 128(1), pp. 29-45.
[92] Dieter, G. E., 1986, Mechanical metallurgy, McGraw-Hill, New York.
[93] Von Turkovich, B. F., "Dislocation Theory of Shear Stress and Strain Rate in Metal Cutting," Proc. 8th International Machine Tool Design and Research Conference.
[94] Ramalingham, S., and Black, J. T., 1971, "On the Metal Physical Considerations in the Machining of Metals," Journal of Engineering for Industry.
[95] Black, J. T., 1979, "Flow Stress Model in Metal Cutting," ASME Journal of Engineering for Industry, 101, pp. 403-415.
[96] Meyers, M. A., and Chawla, K. K., 1984, Mechanical Metallurgy, Principles and Applications, Prentice-Hall, Englewood Cliffs, NJ.
[97] Cottrell, A. H., 1964, Theory of crystal dislocations, Gordon and Breach, New York,.
[98] Gilman, J. J., 1969, Micromechanics of Flow in Solids, McGraw-Hill, New York.
[99] Gillis, P. P., Gilman, J. J., and Taylor, J. W., 1969, Philosophical Magazine, 20, p. 279.
[100] Parameswaran, V. R., and Weertman, J., 1971, Metallurgical Transactions, 2, p. 1233.
[101] Eshelby, J. D., 1953, Physical Review, 90, p. 248.
[102] Weertman, J., and Weertman, R., 1964, Elementary Dislocation Theory, McMillan, New York.
[103] Payton, L. N., 2002, "dislocation Theory of orthogoanl metal cutting of Cu-Zn alloys," Doctoral Dissertation, Auburn University.
[104] Jessell, M., Bons, P., Rey, P., , 2000, "Microstructure Course. In: Stress, Strain and Structure " Lecture notes.
[105] Nabarro, F., R, N.,, 1967, Theory of Crystal Dislocation, Oxford, London.

[106] Meyers, M. A., Chawla, Krishan Kumar.,, 1999, "Mechanical Behavior of Materials ", Prentice Hall, New jersy.
[107] Weertman, J., 1955, "Theory of Steady-state creep based on dislocation climb," journal of Applied Physics, 26(10).
[108] Lee, Y., Basaran, Cemal., , 2010, "A viscoplasticity model for solder alloys," Proceedings of the ASME International mechanical Engineering Confernce & Exposition, , IMECE 2010-37106.

Contents

APPENDIX 1

The calibration certificate for the Kistler 9257A dynamometer is given below.

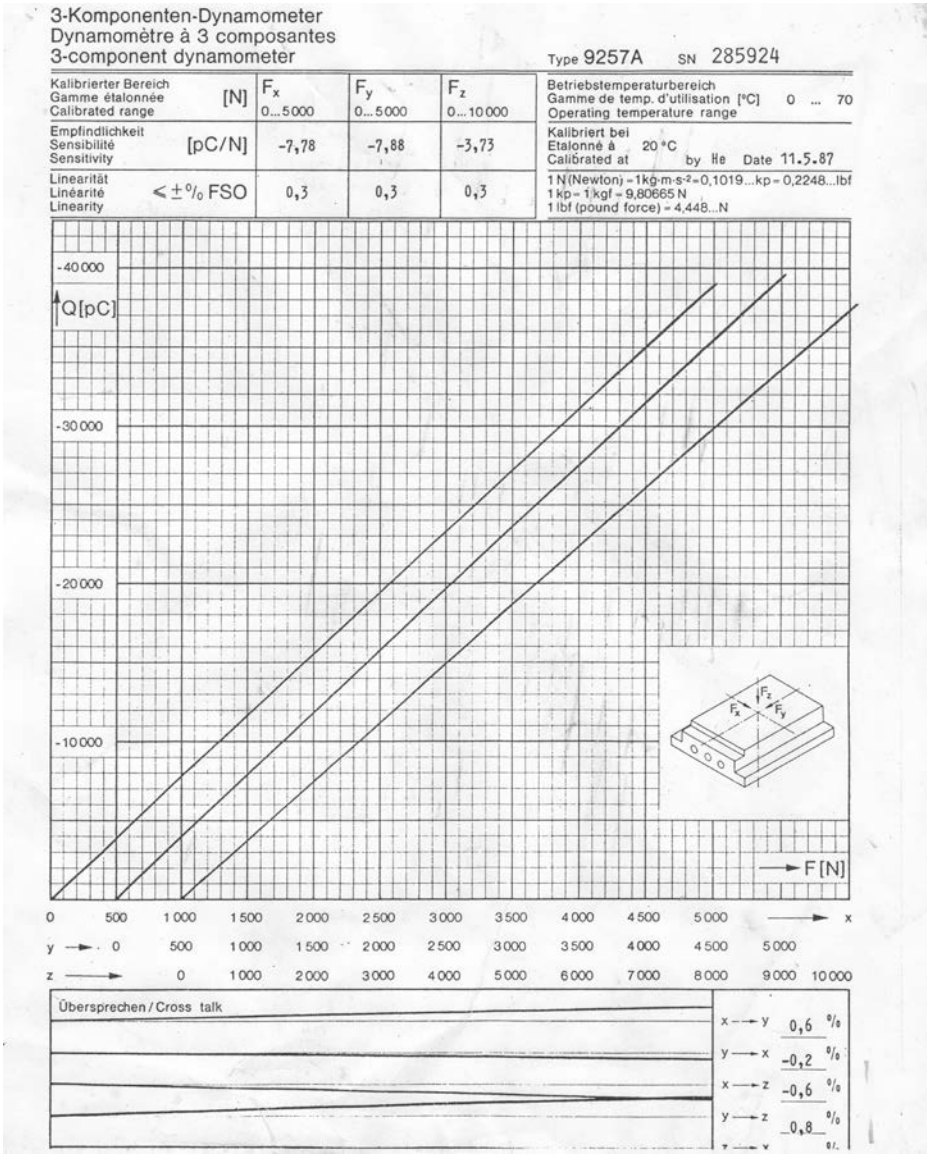

3-Komponenten-Dynamometer
Dynamomètre à 3 composantes
3-component dynamometer

Type 9257A SN 285924

		F_x	F_y	F_z
Kalibrierter Bereich / Gamme étalonnée / Calibrated range	[N]	0...5000	0...5000	0...10000
Empfindlichkeit / Sensibilité / Sensitivity	[pC/N]	-7,78	-7,88	-3,73
Linearität / Linéarité / Linearity	≤ ±% FSO	0,3	0,3	0,3

Betriebstemperaturbereich / Gamme de temp. d'utilisation [°C] / Operating temperature range: 0 ... 70

Kalibriert bei / Etalonné à 20 °C / Calibrated at by He Date 11.5.87

1 N (Newton) = 1 kg·m·s⁻² = 0,1019...kp = 0,2248...lbf
1 kp = 1 kgf = 9,80665 N
1 lbf (pound force) = 4,448...N

-40000
Q[pC]
-30000
-20000
-10000

F[N]

0 500 1000 1500 2000 2500 3000 3500 4000 4500 5000 → x
y → 0 500 1000 1500 2000 2500 3000 3500 4000 4500 5000
z → 0 1000 2000 3000 4000 5000 6000 7000 8000 9000 10000

Übersprechen / Cross talk

x → y	0,6 %
y → x	-0,2 %
x → z	-0,6 %
y → z	-0,8 %
z → x	%

The material certificate provided by the raw material supplier for Aluminum 6061 T6 and AISI 1020 alloy steel materials.

KAISER ALUMINUM
FABRICATED PRODUCTS

CERTIFIED TEST REPORT

			PRODUCT DESCRIPTION: 3 OD X .125 WA STRUCTURAL TUBE		
	LINE ITEM: 001	SHIP DATE: 01/12/2011		ALLOY: 6061	TEMPER: T6
WEIGHT SHIPPED: 5124.000 LB	QUANTITY: 161.000 PCS		DIAM/DAF/THKNS:	WIDTH:	LENGTH: 24.000 FT

Actual Physical Properties

REFERENCE	DASH#	SAMPLE#	UTS (KSI)	YTS (KSI)	%Elong in 2	HARDNESS		CONDUCT.	BEND
XTR100916	0001	0001	47.8	43.1	12.8	RE	96	N/A	N/A
XTR100916	0001	0002	46.6	42.2	12.5	RE	97	N/A	N/A
XTR100916	0001	0003	46.4	42.5	15.0	RE	97	N/A	N/A
XTR100916	0001	0004	46.6	43.0	12.6	RE	97	N/A	N/A

Chemical Composition (wt%), Aluminum Remainder

LIMITS	Si	Fe	Cu	Mn	Mg	Cr	Zn	Ti	Pb	Bi	Zr	Ea	Tot
Maximum	0.8	0.7	0.40	0.15	1.2	0.35	0.25	0.15	NA	NA	NA	0.05	0.15
Minimum	0.40		0.15		0.8	0.04			NA	NA	NA		

Applicable Requirements:

ASTM-B429-02-STENCILED ASTM-B221-06 AMS-QQ-A-200/8 TYPE 2 UNS#96061

Miscellaneous Notes

MANUFACTURED IN USA (LOS ANGELES,CA) MELTED IN USA

CERTIFICATION

Kaiser Aluminum Fabricated Products, LLC hereby certifies that metal shipped under this order has been inspected and tested and found in conformance with applicable specifications forming a part of the description set forth in Kaiser's sales acknowledgement form. Any warranty is limited to that shown on Kaiser's general terms and conditions of sale. Test reports are on file, subject to examination.

Tom G. Small, Jr., QA Manager

Page 1 of 1 Line Item: 001

INNOVENTIVE INDUSTRIES

TEST CERTIFICATE

CUSTOMER NAME :
ADDRESS :
PURCHASE ORDER NO & DATE: 18 MAY. 2011

DATE : 20.07.2011
HEAT NO: 11201477

PRODUCT : ELECTRIC RESISTANCE WELDED CARBON STEEL MECHANICAL ROUND TUBING

SIZE (INCH) :- 3.000 O.D. 2.760 I.D.

Outer Diameter (Inch)	3.000	Specification:	AS PER ASTM A513-T5, 1020 Stress Relieved (2009)
Inside Diameter (Inch)	2.760	Grade:-	1020
Thickness (Inch)	.....	Total Feets :	2778.17'
Length (Feet)	17'-19'	NO.Of Tubes(Nos.):	154

Chemical Analysis	%C		%Mn		%Si	%S		%P		%Al
	Min.	Max	Min.	Max	....	Min.	Max	Min.	Max	
Specification	0.17	0.23	0.3	0.6	....		0.035		0.035	....
Observation	0.210		0.466		0.011	0.008		0.009		0.031

Mechanical Properties	Yield Strength In PSI		Tensile Strength In PSI		% Elongation	Hardness HRB
	Min.	Max.	Min.	Max.	Min.	Min.
Specification	55000		65000		10	75
Observed	81647		91641		17	81

Dimensional Report		Outer Diameter In Inch		Inner Diameter In Inch	
		Min	Max	Min	Max
Specification		3.000	3.009	2.751	2.760
Observations	Sample 1	3.003	3.004	2.754	2.755
	Sample 2	3.004	3.005	2.755	2.756
	Sample 3	3.005	3.006	2.756	2.757

100% ECT(NDT) Done As per S8.2.1 - A513 08 a: Tubes conforms to specification

Packing Details :

AR11142 - 4 - 1 AR11142 - 4 - 5
AR11142 - 4 - 2 AR11142 - 4 - 6
AR11142 - 4 - 3 AR11142 - 4 - 7
AR11142 - 4 - 4 AR11142 - 4 - 8

Prepared By :
Sign
Name : Suhas

Verified By :
Sign
Name : Dipti

Innoventive Industries Limited

APPENDIX 2

The table below lists the radial force, thrust force, cutting force and the cut chip thickness measured during the cutting process.

Run	Environment	Work Piece	Tool	Rake Angle	Feed in/rev	Fr Radial force N	Ft Thrust force N	Fc Cutting force N	Tc inches
1	Dry	Aluminum	HSS	0	0.002	-6.0151	198.82	232.64	0.010583
2	Dry	Aluminum	HSS	0	0.002	-4.5624	172.65	216.1996	0.0099
3	Dry	Aluminum	HSS	0	0.002	-0.6681	175.4492	213.342	0.01002
4	Dry	Aluminum	HSS	0	0.002	-0.6698	177.0113	214.6294	0.01057
5	Dry	Aluminum	HSS	0	0.004	-4.4633	233.3745	335.5765	0.0155
6	Dry	Aluminum	HSS	0	0.004	0.0213	241.8935	339.2945	0.01525
7	Dry	Aluminum	HSS	0	0.004	-0.7817	235.166	338.0937	0.01512
8	Dry	Aluminum	HSS	0	0.004	-0.7213	248.1928	346.0426	0.1575
9	Dry	Aluminum	HSS	7	0.002	-4.21	144.1816	198.5818	0.00868
10	Dry	Aluminum	HSS	7	0.002	-3.5121	140.8573	199.7019	0.0087
11	Dry	Aluminum	HSS	7	0.002	-1.8454	142.4506	200.2728	0.00865
12	Dry	Aluminum	HSS	7	0.002	-4.5089	141.7632	203.0096	0.00858
13	Dry	Aluminum	HSS	7	0.004	-5.2369	197.652	323.2784	0.01473
14	Dry	Aluminum	HSS	7	0.004	-8.77	197.6554	324.414	0.01465
15	Dry	Aluminum	HSS	7	0.004	-5.3018	190.1233	316.9521	0.01455
16	Dry	Aluminum	HSS	7	0.004	-6.7085	190.6575	317.9177	0.01457
17	Dry	Aluminum	HSS	15	0.002	-5.0158	110.4196	181.8978	0.00815
18	Dry	Aluminum	HSS	15	0.002	-1.1007	115.8471	184.4764	0.00803
19	Dry	Aluminum	HSS	15	0.002	-2.5562	115.3726	186.2659	0.00827
20	Dry	Aluminum	HSS	15	0.002	-2.7595	114.2388	183.2786	0.00813
21	Dry	Aluminum	HSS	15	0.004	-2.7689	158.342	302.9938	0.013883
22	Dry	Aluminum	HSS	15	0.004	-3.6254	163.2573	305.7844	0.013933
23	Dry	Aluminum	HSS	15	0.004	-0.6568	155.989	301.6305	0.014017
24	Dry	Aluminum	HSS	15	0.004	-2.5846	157.5041	301.7759	0.013883
25	Cold Comp. Air	Aluminum	HSS	0	0.002	0.9745	201.5471	224.5702	0.011583
26	Cold Comp. Air	Aluminum	HSS	0	0.002	-3.0961	184.1174	226.1335	0.01135
27	Cold Comp. Air	Aluminum	HSS	0	0.002	-1.3147	182.0879	224.3963	0.011183
28	Cold Comp. Air	Aluminum	HSS	0	0.002	-2.2275	174.5485	217.5249	0.011167

29	Cold Comp. Air	Aluminum	HSS	0	0.004	-6.2429	253.7656	351.612	0.016317
30	Cold Comp. Air	Aluminum	HSS	0	0.004	-3.9383	253.2363	353.2215	0.01615
31	Cold Comp. Air	Aluminum	HSS	0	0.004	-5.7878	242.5745	345.3493	0.016333
32	Cold Comp. Air	Aluminum	HSS	0	0.004	-2.3515	255.9373	354.1216	0.016267
33	Cold Comp. Air	Aluminum	HSS	7	0.002	-2.2255	154.953	211.881	0.008267
34	Cold Comp. Air	Aluminum	HSS	7	0.002	-1.7661	140.7721	202.1586	0.008117
35	Cold Comp. Air	Aluminum	HSS	7	0.002	-1.337	141.0843	202.4552	0.008083
36	Cold Comp. Air	Aluminum	HSS	7	0.002	-1.0876	145.9431	204.8002	0.0083
37	Cold Comp. Air	Aluminum	HSS	7	0.004	-2.2186	209.5965	332.5052	0.01435
38	Cold Comp. Air	Aluminum	HSS	7	0.004	-2.0141	205.234	328.6348	0.014283
39	Cold Comp. Air	Aluminum	HSS	7	0.004	-2.0778	205.4657	329.9848	0.014333
40	Cold Comp. Air	Aluminum	HSS	7	0.004	-2.3347	212.1035	337.1219	0.014117
41	Cold Comp. Air	Aluminum	HSS	15	0.002	-2.3525	115.6286	188.6205	0.006633
42	Cold Comp. Air	Aluminum	HSS	15	0.002	-0.7559	120.6224	191.9326	0.006417
43	Cold Comp. Air	Aluminum	HSS	15	0.002	-0.3038	135.2184	189.1384	0.006467
44	Cold Comp. Air	Aluminum	HSS	15	0.002	-1.4492	119.6874	190.0498	0.006667
45	Cold Comp. Air	Aluminum	HSS	15	0.004	-0.8046	154.4841	302.6559	0.012133
46	Cold Comp. Air	Aluminum	HSS	15	0.004	-1.5711	158.3776	303.2566	0.012183
47	Cold Comp. Air	Aluminum	HSS	15	0.004	-2.7572	169.3316	312.4267	0.012216
48	Cold Comp. Air	Aluminum	HSS	15	0.004	-0.4065	171.3214	312.4534	0.012116
49	Nitrogen	Aluminum	HSS	0	0.002	-1.227	181.9404	218.2821	0.009883
50	Nitrogen	Aluminum	HSS	0	0.002	-0.6171	178.8097	221.4708	0.0101
51	Nitrogen	Aluminum	HSS	0	0.002	-1.2583	186.5351	226.3742	0.009983
52	Nitrogen	Aluminum	HSS	0	0.002	-4.7986	192.8114	228.8384	0.009917
53	Nitrogen	Aluminum	HSS	0	0.004	3.0347	240.2491	344.26	0.013817
54	Nitrogen	Aluminum	HSS	0	0.004	-0.7422	240.7294	345.0123	0.0139
55	Nitrogen	Aluminum	HSS	0	0.004	-1.0466	252.3228	352.8082	0.013833
56	Nitrogen	Aluminum	HSS	0	0.004	-1.2305	245.0184	345.4975	0.01395
57	Nitrogen	Aluminum	HSS	7	0.002	-4.5064	145.1312	205.6557	0.006983
58	Nitrogen	Aluminum	HSS	7	0.002	-7.1832	155.8608	206.0906	0.007133
59	Nitrogen	Aluminum	HSS	7	0.002	-4.4421	151.0385	209.7251	0.007183
60	Nitrogen	Aluminum	HSS	7	0.002	-2.479	166.031	209.4929	0.007067
61	Nitrogen	Aluminum	HSS	7	0.004	-4.6636	195.8656	320.531	0.0111
62	Nitrogen	Aluminum	HSS	7	0.004	-3.4635	191.0835	318.0791	0.0107
63	Nitrogen	Aluminum	HSS	7	0.004	-6.1124	206.2003	327.8495	0.010917
64	Nitrogen	Aluminum	HSS	7	0.004	-9.3037	199.0902	323.7054	0.010733
65	Nitrogen	Aluminum	HSS	15	0.002	-1.2685	110.8299	183.0732	0.0049
66	Nitrogen	Aluminum	HSS	15	0.002	-1.924	111.1435	183.2105	0.004717
67	Nitrogen	Aluminum	HSS	15	0.002	-2.7683	111.7645	183.2997	0.004667
68	Nitrogen	Aluminum	HSS	15	0.002	-1.6925	112.6121	183.7805	0.004617
69	Nitrogen	Aluminum	HSS	15	0.004	-3.4704	160.623	305.25	0.008517

70	Nitrogen	Aluminum	HSS	15	0.004	-3.6626	163.9328	308.785	0.0085
71	Nitrogen	Aluminum	HSS	15	0.004	-1.7391	154.3965	299.3457	0.008367
72	Nitrogen	Aluminum	HSS	15	0.004	-3.0999	147.4833	294.3279	0.00855
73	Liquid Nit.	Aluminum	HSS	0	0.002	-4.8824	195.2067	248.5207	0.0075
74	Liquid Nit.	Aluminum	HSS	0	0.002	-4.057	201.0663	239.0119	0.007467
75	Liquid Nit.	Aluminum	HSS	0	0.002	-3.4702	232.1835	268.9921	0.00765
76	Liquid Nit.	Aluminum	HSS	0	0.002	-3.597	221.0488	253.7922	0.007533
77	Liquid Nit.	Aluminum	HSS	0	0.004	-1.8687	272.9195	370.4816	0.015267
78	Liquid Nit.	Aluminum	HSS	0	0.004	-4.2698	262.9523	362.8337	0.015233
79	Liquid Nit.	Aluminum	HSS	0	0.004	-2.9569	398.8132	389.3597	0.01535
80	Liquid Nit.	Aluminum	HSS	0	0.004	-2.6685	247.157	372.2043	0.015367
81	Liquid Nit.	Aluminum	HSS	7	0.002	-1.9686	145.2655	215.6434	0.006033
82	Liquid Nit.	Aluminum	HSS	7	0.002	-2.0211	149.4903	211.5065	0.00625
83	Liquid Nit.	Aluminum	HSS	7	0.002	-3.8036	143.5887	210.2309	0.006217
84	Liquid Nit.	Aluminum	HSS	7	0.002	-4.2575	142.0381	205.4665	0.0062
85	Liquid Nit.	Aluminum	HSS	7	0.004	-2.9378	228.9784	355.1285	0.0124
86	Liquid Nit.	Aluminum	HSS	7	0.004	-5.6133	220.6529	347.1435	0.012433
87	Liquid Nit.	Aluminum	HSS	7	0.004	-4.9536	221.6967	351.6392	0.012517
88	Liquid Nit.	Aluminum	HSS	7	0.004	-2.8576	214.3299	344.3132	0.012567
89	Liquid Nit.	Aluminum	HSS	15	0.002	-0.0308	105.1554	185.5831	0.004767
90	Liquid Nit.	Aluminum	HSS	15	0.002	-1.4157	107.7153	188.4806	0.004883
91	Liquid Nit.	Aluminum	HSS	15	0.002	-2.1106	109.5206	190.7135	0.004833
92	Liquid Nit.	Aluminum	HSS	15	0.002	-1.7544	110.6679	189.1425	0.004783
93	Liquid Nit.	Aluminum	HSS	15	0.004	-2.7138	164.312	316.2855	0.0105
94	Liquid Nit.	Aluminum	HSS	15	0.004	-3.0126	163.1385	311.5762	0.010717
95	Liquid Nit.	Aluminum	HSS	15	0.004	-3.5861	173.1108	323.4123	0.01055
96	Liquid Nit.	Aluminum	HSS	15	0.004	-3.3224	175.2552	323.3191	0.01045
97	Dry	Aluminum	Unctd. Carb.	0	0.002	0.3064	164.0391	203.0355	0.00878
98	Dry	Aluminum	Unctd. Carb.	0	0.002	0.3341	159.1337	198.9311	0.00887
99	Dry	Aluminum	Unctd. Carb.	0	0.002	-0.1586	160.2427	201.4572	0.00863
100	Dry	Aluminum	Unctd. Carb.	0	0.002	-0.0772	166.8888	204.1874	0.00873
101	Dry	Aluminum	Unctd. Carb.	0	0.004	-2.3583	206.6433	317.0022	0.014817
102	Dry	Aluminum	Unctd. Carb.	0	0.004	-2.3679	209.638	319.1074	0.015467
103	Dry	Aluminum	Unctd. Carb.	0	0.004	-2.0586	205.2793	315.952	0.015067
104	Dry	Aluminum	Unctd. Carb.	0	0.004	-2.6078	207.8965	318.1458	0.014917
105	Dry	Aluminum	Unctd. Carb.	7	0.002	-0.5332	130.3931	184.1556	0.0082
106	Dry	Aluminum	Unctd. Carb.	7	0.002	-0.4892	127.9146	182.6282	0.00845
107	Dry	Aluminum	Unctd. Carb.	7	0.002	-2.1231	119.3216	177.8913	0.008222
108	Dry	Aluminum	Unctd. Carb.	7	0.002	-4.4152	123.2089	180.4395	0.00838

109	Dry	Aluminum	Unctd. Carb.	7	0.004	-4.9009	174.3611	300.7586	0.014367
110	Dry	Aluminum	Unctd. Carb.	7	0.004	-5.7671	169.3722	299.6085	0.014333
111	Dry	Aluminum	Unctd. Carb.	7	0.004	-1.9967	170.2859	299.5859	0.01405
112	Dry	Aluminum	Unctd. Carb.	7	0.004	-3.07	173.5985	300.6843	0.014283
113	Dry	Aluminum	Unctd. Carb.	15	0.002	-1.174	105.0722	172.1062	0.00775
114	Dry	Aluminum	Unctd. Carb.	15	0.002	1.6004	103.89	171.0439	0.0075
115	Dry	Aluminum	Unctd. Carb.	15	0.002	1.2804	98.8688	168.1556	0.007533
116	Dry	Aluminum	Unctd. Carb.	15	0.002	-2.5616	101.1252	168.7814	0.007683
117	Dry	Aluminum	Unctd. Carb.	15	0.004	-3.238	136.9912	283.6957	0.013817
118	Dry	Aluminum	Unctd. Carb.	15	0.004	-4.1987	139.0281	283.2382	0.0138
119	Dry	Aluminum	Unctd. Carb.	15	0.004	-4.7009	141.819	285.6196	0.013717
120	Dry	Aluminum	Unctd. Carb.	15	0.004	-2.8123	143.1751	286.5609	0.013727
121	Cold Comp. Air	Aluminum	Unctd. Carb.	0	0.002	-1.2128	164.0185	204.6764	0.007717
122	Cold Comp. Air	Aluminum	Unctd. Carb.	0	0.002	-0.6169	156.9543	198.9473	0.007763
123	Cold Comp. Air	Aluminum	Unctd. Carb.	0	0.002	-1.3003	164.0126	204.252	0.007683
124	Cold Comp. Air	Aluminum	Unctd. Carb.	0	0.002	-2.2223	160.4036	200.0909	0.0077
125	Cold Comp. Air	Aluminum	Unctd. Carb.	0	0.004	-2.7706	220.4736	327.797	0.012233
126	Cold Comp. Air	Aluminum	Unctd. Carb.	0	0.004	-0.0197	215.2296	324.3654	0.012016
127	Cold Comp. Air	Aluminum	Unctd. Carb.	0	0.004	-0.5692	220.194	327.5856	0.012366
128	Cold Comp. Air	Aluminum	Unctd. Carb.	0	0.004	-3.6336	216.082	326.0836	0.012117
129	Cold Comp. Air	Aluminum	Unctd. Carb.	7	0.002	-0.2998	129.9748	185.4433	0.007083
130	Cold Comp. Air	Aluminum	Unctd. Carb.	7	0.002	-0.5104	125.4589	182.6559	0.007217
131	Cold Comp. Air	Aluminum	Unctd. Carb.	7	0.002	-0.0277	125.6079	182.6749	0.007113
132	Cold Comp. Air	Aluminum	Unctd. Carb.	7	0.002	-0.0644	123.2301	180.738	0.007117
133	Cold Comp. Air	Aluminum	Unctd. Carb.	7	0.004	2.4302	200.5658	310.2334	0.01145
134	Cold Comp. Air	Aluminum	Unctd. Carb.	7	0.004	-2.7082	178.0919	307.2361	0.011367
135	Cold Comp. Air	Aluminum	Unctd. Carb.	7	0.004	-2.3261	179.1115	302.0322	0.0114
136	Cold Comp. Air	Aluminum	Unctd. Carb.	7	0.004	-9.5814	192.3043	305.86	0.011333
137	Cold Comp. Air	Aluminum	Unctd. Carb.	15	0.002	2.7307	101.4765	170.7047	0.006217
138	Cold Comp. Air	Aluminum	Unctd. Carb.	15	0.002	-0.4659	102.8787	171.6839	0.006283
139	Cold Comp. Air	Aluminum	Unctd. Carb.	15	0.002	0.3613	98.298	168.6393	0.0062
140	Cold Comp. Air	Aluminum	Unctd. Carb.	15	0.002	-1.2307	101.5145	171.9052	0.006217
141	Cold Comp. Air	Aluminum	Unctd. Carb.	15	0.004	-0.5271	139.3709	286.097	0.010117
142	Cold Comp. Air	Aluminum	Unctd. Carb.	15	0.004	-0.7359	143.2387	288.8304	0.01115
143	Cold Comp. Air	Aluminum	Unctd. Carb.	15	0.004	2.2171	157.5363	275.8365	0.011117
144	Cold Comp. Air	Aluminum	Unctd. Carb.	15	0.004	-0.1173	140.9968	286.9535	0.010283
145	Nitrogen	Aluminum	Unctd. Carb.	0	0.002	-1.7567	169.8755	207.3908	0.007967
146	Nitrogen	Aluminum	Unctd. Carb.	0	0.002	-1.2334	157.3445	198.8675	0.0079
147	Nitrogen	Aluminum	Unctd. Carb.	0	0.002	0.2796	158.3371	199.3261	0.007933
148	Nitrogen	Aluminum	Unctd. Carb.	0	0.002	-2.0804	163.7791	203.6206	0.007967
149	Nitrogen	Aluminum	Unctd. Carb.	0	0.004	-0.1786	221.554	327.4879	0.012683

150	Nitrogen	Aluminum	Unctd. Carb.	0	0.004	-0.1732	212.997	321.9011	0.012517
151	Nitrogen	Aluminum	Unctd. Carb.	0	0.004	10.569	213.2592	323.4945	0.012567
152	Nitrogen	Aluminum	Unctd. Carb.	0	0.004	-0.8363	220.5378	327.7031	0.012667
153	Nitrogen	Aluminum	Unctd. Carb.	7	0.002	-0.5309	126.0515	181.4025	0.0057
154	Nitrogen	Aluminum	Unctd. Carb.	7	0.002	-0.8785	123.4193	179.5451	0.005683
155	Nitrogen	Aluminum	Unctd. Carb.	7	0.002	-1.1604	126.1064	182.2496	0.005583
156	Nitrogen	Aluminum	Unctd. Carb.	7	0.002	-0.9165	124.958	181.9935	0.005553
157	Nitrogen	Aluminum	Unctd. Carb.	7	0.004	-3.5478	171.3413	300.5215	0.0095
158	Nitrogen	Aluminum	Unctd. Carb.	7	0.004	-3.5585	175.9018	302.7127	0.101833
159	Nitrogen	Aluminum	Unctd. Carb.	7	0.004	-2.2219	174.4964	303.3101	0.010067
160	Nitrogen	Aluminum	Unctd. Carb.	7	0.004	-2.6815	176.0999	303.5385	0.010167
161	Nitrogen	Aluminum	Unctd. Carb.	15	0.002	-0.1788	105.7585	171.5087	0.003283
162	Nitrogen	Aluminum	Unctd. Carb.	15	0.002	-1.453	103.3447	169.8758	0.003383
163	Nitrogen	Aluminum	Unctd. Carb.	15	0.002	-0.349	103.3468	170.2746	0.003467
164	Nitrogen	Aluminum	Unctd. Carb.	15	0.002	-1.5968	102.8597	168.7408	0.003567
165	Nitrogen	Aluminum	Unctd. Carb.	15	0.004	-0.359	140.6794	285.7852	0.006967
166	Nitrogen	Aluminum	Unctd. Carb.	15	0.004	-1.1421	142.121	286.0523	0.006683
167	Nitrogen	Aluminum	Unctd. Carb.	15	0.004	-3.053	135.2971	284.0552	0.0066
168	Nitrogen	Aluminum	Unctd. Carb.	15	0.004	-1.4659	135.5228	281.1523	0.006667
169	Liquid Nit.	Aluminum	Unctd. Carb.	0	0.002	-2.0338	169.7086	211.5328	0.008433
170	Liquid Nit.	Aluminum	Unctd. Carb.	0	0.002	-3.9325	168.713	209.5218	0.008533
171	Liquid Nit.	Aluminum	Unctd. Carb.	0	0.002	-0.798	199.2841	238.3424	0.00855
172	Liquid Nit.	Aluminum	Unctd. Carb.	0	0.002	-0.0367	169.0598	208.7949	0.008233
173	Liquid Nit.	Aluminum	Unctd. Carb.	0	0.004	-0.8018	258.7538	356.5159	0.014367
174	Liquid Nit.	Aluminum	Unctd. Carb.	0	0.004	-1.8537	251.5998	351.1933	0.01415
175	Liquid Nit.	Aluminum	Unctd. Carb.	0	0.004	-1.1821	264.3798	362.7055	0.014283
176	Liquid Nit.	Aluminum	Unctd. Carb.	0	0.004	-3.3658	234.6165	336.8478	0.014133
177	Liquid Nit.	Aluminum	Unctd. Carb.	7	0.002	-4.1854	150.9403	209.6872	0.006367
178	Liquid Nit.	Aluminum	Unctd. Carb.	7	0.002	-3.2773	132.3839	191.5607	0.006183
179	Liquid Nit.	Aluminum	Unctd. Carb.	7	0.002	-4.3102	147.9796	206.759	0.006433
180	Liquid Nit.	Aluminum	Unctd. Carb.	7	0.002	-1.8112	136.9174	195.4454	0.006366
181	Liquid Nit.	Aluminum	Unctd. Carb.	7	0.004	-2.1613	199.4016	327.691	0.012117
182	Liquid Nit.	Aluminum	Unctd. Carb.	7	0.004	-4.8925	197.9351	325.9679	0.012167
183	Liquid Nit.	Aluminum	Unctd. Carb.	7	0.004	-4.0812	194.7064	320.8924	0.012183
184	Liquid Nit.	Aluminum	Unctd. Carb.	7	0.004	-6.7533	195.4666	326.8835	0.01225
185	Liquid Nit.	Aluminum	Unctd. Carb.	15	0.002	0.3961	109.8616	182.2131	0.00445
186	Liquid Nit.	Aluminum	Unctd. Carb.	15	0.002	-0.2458	108.2996	177.8009	0.00455
187	Liquid Nit.	Aluminum	Unctd. Carb.	15	0.002	-0.1018	115.4624	181.2228	0.004483
188	Liquid Nit.	Aluminum	Unctd. Carb.	15	0.002	0.7061	121.9578	185.9224	0.0045
189	Liquid Nit.	Aluminum	Unctd. Carb.	15	0.004	-0.9581	149.4618	297.6059	0.010867
190	Liquid Nit.	Aluminum	Unctd. Carb.	15	0.004	-1.3523	151.9104	300.2563	0.01085

191	Liquid Nit.	Aluminum	Unctd. Carb.	15	0.004	-3.997	146.8328	296.6393	0.010817
192	Liquid Nit.	Aluminum	Unctd. Carb.	15	0.004	-2.76	145.3498	296.8043	0.010783
193	Dry	102o steel	HSS	0	0.002	-5.112	517.1114	614.2253	0.012767
194	Dry	102o steel	HSS	0	0.002	2.9467	502.9318	586.9558	0.012833
195	Dry	102o steel	HSS	0	0.002	7.0713	509.7859	594.4569	0.012383
196	Dry	102o steel	HSS	0	0.002	6.4179	495.9598	585.1861	0.01245
197	Dry	102o steel	HSS	0	0.004	-11.1474	720.6149	825.4422	0.021783
198	Dry	102o steel	HSS	0	0.004	-19.8645	706.2889	817.3255	0.021817
199	Dry	102o steel	HSS	0	0.004	-11.2518	707.3873	821.7188	0.0214
200	Dry	102o steel	HSS	0	0.004	-12.6361	701.8244	814.7245	0.0218
201	Dry	102o steel	HSS	7	0.002	-8.3453	395.3014	525.7909	0.010483
202	Dry	102o steel	HSS	7	0.002	-1.1151	381.6591	514.6764	0.010433
203	Dry	102o steel	HSS	7	0.002	-4.5618	386.1393	522.7375	0.0105
204	Dry	102o steel	HSS	7	0.002	-6.4507	397.3696	529.3212	0.01035
205	Dry	102o steel	HSS	7	0.004	-13.1294	670.1289	841.805	0.018617
206	Dry	102o steel	HSS	7	0.004	-3.2559	685.2119	863.6924	0.017667
207	Dry	102o steel	HSS	7	0.004	-7.1401	669.3134	841.3084	0.017383
208	Dry	102o steel	HSS	7	0.004	-5.019	693.5815	857.314	0.01695
209	Dry	102o steel	HSS	15	0.002	-15.1527	277.5093	439.2193	0.008233
210	Dry	102o steel	HSS	15	0.002	-7.9346	279.9663	438.2193	0.008617
211	Dry	102o steel	HSS	15	0.002	-4.9848	293.7584	454.7832	0.00865
212	Dry	102o steel	HSS	15	0.002	-5.634	278.7339	442.2563	0.008167
213	Dry	102o steel	HSS	15	0.004	-30.5509	499.17	752.4931	0.01455
214	Dry	102o steel	HSS	15	0.004	-12.0375	492.8073	731.2637	0.01675
215	Dry	102o steel	HSS	15	0.004	-13.27	492.7373	747.0256	0.014217
216	Dry	102o steel	HSS	15	0.004	-13.704	487.4593	747.1569	0.01535
217	Cold Comp. Air	102oSteel	HSS	0	0.002	-6.4367	249.8309	412.0225	0.00625
218	Cold Comp. Air	102oSteel	HSS	0	0.002	-4.2337	255.8747	420.8744	0.0064
219	Cold Comp. Air	102oSteel	HSS	0	0.002	-2.0097	242.4652	406.1375	0.006067
220	Cold Comp. Air	102oSteel	HSS	0	0.002	-1.4094	254.7599	420.0415	0.006383
221	Cold Comp. Air	102oSteel	HSS	0	0.004	-10.5182	666.452	874.2112	0.0152
222	Cold Comp. Air	102oSteel	HSS	0	0.004	4.6204	662.1535	860.9833	0.015367
223	Cold Comp. Air	102oSteel	HSS	0	0.004	1.174	639.2833	856.6007	0.015317
224	Cold Comp. Air	102oSteel	HSS	0	0.004	-2.9107	649.7263	857.5593	0.015217
225	Cold Comp. Air	102oSteel	HSS	7	0.002	-0.35965	225.8606	390.2726	0.005683
226	Cold Comp. Air	102oSteel	HSS	7	0.002	-16.2731	198.7929	366.5965	0.005567
227	Cold Comp. Air	102oSteel	HSS	7	0.002	-0.9947	224.0428	389.2588	0.0056
228	Cold Comp. Air	102oSteel	HSS	7	0.002	-5.5645	219.0445	390.1992	0.005733
229	Cold Comp. Air	102oSteel	HSS	7	0.004	-2.2124	450.2156	726.9496	0.012633
230	Cold Comp. Air	102oSteel	HSS	7	0.004	-6.0167	460.9629	733.6715	0.0125
231	Cold Comp. Air	102oSteel	HSS	7	0.004	-1.1835	490.7357	748.898	0.01255

232	Cold Comp. Air	102oSteel	HSS	7	0.004	10.339	483.4115	747.3196	0.012483
233	Cold Comp. Air	102oSteel	HSS	15	0.002	-5.1229	218.7219	383.3561	0.00535
234	Cold Comp. Air	102oSteel	HSS	15	0.002	-2.9072	202.7566	369.9832	0.005367
235	Cold Comp. Air	102oSteel	HSS	15	0.002	-5.6833	209.1437	374.4785	0.005367
236	Cold Comp. Air	102oSteel	HSS	15	0.002	-5.5136	198.0666	365.0305	0.005217
237	Cold Comp. Air	102oSteel	HSS	15	0.004	-7.965	407.0889	691.3724	0.009833
238	Cold Comp. Air	102oSteel	HSS	15	0.004	-9.0389	411.0117	694.1164	0.010233
239	Cold Comp. Air	102oSteel	HSS	15	0.004	-13.8139	417.8984	699.9936	0.01
240	Cold Comp. Air	102oSteel	HSS	15	0.004	-9.4511	395.1277	685.4871	0.010117
241	Nitrogen	102oSteel	HSS	0	0.002	28.9436	218.8552	388.7651	0.00645
242	Nitrogen	102oSteel	HSS	0	0.002	10.2591	245.6017	408.7615	0.006267
243	Nitrogen	102oSteel	HSS	0	0.002	-5.9536	223.3659	388.8318	0.006517
244	Nitrogen	102oSteel	HSS	0	0.002	3.5921	308.4203	467.6706	0.00635
245	Nitrogen	102oSteel	HSS	0	0.004	-8.1327	722.1704	907.322	0.016467
246	Nitrogen	102oSteel	HSS	0	0.004	-0.1898	780.8907	928.4949	0.016383
247	Nitrogen	102oSteel	HSS	0	0.004	4.3117	77.6247	920.489	0.016517
248	Nitrogen	102oSteel	HSS	0	0.004	6.8215	789.9367	939.8015	0.01645
249	Nitrogen	102oSteel	HSS	7	0.002	-1.9956	265.1675	429.8416	0.0053
250	Nitrogen	102oSteel	HSS	7	0.002	-2.236	290.1994	452.447	0.005383
251	Nitrogen	102oSteel	HSS	7	0.002	4.013	272.2289	439.5488	0.005233
252	Nitrogen	102oSteel	HSS	7	0.002	-4.3346	243.911	410.8887	0.005283
253	Nitrogen	102oSteel	HSS	7	0.004	-7.698	551.3043	798.6477	0.010317
254	Nitrogen	102oSteel	HSS	7	0.004	-8.3763	583.6562	799.8567	0.010217
255	Nitrogen	102oSteel	HSS	7	0.004	-5.7322	586.1289	808.2166	0.0101
256	Nitrogen	102oSteel	HSS	7	0.004	-10.6722	632.6789	820.8611	0.010183
257	Nitrogen	102oSteel	HSS	15	0.002	-6.2192	239.2638	407.4894	0.003683
258	Nitrogen	102oSteel	HSS	15	0.002	-5.9543	222.521	390.2903	0.00355
259	Nitrogen	102oSteel	HSS	15	0.002	-3.0845	235.9659	402.9293	0.0036
260	Nitrogen	102oSteel	HSS	15	0.002	-5.0371	238.1947	404.5824	0.00375
261	Nitrogen	102oSteel	HSS	15	0.004	0.6855	450.2806	722.0339	0.0087
262	Nitrogen	102oSteel	HSS	15	0.004	-5.9918	451.54	725.2946	0.00865
263	Nitrogen	102oSteel	HSS	15	0.004	0.3178	431.8087	711.5893	0.008733
264	Nitrogen	102oSteel	HSS	15	0.004	-6.1431	427.4748	707.3424	0.00845
265	Liquid Nit.	102oSteel	HSS	0	0.002	-0.9936	233.9084	409.4519	0.005833
266	Liquid Nit.	102oSteel	HSS	0	0.002	-6.1776	222.7882	398.1978	0.006167
267	Liquid Nit.	102oSteel	HSS	0	0.002	-6.5692	226.5024	394.842	0.00615
268	Liquid Nit.	102oSteel	HSS	0	0.002	-2.3798	222.1694	397.9633	0.006317
269	Liquid Nit.	102oSteel	HSS	0	0.004	-19.452	599.3386	832.4204	0.013917
270	Liquid Nit.	102oSteel	HSS	0	0.004	-0.1279	602.5334	836.5058	0.014117
271	Liquid Nit.	102oSteel	HSS	0	0.004	-3.2324	523.1524	787.7618	0.014
272	Liquid Nit.	102oSteel	HSS	0	0.004	-34.4619	601.1962	836.1058	0.013967

273	Liquid Nit.	102oSteel	HSS	7	0.002	0.2513	199.3094	347.2567	0.005303
274	Liquid Nit.	102oSteel	HSS	7	0.002	-3.6243	218.8308	390.5504	0.004983
275	Liquid Nit.	102oSteel	HSS	7	0.002	-5.9063	192.0687	362.943	0.0051
276	Liquid Nit.	102oSteel	HSS	7	0.002	-4.2392	216.4476	385.8445	0.005067
277	Liquid Nit.	102oSteel	HSS	7	0.004	-9.9999	476.6622	753.0843	0.01065
278	Liquid Nit.	102oSteel	HSS	7	0.004	-11.7715	489.5776	758.6761	0.010633
279	Liquid Nit.	102oSteel	HSS	7	0.004	2.9542	480.4437	754.4806	0.010467
280	Liquid Nit.	102oSteel	HSS	7	0.004	-2.1941	511.9545	769.3339	0.0106
281	Liquid Nit.	102oSteel	HSS	15	0.002	-6.109	204.4404	376.8224	0.003967
282	Liquid Nit.	102oSteel	HSS	15	0.002	-6.7699	211.039	386.3852	0.004367
283	Liquid Nit.	102oSteel	HSS	15	0.002	-6.4716	199.5895	376.1318	0.0042
284	Liquid Nit.	102oSteel	HSS	15	0.002	-6.3844	197.3483	368.705	0.004583
285	Liquid Nit.	102oSteel	HSS	15	0.004	-6.0734	394.0755	687.6333	0.0075
286	Liquid Nit.	102oSteel	HSS	15	0.004	-3.0562	412.9907	704.7245	0.007667
287	Liquid Nit.	102oSteel	HSS	15	0.004	-10.7784	421.1492	707.0094	0.007417
288	Liquid Nit.	102oSteel	HSS	15	0.004	-6.614	404.2209	691.2181	0.007383
289	Dry	102o steel	Unctd. Carb.	0	0.002	-2.2294	596.8598	523.5713	0.013567
290	Dry	102o steel	Unctd. Carb.	0	0.002	-4.6507	616.3077	535.1927	0.0135
291	Dry	102o steel	Unctd. Carb.	0	0.002	-3.8218	543.6471	497.6703	0.013217
292	Dry	102o steel	Unctd. Carb.	0	0.002	-1.2763	547.3946	502.9702	0.013517
293	Dry	102o steel	Unctd. Carb.	0	0.004	0.8062	466.1516	656.3718	0.019283
294	Dry	102o steel	Unctd. Carb.	0	0.004	-0.4458	872.2132	871.4515	0.0193
295	Dry	102o steel	Unctd. Carb.	0	0.004	1.3564	594.1015	658.8432	0.01965
296	Dry	102o steel	Unctd. Carb.	0	0.004	0.6086	869.8085	895.6769	0.019417
297	Dry	102o steel	Unctd. Carb.	7	0.002	-1.4931	523.7329	495.9682	0.012717
298	Dry	102o steel	Unctd. Carb.	7	0.002	-2.5415	497.2013	484.0035	0.012433
299	Dry	102o steel	Unctd. Carb.	7	0.002	-3.776	529.2054	494.7562	0.012267
300	Dry	102o steel	Unctd. Carb.	7	0.002	-1.2934	512.1106	482.9916	0.0121
301	Dry	102o steel	Unctd. Carb.	7	0.004	3.325	367.0536	574.5563	0.018233
302	Dry	102o steel	Unctd. Carb.	7	0.004	6.01606	390.1058	573.6699	0.018433
303	Dry	102o steel	Unctd. Carb.	7	0.004	1.2069	416.9256	636.4796	0.0182
304	Dry	102o steel	Unctd. Carb.	7	0.004	-1.073	406.4825	615.2771	0.018483
305	Dry	102o steel	Unctd. Carb.	15	0.002	9.3021	512.6168	244.6355	0.010733
306	Dry	102o steel	Unctd. Carb.	15	0.002	1.8785	354.5089	378.3851	0.011388
307	Dry	102o steel	Unctd. Carb.	15	0.002	2.3068	360.3917	359.408	0.010133
308	Dry	102o steel	Unctd. Carb.	15	0.002	10.5578	337.8878	289.9954	0.0107
309	Dry	102o steel	Unctd. Carb.	15	0.004	1.8668	240.7465	439.7258	0.015817
310	Dry	102o steel	Unctd. Carb.	15	0.004	3.9826	322.9753	492.7041	0.015883
311	Dry	102o steel	Unctd. Carb.	15	0.004	0.086	287.1598	454.693	0.015783
312	Dry	102o steel	Unctd. Carb.	15	0.004	2.5432	273.6629	437.4799	0.016067
313	Cold Comp. Air	102oSteel	Unctd. Carb.	0	0.002	0.6978	338.1305	189.097	0.012633

314	Cold Comp. Air	102oSteel	Unctd. Carb.	0	0.002	-1.1188	348.3737	170.9871	0.012783
315	Cold Comp. Air	102oSteel	Unctd. Carb.	0	0.002	1.0023	333.2833	150.3163	0.0128
316	Cold Comp. Air	102oSteel	Unctd. Carb.	0	0.002	-1.7715	377.2822	364.3751	0.012367
317	Cold Comp. Air	102oSteel	Unctd. Carb.	0	0.004	-2.0723	457.3035	575.1828	0.01905
318	Cold Comp. Air	102oSteel	Unctd. Carb.	0	0.004	1.7254	495.4884	563.8183	0.019267
319	Cold Comp. Air	102oSteel	Unctd. Carb.	0	0.004	-0.8265	460.0241	549.9596	0.019017
320	Cold Comp. Air	102oSteel	Unctd. Carb.	0	0.004	-0.387	455.1406	565.715	0.019217
321	Cold Comp. Air	102oSteel	Unctd. Carb.	7	0.002	3.2196	283.4148	369.1915	0.0113
322	Cold Comp. Air	102oSteel	Unctd. Carb.	7	0.002	-1.6395	160.2749	293.5696	0.011283
323	Cold Comp. Air	102oSteel	Unctd. Carb.	7	0.002	7.9695	234.6311	345.852	0.011167
324	Cold Comp. Air	102oSteel	Unctd. Carb.	7	0.002	-2.3373	225.7492	335.4811	0.011233
325	Cold Comp. Air	102oSteel	Unctd. Carb.	7	0.004	3.0871	101.4971	409.2714	0.016833
326	Cold Comp. Air	102oSteel	Unctd. Carb.	7	0.004	-3.7988	101.5943	389.4993	0.016817
327	Cold Comp. Air	102oSteel	Unctd. Carb.	7	0.004	2.9572	90.4716	396.5178	0.017067
328	Cold Comp. Air	102oSteel	Unctd. Carb.	7	0.004	-2.8441	107.7146	402.7248	0.017
329	Cold Comp. Air	102oSteel	Unctd. Carb.	15	0.002	0.3611	188.7805	316.0091	0.010833
330	Cold Comp. Air	102oSteel	Unctd. Carb.	15	0.002	2.4583	337.6728	395.5955	0.010983
331	Cold Comp. Air	102oSteel	Unctd. Carb.	15	0.002	2.9625	312.1055	377.7923	0.010916
332	Cold Comp. Air	102oSteel	Unctd. Carb.	15	0.002	-3.8674	339.7787	391.0737	0.0115
333	Cold Comp. Air	102oSteel	Unctd. Carb.	15	0.004	-2.3014	174.3373	421.9717	0.01477
334	Cold Comp. Air	102oSteel	Unctd. Carb.	15	0.004	-2.4143	163.4782	415.0167	0.014967
335	Cold Comp. Air	102oSteel	Unctd. Carb.	15	0.004	-2.0272	163.8543	407.3952	0.01465
336	Cold Comp. Air	102oSteel	Unctd. Carb.	15	0.004	-8.0299	210.2706	403.4888	0.014833
337	Nitrogen	102oSteel	Unctd. Carb.	0	0.002	-1.0672	569.192	515.2243	0.010367
338	Nitrogen	102oSteel	Unctd. Carb.	0	0.002	-1.497	573.9338	518.5329	0.0103
339	Nitrogen	102oSteel	Unctd. Carb.	0	0.002	-0.5816	612.6996	530.6029	0.010317
340	Nitrogen	102oSteel	Unctd. Carb.	0	0.002	-1.8225	554.8034	504.8034	0.010367
341	Nitrogen	102oSteel	Unctd. Carb.	0	0.004	-1.7063	119.802	380.7269	0.01833
342	Nitrogen	102oSteel	Unctd. Carb.	0	0.004	-1.8092	110.2787	428.211	0.0184
343	Nitrogen	102oSteel	Unctd. Carb.	0	0.004	-3.1574	94.613	420.5035	0.01835
344	Nitrogen	102oSteel	Unctd. Carb.	0	0.004	-1.0679	149.615	442.9037	0.018317
345	Nitrogen	102oSteel	Unctd. Carb.	7	0.002	1.3847	396.1477	431.4025	0.00835
346	Nitrogen	102oSteel	Unctd. Carb.	7	0.002	-1.8001	184.2387	309.4843	0.0081
347	Nitrogen	102oSteel	Unctd. Carb.	7	0.002	0.1967	178.3388	303.8884	0.00805
348	Nitrogen	102oSteel	Unctd. Carb.	7	0.002	-0.9455	206.0992	316.3875	0.008217
349	Nitrogen	102oSteel	Unctd. Carb.	7	0.004	0.0937	93.0722	407.5095	0.0172
350	Nitrogen	102oSteel	Unctd. Carb.	7	0.004	-4.5185	86.3988	372.9463	0.017217
351	Nitrogen	102oSteel	Unctd. Carb.	7	0.004	-0.9038	131.986	444.2793	0.017267
352	Nitrogen	102oSteel	Unctd. Carb.	7	0.004	-3.1372	88.5143	391.7454	0.017233
353	Nitrogen	102oSteel	Unctd. Carb.	15	0.002	-1.3698	189.9325	315.1837	0.0039
354	Nitrogen	102oSteel	Unctd. Carb.	15	0.002	1.5552	167.8439	292.7292	0.003933

355	Nitrogen	102oSteel	Unctd. Carb.	15	0.002	0.1427	215.3725	337.8947	0.0041
356	Nitrogen	102oSteel	Unctd. Carb.	15	0.002	-2.3676	289.7561	376.0429	0.004
357	Nitrogen	102oSteel	Unctd. Carb.	15	0.004	-3.8146	80.5854	311.0417	0.0084
358	Nitrogen	102oSteel	Unctd. Carb.	15	0.004	-7.8389	76.4343	328.4096	0.00855
359	Nitrogen	102oSteel	Unctd. Carb.	15	0.004	-0.4439	73.6059	346.4909	0.008567
360	Nitrogen	102oSteel	Unctd. Carb.	15	0.004	-8.1946	103.6189	341.8446	0.008417
361	Liquid Nit.	102oSteel	Unctd. Carb.	0	0.002	0.1387	211.057	330.4854	0.007133
362	Liquid Nit.	102oSteel	Unctd. Carb.	0	0.002	1.0517	210.2753	321.8856	0.006883
363	Liquid Nit.	102oSteel	Unctd. Carb.	0	0.002	4.2256	256.9295	352.5296	0.007267
364	Liquid Nit.	102oSteel	Unctd. Carb.	0	0.002	6.5148	394.8416	426.4477	0.007417
365	Liquid Nit.	102oSteel	Unctd. Carb.	0	0.004	14.2632	214.1733	474.0729	0.016083
366	Liquid Nit.	102oSteel	Unctd. Carb.	0	0.004	-1.8032	131.7219	479.6725	0.015517
367	Liquid Nit.	102oSteel	Unctd. Carb.	0	0.004	1.8997	307.9192	536.7797	0.015683
368	Liquid Nit.	102oSteel	Unctd. Carb.	0	0.004	0.8871	206.8685	528.9951	0.01575
369	Liquid Nit.	102oSteel	Unctd. Carb.	7	0.002	0.5609	240.11	348.0906	0.008833
370	Liquid Nit.	102oSteel	Unctd. Carb.	7	0.002	-0.2837	252.9805	357.976	0.008733
371	Liquid Nit.	102oSteel	Unctd. Carb.	7	0.002	1.5127	267.613	364.119	0.00865
372	Liquid Nit.	102oSteel	Unctd. Carb.	7	0.002	-0.3805	341.5222	405.5661	0.0086
373	Liquid Nit.	102oSteel	Unctd. Carb.	7	0.004	7.34	92.014	374.7444	0.0167
374	Liquid Nit.	102oSteel	Unctd. Carb.	7	0.004	-0.187	96.4095	374.8534	0.016767
375	Liquid Nit.	102oSteel	Unctd. Carb.	7	0.004	6.2857	85.2848	366.0598	0.016583
376	Liquid Nit.	102oSteel	Unctd. Carb.	7	0.004	-3.7301	108.0995	383.0404	0.016633
377	Liquid Nit.	102oSteel	Unctd. Carb.	15	0.002	0.4697	204.1102	328.7274	0.0105
378	Liquid Nit.	102oSteel	Unctd. Carb.	15	0.002	-2.8833	179.4327	310.866	0.010005
379	Liquid Nit.	102oSteel	Unctd. Carb.	15	0.002	5.4411	165.3175	311.6137	0.010017
380	Liquid Nit.	102oSteel	Unctd. Carb.	15	0.002	3.9277	201.2311	324.2809	0.0101
381	Liquid Nit.	102oSteel	Unctd. Carb.	15	0.004	4.6177	78.7616	310.2681	0.018367
382	Liquid Nit.	102oSteel	Unctd. Carb.	15	0.004	-10.2938	72.0907	315.8874	0.018533
383	Liquid Nit.	102oSteel	Unctd. Carb.	15	0.004	0.2377	98.6274	344.1799	0.0181
384	Liquid Nit.	102oSteel	Unctd. Carb.	15	0.004	-5.3144	78.1311	316.0656	0.018167

APPENDIX 3

The first table below lists the various parameters like chip thickness ratio, shear plane angle, forces along and normal to the rake face (F, N), shear plane (Fs, Fn, Fsp, Fnp)and the respective ratios. The second table lists the shear area, shear stress, shear strain, normal stress, friction coefficient, tec.,

Run	Chip thickness ratio	Phi radians	Psi degrees	Friction Force (F)	Normal Force (N)	F/N Ratio	Fs (Merchant)	Fn (Merchant)	Fs/Fn (Merchant)	Fs (Payton)	Fn (Payton)	Fs/Fn (Payton)
1	0.188982	0.18678	34.29832	198.82	232.64	0.854625	191.67381	238.56218	0.803454	23.91435	305.0883	0.078385
2	0.20202	0.199337	33.57881	172.65	216.1996	0.798568	177.7303	212.04299	0.838181	30.79422	274.9582	0.111996
3	0.199601	0.197012	33.71206	175.4492	213.342	0.822385	174.87271	213.81479	0.81787	26.79426	274.9169	0.097463
4	0.189215	0.187004	34.28546	177.0113	214.6294	0.82473	177.97826	213.82825	0.832342	26.60001	276.9318	0.096053
5	0.258065	0.252554	30.52971	233.3745	335.5765	0.695444	266.61596	309.82443	0.860539	72.26773	402.3091	0.179632
6	0.262295	0.256517	30.30268	241.8935	339.2945	0.712931	266.82121	320.06197	0.833655	68.87291	410.962	0.167589
7	0.26455	0.258625	30.18185	235.166	338.0937	0.695565	266.70536	313.81308	0.849886	72.78087	405.3558	0.179548
8	0.025397	0.025391	43.54518	248.1928	346.0426	0.717232	339.62978	256.89835	1.32204	69.19026	420.1879	0.164665
9	0.230415	0.231101	35.2589	167.3079	179.5303	0.93192	160.2778	185.8335	0.862481	23.59865	244.2666	0.09661
10	0.229885	0.230573	35.28912	164.1449	181.0472	0.906642	162.22597	182.76861	0.887603	26.8306	242.9028	0.110458
11	0.231214	0.231896	35.21332	165.7959	181.4196	0.913881	162.17348	184.66492	0.878204	26.01558	244.3861	0.106453
12	0.2331	0.233774	35.10576	165.4472	184.2198	0.898096	164.6481	184.93433	0.890306	28.34387	245.9803	0.115228
13	0.271555	0.271855	32.92388	235.5765	296.781	0.793772	258.33269	277.19931	0.931938	66.17815	373.0894	0.177379
14	0.273038	0.273315	32.8402	235.7182	297.9077	0.791246	259.0201	277.88611	0.932109	66.92808	373.9422	0.17898
15	0.274914	0.275162	32.73436	227.3329	291.4194	0.780088	253.37163	269.08794	0.941594	67.62488	363.3626	0.186109
16	0.274537	0.274791	32.75564	227.9808	292.3127	0.779921	254.25597	269.76999	0.942492	67.86462	364.4398	0.186216
17	0.245399	0.247907	38.296	153.7358	147.1211	1.044961	149.24264	151.67707	0.98395	23.13061	211.5284	0.10935
18	0.249066	0.251703	38.0785	159.6457	148.2071	1.077188	149.8114	158.14119	0.947327	20.39443	216.8782	0.094036
19	0.241838	0.244221	38.50716	159.6505	150.0584	1.063923	152.84147	156.98824	0.973586	21.86026	218.0091	0.100272
20	0.246002	0.248531	38.2602	157.7822	147.4664	1.069954	149.54676	155.8118	0.959791	20.94121	214.9489	0.097424
21	0.288122	0.292127	35.76236	231.3672	251.6876	0.919263	244.55616	238.89269	1.023707	58.82978	336.7736	0.174686
22	0.287088	0.291057	35.82364	236.8373	253.111	0.935705	246.07422	244.14038	1.007921	56.62902	341.9798	0.165592
23	0.285368	0.289278	35.92561	228.7415	250.9798	0.911394	244.60037	235.55081	1.038419	59.86662	334.2597	0.179102
24	0.288122	0.292127	35.76236	230.2426	250.7281	0.918296	243.63116	237.73955	1.024782	58.75312	335.2973	0.175227

25	0.172662	0.170977	35.20376	201.5471	224.5702	0.897479	187.00357	236.81781	0.789652	16.27979	301.3104	0.05403
26	0.176211	0.174421	35.00642	184.1174	226.1335	0.814198	190.75109	220.56654	0.864823	29.70987	290.0912	0.102416
27	0.178838	0.176967	34.86052	182.0879	224.3963	0.811457	188.83604	218.74792	0.863259	29.91656	287.4277	0.104084
28	0.179104	0.177225	34.84576	174.5485	217.5249	0.80243	183.3451	210.16383	0.872391	30.3889	277.2378	0.109613
29	0.245148	0.240407	31.22572	253.7656	351.612	0.721721	281.07913	330.18555	0.851276	69.18785	428.0666	0.161629
30	0.247678	0.242792	31.08904	253.2363	353.2215	0.716933	281.9802	330.72831	0.852604	70.70021	428.8304	0.164868
31	0.244903	0.240176	31.23894	242.5745	345.3493	0.702403	277.73446	317.76107	0.874036	72.67276	415.7249	0.17481
32	0.245897	0.241113	31.18525	255.9373	354.1216	0.722738	282.76426	333.09216	0.848907	69.42678	431.3768	0.160942
33	0.241926	0.242546	34.60312	179.6198	191.4177	0.938366	168.4633	201.30601	0.836852	24.34366	261.3645	0.093141
34	0.246406	0.246992	34.34839	164.3597	183.4959	0.895713	161.60636	185.92544	0.8692	28.52227	244.6863	0.116567
35	0.247433	0.248011	34.29001	164.7058	183.7523	0.896347	161.62773	186.46545	0.866797	28.48498	245.1153	0.116211
36	0.240964	0.241591	34.65785	169.8141	185.4877	0.915501	163.93595	190.70269	0.859642	26.3998	250.0911	0.105561
37	0.278746	0.278931	32.51845	248.5564	304.4834	0.816322	261.94625	293.04362	0.893881	63.34611	387.9145	0.163299
38	0.280053	0.280216	32.44482	243.7547	301.1735	0.80935	259.05654	288.11723	0.899136	64.04883	382.1251	0.167612
39	0.279076	0.279256	32.49983	244.1492	302.4852	0.807144	260.56686	288.46323	0.903293	64.76983	383.2897	0.168984
40	0.283352	0.283456	32.25919	251.6073	308.7601	0.814896	264.3489	297.92403	0.887303	64.5276	393.0334	0.164178
41	0.301523	0.305981	34.9686	160.5072	152.2665	1.05412	145.02883	167.07574	0.868042	23.09055	220.0329	0.104941
42	0.311687	0.316477	34.36718	166.1881	154.1733	1.077931	144.86056	174.36544	0.830787	21.14498	225.7006	0.093686
43	0.309277	0.31399	34.50972	179.5636	147.6966	1.21576	138.12825	187.02389	0.738559	7.864193	232.3693	0.033844
44	0.299999	0.304406	35.05884	164.7977	152.5966	1.079956	145.43885	171.14772	0.849786	20.74059	223.6377	0.092742
45	0.329679	0.335028	33.3043	227.5533	252.3597	0.901702	235.03481	245.40694	0.957735	61.68476	334.157	0.184598
46	0.328326	0.333635	33.38413	231.4696	251.9322	0.918777	234.66907	248.95473	0.942617	58.96152	337.0038	0.174958
47	0.327439	0.332721	33.43647	244.4237	257.9548	0.947545	239.98584	262.0886	0.915667	55.85353	350.9473	0.159151
48	0.330142	0.335505	33.27701	246.3527	257.4656	0.956837	238.62552	264.64317	0.901688	54.29117	352.1798	0.154158
49	0.202362	0.199665	33.56002	181.9404	218.2821	0.83351	177.85921	221.62014	0.802541	25.69746	283	0.090804
50	0.19802	0.195491	33.7992	178.8097	221.4708	0.807374	182.5189	218.42408	0.835617	30.16595	283.0411	0.106578
51	0.200335	0.197717	33.67164	186.5351	226.3742	0.824012	185.3225	227.36797	0.815077	28.1705	291.971	0.096484
52	0.201681	0.199011	33.59751	192.8114	228.8384	0.842566	186.20292	234.24714	0.794899	25.47494	298.1514	0.085443
53	0.289505	0.281801	28.85399	240.2491	344.26	0.697871	263.87111	326.50669	0.808164	73.54681	413.3103	0.177946
54	0.28777	0.280199	28.94578	240.7294	345.0123	0.697742	264.984	326.75313	0.810961	73.73915	414.1819	0.178036
55	0.289164	0.281486	28.87206	252.3228	352.8082	0.715184	268.83197	340.39652	0.789761	71.05391	427.8922	0.166056
56	0.286738	0.279246	29.00037	245.0184	345.4975	0.709176	264.57944	330.7571	0.799921	71.04945	417.5578	0.170155
57	0.286398	0.286443	32.08802	169.1125	186.4357	0.907082	156.27057	197.3242	0.791948	27.57475	250.1939	0.110214
58	0.280387	0.280544	32.42603	179.8152	185.5598	0.969042	154.87907	206.8294	0.748825	19.82693	257.6292	0.076959

59	0.278424	0.278614	32.53659	175.4717	189.7549	0.924728	160.09845	202.8934	0.789077	25.84691	257.156	0.100511
60	0.283018	0.283127	32.27802	190.3242	187.6973	1.013995	154.76994	217.94457	0.710134	14.46433	266.9164	0.05419
61	0.36036	0.357985	27.98899	233.4686	294.2718	0.793377	231.58206	295.7587	0.78301	65.69561	369.848	0.177629
62	0.373832	0.370776	27.25608	228.4233	292.421	0.781145	227.22744	293.35117	0.774592	67.65251	364.8429	0.185429
63	0.366411	0.36374	27.65923	244.6181	300.2763	0.814644	233.0389	309.34888	0.753321	62.80476	382.1772	0.164334
64	0.372682	0.369688	27.31843	237.056	297.0296	0.798089	229.89971	302.60241	0.759742	65.38394	374.3622	0.174654
65	0.408163	0.415197	28.71095	154.4363	148.1502	1.04243	122.8132	175.25975	0.70075	23.52063	212.7107	0.110576
66	0.424025	0.431194	27.79438	154.7747	148.2017	1.044352	119.98762	177.54418	0.675818	23.35542	213.0105	0.109644
67	0.428568	0.43576	27.53276	155.3977	148.1271	1.049083	118.99443	178.69082	0.665924	22.91705	213.4593	0.10736
68	0.433213	0.440421	27.26575	156.3408	148.3722	1.053707	118.23396	180.21511	0.656071	22.53729	214.3568	0.105139
69	0.469667	0.476714	25.18629	234.1544	253.2766	0.924501	197.51306	282.78243	0.698463	58.39363	339.9522	0.17177
70	0.470588	0.477624	25.13414	238.2664	255.8345	0.93133	198.87362	287.52639	0.691671	57.91976	344.7716	0.167995
71	0.478087	0.48502	24.71041	226.6119	249.185	0.909412	192.83722	276.15201	0.698301	59.73914	331.4775	0.180221
72	0.467836	0.474904	25.28999	218.6356	246.1274	0.888302	194.31932	265.74469	0.731226	62.1691	323.2882	0.192302
73	0.266667	0.260602	30.06858	195.2067	248.5207	0.785475	189.83191	252.65004	0.751363	37.69869	313.7627	0.12015
74	0.267856	0.261712	30.00498	201.0663	239.0119	0.84124	178.85026	256.0604	0.698469	26.83159	311.1823	0.086225
75	0.261438	0.255714	30.34864	232.1835	268.9921	0.863161	201.51751	292.67152	0.688545	26.02761	354.3847	0.073445
76	0.265488	0.259502	30.13166	221.0488	253.7922	0.870983	188.57386	278.77043	0.676449	23.15308	335.7633	0.068957
77	0.262008	0.256248	30.31806	272.9195	370.4816	0.736661	289.21226	357.90772	0.808064	68.98682	454.9533	0.151635
78	0.262582	0.256785	30.28729	262.9523	362.8337	0.724719	284.15428	346.48023	0.820117	70.62682	442.4975	0.15961
79	0.260586	0.254917	30.39432	398.8132	389.3597	1.02428	276.21039	484.10822	0.570555	-6.6846	557.3224	-0.01199
80	0.260303	0.254652	30.40952	247.157	372.2043	0.664036	297.94012	332.94791	0.894855	88.42179	437.9546	0.201897
81	0.33151	0.330329	29.57356	170.463	196.3326	0.868236	156.86737	207.35663	0.75651	34.09221	257.7632	0.132262
82	0.32	0.319202	30.21108	174.1522	191.7117	0.908407	153.91113	208.31158	0.738851	28.18683	257.4643	0.109479
83	0.321714	0.320862	30.11596	168.1391	191.1648	0.879551	154.21585	202.56411	0.761319	31.76163	252.5984	0.12574
84	0.322581	0.321701	30.06789	166.0194	186.6249	0.889589	150.01615	199.71595	0.751148	29.76597	248.0026	0.120023
85	0.322581	0.321701	30.06789	270.5509	324.576	0.833552	264.51149	329.51636	0.802726	63.82058	417.7012	0.15279
86	0.321716	0.320864	30.11586	261.3143	317.6651	0.822609	259.83553	318.87586	0.814849	64.76499	406.2041	0.15944
87	0.319573	0.318788	30.23479	262.8982	322.0001	0.816454	264.4389	320.73606	0.824475	66.96217	410.2629	0.163218
88	0.318302	0.317556	30.3054	254.6935	315.6265	0.806946	260.17453	311.12393	0.836241	67.62522	399.8946	0.169108
89	0.419577	0.426717	28.05091	149.6048	152.0433	0.983962	125.41954	172.53603	0.726918	29.55045	211.2475	0.139885
90	0.409556	0.416606	28.63026	152.8274	154.1795	0.99123	128.77152	174.77248	0.736795	29.28343	215.1046	0.136136
91	0.413793	0.420885	28.38509	155.1491	155.8691	0.995381	129.32292	177.88194	0.727015	29.21049	217.9751	0.134008

92	0.418119	0.425247	28.13512	155.8507	154.0547	1.011658	126.64124	178.84146	0.70812	27.34391	217.4272	0.125761
93	0.380952	0.387574	30.29366	240.5739	262.9813	0.914795	230.72562	271.66273	0.849309	62.18494	350.953	0.177189
94	0.373249	0.379717	30.74384	238.2215	258.7361	0.920712	228.91406	267.00609	0.857336	60.2491	346.5024	0.173878
95	0.379147	0.385734	30.3991	250.9175	267.5879	0.937701	234.51783	282.07136	0.831413	59.5429	361.9634	0.1645
96	0.382775	0.389431	30.18727	252.9647	266.9429	0.947636	232.57302	284.88491	0.816375	57.7849	363.1949	0.159102
97	0.22779	0.223969	32.16753	164.0391	203.0355	0.807933	161.53116	205.0364	0.787817	27.57462	259.5609	0.106236
98	0.225479	0.22177	32.29349	159.1337	198.9311	0.799944	159.05661	198.99274	0.799309	28.14101	253.19	0.111146
99	0.23175	0.22773	31.95206	160.2427	201.4572	0.795418	160.07848	201.58772	0.794088	29.14305	255.7605	0.113947
100	0.229095	0.225209	32.09649	166.8888	204.1874	0.817332	161.76325	208.2715	0.776694	26.37409	262.3905	0.100515
101	0.26996	0.263675	29.89255	206.6433	317.0022	0.651867	252.18876	282.12174	0.8939	78.03553	370.2733	0.210751
102	0.258615	0.25307	30.50013	209.638	319.1074	0.656951	256.45457	282.85805	0.906655	77.40656	373.8795	0.207036
103	0.265481	0.259495	30.13203	205.2793	315.952	0.649717	252.70071	279.47739	0.90419	78.25742	368.5662	0.212329
104	0.26815	0.261987	29.98924	207.8965	318.1458	0.653463	253.4445	283.20238	0.894924	77.95803	371.9681	0.209583
105	0.243902	0.244509	34.49069	151.8641	166.892	0.909954	147.11264	171.09505	0.85983	24.36653	224.3255	0.108621
106	0.236686	0.23734	34.90139	149.2179	165.678	0.90065	147.43345	167.268	0.881421	25.21074	221.5392	0.113798
107	0.24325	0.243861	34.5278	140.1117	162.0237	0.864761	143.81771	158.74327	0.905977	28.50775	212.2976	0.134282
108	0.238663	0.239306	34.7888	144.2806	164.0791	0.879335	146.0935	162.46703	0.899219	27.28482	216.7819	0.125863
109	0.278416	0.278606	32.53702	209.7147	277.2675	0.756362	241.20911	250.35114	0.963483	68.69993	340.79	0.20159
110	0.279076	0.279256	32.49983	204.6228	276.734	0.739421	241.31613	245.39503	0.983378	71.67432	336.6229	0.212922
111	0.284698	0.284776	32.18356	205.527	276.6002	0.743047	239.6795	247.59389	0.968035	70.97502	337.2114	0.210476
112	0.280053	0.280216	32.44482	208.9487	277.2867	0.753548	240.94543	249.98557	0.963837	69.22186	340.2291	0.203457
113	0.258065	0.261018	37.54476	146.0363	139.0471	1.050265	139.16117	145.92765	0.953631	21.41224	200.5049	0.106792
114	0.266667	0.269924	37.03451	144.6195	138.327	1.04549	137.14753	145.73847	0.941052	21.70345	198.9425	0.109094
115	0.265498	0.268714	37.1038	139.0218	136.8367	1.015969	135.87212	139.96469	0.97076	23.92875	193.5943	0.123603
116	0.260315	0.263348	37.41127	141.3633	136.8572	1.032926	136.63809	141.57507	0.965128	22.51959	195.4644	0.115211
117	0.289498	0.29355	35.6808	205.7492	238.5731	0.862416	231.92119	213.21914	1.087713	64.02057	308.4659	0.207545
118	0.289855	0.293919	35.65967	207.5983	237.604	0.873715	230.81455	215.12168	1.072949	62.12608	309.3429	0.200832
119	0.291609	0.295733	35.55575	210.9104	239.1819	0.881799	231.88862	218.90375	1.059318	61.36162	312.9312	0.196087
120	0.291397	0.295513	35.56834	212.4639	239.7401	0.886226	232.44226	220.42425	1.054522	60.85878	314.5035	0.193507
121	0.259182	0.253601	30.46972	164.0185	204.6764	0.801355	156.97899	210.12399	0.747078	28.74948	260.7067	0.110275
122	0.257622	0.25214	30.55346	156.9543	198.9473	0.788924	153.50033	201.62423	0.761319	29.69354	251.6604	0.11799
123	0.260305	0.254654	30.40943	164.0126	204.252	0.802991	156.34856	210.17645	0.743892	28.45355	260.4024	0.109268
124	0.25974	0.254125	30.43972	160.4036	200.0909	0.801654	153.33952	205.55456	0.74598	28.06316	254.9081	0.110091
125	0.326984	0.316026	26.89306	220.4736	327.797	0.672592	243.04255	311.43185	0.780404	75.8891	387.6859	0.195749

126	0.332889	0.321351	26.58794	215.2296	324.3654	0.663541	239.781	306.6623	0.781906	77.17066	381.5513	0.202255
127	0.323468	0.312845	27.07529	220.194	327.5856	0.672172	243.91672	310.32621	0.786001	75.93733	387.3387	0.196049
128	0.330123	0.318858	26.73076	216.082	326.0836	0.662658	241.90904	307.41172	0.786922	77.78288	383.369	0.202893
129	0.282354	0.282476	32.31533	151.6058	168.2211	0.90123	141.86544	176.51307	0.803711	25.53308	225.0127	0.113474
130	0.277135	0.277347	32.60918	146.7839	166.0048	0.884215	141.32445	170.67663	0.828025	27.0683	219.9328	0.123075
131	0.281163	0.281306	32.38233	146.9341	166.0055	0.885116	140.62448	171.38326	0.820526	26.9693	220.0457	0.122562
132	0.281029	0.281174	32.38989	144.338	164.3728	0.878113	139.44605	168.54282	0.827363	27.46673	217.0195	0.126563
133	0.349345	0.347466	28.59165	236.8788	283.4781	0.835616	223.39742	294.2193	0.759289	55.35197	365.25	0.151545
134	0.351905	0.349916	28.45132	214.2071	283.2421	0.756269	227.56492	272.62603	0.834715	70.19785	348.1135	0.201652
135	0.350877	0.348932	28.50764	214.5849	277.9527	0.772019	222.59393	271.58115	0.819622	65.98601	344.8916	0.191324
136	0.352942	0.350907	28.39452	228.1459	280.1442	0.814387	221.11678	285.72478	0.77388	58.64156	356.5003	0.164492
137	0.321714	0.326821	33.77452	142.2004	138.624	1.025799	129.09146	150.90716	0.855436	23.41172	197.2041	0.118718
138	0.318304	0.323305	33.97598	143.8083	139.2069	1.033054	130.10426	152.09296	0.855426	22.89538	198.8346	0.115148
139	0.322581	0.327715	33.72334	138.5956	137.4517	1.008323	128.02422	147.34826	0.868855	24.67605	193.6306	0.127439
140	0.321714	0.326821	33.77452	142.5478	139.7738	1.019847	130.21621	151.32855	0.860487	24.11239	198.1797	0.121669
141	0.39539	0.402257	29.45238	208.6693	240.2766	0.868454	208.69754	240.25212	0.868661	63.59445	311.8196	0.203946
142	0.358744	0.364883	31.59374	213.1128	241.9158	0.880938	218.70209	236.8749	0.923281	62.18991	316.3428	0.19659
143	0.359819	0.365984	31.53068	223.5601	225.6642	0.990676	201.19126	245.81607	0.818463	42.93667	314.7378	0.13642
144	0.388992	0.395757	29.82481	210.4615	240.6831	0.874434	210.41825	240.72093	0.874117	62.82594	313.4889	0.200409
145	0.251045	0.245962	30.90742	169.8755	207.3908	0.819108	159.78619	215.26032	0.742293	26.52732	266.7676	0.09944
146	0.253165	0.247955	30.79323	157.3445	198.8675	0.791203	154.16963	201.33877	0.765723	29.36119	251.8799	0.116568
147	0.252111	0.246965	30.84995	158.3371	199.3261	0.794362	154.5709	202.26064	0.764216	28.9836	252.9061	0.114602
148	0.251045	0.245962	30.90742	163.7791	203.6206	0.804335	157.61387	208.42939	0.756198	28.17219	259.7908	0.108442
149	0.315383	0.305509	27.49562	221.554	327.4879	0.676526	245.68452	309.79609	0.793052	74.90658	388.2313	0.192943
150	0.319573	0.309316	27.27752	212.997	321.9011	0.661685	241.78662	300.8775	0.803605	77.00683	378.2301	0.203598
151	0.318302	0.308161	27.34365	213.2592	323.4945	0.659236	243.57252	301.33139	0.808321	77.94813	379.5422	0.205374
152	0.315789	0.305878	27.47447	220.5378	327.7031	0.672981	246.08138	308.98252	0.796425	75.77731	387.6649	0.195471
153	0.350877	0.348932	28.50764	147.2193	164.6885	0.893926	127.37452	180.47598	0.70577	25.79394	219.3867	0.117573
154	0.351908	0.349918	28.45115	144.3804	163.1658	0.884869	126.35403	177.49204	0.711886	26.53459	216.2514	0.122703
155	0.358211	0.355936	28.10634	147.3771	165.5226	0.890374	126.88222	181.71033	0.698266	26.31413	220.0575	0.119578
156	0.360146	0.357781	28.00068	146.206	165.4084	0.883909	126.70917	180.77866	0.700908	27.00453	219.1047	0.123249
157	0.421053	0.414941	24.72561	206.6885	277.4002	0.745091	205.94535	277.95238	0.740938	70.80452	338.6115	0.209103
158	0.03928	0.039155	46.2566	211.4821	279.0193	0.757948	295.59506	187.61658	1.575527	68.84084	343.2745	0.200542
159	0.39735	0.392908	25.98805	210.1599	279.7835	0.751152	213.38728	277.32991	0.769435	70.28928	342.7906	0.20505

160	0.393441	0.389248	26.19774	211.7793	279.8148	0.756855	214.00361	278.11734	0.769472	69.23967	344.0242	0.201264
161	0.609143	0.609727	17.56519	146.5446	138.2924	1.059672	80.041557	184.91469	0.432857	20.50402	200.4487	0.102291
162	0.591139	0.593157	18.51459	143.7904	137.3398	1.046968	83.089809	180.64883	0.459952	21.42497	197.6838	0.10838
163	0.576918	0.579933	19.27226	143.8957	137.7245	1.044808	85.803793	179.75458	0.477339	21.66608	198.0015	0.109424
164	0.560742	0.564752	20.14211	143.0282	136.369	1.048832	87.487839	177.19891	0.493727	21.1188	196.4881	0.107481
165	0.57416	0.577356	19.41996	209.8525	239.6368	0.875711	162.67771	273.86098	0.594016	62.36653	312.3688	0.199657
166	0.598507	0.599962	18.12473	211.3141	239.5217	0.882234	155.85228	278.80883	0.558993	61.38544	313.4583	0.195833
167	0.606061	0.606904	17.72695	204.2059	239.3588	0.853137	156.1643	273.13984	0.571738	65.58344	307.7198	0.213127
168	0.59997	0.601309	18.04752	203.6725	236.4964	0.861208	155.16867	270.8057	0.572989	63.63721	305.5542	0.208268
169	0.237164	0.232861	31.65803	169.7086	211.5328	0.80228	166.66117	213.94202	0.779002	29.57418	269.5784	0.109705
170	0.234384	0.230228	31.80889	168.713	209.5218	0.805229	165.49316	212.07422	0.780355	28.85618	267.4524	0.107893
171	0.233918	0.229786	31.83421	199.2841	238.3424	0.836125	186.68672	248.33308	0.751759	27.61839	309.4487	0.08925
172	0.242925	0.238309	31.34592	169.0598	208.7949	0.809693	162.98591	213.56994	0.76315	28.09696	267.1836	0.10516
173	0.278422	0.271544	29.44165	258.7538	356.5159	0.725785	274.04952	344.89706	0.794584	69.12824	435.0614	0.158893
174	0.282686	0.275497	29.21517	251.5998	351.1933	0.716414	269.50827	337.6455	0.798199	70.42324	426.2391	0.16522
175	0.280053	0.273058	29.35493	264.3798	362.7055	0.72891	277.97025	352.39821	0.788796	69.52677	443.4163	0.156798
176	0.28302	0.275807	29.19745	234.6165	336.8478	0.696506	260.22545	317.4808	0.819657	72.28845	404.0863	0.178894
177	0.314134	0.313512	30.53707	175.3697	189.7292	0.924315	152.91602	208.25078	0.734288	25.89534	257.0625	0.100736
178	0.323452	0.322544	30.01958	154.7425	173.9993	0.889328	139.71919	186.27814	0.750057	27.78228	231.1907	0.12017
179	0.310897	0.310367	30.71731	172.0742	187.1837	0.91928	151.6863	204.05517	0.743359	26.17249	252.9076	0.103486
180	0.314169	0.313546	30.53514	159.7156	177.3025	0.900809	143.68671	190.52404	0.754166	26.96097	237.1042	0.113709
181	0.330123	0.32899	29.65024	237.8508	300.9475	0.79034	245.69239	294.58045	0.834042	67.79166	377.5535	0.179555
182	0.328766	0.327681	29.72527	236.1852	299.416	0.78882	244.91853	292.3154	0.837857	67.74824	375.2913	0.180522
183	0.328318	0.327248	29.75005	232.362	294.7718	0.788278	241.27663	287.52061	0.839163	66.80327	369.3506	0.180867
184	0.326531	0.325521	29.849	233.8467	300.6256	0.777867	247.20618	289.73974	0.853201	70.20373	374.3414	0.187539
185	0.449438	0.456639	26.3365	153.2784	147.5701	1.038682	115.1017	178.94911	0.643209	23.76524	211.4389	0.112398
186	0.43956	0.446778	26.90153	150.6276	143.7125	1.048118	113.55658	174.4903	0.65079	22.31848	206.9876	0.107825
187	0.4461	0.453311	26.52721	158.432	145.1639	1.091401	112.35359	183.16643	0.613396	18.71897	214.0628	0.087446
188	0.444444	0.451658	26.62188	165.9224	148.0222	1.120929	114.04947	190.87578	0.597506	16.42676	221.7454	0.074079
189	0.368087	0.374443	31.046	221.3951	248.7817	0.889917	222.31898	247.9564	0.896605	62.59497	327.0932	0.191367
190	0.368664	0.375032	31.01223	224.4462	250.708	0.89525	223.74203	251.33667	0.890208	62.26583	330.6865	0.188293
191	0.3698	0.376193	30.94571	218.6055	248.5284	0.8796	221.95146	245.54489	0.903914	64.09227	324.7259	0.197373
192	0.370944	0.377362	30.87873	217.2157	249.0716	0.872101	222.36406	244.48636	0.909515	65.36926	323.954	0.201786
193	0.156654	0.155391	36.09675	517.1114	614.2253	0.841892	526.79311	605.94219	0.869378	68.6699	799.9759	0.08584

194	0.155848	0.154604	36.14181	502.9318	586.9558	0.856848	502.50876	587.31801	0.855599	59.41394	770.6669	0.077094
195	0.161512	0.160129	35.82529	509.7859	594.4569	0.857566	505.56879	598.04754	0.845366	59.87144	780.8176	0.076678
196	0.160643	0.159282	35.87383	495.9598	585.1861	0.847525	499.11478	582.4975	0.856853	63.09252	764.4856	0.082529
197	0.183629	0.181606	34.59473	720.6149	825.4422	0.873005	681.7177	857.84709	0.794684	74.12409	1093.227	0.067803
198	0.183343	0.181329	34.61059	706.2889	817.3255	0.864146	676.55506	842.10346	0.803411	78.51473	1077.358	0.072877
199	0.186916	0.184784	34.41268	707.3873	821.7188	0.860863	677.7589	846.32231	0.800828	80.84458	1081.241	0.07477
200	0.183486	0.181468	34.60267	701.8244	814.7245	0.861425	674.686	837.33643	0.805753	79.83243	1072.362	0.074445
201	0.190785	0.191495	37.52814	456.4327	473.6966	0.963555	440.94338	488.14773	0.903299	52.33635	655.7287	0.079814
202	0.191699	0.192412	37.47562	441.5375	464.3275	0.950918	432.19508	473.03581	0.913663	55.18913	638.3648	0.086454
203	0.190476	0.191185	37.54589	446.9668	471.7826	0.9474	439.83779	478.43575	0.919325	57.17511	647.3709	0.088319
204	0.193237	0.193953	37.38732	458.9157	476.9485	0.962191	442.80778	491.93984	0.900126	53.1266	659.7432	0.080526
205	0.214857	0.215587	36.14779	767.7241	753.8621	1.018388	678.96369	834.69558	0.813427	55.9	1074.516	0.052023
206	0.226411	0.227113	35.4874	785.3621	773.7482	1.01501	687.22733	862.08962	0.797165	59.10653	1100.903	0.053689
207	0.23011	0.230797	35.27629	766.8541	753.4686	1.017765	665.89267	844.01849	0.788955	56.18171	1073.603	0.05233
208	0.235988	0.236646	34.94117	792.8919	766.3974	1.03457	670.81461	875.24303	0.766432	48.61161	1101.671	0.044125
209	0.242925	0.245346	38.44271	381.7317	352.4286	1.083146	358.66138	375.88165	0.954187	47.21684	517.3931	0.091259
210	0.232099	0.234144	39.08453	383.8462	350.8267	1.094119	361.30658	373.99845	0.966064	44.65881	518.0954	0.086198
211	0.231214	0.233228	39.13701	401.4554	363.2566	1.105157	374.57682	390.91427	0.958207	43.80026	539.6326	0.081167
212	0.244888	0.247378	38.32629	383.7006	355.0451	1.080709	360.54157	378.54061	0.952451	48.09411	520.548	0.092391
213	0.274914	0.278461	36.54538	676.9207	597.6578	1.132623	586.29702	686.78407	0.853685	62.07059	900.8684	0.068901
214	0.238806	0.241083	38.68694	665.2803	578.7986	1.149416	592.45541	653.14793	0.907077	54.19482	880.1526	0.061574
215	0.281353	0.285124	36.16358	669.2921	594.0415	1.126676	578.27014	682.96482	0.846706	63.84559	892.6147	0.071526
216	0.260586	0.263629	37.39517	664.228	595.5344	1.115348	594.31812	665.31645	0.893286	68.11284	889.5058	0.076574
217	0.32	0.309703	27.25533	249.8309	412.0225	0.606353	316.27778	363.51944	0.870044	114.6868	468.001	0.245057
218	0.3125	0.302885	27.64598	255.8747	420.8744	0.60796	325.39516	369.76359	0.880009	116.6724	478.5339	0.243812
219	0.329652	0.318434	26.75508	242.4652	406.1375	0.597003	309.80881	357.42908	0.86677	115.7338	458.6314	0.252346
220	0.313332	0.303643	27.60254	254.7599	420.0415	0.606511	324.65329	368.69731	0.880542	116.8717	477.1566	0.244934
221	0.263158	0.257324	30.25644	666.452	874.2112	0.762347	675.81982	866.98965	0.779502	146.9079	1089.413	0.13485
222	0.260298	0.254647	30.40979	662.1535	860.9833	0.769067	666.41938	857.68567	0.776997	140.5939	1077.02	0.13054
223	0.261153	0.255448	30.36393	639.2833	856.6007	0.746303	667.27109	834.98334	0.799143	153.6666	1057.75	0.145277
224	0.262869	0.257054	30.27191	649.7263	857.5593	0.757646	664.20143	846.39747	0.784739	146.9601	1065.812	0.137886
225	0.351927	0.349936	28.45013	271.7393	359.8381	0.755171	289.18639	345.97246	0.835865	89.44286	441.9567	0.202379
226	0.359279	0.356955	28.048	241.988	339.6372	0.71249	274.02547	314.35911	0.871696	94.02711	406.2887	0.231429
227	0.357143	0.354918	28.16471	269.8115	359.0534	0.751452	287.14044	345.35193	0.831443	90.13255	439.9929	0.20485

228	0.348857	0.347	28.61839	264.9651	360.5959	0.734798	292.45013	338.68692	0.863482	94.49918	437.3852	0.216055
229	0.316631	0.315936	30.39823	535.4526	666.6635	0.803183	551.08543	653.80017	0.842896	144.4998	842.7749	0.171457
230	0.32	0.319202	30.21108	546.939	672.0256	0.813866	551.95674	667.91049	0.826393	140.9046	854.9307	0.164814
231	0.318725	0.317966	30.28187	578.3455	683.5102	0.84614	557.93677	700.26874	0.796747	128.6955	886.0628	0.145244
232	0.320428	0.319617	30.18732	570.8836	682.8362	0.836048	557.58318	693.73934	0.803736	133.1351	880.0274	0.151285
233	0.373832	0.380311	30.70976	310.489	313.6842	0.989814	274.77329	345.39949	0.795523	59.84866	437.2863	0.136864
234	0.372648	0.379102	30.77903	291.6065	304.8991	0.956404	268.67581	325.2862	0.825967	64.37388	416.9578	0.154389
235	0.372648	0.379102	30.77903	298.9395	307.5881	0.971882	270.48815	332.88345	0.812561	62.04321	424.4124	0.146186
236	0.383384	0.390051	30.15173	285.7945	301.329	0.948447	262.30103	321.98729	0.814632	65.07969	410.1735	0.158664
237	0.406793	0.413812	28.79032	572.158	562.4521	1.017256	469.32546	650.73096	0.721228	97.91551	796.3226	0.12296
238	0.390892	0.397689	29.7141	576.6574	564.0873	1.022284	480.76635	647.75915	0.742199	96.47379	800.8876	0.120459
239	0.4	0.406933	29.18446	584.8305	567.9818	1.029664	477.42951	660.82613	0.722474	94.58801	809.7427	0.116812
240	0.39539	0.402257	29.45238	559.0812	559.8631	0.998603	476.08049	631.95398	0.753347	103.8222	784.372	0.132364
241	0.310078	0.300676	27.77251	218.8552	388.7651	0.56295	306.50615	324.17569	0.945494	120.1444	429.6524	0.279632
242	0.319132	0.308915	27.30045	245.6017	408.7615	0.600844	314.74314	358.24979	0.878558	115.3714	462.7047	0.249341
243	0.306904	0.297778	27.93855	223.3659	388.8318	0.574454	306.18464	327.61786	0.934579	117.0021	432.8891	0.270282
244	0.314961	0.305125	27.51762	308.4203	467.6706	0.659482	353.41533	434.66824	0.813069	112.607	548.7791	0.205195
245	0.242914	0.238299	31.34648	722.1704	907.322	0.795936	711.21363	915.93584	0.776488	130.922	1152.225	0.113625
246	0.244151	0.239466	31.27959	780.8907	928.4949	0.841029	716.78514	978.83202	0.732286	104.3719	1208.718	0.086349
247	0.24218	0.237605	31.38625	77.6247	920.489	0.08433	876.35648	292.10428	3.000149	595.9951	705.773	0.844457
248	0.243161	0.238532	31.33314	789.9367	939.8015	0.840536	726.54864	989.62312	0.734167	105.9704	1223.11	0.08664
249	0.377358	0.374112	27.06499	315.5755	394.3218	0.800299	303.20629	403.91032	0.750677	86.22295	497.6376	0.173265
250	0.371519	0.368586	27.38156	343.1757	413.7081	0.829512	317.5016	433.72424	0.732036	82.45395	531.1547	0.155235
251	0.38219	0.378671	26.80373	323.7673	403.0961	0.803201	307.77038	415.43846	0.740833	87.36646	509.5869	0.171446
252	0.378551	0.375238	27.00043	292.1677	378.1007	0.772724	292.90722	377.52809	0.775855	89.58455	469.3578	0.190866
253	0.387721	0.383878	26.50541	644.5256	725.5076	0.888379	534.04751	810.28874	0.659083	116.2975	963.457	0.120709
254	0.391516	0.387442	26.3012	676.7837	722.7649	0.936382	520.05231	842.5977	0.617201	92.86844	985.7996	0.094206
255	0.39604	0.391682	26.05829	680.2568	730.7611	0.930888	523.25827	850.27169	0.615401	96.55593	993.6992	0.097168
256	0.392812	0.388657	26.23157	728.0008	737.6384	0.986935	519.88881	896.55516	0.579874	70.07054	1034.014	0.067766
257	0.542991	0.547924	21.10629	336.5771	331.6785	1.014769	223.19985	416.50523	0.535887	58.24309	468.9376	0.124202
258	0.56338	0.567238	19.99968	315.9533	319.3988	0.989213	209.60481	397.37632	0.527472	61.0559	445.1003	0.137173
259	0.555556	0.559852	20.42282	332.2113	328.1273	1.012446	216.10318	413.92191	0.522087	58.08348	463.3122	0.125366
260	0.533333	0.538697	21.63495	334.792	329.1473	1.01715	225.08653	412.01904	0.546301	57.3216	465.9805	0.123013
261	0.45977	0.466913	25.74783	621.8138	580.89	1.07045	442.0629	727.09419	0.607986	82.31477	846.9415	0.097191

262	0.462428	0.469549	25.59681	623.8742	583.7136	1.068802	442.48285	730.85536	0.605431	83.30061	850.295	0.097967
263	0.458033	0.465189	25.84664	601.268	575.5822	1.044626	442.26785	705.13633	0.627209	90.61124	827.4102	0.109512
264	0.473373	0.480373	24.97664	595.9826	572.6017	1.040833	429.74673	705.96439	0.608737	91.46421	821.4026	0.111351
265	0.342877	0.330315	26.07435	233.9084	409.4519	0.571272	311.45097	354.06537	0.879643	124.128	454.9244	0.272854
266	0.324323	0.313619	27.03095	222.7882	398.1978	0.559491	310.04416	334.76662	0.92615	124.0333	439.1034	0.282469
267	0.325203	0.314416	26.98531	226.5024	394.842	0.573653	305.43742	337.50781	0.904979	119.0341	439.3568	0.270928
268	0.316623	0.306636	27.43104	222.1694	397.9633	0.558266	312.33744	331.93276	0.940966	124.3051	438.5	0.283478
269	0.287424	0.27988	28.96405	599.3386	832.4204	0.719995	634.46823	805.9656	0.787215	164.8137	1012.406	0.162794
270	0.283352	0.276115	29.1798	602.5334	836.5058	0.720298	640.55822	807.75839	0.793007	165.4435	1017.554	0.162589
271	0.285714	0.2783	29.0546	523.1524	787.7618	0.6641	613.73082	719.43837	0.853069	187.1071	926.9563	0.201851
272	0.286395	0.278929	29.01853	601.1962	836.1058	0.719043	638.26569	808.16254	0.789774	166.1062	1016.326	0.163438
273	0.377124	0.37389	27.0777	240.1437	320.3786	0.749562	250.47044	312.37159	0.801835	80.82534	392.1463	0.20611
274	0.40134	0.396637	25.77438	264.7958	360.9705	0.733566	275.69178	352.71883	0.781619	94.89195	437.5066	0.216893
275	0.392157	0.388043	26.26675	234.8687	336.8304	0.697291	263.28401	315.11829	0.835508	96.64236	399.0968	0.242153
276	0.394734	0.390459	26.12833	261.8568	356.5901	0.734336	274.42083	347.01405	0.790806	93.55863	432.403	0.216369
277	0.375587	0.372437	27.16094	564.8871	689.3804	0.819413	528.00458	718.02088	0.735361	142.0099	879.8727	0.161398
278	0.376187	0.373005	27.12841	578.3877	693.3565	0.834185	528.09752	732.3856	0.721065	136.042	892.6187	0.152408
279	0.382164	0.378647	26.80511	568.8106	690.3055	0.823998	523.43466	725.31599	0.721664	140.1029	883.4242	0.158591
280	0.377358	0.374112	27.06499	601.8967	701.2078	0.858371	529.02958	757.69371	0.69821	126.3448	915.4283	0.138017
281	0.504197	0.510572	23.24641	295.0031	311.0694	0.948351	228.85938	362.51122	0.631317	67.20147	423.4087	0.158715
282	0.458012	0.465168	25.84784	303.8519	318.5985	0.953714	250.66392	361.93726	0.692562	67.78791	435.0124	0.15583
283	0.47619	0.483151	24.81746	290.1387	311.6579	0.930953	240.35425	351.4839	0.683827	70.62954	419.9078	0.168202
284	0.436367	0.443581	27.08467	286.0517	305.0642	0.937677	248.32458	336.48868	0.737988	67.88645	412.6514	0.164513
285	0.533333	0.538697	21.63495	558.6203	562.2085	0.993618	388.08158	691.03382	0.561596	105.9635	785.4341	0.134911
286	0.521716	0.527534	22.27453	581.3145	573.8217	1.013058	401.01676	711.60628	0.563537	101.3615	810.5083	0.125059
287	0.539326	0.544427	21.30661	589.7864	573.9172	1.027651	386.66772	726.44133	0.532277	96.27993	817.2877	0.117804
288	0.541763	0.546753	21.17336	569.3478	563.0453	1.011194	380.28929	704.66805	0.539672	100.0969	794.4543	0.125995
289	0.147417	0.146362	36.61405	596.8598	523.5713	1.139978	430.92709	666.83609	0.646226	-51.8228	792.2644	-0.06541
290	0.148148	0.147078	36.57303	616.3077	535.1927	1.151562	439.0954	688.08548	0.638141	-57.357	814.2337	-0.07044
291	0.151324	0.150184	36.39508	543.6471	497.6703	1.092384	410.72763	611.98915	0.671135	-32.5105	736.3226	-0.04415
292	0.147965	0.146899	36.58329	547.3946	502.9702	1.088324	417.4301	615.11949	0.678616	-31.4128	742.7201	-0.04229
293	0.207437	0.204536	33.28096	466.1516	656.3718	0.710194	548.00868	589.75227	0.929218	134.506	793.7439	0.169458

294	0.207254	0.204361	33.291	872.2132	871.4515	1.000874	676.30948	1030.9166	0.656027	-0.5386	1232.957	-0.00044
295	0.203562	0.200819	33.49395	594.1015	658.8432	0.901734	527.09654	713.58264	0.738662	45.7793	885.9657	0.051672
296	0.206009	0.203167	33.35939	869.8085	895.6769	0.971119	701.75188	1032.6414	0.67957	18.29172	1248.387	0.014652
297	0.157274	0.157828	39.45712	580.2724	428.4443	1.354371	407.48685	595.1765	0.684649	-63.6143	718.4941	-0.08854
298	0.160862	0.161439	39.25025	552.4804	419.8022	1.316049	397.79078	568.53409	0.699678	-51.6713	691.9527	-0.07467
299	0.163039	0.163628	39.1248	585.5564	426.5744	1.372694	401.9406	602.73195	0.666865	-68.516	721.2126	-0.095
300	0.165289	0.165891	38.99514	567.1553	416.9809	1.360147	391.79539	584.83718	0.669922	-63.5082	701.0741	-0.09059
301	0.219382	0.220104	35.88896	434.3384	525.5411	0.82646	480.55568	483.64194	0.993619	105.8056	673.5343	0.157009
302	0.217002	0.217728	36.02508	457.1108	521.8519	0.87594	475.85834	504.81534	0.942638	87.95321	688.1453	0.127812
303	0.21978	0.220501	35.86622	491.3853	580.9249	0.845867	529.87975	546.04092	0.970403	109.4853	752.9583	0.145407
304	0.216415	0.217142	36.05866	478.4361	561.1532	0.852594	513.25607	529.49234	0.969336	103.2575	730.1588	0.141418
305	0.186341	0.186905	41.79112	558.4661	103.6248	5.389312	145.12108	549.14696	0.264266	-257.762	506.1437	-0.50927
306	0.175623	0.175881	42.42276	440.3626	273.7383	1.608699	310.51724	415.24798	0.747787	-50.9046	516.0044	-0.09865
307	0.197375	0.198273	41.13977	441.1333	253.8852	1.737533	281.37773	424.12599	0.66343	-67.1242	504.5301	-0.13304
308	0.186916	0.187497	41.75722	401.4309	192.6622	2.083599	221.93058	386.02114	0.574918	-91.5264	435.7619	-0.21004
309	0.252892	0.255664	37.85154	346.3527	362.4327	0.955633	364.55097	344.12243	1.059364	76.69107	495.4151	0.154802
310	0.251842	0.254576	37.91387	439.4914	392.3235	1.120227	395.48784	436.64601	0.90574	43.70572	587.5033	0.074392
311	0.253437	0.256228	37.81923	395.0583	364.8773	1.082715	367.07272	393.01921	0.933982	48.98037	535.544	0.091459
312	0.248957	0.25159	38.08494	377.5662	351.744	1.073412	355.58017	373.9556	0.950862	49.20951	513.6716	0.0958
313	0.158316	0.157012	36.00385	338.1305	189.097	1.788133	133.89808	363.53984	0.368317	-105.383	372.8061	-0.28267
314	0.156458	0.1552	36.10772	348.3737	170.9871	2.037427	115.08129	370.61721	0.310513	-125.431	367.2435	-0.34155
315	0.15625	0.154997	36.11934	333.2833	150.3163	2.217213	97.063077	352.49327	0.275362	-129.377	341.9566	-0.37834
316	0.161725	0.160336	35.8134	377.2822	364.3751	1.035423	299.46828	430.61563	0.695442	-9.1267	524.4309	-0.0174
317	0.209974	0.206967	33.14166	457.3035	575.1828	0.795058	468.93513	565.73986	0.828888	83.35325	730.0781	0.11417
318	0.207612	0.204704	33.27132	495.4884	563.8183	0.878809	451.32485	599.75471	0.752516	48.31654	749.043	0.064504
319	0.210341	0.207319	33.12149	460.0241	549.9596	0.836469	443.49281	563.37542	0.787207	63.594	714.1663	0.089046
320	0.208152	0.205222	33.24165	455.1406	565.715	0.80454	461.09338	560.87371	0.822098	78.18791	721.8539	0.108315
321	0.176991	0.177652	38.3213	326.2954	331.9	0.983113	313.2962	344.19733	0.910223	32.36855	464.3044	0.069714

322	0.177253	0.177915	38.30623	194.8574	271.8488	0.716786	260.57046	209.70024	1.242585	74.4863	326.072	0.228435
323	0.179104	0.179774	38.19973	275.031	314.6797	0.874003	298.32465	292.69055	1.019249	53.44016	414.4991	0.128927
324	0.178047	0.178712	38.26055	264.9514	305.4686	0.86736	290.00834	281.78969	1.029166	53.22035	400.8464	0.13277
325	0.237628	0.238277	34.84773	150.6182	393.8514	0.382424	373.75166	195.22918	1.914425	195.1746	373.7802	0.522164
326	0.23786	0.238507	34.83454	148.3051	374.2148	0.39631	354.47134	190.73851	1.858415	182.0004	359.0361	0.506914
327	0.234375	0.235041	35.03312	138.1206	382.5365	0.361065	364.5461	180.32641	2.02159	194.9814	356.9226	0.546285
328	0.235294	0.235956	34.98072	155.9915	386.5958	0.4035	366.38509	198.87601	1.842279	186.1801	372.9969	0.499146
329	0.184621	0.185135	41.89257	264.1371	256.3814	1.030251	275.85849	243.72509	1.131843	42.60451	365.6292	0.116524
330	0.1821	0.18254	42.04123	428.5545	294.7198	1.454109	327.72595	403.87426	0.811455	-27.0706	519.4092	-0.05212
331	0.183217	0.183689	41.97534	399.2506	284.1405	1.405117	314.42769	375.8618	0.836551	-17.6246	489.7206	-0.03599
332	0.173913	0.174124	42.52345	429.4183	289.807	1.481739	326.29521	402.3924	0.810888	-31.494	517.1038	-0.0609
333	0.270819	0.274222	36.78822	277.6112	362.4715	0.765884	358.99494	282.09261	1.272614	118.569	440.9025	0.268923
334	0.267255	0.270532	36.99964	265.322	358.5641	0.739957	356.23339	268.4432	1.327035	122.9502	428.7741	0.286748
335	0.273038	0.276518	36.65666	263.7127	351.1049	0.751094	347.18545	268.8519	1.291363	118.0121	422.9565	0.279017
336	0.269669	0.273032	36.85644	307.5364	335.3182	0.917148	331.84282	311.28327	1.066048	78.80954	448.1138	0.175869
337	0.192925	0.190584	34.08035	569.192	515.2243	1.104746	398.0722	656.4862	0.606368	-38.1609	766.7981	-0.04977
338	0.194175	0.191788	34.01135	573.9338	518.5329	1.106842	399.62544	662.25062	0.603435	-39.1744	772.4906	-0.05071
339	0.193862	0.191487	34.0286	612.6996	530.6029	1.154723	404.29635	702.48466	0.575523	-58.0511	808.437	-0.07181
340	0.192925	0.190584	34.08035	554.8034	504.8034	1.099048	390.56565	640.38407	0.609893	-35.3553	749.2552	-0.04719
341	0.218221	0.214853	32.68981	119.802	380.7269	0.314666	346.43083	198.22	1.747709	184.5018	353.9274	0.521298
342	0.217391	0.214061	32.73523	110.2787	428.211	0.257534	395.0112	198.72645	1.987713	224.8121	380.7697	0.590415
343	0.217984	0.214626	32.70282	94.613	420.5035	0.224999	390.70461	182.00199	2.146705	230.4394	364.2424	0.632654
344	0.21838	0.215005	32.68115	149.615	442.9037	0.337805	400.7854	240.6645	1.665328	207.3864	418.974	0.494986
345	0.239521	0.240158	34.73998	445.7696	379.9086	1.17336	324.79544	487.39003	0.666397	-10.8411	585.5968	-0.01851
346	0.246914	0.247496	34.31952	220.5821	284.7244	0.774721	254.91969	254.44131	1.00188	67.08387	353.8703	0.189572
347	0.248447	0.249017	34.23239	214.0442	279.8892	0.764746	250.56321	247.73164	1.01143	67.79468	345.7698	0.196069
348	0.243408	0.244017	34.51883	243.1209	288.912	0.841505	257.22039	276.43372	0.930496	55.28553	373.5257	0.14801
349	0.232558	0.233234	35.13666	142.0414	393.1293	0.36131	374.96442	184.73795	2.02971	200.317	366.8781	0.546004
350	0.232333	0.23301	35.1495	131.2055	359.637	0.364828	342.91759	170.17997	2.015029	182.4128	336.5698	0.541976
351	0.23166	0.23234	35.18789	185.1462	424.8827	0.435758	401.95113	230.73728	1.742029	195.5367	420.2021	0.46534

352	0.232113	0.232791	35.16206	135.5963	378.0382	0.358684	360.75885	176.50011	2.043958	193.2851	352.0513	0.549025
353	0.512821	0.51894	22.76695	265.0363	255.2859	1.038194	179.48953	321.24543	0.55873	41.1881	365.6756	0.112636
354	0.508518	0.514769	23.00594	237.8886	239.3135	0.994046	172.15831	290.21281	0.593214	45.04273	334.4146	0.134691
355	0.487805	0.494566	24.16345	295.4874	270.6387	1.091815	195.17989	349.94707	0.557741	34.83077	399.1804	0.087256
356	0.5	0.506485	23.48053	377.21	288.2352	1.308688	188.26994	435.7996	0.43201	-0.95856	474.7272	-0.00202
357	0.47619	0.483151	24.81746	158.343	279.5862	0.566348	238.00066	215.86252	1.102557	125.4175	295.8233	0.423961
358	0.467836	0.474904	25.28999	158.8285	297.4367	0.533991	257.11681	218.14219	1.178666	139.2837	307.0751	0.453582
359	0.466924	0.474002	25.34168	160.7763	315.6339	0.509376	274.69233	223.64681	1.228242	152.5348	319.6981	0.477121
360	0.475246	0.48222	24.87082	188.5641	303.378	0.621548	254.81022	250.3325	1.017887	125.8954	334.2827	0.376614
361	0.280387	0.273367	29.3372	211.057	330.4854	0.638627	261.23336	292.44279	0.89328	84.44863	382.9283	0.220534
362	0.290558	0.282772	28.79834	210.2753	321.8856	0.653261	250.43131	291.73653	0.858416	78.9204	376.2946	0.20973
363	0.275228	0.268578	29.6116	256.9295	352.5296	0.728817	271.71206	341.26594	0.796189	67.59948	430.9527	0.156861
364	0.269663	0.263398	29.90843	394.8416	426.4477	0.925885	308.93803	492.25484	0.627598	22.34889	580.7392	0.038484
365	0.248705	0.24376	31.03316	214.1733	474.0729	0.451773	408.36676	322.26062	1.267194	183.7768	486.6636	0.377626
366	0.257787	0.252294	30.5446	131.7219	479.6725	0.274608	431.6059	247.29075	1.745338	246.0382	432.3211	0.56911
367	0.255048	0.249724	30.69185	307.9192	536.7797	0.573642	444.0309	431.0258	1.030172	161.8288	597.2923	0.270937
368	0.253968	0.24871	30.74997	206.8685	528.9951	0.391059	461.79685	330.71749	1.396348	227.7779	520.3341	0.437753
369	0.226416	0.227118	35.48711	280.7418	316.2339	0.887766	285.0858	312.3235	0.91279	50.82005	419.8061	0.121056
370	0.229009	0.2297	35.33913	294.7211	324.4771	0.908296	290.97355	327.84195	0.887542	47.73088	435.7381	0.10954
371	0.231214	0.231896	35.21332	309.9932	328.7911	0.942827	292.86864	344.13271	0.851034	40.84226	450.0347	0.090754
372	0.232558	0.233234	35.13666	388.4026	360.922	1.07614	315.65054	426.01175	0.740943	12.95122	530.0505	0.024434
373	0.239521	0.240158	34.73998	136.998	360.7374	0.379772	342.10335	178.50836	1.916456	179.3987	341.6373	0.525115
374	0.238569	0.239211	34.7942	141.374	360.3099	0.392368	341.33658	182.48069	1.870535	176.1789	344.6315	0.51121
375	0.241206	0.241832	34.64407	129.2606	352.9376	0.366242	334.9837	170.46758	1.965087	178.684	330.674	0.540363
376	0.240481	0.241112	34.68531	153.9746	367.0113	0.419537	346.14796	196.43585	1.762143	172.8485	358.5092	0.482131
377	0.190476	0.191163	41.54715	282.2362	264.6987	1.066255	283.95807	262.8507	1.080302	38.18505	385.0514	0.099169
378	0.1999	0.200877	40.99057	253.7767	253.8329	0.999779	268.81301	237.85149	1.130172	46.8897	355.8583	0.131765
379	0.199667	0.200637	41.00433	240.336	258.2084	0.930783	272.41591	224.10388	1.215579	58.54321	347.8587	0.168296
380	0.19802	0.198938	41.10167	278.3044	261.1489	1.065693	278.11605	261.34942	1.064154	37.76234	379.7711	0.099434
381	0.217785	0.219344	39.93253	156.3812	279.311	0.559882	285.69654	144.38549	1.978707	126.3935	294.0993	0.429765
382	0.215831	0.217324	40.04823	151.3919	286.4654	0.528483	292.91301	138.50592	2.114805	135.1067	294.4964	0.458772
383	0.220994	0.222661	39.74249	184.3471	306.9256	0.600625	313.90385	172.19623	1.822943	131.2771	333.0968	0.394111
384	0.220183	0.221822	39.79055	157.2726	285.0741	0.55169	291.13204	145.75345	1.997428	130.423	298.3149	0.437199

Run	Beta (degrees)	Shear Area, As	Shear Area, As P	Shear Stress, Ts Merchant (Mpa)	Shear Stress, Ts (Payton) (Mpa)	Shear Stress, Ts (Payton) corrected (Mpa)	χ	λ	Friction Co-efficient	Normal Stress σ (Merchant)	Shear Strain ϒ (Merchant)	Normal Stress σ (Payton)	Shear Strain ϒ (Payton)
1	40.51803	0.001292	0.001796	229.8716	28.68013	20.63888	4.481966	85.51803	0.707173	184582.9	5.480482	236056.3	2
2	38.60973	0.001212	0.00168	227.2958	39.38212	28.40994	6.390269	83.60973	0.673867	174953	5.15202	226863.2	2
3	39.43336	0.001226	0.0017	221.0662	33.87209	24.42364	5.566643	84.43336	0.688242	174383.5	5.209601	224217.3	2
4	39.51342	0.001291	0.001794	213.7002	31.93889	22.98493	5.486576	84.51342	0.689639	165642	5.474215	214525.1	2
5	34.81643	0.001921	0.00263	215.1323	58.31278	42.58425	10.18357	79.81643	0.607661	161288.2	4.133065	209433.8	2
6	35.48624	0.001892	0.002588	218.6019	56.42635	41.24914	9.513759	80.48624	0.619352	169174.5	4.074795	217221.4	2
7	34.82111	0.001877	0.002566	220.2633	60.10735	43.96447	10.17889	79.82111	0.607743	167204.8	4.04455	215980.3	2
8	35.6493	0.018906	0.026729	27.84431	5.672516	4.012368	9.350701	80.6493	0.622198	13588.12	39.4004	22225	2
9	42.98177	0.001048	0.001391	237.0955	34.90898	26.30116	5.518232	84.48177	0.750173	177354.2	4.359169	233121	1.769451
10	42.19676	0.00105	0.001394	239.4395	39.60097	29.83449	6.303237	83.69676	0.736472	174038.2	4.36871	231299.8	1.769451
11	42.42359	0.001044	0.001386	240.7108	38.61439	29.09544	6.076412	83.92359	0.740431	176834.7	4.344861	234023.6	1.769451
12	41.9269	0.001036	0.001375	246.3262	42.40461	31.95798	6.5731	83.4269	0.731762	178500.3	4.311499	237422.4	1.769451
13	38.44156	0.001788	0.00236	223.9982	57.38255	43.46297	10.05844	79.94156	0.670932	155068.9	3.73818	208711.1	1.769451
14	38.35266	0.001778	0.002347	225.7707	58.33679	44.19551	10.14734	79.85266	0.66938	156267.4	3.719524	210283.9	1.769451
15	37.95738	0.001767	0.002331	222.3023	59.33247	44.96256	10.54262	79.45738	0.662481	152316.7	3.696227	205680.7	1.769451
16	37.95142	0.001769	0.002334	222.7847	59.46447	45.06001	10.54858	79.45142	0.662377	152501.9	3.700884	206019	1.769451
17	46.25951	0.000978	0.001233	236.5074	36.65547	29.08355	6.240492	83.75951	0.807381	155074.1	3.936908	216265.9	1.534654
18	47.12791	0.000964	0.001215	240.9675	32.80388	26.0264	5.372088	84.62791	0.822537	164106.6	3.878588	225059.3	1.534654
19	46.77396	0.000993	0.001251	238.6821	34.13768	27.08743	5.726037	84.27396	0.81636	158166	3.995338	219644.7	1.534654
20	46.93557	0.000976	0.00123	237.5743	33.26782	26.39546	5.564432	84.43557	0.81918	159694.6	3.92718	220305.4	1.534654
21	42.59119	0.001667	0.0021	227.4295	54.70985	43.42421	9.908812	80.09119	0.743356	143330.5	3.355572	202056.9	1.534654
22	43.09761	0.001673	0.002107	228.0273	52.47589	41.64975	9.402386	80.59761	0.752195	145958	3.367443	204450.7	1.534654
23	42.34586	0.001683	0.00212	225.3146	55.14638	43.76709	10.15414	79.84586	0.739075	139985.9	3.387403	198647.8	1.534654
24	42.56114	0.001667	0.0021	226.5693	54.63856	43.36762	9.938861	80.06114	0.742832	142638.6	3.355572	201171.2	1.534654
25	41.90732	0.001411	0.001966	205.4896	17.88911	12.83668	3.092682	86.90732	0.731421	167888.8	5.964312	213610	2
26	39.15241	0.001383	0.001926	213.7876	33.29785	23.90789	5.847595	84.15241	0.683338	159486	5.851211	209757.5	2
27	39.05784	0.001363	0.001898	214.699	34.01392	24.43307	5.942163	84.05784	0.681688	160456.2	5.770488	210834.3	2
28	38.7	0.001	0.001	208.75	34.60	24.855	6.255	83.74	0.676	154381.	5.76245	20365	2

	446	361	895	62	073	73	398	46	221	6	4	2.6	
29	35.81876	0.002016	0.002769	216.1099	53.19563	38.72878	9.181243	80.81876	0.625155	163784.1	4.324323	21233 6.6	2
30	35.638	0.001997	0.002741	218.9118	54.88723	39.98384	9.361996	80.638	0.622001	165649.2	4.285178	21478 4.9	2
31	35.08433	0.002018	0.002772	213.3373	55.82242	40.63891	9.915667	80.08433	0.612337	157472.7	4.328153	20602 0.5	2
32	35.85709	0.00201	0.002761	218.032	53.53314	38.98126	9.142913	80.85709	0.625824	165701.9	4.312647	21459 5.1	2
33	43.17878	0.000999	0.001325	261.3092	37.76029	28.48692	5.321216	84.67878	0.753612	201452.9	4.162715	26155 5.2	1.769451
34	41.85123	0.000982	0.0013	255.1751	45.03643	33.99477	6.648775	83.35123	0.730442	189402.7	4.091514	24926 2.5	1.769451
35	41.87136	0.000978	0.001295	256.24	45.15928	34.09187	6.628641	83.37136	0.730793	190720.3	4.075573	25070 8.4	1.769451
36	42.47413	0.001003	0.00133	253.3048	40.79151	30.77018	6.025868	83.97413	0.741313	190105	4.17837	24930 7.2	1.769451
37	39.22551	0.001743	0.002299	232.8915	56.31984	42.70469	9.274491	80.72551	0.684614	168089.7	3.649711	22250 7.6	1.769451
38	38.98497	0.001736	0.002288	231.3555	57.20007	43.38097	9.515026	80.48497	0.680416	166005.3	3.634153	22017 0.1	1.769451
39	38.90854	0.001741	0.002296	231.928	57.65098	43.71627	9.591459	80.40854	0.679082	165650.1	3.645763	22010 4.3	1.769451
40	39.17645	0.001716	0.002262	238.7385	58.27611	44.22011	9.323553	80.67645	0.683758	173587.3	3.59559	22900 3.4	1.769451
41	46.50923	0.000797	0.001003	282.1445	44.92122	35.67321	5.990768	84.00923	0.811739	209699.9	3.209754	27616 7.4	1.534654
42	47.14781	0.000771	0.000971	291.1657	42.50082	33.76864	5.352188	84.64781	0.822885	226109	3.108312	29267 8.1	1.534654
43	50.56165	0.000777	0.000978	275.524	15.68668	12.46205	1.938 35	88.06165	0.882467	240680.8	3.131699	29903 5.7	1.534654
44	47.20144	0.000801	0.001008	281.5312	40.1483	31.88072	5.298564	84.70144	0.823 82	213739.4	3.225621	27929 2.1	1.534654
45	42.04105	0.001 46	0.001835	249.5456	65.4931	52.09879	10.45895	79.54105	0.733755	168101.6	2.945662	22889 4.7	1.534654
46	42.57609	0.001466	0.001843	248.1598	62.35112	49.59438	9.923912	80.07609	0.743093	169849.1	2.957202	22992 0.6	1.534654
47	43.45717	0.001 47	0.001848	253.1132	58.90875	46.85324	9.042828	80.95717	0.758471	178338.3	2.964825	23880 2.3	1.534654
48	43.73641	0.001458	0.001833	253.7045	57.72189	45.91853	8.763 59	81.23641	0.763344	181526.3	2.941741	24157 0.1	1.534654
49	39.81156	0.001 21	0.001677	227.8299	32.91733	23.74787	5.188442	84.81156	0.694843	183151.7	5.144012	23387 7.4	2
50	38.91649	0.001236	0.001714	228.9738	37.84382	27.27922	6.083506	83.91649	0.679221	176785.2	5.24802	22908 4	2
51	39.48894	0.001222	0.001694	235.1044	35.73774	25.77251	5.511061	84.48894	0.689212	186092.7	5.191985	23896 8	2
52	40.11634	0.001214	0.001683	237.7466	32.52677	23.463	4.883659	85.11634	0.700162	192961	5.160016	24560 2.2	2
53	34.91007	0.001726	0.002345	236.9532	66.04418	48.61797	10.08993	79.91007	0.609296	189160.4	3.743673	23944 9.8	2
54	34.90508	0.001736	0.002359	236.6354	65.85037	48.45288	10.09492	79.90508	0.609209	188255.3	3.76277	23862 6.5	2
55	35.57175	0.001728	0.002348	241.145	63.73607	46.91459	9.428254	80.57175	0.620844	196992.6	3.747414	24762 7.7	2
56	35.34334	0.001741	0.002367	235.4917	63.23832	46.51819	9.656664	80.34334	0.616858	189931.1	3.774238	23977 4.8	2
57	42.21061	0.000849	0.001119	285.1554	50.31714	38.19956	6.289386	83.71061	0.736714	232301.6	3.560851	29454 2.9	1.769451
58	44.09924	0.000867	0.001143	276.9508	35.454	26.88999	4.400 76	85.59924	0.769677	238610.5	3.630207	29721 6.2	1.769451
59	42.76044	0.000873	0.001151	284.3663	45.90919	34.80904	5.739559	84.26044	0.746 31	232501.9	3.653568	29468 3	1.769451
60	45.39815	0.000859	0.001132	279.236	26.09655	19.80109	3.101852	86.89815	0.792347	253687	3.599459	31069 0.1	1.769451
61	38.42768	0.001 37	0.001778	262.0262	74.33205	57.25597	10.07232	79.92768	0.670 69	215896.1	2.913337	26997 9.3	1.769451

62	37.99501	0.001325	0.001714	265.8687	79.1572	61.16565	10.50499	79.49501	0.663138	221442.9	2.826159	275410.1	1.769451
63	39.16776	0.001349	0.001749	267.7267	72.15322	55.65557	9.33224	80.66776	0.683606	229286.9	2.873264	283266.6	1.769451
64	38.59298	0.001328	0.00172	268.2423	76.28866	58.93285	9.907023	80.09298	0.673575	227786.9	2.833313	281804.7	1.769451
65	46.19011	0.000595	0.000741	319.9414	61.27374	49.18933	6.309886	83.69011	0.80617	294560.9	2.42309	357505	1.534654
66	46.24283	0.000574	0.000713	323.8833	63.04341	50.74198	6.257169	83.74283	0.80709	309190.4	2.344628	370954.5	1.534654
67	46.37218	0.000569	0.000706	324.3868	62.47342	50.32303	6.127817	83.87218	0.809347	314272.4	2.32345	375421.6	1.534654
68	46.49802	0.000563	0.000698	325.5363	62.05244	50.02544	6.00198	83.99802	0.811544	320122.2	2.302361	380769.2	1.534654
69	42.75341	0.001046	0.001288	292.6641	86.52451	70.26089	9.746589	80.25341	0.746188	270329.5	2.154613	324981.7	1.534654
70	42.96367	0.001044	0.001286	295.1993	85.97355	69.82739	9.536335	80.46367	0.749857	275348.8	2.151252	330169.5	1.534654
71	42.28377	0.00103	0.001266	290.3211	89.93872	73.16852	10.21623	79.78377	0.737991	268227.5	2.124508	321965.5	1.534654
72	41.61476	0.00105	0.001293	286.9222	91.7958	74.51204	10.88524	79.11476	0.726315	253151.3	2.161344	307967.9	1.534654
73	38.14873	0.000931	0.001273	315.8945	62.73343	45.90937	6.851265	83.14873	0.665821	271243.7	4.016667	336853.8	2
74	40.07188	0.000928	0.001267	298.8588	44.8356	32.82117	4.928121	85.07188	0.699386	276049.1	4.001206	335474	2
75	40.79948	0.000949	0.001298	329.1895	42.51747	31.07486	4.200519	85.79948	0.712085	308447.4	4.086438	373487	2
76	41.05532	0.000935	0.001278	312.5054	38.36938	28.07113	3.944675	86.05532	0.716551	298050.7	4.032138	358985.3	2
77	36.37764	0.001894	0.002591	236.7039	56.46182	41.27217	8.622359	81.37764	0.63491	188985	4.078683	240227.6	2
78	35.93154	0.00189	0.002585	233.0409	57.92253	42.34587	9.068461	80.93154	0.627124	183325.9	4.070915	234129.5	2
79	45.68718	0.001904	0.002605	224.9141	-5.4432	-3.97746	-0.68718	90.68718	0.797392	254323.5	4.098086	292786.1	2
80	33.58559	0.001905	0.002608	242.3613	71.92729	52.55512	11.41441	78.58559	0.586179	174734.3	4.101978	229842.8	2
81	40.96569	0.00074	0.000967	328.6042	71.41603	54.66751	7.534311	82.46569	0.714986	280237.3	3.127584	348360.5	1.769451
82	42.25222	0.000765	0.001001	311.9295	57.12586	43.62884	6.247781	83.75222	0.73744	272375	3.225302	336644	1.769451
83	41.33326	0.000761	0.000996	314.1167	64.69412	49.42542	7.166739	82.83326	0.721401	266190.1	3.210254	331940.3	1.769451
84	41.65594	0.000759	0.000993	306.3337	60.78226	46.44467	6.844063	83.15594	0.727033	263109.7	3.202715	326723.5	1.769451
85	39.81296	0.001518	0.001987	270.0668	65.16096	49.79051	8.687041	81.31296	0.694867	217055.7	3.202715	275143.9	1.769451
86	39.44104	0.001522	0.001992	264.6262	65.95908	50.39185	9.058962	80.94104	0.688376	209519	3.210238	266898.5	1.769451
87	39.23005	0.001532	0.002005	267.6319	67.7707	51.75438	9.269946	80.73005	0.684694	209424.6	3.229078	267881.1	1.769451
88	38.90166	0.001537	0.002013	262.3325	68.18613	52.05889	9.598344	80.40166	0.678962	202389.6	3.240391	260135.9	1.769451
89	44.53683	0.00058	0.000721	335.2477	78.98864	63.52785	7.963171	82.03683	0.777314	297541.7	2.365906	364300.4	1.534654
90	44.74765	0.000593	0.000739	336.5348	76.53006	61.45023	7.752346	82.24765	0.780994	294680	2.415905	362683.1	1.534654
91	44.86736	0.000587	0.000731	341.241	77.07695	61.93128	7.632641	82.36736	0.783083	302820.3	2.394409	371073.6	1.534654
92	45.33204	0.000582	0.000724	337.4186	72.85418	58.57985	7.167957	82.83204	0.791193	307418.1	2.373004	373744.7	1.534654
93	42.45212	0.00127	0.001588	281.5877	75.89323	60.68955	10.04788	79.95212	0.740929	213902.2	2.576093	276333.9	1.534654
94	42.63615	0.001295	0.001621	273.991	72.11315	57.61127	9.863849	80.13615	0.744141	206182.8	2.624204	267570.1	1.534654

95	43.15852	0.001276	0.001596	284.9252	72.34108	57.83564	9.341482	80.65852	0.753258	221096.3	2.587164	283718.1	1.534654
96	43.45992	0.001264	0.001581	285.133	70.8439	56.66515	9.040082	80.95992	0.758519	225333.1	2.565039	287273.3	1.534654
97	38.93589	0.001081	0.001049	231.7012	39.55319	28.68477	6.064108	83.93589	0.67956	189745	4.617794	240203.2	2
98	38.65784	0.001091	0.001505	225.9493	39.97596	28.97693	6.342155	83.65784	0.674707	182374.4	4.660479	232045.6	2
99	38.49937	0.001063	0.001465	233.4067	42.49281	30.84328	6.500626	83.49937	0.671941	189632.1	4.546752	240592	2
100	39.26021	0.001075	0.001482	233.297	38.03704	27.59304	5.739788	84.26021	0.68522	193787.8	4.594095	244143.3	2
101	33.09901	0.001842	0.002515	212.247	65.67622	48.10258	11.90099	78.09901	0.577687	153186.2	3.97421	201050.7	2
102	33.30296	0.001917	0.002625	207.3469	62.58422	45.70966	11.69704	78.30296	0.581246	147544.5	4.125365	195023.1	2
103	33.01246	0.001871	0.002557	209.3831	64.84265	47.43895	11.98754	78.01246	0.576176	149399.6	4.032231	197023.6	2
104	33.16313	0.001853	0.002531	211.9701	65.20075	47.73266	11.83687	78.16313	0.578806	152811.5	3.9974	200708.1	2
105	42.30076	0.000991	0.001314	230.0009	38.09546	28.74666	6.19924	83.80076	0.738288	172577.6	4.130955	226269.2	1.769451
106	42.00778	0.001021	0.001354	223.8742	38.28191	28.86265	6.492221	83.50778	0.733174	163865.8	4.249624	217033.2	1.769451
107	40.85196	0.000994	0.001317	224.2656	44.45425	33.5423	7.648042	82.35196	0.713001	159703	4.141381	213581.1	1.769451
108	41.3263	0.001013	0.001343	223.6413	41.76787	31.49811	7.173697	82.8263	0.72128	160455.2	4.216353	214097.5	1.769451
109	37.10249	0.001745	0.002302	214.2117	61.01068	46.25916	11.39751	78.60249	0.647561	143438.8	3.653661	195255.7	1.769451
110	36.47999	0.001741	0.002296	214.7931	63.7966	48.37644	12.02001	77.97999	0.636696	140918.2	3.645763	193305.9	1.769451
111	36.61408	0.001709	0.002251	217.4398	64.38931	48.86936	11.88592	78.11408	0.639036	144915.7	3.580145	197368.5	1.769451
112	36.99976	0.001736	0.002288	215.1811	61.81994	46.88471	11.50024	78.49976	0.645768	144034.9	3.634153	196030.8	1.769451
113	46.4044	0.00093	0.001172	231.9357	35.68712	28.3125	6.095604	83.9044	0.80991	156911.4	3.742965	215596.6	1.534654
114	46.27399	0.0009	0.001134	236.1912	37.37701	29.65415	6.22601	83.77399	0.807633	161926.3	3.622461	221039.9	1.534654
115	45.45383	0.000904	0.001139	232.9718	41.02919	32.55143	7.046166	82.95383	0.793319	154831.3	3.638334	214157.4	1.534654
116	45.92789	0.000922	0.001162	229.7163	37.85999	30.03638	6.572111	83.42789	0.801593	153558.6	3.710613	212009.4	1.534654
117	40.775	0.001659	0.00209	216.7001	59.81887	47.48143	11.725	78.275	0.711658	128532.3	3.339915	185948.7	1.534654
118	41.14422	0.001657	0.002087	215.9292	58.11954	46.13312	11.35578	78.64422	0.718102	129837.4	3.335884	186704.9	1.534654
119	41.40583	0.001647	0.002075	218.2336	57.74826	45.84116	11.09417	78.90583	0.722668	132911.6	3.316218	190002.1	1.534654
120	41.5482	0.001648	0.002076	218.5969	57.23373	45.43239	10.9518	79.0482	0.725153	133738.3	3.318587	190819.1	1.534654
121	38.70712	0.000957	0.00131	254.3601	46.58407	34.0283	6.292877	83.70712	0.675567	219659.8	4.117482	272538	2
122	38.27076	0.000962	0.001317	247.3207	47.84241	34.93428	6.729244	83.27076	0.667951	209585.5	4.139272	261597.5	2
123	38.76416	0.000953	0.001304	254.3671	46.29174	33.82401	6.235835	83.76416	0.676562	220606.6	4.101955	273325	2
124	38.71753	0.000955	0.001307	248.9648	45.56384	33.28757	6.282466	83.71753	0.675748	215317	4.10974	267014.5	2
125	33.92446	0.001544	0.002076	243.9174	76.16227	56.66081	11.07554	78.92446	0.592093	201646.6	3.385234	251019.7	2
126	33.56589	0.001552	0.002039	244.5599	78.70869	58.65819	11.43411	78.56589	0.585835	201789.4	3.336889	251067.7	2
127	33.90791	0.001556	0.002099	242.4125	75.46902	56.08702	11.09209	78.90791	0.591805	198975.4	3.414968	248354.3	2
128	33.53078	0.001531	0.002056	244.8821	78.73882	58.63217	11.46922	78.53078	0.585222	200767.2	3.359298	250374	2

129	42.02611	0.000861	0.001135	255.3808	45.96368	34.87185	6.473885	83.52611	0.733494	205001	3.607153	26132	8.1	1.769451
130	41.48359	0.000877	0.001156	249.908	47.86564	36.28522	7.016413	82.98359	0.724025	194717.2	3.669095	25091	1.3	1.769451
131	41.51255	0.000865	0.001 14	252.1267	48.35346	36.67803	6.987451	83.01255	0.724531	198241.1	3.621066	25452	9.6	1.769451
132	41.2868	0.000865	0.001 14	249.8997	49.22283	37.33669	7.2132	82.7868	0.720591	194866.5	3.622643	25091	4.5	1.769451
133	39.88266	0.001 41	0.001835	245.6449	60.8643	46.76652	8.617344	81.38266	0.696084	208722	2.990396	25911	1.8	1.769451
134	37.09907	0.001 4	0.001821	251.9189	77.71043	59.74436	11.40093	78.59907	0.647501	194710.9	2.971994	24862	4.4	1.769451
135	37.66884	0.001404	0.001827	245.752	72.85102	55.99567	10.83116	79.16884	0.657445	193442	2.979346	24565	9.7	1.769451
136	39.15893	0.001396	0.001816	245.4456	65.09371	50.05605	9.341066	80.65893	0.683452	204620.4	2.964626	25530	5.9	1.769451
137	45.72964	0.000748	0.000 94	267.6518	48.54069	38.59147	6.770363	83.22964	0.798133	201859.9	3.015165	26378	8.7	1.534654
138	45.93144	0.000755	0.000 95	266.9519	46.97744	37.34031	6.568557	83.43144	0.801655	201334.5	3.04611	26320	9.1	1.534654
139	45.23744	0.000746	0.000938	266.1384	51.29691	40.78514	7.26256	82.73744	0.789542	197618.7	3.007418	25969	1	1.534654
140	45.56296	0.000748	0.000 94	269.9838	49.99343	39.74644	6.937042	83.06296	0.795224	202423.5	3.015165	26509	3.6	1.534654
141	40.97283	0.001226	0.001 53	263.8372	80.39663	64.41731	11.52717	78.47283	0.715111	195953.6	2.491808	25432	5.3	1.534654
142	41.37804	0.001345	0.001687	252.01	71.66132	57.15616	11.12196	78.87804	0.722183	176096.8	2.721333	23517	4.5	1.534654
143	44.73164	0.001341	0.001681	232.5002	49.61838	39.57952	7.768361	82.23164	0.780714	183270.2	2.713827	23465	5.4	1.534654
144	41.16755	0.001245	0.001555	261.9429	78.20998	62.60905	11.33245	78.66755	0.718509	193332.3	2.528252	25177	5.1	1.534654
145	39.32119	0.000986	0.001352	251.27	41.71525	30.41244	5.678814	84.32119	0.686284	218390	4.234395	27064	6.2	2
146	38.35114	0.000978	0.001341	244.3619	46.53806	33.94556	6.648 86	83.35114	0.669354	205887.2	4.203165	25757	0.2	2
147	38.4623	0.000982	0.001346	244.0397	45.75991	33.36961	6.537702	83.4623	0.671294	206021.1	4.218611	25760	8.1	2
148	38.81092	0.000986	0.001352	247.8539	44.30187	32.29822	6.189075	83.81092	0.677378	211459.8	4.234395	26356	8	2
149	34.07936	0.001596	0.002152	238.6251	72.75424	53.9429	10.92064	79.07936	0.594797	194125.1	3.486133	24327	4.3	2
150	33.49199	0.001577	0.002124	237.672	75.69634	56.19216	11.50801	78.49199	0.584546	190810.7	3.448748	23986	6.3	2
151	33.39431	0.001583	0.002133	238.5626	76.34486	56.65272	11.60569	78.39431	0.582841	190408.3	3.459977	23982	9	2
152	33.93979	0.001594	0.002 15	239.2903	73.68608	54.64017	11.06021	78.93979	0.592361	193841.9	3.482464	24320	3.7	2
153	41.79435	0.000702	0.000913	281.2525	56.95495	43.77744	6.705649	83.29435	0.729449	257099.1	2.979346	31252	9.8	1.769451
154	41.50463	0.000 7	0.000911	279.7552	58.74913	45.1668	6.995368	83.00463	0.724392	253533.5	2.971972	30889	8.2	1.769451
155	41.68104	0.000689	0.000895	285.5521	59.22071	45.59377	6.818 96	83.18104	0.727471	263834.5	2.927947	31951	2.8	1.769451
156	41.47376	0.000685	0.000 89	286.5768	61.07586	47.04278	7.026237	82.97376	0.723854	263783.4	2.914784	31970	7	1.769451
157	36.68948	0.001191	0.001522	268.099	92.17 31	72.10159	11.81052	78.18948	0.640352	233443.1	2.571481	28438	8.7	1.769451
158	37.16023	0.012262	0.016316	37.3641	8.701831	6.53981	11.33977	78.66023	0.648568	15300.41	25.44344	27994	.54	1.769451
159	36.91212	0.001254	0.001613	263.8263	86.90378	67.54752	11.58788	78.41212	0.644238	221214.6	2.690339	27342	9.9	1.769451
160	37.12045	0.001265	0.001629	262.2502	84.84958	65.88438	11.37955	78.62045	0.647874	219882.3	2.711589	27198	8.9	1.769451
161	46.65949	0.000419	0.000497	296.0204	75.83072	63.99506	5.840507	84.15949	0.814362	441209.6	1.794294	47827	4	1.534654
162	46.31443	0.000429	0.000512	299.9623	77.34624	64.89298	6.185573	83.81443	0.808339	420747.5	1.827419	46042	3.5	1.534654

163	46.25532	0.000438	0.000524	303.6569	76.67558	64.04453	6.244679	83.75532	0.807308	410415.8	1.855867	452077.1	1.534654
164	46.36532	0.000448	0.000539	302.4058	72.99813	60.67653	6.134676	83.86532	0.809228	395158.1	1.890885	438173.5	1.534654
165	41.20898	0.000879	0.001054	286.722	109.922	91.73657	11.29102	78.70898	0.719232	311408.5	1.86163	355196	1.534654
166	41.41983	0.00085	0.001011	284.154	111.9195	94.12227	11.08017	78.91983	0.722912	327955.2	1.813487	368712.4	1.534654
167	40.46872	0.000842	0.000998	287.6055	120.7841	101.8282	12.03128	77.96872	0.706312	324539.8	1.799747	365627.1	1.534654
168	40.73529	0.000848	0.001008	283.4646	116.2535	97.81347	11.76471	78.23529	0.710965	319168.5	1.810783	360122.7	1.534654
169	38.73939	0.00104	0.001431	248.3825	44.0757	32.03073	6.260614	83.73939	0.67613	205707.5	4.453664	259202.4	2
170	38.84202	0.001052	0.001448	243.9027	42.52804	30.88683	6.157979	83.84202	0.677921	201647	4.500884	254302.4	2
171	39.89985	0.001054	0.001451	274.619	40.62706	29.50316	5.100153	84.89985	0.696384	235678	4.508918	293679.2	2
172	38.99685	0.001017	0.001397	248.4807	42.83532	31.17005	6.003145	83.99685	0.680624	210063.3	4.359425	262796.7	2
173	35.97157	0.00179	0.002438	237.3619	59.87388	43.94757	9.028428	80.97157	0.627822	192725.3	3.870097	243108.3	2
174	35.61834	0.001765	0.002401	236.7407	61.86099	45.45649	9.381658	80.61834	0.621657	191350.4	3.820186	241558.1	2
175	36.0887	0.00178	0.002424	242.0663	60.54635	44.45995	8.911305	81.0887	0.629867	197987.2	3.850803	249123.7	2
176	34.85744	0.001763	0.002399	228.8366	63.56889	46.71557	10.14256	79.85744	0.608377	180119.5	3.816345	229254.2	2
177	42.74768	0.000778	0.00102	304.5727	51.57743	39.34728	5.752319	84.24768	0.746088	267603.7	3.278181	330327.1	1.769451
178	41.6476	0.000757	0.000991	286.0289	56.87505	43.46654	6.852398	83.1476	0.726888	246027.3	3.19518	305345.6	1.769451
179	42.5917	0.000786	0.001031	299.1904	51.62337	39.35854	5.908301	84.0917	0.743365	259666.7	3.308318	321833	1.769451
180	42.0128	0.000778	0.00102	286.2197	53.70546	40.97098	6.487205	83.5128	0.733262	244850	3.277863	304712	1.769451
181	38.32072	0.001486	0.001941	256.3324	70.72747	54.12518	10.17928	79.82072	0.668823	198282	3.138957	254131.1	1.769451
182	38.26707	0.001491	0.001949	254.5447	70.41098	53.86823	10.23293	79.76707	0.667886	196002.4	3.150184	251639.2	1.769451
183	38.24793	0.001493	0.001952	250.4405	69.34051	53.04448	10.25207	79.74793	0.667552	192542.1	3.153913	247340.7	1.769451
184	37.87817	0.001501	0.001963	255.2894	72.49928	55.44107	10.62183	79.37817	0.661099	193040.8	3.168913	249407.1	1.769451
185	46.087	0.000544	0.000673	327.7758	67.67642	54.72681	6.412998	83.587	0.80437	328770	2.232884	388461	1.534654
186	46.34585	0.000555	0.000688	316.8687	62.27757	50.26564	6.154154	83.84585	0.808888	314127.4	2.274421	372630.8	1.534654
187	47.50242	0.000548	0.000678	317.7804	52.94465	42.78604	4.997584	85.00242	0.829074	334236.2	2.246665	390614.8	1.534654
188	48.2633	0.00055	0.000681	321.4824	46.30371	37.40738	4.236697	85.7633	0.842354	347122	2.253596	403260.7	1.534654
189	41.66644	0.001312	0.001644	262.5772	73.92988	59.0266	10.83356	79.16644	0.727216	188939.7	2.65776	249241	1.534654
190	41.83648	0.00131	0.001641	264.6543	73.65143	58.80822	10.66352	79.33648	0.730184	191802.7	2.653957	252357	1.534654
191	41.33484	0.001307	0.001636	263.3104	76.03536	60.71976	11.16516	78.83484	0.721429	187935.3	2.646507	248538.9	1.534654
192	41.09173	0.001303	0.001631	264.5805	77.77979	62.1212	11.40827	78.59173	0.717186	187678.8	2.639054	248681.8	1.534654
193	40.09376	0.001551	0.002167	526.548	68.63795	49.12628	4.906241	85.09376	0.699768	390747.8	6.540154	515872.3	2
194	40.59155	0.001559	0.002178	499.7532	59.08814	42.28599	4.408452	85.59155	0.708456	376836.3	6.572348	494477	2
195	40.61526	0.001505	0.002101	520.6116	61.65286	44.16011	4.384739	85.61526	0.70887	397316.6	6.353012	518741	2
196	40.28211	0.001513	0.002113	511.2694	64.62897	46.28549	4.717893	85.28211	0.703055	384955.8	6.385643	505226.5	2

197	41.12111	0.002658	0.003697	397.5912	43.23064	31.07979	3.878889	86.12111	0.717699	322782.2	5.629379	41134 8.8	2
198	40.83182	0.002662	0.003702	393.9854	45.7223	32.86945	4.168182	85.83182	0.71265	316380.6	5.637593	40476 6.4	2
199	40.72394	0.002612	0.003632	402.12	47.96577	34.50432	4.276058	85.72394	0.710767	323954.3	5.536916	41387 6.3	2
200	40.74245	0.002 66	0.003 7	393.1933	46.52472	33.44715	4.257554	85.74245	0.711 09	314826.9	5.633486	40319 3.3	2
201	43.93667	0.001261	0.00168	542.0062	64.33166	48.29757	4.563333	85.43667	0.766 84	387115.1	5.227511	52001 1.6	1.769451
202	43.55884	0.001255	0.001672	533.7646	68.15905	51.17429	4.941158	85.05884	0.760245	376904.6	5.203245	50863 5.1	1.769451
203	43.45279	0.001263	0.001682	539.7834	70.16718	52.6775	5.047207	84.95279	0.758394	378807	5.235764	51256 3.4	1.769451
204	43.89612	0.001245	0.001658	551.1965	66.13072	49.65685	4.603877	85.39612	0.766132	395066.9	5.162982	52982 6.3	1.769451
205	45.52196	0.002244	0.002983	469.0191	38.61498	29.04755	2.978039	87.02196	0.794508	371997.1	4.660104	47887 7.2	1.769451
206	45.42679	0.002132	0.002831	499.6815	42.97622	32.36533	3.073211	86.92679	0.792847	404401.4	4.432461	51642 7.2	1.769451
207	45.50444	0.002098	0.002785	491.885	41.5006	31.26639	2.995559	87.00444	0.794202	402234	4.364655	51164 7.2	1.769451
208	45.97344	0.002047	0.002716	507.8464	36.80187	27.74456	2.526557	87.47344	0.802388	427490	4.261514	53808 3	1.769451
209	47.28568	0.000988	0.001245	562.625	74.06812	58.77015	5.214319	84.78568	0.825291	380410.9	3.977317	52362 7.5	1.534654
210	47.57339	0.001034	0.001303	541.3835	66.91697	53.10911	4.926606	85.07339	0.830312	361548.3	4.164876	50084 8.4	1.534654
211	47.85966	0.001038	0.001308	559.112	65.37845	51.88939	4.640344	85.35966	0.835309	376449.6	4.181041	51966 5	1.534654
212	47.22135	0.000 98	0.001235	570.1629	76.05635	60.34583	5.278646	84.72135	0.824168	386210	3.945179	53109 4.5	1.534654
213	48.5585	0.001746	0.002201	520.4101	55.09522	43.71604	3.941498	86.0585	0.847506	393292.5	3.514531	51588 9.6	1.534654
214	48.9765	0.002 01	0.002534	456.7715	41.78314	33.15591	3.523502	86.4765	0.854801	324879.5	4.046551	43779 2.9	1.534654
215	48.4088	0.001707	0.002 15	525.2378	57.9904	46.0194	4.091198	85.9088	0.844893	400212.8	3.43501	52306 6.2	1.534654
216	48.12119	0.001842	0.002322	500.105	57.31538	45.47143	4.37881	85.62119	0.839873	361191.8	3.706753	48290 1.4	1.534654
217	31.23064	0.000787	0.001061	622.5445	225.7434	167.5983	13.76936	76.23064	0.545077	461632.9	3.445	59431 4	2
218	31.29792	0.000805	0.001086	626.8293	224.7534	166.5039	13.70208	76.29792	0.546252	459546.8	3.5125	59472 7.9	2
219	30.83732	0.000767	0.00103	626.4261	234.011	174.2298	14.16268	75.83732	0.538213	466265.6	3.363152	59828 3.8	2
220	31.23728	0.000803	0.001083	626.9171	225.6835	167.2326	13.76272	76.23728	0.545193	459333	3.504832	59445 4.6	2
221	37.31996	0.001886	0.002 58	555.3907	120.7294	88.27506	7.680035	82.31996	0.651356	459673	4.063158	57760 0.9	2
222	37.56268	0.001905	0.002608	542.0933	114.3649	83.56294	7.437318	82.56268	0.655592	450113.5	4.102048	56522 0.3	2
223	36.73407	0.001 9	0.002599	544.455	125.3831	91.63273	8.265925	81.73407	0.641131	439546.6	4.090328	55681 3.8	2
224	37.14924	0.001888	0.002582	545.2824	120.6483	88.2095	7.850759	82.14924	0.648377	448294.5	4.067044	56450 7.4	2
225	37.05905	0.000 7	0.000911	640.3066	198.0413	152.2564	11.44095	78.55905	0.646802	494218.6	2.97184	63133 1.2	1.769451
226	35.46948	0.000687	0.000892	618.391	212.1902	163.404	13.03052	76.96948	0.619059	457684	2.920661	59152 6.8	1.769451
227	36.92312	0.000691	0.000897	644.4467	202.2899	155.7045	11.57688	78.42312	0.64443	500059.8	2.935283	63709 7.2	1.769451
228	36.30837	0.000706	0.000919	642.3198	207.5523	159.4607	12.19163	77.80837	0.633701	479916.2	2.993935	61977 0.7	1.769451
229	38.77083	0.001545	0.002024	552.9167	144.98	110.6543	9.729172	80.27083	0.676679	423207.3	3.255408	54553 1.4	1.769451
230	39.14098	0.001 53	0.002003	559.3215	142.7847	109.0493	9.359016	80.64098	0.683139	436658.7	3.225302	55892 6.7	1.769451

231	40.23591	0.001535	0.002011	563.2673	129.9251	99.20354	8.264093	81.73591	0.702249	456101.7	3.236612	57711 3.8	1.769451
232	39.89723	0.001528	0.002	565.732	135.0808	103.1741	8.602769	81.39723	0.696338	454113.9	3.221527	576056	1.769451
233	44.7067	0.000647	0.000809	658.7415	143.4812	114.6354	7.793297	82.2067	0.780279	534231.7	2.620485	676353.6	1.534654
234	43.72343	0.000648	0.000812	642.1751	153.8631	122.9125	8.776567	81.22343	0.763118	501600.5	2.628058	642960.7	1.534654
235	44.18306	0.000648	0.000812	646.5069	148.2925	118.4624	8.316938	81.68306	0.77114	513315.7	2.628058	654455.9	1.534654
236	43.48439	0.000631	0.000789	644.1305	159.8157	127.8402	9.015615	80.98439	0.758946	510129	2.561373	649843.7	1.534654
237	45.49012	0.001194	0.001487	609.3996	127.1392	102.0431	7.00988	82.99012	0.793952	545126.1	2.430213	667090.1	1.534654
238	45.63133	0.001239	0.001548	601.257	120.6523	96.6105	6.868674	83.13133	0.796417	522645.4	2.517278	646197.3	1.534654
239	45.83734	0.001213	0.001513	610.1976	120.8919	96.92908	6.662664	83.33734	0.800012	544898.8	2.466403	667691.3	1.534654
240	44.95996	0.001226	0.001 53	601.8649	131.2529	105.1656	7.54004	82.45996	0.784699	515432.2	2.491808	639746.8	1.534654
241	29.37732	0.000 81	0.001095	586.268	229.8056	170.1298	15.62268	74.37732	0.512731	400041.3	3.535078	530202.4	2
242	30.99928	0.000789	0.001064	617.9988	226.532	168.1415	14.00072	75.99928	0.54104	453821.1	3.452632	586141.7	2
243	29.87538	0.000818	0.001106	580.1772	221.7026	163.9842	15.12462	74.87538	0.521424	400509	3.565254	529201.9	2
244	33.40413	0.000799	0.001078	685.6849	218.4764	161.9675	11.59587	78.40413	0.583012	544082.2	3.489961	686916.9	2
245	38.51755	0.002033	0.002794	542.1199	99.79475	72.61766	6.482449	83.51755	0.672258	450430.4	4.359589	566630.6	2
246	40.06479	0.002024	0.002 78	548.9919	79.93936	58.18602	4.935207	85.06479	0.699263	483673.8	4.339976	597268.3	2
247	4.820339	0.002039	0.002803	666.0905	452.9968	329.5767	40.17966	49.82034	0.084131	143237.8	4.371347	346086.7	2
248	40.04825	0.002032	0.002792	554.3398	80.85297	58.83762	4.95175	85.04825	0.698974	487134.2	4.355661	602066.1	2
249	38.67026	0.000657	0.000849	715.6198	203.5012	157.3818	9.829736	80.17026	0.674923	615030.3	2.804524	757748	1.769451
250	39.6761	0.000666	0.000863	738.8018	191.864	148.1734	8.823897	81.1761	0.692479	651123.2	2.840604	797389.5	1.769451
251	38.77147	0.000649	0.000838	734.8209	208.5929	161.5108	9.728529	80.27147	0.67669	639924.7	2.77564	784947.1	1.769451
252	37.69414	0.000655	0.000847	693.2958	212.0419	164.0345	10.80586	79.19414	0.657887	576507.8	2.797313	716737.2	1.769451
253	41.61721	0.001282	0.001653	645.8701	140.6486	109.0528	6.882789	83.11721	0.726357	632226.2	2.743608	751735.5	1.769451
254	43.11827	0.001 27	0.001637	634.4902	113.3042	87.93564	5.381735	84.61827	0.752556	663232.2	2.722243	775950.4	1.769451
255	42.9501	0.001257	0.001618	645.0284	119.026	92.48367	5.549903	84.4501	0.749621	676219.8	2.697407	790287.5	1.769451
256	44.62325	0.001267	0.001632	636.1793	85.74415	66.56826	3.876752	86.12325	0.778823	707804.8	2.715061	816324.9	1.769451
257	45.41999	0.000461	0.000557	750.9014	195.9447	162.0412	7.080005	82.91999	0.792728	904017.6	1.932864	1017821	1.534654
258	44.68929	0.000447	0.000537	727.3492	211.8699	176.2452	7.810707	82.18929	0.779975	889633.5	1.884971	996476.4	1.534654
259	45.35435	0.000452	0.000545	741.1856	199.2134	165.3363	7.145648	82.85435	0.791583	915907.7	1.902752	1025196	1.534654
260	45.48711	0.000468	0.000567	745.7671	189.9206	156.6408	7.012886	82.98711	0.7939	880721.1	1.957392	996067.8	1.534654
261	46.94882	0.001066	0.001316	642.5628	119.6491	96.9564	5.551178	84.44882	0.819412	681851.2	2.191816	794241.1	1.534654
262	46.90478	0.001061	0.001308	646.534	121.7147	98.68475	5.595225	84.40478	0.818643	688959.7	2.181627	801552.6	1.534654
263	46.25034	0.001 07	0.001321	640.6603	131.2576	106.3253	6.249664	83.75034	0.807221	658996.3	2.198559	773269.3	1.534654
264	46.14622	0.001039	0.001278	641.2826	136.486	110.9207	6.353783	83.64622	0.805403	679652.7	2.141194	790788.5	1.534654

265	29.73812	0.00074	0.00099	652.3982	260.0117	194.3632	15.26188	74.73812	0.519028	478491.2	3.259377	614794.2	2
266	29.22663	0.000778	0.001047	617.7383	247.1265	183.7054	15.77337	74.22663	0.510101	430319	3.407673	564436.7	2
267	29.84088	0.000776	0.001044	610.0544	237.7484	176.7797	15.15912	74.84088	0.520822	434908.2	3.400203	566149.5	2
268	29.17314	0.000795	0.001072	608.8938	242.3295	179.7368	15.82686	74.17314	0.509167	417479.4	3.474958	551511.5	2
269	35.7537	0.001738	0.002362	565.9634	147.0184	108.1667	9.246298	80.7537	0.62402	463833.8	3.766599	582640.7	2
270	35.76513	0.001761	0.002396	563.9062	145.6458	107.0416	9.234872	80.76513	0.624219	458772.3	3.812527	577927.4	2
271	33.58813	0.001747	0.002376	544.4542	165.9868	122.0671	11.41187	78.58813	0.586223	411760.3	3.785714	530530.2	2
272	35.71777	0.001743	0.00237	567.4674	147.6812	108.6246	9.282233	80.71777	0.623393	463559.6	3.77807	582961.5	2
273	36.85384	0.000657	0.00085	590.8199	190.6541	147.4378	11.64616	78.35384	0.643221	475376.3	2.80595	596779.9	1.769451
274	36.26251	0.000621	0.000798	687.8452	236.7534	184.2128	12.23749	77.76251	0.6329	567757.6	2.669147	704237.2	1.769451
275	34.8877	0.000634	0.000817	643.3863	236.1646	183.3179	13.6123	76.3877	0.608905	496807.8	2.718683	629206.2	1.769451
276	36.29116	0.000631	0.000812	674.5627	229.9795	178.6348	12.20884	77.79116	0.6334	550325.6	2.704505	685742.9	1.769451
277	39.33163	0.001319	0.001706	620.4327	166.8689	128.996	9.168371	80.83163	0.686466	544329	2.815333	667028.3	1.769451
278	39.83436	0.001317	0.001704	621.4437	160.0888	123.7727	8.665638	81.33436	0.695241	556025.7	2.811656	677674.4	1.769451
279	39.48847	0.001298	0.001677	624.8286	167.2421	129.4926	9.011532	80.98847	0.689204	558589.9	2.775791	680354.3	1.769451
280	40.64184	0.001313	0.001698	624.3011	149.0979	115.3079	7.858155	82.14184	0.709334	576866.4	2.804524	696956.9	1.769451
281	43.4815	0.000491	0.0006	722.289	212.0904	173.6071	9.018495	80.9815	0.758895	738127.2	2.0394	862123.6	1.534654
282	43.64284	0.000535	0.00066	726.1833	196.3843	159.0805	8.857158	81.14284	0.761711	676480.3	2.198641	813061.7	1.534654
283	42.95208	0.000517	0.000635	721.1512	211.9146	172.3277	9.547918	80.45208	0.749655	680373.5	2.13117	812822.8	1.534654
284	43.15779	0.000559	0.000693	688.2993	188.1658	151.7829	9.342211	80.65779	0.753246	601721.5	2.288352	737918.4	1.534654
285	44.81657	0.000936	0.001134	642.9049	175.5416	144.7815	7.683426	82.31657	0.782197	738567.9	1.957392	839461.8	1.534654
286	45.37164	0.000954	0.00116	651.8844	164.7712	135.477	7.128357	82.87164	0.791885	746303.2	1.988588	850027.6	1.534654
287	45.78128	0.000927	0.001122	646.6941	161.0263	133.0285	6.718718	83.28128	0.799034	783842.8	1.942028	881867.6	1.534654
288	45.31888	0.000923	0.001117	638.4677	168.0527	138.9275	7.181117	82.81888	0.790964	763267.6	1.935915	860520.4	1.534654
289	48.74244	0.001646	0.002302	405.8849	-48.8112	-34.8878	-3.74244	93.74244	0.850716	405215.1	6.930917	481433.9	2
290	49.02942	0.001638	0.002291	415.5871	-54.2862	-38.8051	-4.02942	94.02942	0.855725	420158.4	6.898148	497186.9	2
291	47.52811	0.001604	0.002243	396.8861	-31.4149	-22.4666	-2.52811	92.52811	0.829522	381525.1	6.759674	459036.8	2
292	47.42184	0.001664	0.002294	394.6041	-29.6951	-21.2262	-2.42184	92.42184	0.827667	375149.8	6.906315	452971	2
293	35.38216	0.002363	0.003272	359.4312	88.22059	63.70938	9.617842	80.38216	0.617535	249554.5	5.028187	335873.8	2
294	45.02503	0.002365	0.003275	443.2073	-0.35296	-0.25489	-0.02503	90.02503	0.785835	435865.4	5.032254	521286.9	2
295	42.04206	0.002406	0.003335	339.5176	29.48772	21.27859	2.957936	87.04206	0.733772	296540.4	5.116062	368176.8	2

296	44.16055	0.002379	0.003295	457.2316	11.91811	8.604343	0.839454	89.16055	0.770747	434079.8	5.060159	524770.2	2
297	53.55968	0.001527	0.002038	413.6322	-64.5737	-48.3936	-5.05968	95.05968	0.934793	389775	6.318986	470534.5	1.769451
298	52.77062	0.001493	0.001992	412.9479	-53.6402	-40.2051	-4.27062	94.27062	0.921021	380771.5	6.179686	463430.2	1.769451
299	53.92688	0.001473	0.001965	422.8648	-72.0828	-54.0333	-5.42688	95.42688	0.941202	409101.7	6.098256	489520	1.769451
300	53.67613	0.001453	0.001939	417.8401	-67.73	-50.7753	-5.17613	95.17613	0.936825	402395.6	6.016396	482372	1.769451
301	39.57235	0.002198	0.002921	338.8059	74.59609	56.13815	8.927645	81.07235	0.690668	219987.8	4.567943	306361.7	1.769451
302	41.2164	0.002222	0.002953	331.9306	61.35094	46.15971	7.283597	82.71764	0.719362	227179.7	4.61592	309682.8	1.769451
303	40.22678	0.002195	0.002916	374.2436	77.32733	58.19585	8.273219	81.72678	0.70209	248811.1	4.560031	343095.8	1.769451
304	40.45072	0.002228	0.002961	357.0685	71.83552	54.04516	8.049275	81.95072	0.705998	237653.7	4.627922	327719.4	1.769451
305	79.48818	0.001292	0.001623	174.1572	-309.335	-246.102	-26.9882	116.9882	1.38733	425174.4	5.212826	391879.3	1.534654
306	58.13408	0.001372	0.001723	350.901	-57.5249	-45.8065	-5.63408	95.63408	1.014631	302742.8	5.540783	376200.9	1.534654
307	60.0783	0.001218	0.001533	357.9531	-85.3917	-67.8827	-7.5783	97.5783	1.048564	348095.7	4.913666	414086.3	1.534654
308	64.36185	0.001288	0.001618	267.1682	-110.183	-87.6558	-11.8618	101.8618	1.123326	299810	5.196339	338442	1.534654
309	43.70037	0.001898	0.002392	297.6989	62.62732	49.68653	8.799633	81.20037	0.762715	181300.7	3.819656	261009.1	1.534654
310	48.24547	0.001906	0.002402	321.6182	35.54232	28.19835	4.254527	85.74547	0.842042	229089.1	3.83565	308237.3	1.534654
311	47.27432	0.001894	0.002387	300.405	40.08456	31.80171	5.225682	84.77432	0.825092	207508.7	3.81142	282759.8	1.534654
312	47.02779	0.001928	0.002431	285.8455	39.55879	31.38573	5.472211	84.52779	0.82079	193946.2	3.880287	266407.7	1.534654
313	60.78422	0.001535	0.002144	135.2209	-106.424	-76.1901	-15.7842	105.7842	1.060885	236858.4	6.474816	242895.7	2
314	63.85749	0.001553	0.002169	114.8872	-125.22	-89.6209	-18.8575	108.8575	1.114524	238704.2	6.547958	236531.3	2
315	65.72384	0.001555	0.002172	96.77377	-128.992	-92.3175	-20.7238	110.7238	1.147097	226736.7	6.55625	219959.1	2
316	45.99702	0.001503	0.002099	308.7748	-9.41033	-6.74056	-0.99702	90.99702	0.802799	286449.6	6.345075	348856.4	2
317	38.48672	0.002336	0.003233	311.1719	55.31082	39.96353	6.513276	83.48672	0.671772	242198.7	4.972474	312553.5	2
318	41.30929	0.002361	0.00327	296.2577	31.71584	22.90471	3.690714	86.30929	0.720983	253992.9	5.024287	317215.6	2
319	39.91143	0.002332	0.003227	294.7826	42.26992	30.5434	5.088567	84.91143	0.696586	241590.9	4.964516	306254.2	2
320	38.81808	0.002355	0.003261	303.4248	51.45195	37.16183	6.181916	83.81808	0.677503	238119.4	5.012327	306463.6	2
321	44.51213	0.001358	0.001811	357.5685	36.9426	27.71101	3.98787	86.01213	0.776883	253442.3	5.625182	341880.6	1.769451
322	35.63242	0.001356	0.001808	297.8278	85.13664	63.86277	12.86758	77.13242	0.621903	154634.5	5.617033	240447.9	1.769451
323	41.15355	0.001342	0.001789	344.5044	61.71254	46.29674	7.346452	82.65355	0.718265	218062.9	5.56016	308813.8	1.769451

324	40.93708	0.00135	0.0018	332.9443	61.09965	45.83417	7.562924	82.43708	0.714487	208715	5.592494	296897.5	1.769451
325	20.92805	0.002034	0.002697	284.865	148.7577	112.1681	27.57195	62.42805	0.365263	95999.33	4.233697	183797.5	1.769451
326	21.61892	0.002032	0.002694	270.4262	138.8481	104.6988	26.88108	63.11892	0.377321	93880.09	4.2298	176714.9	1.769451
327	19.85289	0.002061	0.002734	274.1461	146.63	110.5226	28.64711	61.35289	0.346498	87489.58	4.289283	173169.3	1.769451
328	21.97409	0.002053	0.002724	276.5813	140.5459	105.9477	26.52591	63.47409	0.383052	96857.85	4.273409	181659.3	1.769451
329	45.85365	0.001304	0.001639	327.9528	50.65014	40.30183	6.646351	83.35365	0.800297	186935.9	5.262809	280435.7	1.534654
330	55.48344	0.001322	0.001661	384.2161	-31.7367	-25.2577	-2.98344	92.98344	0.968369	305476.9	5.337844	392863.6	1.534654
331	54.56113	0.001314	0.001651	370.9218	-20.7912	-16.5452	-2.06113	92.06113	0.952271	286060.1	5.30432	372715.4	1.534654
332	55.98527	0.001385	0.001739	365.084	-35.2379	-28.0639	-3.48527	93.48527	0.977127	290468.7	5.596988	373273.6	1.534654
333	37.44793	0.001773	0.002234	313.9248	103.6832	82.26379	15.05207	74.94793	0.653059	159146.3	3.567232	248741	1.534654
334	36.49985	0.001796	0.002264	307.4218	106.1034	84.18067	16.00015	73.99985	0.637043	149458.2	3.614529	238723.9	1.534654
335	36.90999	0.001758	0.002216	306.0752	104.0383	82.54808	15.59001	74.40999	0.644201	152914	3.53847	240563.5	1.534654
336	42.52543	0.00178	0.002244	288.9531	68.62363	54.44622	9.974575	80.02543	0.742209	174871.1	3.582346	251739.1	1.534654
337	47.84906	0.001267	0.001759	487.0092	-46.6868	-33.6213	-2.84906	92.84906	0.835124	518165.3	5.376275	605234.6	2
338	47.90308	0.001259	0.001748	491.9608	-48.2258	-34.7377	-2.90308	92.90308	0.836067	525977.5	5.344175	613533.1	2
339	49.10717	0.001261	0.001751	496.9391	-71.3533	-51.3938	-4.10717	94.10717	0.857082	557067.3	5.352162	641087	2
340	47.70163	0.001267	0.001759	477.8255	-43.2544	-31.1495	-2.70163	92.70163	0.832551	505455.9	5.376275	591388	2
341	17.46704	0.002251	0.003111	238.5082	127.0245	91.93363	27.53296	62.46704	0.304857	88044.41	4.800721	157205.8	2
342	14.44177	0.00226	0.003123	270.9667	154.2148	111.5933	30.55823	59.44177	0.252056	87948.73	4.817391	168514.1	2
343	12.68035	0.002254	0.003114	268.7097	158.4862	114.6983	32.31965	57.68035	0.221314	80756.65	4.805484	161619.1	2
344	18.66522	0.00225	0.003108	276.1211	142.8789	103.4116	26.33478	63.66522	0.325769	106971.3	4.797555	186226.8	2
345	49.56059	0.001009	0.001338	498.9361	-16.6537	-12.5602	-1.06059	91.06059	0.864996	483035.6	4.202104	580364.9	1.769451
346	37.76571	0.00098	0.001298	403.3204	106.1366	80.11993	10.73429	79.26571	0.659136	259717.9	4.083614	361208.9	1.769451
347	37.40681	0.000974	0.00129	398.8133	107.9066	81.47178	11.09319	78.90681	0.652872	254390.7	4.059971	355064.1	1.769451
348	40.08078	0.000993	0.001317	401.3554	86.2651	65.09132	8.419222	81.58078	0.699542	278280.1	4.138854	376020.6	1.769451
349	19.86527	0.002077	0.002756	279.8524	149.5054	112.667	28.63473	61.36527	0.346714	88953.39	4.321028	176655.9	1.769451
350	20.04336	0.002079	0.002759	255.693	136.0143	102.4976	28.45664	61.54336	0.349823	81866.26	4.325	161909.3	1.769451
351	23.54557	0.002085	0.002767	298.8646	145.3883	109.5535	24.95443	65.04557	0.410948	110684.4	4.336923	201570.4	1.769451
352	19.7321	0.002081	0.002761	268.7478	143.988	108.5038	28.7679	61.2321	0.344839	84828.22	4.328891	169200.4	1.769451
353	46.07354	0.000484	0.00059	574.9191	131.9287	108.2244	6.426459	83.57354	0.804135	663853.2	2.013801	755668.1	1.534654

354	44.82892	0.000487	0.000595	547.40 48	143.2205	117.35 96	7.671075	82.32892	0.782412	595339.4	2.026428	68601 4.4	1.534654
355	47.51325	0.000506	0.00062	598.31 47	106.7721	87.055 69	4.986754	85.01325	0.829263	692092.8	2.091431	78946 1.9	1.534654
356	52.61569	0.000495	0.000605	589.84 73	-3.00315	-2.4557	-0.115 69	90.11569	0.918317	880872.2	2.052292	95955 5.7	1.534654
357	29.52495	0.001033	0.001271	357.04 48	188.1493	153.00 19	22.97505	67.02495	0.515308	208924.4	2.13117	28631 5.1	1.534654
358	28.10182	0.001 05	0.001293	379.64 58	205.6593	166.93 68	24.39818	65.60182	0.490469	207804.7	2.161344	29252 3.1	1.534654
359	26.99319	0.001052	0.001296	404.88 52	224.83	182.46 24	25.50681	64.49319	0.47112	212674.5	2.164722	30401 3.5	1.534654
360	31.86295	0.001035	0.001273	381.58 35	188.5309	153.28 02	20.63705	69.36295	0.556113	241856.3	2.134514	32296 4	1.534654
361	32.56341	0.000889	0.001211	455.48 51	147.2442	108.13 26	12.43659	77.56341	0.568339	328968.2	3.846887	43075 5.1	2
362	33.15502	0.000 86	0.001168	451.27 75	142.2146	104.71 98	11.84498	78.15502	0.578664	339166.8	3.732208	43747 2.2	2
363	36.08519	0.000904	0.001233	465.65 82	115.8515	84.965 47	8.914805	81.08519	0.629805	377327.7	3.908578	47649 1.7	2
364	42.79614	0.000922	0.001259	519.48 25	37.57989	27.522 21	2.203856	87.79614	0.746934	534019.4	3.977998	63001 1.1	2
365	24.31216	0.001989	0.002729	318.26 88	143.2301	104.36 43	20.68784	69.31216	0.424327	162038.6	4.26953	24470 3.4	2
366	15.35537	0.001923	0.002633	347.91 17	198.3281	144.82 4	29.64463	60.35537	0.268002	128604.7	4.136955	22483 0.7	2
367	29.84038	0.001942	0.002662	354.35 79	129.1471	94.244 22	15.15962	74.84038	0.520813	221921.6	4.175873	30752 7	2
368	21.35845	0.001 95	0.002673	367.07	181.0546	132.08 92	23.64155	66.35845	0.372775	169598.7	4.191468	26683 8	2
369	41.59759	0.001066	0.001415	414.57 97	73.90393	55.656 97	6.902411	83.09759	0.726015	293024.9	4.432365	39386 6.1	1.769451
370	42.24873	0.001054	0.001399	427.86 91	70.18703	52.872 34	6.251273	83.74873	0.737379	311020.7	4.384602	41338 0.9	1.769451
371	43.31441	0.001044	0.001386	434.69 89	60.62133	45.677 38	5.185591	84.81441	0.755979	329540.7	4.344861	43095 2.3	1.769451
372	47.10032	0.001038	0.001378	471.16 77	19.33213	14.568 67	1.399683	88.60032	0.822056	410258.8	4.321028	51045 0.5	1.769451
373	20.79538	0.002018	0.002676	262.76 19	137.7921	103.92 27	27.70462	62.29538	0.362948	88456.76	4.202104	16929 2.5	1.769451
374	21.42344	0.002026	0.002686	261.15 96	134.7961	101.65 17	27.07656	62.92344	0.37391	90075.68	4.217937	17011 6.2	1.769451
375	20.11485	0.002004	0.002657	259.05 18	138.1811	104.23 69	28.38515	61.61485	0.35107	85049.59	4.174415	16497 9.7	1.769451
376	22.75983	0.002 01	0.002665	266.90 43	133.2783	100.52 98	25.74017	64.25983	0.397234	97719.66	4.186272	17834 5.2	1.769451
377	46.83657	0.001263	0.001588	348.44 31	46.85663	37.266 8	5.663432	84.33657	0.817452	208091.5	5.096497	30483 4.3	1.534654
378	44.99366	0.001203	0.001513	346.40 01	60.42341	48.026 21	7.506341	82.49366	0.785287	197743	4.850022	29585 0.5	1.534654
379	42.94687	0.001204	0.001515	350.62 88	75.35146	59.892 32	9.553127	80.44687	0.749564	186093.8	4.855822	28885 8.7	1.534654
380	46.82149	0.001214	0.001528	354.97 47	48.19813	38.313 82	5.678 51	84.32149	0.817189	215208.9	4.897252	31272 3.6	1.534654
381	29.24368	0.002206	0.002778	200.73 99	88.80825	70.519 87	23.25632	66.74368	0.510398	65451.51	4.443221	13331 8.4	1.534654
382	27.85567	0.002226	0.002803	203.94 57	94.07034	74.704 89	24.64433	65.35567	0.486173	62217.38	4.48424	13228 8.9	1.534654
383	30.99006	0.002174	0.002738	223.83 95	93.61143	74.323 86	21.50994	68.49006	0.540879	79219.32	4.377517	15324 2.1	1.534654
384	28.8851	0.002182	0.002748	206.83 22	92.65786	73.569 2	23.6149	66.3851	0.50414	66805.84	4.39394	13673 2.1	1.534654

Appendix 4

The spindle speed was calculated considering the material hardness and the geometrical dimensions of the alloy as shown below.

Alloy: Aluminum 6061

Hardness: 33.5 HRB

Diameter: 3 inches

Wall thickness: 0.125 inches

Considering a feed of 0.002 inch/rev to 0.005 inch/rev from "Machinery's Handbook" 27th Edition, pp 1038 for an Aluminum 6061 alloy being machined by a HSS tool the speed is 500 feet/minute.

Volume Swept by the tool in 1 revolution = 2 x π x 1.5 = 9.426 inches

= 0.7855 feet.

$$\text{RPM} = \frac{\text{Cutting Speed}}{\text{Volume Swept by the tool in 1 revolution}}$$

$$= \frac{500 \frac{feet}{minute}}{0.7855 \frac{feet}{rev}} = 636.5372 \text{ RPM}$$

The spindle speed for the other scenarios were calculated similarly.

Sample calculations for Run 1 from the previous appendices are discussed below.

Friction Force, $F = F_c \times \sin\alpha + F_t \times \cos\alpha$

$$F = 232.64 \times \sin(0) + 198.82 \times \cos(0) = 198.82 \text{ N}$$

Normal Force, $N = F_c \times \cos\alpha + F_t \times \sin\alpha$

$$N = 232.64 \times \cos(0) + 198.82 \times \sin(0) = 232.64 \text{ N}$$

Merchant's Shear Force along the onset of Shear Plane, $F_s = F_c \times \cos\phi - F_t \times \sin\phi$

$$F_s = 232.64 \times \cos(0.18678) - 198.82 \times \sin(0.18678) = 191.67381 \text{ N}$$

Merchant's Normal Force along the onset of Shear Plane, $F_n = F_c \times \sin\phi - F_t \times \cos\phi$

$$F_n = 232.64 \times \sin(0.18678) - 198.82 \times \cos(0.18678) = 238.56218 \text{ N}$$

Onset of Shear Plane Angle, $\phi = \tan^{-1}\left[\dfrac{r_c \times \cos\alpha}{1 - r_c \times \sin\alpha}\right]$

$$\phi = \tan^{-1}\left[\frac{0.188982 \times \cos(0)}{1 - 0.188982 \times \sin(0)}\right] = 0.18678 \text{ radians}$$

Friction Angle, $\beta = \tan^{-1}\left[\dfrac{F}{N}\right]$

$$\beta = \tan^{-1}\left[\frac{198.82}{232.64}\right] = 40.51803^{\circ}$$

Merchant's Shear Area, $A_s = \frac{t \times w}{\sin \phi}$; $A_s = \frac{0.002 \times 0.125}{\sin(0.18678)} = 0.001292$ inch^2

Merchant's Shear Stress, $\tau_s = \frac{F_s}{A_s} = \frac{F_s \times \sin \phi}{t \times w}$;

$$\tau_s = \frac{191.67381}{0.001292} = 229.8716 \text{ MPa}$$

APPENDIX 5

Minitab Project Report
Aluminum 6061; HSS

General Linear Model: Fy Thrust, Fz Cutting, ... versus Environment, Rake Angle

Factor	Type	Levels	Values
Environment	fixed	4	Cold Comp. Air, Dry, Liquid Nit., Nitrogen
Rake Angle	fixed	3	0, 7, 15
Feed in/rev	fixed	2	0.002, 0.004

Analysis of Variance for **Fy Thrust**, using Adjusted SS for Tests

Source	DF	Seq SS	Adj SS	Adj MS	F	P
Environment	3	5669.7	5669.7	1889.9	7.47	0.000
Rake Angle	2	119815.4	119815.4	59907.7	236.70	0.000
Feed in/rev	1	79858.0	79858.0	79858.0	315.53	0.000
Environment*Rake Angle	6	5175.6	5175.6	862.6	3.41	0.005
Environment*Feed in/rev	3	2114.4	2114.4	704.8	2.78	0.047
Rake Angle*Feed in/rev	2	1452.4	1452.4	726.2	2.87	0.063
Environment*Rake Angle*Feed in/rev	6	329.8	329.8	55.0	0.22	0.970
Error	72	18222.8	18222.8	253.1		
Total	95	232638.0				

S = 15.9089 R-Sq = 92.17% R-Sq(adj) = 89.66%

Unusual Observations for Fy Thrust

Obs	Fy Thrust	Fit	SE Fit	Residual	St Resid	
78	262.952	295.460	7.954	-32.508	-2.36	R
79	398.813	295.460	7.954	103.353	7.50	R
80	247.157	295.460	7.954	-48.303	-3.51	R

R denotes an observation with a large standardized residual.

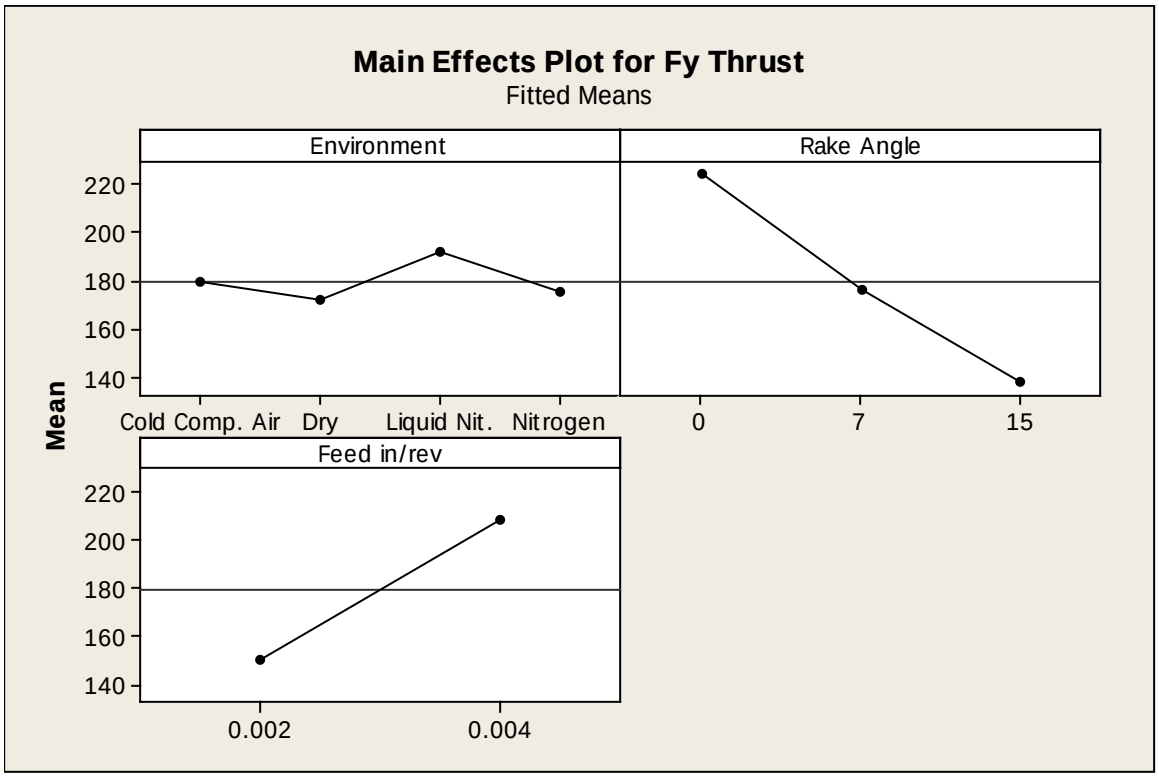
Main Effects Plot for Fy Thrust
Fitted Means
Environment
Rake Angle
Feed in/rev
Mean
220
200
180
160
140
Cold Comp. Air
Dry
Liquid Nit.
Nitrogen
0
7
15
0.002
0.004

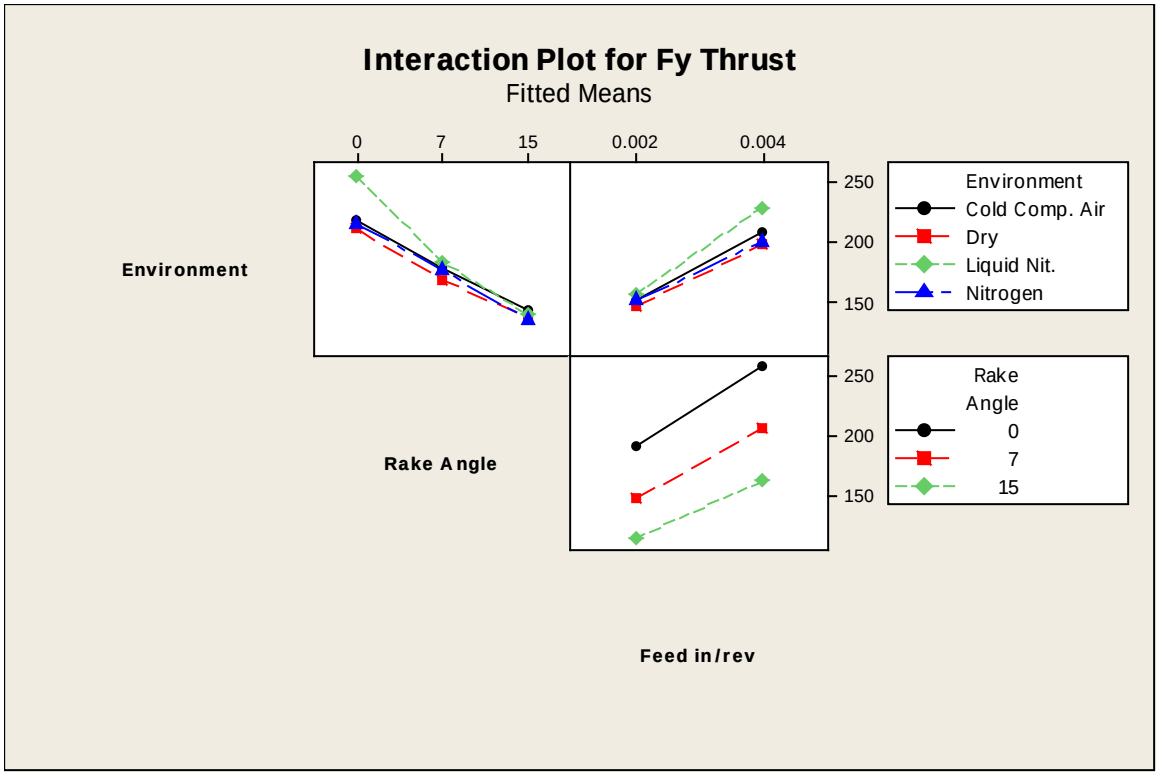
Interaction Plot for Fy Thrust
Fitted Means
Environment
Rake Angle
Feed in/rev
0
7
15
0.002
0.004
250
200
150
Environment
Cold Comp. Air
Dry
Liquid Nit.
Nitrogen
Rake Angle
0
7
15

Analysis of Variance for **Fz Cutting**, using Adjusted SS for Tests

Source	DF	Seq SS	Adj SS	Adj MS	F	P
Environment	3	6237	6237	2079	72.73	0.000
Rake Angle	2	31171	31171	15586	545.21	0.000
Feed in/rev	1	364563	364563	364563	12752.96	0.000
Environment*Rake Angle	6	1430	1430	238	8.34	0.000
Environment*Feed in/rev	3	464	464	155	5.41	0.002
Rake Angle*Feed in/rev	2	57	57	28	0.99	0.376
Environment*Rake Angle*Feed in/rev	6	453	453	75	2.64	0.023
Error	72	2058	2058	29		
Total	95	406432				

S = 5.34664 R-Sq = 99.49% R-Sq(adj) = 99.33%

Unusual Observations for Fz Cutting

Obs	Fz Cutting	Fit	SE Fit	Residual	St Resid	
1	232.640	219.203	2.673	13.437	2.90	R
74	239.012	252.579	2.673	-13.567	-2.93	R
75	268.992	252.579	2.673	16.413	3.54	R
78	362.834	373.720	2.673	-10.886	-2.35	R
79	389.360	373.720	2.673	15.640	3.38	R

R denotes an observation with a large standardized residual.

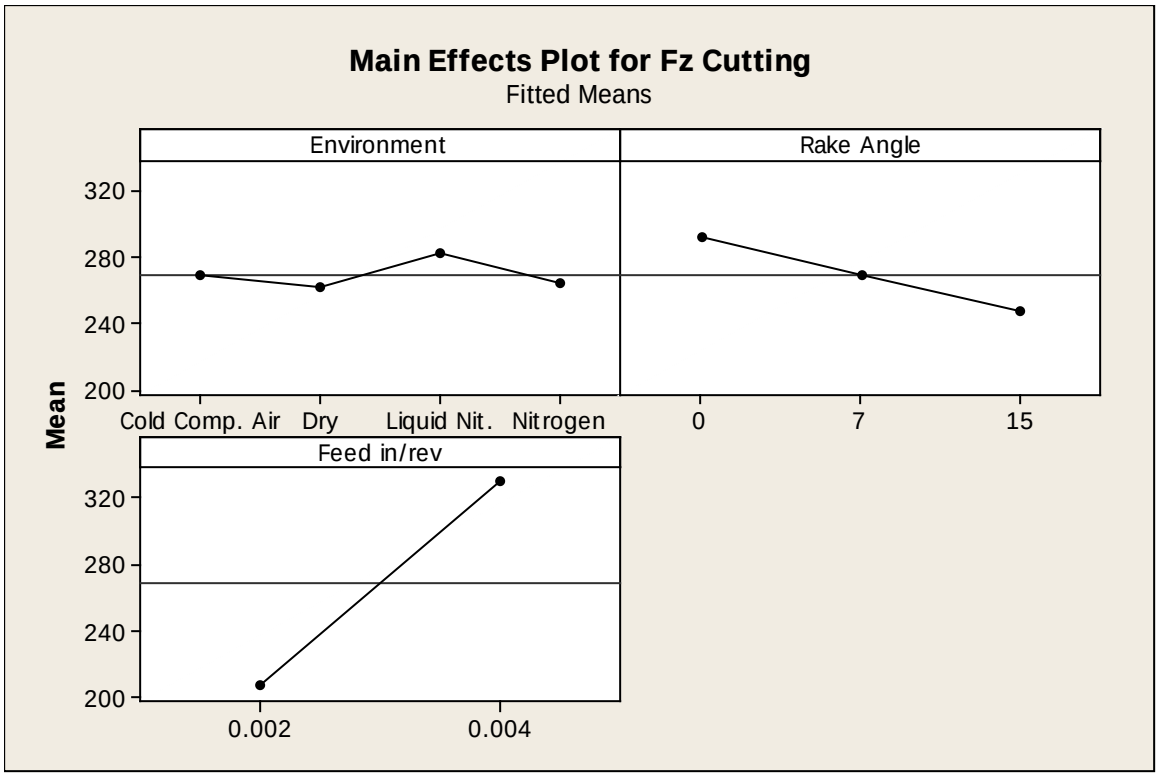
Main Effects Plot for Fz Cutting
Fitted Means
Environment
Rake Angle
Feed in/rev
Mean
320
280
240
200
Cold Comp. Air
Dry
Liquid Nit.
Nitrogen
0
7
15
0.002
0.004

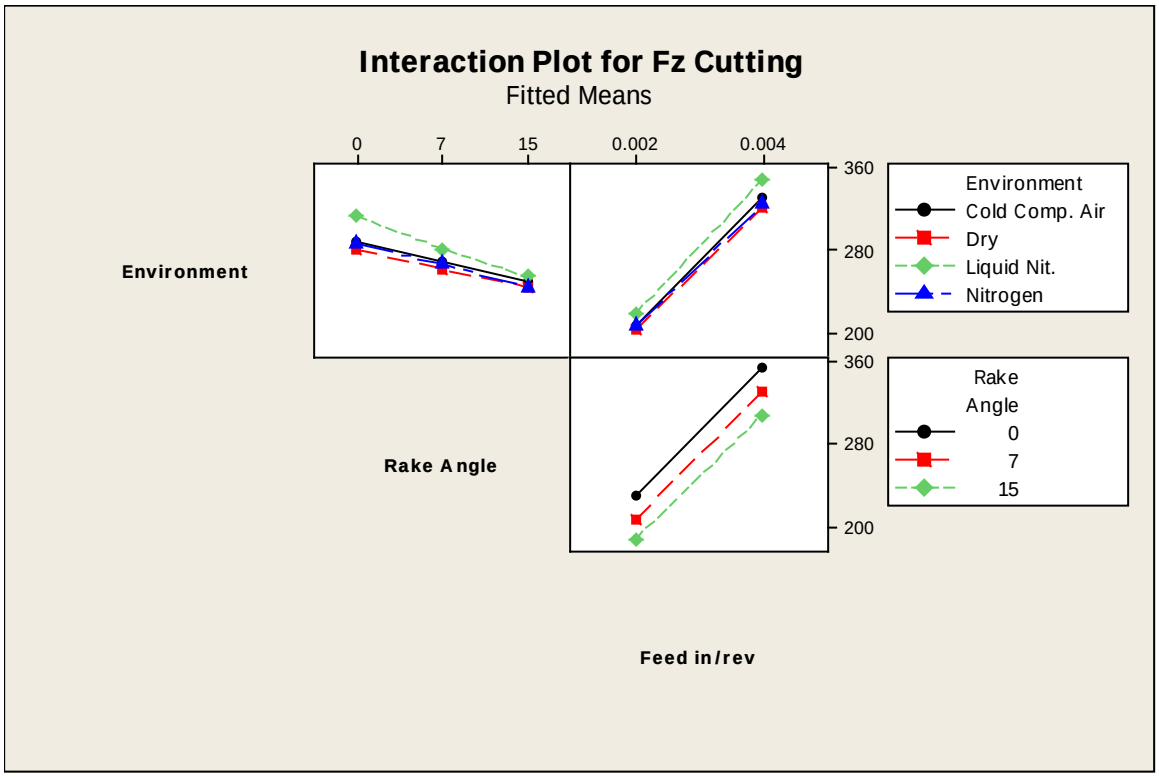
Interaction Plot for Fz Cutting
Fitted Means
Environment
Rake Angle
Feed in/rev
0
7
15
0.002
0.004
360
280
200
Environment
Cold Comp. Air
Dry
Liquid Nit.
Nitrogen
Rake Angle
0
7
15

Analysis of Variance for **Resultant force**, using Adjusted SS for Tests

Analysis of Variance for Resultant, using Adjusted SS for Tests

Source	DF	Seq SS	Adj SS	Adj MS	F	P
Environment	3	12052	12052	4017	22.64	0.000
Rake Angle	2	115688	115688	57844	325.95	0.000
Feed in/rev	1	436533	436533	436533	2459.83	0.000
Environment*Rake Angle	6	5519	5519	920	5.18	0.000
Environment*Feed in/rev	3	1990	1990	663	3.74	0.015
Rake Angle*Feed in/rev	2	408	408	204	1.15	0.323
Environment*Rake Angle*Feed in/rev	6	529	529	88	0.50	0.809
Error	72	12777	12777	177		
Total	95	585497				

S = 13.3216 R-Sq = 97.82% R-Sq(adj) = 97.12%

Unusual Observations for Resultant

Obs	Resultant	Fit	SE Fit	Residual	St Resid
75	355.339	330.064	6.661	25.275	2.19 R
78	448.098	478.102	6.661	-30.003	-2.60 R
79	557.362	478.102	6.661	79.261	6.87 R
80	446.791	478.102	6.661	-31.310	-2.71 R

R denotes an observation with a large standardized residual.

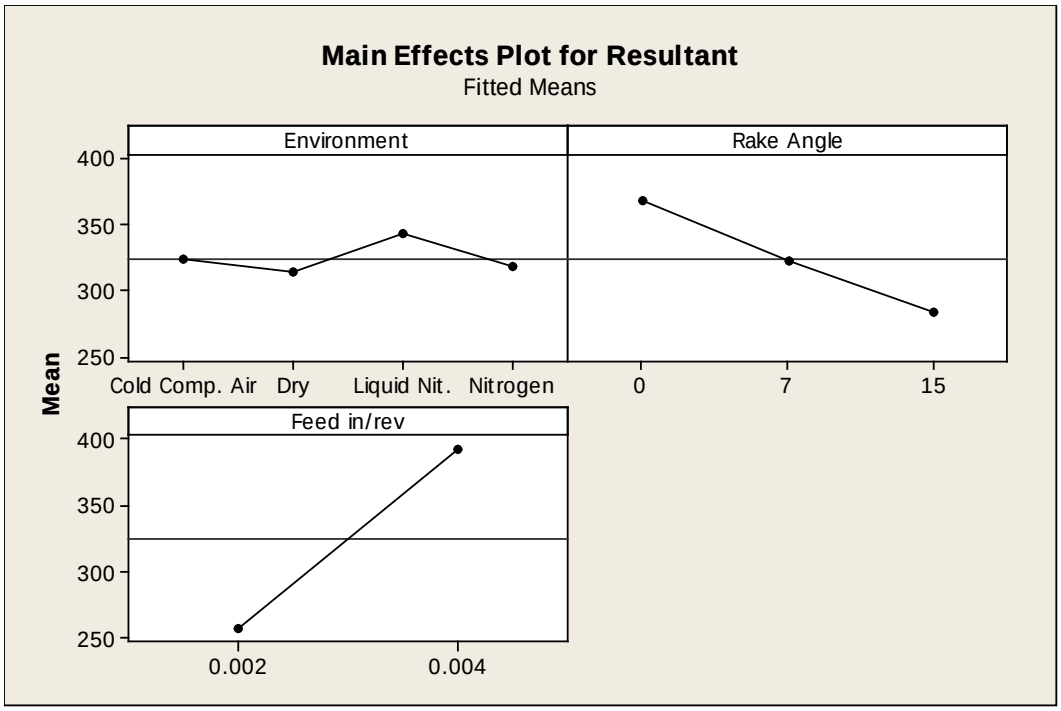
Main Effects Plot for Resultant
Fitted Means
Environment
Rake Angle
Feed in/rev
Mean
400
350
300
250
Cold Comp. Air
Dry
Liquid Nit.
Nitrogen
0
7
15
0.002
0.004

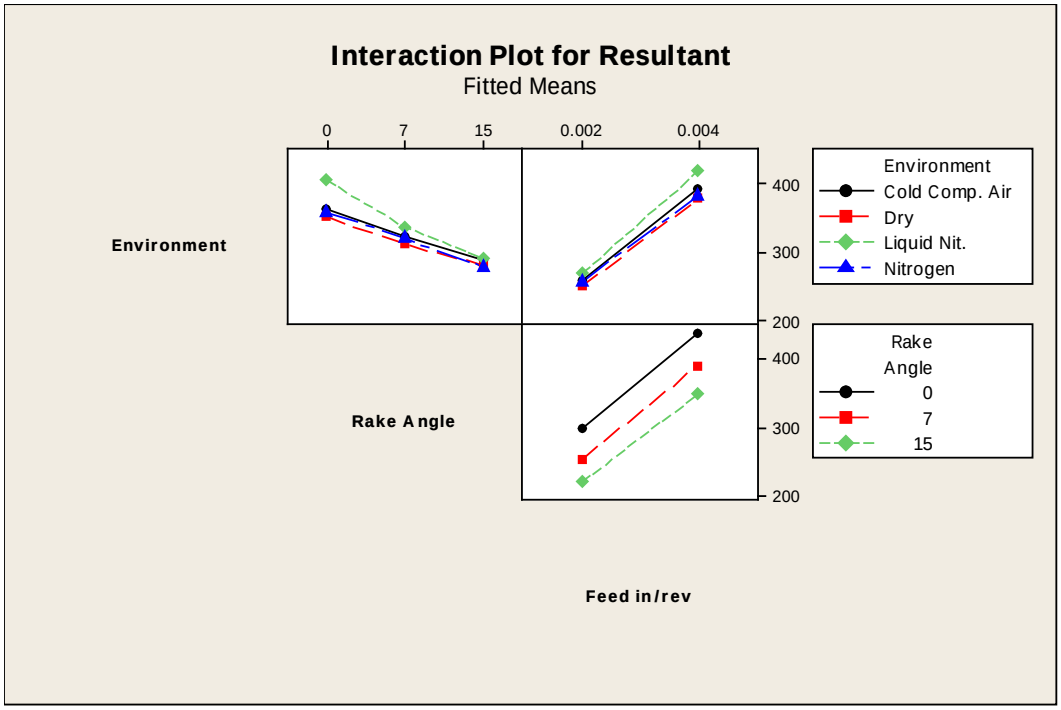
Interaction Plot for Resultant
Fitted Means
Environment
Rake Angle
Feed in/rev
0
7
15
0.002
0.004
400
300
200
Environment
Cold Comp. Air
Dry
Liquid Nit.
Nitrogen
Rake Angle
0
7
15

Analysis of Variance for **Chip thickness ratio**, using Adjusted SS for Tests

Source	DF	Seq SS	Adj SS	Adj MS	F
Environment	3	0.169882	0.169882	0.056627	94.69
Rake Angle	2	0.260688	0.260688	0.130344	217.96
Feed in/rev	1	0.026475	0.026475	0.026475	44.27
Environment*Rake Angle	6	0.043796	0.043796	0.007299	12.21
Environment*Feed in/rev	3	0.024270	0.024270	0.008090	13.53
Rake Angle*Feed in/rev	2	0.002365	0.002365	0.001183	1.98
Environment*Rake Angle*Feed in/rev	6	0.004888	0.004888	0.000815	1.36
Error	72	0.043058	0.043058	0.000598	
Total	95	0.575423			

Source	P
Environment	0.000
Rake Angle	0.000
Feed in/rev	0.000
Environment*Rake Angle	0.000
Environment*Feed in/rev	0.000
Rake Angle*Feed in/rev	0.146
Environment*Rake Angle*Feed in/rev	0.242
Error	
Total	

S = 0.0244545 R-Sq = 92.52% R-Sq(adj) = 90.13%

Unusual Observations for Chip thickness ratio

Obs	Chip thickness ratio	Fit	SE Fit	Residual	St Resid
5	0.258065	0.202577	0.012227	0.055488	2.62 R
6	0.262295	0.202577	0.012227	0.059718	2.82 R
7	0.264550	0.202577	0.012227	0.061974	2.93 R
8	0.025397	0.202577	0.012227	-0.177180	-8.37 R

R denotes an observation with a large standardized residual.

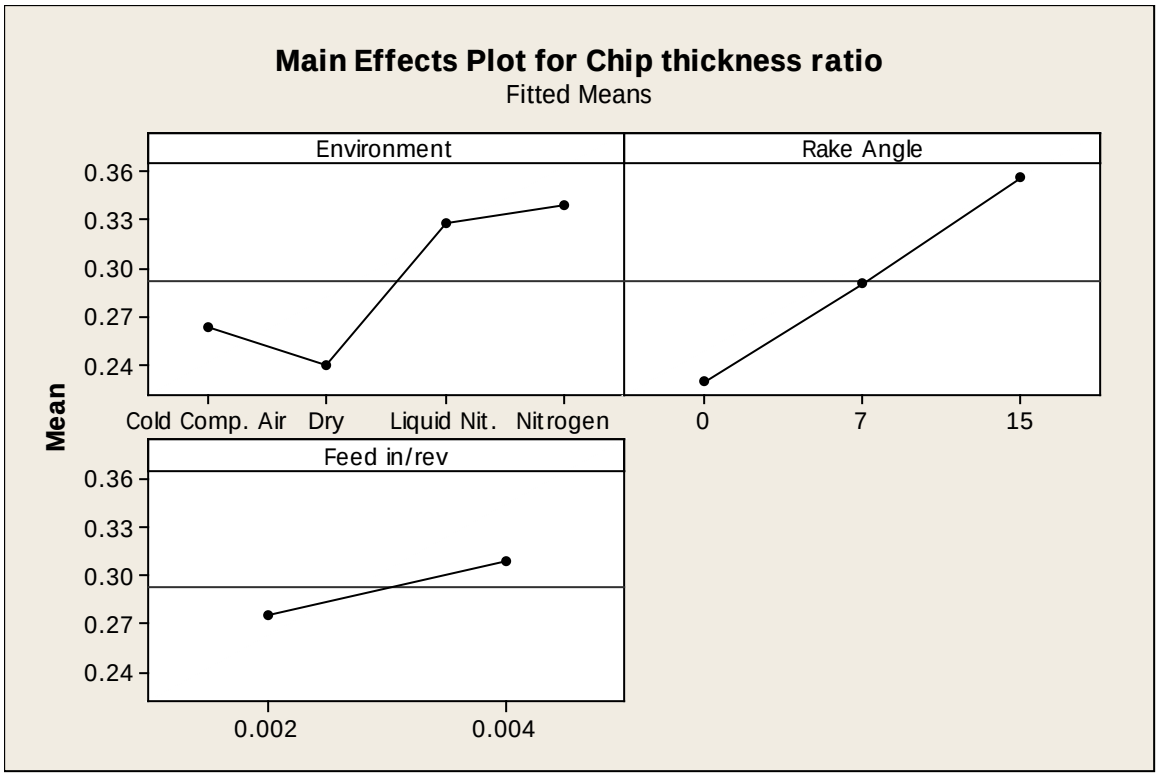
Main Effects Plot for Chip thickness ratio
Fitted Means
Environment
Rake Angle
Feed in/rev
Mean
0.36
0.33
0.30
0.27
0.24
Cold Comp. Air
Dry
Liquid Nit.
Nitrogen
0
7
15
0.002
0.004

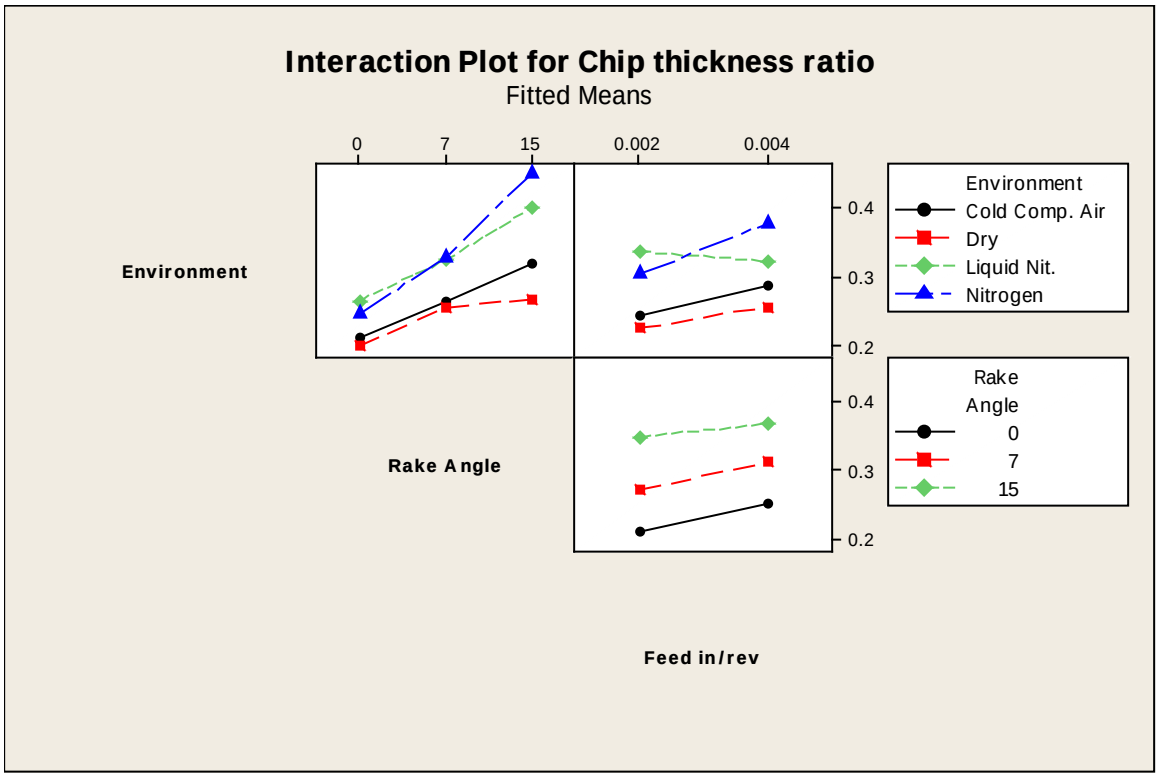
Interaction Plot for Chip thickness ratio
Fitted Means
Environment
Rake Angle
Feed in/rev
0
7
15
0.002
0.004
0.4
0.3
0.2
Environment
Cold Comp. Air
Dry
Liquid Nit.
Nitrogen
Rake Angle
0
7
15

Analysis of Variance for **Phi** degrees, using Adjusted SS for Tests

Source	DF	Seq SS	Adj SS	Adj MS	F
Environment	3	555.429	555.429	185.143	98.97
Rake Angle	2	994.619	994.619	497.309	265.86
Feed in/rev	1	81.890	81.890	81.890	43.78
Environment*Rake Angle	6	157.467	157.467	26.244	14.03
Environment*Feed in/rev	3	75.247	75.247	25.082	13.41
Rake Angle*Feed in/rev	2	6.371	6.371	3.186	1.70
Environment*Rake Angle*Feed in/rev	6	16.023	16.023	2.671	1.43
Error	72	134.683	134.683	1.871	
Total	95	2021.730			

Source	P
Environment	0.000
Rake Angle	0.000
Feed in/rev	0.000
Environment*Rake Angle	0.000
Environment*Feed in/rev	0.000
Rake Angle*Feed in/rev	0.189
Environment*Rake Angle*Feed in/rev	0.216
Error	
Total	

S = 1.36770 R-Sq = 93.34% R-Sq(adj) = 91.21%

Unusual Observations for Phi degrees

Obs	Phi degrees	Fit	SE Fit	Residual	St Resid
5	14.4703	11.3601	0.6839	3.1101	2.63 R
6	14.6973	11.3601	0.6839	3.3372	2.82 R
7	14.8181	11.3601	0.6839	3.4580	2.92 R
8	1.4548	11.3601	0.6839	-9.9053	-8.36 R

R denotes an observation with a large standardized residual.

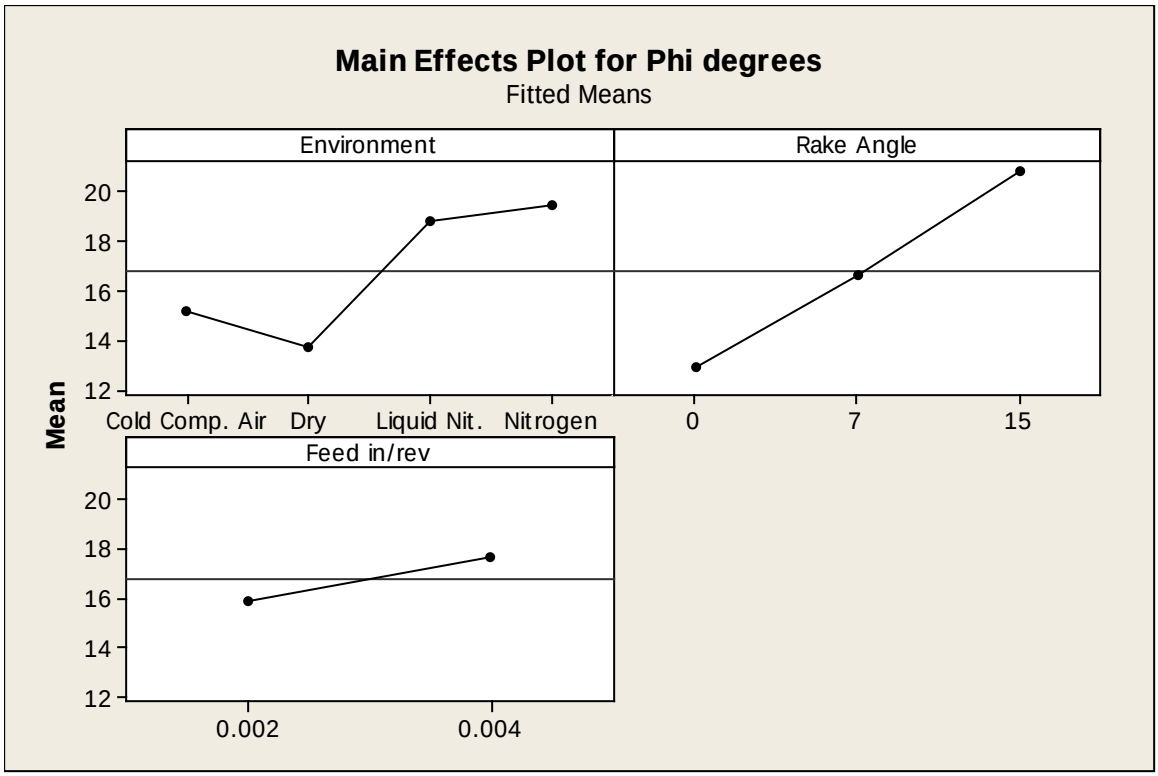
Main Effects Plot for Phi degrees
Fitted Means
Environment
Rake Angle
Feed in/rev
Mean
20
18
16
14
12
Cold Comp. Air
Dry
Liquid Nit.
Nitrogen
0
7
15
0.002
0.004

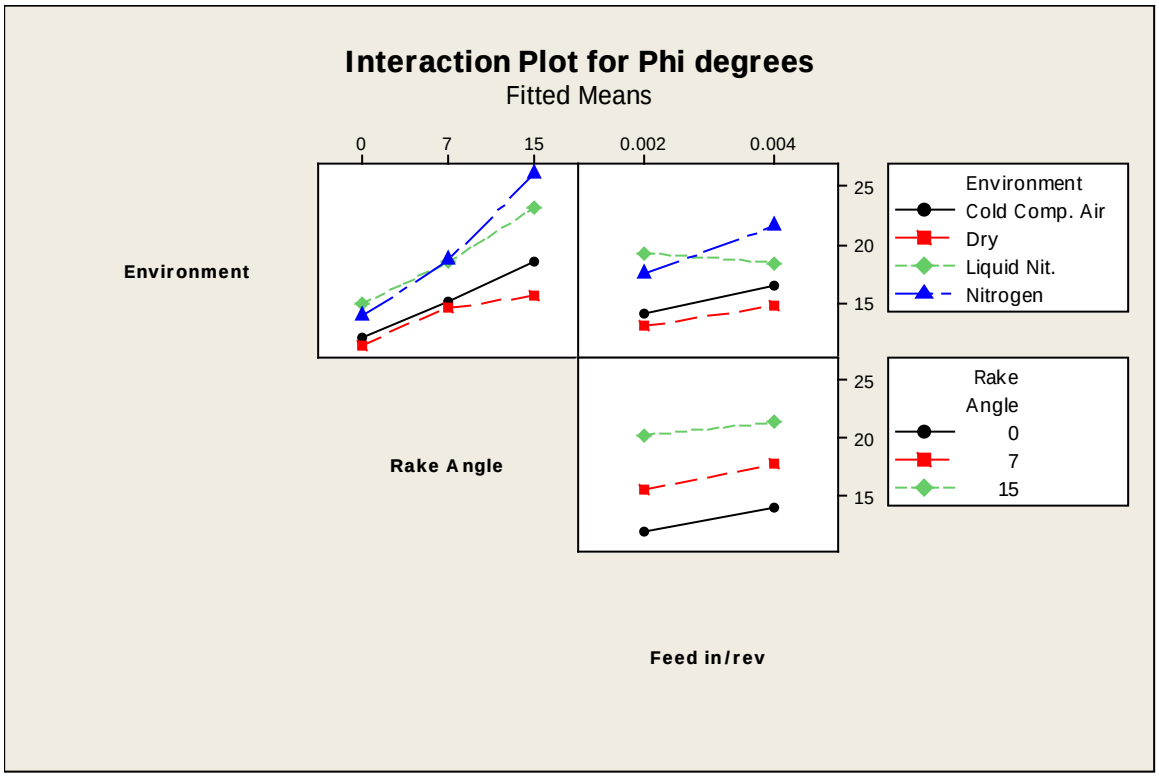
Interaction Plot for Phi degrees
Fitted Means
0
7
15
0.002
0.004
Environment
Rake Angle
25
20
15
Environment
Cold Comp. Air
Dry
Liquid Nit.
Nitrogen
Rake Angle
0
7
15
Feed in/rev

Analysis of Variance for **Psi** degrees, using Adjusted SS for Tests

Source	DF	Seq SS	Adj SS	Adj MS	F
Environment	3	555.429	555.429	185.143	98.97
Rake Angle	2	2.352	2.352	1.176	0.63
Feed in/rev	1	81.890	81.890	81.890	43.78
Environment*Rake Angle	6	157.467	157.467	26.244	14.03
Environment*Feed in/rev	3	75.247	75.247	25.082	13.41
Rake Angle*Feed in/rev	2	6.371	6.371	3.186	1.70
Environment*Rake Angle*Feed in/rev	6	16.023	16.023	2.671	1.43
Error	72	134.683	134.683	1.871	
Total	95	1029.463			

Source	P
Environment	0.000
Rake Angle	0.536
Feed in/rev	0.000
Environment*Rake Angle	0.000
Environment*Feed in/rev	0.000
Rake Angle*Feed in/rev	0.189
Environment*Rake Angle*Feed in/rev	0.216
Error	
Total	

S = 1.36770 R-Sq = 86.92% R-Sq(adj) = 82.74%

Unusual Observations for Psi degrees

Obs	Psi degrees	Fit	SE Fit	Residual	St Resid	
5	30.5297	33.6399	0.6839	-3.1101	-2.63	R
6	30.3027	33.6399	0.6839	-3.3372	-2.82	R
7	30.1819	33.6399	0.6839	-3.4580	-2.92	R
8	43.5452	33.6399	0.6839	9.9053	8.36	R

R denotes an observation with a large standardized residual.

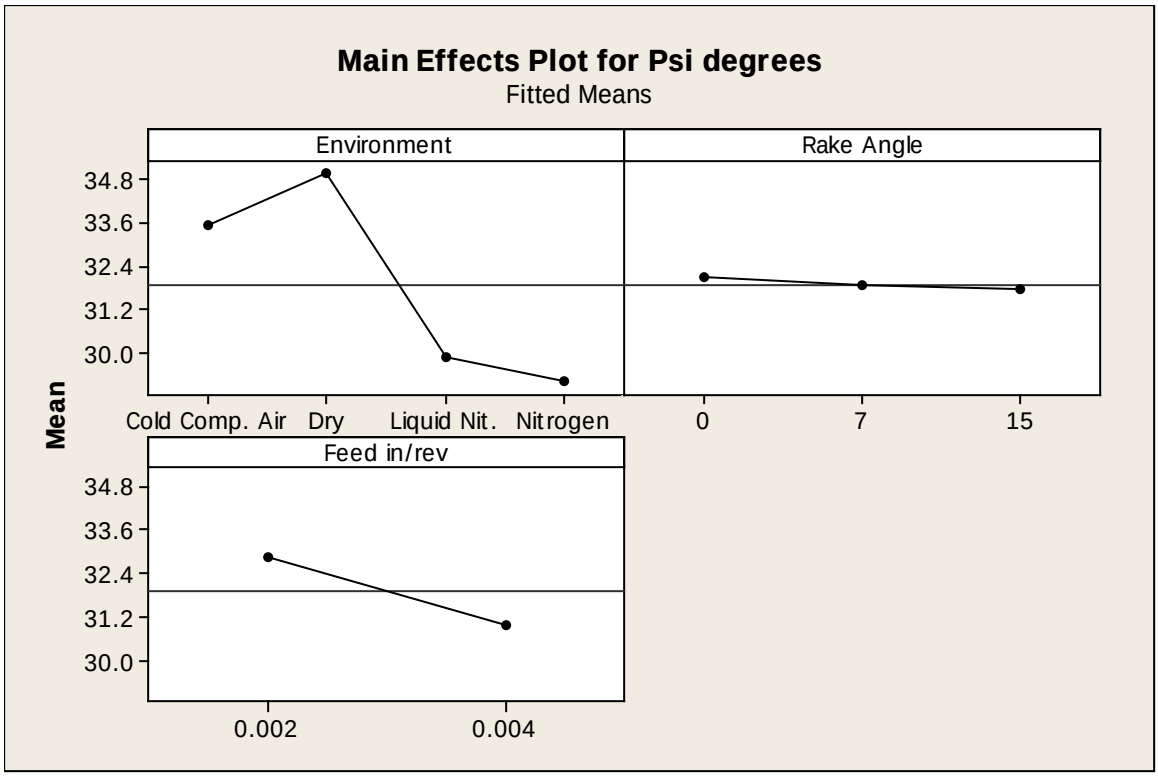
Main Effects Plot for Psi degrees
Fitted Means
Environment
Rake Angle
Feed in/rev
Mean
34.8
33.6
32.4
31.2
30.0
Cold Comp. Air
Dry
Liquid Nit.
Nitrogen
0
7
15
0.002
0.004

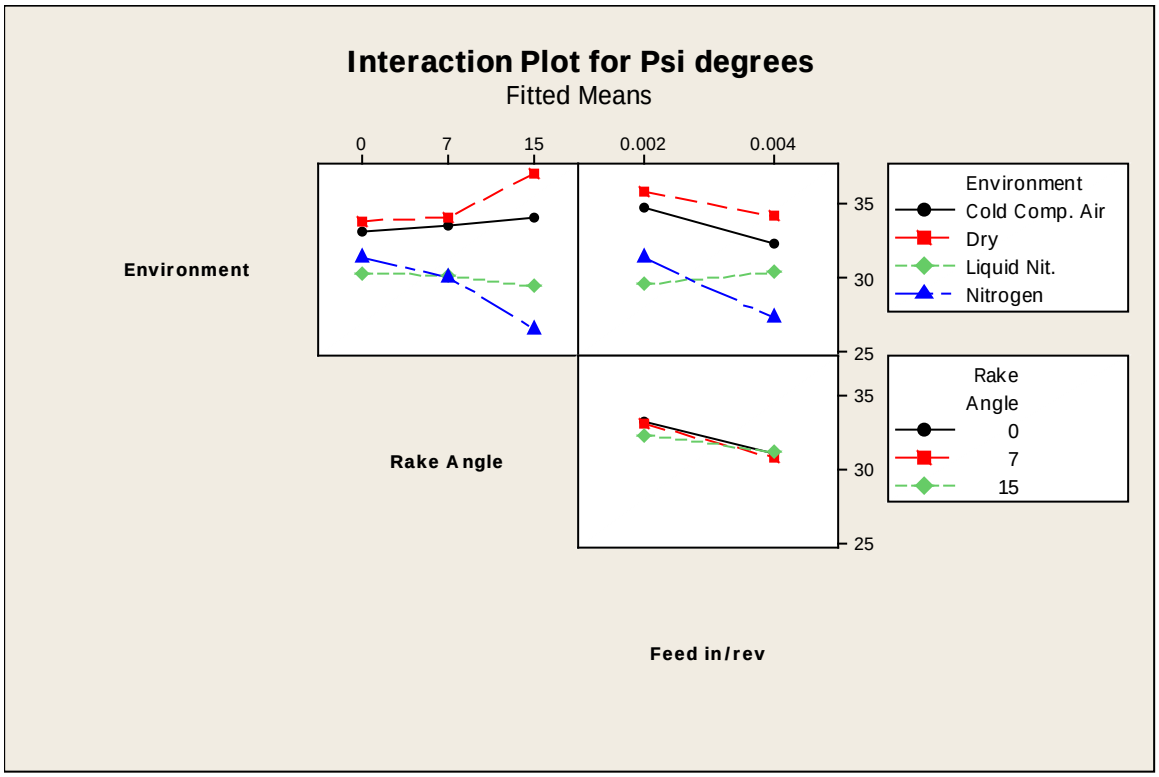
Interaction Plot for Psi degrees
Fitted Means
Environment
Rake Angle
Feed in/rev
0
7
15
0.002
0.004
35
30
25
Environment
Cold Comp. Air
Dry
Liquid Nit.
Nitrogen
Rake Angle
0
7
15

Analysis of Variance for **Friction Force (F)**, using Adjusted SS for Tests

Source	DF	Seq SS	Adj SS	Adj MS	F
Environment	3	6635.0	6635.0	2211.7	8.61
Rake Angle	2	11960.3	11960.3	5980.2	23.29
Feed in/rev	1	126335.4	126335.4	126335.4	492.00
Environment*Rake Angle	6	4666.0	4666.0	777.7	3.03
Environment*Feed in/rev	3	2423.4	2423.4	807.8	3.15
Rake Angle*Feed in/rev	2	472.5	472.5	236.2	0.92
Environment*Rake Angle*Feed in/rev	6	361.0	361.0	60.2	0.23
Error	72	18488.0	18488.0	256.8	
Total	95	171341.5			

Source	P
Environment	0.000
Rake Angle	0.000
Feed in/rev	0.000
Environment*Rake Angle	0.011
Environment*Feed in/rev	0.030
Rake Angle*Feed in/rev	0.403
Environment*Rake Angle*Feed in/rev	0.964
Error	
Total	

S = 16.0243 R-Sq = 89.21% R-Sq(adj) = 85.76%

Unusual Observations for Friction Force (F)

Obs	Friction Force (F)	Fit	SE Fit	Residual	St Resid
78	262.952	295.460	8.012	-32.508	-2.34 R
79	398.813	295.460	8.012	103.353	7.45 R
80	247.157	295.460	8.012	-48.303	-3.48 R

R denotes an observation with a large standardized residual.

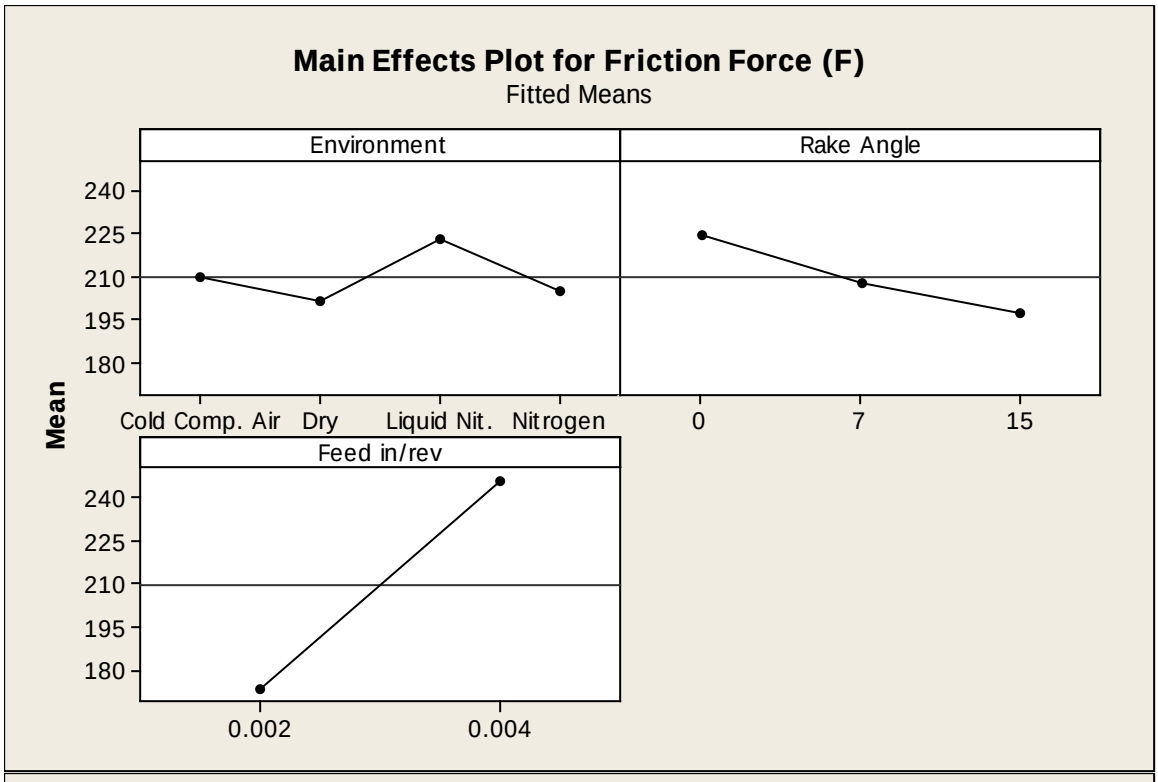
Main Effects Plot for Friction Force (F)
Fitted Means
Environment
Rake Angle
Feed in/rev
Mean
240
225
210
195
180
Cold Comp. Air
Dry
Liquid Nit.
Nitrogen
0
7
15
0.002
0.004

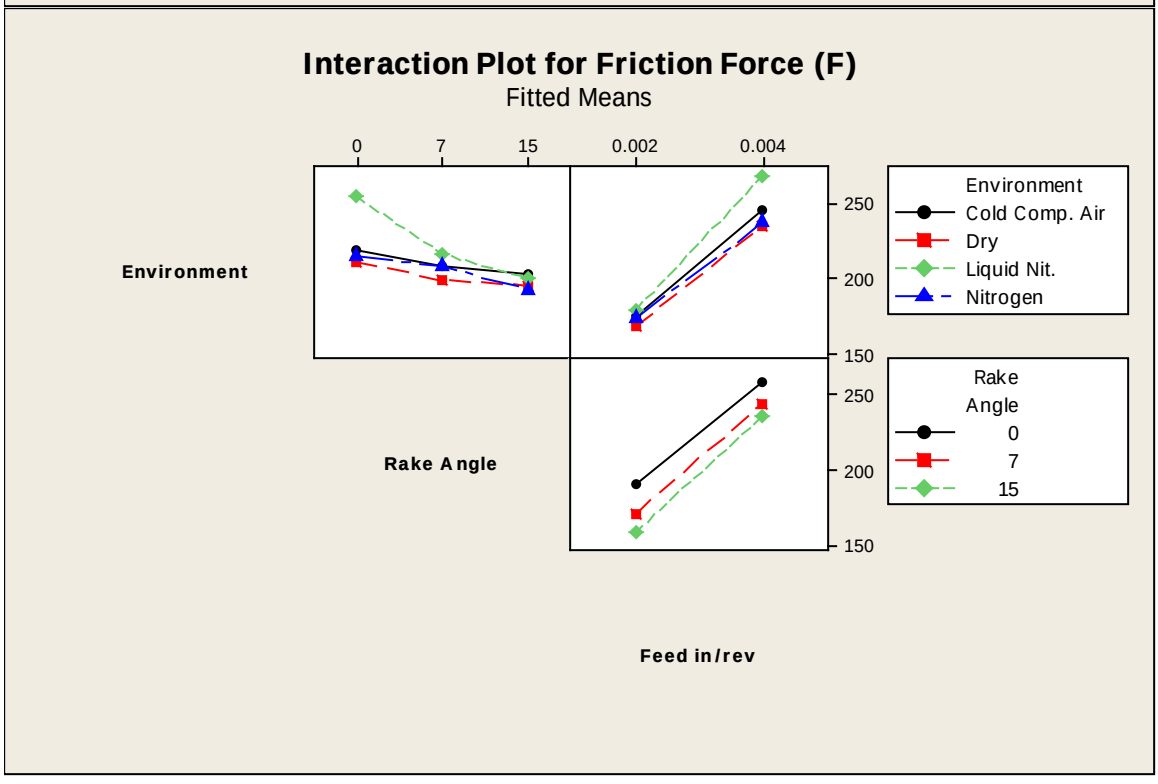
Interaction Plot for Friction Force (F)
Fitted Means
Environment
Rake Angle
Feed in/rev
0
7
15
0.002
0.004
250
200
150
Environment
Cold Comp. Air
Dry
Liquid Nit.
Nitrogen
Rake Angle
0
7
15

Analysis of Variance for **Normal Force (N)**, using Adjusted SS for Tests

Source	DF	Seq SS	Adj SS	Adj MS	F	P
Environment	3	5709	5709	1903	76.42	0.000
Rake Angle	2	124781	124781	62391	2505.40	0.000
Feed in/rev	1	317733	317733	317733	12759.08	0.000
Environment*Rake Angle	6	1502	1502	250	10.05	0.000
Environment*Feed in/rev	3	270	270	90	3.61	0.017
Rake Angle*Feed in/rev	2	1389	1389	694	27.88	0.000
Environment*Rake Angle*Feed in/rev	6	307	307	51	2.05	0.070
Error	72	1793	1793	25		
Total	95	453484				

S = 4.99024   R-Sq = 99.60%   R-Sq(adj) = 99.48%

Unusual Observations for Normal Force (N)

Obs	Normal Force (N)	Fit	SE Fit	Residual	St Resid	
1	232.640	219.203	2.495	13.437	3.11	R
74	239.012	252.579	2.495	-13.567	-3.14	R
75	268.992	252.579	2.495	16.413	3.80	R
78	362.834	373.720	2.495	-10.886	-2.52	R
79	389.360	373.720	2.495	15.640	3.62	R

R denotes an observation with a large standardized residual.

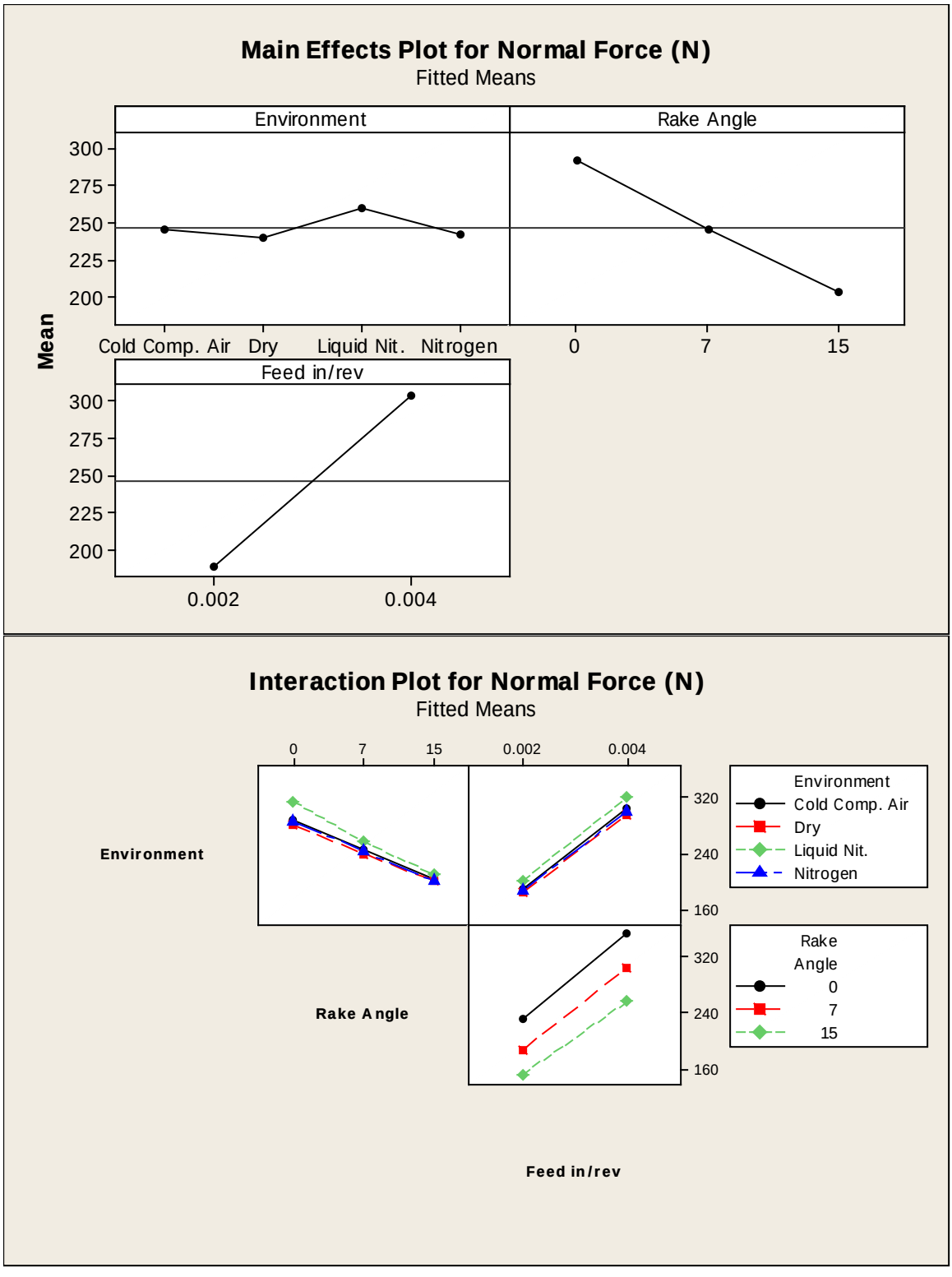
Main Effects Plot for Normal Force (N)
Fitted Means
Environment
Rake Angle
Feed in/rev
Mean
300
275
250
225
200
Cold Comp. Air
Dry
Liquid Nit.
Nitrogen
0
7
15
0.002
0.004
Interaction Plot for Normal Force (N)
Fitted Means
Environment
Rake Angle
Feed in/rev
320
240
160
Environment
Cold Comp. Air
Dry
Liquid Nit.
Nitrogen
Rake Angle
0
7
15

Analysis of Variance for **F/N Ratio**, using Adjusted SS for Tests

Source	DF	Seq SS	Adj SS	Adj MS	F
Environment	3	0.003136	0.003136	0.001045	0.61
Rake Angle	2	0.712049	0.712049	0.356024	207.70
Feed in/rev	1	0.316110	0.316110	0.316110	184.42
Environment*Rake Angle	6	0.026209	0.026209	0.004368	2.55
Environment*Feed in/rev	3	0.022878	0.022878	0.007626	4.45
Rake Angle*Feed in/rev	2	0.002988	0.002988	0.001494	0.87
Environment*Rake Angle*Feed in/rev	6	0.005533	0.005533	0.000922	0.54
Error	72	0.123415	0.123415	0.001714	
Total	95	1.212318			

Source	P
Environment	0.611
Rake Angle	0.000
Feed in/rev	0.000
Environment*Rake Angle	0.027
Environment*Feed in/rev	0.006
Rake Angle*Feed in/rev	0.423
Environment*Rake Angle*Feed in/rev	0.778
Error	
Total	

S = 0.0414016 R-Sq = 89.82% R-Sq(adj) = 86.57%

Unusual Observations for F/N Ratio

Obs	F/N Ratio	Fit	SE Fit	Residual	St Resid	
43	1.21576	1.10694	0.02070	0.10882	3.03	R
79	1.02428	0.78742	0.02070	0.23686	6.61	R
80	0.66404	0.78742	0.02070	-0.12339	-3.44	R

R denotes an observation with a large standardized residual.

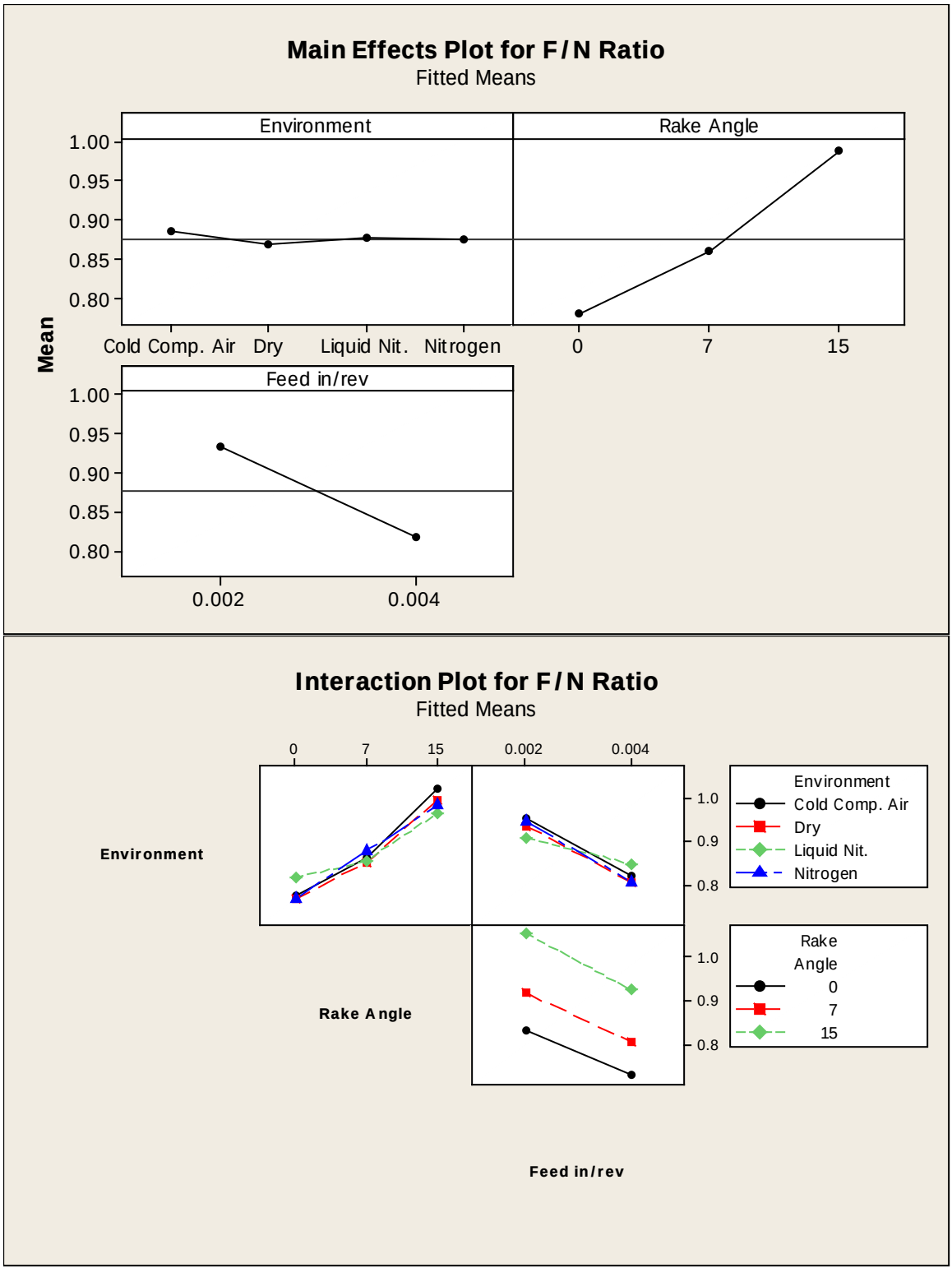
Main Effects Plot for F/N Ratio
Fitted Means
Environment
Rake Angle
Feed in/rev
Mean
1.00
0.95
0.90
0.85
0.80
Cold Comp. Air
Dry
Liquid Nit.
Nitrogen
0
7
15
0.002
0.004
Interaction Plot for F/N Ratio
Fitted Means
Environment
Rake Angle
Feed in/rev
Cold Comp. Air
Dry
Liquid Nit.
Nitrogen
Rake Angle
0
7
15

Analysis of Variance for **Fs (Merchant)**, using Adjusted SS for Tests

Source	DF	Seq SS	Adj SS	Adj MS	F	P
Environment	3	7129	7129	2376	33.81	0.000
Rake Angle	2	41711	41711	20855	296.71	0.000
Feed in/rev	1	208902	208902	208902	2972.06	0.000
Environment*Rake Angle	6	2568	2568	428	6.09	0.000
Environment*Feed in/rev	3	2224	2224	741	10.55	0.000
Rake Angle*Feed in/rev	2	23	23	11	0.16	0.851
Environment*Rake Angle*Feed in/rev	6	351	351	59	0.83	0.548
Error	72	5061	5061	70		
Total	95	267968				

S = 8.38383 R-Sq = 98.11% R-Sq(adj) = 97.51%

Unusual Observations for Fs (Merchant)

Obs	Fs (Merchant)	Fit	SE Fit	Residual	St Resid	
5	266.616	284.943	4.192	-18.327	-2.52	R
6	266.821	284.943	4.192	-18.122	-2.50	R
7	266.705	284.943	4.192	-18.238	-2.51	R
8	339.630	284.943	4.192	54.687	7.53	R

R denotes an observation with a large standardized residual.

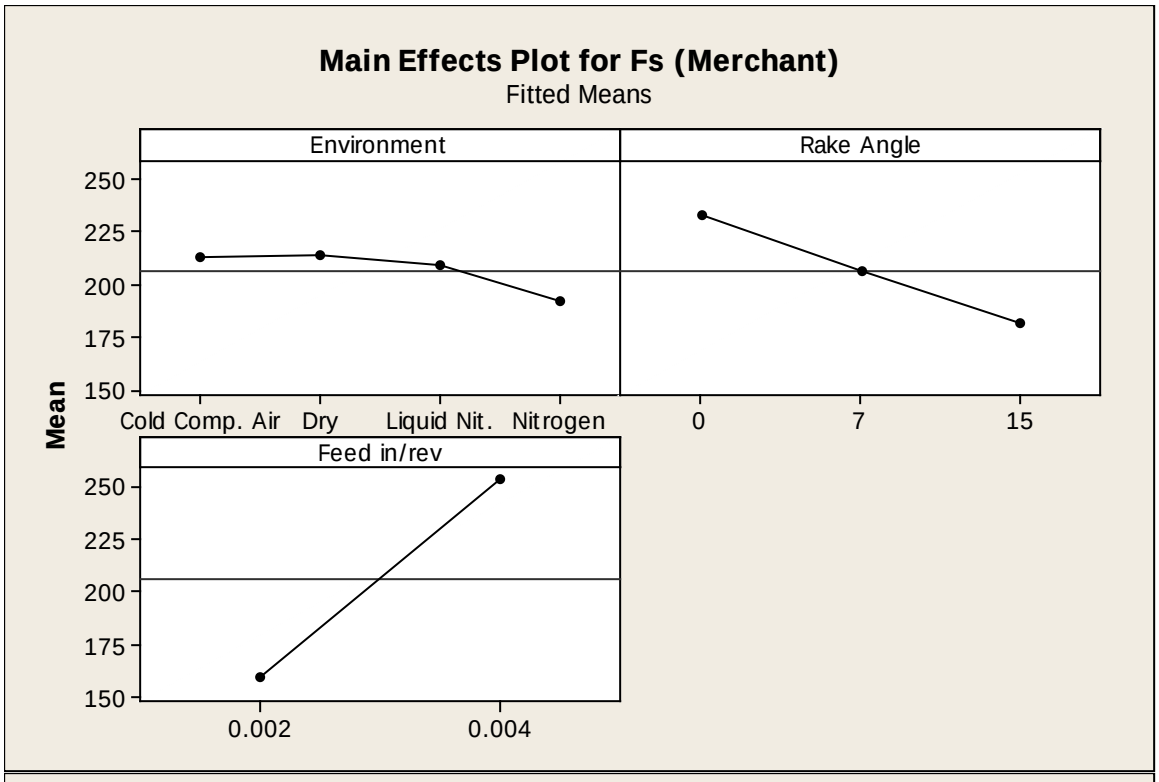
Main Effects Plot for Fs (Merchant)
Fitted Means
Environment
Rake Angle
Feed in/rev
Mean
250
225
200
175
150
Cold Comp. Air
Dry
Liquid Nit.
Nitrogen
0
7
15
0.002
0.004

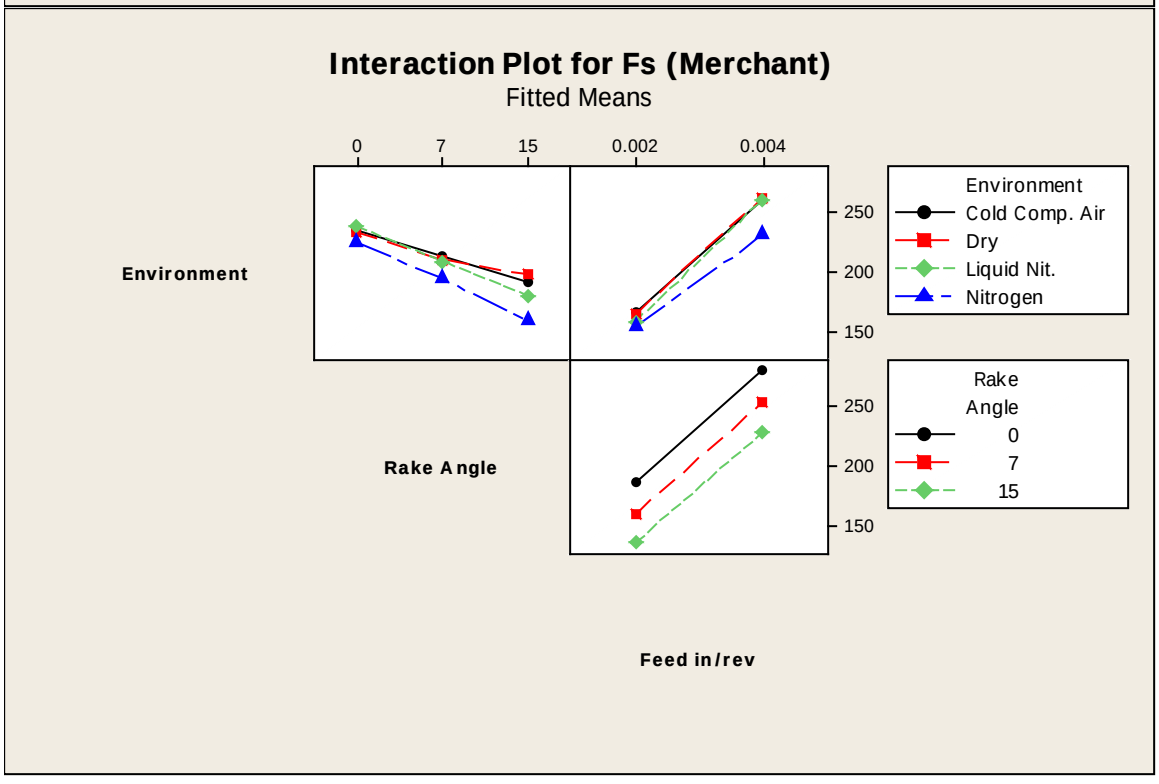
Interaction Plot for Fs (Merchant)
Fitted Means
Environment
Rake Angle
Feed in/rev
0
7
15
0.002
0.004
250
200
150
Environment
Cold Comp. Air
Dry
Liquid Nit.
Nitrogen
Rake Angle
0
7
15

Analysis of Variance for **Fn (Merchant)**, using Adjusted SS for Tests

Source	DF	Seq SS	Adj SS	Adj MS	F	P
Environment	3	22767	22767	7589	25.37	0.000
Rake Angle	2	74024	74024	37012	123.73	0.000
Feed in/rev	1	226826	226826	226826	758.30	0.000
Environment*Rake Angle	6	6169	6169	1028	3.44	0.005
Environment*Feed in/rev	3	1855	1855	618	2.07	0.112
Rake Angle*Feed in/rev	2	455	455	228	0.76	0.471
Environment*Rake Angle*Feed in/rev	6	740	740	123	0.41	0.869
Error	72	21537	21537	299		
Total	95	354373				

S = 17.2953 R-Sq = 93.92% R-Sq(adj) = 91.98%

Unusual Observations for Fn (Merchant)

Obs	Fn (Merchant)	Fit	SE Fit	Residual	St Resid	
8	256.898	300.149	8.648	-43.251	-2.89	R
78	346.480	380.361	8.648	-33.881	-2.26	R
79	484.108	380.361	8.648	103.747	6.93	R
80	332.948	380.361	8.648	-47.413	-3.17	R

R denotes an observation with a large standardized residual.

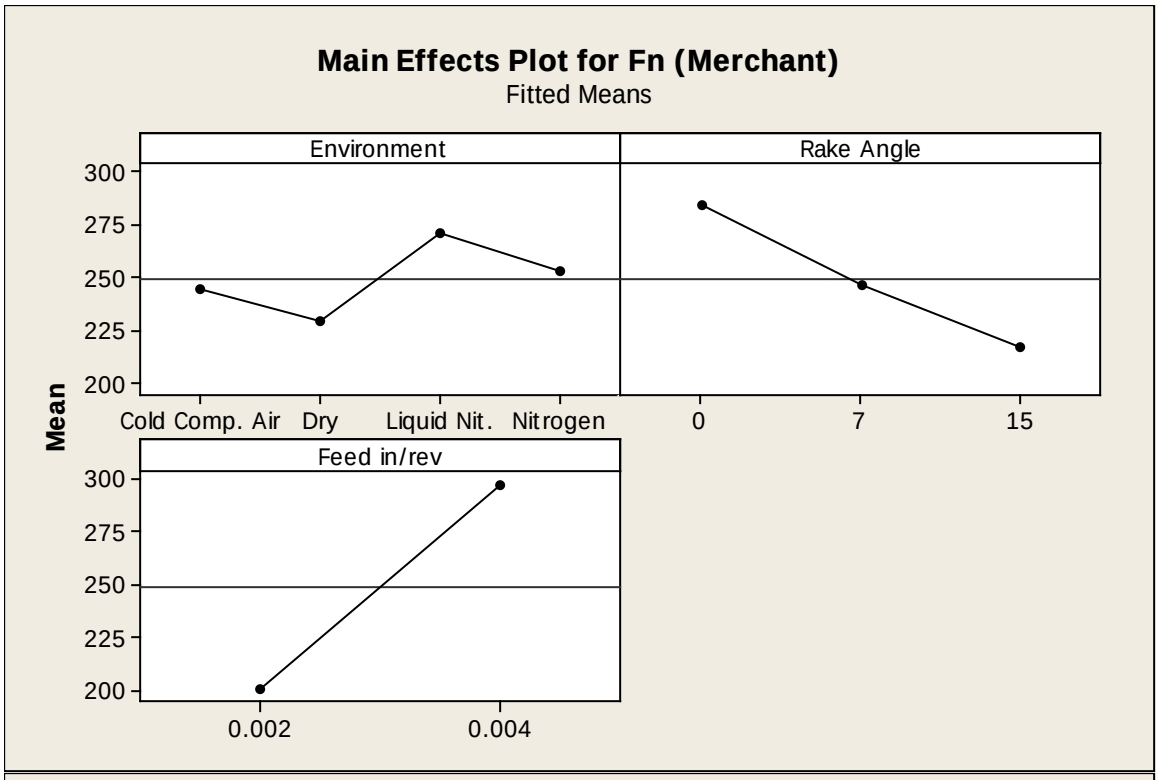
Main Effects Plot for Fn (Merchant)
Fitted Means
Environment
Rake Angle
Feed in/rev
Mean
300
275
250
225
200
Cold Comp. Air
Dry
Liquid Nit.
Nitrogen
0
7
15
0.002
0.004

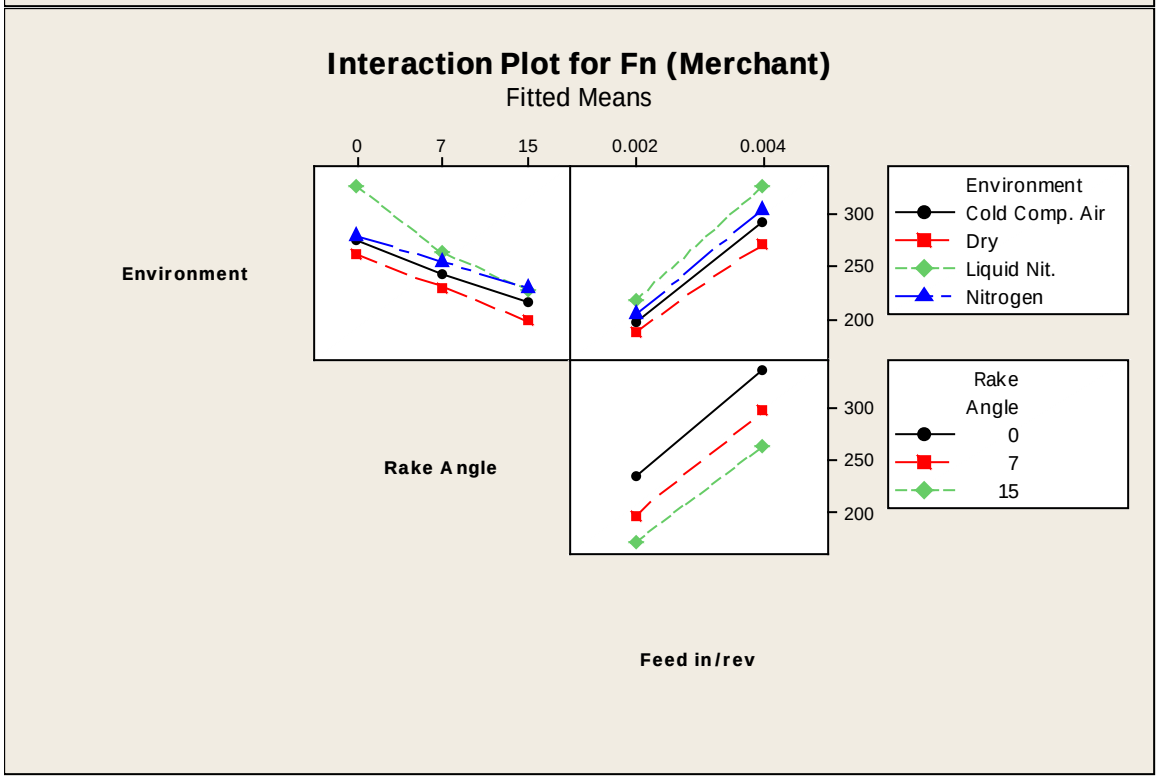
Interaction Plot for Fn (Merchant)
Fitted Means
Environment
Rake Angle
Feed in/rev
0
7
15
0.002
0.004
300
250
200
Environment
Cold Comp. Air
Dry
Liquid Nit.
Nitrogen
Rake Angle
0
7
15

Analysis of Variance for **Fs/Fn (Merchant)**, using Adjusted SS for Tests

Source	DF	Seq SS	Adj SS	Adj MS	F
Environment	3	0.518537	0.518537	0.172846	47.46
Rake Angle	2	0.002863	0.002863	0.001431	0.39
Feed in/rev	1	0.079903	0.079903	0.079903	21.94
Environment*Rake Angle	6	0.114805	0.114805	0.019134	5.25
Environment*Feed in/rev	3	0.023171	0.023171	0.007724	2.12
Rake Angle*Feed in/rev	2	0.005071	0.005071	0.002536	0.70
Environment*Rake Angle*Feed in/rev	6	0.019426	0.019426	0.003238	0.89
Error	72	0.262192	0.262192	0.003642	
Total	95	1.025969			

Source	P
Environment	0.000
Rake Angle	0.676
Feed in/rev	0.000
Environment*Rake Angle	0.000
Environment*Feed in/rev	0.105
Rake Angle*Feed in/rev	0.502
Environment*Rake Angle*Feed in/rev	0.508
Error	
Total	

S = 0.0603454 R-Sq = 74.44% R-Sq(adj) = 66.28%

Unusual Observations for Fs/Fn (Merchant)

Obs	Fs/Fn (Merchant)	Fit	SE Fit	Residual	St Resid	
5	0.86054	0.96653	0.03017	-0.10599	-2.03	R
6	0.83365	0.96653	0.03017	-0.13288	-2.54	R
7	0.84989	0.96653	0.03017	-0.11664	-2.23	R
8	1.32204	0.96653	0.03017	0.35551	6.80	R
79	0.57056	0.77340	0.03017	-0.20284	-3.88	R
80	0.89486	0.77340	0.03017	0.12146	2.32	R

R denotes an observation with a large standardized residual.

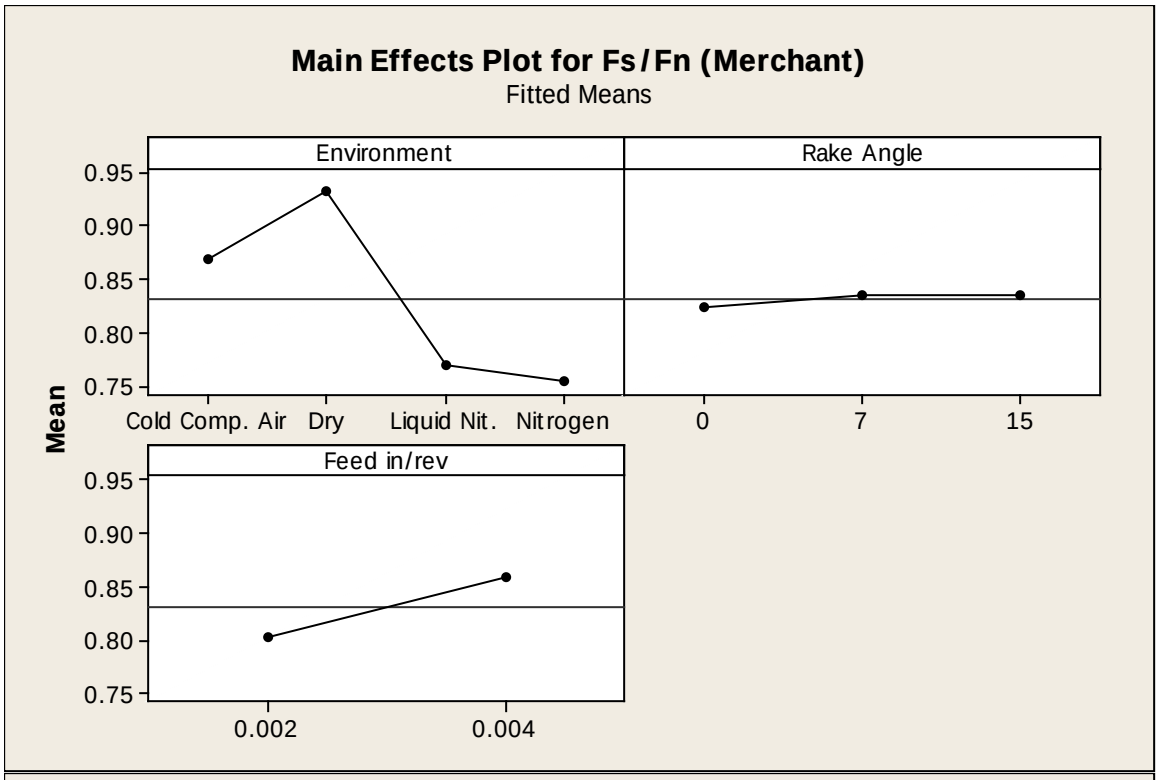
Main Effects Plot for Fs/Fn (Merchant)
Fitted Means
Environment
Rake Angle
Feed in/rev
Mean
0.95
0.90
0.85
0.80
0.75
Cold Comp. Air
Dry
Liquid Nit.
Nitrogen
0
7
15
0.002
0.004

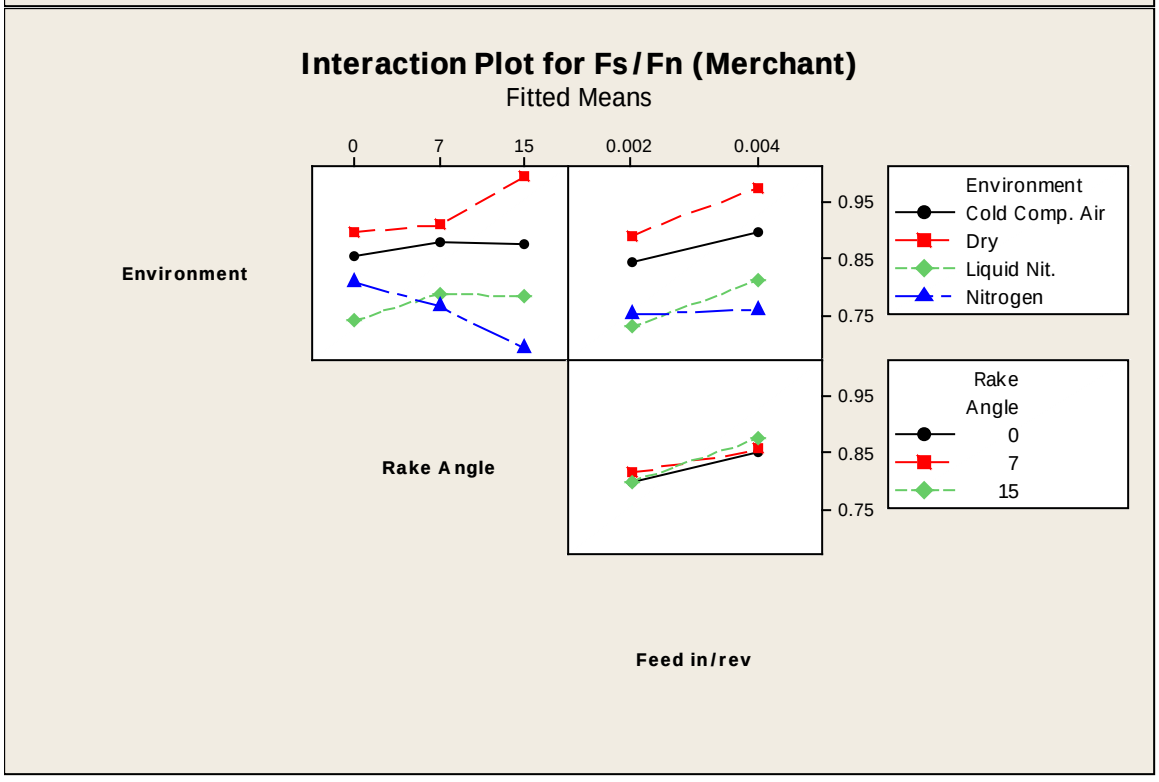
Interaction Plot for Fs/Fn (Merchant)
Fitted Means
Environment
Rake Angle
Feed in/rev
0
7
15
0.002
0.004
0.95
0.85
0.75
Environment
Cold Comp. Air
Dry
Liquid Nit.
Nitrogen
Rake Angle
0
7
15

Analysis of Variance for **Fs (Payton)**, using Adjusted SS for Tests

Source	DF	Seq SS	Adj SS	Adj MS	F
Environment	3	19.3	19.3	6.4	0.08
Rake Angle	2	729.7	729.7	364.9	4.32
Feed in/rev	1	35271.6	35271.6	35271.6	417.79
Environment*Rake Angle	6	569.0	569.0	94.8	1.12
Environment*Feed in/rev	3	443.2	443.2	147.7	1.75
Rake Angle*Feed in/rev	2	68.0	68.0	34.0	0.40
Environment*Rake Angle*Feed in/rev	6	170.4	170.4	28.4	0.34
Error	72	6078.5	6078.5	84.4	
Total	95	43349.8			

Source	P
Environment	0.973
Rake Angle	0.017
Feed in/rev	0.000
Environment*Rake Angle	0.358
Environment*Feed in/rev	0.164
Rake Angle*Feed in/rev	0.670
Environment*Rake Angle*Feed in/rev	0.915
Error	
Total	

S = 9.18826 R-Sq = 85.98% R-Sq(adj) = 81.50%

Unusual Observations for Fs (Payton)

Obs	Fs (Payton)	Fit	SE Fit	Residual	St Resid
79	-6.6846	55.3377	4.5941	-62.0223	-7.79 R
80	88.4218	55.3377	4.5941	33.0841	4.16 R

R denotes an observation with a large standardized residual.

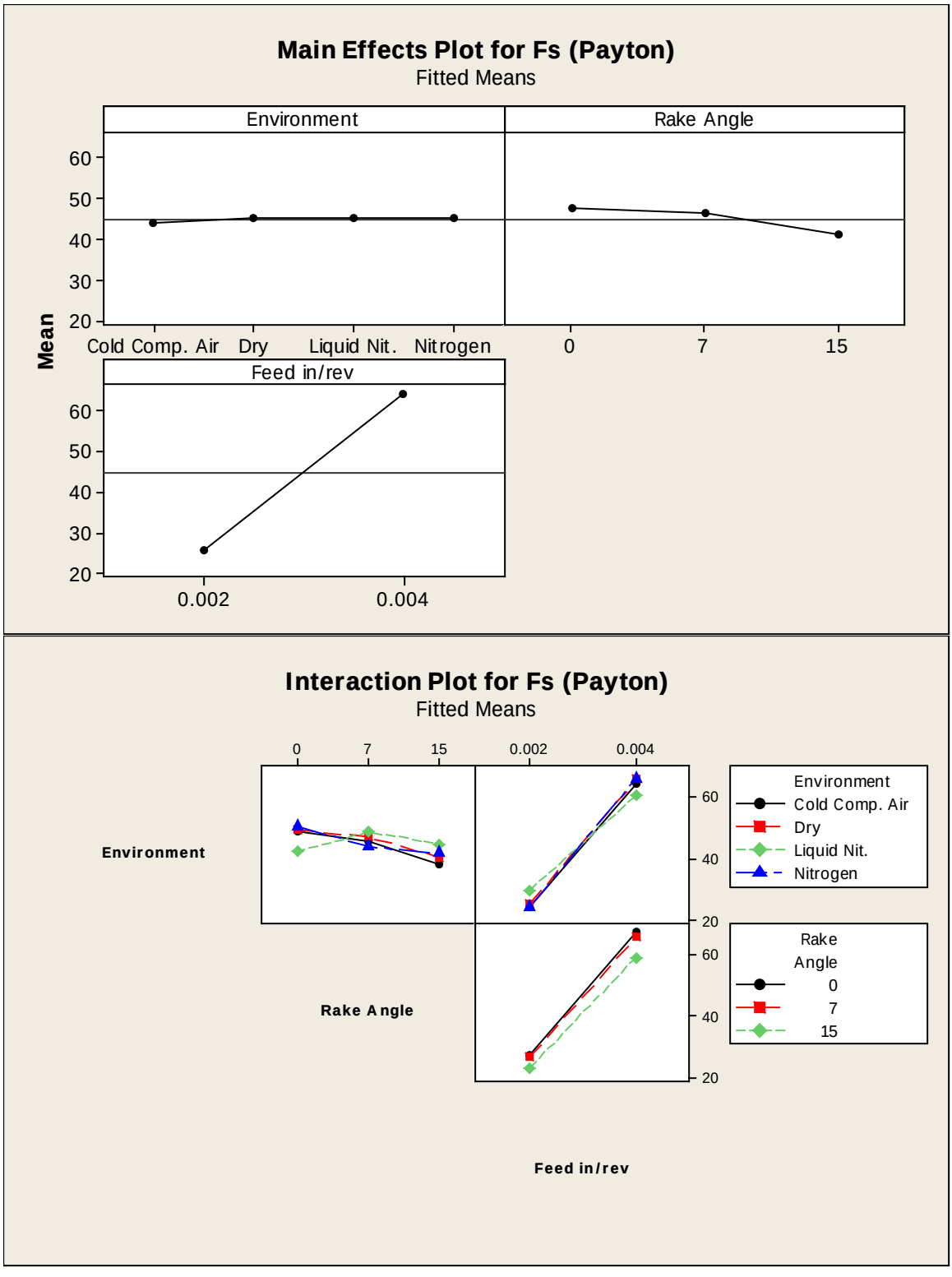
Main Effects Plot for Fs (Payton)
Fitted Means
Environment
Rake Angle
Feed in/rev
Mean
60
50
40
30
20
Cold Comp. Air
Dry
Liquid Nit.
Nitrogen
0
7
15
0.002
0.004
Interaction Plot for Fs (Payton)
Fitted Means
Environment
Rake Angle
Feed in/rev
Environment
Cold Comp. Air
Dry
Liquid Nit.
Nitrogen
Rake Angle
0
7
15

Analysis of Variance for **Fn (Payton)**, using Adjusted SS for Tests

Source	DF	Seq SS	Adj SS	Adj MS	F	P
Environment	3	12128	12128	4043	20.49	0.000
Rake Angle	2	114717	114717	57359	290.78	0.000
Feed in/rev	1	410234	410234	410234	2079.70	0.000
Environment*Rake Angle	6	5796	5796	966	4.90	0.000
Environment*Feed in/rev	3	2198	2198	733	3.71	0.015
Rake Angle*Feed in/rev	2	356	356	178	0.90	0.410
Environment*Rake Angle*Feed in/rev	6	549	549	92	0.46	0.833
Error	72	14202	14202	197		
Total	95	560181				

S = 14.0448 R-Sq = 97.46% R-Sq(adj) = 96.65%

Unusual Observations for Fn (Payton)

Obs	Fn (Payton)	Fit	SE Fit	Residual	St Resid	
75	354.385	328.773	7.022	25.611	2.11	R
78	442.498	473.182	7.022	-30.684	-2.52	R
79	557.322	473.182	7.022	84.140	6.92	R
80	437.955	473.182	7.022	-35.227	-2.90	R

R denotes an observation with a large standardized residual.

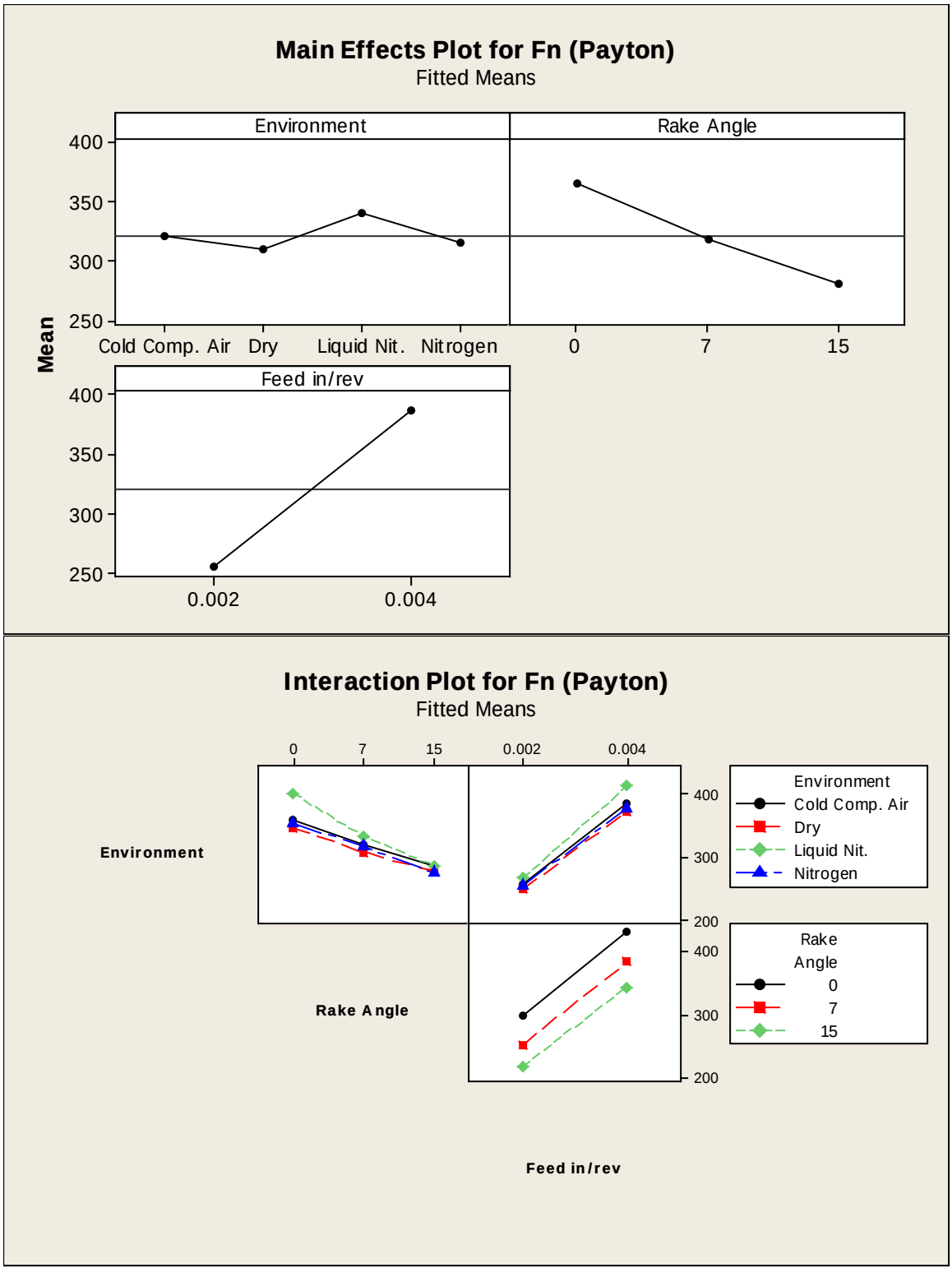
Main Effects Plot for Fn (Payton)
Fitted Means
Environment
Rake Angle
Feed in/rev
Mean
400
350
300
250
Cold Comp. Air
Dry
Liquid Nit.
Nitrogen
0
7
15
0.002
0.004
Interaction Plot for Fn (Payton)
Fitted Means
Environment
Rake Angle
Feed in/rev
Environment
Cold Comp. Air
Dry
Liquid Nit.
Nitrogen
Rake Angle
0
7
15

Analysis of Variance for **Fs/Fn (Payton)**, using Adjusted SS for Tests

Source	DF	Seq SS	Adj SS	Adj MS	F
Environment	3	0.0009501	0.0009501	0.0003167	0.58
Rake Angle	2	0.0035077	0.0035077	0.0017538	3.22
Feed in/rev	1	0.1049585	0.1049585	0.1049585	192.74
Environment*Rake Angle	6	0.0072319	0.0072319	0.0012053	2.21
Environment*Feed in/rev	3	0.0067607	0.0067607	0.0022536	4.14
Rake Angle*Feed in/rev	2	0.0000037	0.0000037	0.0000018	0.00
Environment*Rake Angle*Feed in/rev	6	0.0012687	0.0012687	0.0002115	0.39
Error	72	0.0392084	0.0392084	0.0005446	
Total	95	0.1638897			

Source	P
Environment	0.629
Rake Angle	0.046
Feed in/rev	0.000
Environment*Rake Angle	0.051
Environment*Feed in/rev	0.009
Rake Angle*Feed in/rev	0.997
Environment*Rake Angle*Feed in/rev	0.884
Error	
Total	

S = 0.0233358 R-Sq = 76.08% R-Sq(adj) = 68.43%

Unusual Observations for Fs/Fn (Payton)

Obs	Fs/Fn (Payton)	Fit	SE Fit	Residual	St Resid
43	0.033844	0.081303	0.011668	-0.047460	-2.35 R
79	-0.011994	0.125287	0.011668	-0.137281	-6.79 R
80	0.201897	0.125287	0.011668	0.076610	3.79 R

R denotes an observation with a large standardized residual.

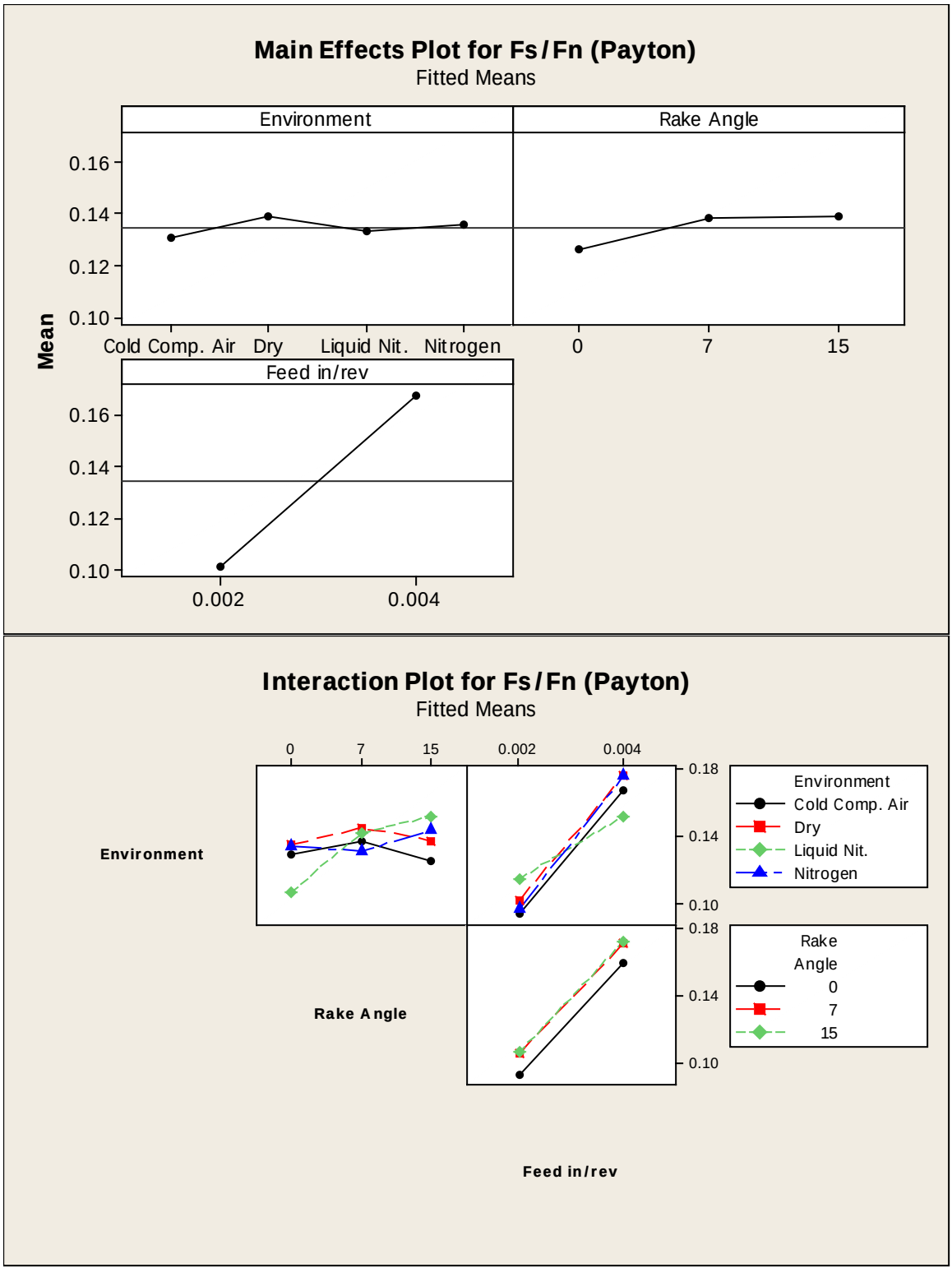
Main Effects Plot for Fs/Fn (Payton)
Fitted Means
Environment
Rake Angle
Feed in/rev
Mean
0.16
0.14
0.12
0.10
Cold Comp. Air
Dry
Liquid Nit.
Nitrogen
0
7
15
0.002
0.004
Interaction Plot for Fs/Fn (Payton)
Fitted Means
Environment
Rake Angle
Feed in/rev
0.18
Environment
Cold Comp. Air
Dry
Liquid Nit.
Nitrogen
Rake Angle
0
7
15

Analysis of Variance for **Beta** (degrees), using Adjusted SS for Tests

Source	DF	Seq SS	Adj SS	Adj MS	F
Environment	3	3.005	3.005	1.002	0.57
Rake Angle	2	737.728	737.728	368.864	210.81
Feed in/rev	1	331.712	331.712	331.712	189.58
Environment*Rake Angle	6	23.363	23.363	3.894	2.23
Environment*Feed in/rev	3	21.592	21.592	7.197	4.11
Rake Angle*Feed in/rev	2	0.012	0.012	0.006	0.00
Environment*Rake Angle*Feed in/rev	6	4.099	4.099	0.683	0.39
Error	72	125.981	125.981	1.750	
Total	95	1247.492			

Source	P
Environment	0.635
Rake Angle	0.000
Feed in/rev	0.000
Environment*Rake Angle	0.050
Environment*Feed in/rev	0.009
Rake Angle*Feed in/rev	0.997
Environment*Rake Angle*Feed in/rev	0.883
Error	
Total	

S = 1.32278 R-Sq = 89.90% R-Sq(adj) = 86.68%

Unusual Observations for Beta (degrees)

Obs	Beta (degrees)	Fit	SE Fit	Residual	St Resid	
43	50.5616	47.8550	0.6614	2.7066	2.36	R
79	45.6872	37.8955	0.6614	7.7917	6.80	R
80	33.5856	37.8955	0.6614	-4.3099	-3.76	R

R denotes an observation with a large standardized residual.

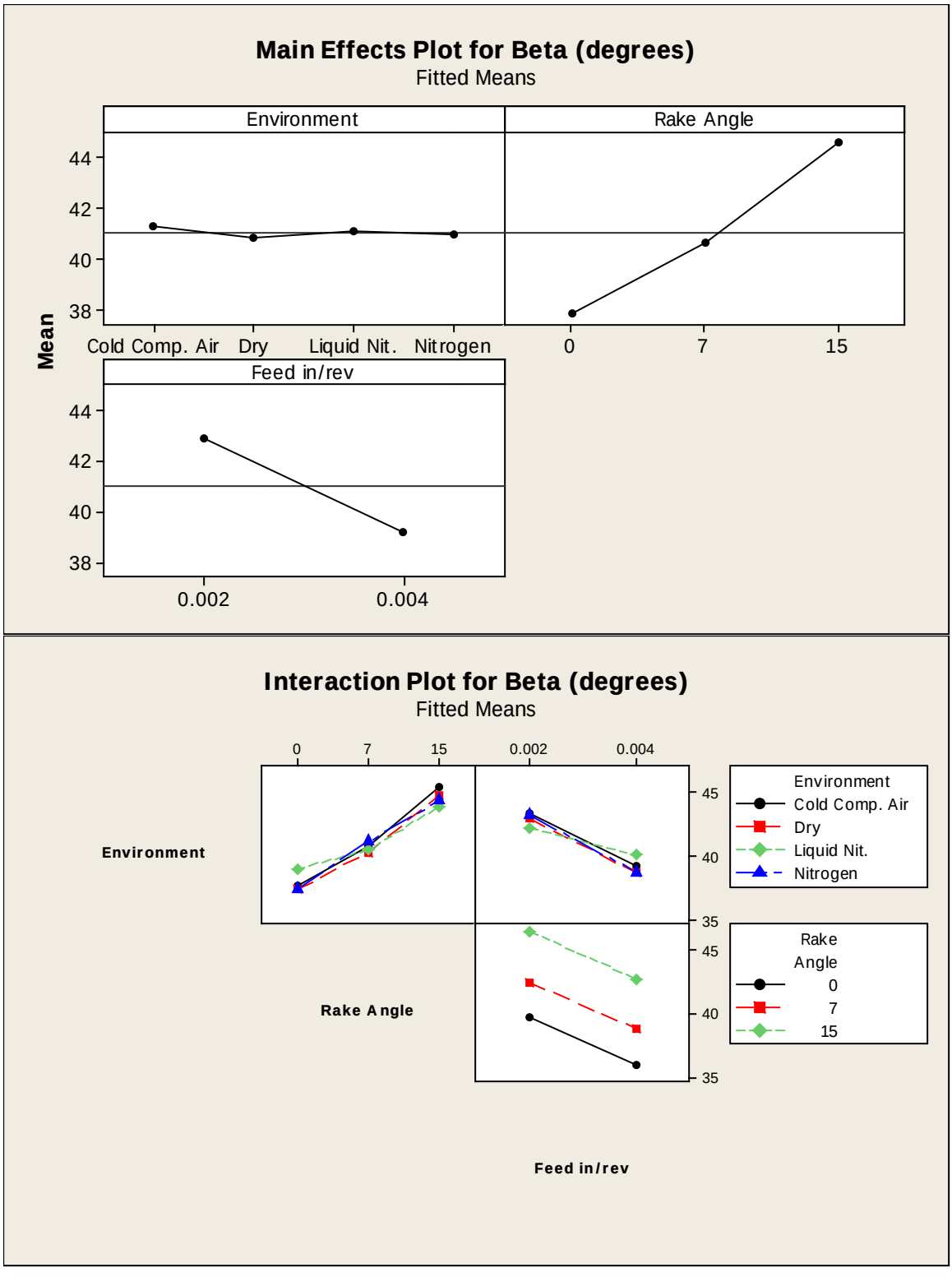
Main Effects Plot for Beta (degrees)
Fitted Means
Environment
Rake Angle
Feed in/rev
Mean
44
42
40
38
Cold Comp. Air
Dry
Liquid Nit.
Nitrogen
0
7
15
0.002
0.004
Interaction Plot for Beta (degrees)
Fitted Means
Environment
Rake Angle
Feed in/rev
45
40
35
Environment
Cold Comp. Air
Dry
Liquid Nit.
Nitrogen
Rake Angle
0
7
15

Analysis of Variance for **Shear Area, As**, using Adjusted SS for Tests

Source	DF	Seq SS	Adj SS	Adj MS	F
Environment	3	0.0000161	0.0000161	0.0000054	1.78
Rake Angle	2	0.0000188	0.0000188	0.0000094	3.12
Feed in/rev	1	0.0000250	0.0000250	0.0000250	8.31
Environment*Rake Angle	6	0.0000143	0.0000143	0.0000024	0.79
Environment*Feed in/rev	3	0.0000097	0.0000097	0.0000032	1.08
Rake Angle*Feed in/rev	2	0.0000064	0.0000064	0.0000032	1.06
Environment*Rake Angle*Feed in/rev	6	0.0000170	0.0000170	0.0000028	0.94
Error	72	0.0002170	0.0002170	0.0000030	
Total	95	0.0003245			

Source	P
Environment	0.158
Rake Angle	0.050
Feed in/rev	0.005
Environment*Rake Angle	0.578
Environment*Feed in/rev	0.365
Rake Angle*Feed in/rev	0.352
Environment*Rake Angle*Feed in/rev	0.471
Error	
Total	

S = 0.00173609 R-Sq = 33.12% R-Sq(adj) = 11.75%

Unusual Observations for Shear Area, As

Obs	Shear Area, As	Fit	SE Fit	Residual	St Resid	
5	0.001921	0.006149	0.000868	-0.004228	-2.81	R
6	0.001892	0.006149	0.000868	-0.004257	-2.83	R
7	0.001877	0.006149	0.000868	-0.004272	-2.84	R
8	0.018906	0.006149	0.000868	0.012757	8.48	R

R denotes an observation with a large standardized residual.

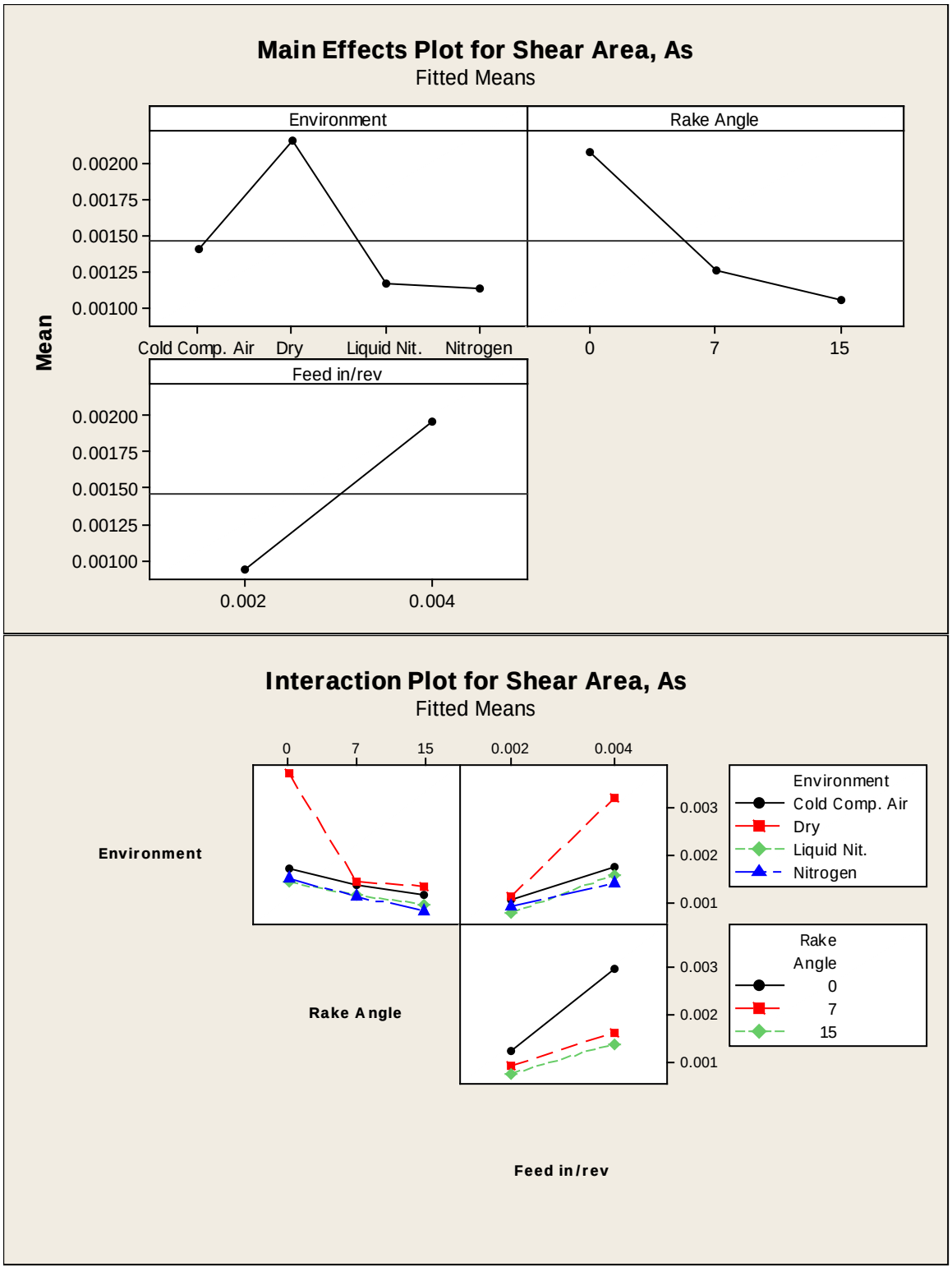
Main Effects Plot for Shear Area, As
Fitted Means
Environment
Rake Angle
Feed in/rev
Mean
0.00200
0.00175
0.00150
0.00125
0.00100
Cold Comp. Air
Dry
Liquid Nit.
Nitrogen
0
7
15
0.002
0.004
Interaction Plot for Shear Area, As
Fitted Means
Environment
Rake Angle
Feed in/rev
0.003
0.002
0.001
Environment
Cold Comp. Air
Dry
Liquid Nit.
Nitrogen
Rake Angle
0
7
15

Analysis of Variance for **Shear Stress, Ts Merchant** (Mpa), using Adjusted SS for
Tests

Source	DF	Seq SS	Adj SS	Adj MS	F
Environment	3	71265.6	71265.6	23755.2	59.20
Rake Angle	2	39502.5	39502.5	19751.3	49.22
Feed in/rev	1	21270.5	21270.5	21270.5	53.00
Environment*Rake Angle	6	4752.6	4752.6	792.1	1.97
Environment*Feed in/rev	3	8747.0	8747.0	2915.7	7.27
Rake Angle*Feed in/rev	2	184.9	184.9	92.5	0.23
Environment*Rake Angle*Feed in/rev	6	5750.5	5750.5	958.4	2.39
Error	72	28893.3	28893.3	401.3	
Total	95	180366.9			

Source	P
Environment	0.000
Rake Angle	0.000
Feed in/rev	0.000
Environment*Rake Angle	0.081
Environment*Feed in/rev	0.000
Rake Angle*Feed in/rev	0.795
Environment*Rake Angle*Feed in/rev	0.037
Error	
Total	

S = 20.0324 R-Sq = 83.98% R-Sq(adj) = 78.86%

Unusual Observations for Shear Stress, Ts Merchant (Mpa)

Obs	Shear Stress, Ts Merchant (Mpa)	Fit	SE Fit	Residual	St Resid
5	215.132	170.460	10.016	44.672	2.57 R
6	218.602	170.460	10.016	48.141	2.77 R
7	220.263	170.460	10.016	49.803	2.87 R
8	27.844	170.460	10.016	-142.616	-8.22 R

R denotes an observation with a large standardized residual.

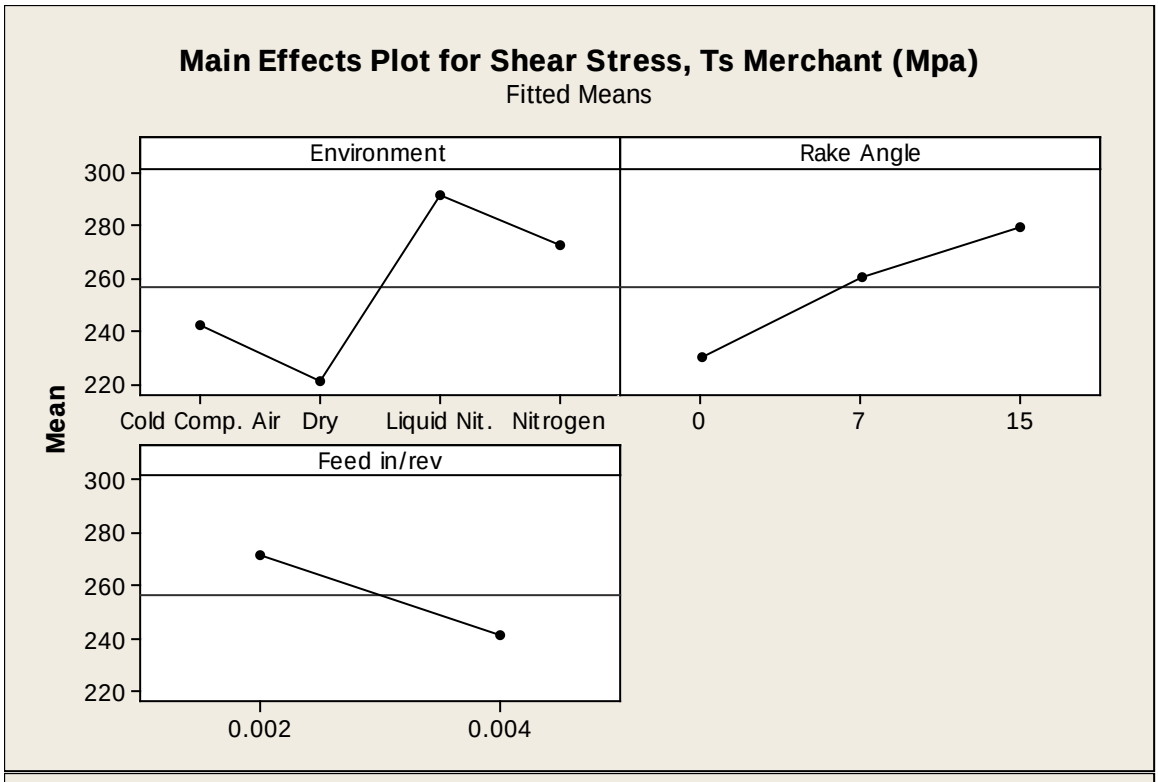
Main Effects Plot for Shear Stress, Ts Merchant (Mpa)
Fitted Means
Environment
Rake Angle
Feed in/rev
Mean
300
280
260
240
220
Cold Comp. Air
Dry
Liquid Nit.
Nitrogen
0
7
15
0.002
0.004

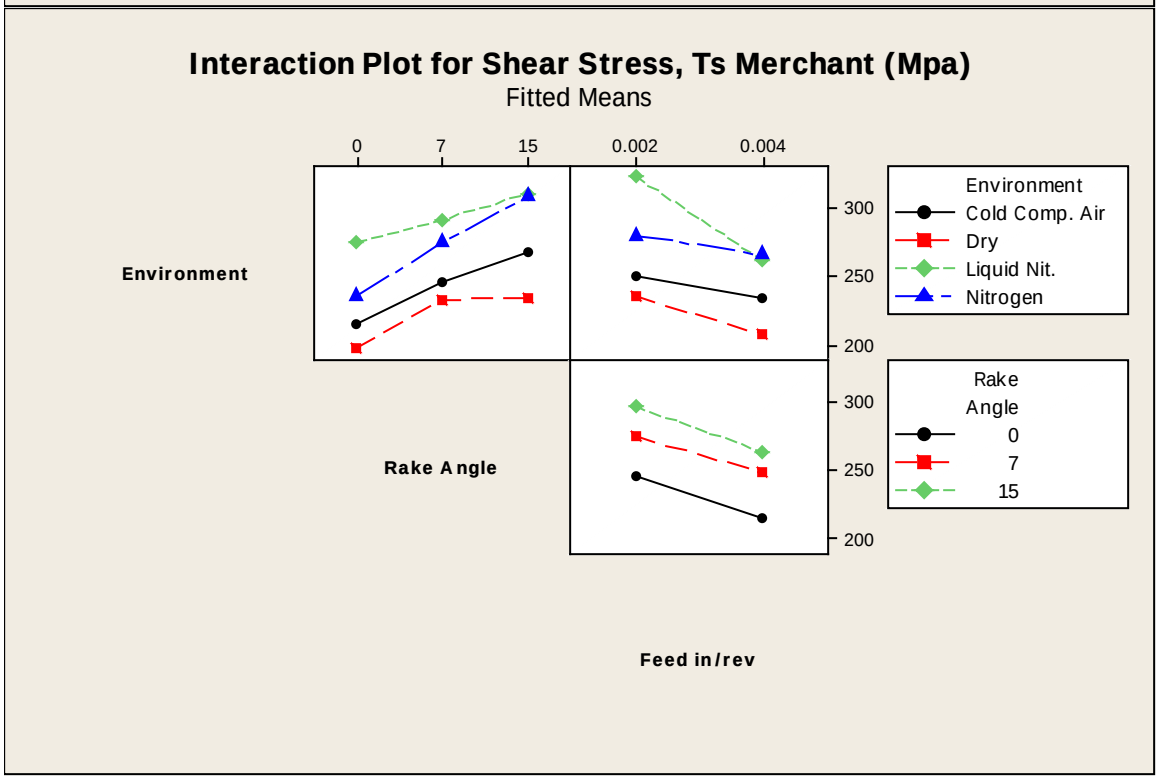
Interaction Plot for Shear Stress, Ts Merchant (Mpa)
Fitted Means
Environment
Rake Angle
Feed in/rev
0
7
15
0.002
0.004
300
250
200
Environment
Cold Comp. Air
Dry
Liquid Nit.
Nitrogen
Rake Angle
0
7
15

Analysis of Variance for **Shear Stress, Ts (Payton)** (Mpa), using Adjusted SS for
Tests

Source	DF	Seq SS	Adj SS	Adj MS	F	P
Environment	3	6219.1	6219.1	2073.0	19.87	0.000
Rake Angle	2	4429.6	4429.6	2214.8	21.22	0.000
Feed in/rev	1	7105.2	7105.2	7105.2	68.09	0.000
Environment*Rake Angle	6	2314.3	2314.3	385.7	3.70	0.003
Environment*Feed in/rev	3	3154.0	3154.0	1051.3	10.07	0.000
Rake Angle*Feed in/rev	2	25.8	25.8	12.9	0.12	0.884
Environment*Rake Angle*Feed in/rev	6	336.9	336.9	56.1	0.54	0.778
Error	72	7513.5	7513.5	104.4		
Total	95	31098.4				

S = 10.2154 R-Sq = 75.84% R-Sq(adj) = 68.12%

Unusual Observations for Shear Stress, Ts (Payton) (Mpa)

Obs	Shear Stress, Ts (Payton) (Mpa)	Fit	SE Fit	Residual	St Resid	
8	5.6725	45.1297	5.1077	-39.4572	-4.46	R
43	15.6867	35.8143	5.1077	-20.1276	-2.28	R
79	-5.4432	45.2171	5.1077	-50.6603	-5.73	R
80	71.9273	45.2171	5.1077	26.7102	3.02	R

R denotes an observation with a large standardized residual.

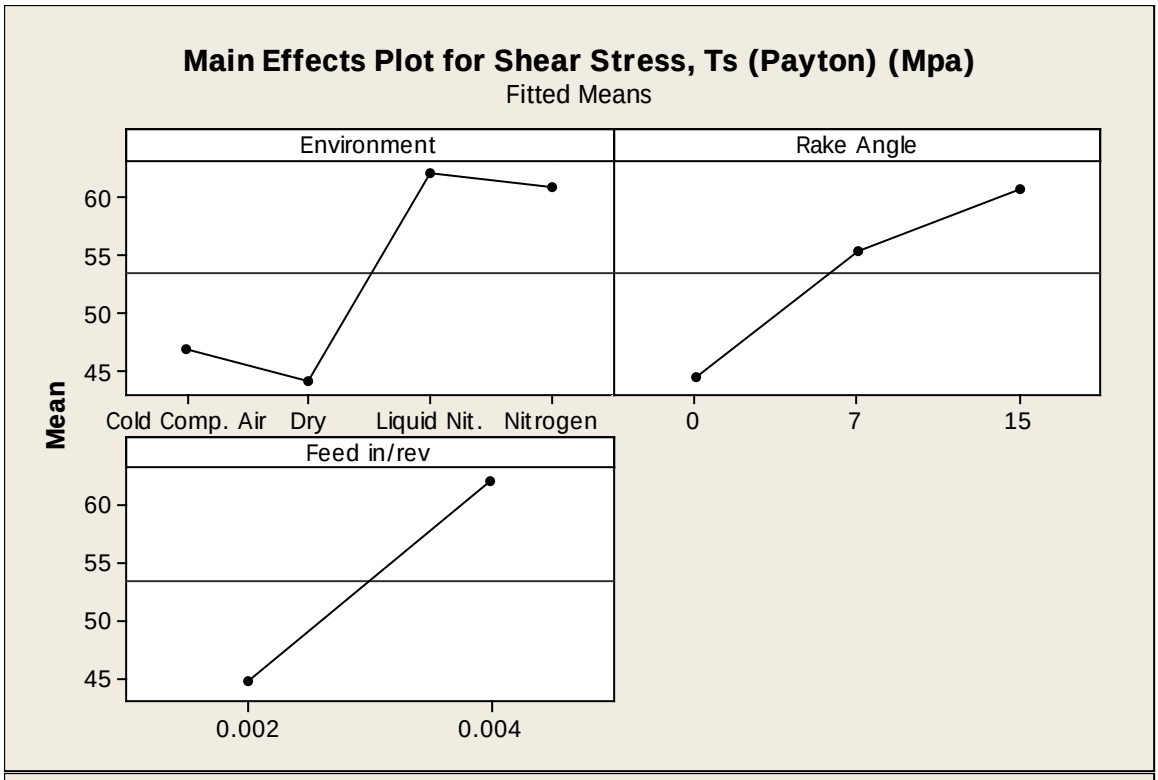
Main Effects Plot for Shear Stress, Ts (Payton) (Mpa)
Fitted Means
Environment
Rake Angle
Feed in/rev
Mean
60
55
50
45
Cold Comp. Air
Dry
Liquid Nit.
Nitrogen
0
7
15
0.002
0.004

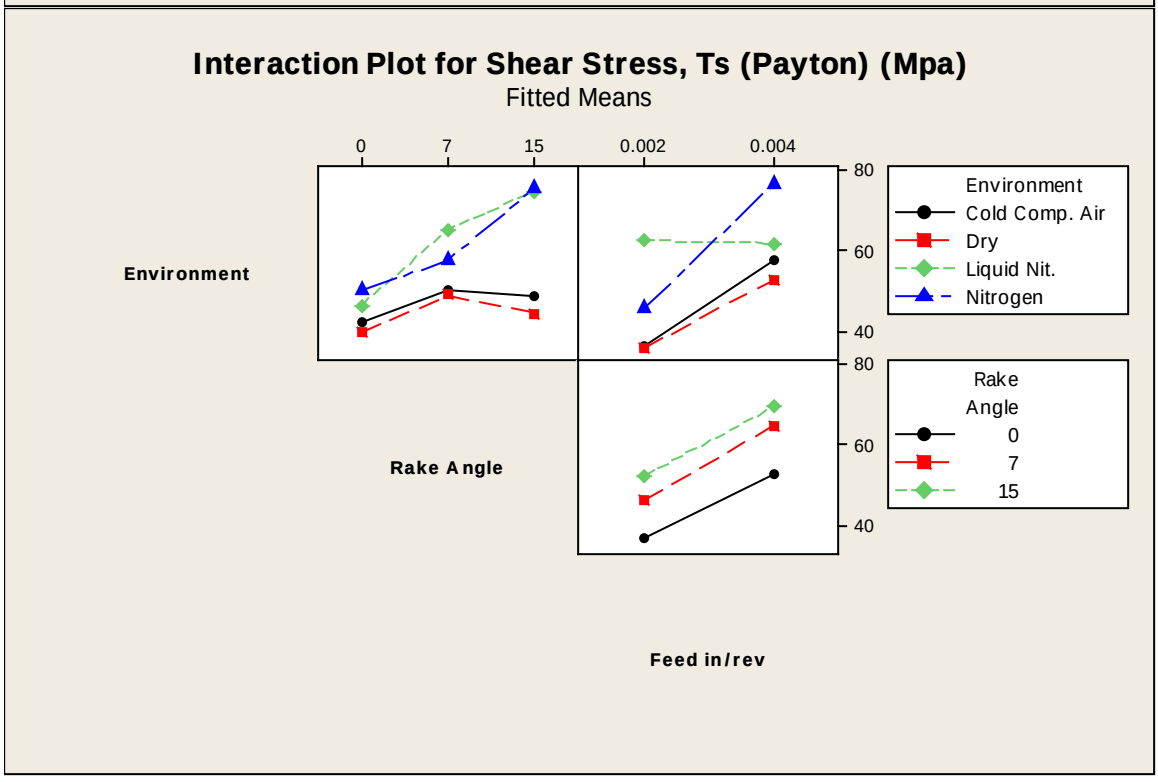
Interaction Plot for Shear Stress, Ts (Payton) (Mpa)
Fitted Means
Environment
Rake Angle
Feed in/rev
0
7
15
0.002
0.004
80
60
40
Environment
Cold Comp. Air
Dry
Liquid Nit.
Nitrogen
Rake Angle
0
7
15

Analysis of Variance for **Friction Co-efficient**, using Adjusted SS for Tests

Source	DF	Seq SS	Adj SS	Adj MS	F
Environment	3	0.000915	0.000915	0.000305	0.57
Rake Angle	2	0.224725	0.224725	0.112362	210.81
Feed in/rev	1	0.101045	0.101045	0.101045	189.58
Environment*Rake Angle	6	0.007117	0.007117	0.001186	2.23
Environment*Feed in/rev	3	0.006577	0.006577	0.002192	4.11
Rake Angle*Feed in/rev	2	0.000004	0.000004	0.000002	0.00
Environment*Rake Angle*Feed in/rev	6	0.001249	0.001249	0.000208	0.39
Error	72	0.038376	0.038376	0.000533	
Total	95	0.380008			

Source	P
Environment	0.635
Rake Angle	0.000
Feed in/rev	0.000
Environment*Rake Angle	0.050
Environment*Feed in/rev	0.009
Rake Angle*Feed in/rev	0.997
Environment*Rake Angle*Feed in/rev	0.883
Error	
Total	

S = 0.0230868 R-Sq = 89.90% R-Sq(adj) = 86.68%

Unusual Observations for Friction Co-efficient

Obs	Friction Co-efficient	Fit	SE Fit	Residual	St Resid	
43	0.882467	0.835228	0.011543	0.047239	2.36	R
79	0.797392	0.661401	0.011543	0.135991	6.80	R
80	0.586179	0.661401	0.011543	-0.075222	-3.76	R

R denotes an observation with a large standardized residual.

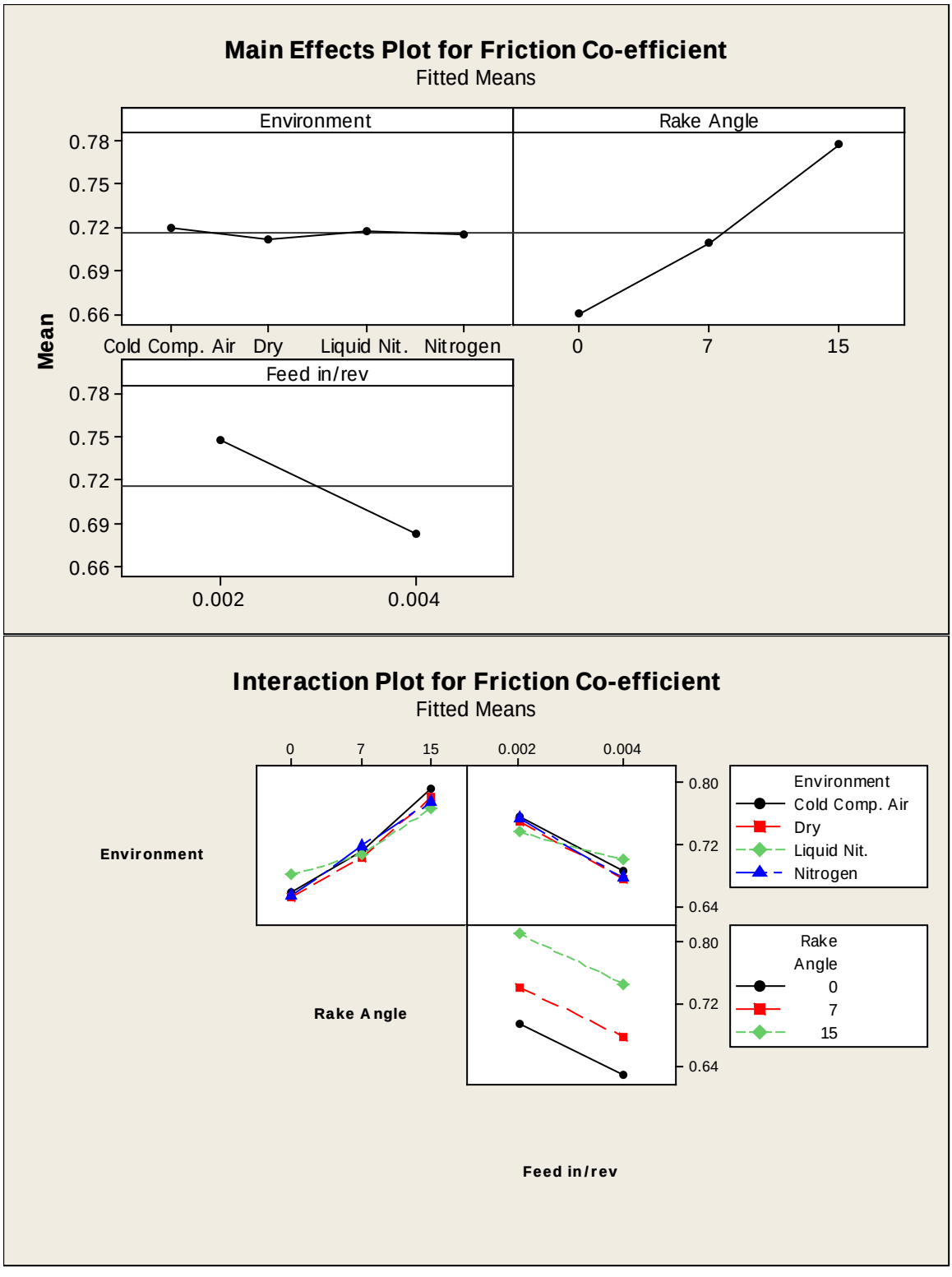
Main Effects Plot for Friction Co-efficient
Fitted Means
Environment
Rake Angle
Feed in/rev
Mean
0.78
0.75
0.72
0.69
0.66
Cold Comp. Air
Dry
Liquid Nit.
Nitrogen
0
7
15
0.002
0.004
Interaction Plot for Friction Co-efficient
Fitted Means
Environment
Rake Angle
Feed in/rev
0.80
0.72
0.64
Environment
Cold Comp. Air
Dry
Liquid Nit.
Nitrogen
Rake Angle
0
7
15

Analysis of Variance for **Normal Stress (Merchant)**, using Adjusted SS for Tests

Source	DF	Seq SS	Adj SS	Adj MS
Environment	3	1.38912E+11	1.38912E+11	46303927054
Rake Angle	2	22781391814	22781391814	11390695907
Feed in/rev	1	32438951465	32438951465	32438951465
Environment*Rake Angle	6	25588474005	25588474005	4264745668
Environment*Feed in/rev	3	13761438174	13761438174	4587146058
Rake Angle*Feed in/rev	2	1459222928	1459222928	729611464
Environment*Rake Angle*Feed in/rev	6	5454859385	5454859385	909143231
Error	72	25430048683	25430048683	353195121
Total	95	2.65826E+11		

Source	F	P
Environment	131.10	0.000
Rake Angle	32.25	0.000
Feed in/rev	91.84	0.000
Environment*Rake Angle	12.07	0.000
Environment*Feed in/rev	12.99	0.000
Rake Angle*Feed in/rev	2.07	0.134
Environment*Rake Angle*Feed in/rev	2.57	0.026
Error		
Total		

S = 18793.5 R-Sq = 90.43% R-Sq(adj) = 87.38%

Unusual Observations for Normal Stress (Merchant)

Obs	Normal Stress (Merchant)	Fit	SE Fit	Residual	St Resid	
5	161288	127814	9397	33474	2.06	R
6	169175	127814	9397	41361	2.54	R
7	167205	127814	9397	39391	2.42	R
8	13588	127814	9397	-114226	-7.02	R
79	254323	200342	9397	53981	3.32	R

R denotes an observation with a large standardized residual.

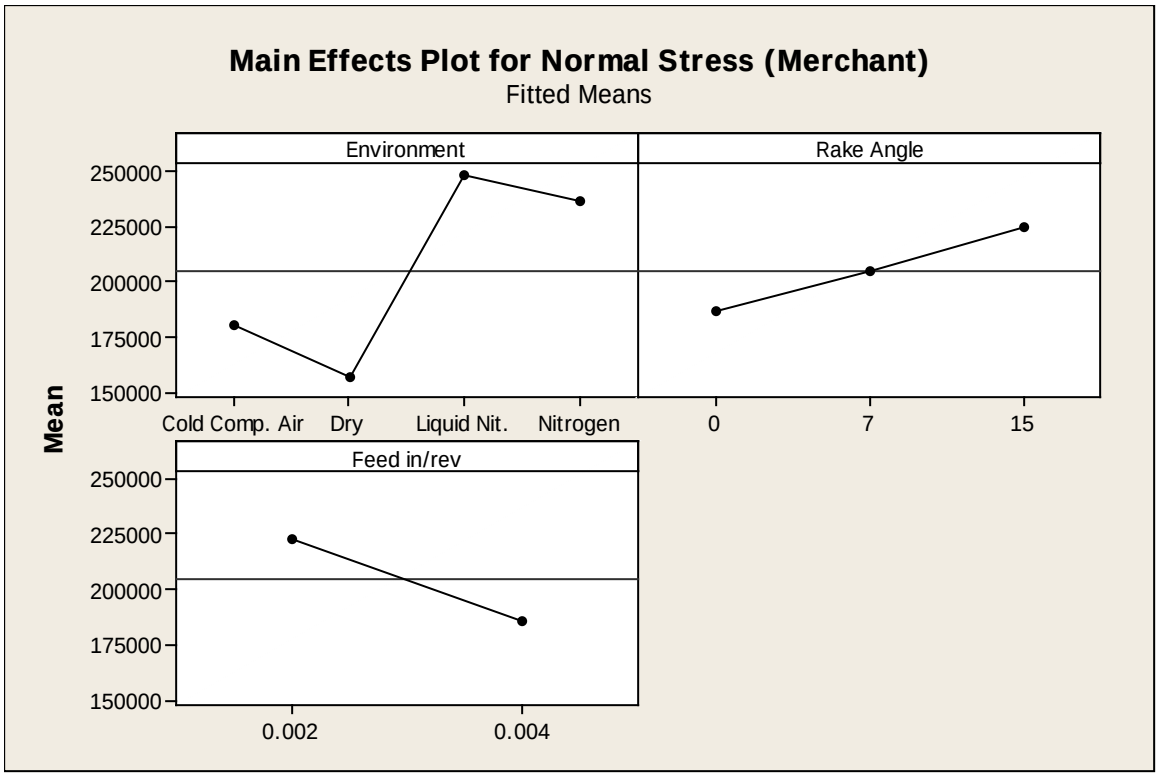
Main Effects Plot for Normal Stress (Merchant)
Fitted Means
Environment
Rake Angle
Feed in/rev
Mean
250000
225000
200000
175000
150000
Cold Comp. Air
Dry
Liquid Nit.
Nitrogen
0
7
15
0.002
0.004

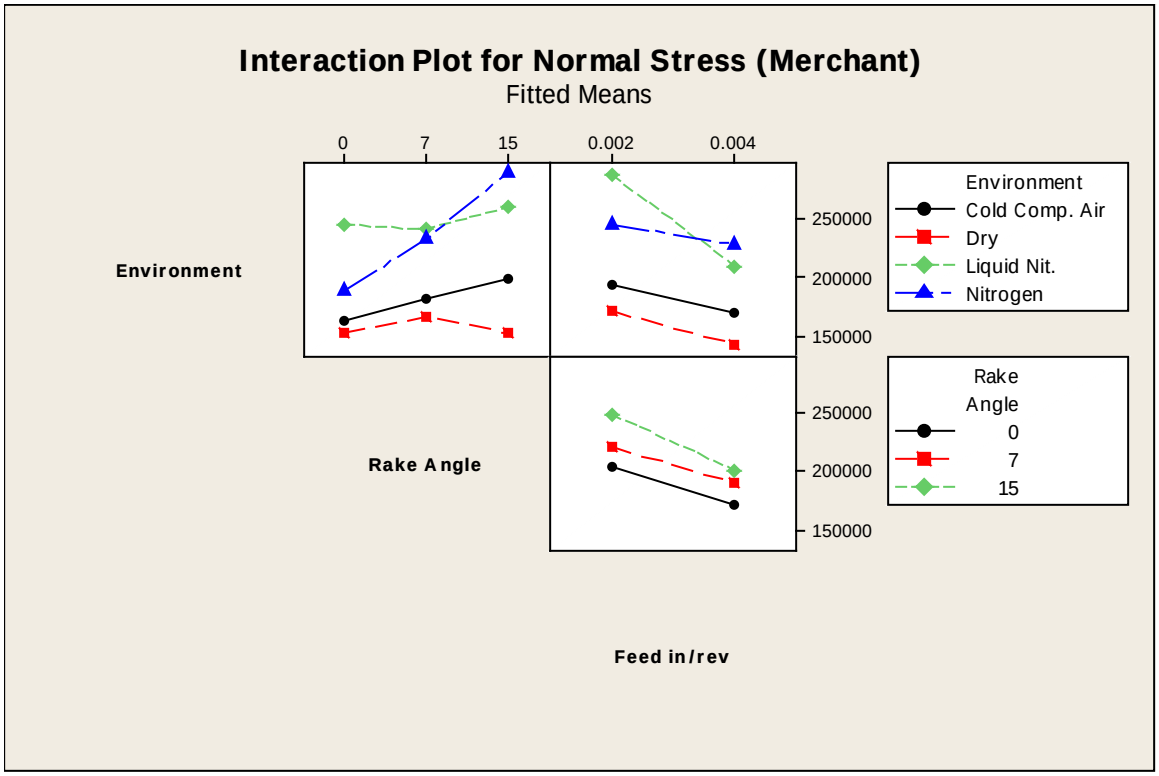
Interaction Plot for Normal Stress (Merchant)
Fitted Means
Environment
Rake Angle
Feed in/rev
0
7
15
0.002
0.004
250000
200000
150000
Environment
Cold Comp. Air
Dry
Liquid Nit.
Nitrogen
Rake Angle
0
7
15

Analysis of Variance for **Shear strain (Merchant)**, using Adjusted SS for Tests

Source	DF	Seq SS	Adj SS	Adj MS	F	P
Environment	3	85.88	85.88	28.63	2.20	0.095
Rake Angle	2	137.25	137.25	68.63	5.28	0.007
Feed in/rev	1	0.70	0.70	0.70	0.05	0.817
Environment*Rake Angle	6	58.26	58.26	9.71	0.75	0.614
Environment*Feed in/rev	3	33.63	33.63	11.21	0.86	0.465
Rake Angle*Feed in/rev	2	12.28	12.28	6.14	0.47	0.625
Environment*Rake Angle*Feed in/rev	6	80.48	80.48	13.41	1.03	0.412
Error	72	935.62	935.62	12.99		
Total	95	1344.11				

S = 3.60482 R-Sq = 30.39% R-Sq(adj) = 8.15%

Unusual Observations for Shear strain (Merchant)

Obs	Shear strain (Merchant)	Fit	SE Fit	Residual	St Resid
5	4.1331	12.9132	1.8024	-8.7801	-2.81 R
6	4.0748	12.9132	1.8024	-8.8384	-2.83 R
7	4.0446	12.9132	1.8024	-8.8687	-2.84 R
8	39.4004	12.9132	1.8024	26.4872	8.48 R

R denotes an observation with a large standardized residual.

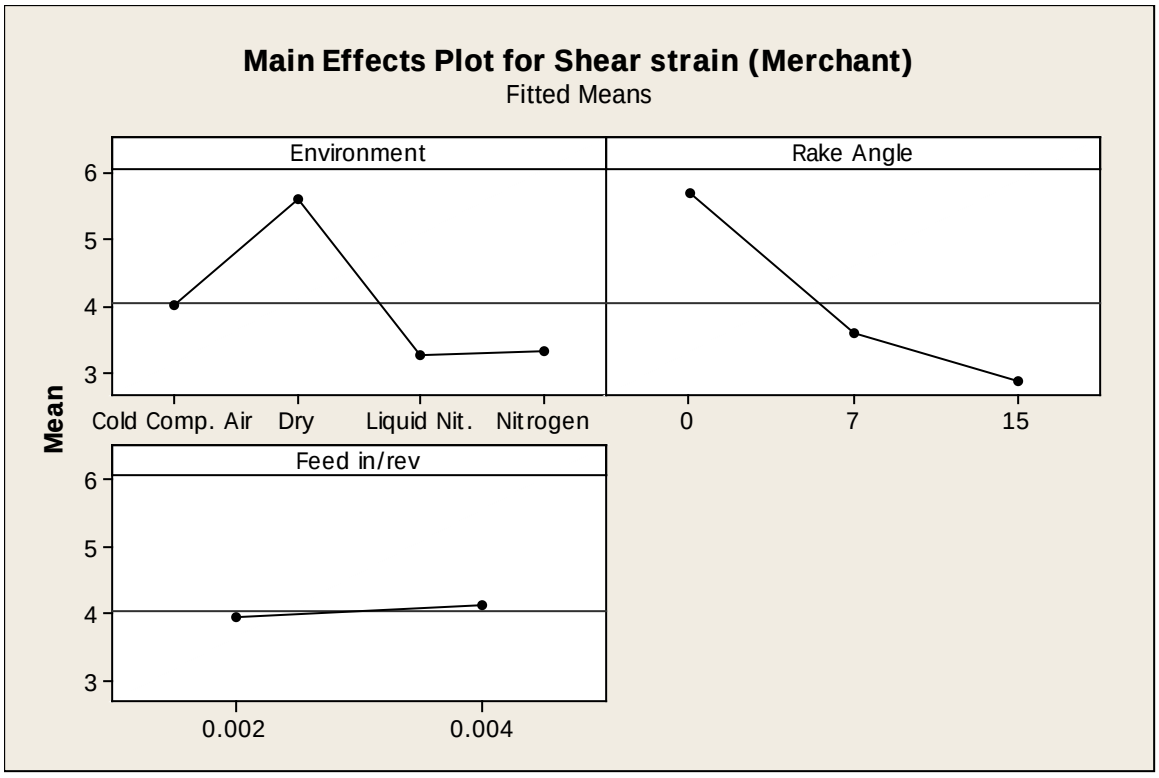
Main Effects Plot for Shear strain (Merchant)
Fitted Means
Environment
Rake Angle
Feed in/rev
Mean
6
5
4
3
Cold Comp. Air
Dry
Liquid Nit.
Nitrogen
0
7
15
0.002
0.004

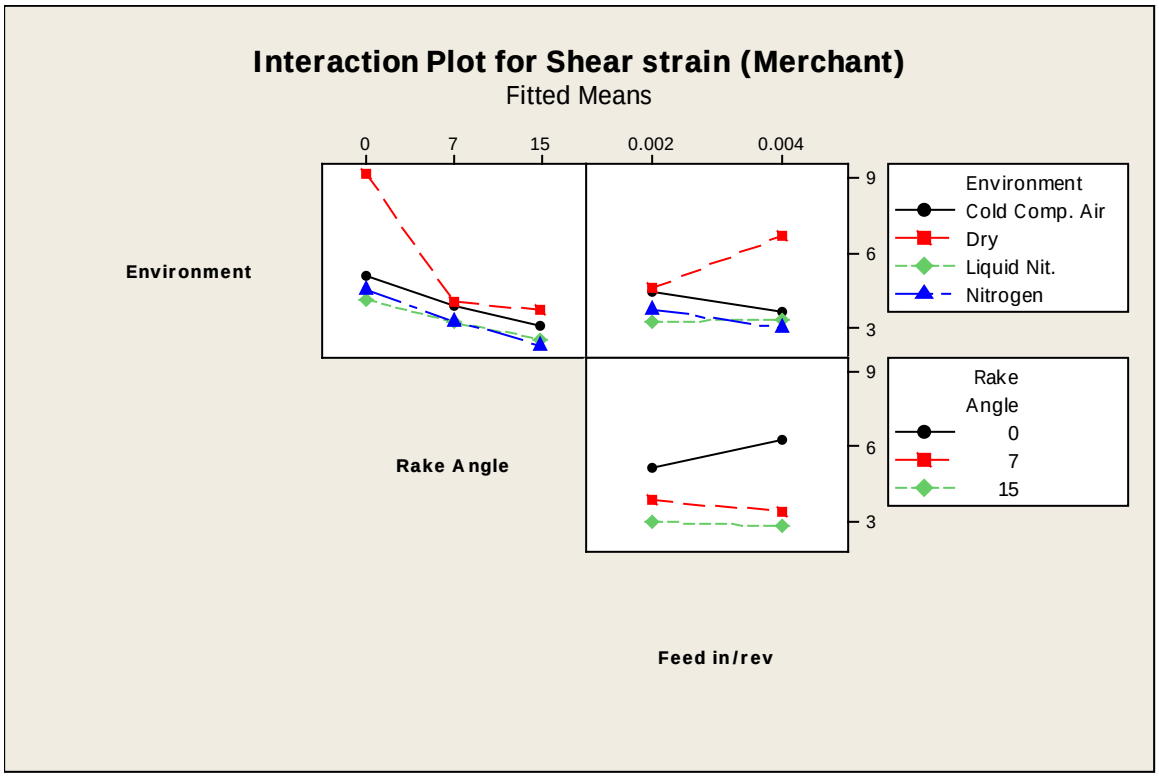
Interaction Plot for Shear strain (Merchant)
Fitted Means
Environment
Rake Angle
Feed in/rev
0
7
15
0.002
0.004
9
6
3
Environment
Cold Comp. Air
Dry
Liquid Nit.
Nitrogen
Rake Angle
0
7
15

Analysis of Variance for **Normal Stress (Payton)**, using Adjusted SS for Tests

Source	DF	Seq SS	Adj SS	Adj MS
Environment	3	1.54837E+11	1.54837E+11	51612434517
Rake Angle	2	38231554604	38231554604	19115777302
Feed in/rev	1	43379410155	43379410155	43379410155
Environment*Rake Angle	6	23013841011	23013841011	3835640168
Environment*Feed in/rev	3	15975407884	15975407884	5325135961
Rake Angle*Feed in/rev	2	1203953978	1203953978	601976989
Environment*Rake Angle*Feed in/rev	6	7753498291	7753498291	1292249715
Error	72	34076556343	34076556343	473285505
Total	95	3.18472E+11		

Source	F	P
Environment	109.05	0.000
Rake Angle	40.39	0.000
Feed in/rev	91.66	0.000
Environment*Rake Angle	8.10	0.000
Environment*Feed in/rev	11.25	0.000
Rake Angle*Feed in/rev	1.27	0.287
Environment*Rake Angle*Feed in/rev	2.73	0.019
Error		
Total		

S = 21755.1 R-Sq = 89.30% R-Sq(adj) = 85.88%

Unusual Observations for Narmal Stress (Payton)

Obs	Narmal Stress (Payton)	Fit	SE Fit	Residual	St Resid	
5	209434	166215	10878	43219	2.29	R
6	217221	166215	10878	51006	2.71	R
7	215980	166215	10878	49765	2.64	R
8	22225	166215	10878	-143990	-7.64	R
79	292786	249247	10878	43540	2.31	R

R denotes an observation with a large standardized residual.

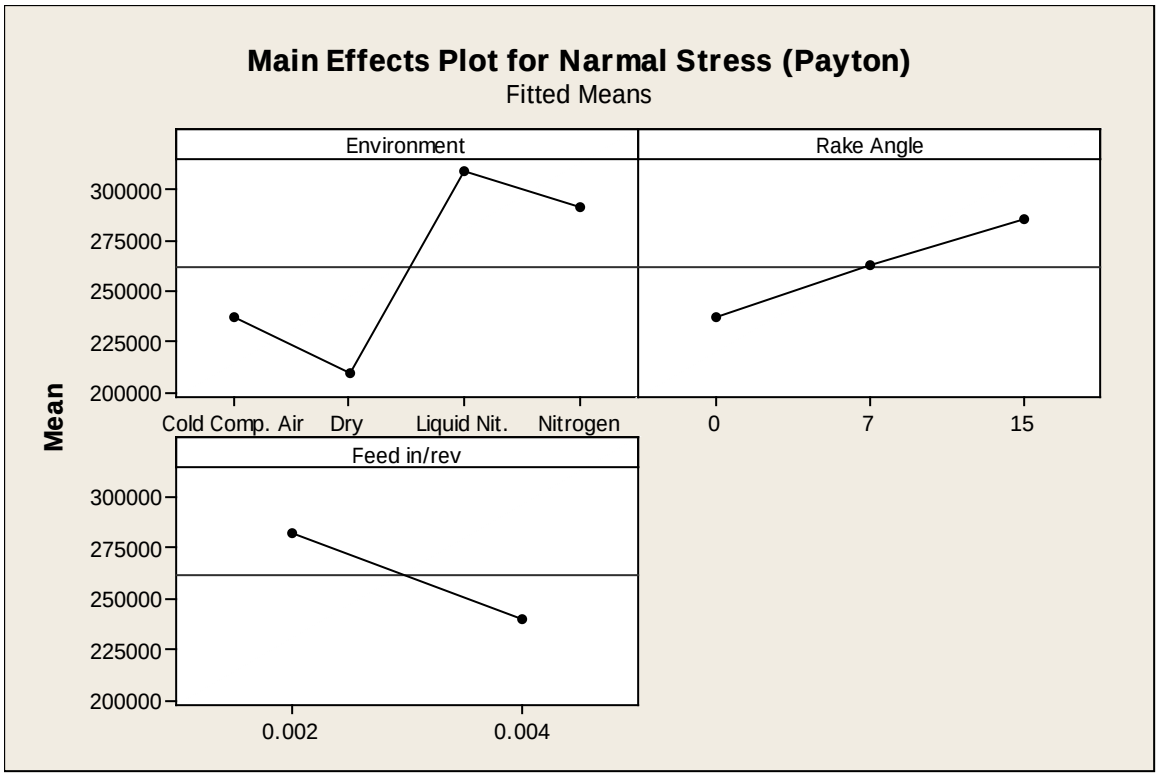
Main Effects Plot for Narmal Stress (Payton)
Fitted Means
Environment
Rake Angle
Feed in/rev
Mean
300000
275000
250000
225000
200000
Cold Comp. Air
Dry
Liquid Nit.
Nitrogen
0
7
15
0.002
0.004

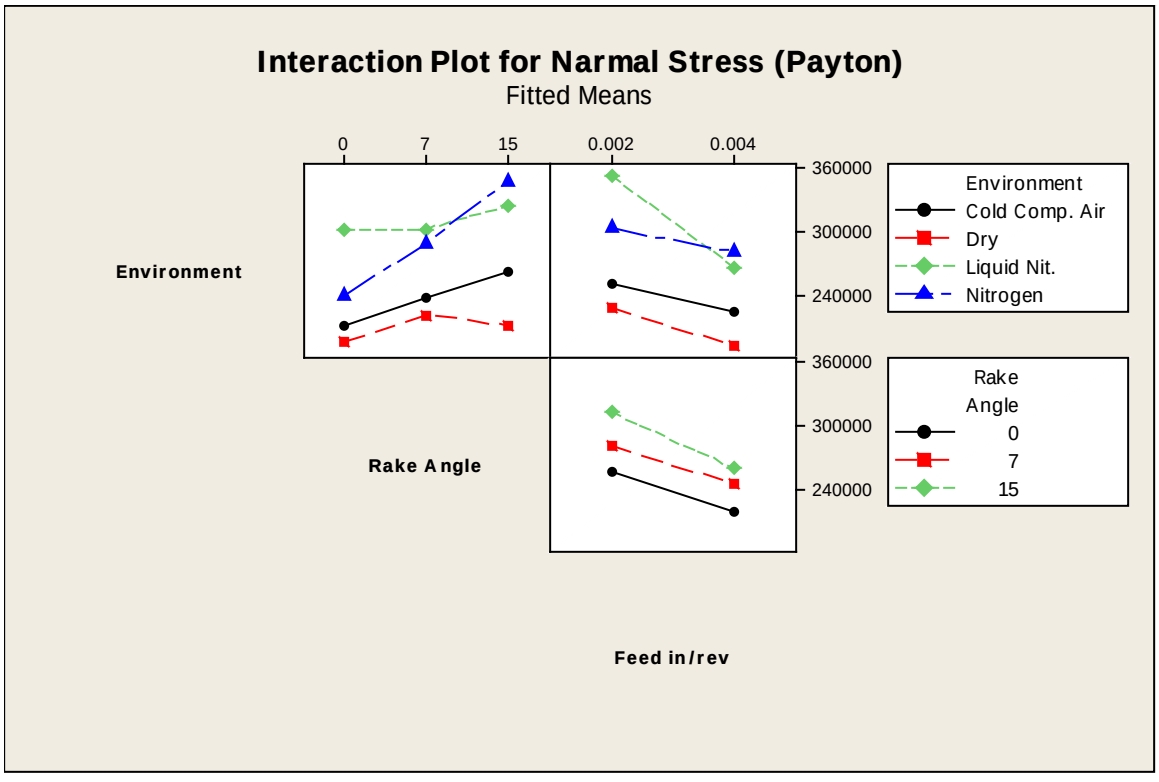
Interaction Plot for Narmal Stress (Payton)
Fitted Means
Environment
Rake Angle
Feed in/rev
0
7
15
0.002
0.004
360000
300000
240000
Environment
Cold Comp. Air
Dry
Liquid Nit.
Nitrogen
Rake Angle
0
7
15

Analysis of Variance for **Shear strain (Payton)**, using Adjusted SS for Tests

Source	DF	Seq SS	Adj SS	Adj MS	F	P
Environment	3	0.00000	0.00000	0.00000	**	
Rake Angle	2	3.46485	3.46485	1.73242	**	
Feed in/rev	1	0.00000	0.00000	0.00000	**	
Environment*Rake Angle	6	0.00000	0.00000	0.00000	**	
Environment*Feed in/rev	3	0.00000	0.00000	0.00000	**	
Rake Angle*Feed in/rev	2	0.00000	0.00000	0.00000	**	
Environment*Rake Angle*Feed in/rev	6	0.00000	0.00000	0.00000	**	
Error	72	0.00000	0.00000	0.00000		
Total	95	3.46485				

** Denominator of F-test is zero.

S = 8.576051E-17 R-Sq = 100.00% R-Sq(adj) = 100.00%

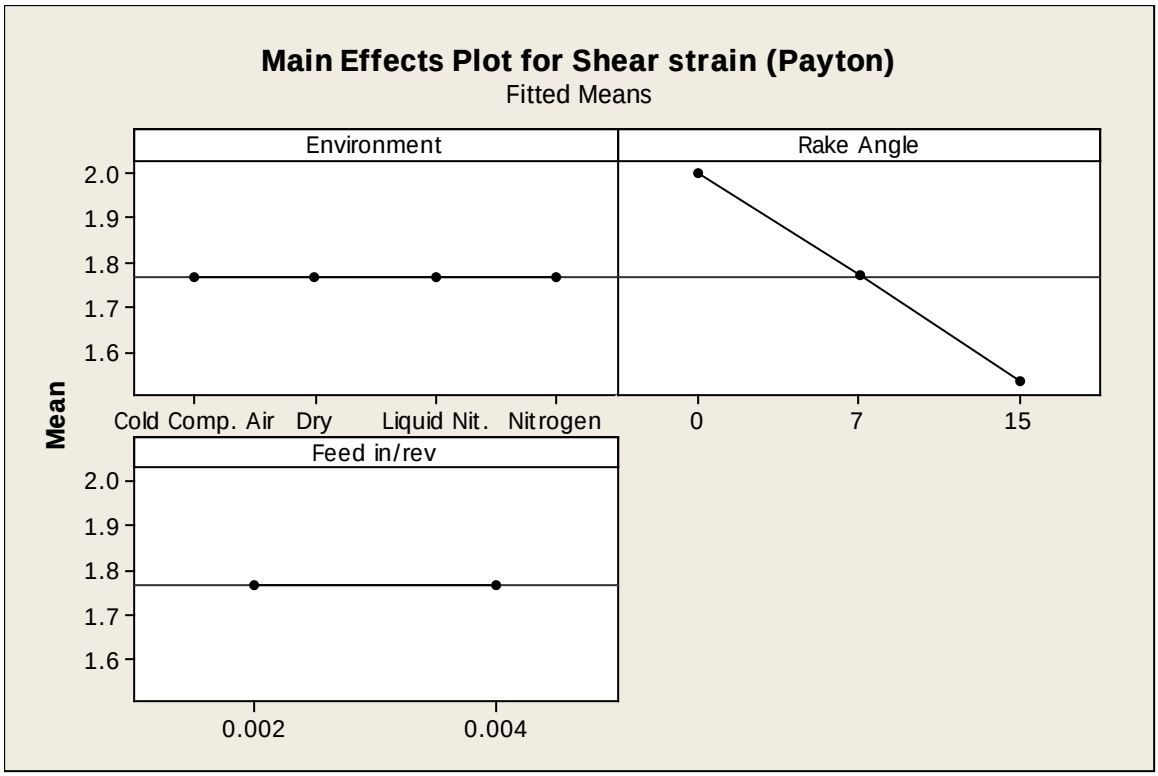
Main Effects Plot for Shear strain (Payton)
Fitted Means
Environment
Rake Angle
Feed in/rev
Mean
2.0
1.9
1.8
1.7
1.6
Cold Comp. Air
Dry
Liquid Nit.
Nitrogen
0
7
15
0.002
0.004

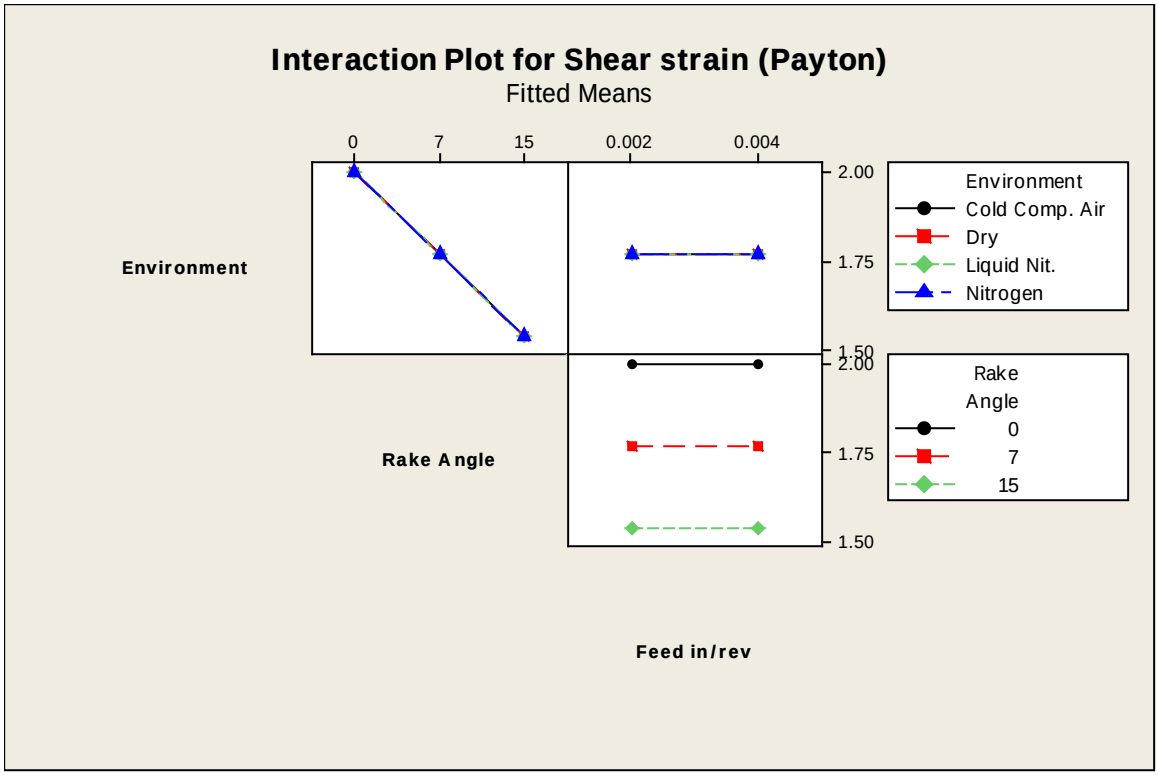
Interaction Plot for Shear strain (Payton)
Fitted Means
Environment
Rake Angle
Feed in/rev
0
7
15
0.002
0.004
2.00
1.75
1.50
Environment
Cold Comp. Air
Dry
Liquid Nit.
Nitrogen
Rake Angle
0
7
15

Analysis of Variance for **Shear strain new**, using Adjusted SS for Tests

Source	DF	Seq SS	Adj SS	Adj MS	F
Environment	3	1.19275	1.19275	0.39758	2371.87
Rake Angle	2	1.07829	1.07829	0.53915	3216.39
Feed in/rev	1	0.22995	0.22995	0.22995	1371.82
Environment*Rake Angle	6	0.56515	0.56515	0.09419	561.92
Environment*Feed in/rev	3	0.21889	0.21889	0.07296	435.27
Rake Angle*Feed in/rev	2	0.02274	0.02274	0.01137	67.84
Environment*Rake Angle*Feed in/rev	6	0.01174	0.01174	0.00196	11.67
Error	72	0.01207	0.01207	0.00017	
Total	95	3.33158			

Source	P
Environment	0.000
Rake Angle	0.000
Feed in/rev	0.000
Environment*Rake Angle	0.000
Environment*Feed in/rev	0.000
Rake Angle*Feed in/rev	0.000
Environment*Rake Angle*Feed in/rev	0.000
Error	
Total	

S = 0.0129470 R-Sq = 99.64% R-Sq(adj) = 99.52%

Unusual Observations for Shear strain new

Obs	Shear strain new	Fit	SE Fit	Residual	St Resid	
61	0.74661	0.77288	0.00647	-0.02626	-2.34	R
65	0.83967	0.89493	0.00647	-0.05526	-4.93	R
68	0.93059	0.89493	0.00647	0.03566	3.18	R
71	1.11529	1.08653	0.00647	0.02876	2.56	R

R denotes an observation with a large standardized residual.

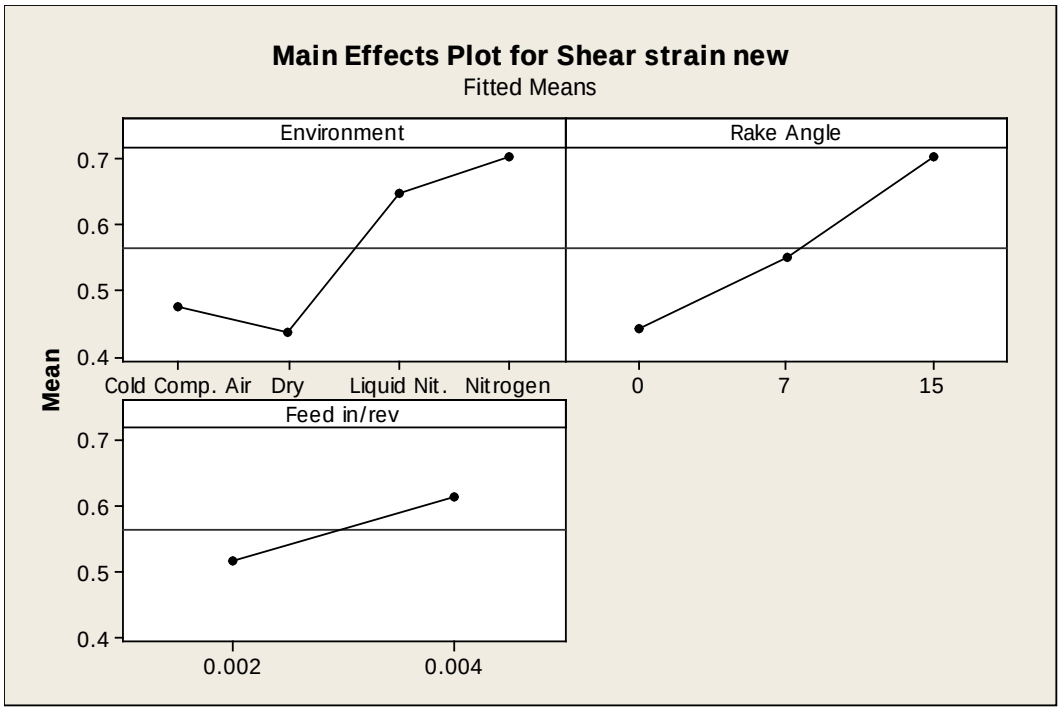
Main Effects Plot for Shear strain new
Fitted Means
Environment
Rake Angle
Feed in/rev
Mean
0.7
0.6
0.5
0.4
Cold Comp. Air
Dry
Liquid Nit.
Nitrogen
0
7
15
0.002
0.004

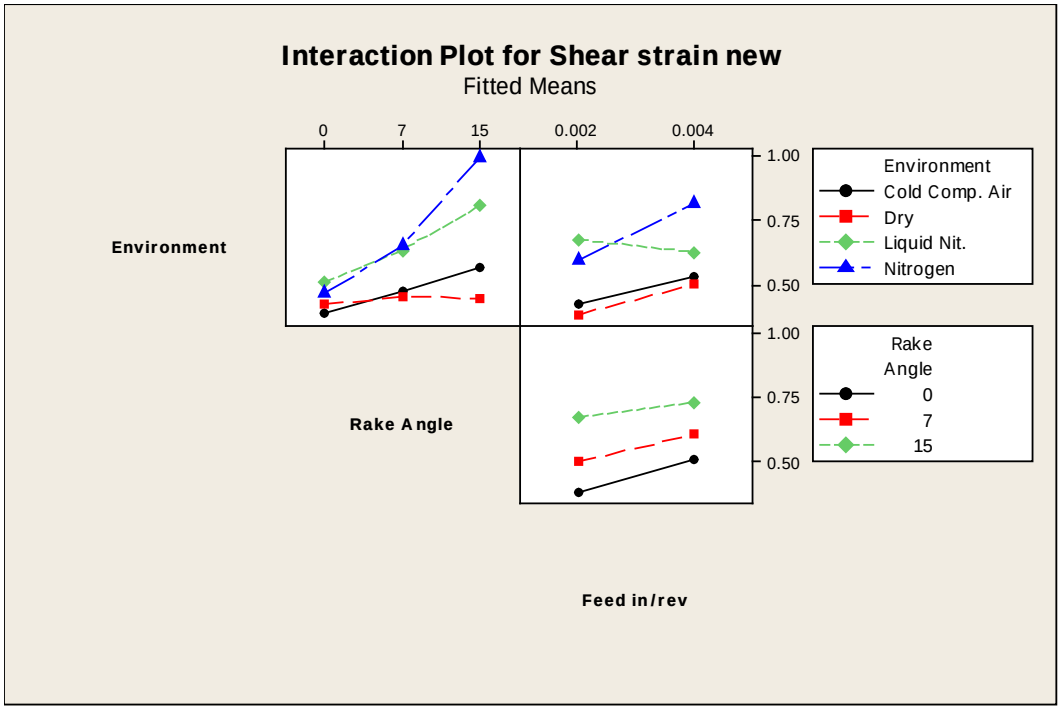
Interaction Plot for Shear strain new
Fitted Means
Environment
Rake Angle
Feed in/rev
0
7
15
0.002
0.004
1.00
0.75
0.50
Environment
Cold Comp. Air
Dry
Liquid Nit.
Nitrogen
Rake Angle
0
7
15

Analysis of Variance for **Shear Area, As P**, using Adjusted SS for Tests

Source	DF	Seq SS	Adj SS	Adj MS
Environment	3	0.0000036	0.0000036	0.0000012
Rake Angle	2	0.0000115	0.0000115	0.0000057
Feed in/rev	1	0.0000196	0.0000196	0.0000196
Environment*Rake Angle	6	0.0000007	0.0000007	0.0000001
Environment*Feed in/rev	3	0.0000007	0.0000007	0.0000002
Rake Angle*Feed in/rev	2	0.0000001	0.0000001	0.0000000
Environment*Rake Angle*Feed in/rev	6	0.0000002	0.0000002	0.0000000
Error	72	0.0000000	0.0000000	0.0000000
Total	95	0.0000363		

Source	F	P
Environment	2254.92	0.000
Rake Angle	10760.76	0.000
Feed in/rev	36717.10	0.000
Environment*Rake Angle	206.05	0.000
Environment*Feed in/rev	432.36	0.000
Rake Angle*Feed in/rev	76.63	0.000
Environment*Rake Angle*Feed in/rev	60.28	0.000
Error		
Total		

S = 0.0000230754 R-Sq = 99.89% R-Sq(adj) = 99.86%

Unusual Observations for Shear Area, As P

Obs	Shear Area, As P	Fit	SE Fit	Residual	St Resid	
1	0.001871	0.001815	0.000012	0.000056	2.78	R
2	0.001750	0.001815	0.000012	-0.000065	-3.26	R
3	0.001771	0.001815	0.000012	-0.000044	-2.20	R
4	0.001869	0.001815	0.000012	0.000053	2.67	R
7	0.002673	0.002723	0.000012	-0.000050	-2.52	R
8	0.002784	0.002723	0.000012	0.000061	3.05	R
25	0.002048	0.002001	0.000012	0.000046	2.32	R

R denotes an observation with a large standardized residual.

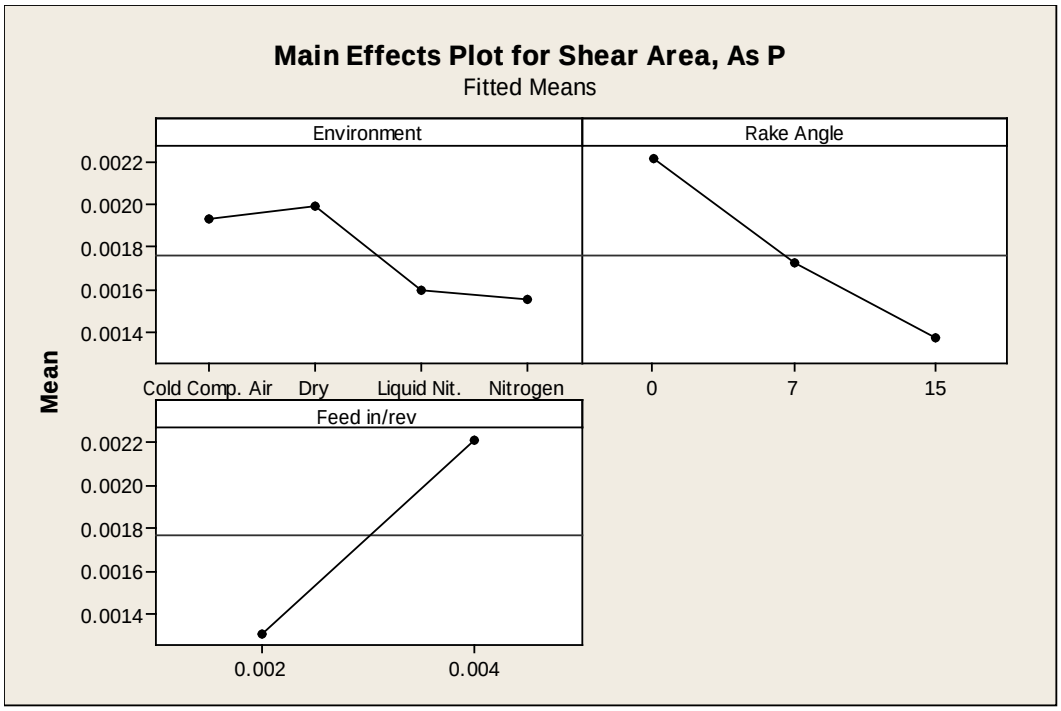
Main Effects Plot for Shear Area, As P
Fitted Means
Environment
Rake Angle
Feed in/rev
Mean
0.0022
0.0020
0.0018
0.0016
0.0014
Cold Comp. Air
Dry
Liquid Nit.
Nitrogen
0
7
15
0.002
0.004

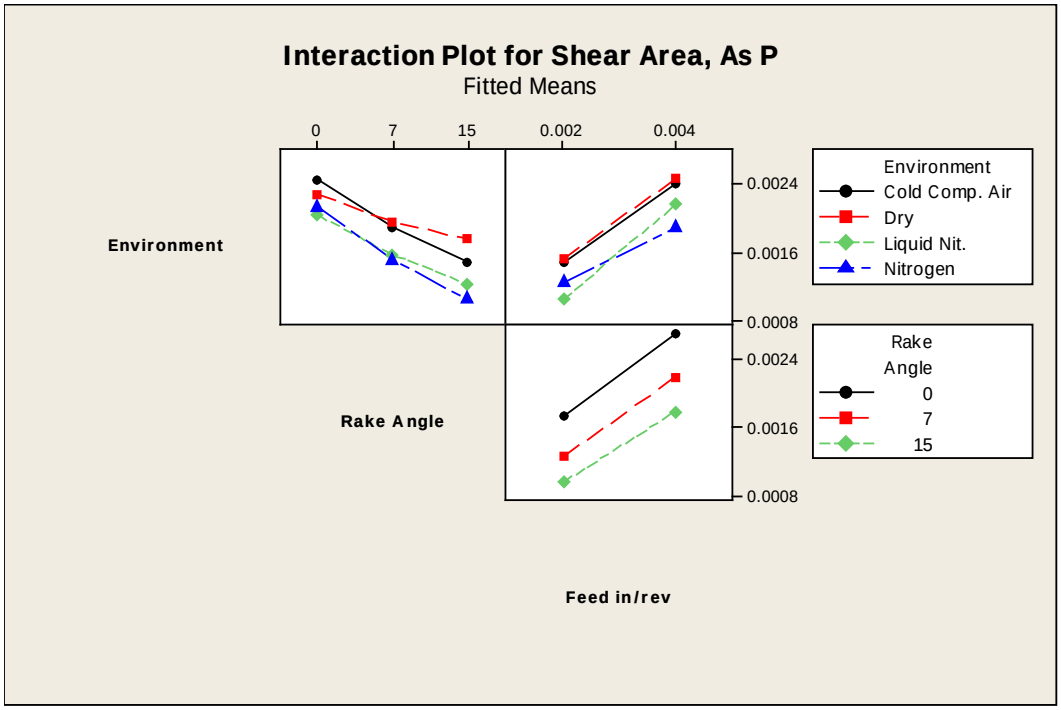
Interaction Plot for Shear Area, As P
Fitted Means
Environment
Rake Angle
Feed in/rev
0
7
15
0.002
0.004
0.0024
0.0016
0.0008
Environment
Cold Comp. Air
Dry
Liquid Nit.
Nitrogen
Rake Angle
0
7
15

Analysis of Variance for **Shear Stress, Ts (Payton) cor_1**, using Adjusted SS for
Tests

Source	DF	Seq SS	Adj SS	Adj MS	F
Environment	3	3282.38	3282.38	1094.13	28.51
Rake Angle	2	3421.53	3421.53	1710.77	44.57
Feed in/rev	1	4409.47	4409.47	4409.47	114.89
Environment*Rake Angle	6	1802.07	1802.07	300.34	7.83
Environment*Feed in/rev	3	1845.48	1845.48	615.16	16.03
Rake Angle*Feed in/rev	2	2.06	2.06	1.03	0.03
Environment*Rake Angle*Feed in/rev	6	154.52	154.52	25.75	0.67
Error	72	2763.39	2763.39	38.38	
Total	95	17680.91			

Source	P
Environment	0.000
Rake Angle	0.000
Feed in/rev	0.000
Environment*Rake Angle	0.000
Environment*Feed in/rev	0.000
Rake Angle*Feed in/rev	0.974
Environment*Rake Angle*Feed in/rev	0.673
Error	
Total	

S = 6.19520 R-Sq = 84.37% R-Sq(adj) = 79.38%

Unusual Observations for Shear Stress, Ts (Payton) cor_1

Obs	Shear Stress, Ts (Payton) cor_1	Fit	SE Fit	Residual	St Resid
43	11.9636	27.3083	3.0976	-15.3447	-2.86 R
73	44.0730	33.0904	3.0976	10.9826	2.05 R
79	-3.8184	31.7270	3.0976	-35.5453	-6.63 R
80	50.4529	31.7270	3.0976	18.7259	3.49 R

R denotes an observation with a large standardized residual.

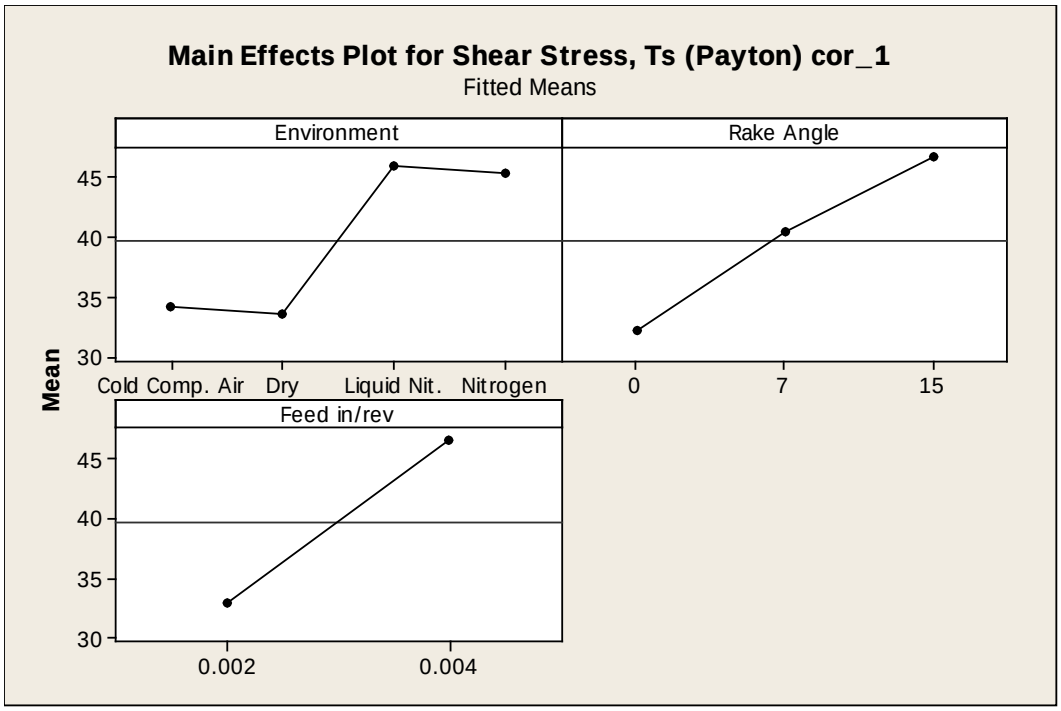
Main Effects Plot for Shear Stress, Ts (Payton) cor_1
Fitted Means
Environment
Rake Angle
Feed in/rev
Mean
45
40
35
30
Cold Comp. Air
Dry
Liquid Nit.
Nitrogen
0
7
15
0.002
0.004

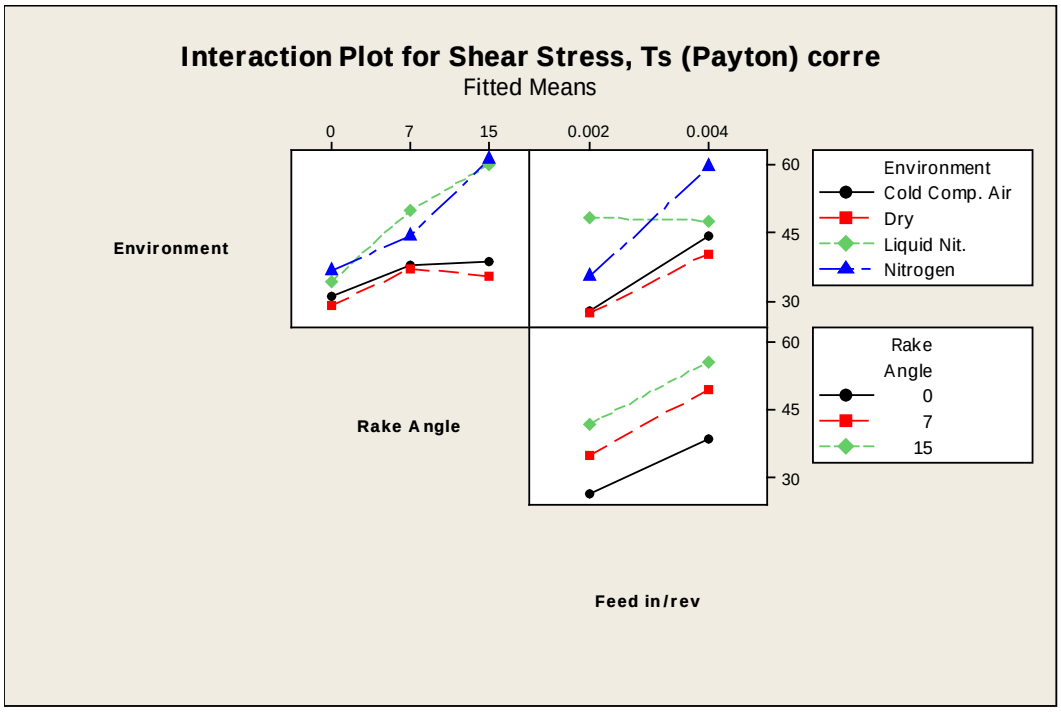
Interaction Plot for Shear Stress, Ts (Payton) corre
Fitted Means
Environment
Rake Angle
Feed in/rev
0
7
15
0.002
0.004
60
45
30
Environment
Cold Comp. Air
Dry
Liquid Nit.
Nitrogen
Rake Angle
0
7
15

ALUMINUM 6061; UNCOATED CARBIDE

Factor	Type	Levels	Values
Environment	fixed	4	Cold Comp. Air, Dry, Liquid Nit., Nitrogen
Rake Angle	fixed	3	0, 7, 15
Feed in/rev	fixed	2	0.002, 0.004

Analysis of Variance for **Fy Thrust**, using Adjusted SS for Tests

Source	DF	Seq SS	Adj SS	Adj MS	F	P
Environment	3	6012.0	6012.0	2004.0	54.81	0.000
Rake Angle	2	79866.3	79866.3	39933.2	1092.17	0.000
Feed in/rev	1	59094.9	59094.9	59094.9	1616.24	0.000
Environment*Rake Angle	6	1033.8	1033.8	172.3	4.71	0.000
Environment*Feed in/rev	3	613.4	613.4	204.5	5.59	0.002
Rake Angle*Feed in/rev	2	1763.3	1763.3	881.6	24.11	0.000
Environment*Rake Angle*Feed in/rev	6	764.9	764.9	127.5	3.49	0.004
Error	72	2632.6	2632.6	36.6		
Total	95	151781.1				

S = 6.04676 R-Sq = 98.27% R-Sq(adj) = 97.71%

Unusual Observations for Fy Thrust

Obs	Fy Thrust	Fit	SE Fit	Residual	St Resid	
37	200.566	187.518	3.023	13.047	2.49	R
47	157.536	145.286	3.023	12.251	2.34	R
75	199.284	176.691	3.023	22.593	4.31	R
79	264.380	252.337	3.023	12.042	2.30	R
80	234.617	252.337	3.023	-17.721	-3.38	R

R denotes an observation with a large standardized residual.

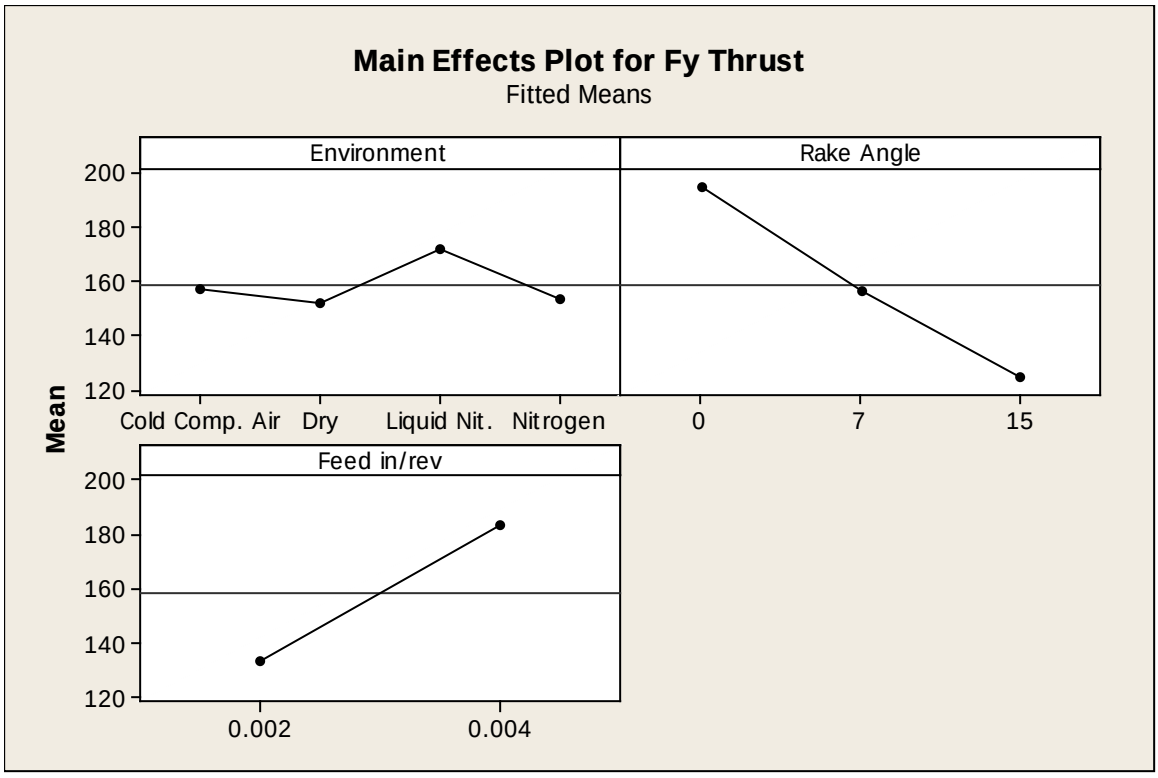
Main Effects Plot for Fy Thrust
Fitted Means
Environment
Rake Angle
Feed in/rev
Mean
200
180
160
140
120
Cold Comp. Air
Dry
Liquid Nit.
Nitrogen
0
7
15
0.002
0.004

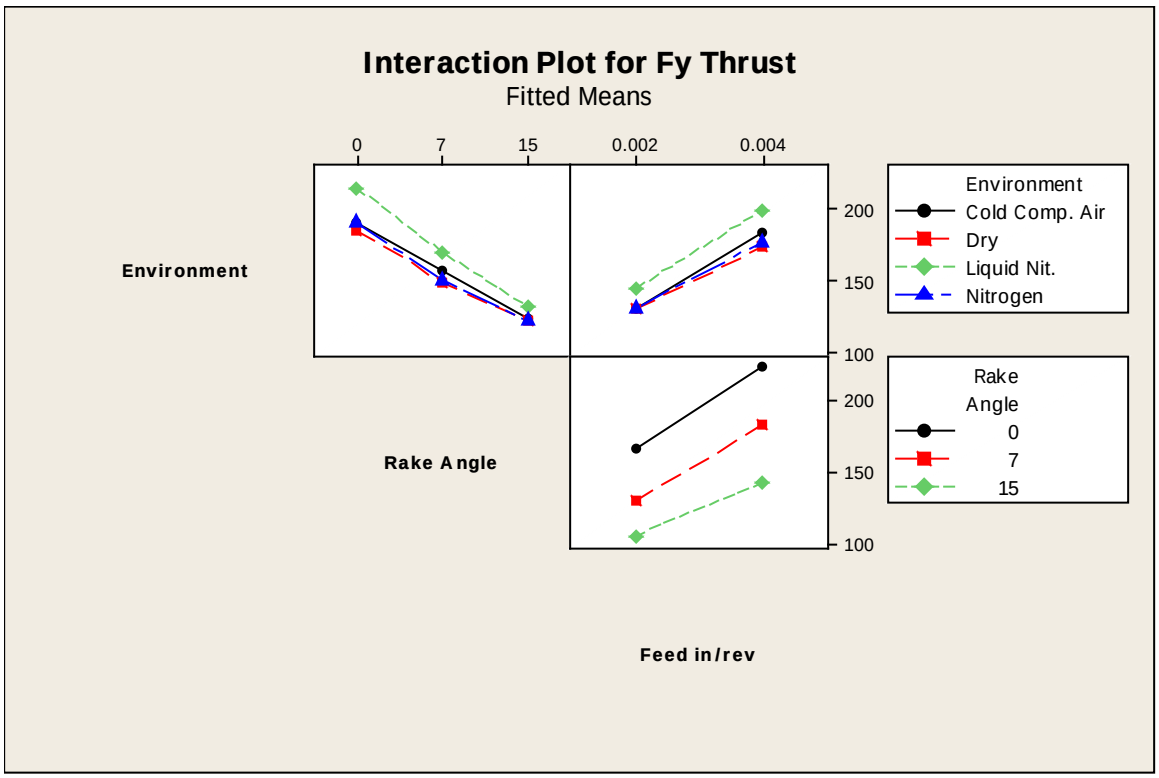
Interaction Plot for Fy Thrust
Fitted Means
Environment
Rake Angle
Feed in/rev
0
7
15
0.002
0.004
200
150
100
Environment
Cold Comp. Air
Dry
Liquid Nit.
Nitrogen
Rake Angle
0
7
15

Analysis of Variance for **Fz Cutting**, using Adjusted SS for Tests

Source	DF	Seq SS	Adj SS	Adj MS	F	P
Environment	3	6147	6147	2049	90.76	0.000
Rake Angle	2	22601	22601	11300	500.56	0.000
Feed in/rev	1	347735	347735	347735	15402.97	0.000
Environment*Rake Angle	6	381	381	64	2.81	0.016
Environment*Feed in/rev	3	233	233	78	3.44	0.021
Rake Angle*Feed in/rev	2	414	414	207	9.17	0.000
Environment*Rake Angle*Feed in/rev	6	183	183	31	1.35	0.245
Error	72	1625	1625	23		
Total	95	379320				

S = 4.75140 R-Sq = 99.57% R-Sq(adj) = 99.43%

Unusual Observations for Fz Cutting

Obs	Fz Cutting	Fit	SE Fit	Residual	St Resid	
47	275.837	284.429	2.376	-8.593	-2.09	R
75	238.342	217.048	2.376	21.294	5.18	R
76	208.795	217.048	2.376	-8.253	-2.01	R
79	362.705	351.816	2.376	10.890	2.65	R
80	336.848	351.816	2.376	-14.968	-3.64	R
81	209.687	200.863	2.376	8.824	2.14	R
82	191.561	200.863	2.376	-9.302	-2.26	R

R denotes an observation with a large standardized residual.

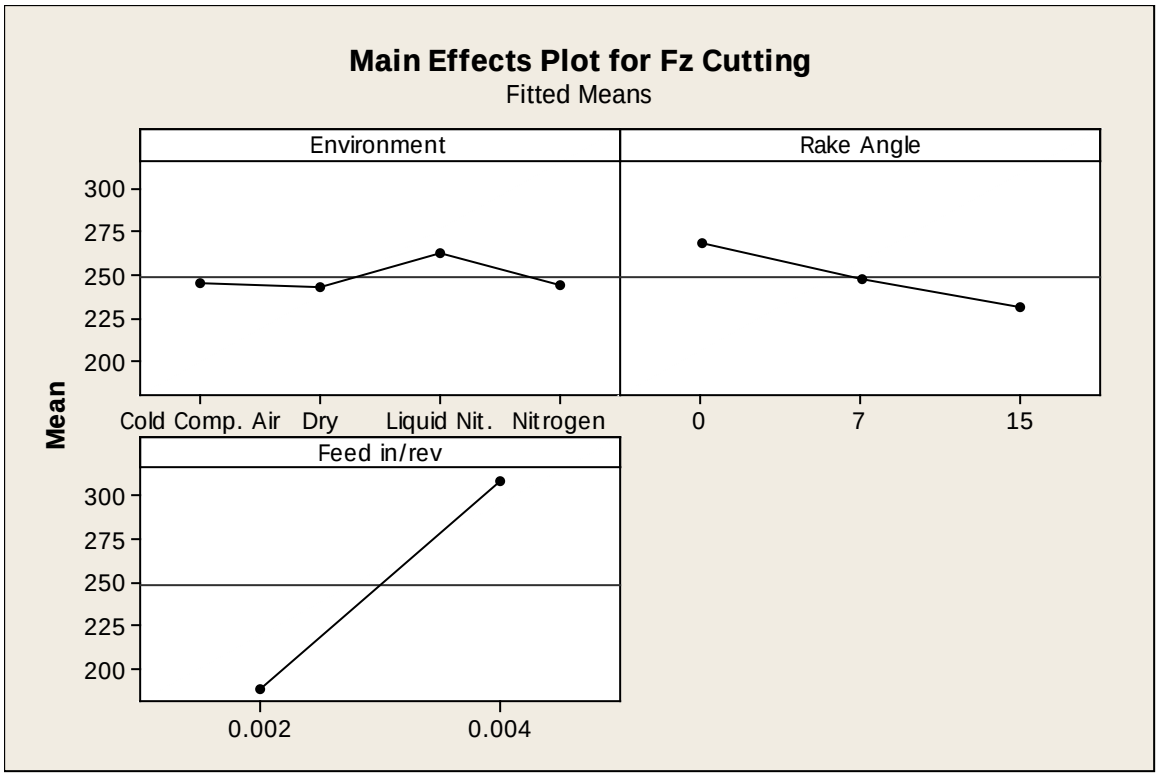
Main Effects Plot for Fz Cutting
Fitted Means
Environment
Rake Angle
Feed in/rev
Mean
300
275
250
225
200
Cold Comp. Air
Dry
Liquid Nit.
Nitrogen
0
7
15
0.002
0.004

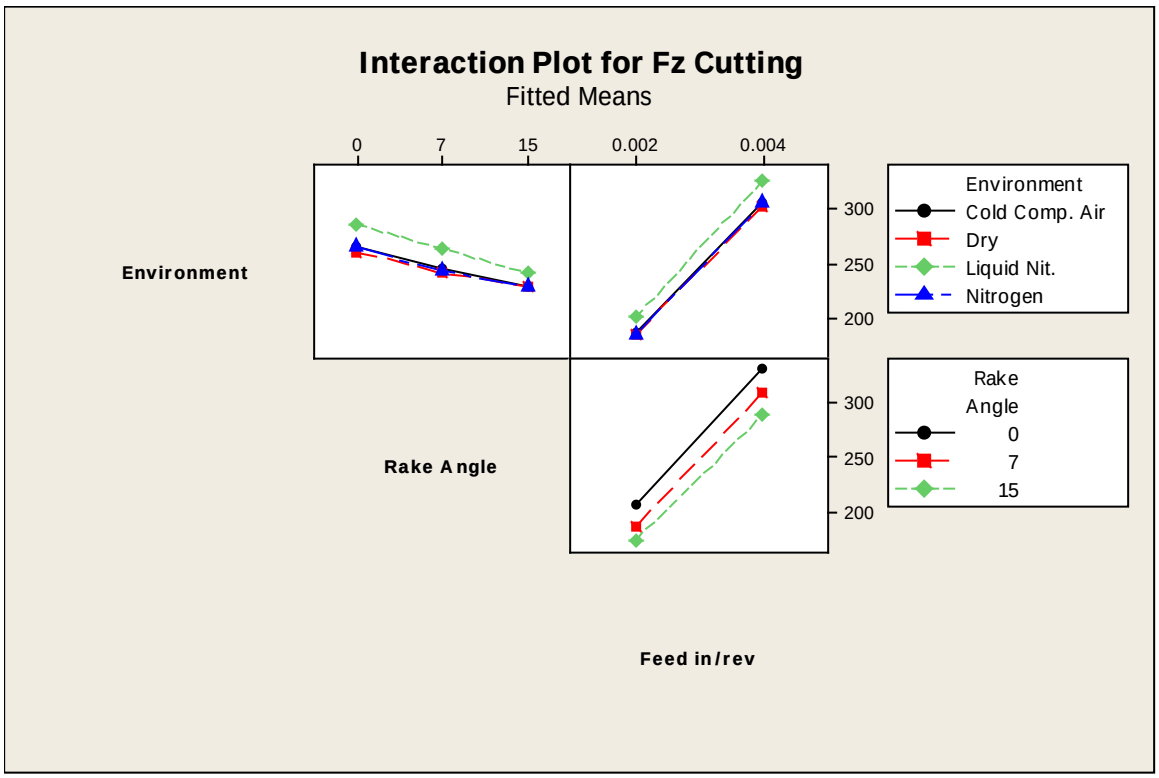
Interaction Plot for Fz Cutting
Fitted Means
Environment
Rake Angle
Feed in/rev
0
7
15
0.002
0.004
300
250
200
Environment
Cold Comp. Air
Dry
Liquid Nit.
Nitrogen
Rake Angle
0
7
15

Analysis of Variance for **Resultant force**, using Adjusted SS for Tests

Source	DF	Seq SS	Adj SS	Adj MS	F	P
Environment	3	11705	11705	3902	80.44	0.000
Rake Angle	2	77683	77683	38841	800.75	0.000
Feed in/rev	1	395199	395199	395199	8147.43	0.000
Environment*Rake Angle	6	1129	1129	188	3.88	0.002
Environment*Feed in/rev	3	631	631	210	4.34	0.007
Rake Angle*Feed in/rev	2	1127	1127	563	11.61	0.000
Environment*Rake Angle*Feed in/rev	6	676	676	113	2.32	0.042
Error	72	3492	3492	49		
Total	95	491642				

S = 6.96462 R-Sq = 99.29% R-Sq(adj) = 99.06%

Unusual Observations for Resultant

Obs	Resultant	Fit	SE Fit	Residual	St Resid	
75	310.679	279.884	3.482	30.795	5.11	R
79	448.834	432.968	3.482	15.866	2.63	R
80	410.501	432.968	3.482	-22.467	-3.72	R
81	258.363	246.027	3.482	12.337	2.05	R
82	232.854	246.027	3.482	-13.173	-2.18	R

R denotes an observation with a large standardized residual.

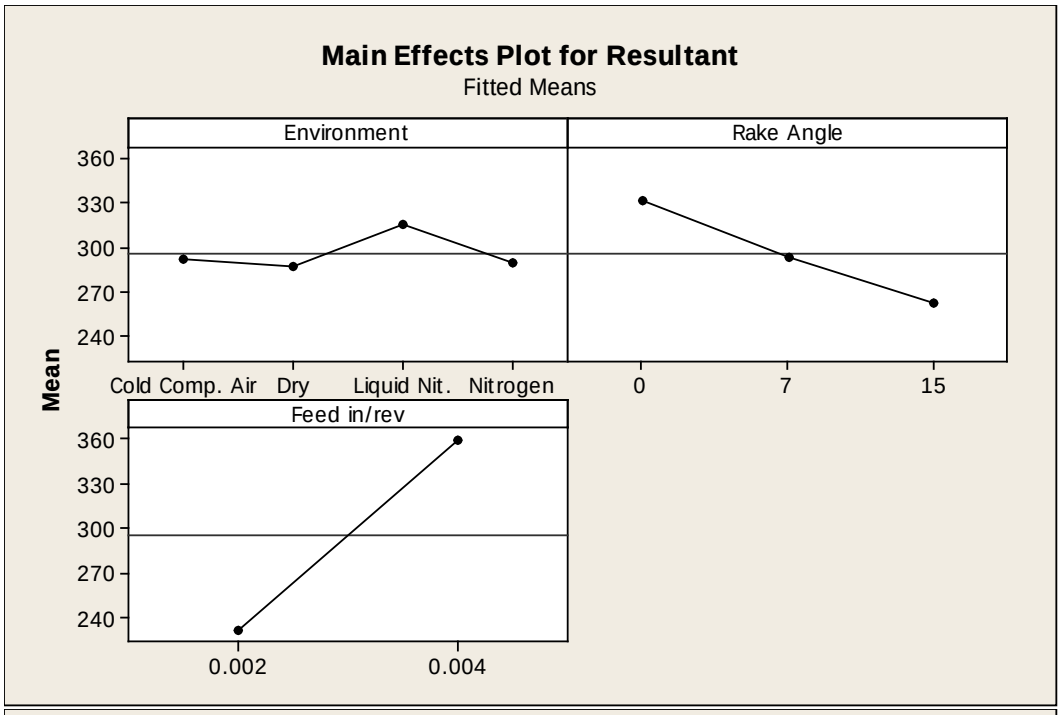
Main Effects Plot for Resultant
Fitted Means
Environment
Rake Angle
Feed in/rev
Mean
360
330
300
270
240
Cold Comp. Air
Dry
Liquid Nit.
Nitrogen
0
7
15
0.002
0.004

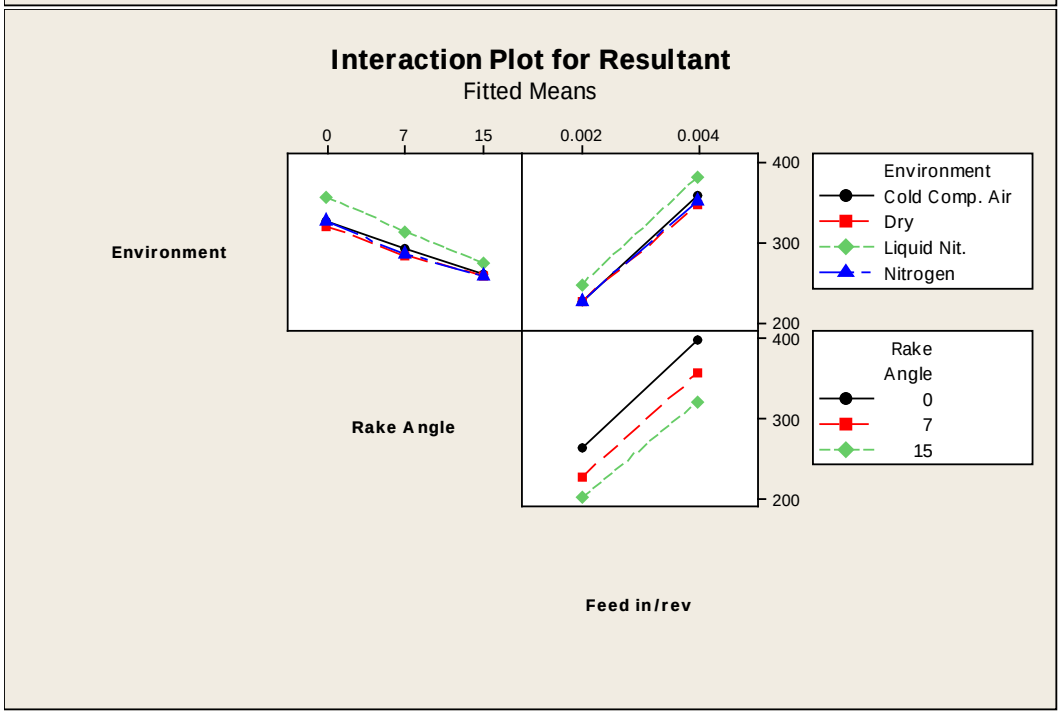
Interaction Plot for Resultant
Fitted Means
Environment
Rake Angle
Feed in/rev
0
7
15
0.002
0.004
400
300
200
Environment
Cold Comp. Air
Dry
Liquid Nit.
Nitrogen
Rake Angle
0
7
15

Analysis of Variance for **Chip thickness ratio**, using Adjusted SS for Tests

Source	DF	Seq SS	Adj SS	Adj MS	F
Environment	3	0.242244	0.242244	0.080748	56.04
Rake Angle	2	0.308051	0.308051	0.154025	106.89
Feed in/rev	1	0.016420	0.016420	0.016420	11.40
Environment*Rake Angle	6	0.224658	0.224658	0.037443	25.99
Environment*Feed in/rev	3	0.017145	0.017145	0.005715	3.97
Rake Angle*Feed in/rev	2	0.010243	0.010243	0.005122	3.55
Environment*Rake Angle*Feed in/rev	6	0.017237	0.017237	0.002873	1.99
Error	72	0.103745	0.103745	0.001441	
Total	95	0.939744			

Source	P
Environment	0.000
Rake Angle	0.000
Feed in/rev	0.001
Environment*Rake Angle	0.000
Environment*Feed in/rev	0.011
Rake Angle*Feed in/rev	0.034
Environment*Rake Angle*Feed in/rev	0.078
Error	
Total	

S = 0.0379593 R-Sq = 88.96% R-Sq(adj) = 85.43%

Unusual Observations for Chip thickness ratio

Obs	Chip thickness ratio	Fit	SE Fit	Residual	St Resid	
61	0.421053	0.312781	0.018980	0.108272	3.29	R
62	0.039280	0.312781	0.018980	-0.273501	-8.32	R
63	0.397350	0.312781	0.018980	0.084569	2.57	R
64	0.393441	0.312781	0.018980	0.080660	2.45	R

R denotes an observation with a large standardized residual.

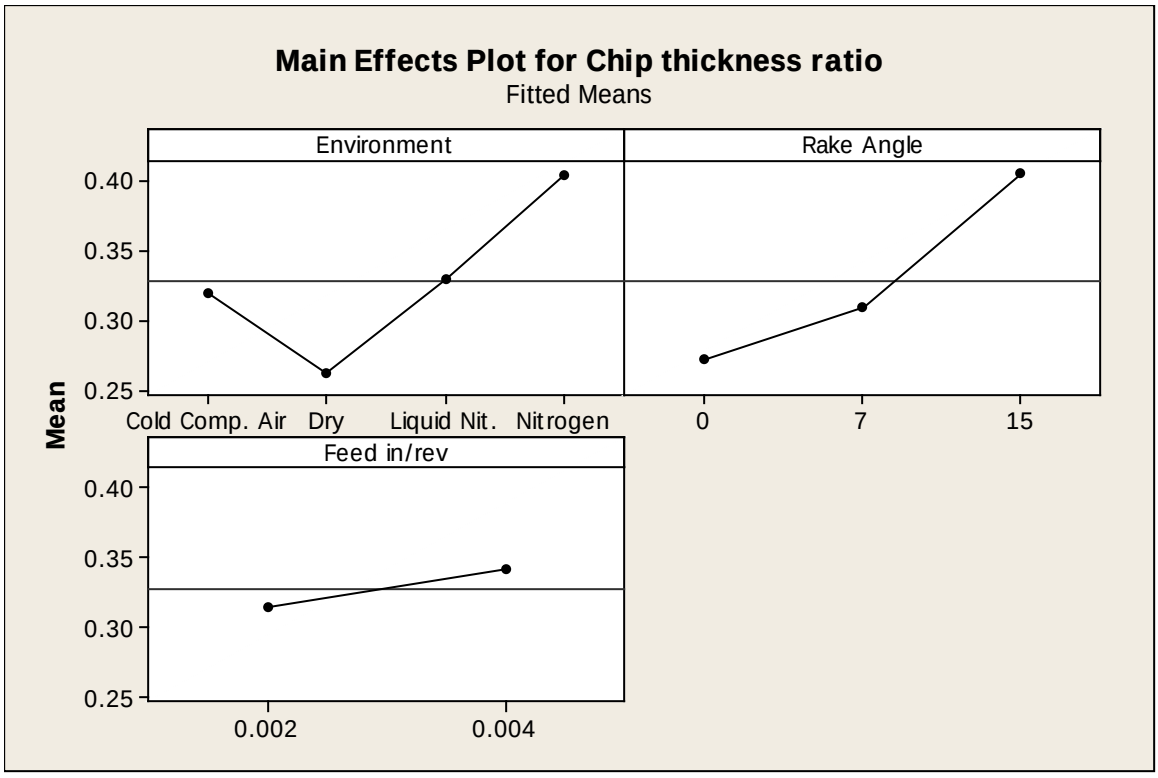
Main Effects Plot for Chip thickness ratio
Fitted Means
Environment
Rake Angle
Feed in/rev
Mean
0.40
0.35
0.30
0.25
Cold Comp. Air
Dry
Liquid Nit.
Nitrogen
0
7
15
0.002
0.004

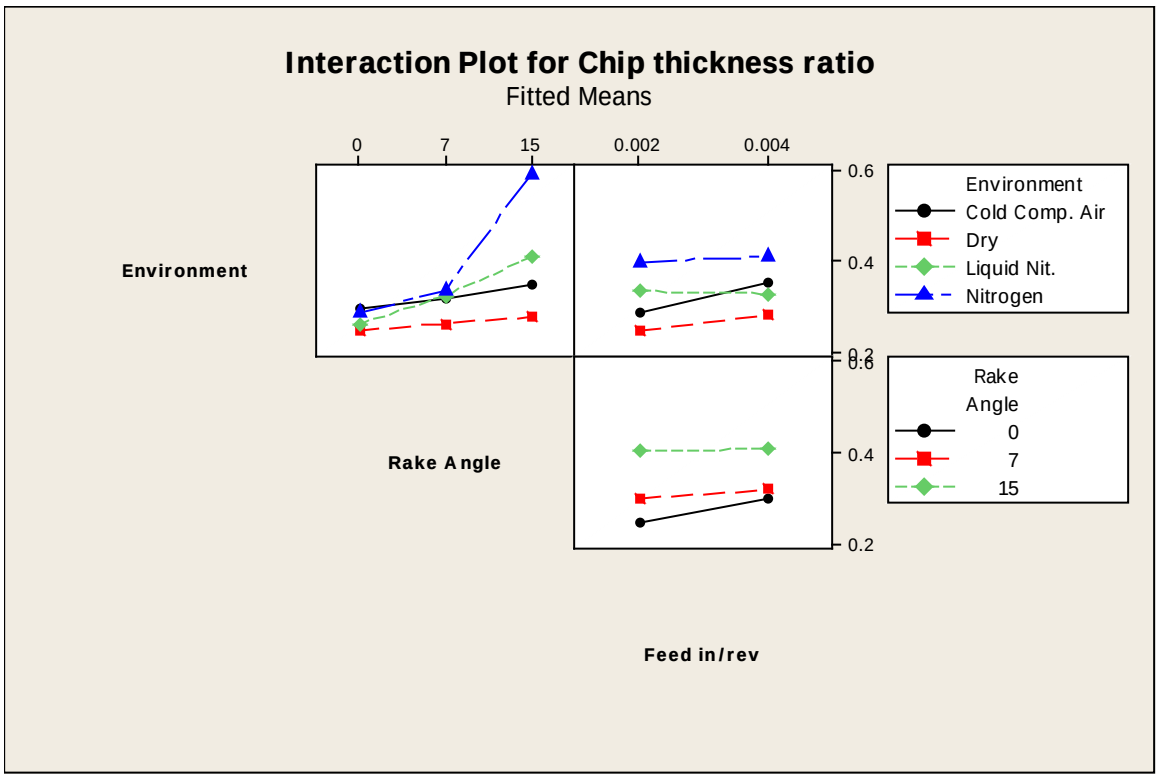
Interaction Plot for Chip thickness ratio
Fitted Means
Environment
Rake Angle
Feed in/rev
0
7
15
0.002
0.004
0.6
0.4
0.2
Environment
Cold Comp. Air
Dry
Liquid Nit.
Nitrogen
Rake Angle
0
7
15

Analysis of Variance for **Phi** degrees, using Adjusted SS for Tests

Source	DF	Seq SS	Adj SS	Adj MS	F	P
Environment	3	767.43	767.43	255.81	55.64	0.000
Rake Angle	2	1176.00	1176.00	588.00	127.90	0.000
Feed in/rev	1	47.56	47.56	47.56	10.34	0.002
Environment*Rake Angle	6	733.41	733.41	122.23	26.59	0.000
Environment*Feed in/rev	3	56.09	56.09	18.70	4.07	0.010
Rake Angle*Feed in/rev	2	28.38	28.38	14.19	3.09	0.052
Environment*Rake Angle*Feed in/rev	6	57.70	57.70	9.62	2.09	0.065
Error	72	331.00	331.00	4.60		
Total	95	3197.57				

S = 2.14412 R-Sq = 89.65% R-Sq(adj) = 86.34%

Unusual Observations for Phi degrees

Obs	Phi degrees	Fit	SE Fit	Residual	St Resid
61	23.7744	17.7080	1.0721	6.0664	3.27 R
62	2.2434	17.7080	1.0721	-15.4646	-8.33 R
63	22.5119	17.7080	1.0721	4.8039	2.59 R
64	22.3023	17.7080	1.0721	4.5943	2.47 R

R denotes an observation with a large standardized residual.

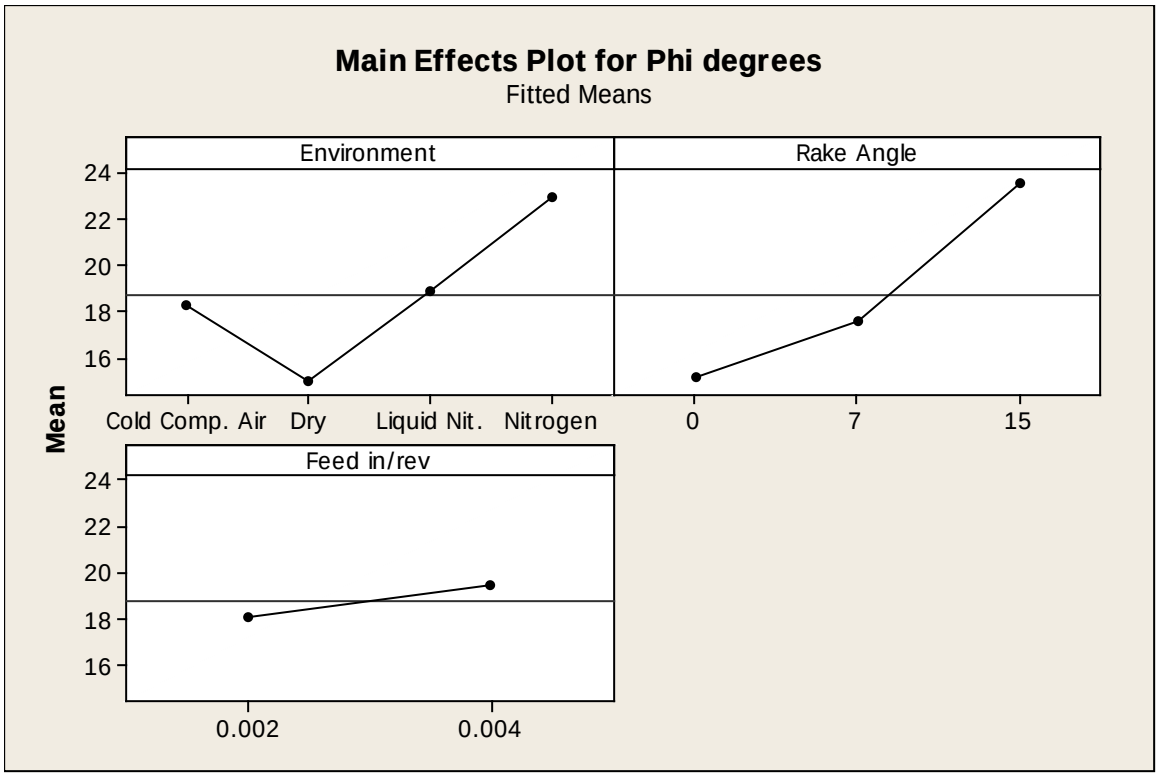
Main Effects Plot for Phi degrees
Fitted Means
Environment
Rake Angle
Feed in/rev
Mean
24
22
20
18
16
Cold Comp. Air
Dry
Liquid Nit.
Nitrogen
0
7
15
0.002
0.004

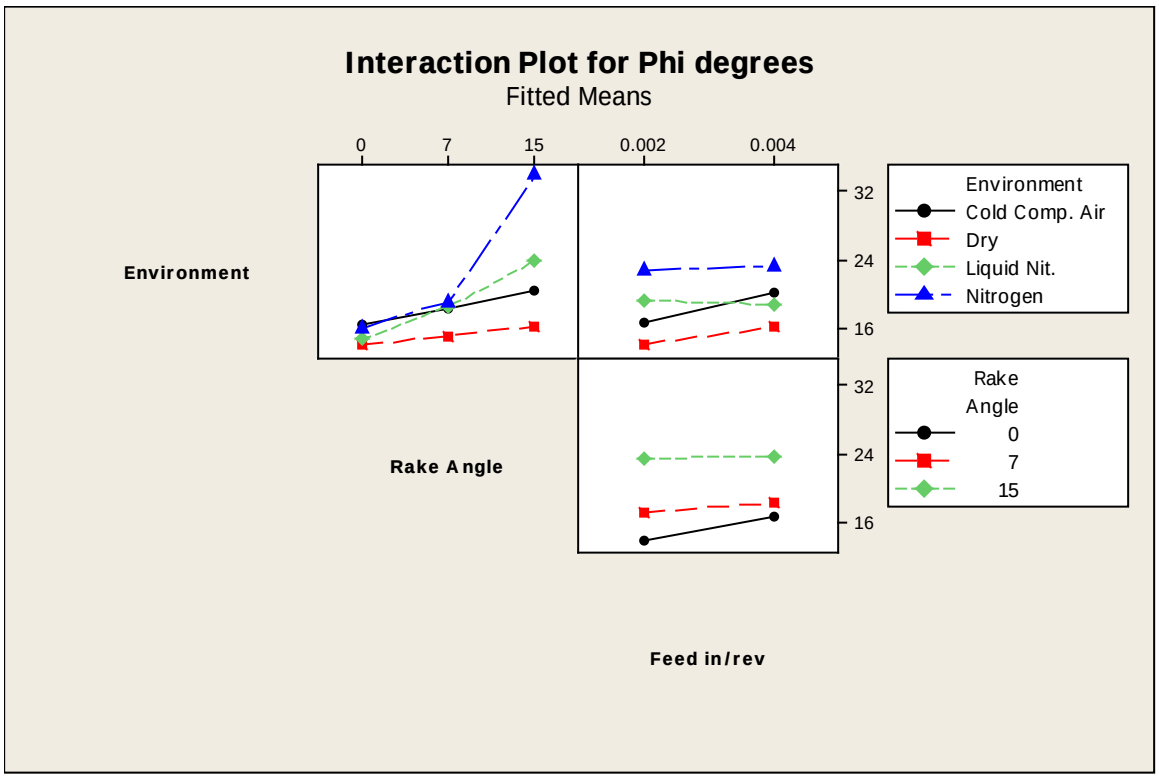
Interaction Plot for Phi degrees
Fitted Means
0
7
15
0.002
0.004
Environment
Rake Angle
Feed in/rev
32
24
16
Environment
Cold Comp. Air
Dry
Liquid Nit.
Nitrogen
Rake Angle
0
7
15

Analysis of Variance for **Psi** degrees, using Adjusted SS for Tests

Source	DF	Seq SS	Adj SS	Adj MS	F
Environment	3	767.430	767.430	255.810	55.64
Rake Angle	2	57.915	57.915	28.957	6.30
Feed in/rev	1	47.558	47.558	47.558	10.34
Environment*Rake Angle	6	733.405	733.405	122.234	26.59
Environment*Feed in/rev	3	56.092	56.092	18.697	4.07
Rake Angle*Feed in/rev	2	28.378	28.378	14.189	3.09
Environment*Rake Angle*Feed in/rev	6	57.700	57.700	9.617	2.09
Error	72	331.003	331.003	4.597	
Total	95	2079.481			

Source	P
Environment	0.000
Rake Angle	0.003
Feed in/rev	0.002
Environment*Rake Angle	0.000
Environment*Feed in/rev	0.010
Rake Angle*Feed in/rev	0.052
Environment*Rake Angle*Feed in/rev	0.065
Error	
Total	

S = 2.14412 R-Sq = 84.08% R-Sq(adj) = 79.00%

Unusual Observations for Psi degrees

Obs	Psi degrees	Fit	SE Fit	Residual	St Resid
61	24.7256	30.7920	1.0721	-6.0664	-3.27 R
62	46.2566	30.7920	1.0721	15.4646	8.33 R
63	25.9881	30.7920	1.0721	-4.8039	-2.59 R
64	26.1977	30.7920	1.0721	-4.5943	-2.47 R

R denotes an observation with a large standardized residual.

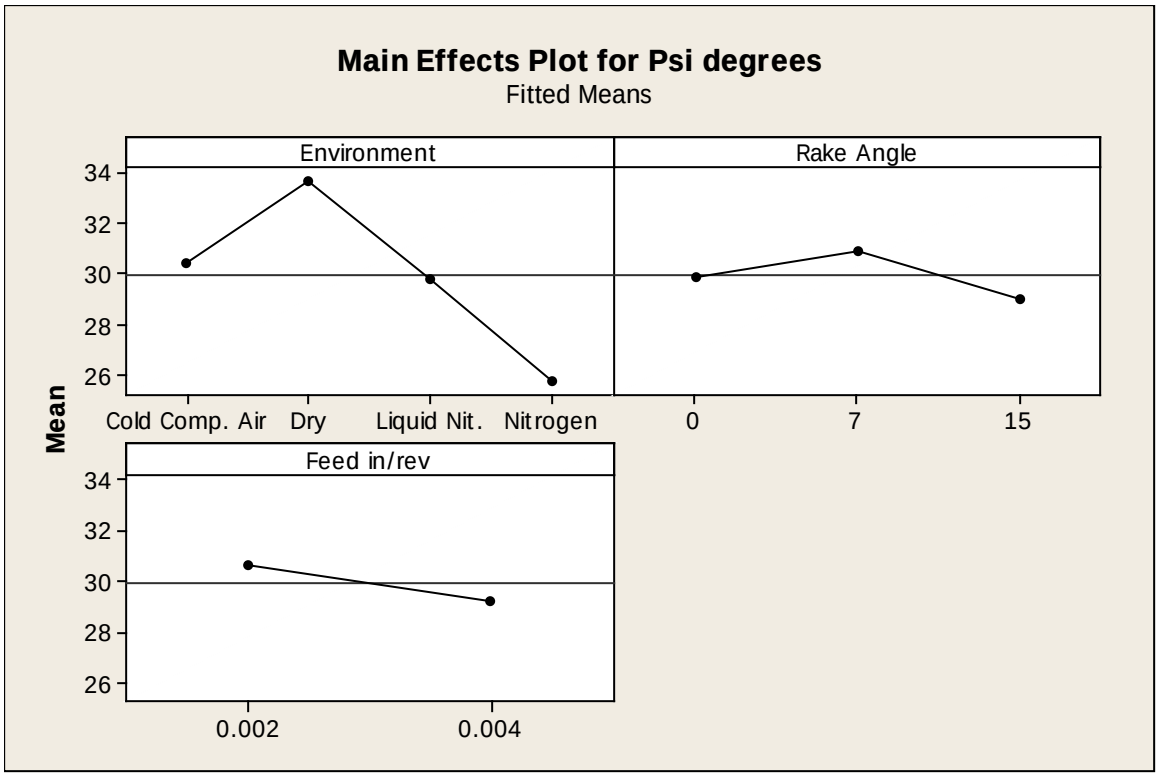
Main Effects Plot for Psi degrees
Fitted Means
Environment
Rake Angle
Feed in/rev
Mean
34
32
30
28
26
Cold Comp. Air
Dry
Liquid Nit.
Nitrogen
0
7
15
0.002
0.004

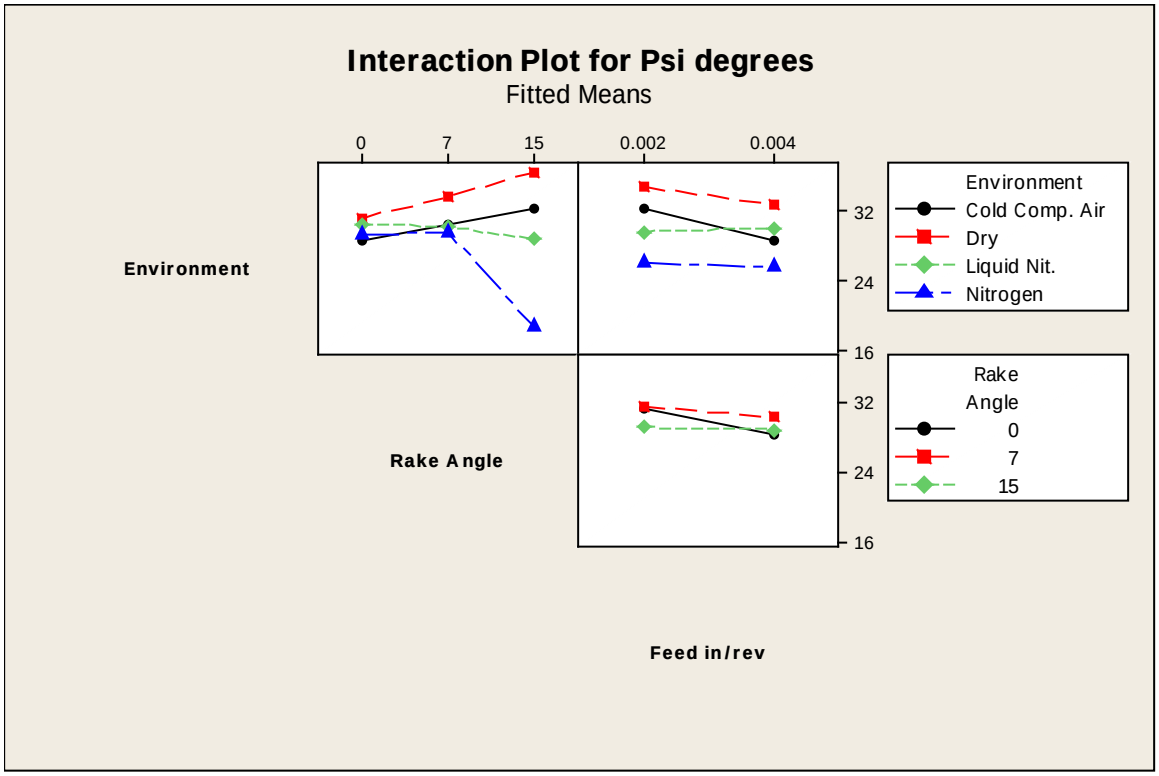
Interaction Plot for Psi degrees
Fitted Means
0
7
15
0.002
0.004
Environment
Rake Angle
Feed in/rev
32
24
16
Environment
Cold Comp. Air
Dry
Liquid Nit.
Nitrogen
Rake Angle
0
7
15

Analysis of Variance for **Friction Force (F)**, using Adjusted SS for Tests

Source	DF	Seq SS	Adj SS	Adj MS	F
Environment	3	7214.9	7214.9	2405.0	64.13
Rake Angle	2	3744.6	3744.6	1872.3	49.93
Feed in/rev	1	98024.1	98024.1	98024.1	2614.05
Environment*Rake Angle	6	778.3	778.3	129.7	3.46
Environment*Feed in/rev	3	633.2	633.2	211.1	5.63
Rake Angle*Feed in/rev	2	431.9	431.9	215.9	5.76
Environment*Rake Angle*Feed in/rev	6	743.8	743.8	124.0	3.31
Error	72	2699.9	2699.9	37.5	
Total	95	114270.7			

Source	P
Environment	0.000
Rake Angle	0.000
Feed in/rev	0.000
Environment*Rake Angle	0.005
Environment*Feed in/rev	0.002
Rake Angle*Feed in/rev	0.005
Environment*Rake Angle*Feed in/rev	0.006
Error	
Total	

S = 6.12364 R-Sq = 97.64% R-Sq(adj) = 96.88%

Unusual Observations for Friction Force (F)

Obs	Friction Force (F)	Fit	SE Fit	Residual	St Resid	
37	236.879	223.454	3.062	13.425	2.53	R
75	199.284	176.691	3.062	22.593	4.26	R
79	264.380	252.337	3.062	12.042	2.27	R
80	234.617	252.337	3.062	-17.721	-3.34	R
82	154.743	165.475	3.062	-10.733	-2.02	R

R denotes an observation with a large standardized residual.

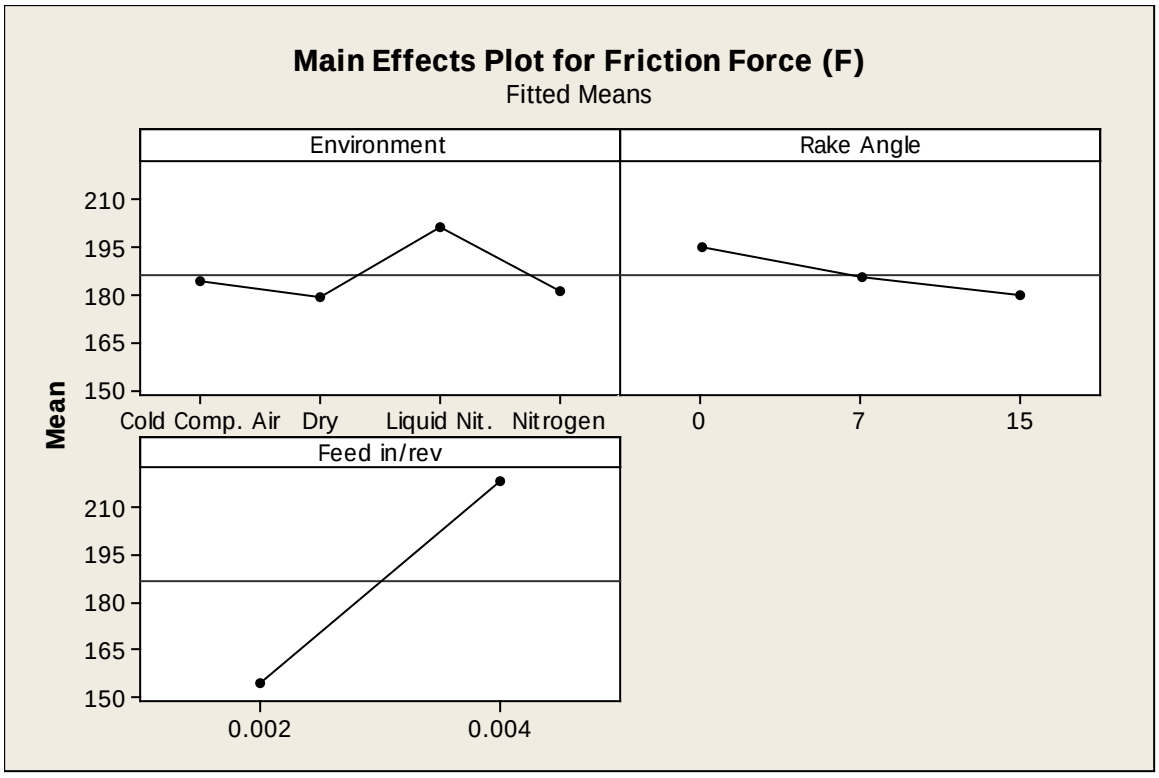
Main Effects Plot for Friction Force (F)
Fitted Means
Environment
Rake Angle
Feed in/rev
Mean
210
195
180
165
150
Cold Comp. Air
Dry
Liquid Nit.
Nitrogen
0
7
15
0.002
0.004

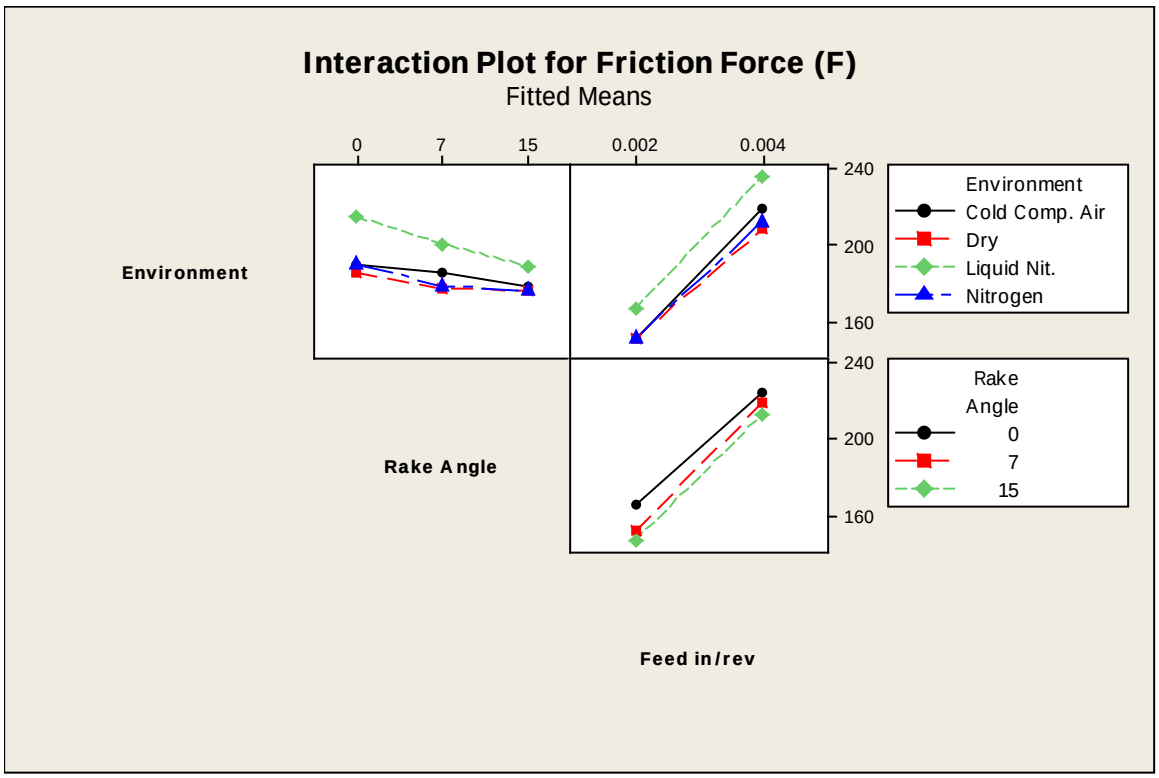
Interaction Plot for Friction Force (F)
Fitted Means
Environment
Rake Angle
Feed in/rev
0
7
15
0.002
0.004
240
200
160
Environment
Cold Comp. Air
Dry
Liquid Nit.
Nitrogen
Rake Angle
0
7
15

Analysis of Variance for **Normal Force (N)**, using Adjusted SS for Tests

Source	DF	Seq SS	Adj SS	Adj MS	F	P
Environment	3	5038	5038	1679	77.60	0.000
Rake Angle	2	96301	96301	48151	2225.06	0.000
Feed in/rev	1	308328	308328	308328	14247.98	0.000
Environment*Rake Angle	6	543	543	90	4.18	0.001
Environment*Feed in/rev	3	232	232	77	3.57	0.018
Rake Angle*Feed in/rev	2	2223	2223	1112	51.36	0.000
Environment*Rake Angle*Feed in/rev	6	186	186	31	1.43	0.215
Error	72	1558	1558	22		
Total	95	414409				

S = 4.65190 R-Sq = 99.62% R-Sq(adj) = 99.50%

Unusual Observations for Normal Force (N)

Obs	Normal Force (N)	Fit	SE Fit	Residual	St Resid
47	225.664	237.135	2.326	-11.471	-2.85 R
75	238.342	217.048	2.326	21.294	5.29 R
76	208.795	217.048	2.326	-8.253	-2.05 R
79	362.705	351.816	2.326	10.890	2.70 R
80	336.848	351.816	2.326	-14.968	-3.72 R

R denotes an observation with a large standardized residual.

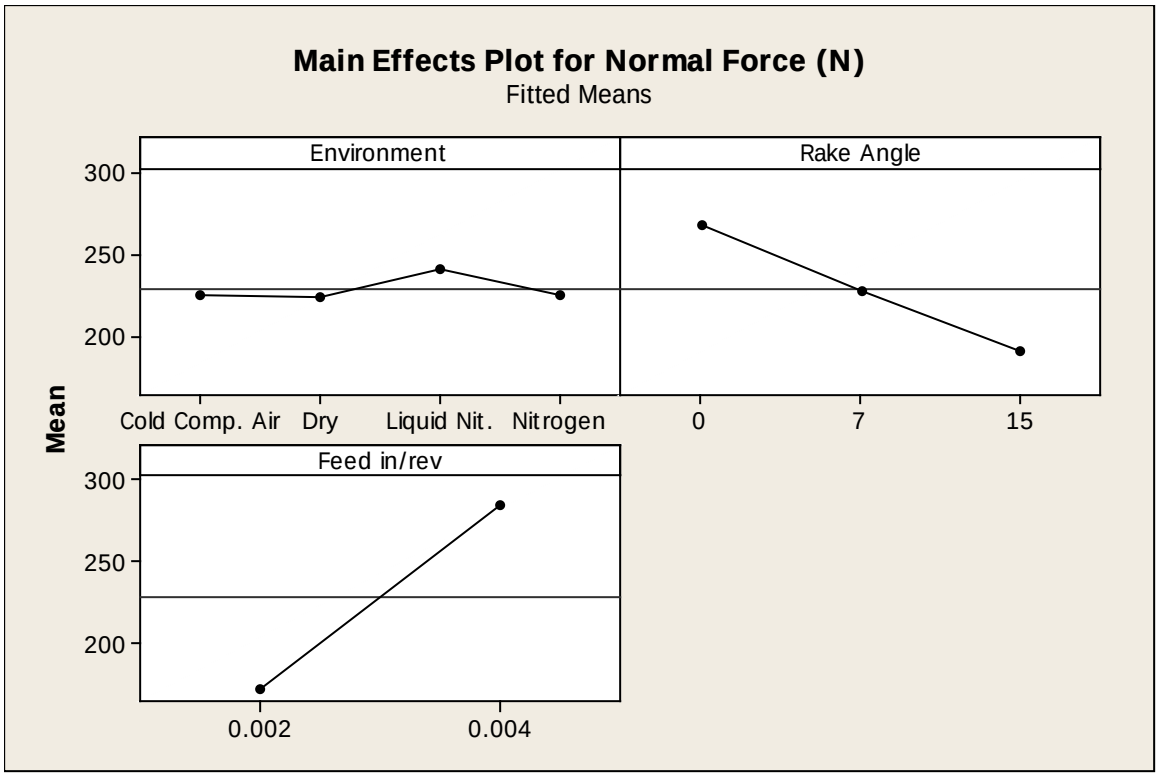
Main Effects Plot for Normal Force (N)
Fitted Means
Environment
Rake Angle
Feed in/rev
Mean
300
250
200
Cold Comp. Air
Dry
Liquid Nit.
Nitrogen
0
7
15
0.002
0.004

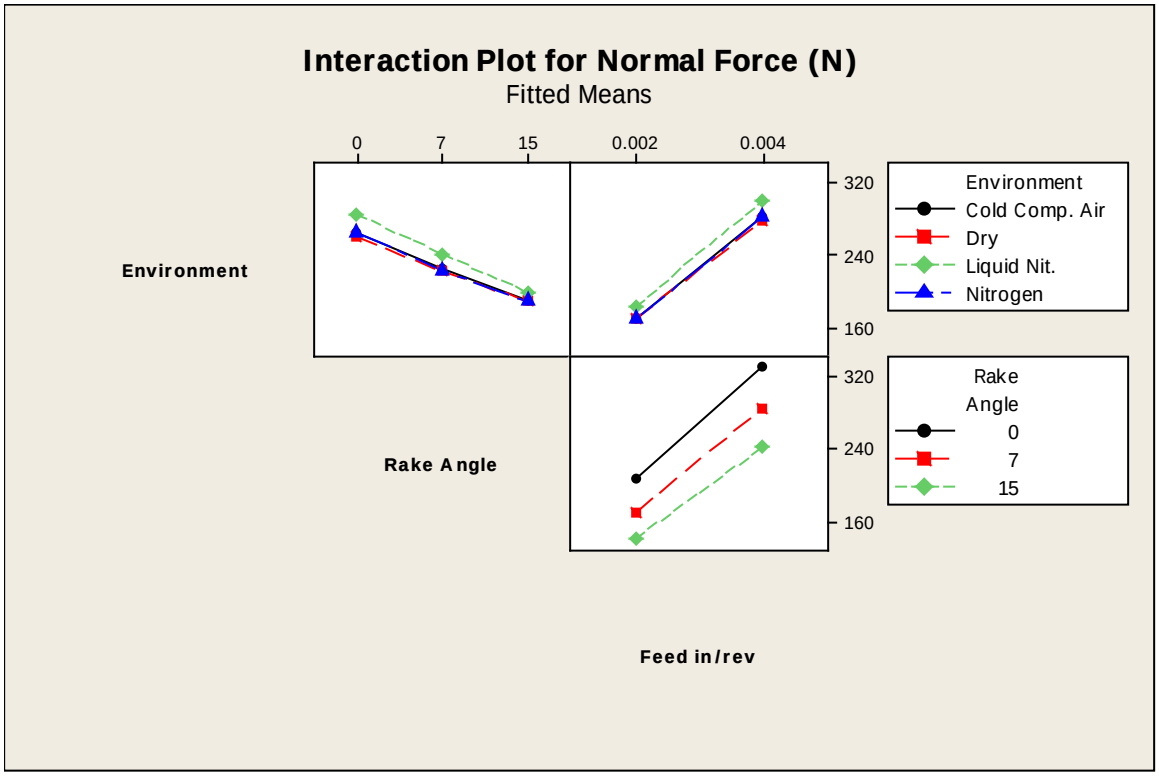
Interaction Plot for Normal Force (N)
Fitted Means
Environment
Rake Angle
Feed in/rev
0
7
15
0.002
0.004
320
240
160
Environment
Cold Comp. Air
Dry
Liquid Nit.
Nitrogen
Rake Angle
0
7
15

Analysis of Variance for **F/N Ratio**, using Adjusted SS for Tests

Source	DF	Seq SS	Adj SS	Adj MS	F
Environment	3	0.012395	0.012395	0.004132	11.28
Rake Angle	2	0.810148	0.810148	0.405074	1105.78
Feed in/rev	1	0.456961	0.456961	0.456961	1247.42
Environment*Rake Angle	6	0.001852	0.001852	0.000309	0.84
Environment*Feed in/rev	3	0.005476	0.005476	0.001825	4.98
Rake Angle*Feed in/rev	2	0.007469	0.007469	0.003735	10.19
Environment*Rake Angle*Feed in/rev	6	0.006853	0.006853	0.001142	3.12
Error	72	0.026375	0.026375	0.000366	
Total	95	1.327529			

Source	P
Environment	0.000
Rake Angle	0.000
Feed in/rev	0.000
Environment*Rake Angle	0.541
Environment*Feed in/rev	0.003
Rake Angle*Feed in/rev	0.000
Environment*Rake Angle*Feed in/rev	0.009
Error	
Total	

S = 0.0191396 R-Sq = 98.01% R-Sq(adj) = 97.38%

Unusual Observations for F/N Ratio

Obs	F/N Ratio	Fit	SE Fit	Residual	St Resid	
37	0.83562	0.79457	0.00957	0.04104	2.48	R
38	0.75627	0.79457	0.00957	-0.03830	-2.31	R
45	0.86845	0.90363	0.00957	-0.03517	-2.12	R
47	0.99068	0.90363	0.00957	0.08705	5.25	R
89	1.03868	1.07478	0.00957	-0.03610	-2.18	R
92	1.12093	1.07478	0.00957	0.04615	2.78	R

R denotes an observation with a large standardized residual.

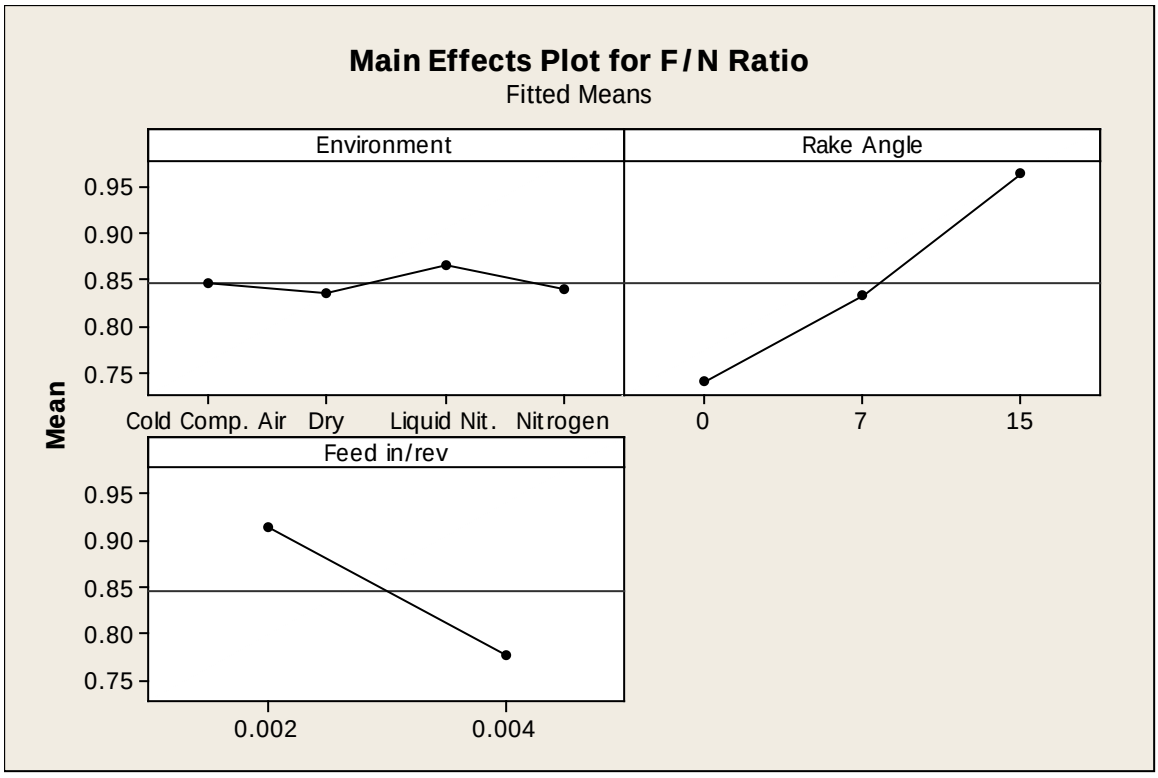
Main Effects Plot for F/N Ratio
Fitted Means
Environment
Rake Angle
Feed in/rev
Mean
0.95
0.90
0.85
0.80
0.75
Cold Comp. Air
Dry
Liquid Nit.
Nitrogen
0
7
15
0.002
0.004

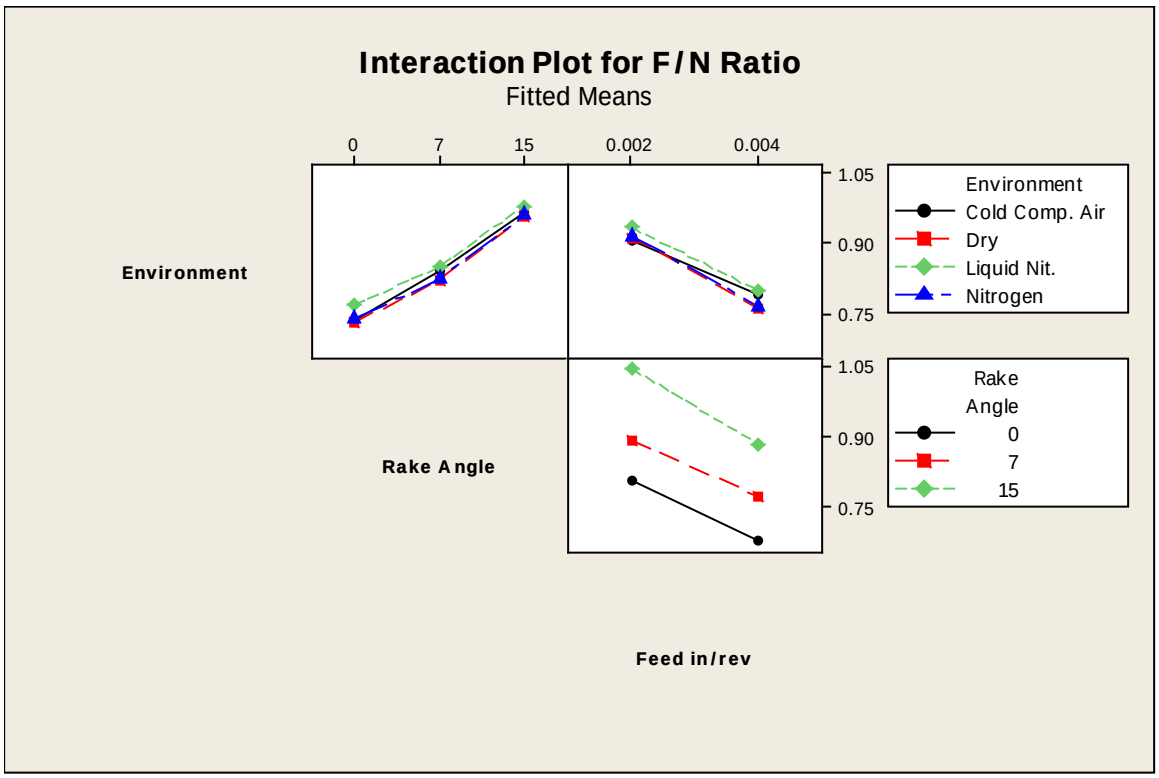
Interaction Plot for F/N Ratio
Fitted Means
Environment
Rake Angle
Feed in/rev
0
7
15
0.002
0.004
1.05
0.90
0.75
Environment
Cold Comp. Air
Dry
Liquid Nit.
Nitrogen
Rake Angle
0
7
15

Analysis of Variance for **Fs (Merchant)**, using Adjusted SS for Tests

Source	DF	Seq SS	Adj SS	Adj MS	F	P
Environment	3	12649	12649	4216	47.34	0.000
Rake Angle	2	34065	34065	17032	191.26	0.000
Feed in/rev	1	203793	203793	203793	2288.40	0.000
Environment*Rake Angle	6	9625	9625	1604	18.01	0.000
Environment*Feed in/rev	3	1148	1148	383	4.30	0.008
Rake Angle*Feed in/rev	2	139	139	70	0.78	0.462
Environment*Rake Angle*Feed in/rev	6	1078	1078	180	2.02	0.074
Error	72	6412	6412	89		
Total	95	268907				

S = 9.43688 R-Sq = 97.62% R-Sq(adj) = 96.85%

Unusual Observations for Fs (Merchant)

Obs	Fs (Merchant)	Fit	SE Fit	Residual	St Resid
61	205.945	232.233	4.718	-26.287	-3.22 R
62	295.595	232.233	4.718	63.362	7.75 R
63	213.387	232.233	4.718	-18.846	-2.31 R
64	214.004	232.233	4.718	-18.229	-2.23 R

R denotes an observation with a large standardized residual.

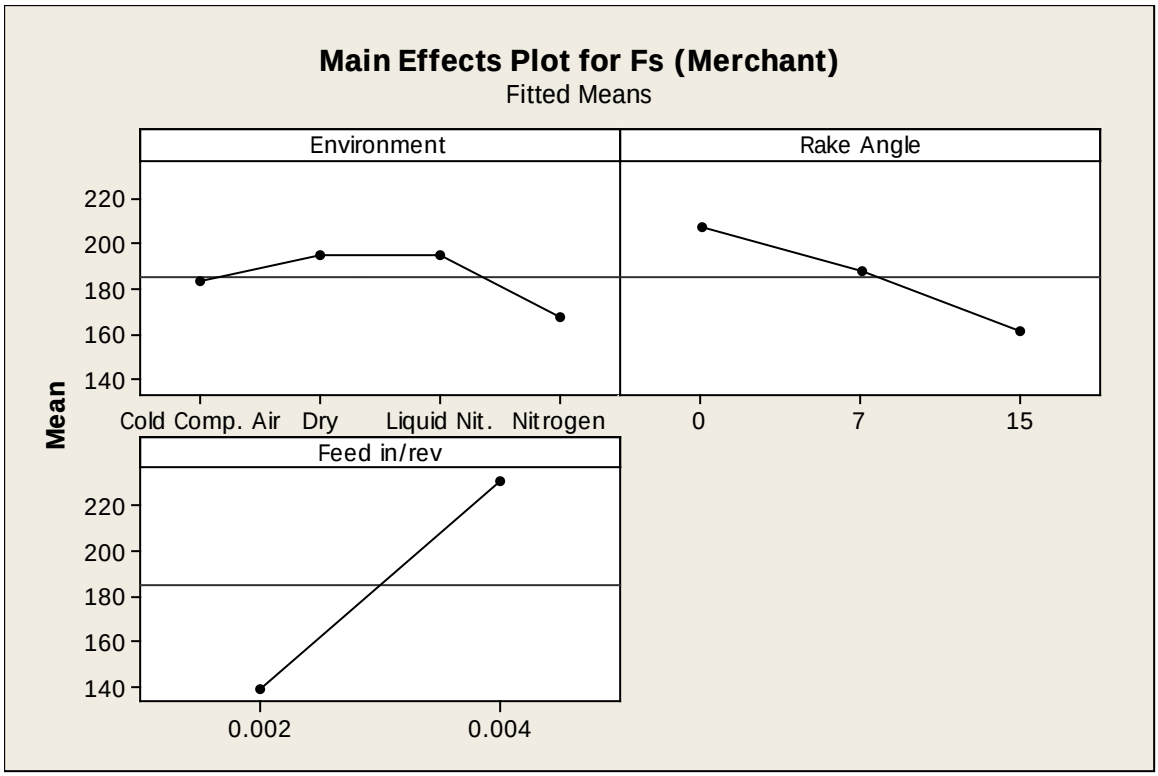
Main Effects Plot for Fs (Merchant)
Fitted Means
Environment
Rake Angle
Feed in/rev
Mean
220
200
180
160
140
Cold Comp. Air
Dry
Liquid Nit.
Nitrogen
0
7
15
0.002
0.004

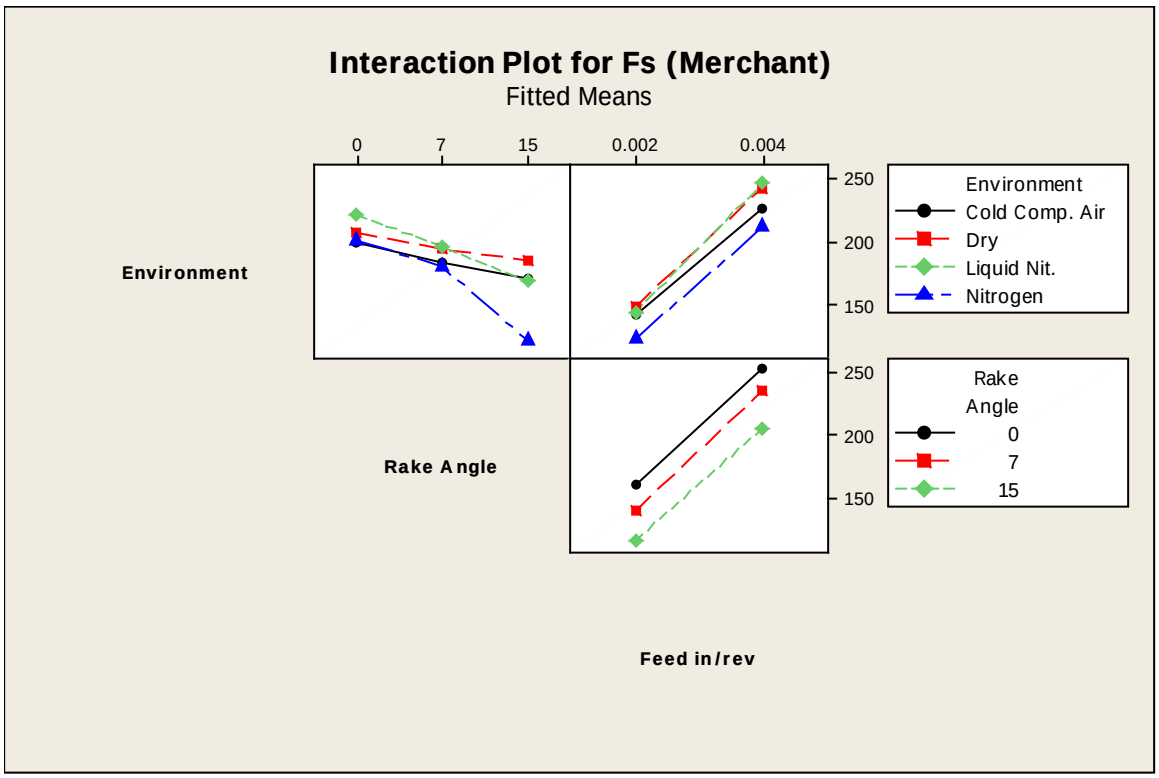
Interaction Plot for Fs (Merchant)
Fitted Means
Environment
Rake Angle
Feed in/rev
0
7
15
0.002
0.004
250
200
150
Environment
Cold Comp. Air
Dry
Liquid Nit.
Nitrogen
Rake Angle
0
7
15

Analysis of Variance for **Fn (Merchant)**, using Adjusted SS for Tests

Source	DF	Seq SS	Adj SS	Adj MS	F	P
Environment	3	16659	16659	5553	43.27	0.000
Rake Angle	2	49320	49320	24660	192.17	0.000
Feed in/rev	1	194320	194320	194320	1514.25	0.000
Environment*Rake Angle	6	5513	5513	919	7.16	0.000
Environment*Feed in/rev	3	1494	1494	498	3.88	0.012
Rake Angle*Feed in/rev	2	1298	1298	649	5.06	0.009
Environment*Rake Angle*Feed in/rev	6	2339	2339	390	3.04	0.011
Error	72	9240	9240	128		
Total	95	280183				

S = 11.3282 R-Sq = 96.70% R-Sq(adj) = 95.65%

Unusual Observations for Fn (Merchant)

Obs	Fn (Merchant)	Fit	SE Fit	Residual	St Resid	
61	277.952	255.254	5.664	22.698	2.31	R
62	187.617	255.254	5.664	-67.637	-6.89	R
63	277.330	255.254	5.664	22.076	2.25	R
64	278.117	255.254	5.664	22.863	2.33	R
75	248.333	221.980	5.664	26.353	2.69	R
80	317.481	338.105	5.664	-20.625	-2.10	R

R denotes an observation with a large standardized residual.

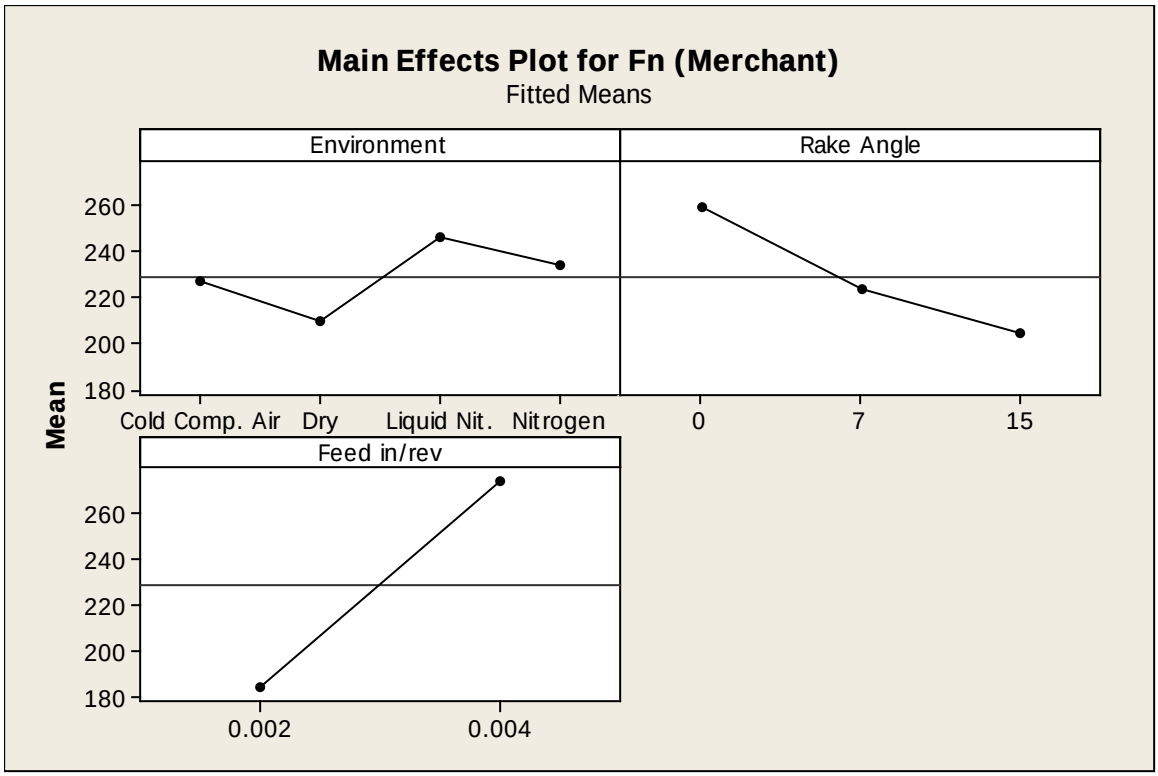
Main Effects Plot for Fn (Merchant)
Fitted Means
Environment
Rake Angle
Feed in/rev
Mean
260
240
220
200
180
Cold Comp. Air
Dry
Liquid Nit.
Nitrogen
0
7
15
0.002
0.004

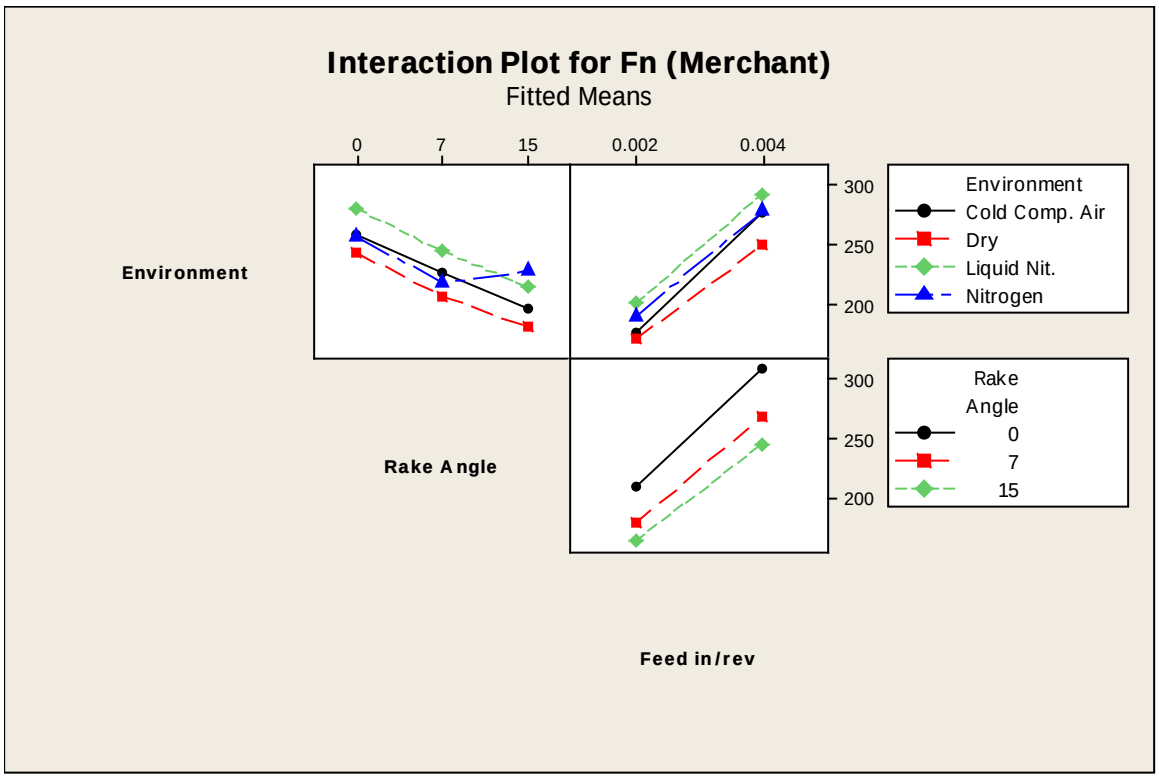
Interaction Plot for Fn (Merchant)
Fitted Means
Environment
Rake Angle
Feed in/rev
0
7
15
0.002
0.004
300
250
200
Environment
Cold Comp. Air
Dry
Liquid Nit.
Nitrogen
Rake Angle
0
7
15

Analysis of Variance for **Fs/Fn (Merchant)**, using Adjusted SS for Tests

Source	DF	Seq SS	Adj SS	Adj MS	F
Environment	3	0.594461	0.594461	0.198154	27.46
Rake Angle	2	0.051127	0.051127	0.025563	3.54
Feed in/rev	1	0.216336	0.216336	0.216336	29.98
Environment*Rake Angle	6	0.554658	0.554658	0.092443	12.81
Environment*Feed in/rev	3	0.065904	0.065904	0.021968	3.04
Rake Angle*Feed in/rev	2	0.021208	0.021208	0.010604	1.47
Environment*Rake Angle*Feed in/rev	6	0.095388	0.095388	0.015898	2.20
Error	72	0.519574	0.519574	0.007216	
Total	95	2.118656			

Source	P
Environment	0.000
Rake Angle	0.034
Feed in/rev	0.000
Environment*Rake Angle	0.000
Environment*Feed in/rev	0.034
Rake Angle*Feed in/rev	0.237
Environment*Rake Angle*Feed in/rev	0.052
Error	
Total	

S = 0.0849488 R-Sq = 75.48% R-Sq(adj) = 67.64%

Unusual Observations for Fs/Fn (Merchant)

Obs	Fs/Fn (Merchant)	Fit	SE Fit	Residual	St Resid	
61	0.74094	0.96384	0.04247	-0.22291	-3.03	R
62	1.57553	0.96384	0.04247	0.61168	8.31	R
63	0.76943	0.96384	0.04247	-0.19441	-2.64	R
64	0.76947	0.96384	0.04247	-0.19437	-2.64	R

R denotes an observation with a large standardized residual.

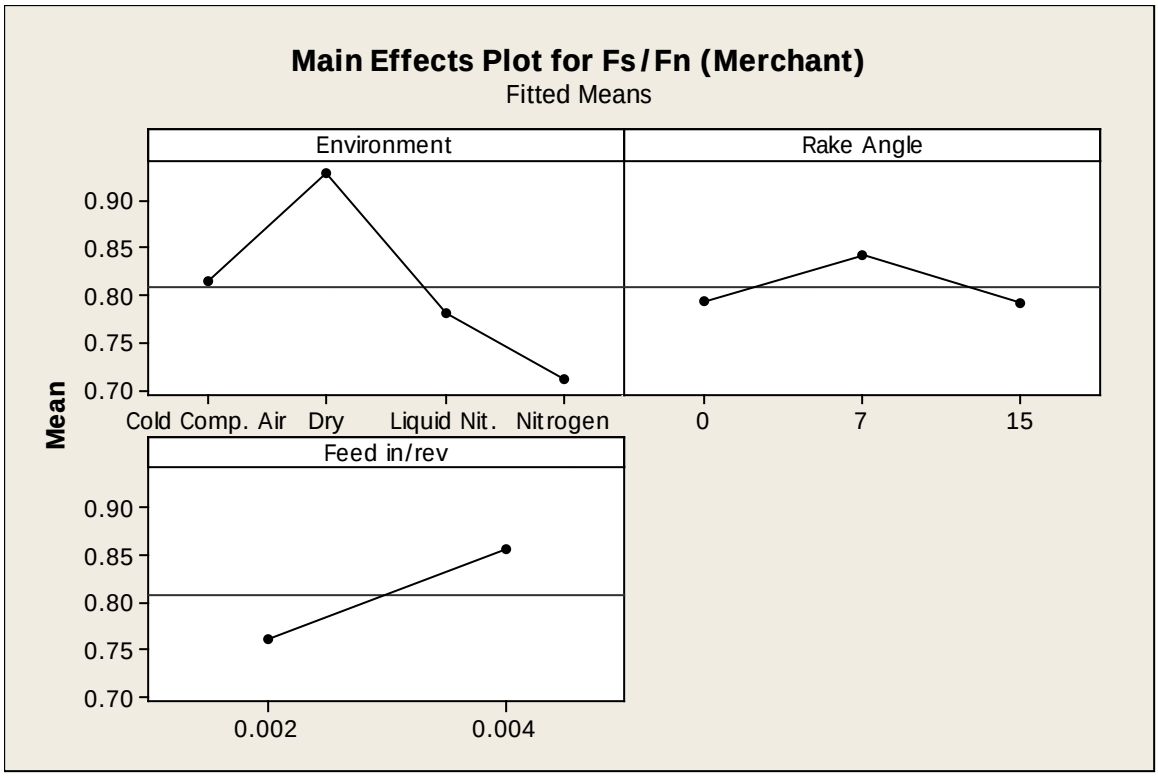
Main Effects Plot for Fs/Fn (Merchant)
Fitted Means
Environment
Rake Angle
Feed in/rev
Mean
0.90
0.85
0.80
0.75
0.70
Cold Comp. Air
Dry
Liquid Nit.
Nitrogen
0
7
15
0.002
0.004

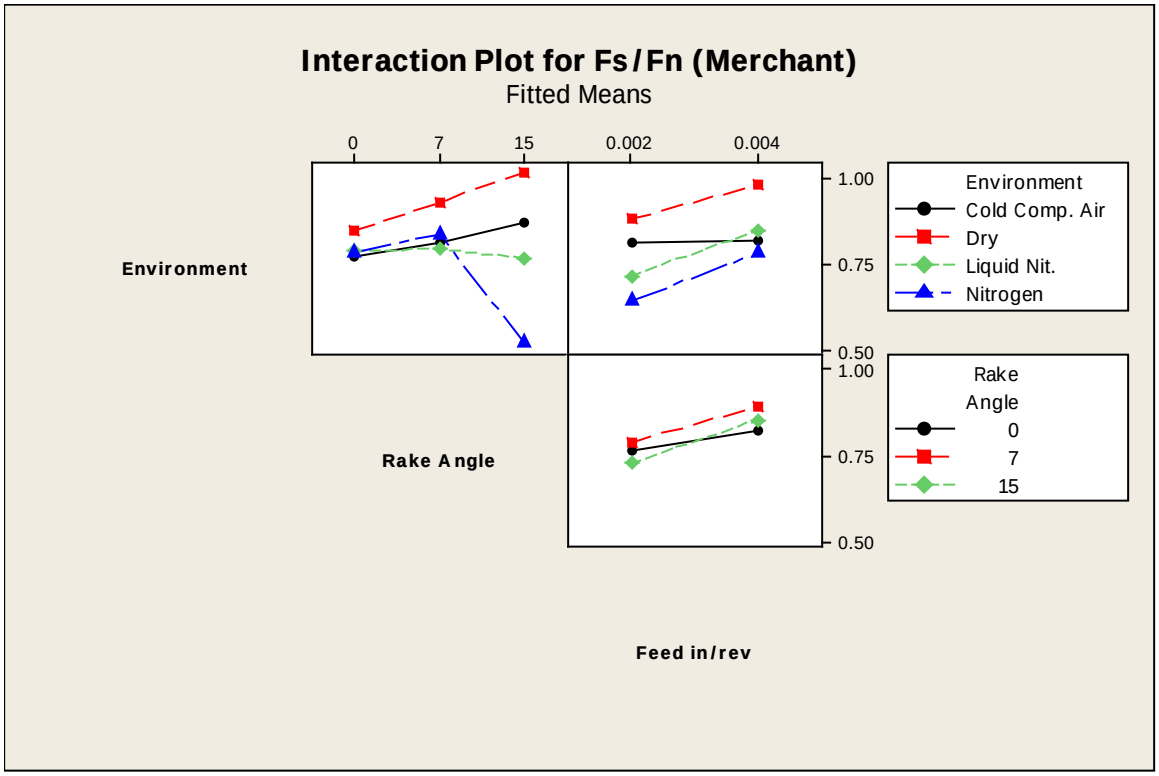
Interaction Plot for Fs/Fn (Merchant)
Fitted Means
Environment
Rake Angle
Feed in/rev
0
7
15
0.002
0.004
1.00
0.75
0.50
Environment
Cold Comp. Air
Dry
Liquid Nit.
Nitrogen
Rake Angle
0
7
15

Analysis of Variance for **Fs (Payton)**, using Adjusted SS for Tests

Source	DF	Seq SS	Adj SS	Adj MS	F	P
Environment	3	55.0	55.0	18.3	2.38	0.077
Rake Angle	2	1611.8	1611.8	805.9	104.46	0.000
Feed in/rev	1	43616.9	43616.9	43616.9	5653.27	0.000
Environment*Rake Angle	6	85.4	85.4	14.2	1.84	0.102
Environment*Feed in/rev	3	111.9	111.9	37.3	4.84	0.004
Rake Angle*Feed in/rev	2	236.4	236.4	118.2	15.32	0.000
Environment*Rake Angle*Feed in/rev	6	146.6	146.6	24.4	3.17	0.008
Error	72	555.5	555.5	7.7		
Total	95	46419.6				

S = 2.77765 R-Sq = 98.80% R-Sq(adj) = 98.42%

Unusual Observations for Fs (Payton)

Obs	Fs (Payton)	Fit	SE Fit	Residual	St Resid	
37	55.3520	62.5443	1.3888	-7.1924	-2.99	R
38	70.1979	62.5443	1.3888	7.6535	3.18	R
45	63.5944	57.8867	1.3888	5.7077	2.37	R
47	42.9367	57.8867	1.3888	-14.9501	-6.21	R
48	62.8259	57.8867	1.3888	4.9392	2.05	R

R denotes an observation with a large standardized residual.

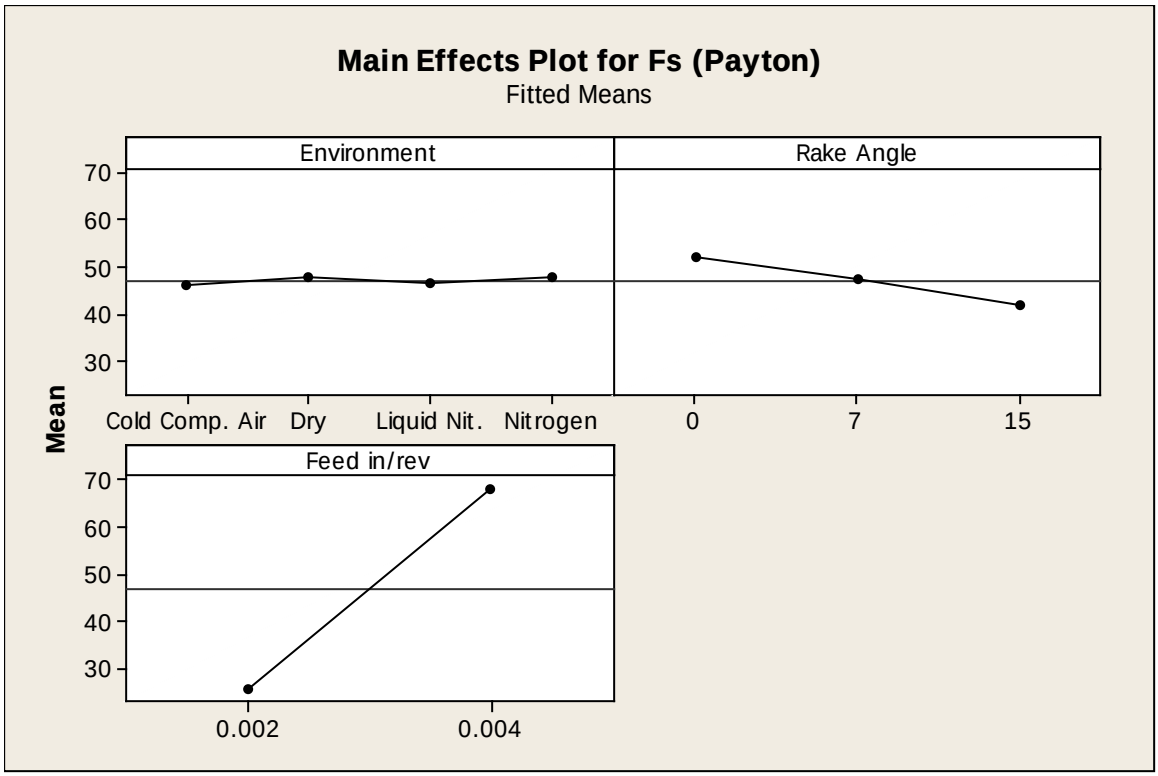
Main Effects Plot for Fs (Payton)
Fitted Means
Environment
Rake Angle
Feed in/rev
Mean
70
60
50
40
30
Cold Comp. Air
Dry
Liquid Nit.
Nitrogen
0
7
15
0.002
0.004

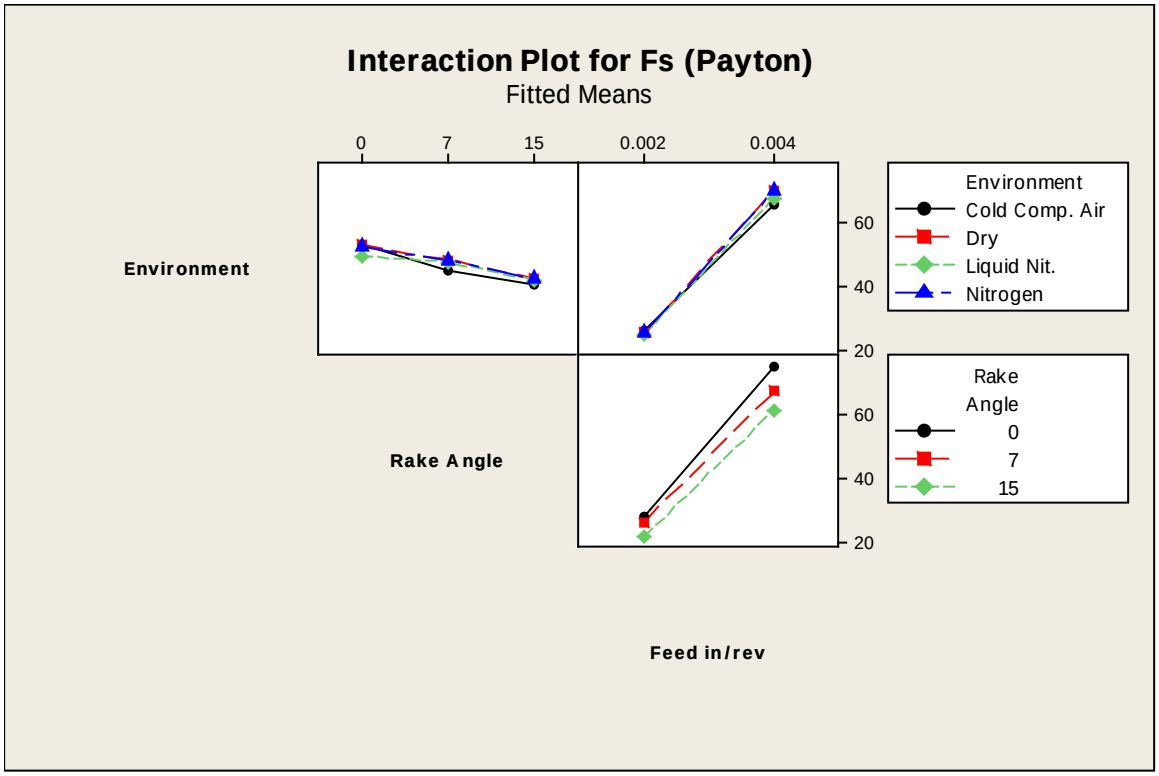
Interaction Plot for Fs (Payton)
Fitted Means
Environment
Rake Angle
Feed in/rev
0
7
15
0.002
0.004
60
40
20
Environment
Cold Comp. Air
Dry
Liquid Nit.
Nitrogen
Rake Angle
0
7
15

Analysis of Variance for **Fn (Payton)**, using Adjusted SS for Tests

Source	DF	Seq SS	Adj SS	Adj MS	F	P
Environment	3	12181	12181	4060	78.96	0.000
Rake Angle	2	75974	75974	37987	738.70	0.000
Feed in/rev	1	364121	364121	364121	7080.78	0.000
Environment*Rake Angle	6	1253	1253	209	4.06	0.001
Environment*Feed in/rev	3	744	744	248	4.82	0.004
Rake Angle*Feed in/rev	2	1033	1033	517	10.05	0.000
Environment*Rake Angle*Feed in/rev	6	792	792	132	2.57	0.026
Error	72	3703	3703	51		
Total	95	459800				

S = 7.17104 R-Sq = 99.19% R-Sq(adj) = 98.94%

Unusual Observations for Fn (Payton)

Obs	Fn (Payton)	Fit	SE Fit	Residual	St Resid	
75	309.449	278.416	3.586	31.033	5.00	R
79	443.416	427.201	3.586	16.216	2.61	R
80	404.086	427.201	3.586	-23.114	-3.72	R
81	257.062	244.566	3.586	12.496	2.01	R
82	231.191	244.566	3.586	-13.376	-2.15	R

R denotes an observation with a large standardized residual.

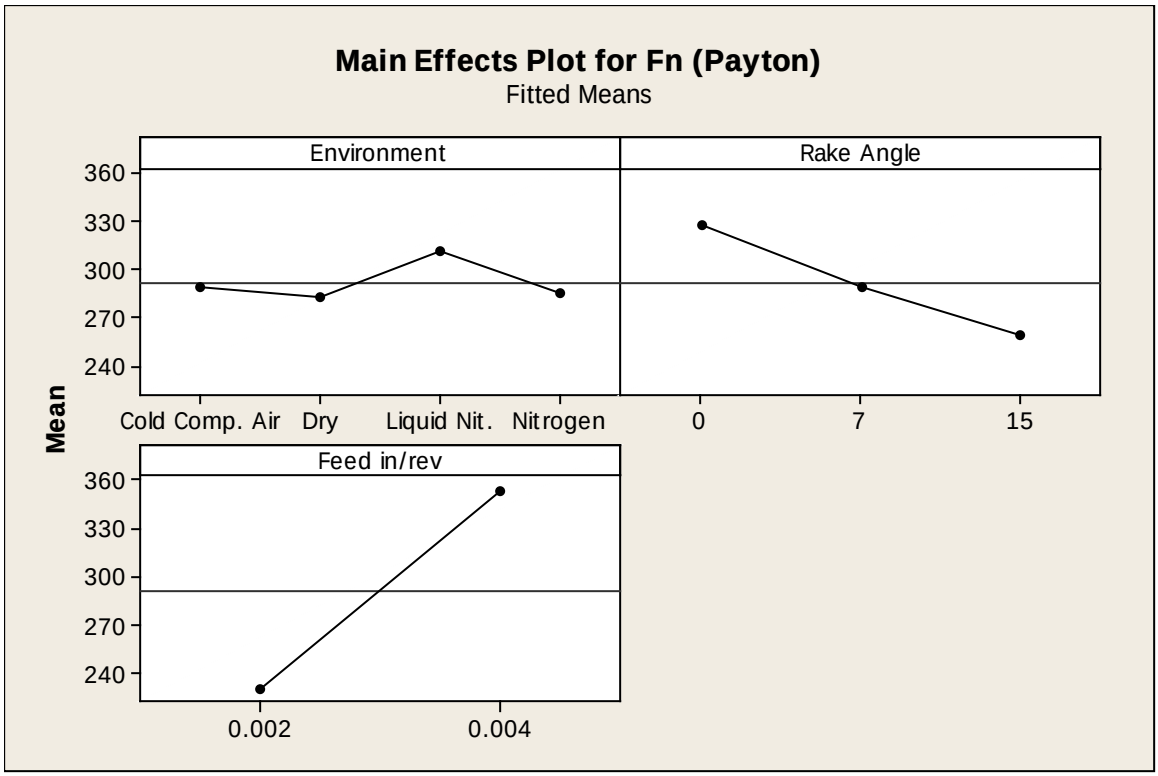
Main Effects Plot for Fn (Payton)
Fitted Means
Environment
Rake Angle
Feed in/rev
Mean
360
330
300
270
240
Cold Comp. Air
Dry
Liquid Nit.
Nitrogen
0
7
15
0.002
0.004

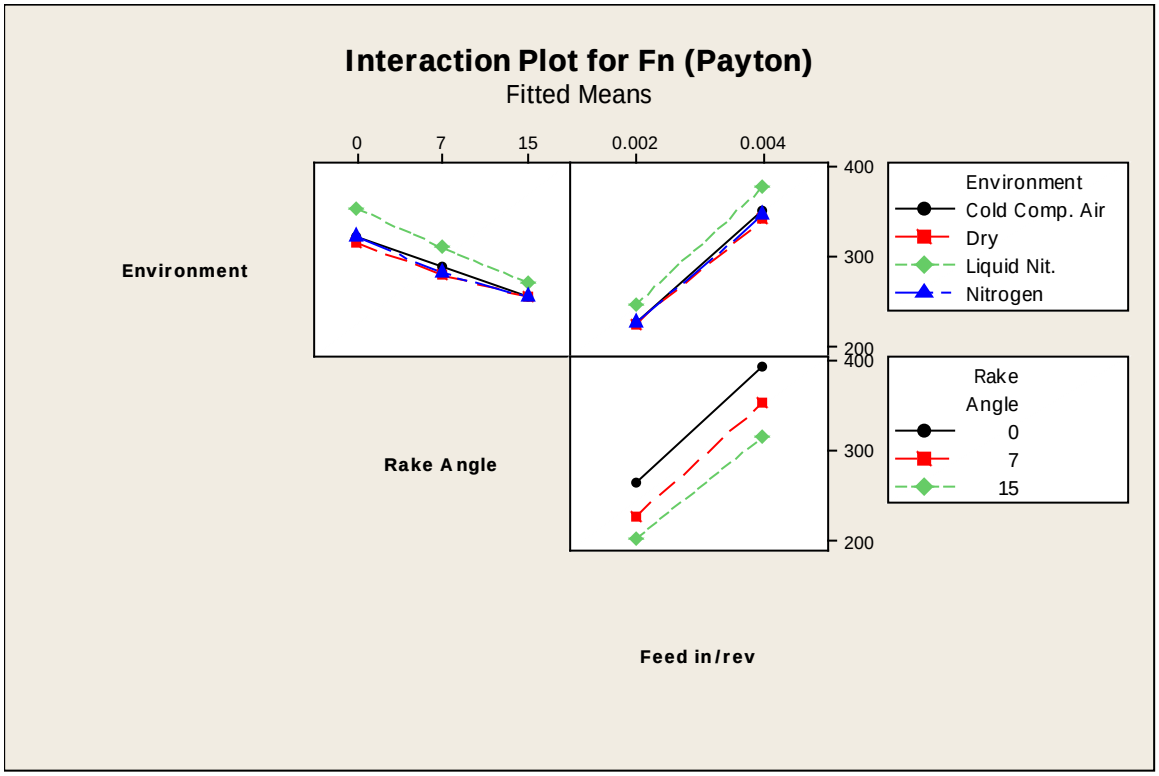
Interaction Plot for Fn (Payton)
Fitted Means
Environment
Rake Angle
Feed in/rev
0
7
15
0.002
0.004
400
300
200
Environment
Cold Comp. Air
Dry
Liquid Nit.
Nitrogen
Rake Angle
0
7
15

Analysis of Variance for **Fs/Fn (Payton)**, using Adjusted SS for Tests

Source	DF	Seq SS	Adj SS	Adj MS
Environment	3	0.0047062	0.0047062	0.0015687
Rake Angle	2	0.0003457	0.0003457	0.0001729
Feed in/rev	1	0.1616884	0.1616884	0.1616884
Environment*Rake Angle	6	0.0010256	0.0010256	0.0001709
Environment*Feed in/rev	3	0.0020454	0.0020454	0.0006818
Rake Angle*Feed in/rev	2	0.0006909	0.0006909	0.0003455
Environment*Rake Angle*Feed in/rev	6	0.0023983	0.0023983	0.0003997
Error	72	0.0083608	0.0083608	0.0001161
Total	95	0.1812614		

Source	F	P
Environment	13.51	0.000
Rake Angle	1.49	0.233
Feed in/rev	1392.39	0.000
Environment*Rake Angle	1.47	0.200
Environment*Feed in/rev	5.87	0.001
Rake Angle*Feed in/rev	2.97	0.057
Environment*Rake Angle*Feed in/rev	3.44	0.005
Error		
Total		

S = 0.0107760 R-Sq = 95.39% R-Sq(adj) = 93.91%

Unusual Observations for Fs/Fn (Payton)

Obs	Fs/Fn (Payton)	Fit	SE Fit	Residual	St Resid	
37	0.151545	0.177253	0.005388	-0.025708	-2.75	R
38	0.201652	0.177253	0.005388	0.024399	2.61	R
45	0.203946	0.184341	0.005388	0.019605	2.10	R
47	0.136420	0.184341	0.005388	-0.047921	-5.13	R
92	0.074079	0.095437	0.005388	-0.021358	-2.29	R

R denotes an observation with a large standardized residual.

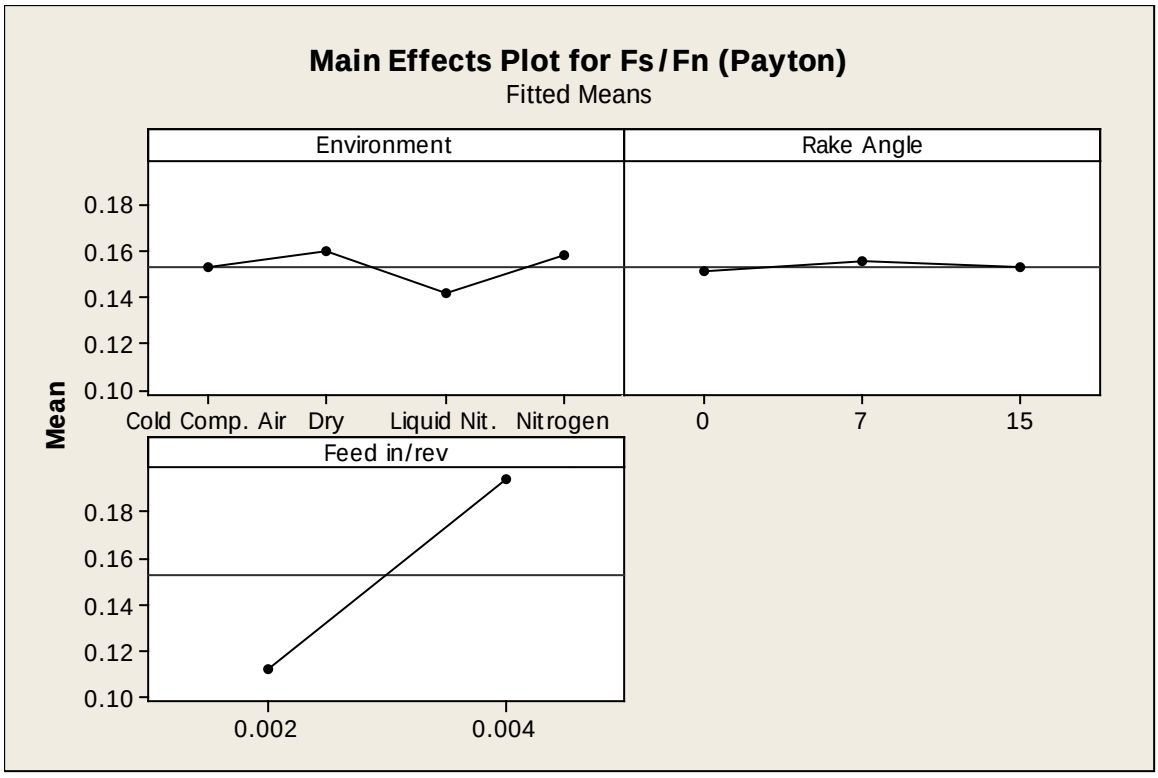
Main Effects Plot for Fs/Fn (Payton)
Fitted Means
Environment
Rake Angle
Feed in/rev
Mean
0.18
0.16
0.14
0.12
0.10
Cold Comp. Air
Dry
Liquid Nit.
Nitrogen
0
7
15
0.002
0.004

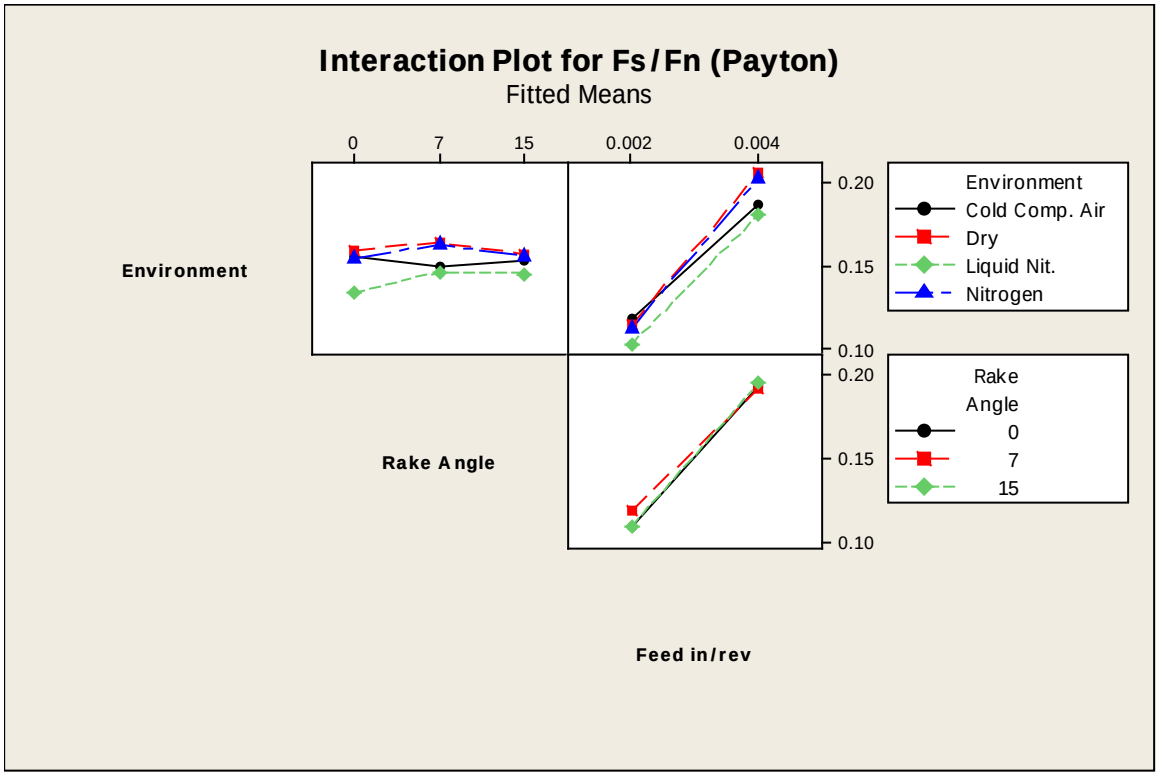
Interaction Plot for Fs/Fn (Payton)
Fitted Means
Environment
Rake Angle
Feed in/rev
0
7
15
0.002
0.004
0.20
0.15
0.10
Environment
Cold Comp. Air
Dry
Liquid Nit.
Nitrogen
Rake Angle
0
7
15

Analysis of Variance for **Beta** (degrees), using Adjusted SS for Tests

Source	DF	Seq SS	Adj SS	Adj MS	F
Environment	3	14.614	14.614	4.871	13.42
Rake Angle	2	882.346	882.346	441.173	1215.27
Feed in/rev	1	505.841	505.841	505.841	1393.41
Environment*Rake Angle	6	3.137	3.137	0.523	1.44
Environment*Feed in/rev	3	6.288	6.288	2.096	5.77
Rake Angle*Feed in/rev	2	2.193	2.193	1.096	3.02
Environment*Rake Angle*Feed in/rev	6	7.458	7.458	1.243	3.42
Error	72	26.138	26.138	0.363	
Total	95	1448.015			

Source	P
Environment	0.000
Rake Angle	0.000
Feed in/rev	0.000
Environment*Rake Angle	0.211
Environment*Feed in/rev	0.001
Rake Angle*Feed in/rev	0.055
Environment*Rake Angle*Feed in/rev	0.005
Error	
Total	

S = 0.602515 R-Sq = 98.19% R-Sq(adj) = 97.62%

Unusual Observations for Beta (degrees)

Obs	Beta (degrees)	Fit	SE Fit	Residual	St Resid	
37	39.8827	38.4524	0.3013	1.4303	2.74	R
38	37.0991	38.4524	0.3013	-1.3533	-2.59	R
45	40.9728	42.0625	0.3013	-1.0897	-2.09	R
47	44.7316	42.0625	0.3013	2.6691	5.12	R
92	48.2633	47.0496	0.3013	1.2137	2.33	R

R denotes an observation with a large standardized residual.

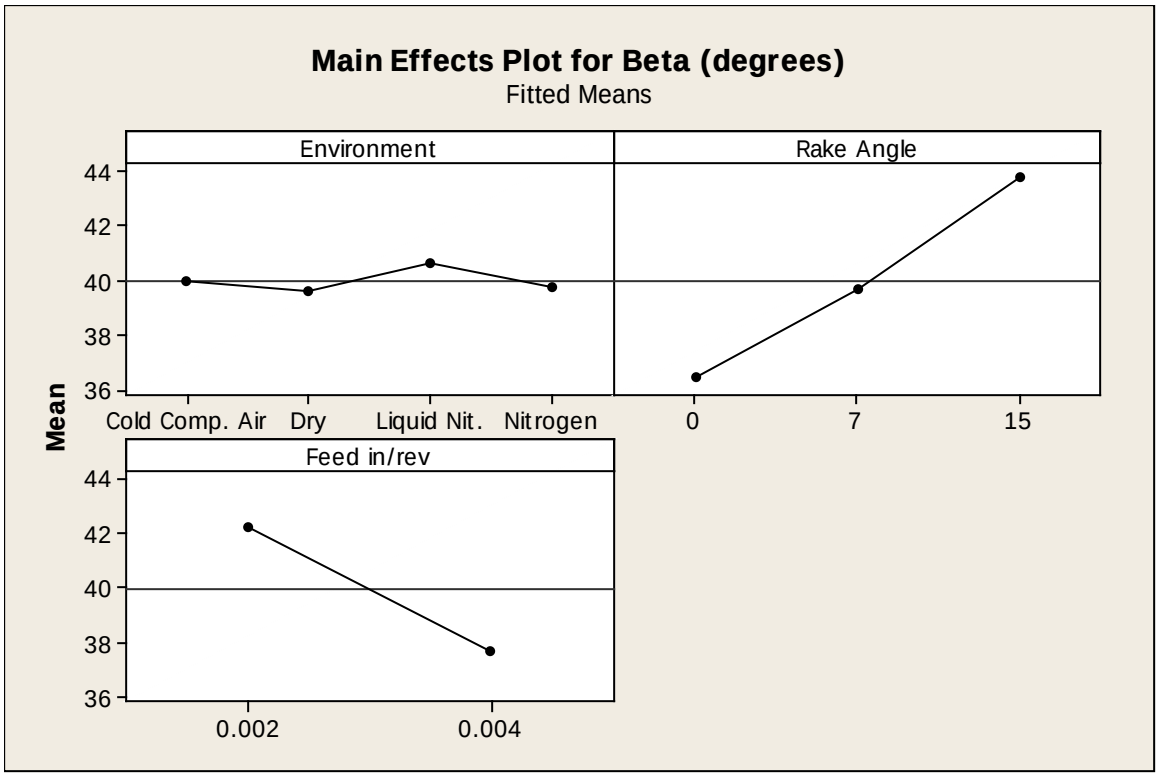
Main Effects Plot for Beta (degrees)
Fitted Means
Environment
Rake Angle
Feed in/rev
Mean
44
42
40
38
36
Cold Comp. Air
Dry
Liquid Nit.
Nitrogen
0
7
15
0.002
0.004

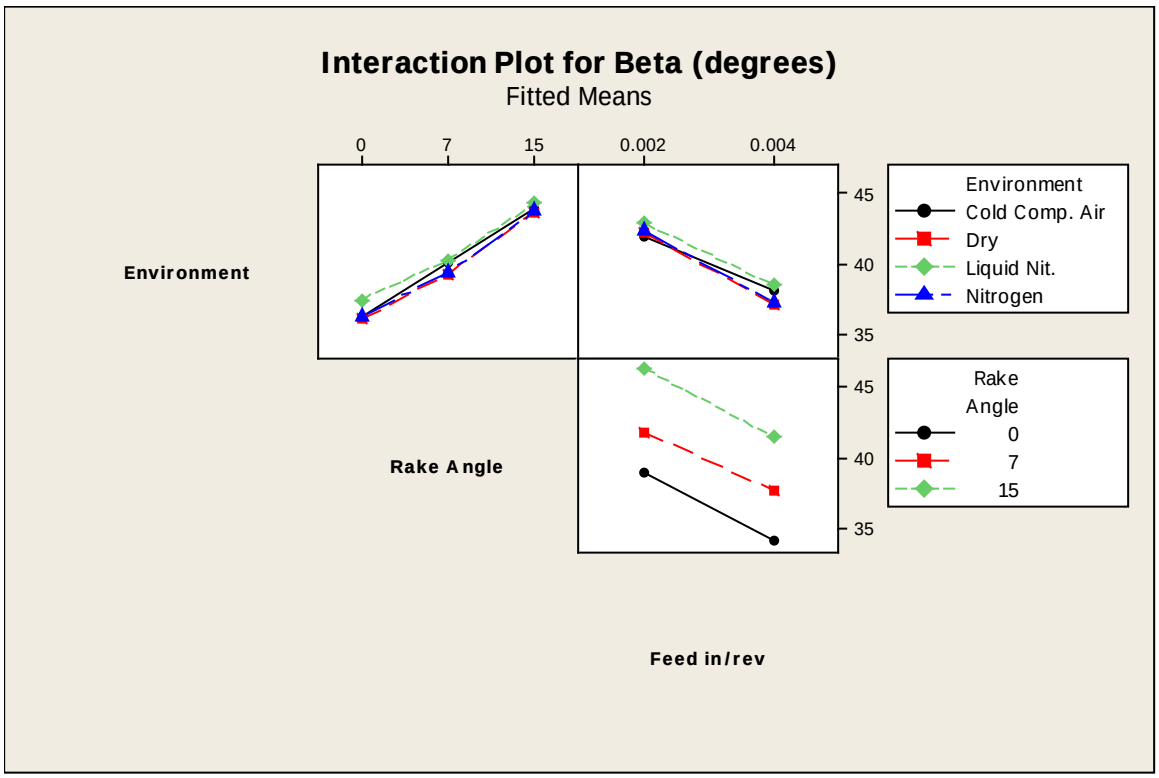
Interaction Plot for Beta (degrees)
Fitted Means
0
7
15
0.002
0.004
Environment
Rake Angle
Feed in/rev
45
40
35
Environment
Cold Comp. Air
Dry
Liquid Nit.
Nitrogen
Rake Angle
0
7
15

Analysis of Variance for **Shear Area**, As, using Adjusted SS for Tests

Source	DF	Seq SS	Adj SS	Adj MS	F
Environment	3	0.0000016	0.0000016	0.0000005	0.42
Rake Angle	2	0.0000047	0.0000047	0.0000024	1.87
Feed in/rev	1	0.0000182	0.0000182	0.0000182	14.38
Environment*Rake Angle	6	0.0000083	0.0000083	0.0000014	1.09
Environment*Feed in/rev	3	0.0000028	0.0000028	0.0000009	0.72
Rake Angle*Feed in/rev	2	0.0000024	0.0000024	0.0000012	0.96
Environment*Rake Angle*Feed in/rev	6	0.0000080	0.0000080	0.0000013	1.05
Error	72	0.0000912	0.0000912	0.0000013	
Total	95	0.0001372			

Source	P
Environment	0.740
Rake Angle	0.161
Feed in/rev	0.000
Environment*Rake Angle	0.375
Environment*Feed in/rev	0.541
Rake Angle*Feed in/rev	0.387
Environment*Rake Angle*Feed in/rev	0.403
Error	
Total	

S = 0.00112548 R-Sq = 33.53% R-Sq(adj) = 12.29%

Unusual Observations for Shear Area, As

Obs	Shear Area, As	Fit	SE Fit	Residual	St Resid
61	0.001191	0.003993	0.000563	-0.002802	-2.87 R
62	0.012262	0.003993	0.000563	0.008269	8.48 R
63	0.001254	0.003993	0.000563	-0.002739	-2.81 R
64	0.001265	0.003993	0.000563	-0.002728	-2.80 R

R denotes an observation with a large standardized residual.

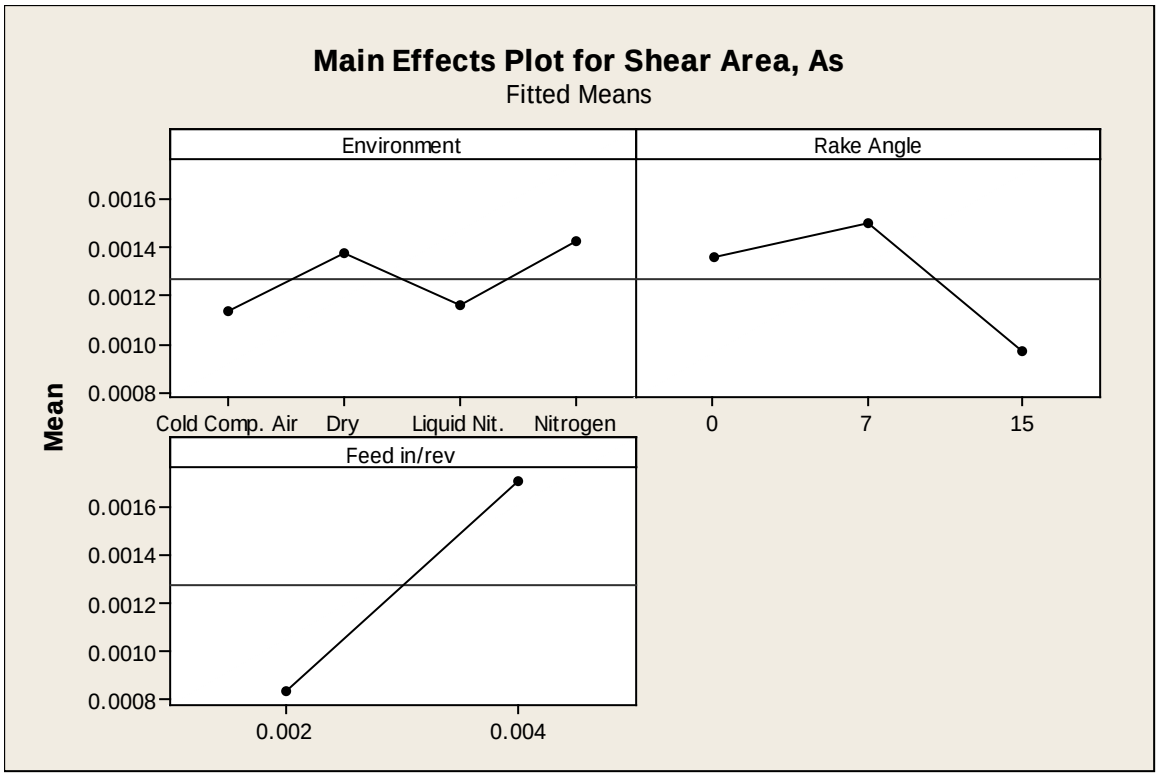
Main Effects Plot for Shear Area, As
Fitted Means
Environment
Rake Angle
Feed in/rev
Mean
0.0016
0.0014
0.0012
0.0010
0.0008
Cold Comp. Air
Dry
Liquid Nit.
Nitrogen
0
7
15
0.002
0.004

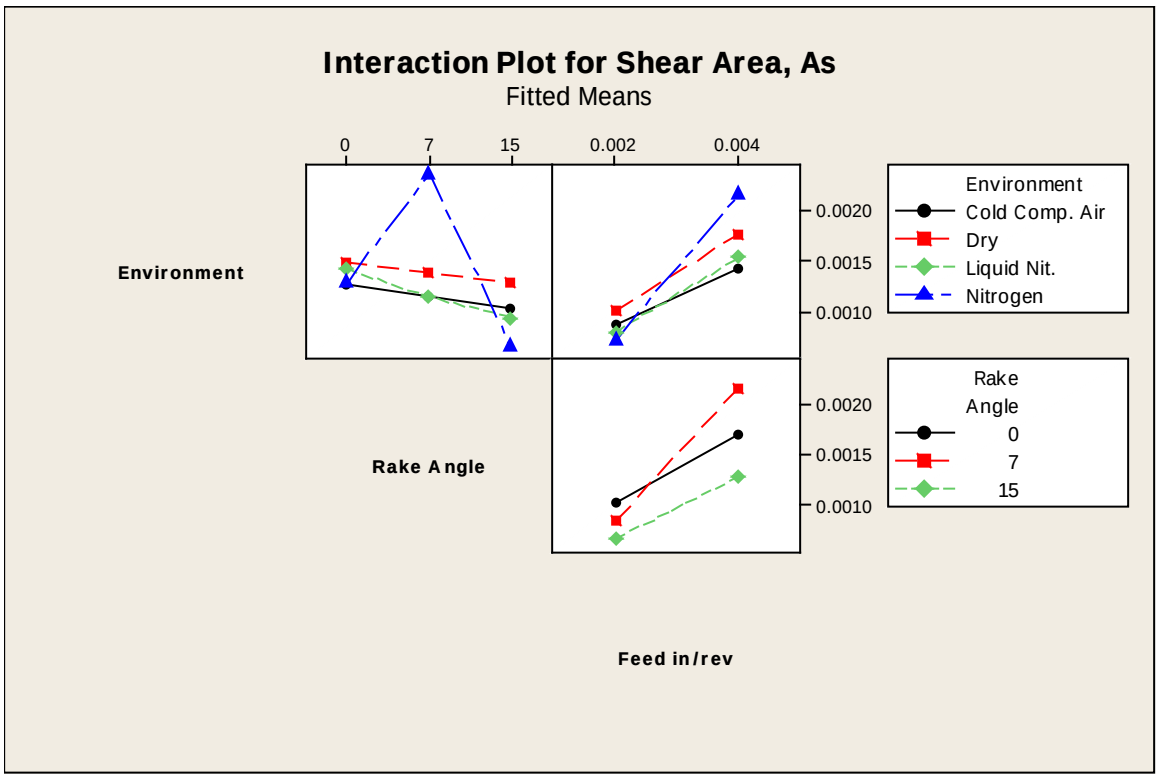
Interaction Plot for Shear Area, As
Fitted Means
Environment
Rake Angle
Feed in/rev
0
7
15
0.002
0.004
0.0020
0.0015
0.0010
Environment
Cold Comp. Air
Dry
Liquid Nit.
Nitrogen
Rake Angle
0
7
15

Analysis of Variance for **Shear Stress, Ts Merchant** (Mpa), using Adjusted SS for Tests

Source	DF	Seq SS	Adj SS	Adj MS	F
Environment	3	31425.5	31425.5	10475.2	18.50
Rake Angle	2	13862.6	13862.6	6931.3	12.24
Feed in/rev	1	13699.2	13699.2	13699.2	24.19
Environment*Rake Angle	6	8849.1	8849.1	1474.9	2.60
Environment*Feed in/rev	3	3478.9	3478.9	1159.6	2.05
Rake Angle*Feed in/rev	2	1475.3	1475.3	737.6	1.30
Environment*Rake Angle*Feed in/rev	6	5793.7	5793.7	965.6	1.71
Error	72	40774.3	40774.3	566.3	
Total	95	119358.6			

Source	P
Environment	0.000
Rake Angle	0.000
Feed in/rev	0.000
Environment*Rake Angle	0.024
Environment*Feed in/rev	0.115
Rake Angle*Feed in/rev	0.278
Environment*Rake Angle*Feed in/rev	0.132
Error	
Total	

S = 23.7973 R-Sq = 65.84% R-Sq(adj) = 54.93%

Unusual Observations for Shear Stress, Ts Merchant (Mpa)

Obs	Shear Stress, Ts Merchant (Mpa)	Fit	SE Fit	Residual	St Resid
61	268.099	207.885	11.899	60.214	2.92 R
62	37.365	207.885	11.899	-170.520	-8.27 R
63	263.826	207.885	11.899	55.941	2.71 R
64	262.250	207.885	11.899	54.365	2.64 R

R denotes an observation with a large standardized residual.

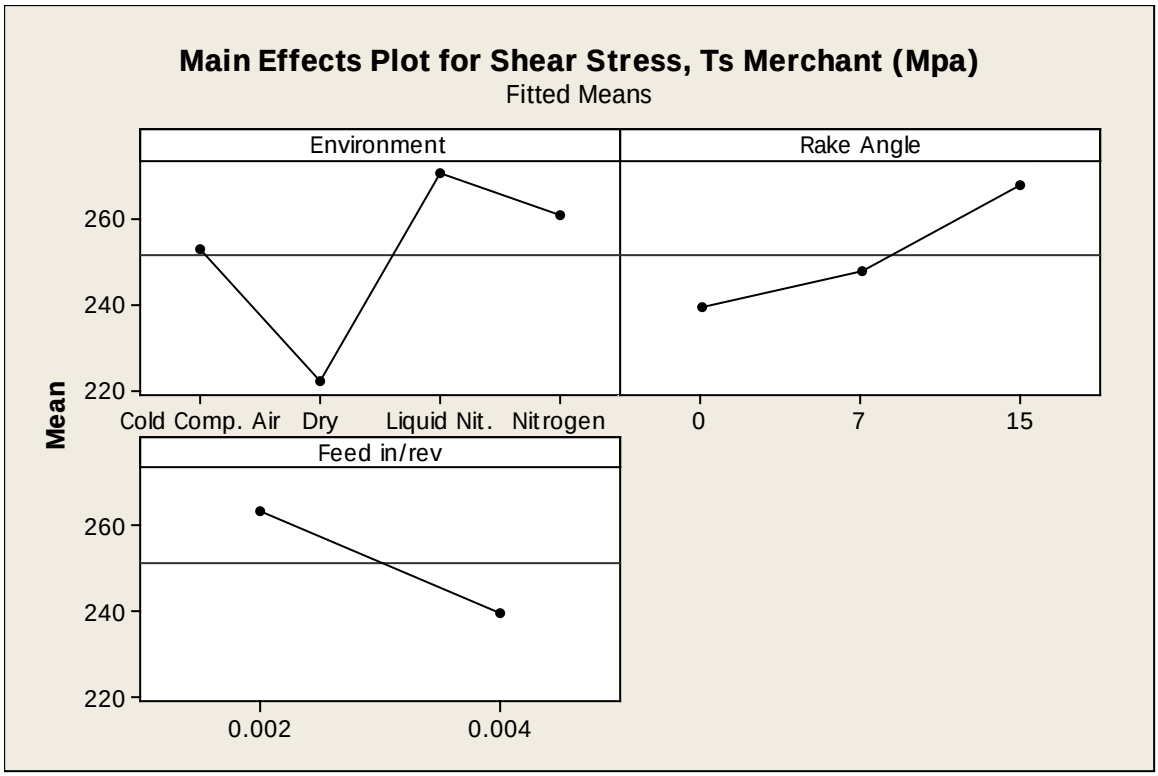
Main Effects Plot for Shear Stress, Ts Merchant (Mpa)
Fitted Means
Environment
Rake Angle
Feed in/rev
Mean
260
240
220
Cold Comp. Air
Dry
Liquid Nit.
Nitrogen
0
7
15
0.002
0.004

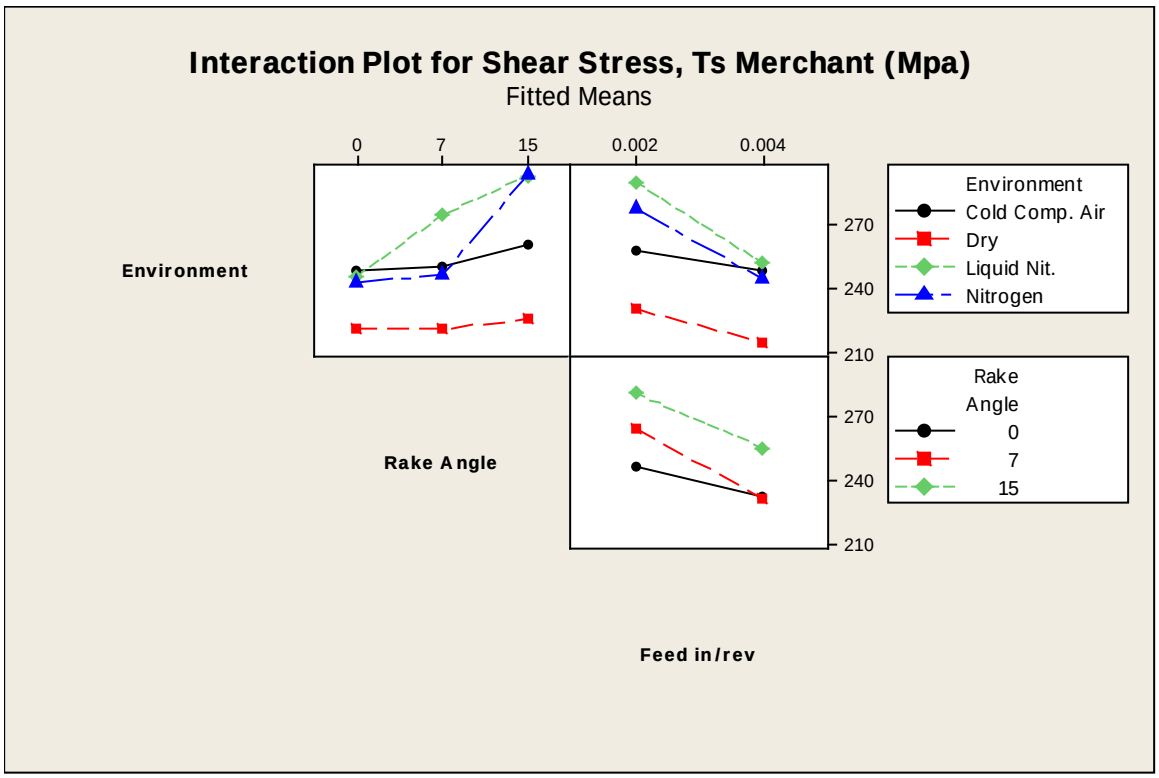
Interaction Plot for Shear Stress, Ts Merchant (Mpa)
Fitted Means
Environment
Rake Angle
Feed in/rev
0
7
15
0.002
0.004
270
240
210
Environment
Cold Comp. Air
Dry
Liquid Nit.
Nitrogen
Rake Angle
0
7
15

Analysis of Variance for **Shear Stress, Ts (Payton)** (Mpa), using Adjusted SS for
Tests

Source	DF	Seq SS	Adj SS	Adj MS	F
Environment	3	5926.9	5926.9	1975.6	23.56
Rake Angle	2	2067.5	2067.5	1033.7	12.33
Feed in/rev	1	12344.6	12344.6	12344.6	147.20
Environment*Rake Angle	6	5025.9	5025.9	837.6	9.99
Environment*Feed in/rev	3	210.5	210.5	70.2	0.84
Rake Angle*Feed in/rev	2	336.5	336.5	168.3	2.01
Environment*Rake Angle*Feed in/rev	6	748.5	748.5	124.7	1.49
Error	72	6038.2	6038.2	83.9	
Total	95	32698.6			

Source	P
Environment	0.000
Rake Angle	0.000
Feed in/rev	0.000
Environment*Rake Angle	0.000
Environment*Feed in/rev	0.478
Rake Angle*Feed in/rev	0.142
Environment*Rake Angle*Feed in/rev	0.195
Error	
Total	

S = 9.15771 R-Sq = 81.53% R-Sq(adj) = 75.63%

Unusual Observations for Shear Stress, Ts (Payton) (Mpa)

Obs	Shear Stress, Ts (Payton) (Mpa)	Fit	SE Fit	Residual	St Resid
47	49.618	69.972	4.579	-20.353	-2.57 R
61	92.173	68.157	4.579	24.016	3.03 R
62	8.702	68.157	4.579	-59.455	-7.50 R
63	86.904	68.157	4.579	18.747	2.36 R
64	84.850	68.157	4.579	16.693	2.10 R

R denotes an observation with a large standardized residual.

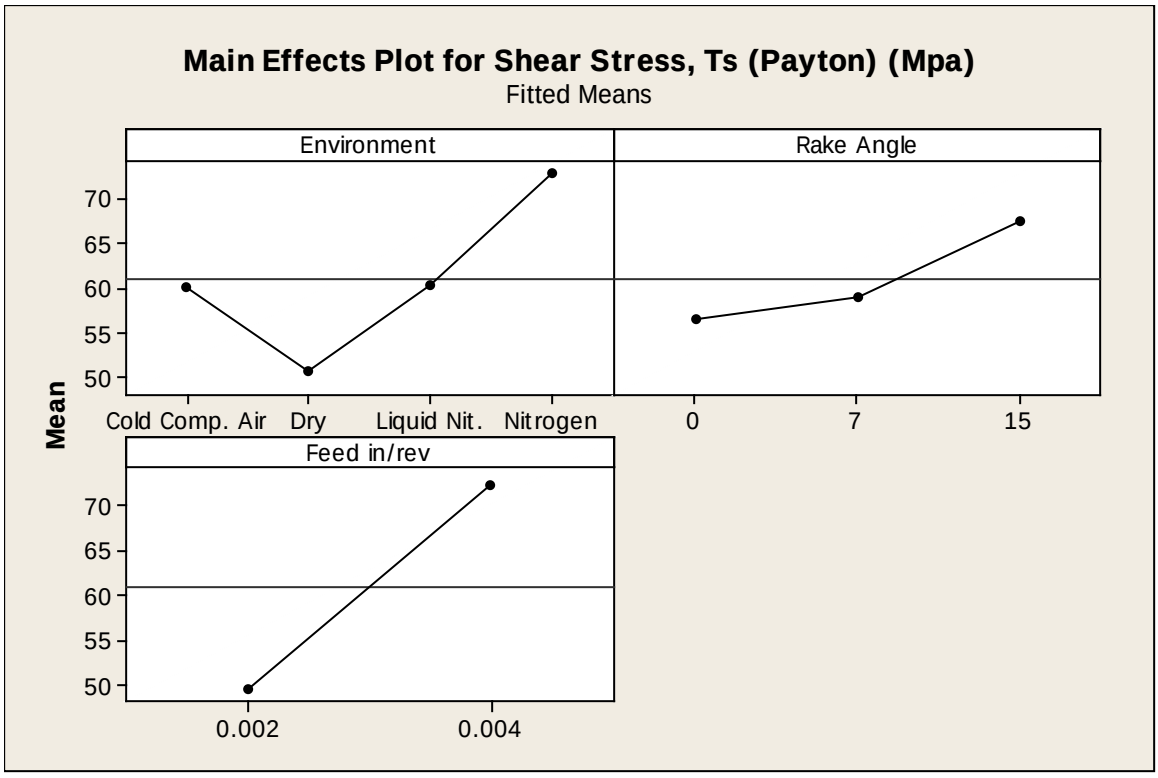
Main Effects Plot for Shear Stress, Ts (Payton) (Mpa)
Fitted Means
Environment
Rake Angle
Feed in/rev
Mean
70
65
60
55
50
Cold Comp. Air
Dry
Liquid Nit.
Nitrogen
0
7
15
0.002
0.004

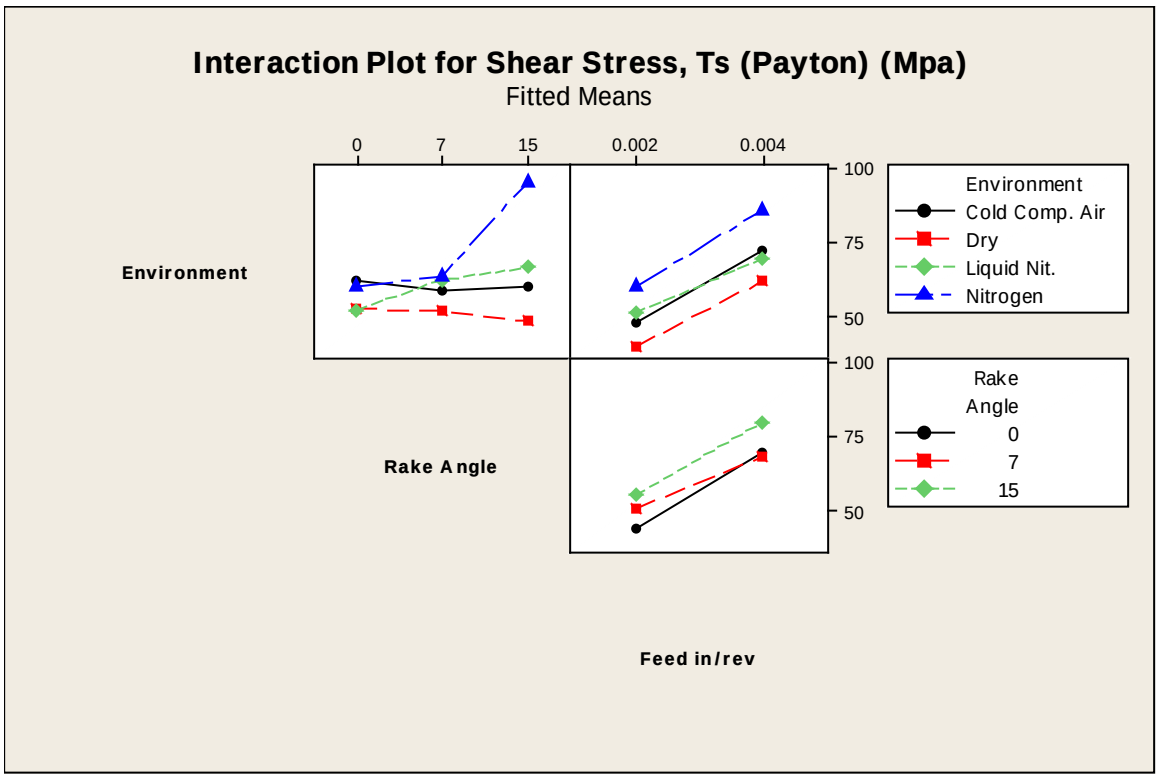
Interaction Plot for Shear Stress, Ts (Payton) (Mpa)
Fitted Means
Environment
Rake Angle
Feed in/rev
0
7
15
0.002
0.004
100
75
50
Environment
Cold Comp. Air
Dry
Liquid Nit.
Nitrogen
Rake Angle
0
7
15

Analysis of Variance for **Friction Co-efficient**, using Adjusted SS for Tests

Source	DF	Seq SS	Adj SS	Adj MS	F
Environment	3	0.004452	0.004452	0.001484	13.42
Rake Angle	2	0.268778	0.268778	0.134389	1215.27
Feed in/rev	1	0.154088	0.154088	0.154088	1393.41
Environment*Rake Angle	6	0.000956	0.000956	0.000159	1.44
Environment*Feed in/rev	3	0.001915	0.001915	0.000638	5.77
Rake Angle*Feed in/rev	2	0.000668	0.000668	0.000334	3.02
Environment*Rake Angle*Feed in/rev	6	0.002272	0.002272	0.000379	3.42
Error	72	0.007962	0.007962	0.000111	
Total	95	0.441090			

Source	P
Environment	0.000
Rake Angle	0.000
Feed in/rev	0.000
Environment*Rake Angle	0.211
Environment*Feed in/rev	0.001
Rake Angle*Feed in/rev	0.055
Environment*Rake Angle*Feed in/rev	0.005
Error	
Total	

S = 0.0105159 R-Sq = 98.19% R-Sq(adj) = 97.62%

Unusual Observations for Friction Co-efficient

Obs	Friction Co-efficient	Fit	SE Fit	Residual	St Resid	
37	0.696084	0.671121	0.005258	0.024963	2.74	R
38	0.647501	0.671121	0.005258	-0.023620	-2.59	R
45	0.715111	0.734129	0.005258	-0.019019	-2.09	R
47	0.780714	0.734129	0.005258	0.046585	5.12	R
92	0.842354	0.821171	0.005258	0.021182	2.33	R

R denotes an observation with a large standardized residual.

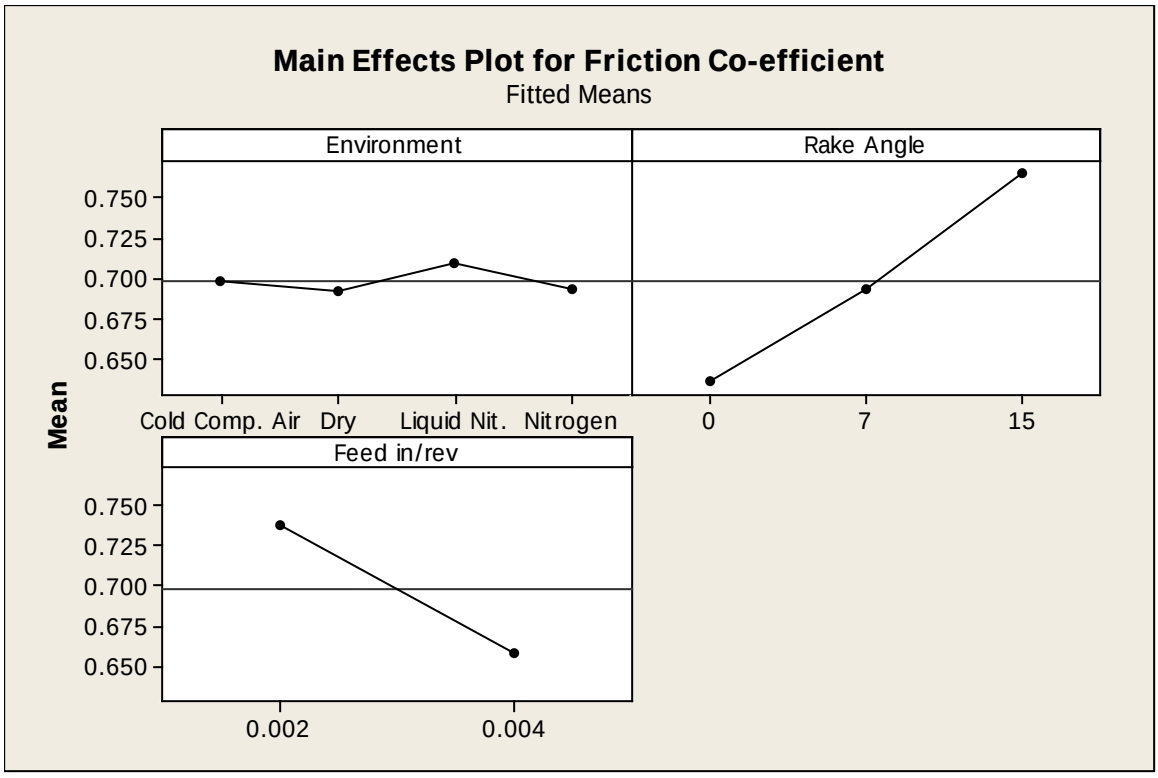
Main Effects Plot for Friction Co-efficient
Fitted Means
Environment
Rake Angle
Feed in/rev
Mean
0.750
0.725
0.700
0.675
0.650
Cold Comp. Air
Dry
Liquid Nit.
Nitrogen
0
7
15
0.002
0.004

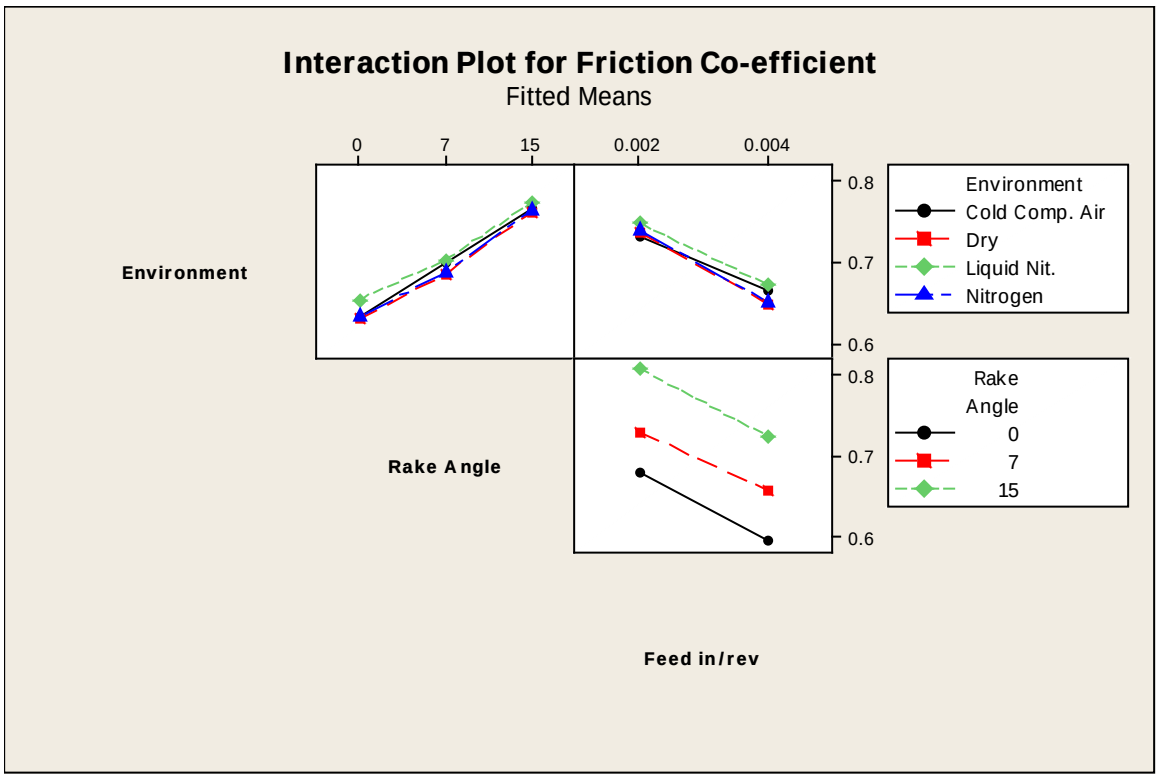
Interaction Plot for Friction Co-efficient
Fitted Means
Environment
Rake Angle
Feed in/rev
0
7
15
0.002
0.004
0.8
0.7
0.6
Environment
Cold Comp. Air
Dry
Liquid Nit.
Nitrogen
Rake Angle
0
7
15

Analysis of Variance for **Normal Stress (Merchant)**, using Adjusted SS for Tests

Source	DF	Seq SS	Adj SS	Adj MS
Environment	3	1.45784E+11	1.45784E+11	48594519489
Rake Angle	2	42968195302	42968195302	21484097651
Feed in/rev	1	48085604921	48085604921	48085604921
Environment*Rake Angle	6	1.11976E+11	1.11976E+11	18662743985
Environment*Feed in/rev	3	17725494158	17725494158	5908498053
Rake Angle*Feed in/rev	2	8492230746	8492230746	4246115373
Environment*Rake Angle*Feed in/rev	6	14394797554	14394797554	2399132926
Error	72	37192610473	37192610473	516564034
Total	95	4.26619E+11		

Source	F	P
Environment	94.07	0.000
Rake Angle	41.59	0.000
Feed in/rev	93.09	0.000
Environment*Rake Angle	36.13	0.000
Environment*Feed in/rev	11.44	0.000
Rake Angle*Feed in/rev	8.22	0.001
Environment*Rake Angle*Feed in/rev	4.64	0.000
Error		
Total		

S = 22728.0 R-Sq = 91.28% R-Sq(adj) = 88.50%

Unusual Observations for Normal Stress (Merchant)

Obs	Normal Stress (Merchant)	Fit	SE Fit	Residual	St Resid	
61	233443	172460	11364	60983	3.10	R
62	15300	172460	11364	-157160	-7.98	R
63	221215	172460	11364	48754	2.48	R
64	219882	172460	11364	47422	2.41	R

R denotes an observation with a large standardized residual.

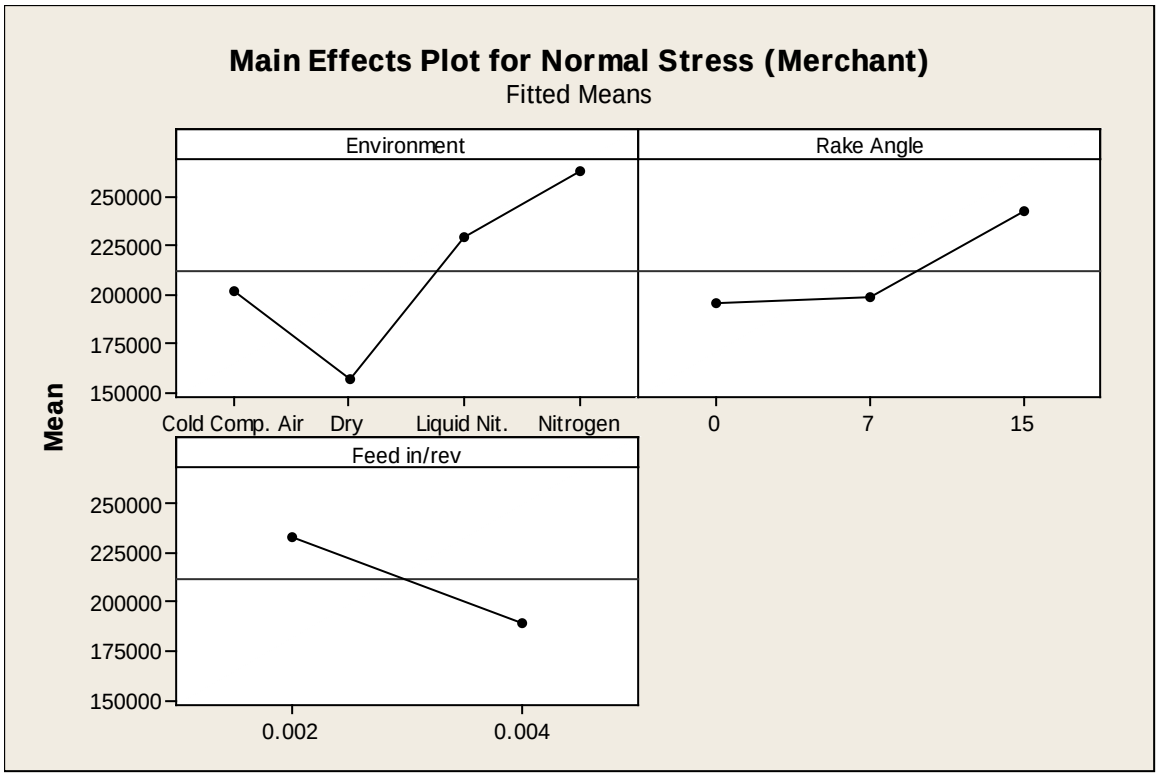
Main Effects Plot for Normal Stress (Merchant)
Fitted Means
Environment
Rake Angle
Feed in/rev
Mean
250000
225000
200000
175000
150000
Cold Comp. Air
Dry
Liquid Nit.
Nitrogen
0
7
15
0.002
0.004

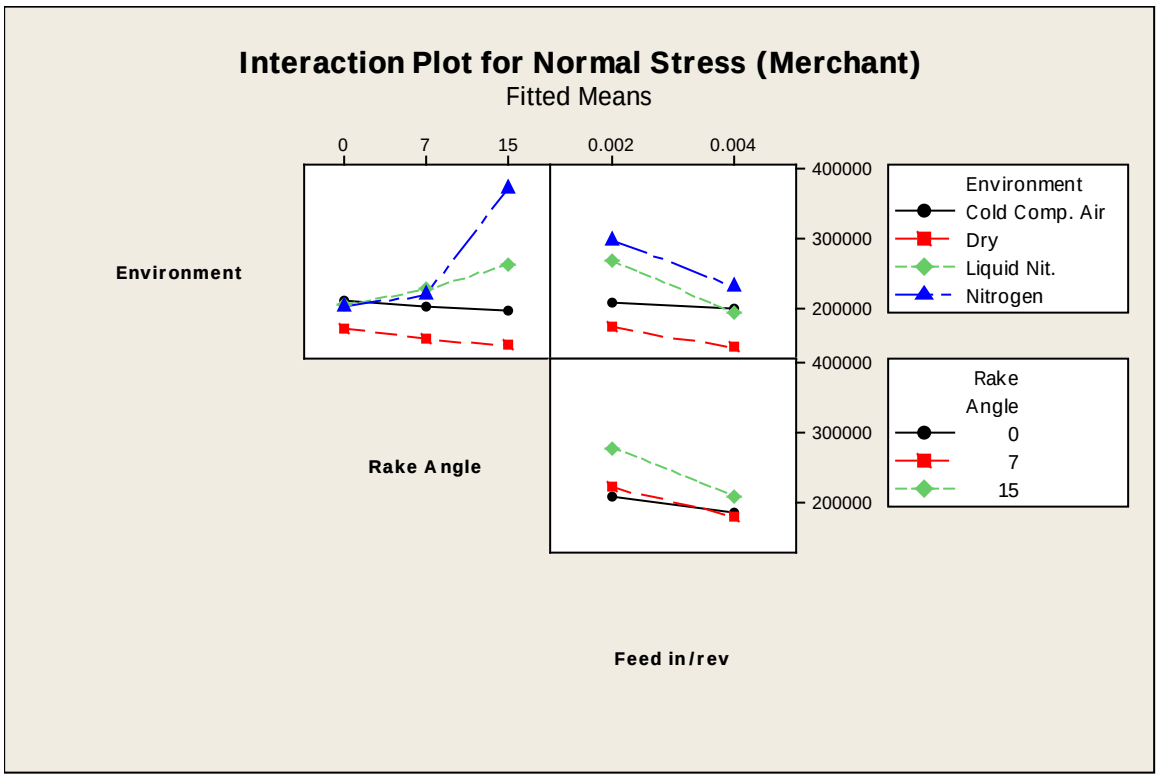
Interaction Plot for Normal Stress (Merchant)
Fitted Means
Environment
Rake Angle
Feed in/rev
0
7
15
0.002
0.004
400000
300000
200000
Environment
Cold Comp. Air
Dry
Liquid Nit.
Nitrogen
Rake Angle
0
7
15

Analysis of Variance for **Shear strain (Merchant)**, using Adjusted SS for Tests

Source	DF	Seq SS	Adj SS	Adj MS	F	P
Environment	3	7.851	7.851	2.617	0.48	0.695
Rake Angle	2	39.764	39.764	19.882	3.67	0.030
Feed in/rev	1	0.173	0.173	0.173	0.03	0.859
Environment*Rake Angle	6	36.322	36.322	6.054	1.12	0.360
Environment*Feed in/rev	3	17.830	17.830	5.943	1.10	0.355
Rake Angle*Feed in/rev	2	11.846	11.846	5.923	1.09	0.340
Environment*Rake Angle*Feed in/rev	6	34.641	34.641	5.774	1.07	0.390
Error	72	389.532	389.532	5.410		
Total	95	537.959				

S = 2.32598 R-Sq = 27.59% R-Sq(adj) = 4.46%

Unusual Observations for Shear strain (Merchant)

Obs	Shear strain (Merchant)	Fit	SE Fit	Residual	St Resid	
61	2.5715	8.3542	1.1630	-5.7827	-2.87	R
62	25.4434	8.3542	1.1630	17.0892	8.48	R
63	2.6903	8.3542	1.1630	-5.6639	-2.81	R
64	2.7116	8.3542	1.1630	-5.6426	-2.80	R

R denotes an observation with a large standardized residual.

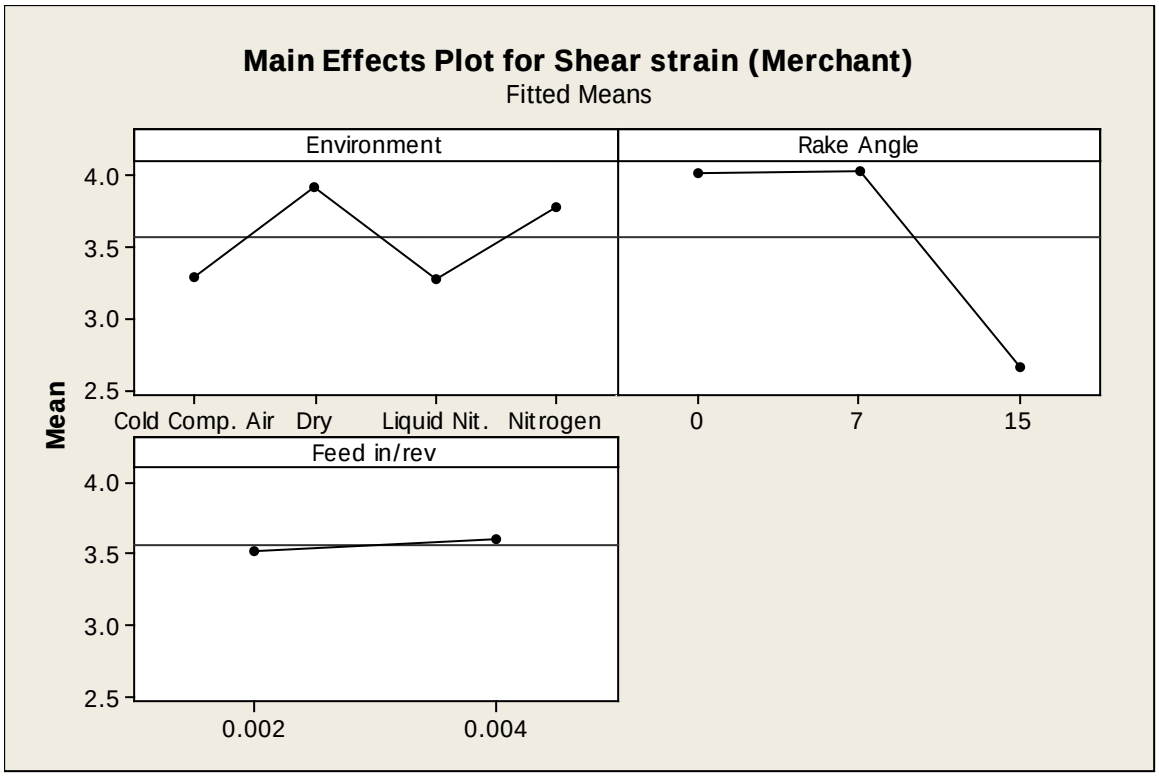
Main Effects Plot for Shear strain (Merchant)
Fitted Means
Environment
Rake Angle
Feed in/rev
Mean
4.0
3.5
3.0
2.5
Cold Comp. Air
Dry
Liquid Nit.
Nitrogen
0
7
15
0.002
0.004

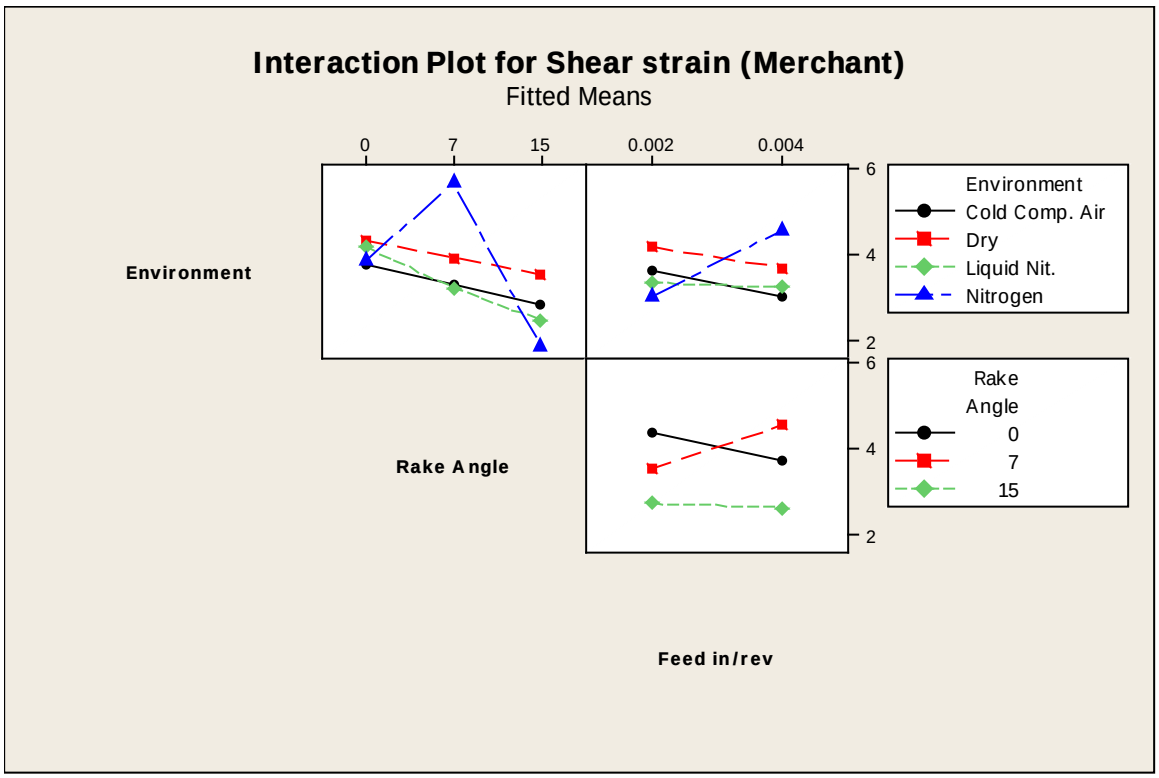
Interaction Plot for Shear strain (Merchant)
Fitted Means
0
7
15
0.002
0.004
Environment
Rake Angle
6
4
2
Environment
Cold Comp. Air
Dry
Liquid Nit.
Nitrogen
Rake Angle
0
7
15
Feed in/rev

Analysis of Variance for **Normal Stress (Payton)**, using Adjusted SS for Tests

Source	DF	Seq SS	Adj SS	Adj MS
Environment	3	1.33259E+11	1.33259E+11	44419610932
Rake Angle	2	47914531844	47914531844	23957265922
Feed in/rev	1	55495851760	55495851760	55495851760
Environment*Rake Angle	6	93498820934	93498820934	15583136822
Environment*Feed in/rev	3	17678845553	17678845553	5892948518
Rake Angle*Feed in/rev	2	7521109068	7521109068	3760554534
Environment*Rake Angle*Feed in/rev	6	14181206518	14181206518	2363534420
Error	72	50663299631	50663299631	703656939
Total	95	4.20212E+11		

Source	F	P
Environment	63.13	0.000
Rake Angle	34.05	0.000
Feed in/rev	78.87	0.000
Environment*Rake Angle	22.15	0.000
Environment*Feed in/rev	8.37	0.000
Rake Angle*Feed in/rev	5.34	0.007
Environment*Rake Angle*Feed in/rev	3.36	0.006
Error		
Total		

S = 26526.5 R-Sq = 87.94% R-Sq(adj) = 84.09%

Unusual Observations for Narmal Stress (Payton)

Obs	Narmal Stress (Payton)	Fit	SE Fit	Residual	St Resid	
61	284389	214450	13263	69938	3.04	R
62	27995	214450	13263	-186456	-8.12	R
63	273430	214450	13263	58979	2.57	R
64	271989	214450	13263	57538	2.50	R

R denotes an observation with a large standardized residual.

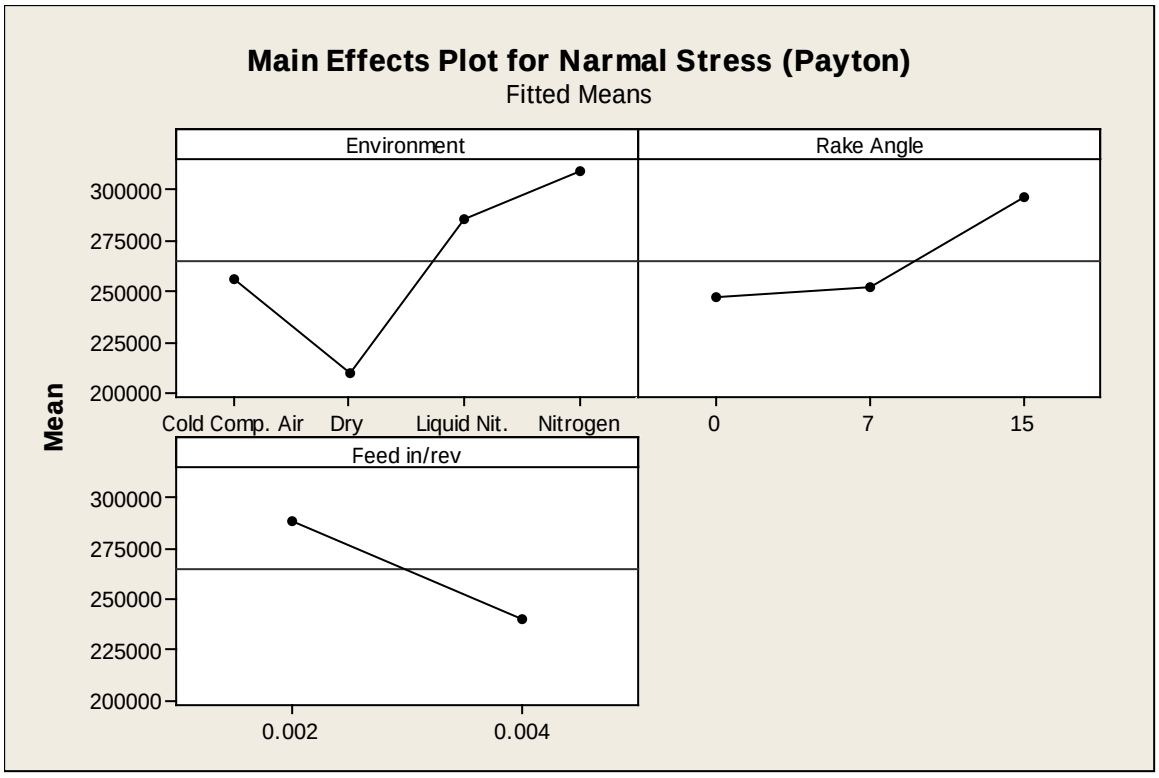
Main Effects Plot for Narmal Stress (Payton)
Fitted Means
Environment
Rake Angle
Feed in/rev
Mean
300000
275000
250000
225000
200000
Cold Comp. Air
Dry
Liquid Nit.
Nitrogen
0
7
15
0.002
0.004

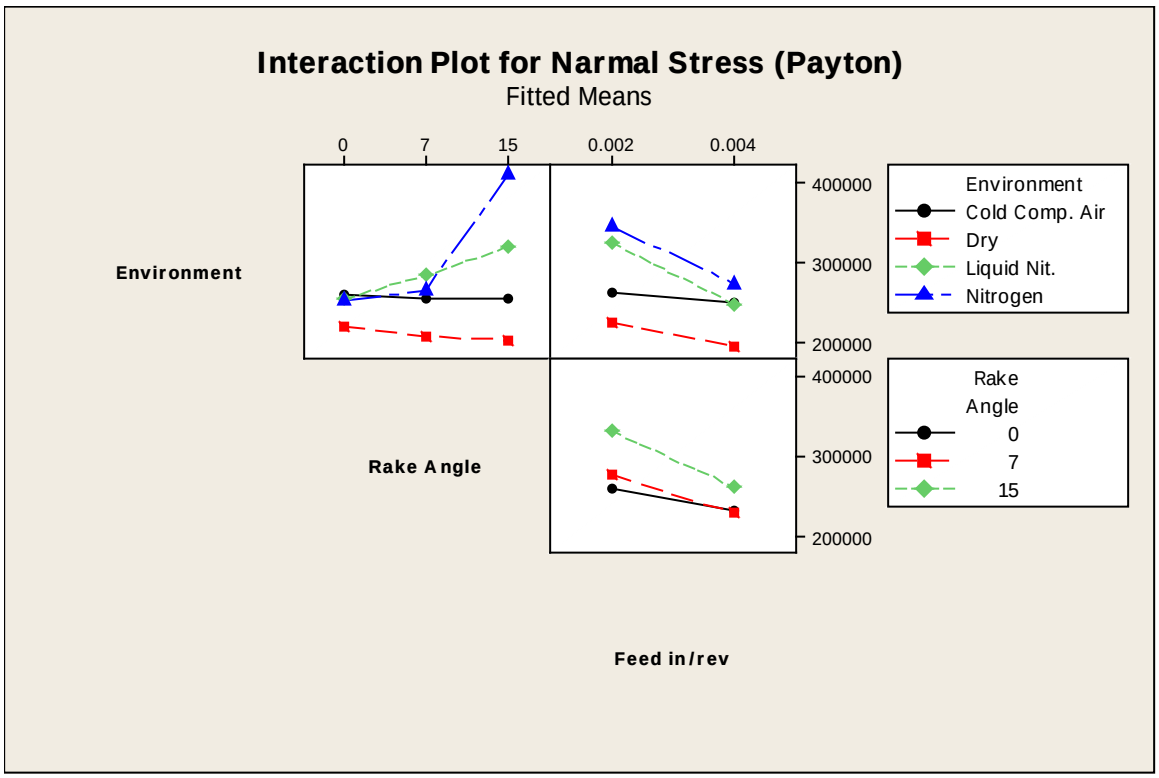
Interaction Plot for Narmal Stress (Payton)
Fitted Means
Environment
Rake Angle
Feed in/rev
0
7
15
0.002
0.004
400000
300000
200000
Environment
Cold Comp. Air
Dry
Liquid Nit.
Nitrogen
Rake Angle
0
7
15

Analysis of Variance for **Shear strain (Payton)**, using Adjusted SS for Tests

Source	DF	Seq SS	Adj SS	Adj MS	F	P
Environment	3	0.00000	0.00000	0.00000	**	
Rake Angle	2	3.46485	3.46485	1.73242	**	
Feed in/rev	1	0.00000	0.00000	0.00000	**	
Environment*Rake Angle	6	0.00000	0.00000	0.00000	**	
Environment*Feed in/rev	3	0.00000	0.00000	0.00000	**	
Rake Angle*Feed in/rev	2	0.00000	0.00000	0.00000	**	
Environment*Rake Angle*Feed in/rev	6	0.00000	0.00000	0.00000	**	
Error	72	0.00000	0.00000	0.00000		
Total	95	3.46485				

** Denominator of F-test is zero.

S = 8.576051E-17 R-Sq = 100.00% R-Sq(adj) = 100.00%

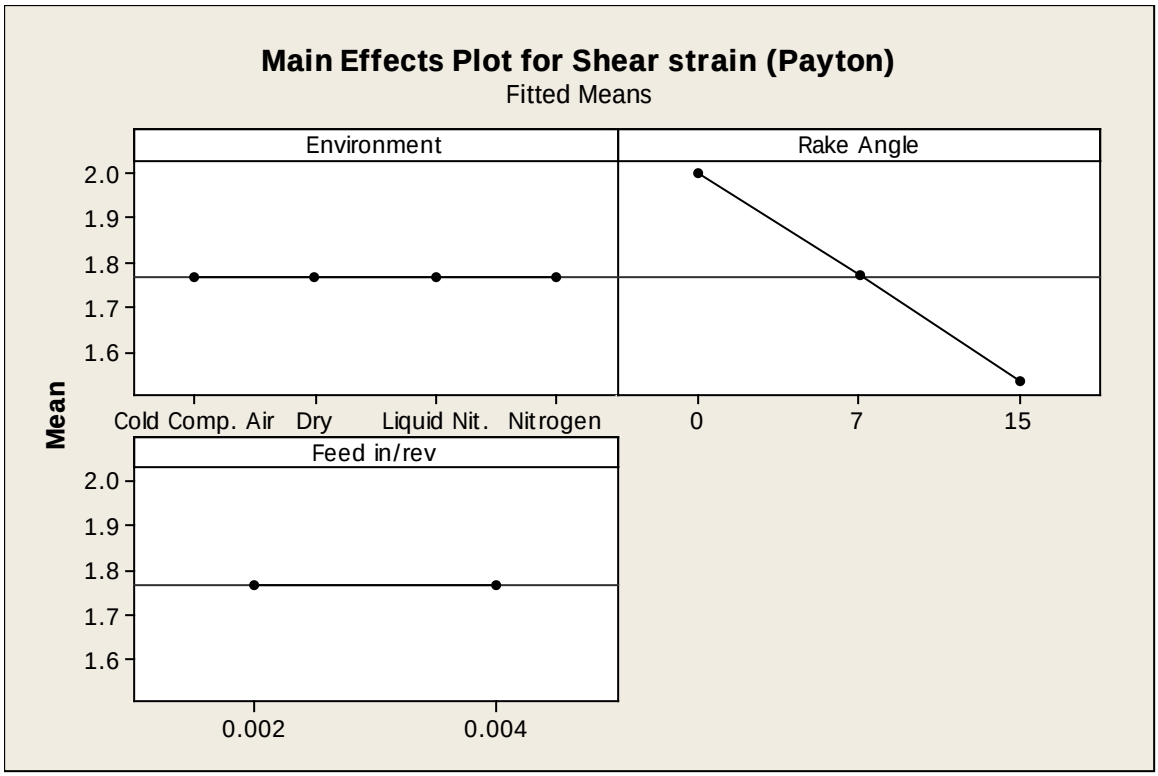
Main Effects Plot for Shear strain (Payton)
Fitted Means
Environment
Rake Angle
Feed in/rev
Mean
2.0
1.9
1.8
1.7
1.6
Cold Comp. Air
Dry
Liquid Nit.
Nitrogen
0
7
15
0.002
0.004

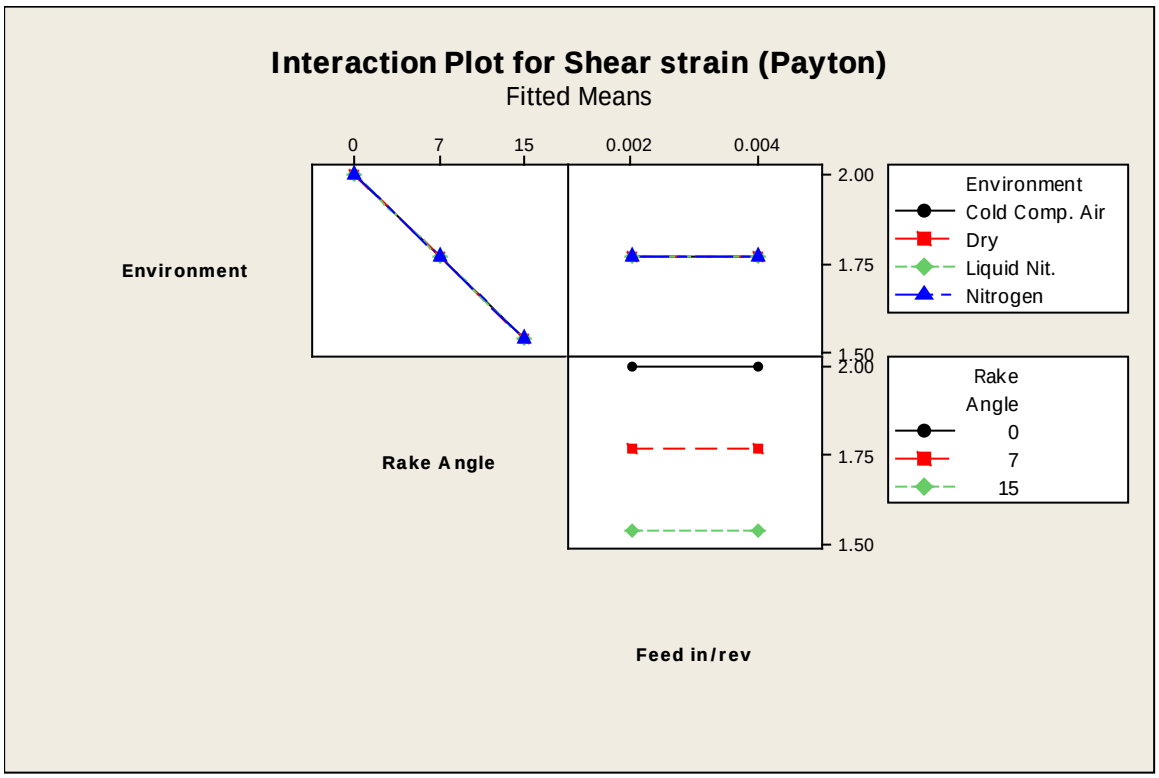
Interaction Plot for Shear strain (Payton)
Fitted Means
Environment
Rake Angle
Feed in/rev
0
7
15
0.002
0.004
2.00
1.75
1.50
Environment
Cold Comp. Air
Dry
Liquid Nit.
Nitrogen
Rake Angle
0
7
15

Analysis of Variance for **Shear Stress, Ts (Payton) corre**, using Adjusted SS for
Tests

Source	DF	Seq SS	Adj SS	Adj MS	F
Environment	3	4513.67	4513.67	1504.56	28.97
Rake Angle	2	2993.38	2993.38	1496.69	28.81
Feed in/rev	1	7583.05	7583.05	7583.05	145.99
Environment*Rake Angle	6	4019.60	4019.60	669.93	12.90
Environment*Feed in/rev	3	174.97	174.97	58.32	1.12
Rake Angle*Feed in/rev	2	200.99	200.99	100.50	1.93
Environment*Rake Angle*Feed in/rev	6	514.83	514.83	85.80	1.65
Error	72	3739.95	3739.95	51.94	
Total	95	23740.44			

Source	P
Environment	0.000
Rake Angle	0.000
Feed in/rev	0.000
Environment*Rake Angle	0.000
Environment*Feed in/rev	0.346
Rake Angle*Feed in/rev	0.152
Environment*Rake Angle*Feed in/rev	0.145
Error	
Total	

S = 7.20720 R-Sq = 84.25% R-Sq(adj) = 79.21%

Unusual Observations for Shear Stress, Ts (Payton) corre

Obs	Shear Stress, Ts (Payton) corre	Fit	SE Fit	Residual	St Resid
47	39.580	55.941	3.604	-16.361	-2.62 R
61	72.102	53.018	3.604	19.083	3.06 R
62	6.540	53.018	3.604	-46.479	-7.45 R
63	67.548	53.018	3.604	14.529	2.33 R
64	65.884	53.018	3.604	12.866	2.06 R

R denotes an observation with a large standardized residual.

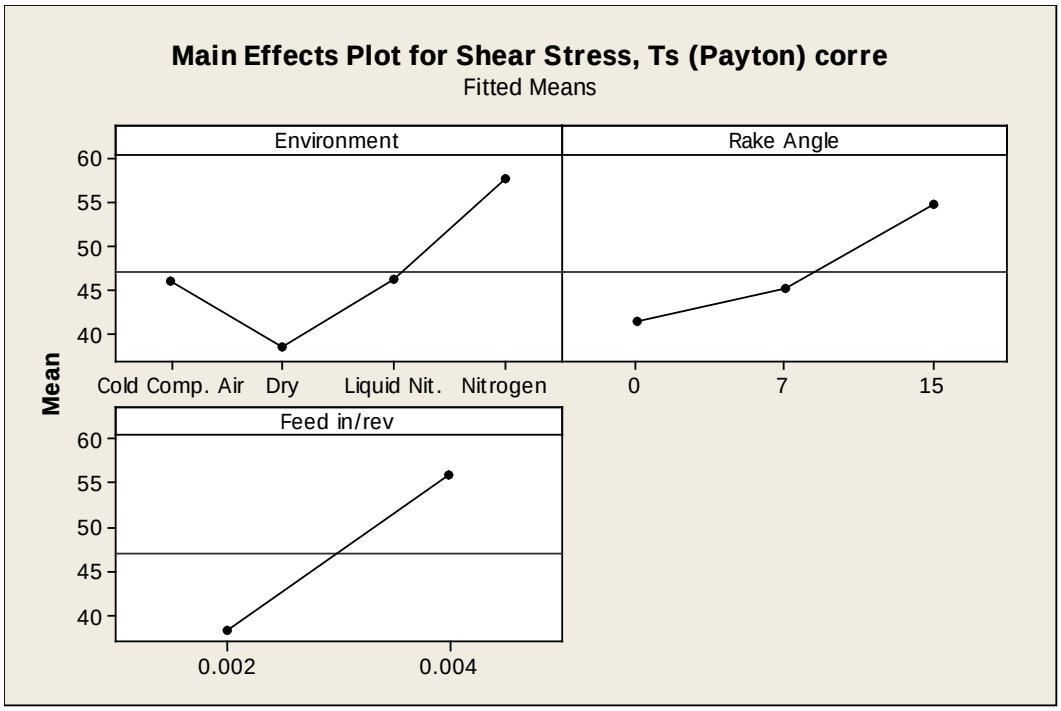
Main Effects Plot for Shear Stress, Ts (Payton) corre
Fitted Means
Environment
Rake Angle
Feed in/rev
Mean
60
55
50
45
40
Cold Comp. Air
Dry
Liquid Nit.
Nitrogen
0
7
15
0.002
0.004

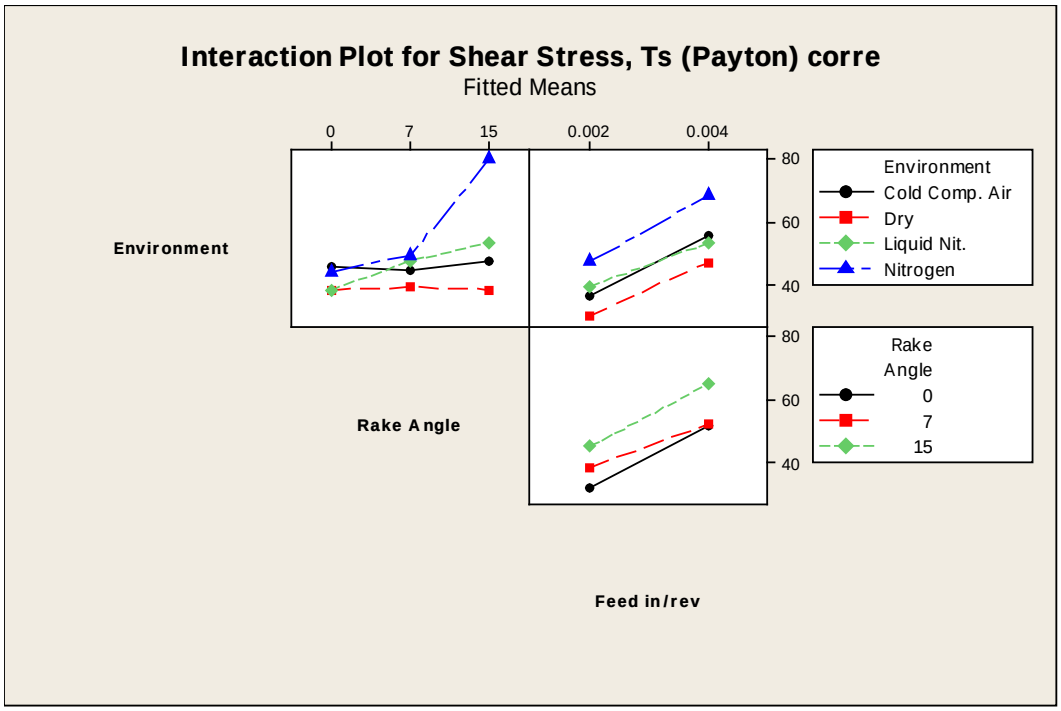
Interaction Plot for Shear Stress, Ts (Payton) corre
Fitted Means
Environment
Rake Angle
Feed in/rev
0
7
15
0.002
0.004
80
60
40
Environment
Cold Comp. Air
Dry
Liquid Nit.
Nitrogen
Rake Angle
0
7
15

Analysis of Variance for **Shear Area, As P**, using Adjusted SS for Tests

Source	DF	Seq SS	Adj SS	Adj MS	F
Environment	3	0.0000028	0.0000028	0.0000009	0.41
Rake Angle	2	0.0000107	0.0000107	0.0000053	2.36
Feed in/rev	1	0.0000308	0.0000308	0.0000308	13.64
Environment*Rake Angle	6	0.0000147	0.0000147	0.0000024	1.08
Environment*Feed in/rev	3	0.0000048	0.0000048	0.0000016	0.71
Rake Angle*Feed in/rev	2	0.0000044	0.0000044	0.0000022	0.98
Environment*Rake Angle*Feed in/rev	6	0.0000142	0.0000142	0.0000024	1.05
Error	72	0.0001627	0.0001627	0.0000023	
Total	95	0.0002451			

Source	P
Environment	0.745
Rake Angle	0.102
Feed in/rev	0.000
Environment*Rake Angle	0.381
Environment*Feed in/rev	0.548
Rake Angle*Feed in/rev	0.382
Environment*Rake Angle*Feed in/rev	0.403
Error	
Total	

S = 0.00150340 R-Sq = 33.62% R-Sq(adj) = 12.41%

Unusual Observations for Shear Area, As P

Obs	Shear Area, As P	Fit	SE Fit	Residual	St Resid	
61	0.001522	0.005270	0.000752	-0.003748	-2.88	R
62	0.016316	0.005270	0.000752	0.011046	8.48	R
63	0.001613	0.005270	0.000752	-0.003657	-2.81	R
64	0.001629	0.005270	0.000752	-0.003641	-2.80	R

R denotes an observation with a large standardized residual.

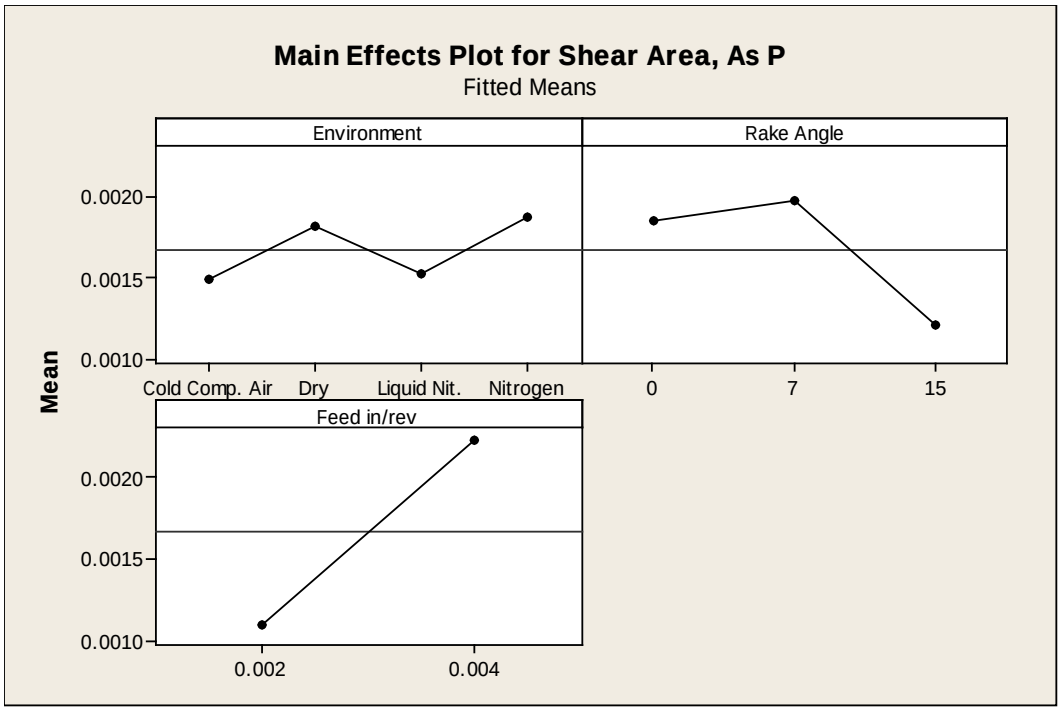
Main Effects Plot for Shear Area, As P
Fitted Means
Environment
Rake Angle
Feed in/rev
Mean
0.0020
0.0015
0.0010
Cold Comp. Air
Dry
Liquid Nit.
Nitrogen
0
7
15
0.002
0.004

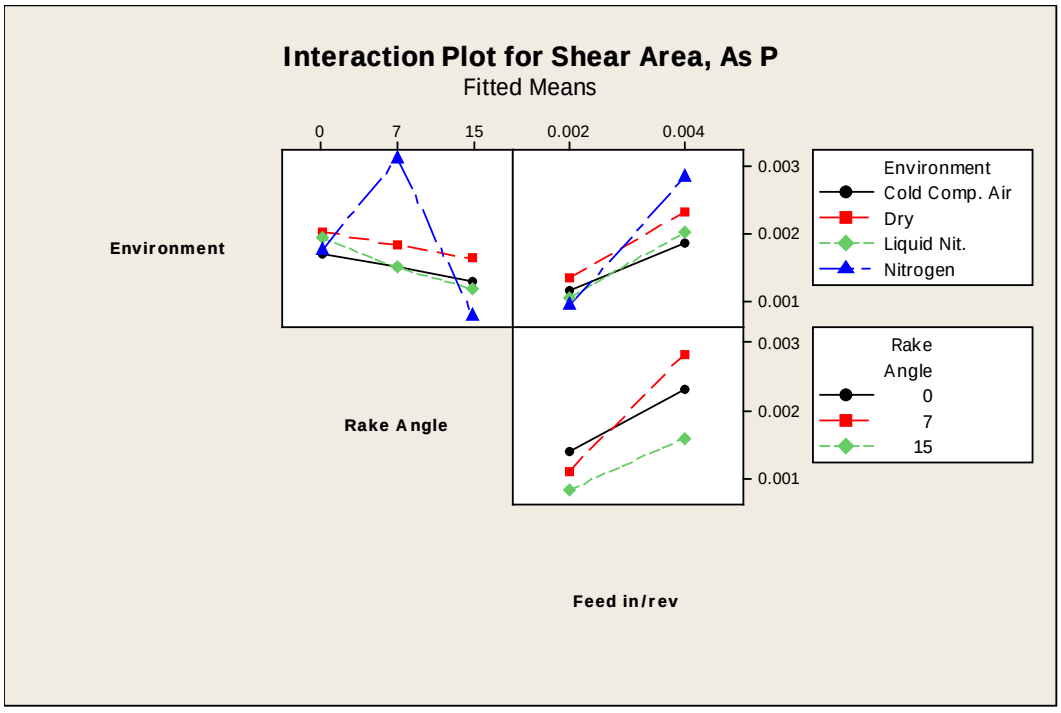
Interaction Plot for Shear Area, As P
Fitted Means
Environment
Rake Angle
Feed in/rev
0
7
15
0.002
0.004
0.003
0.002
0.001
Environment
Cold Comp. Air
Dry
Liquid Nit.
Nitrogen
Rake Angle
0
7
15

Analysis of Variance for **Shear strain new**, using Adjusted SS for Tests

Source	DF	Seq SS	Adj SS	Adj MS	F
Environment	3	4.32546	4.32546	1.44182	877.29
Rake Angle	2	2.76235	2.76235	1.38118	840.39
Feed in/rev	1	0.20462	0.20462	0.20462	124.51
Environment*Rake Angle	6	4.03744	4.03744	0.67291	409.44
Environment*Feed in/rev	3	0.16535	0.16535	0.05512	33.54
Rake Angle*Feed in/rev	2	0.08762	0.08762	0.04381	26.66
Environment*Rake Angle*Feed in/rev	6	0.08726	0.08726	0.01454	8.85
Error	72	0.11833	0.11833	0.00164	
Total	95	11.78844			

Source	P
Environment	0.000
Rake Angle	0.000
Feed in/rev	0.000
Environment*Rake Angle	0.000
Environment*Feed in/rev	0.000
Rake Angle*Feed in/rev	0.000
Environment*Rake Angle*Feed in/rev	0.000
Error	
Total	

S = 0.0405400 R-Sq = 99.00% R-Sq(adj) = 98.68%

Unusual Observations for Shear strain new

Obs	Shear strain new	Fit	SE Fit	Residual	St Resid	
61	0.96381	0.88863	0.02027	0.07518	2.14	R
65	1.89749	1.71807	0.02027	0.17942	5.11	R
68	1.55425	1.71807	0.02027	-0.16382	-4.67	R
69	1.64159	1.78893	0.02027	-0.14734	-4.20	R
71	1.87311	1.78893	0.02027	0.08418	2.40	R

R denotes an observation with a large standardized residual.

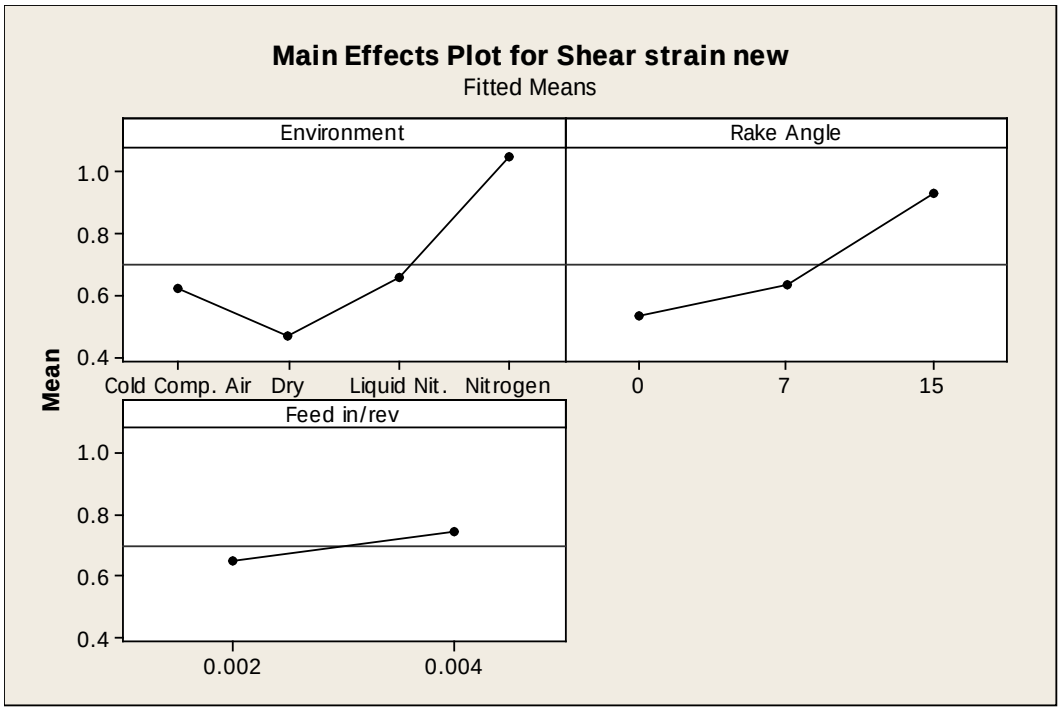
Main Effects Plot for Shear strain new
Fitted Means
Environment
Rake Angle
Feed in/rev
Mean
1.0
0.8
0.6
0.4
Cold Comp. Air
Dry
Liquid Nit.
Nitrogen
0
7
15
0.002
0.004

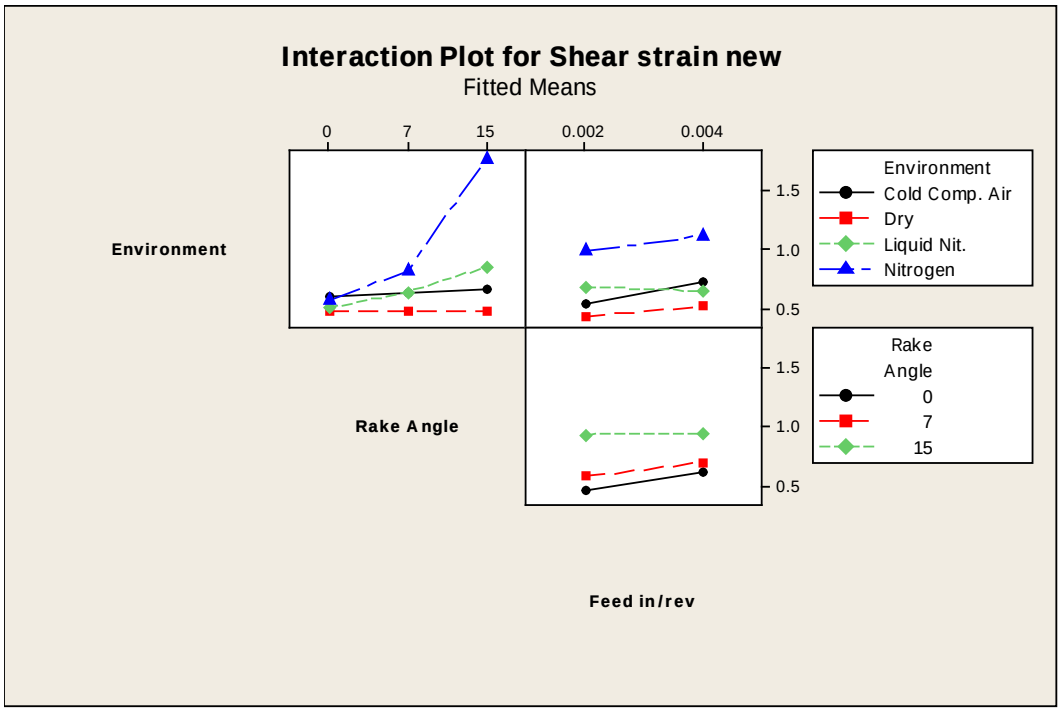
Interaction Plot for Shear strain new
Fitted Means
Environment
Rake Angle
Feed in/rev
0
7
15
0.002
0.004
1.5
1.0
0.5
Environment
Cold Comp. Air
Dry
Liquid Nit.
Nitrogen
Rake Angle
0
7
15

1020 Steel ;HSS

General Linear Model: Fy Thrust, Fz Cutting, ... versus Environment, Rake Angle

Factor	Type	Levels	Values
Environment	fixed	4	Cold Comp. Air, Dry, Liquid Nit., Nitrogen
Rake Angle	fixed	3	0, 7, 15
Feed in/rev	fixed	2	0.002, 0.004

Analysis of Variance for **Fy Thrust**, using Adjusted SS for Tests

Source	DF	Seq SS	Adj SS	Adj MS	F	P
Environment	3	365891	365891	121964	23.30	0.000
Rake Angle	2	301903	301903	150952	28.84	0.000
Feed in/rev	1	1787511	1787511	1787511	341.46	0.000
Environment*Rake Angle	6	69905	69905	11651	2.23	0.050
Environment*Feed in/rev	3	12241	12241	4080	0.78	0.509
Rake Angle*Feed in/rev	2	60559	60559	30279	5.78	0.005
Environment*Rake Angle*Feed in/rev	6	37137	37137	6190	1.18	0.325
Error	72	376911	376911	5235		
Total	95	3012058				

S = 72.3524 R-Sq = 87.49% R-Sq(adj) = 83.49%

Unusual Observations for Fy Thrust

Obs	Fy Thrust	Fit	SE Fit	Residual	St Resid	
53	722.170	592.656	36.176	129.515	2.07	R
54	780.891	592.656	36.176	188.235	3.00	R
55	77.625	592.656	36.176	-515.031	-8.22	R
56	789.937	592.656	36.176	197.281	3.15	R

R denotes an observation with a large standardized residual.

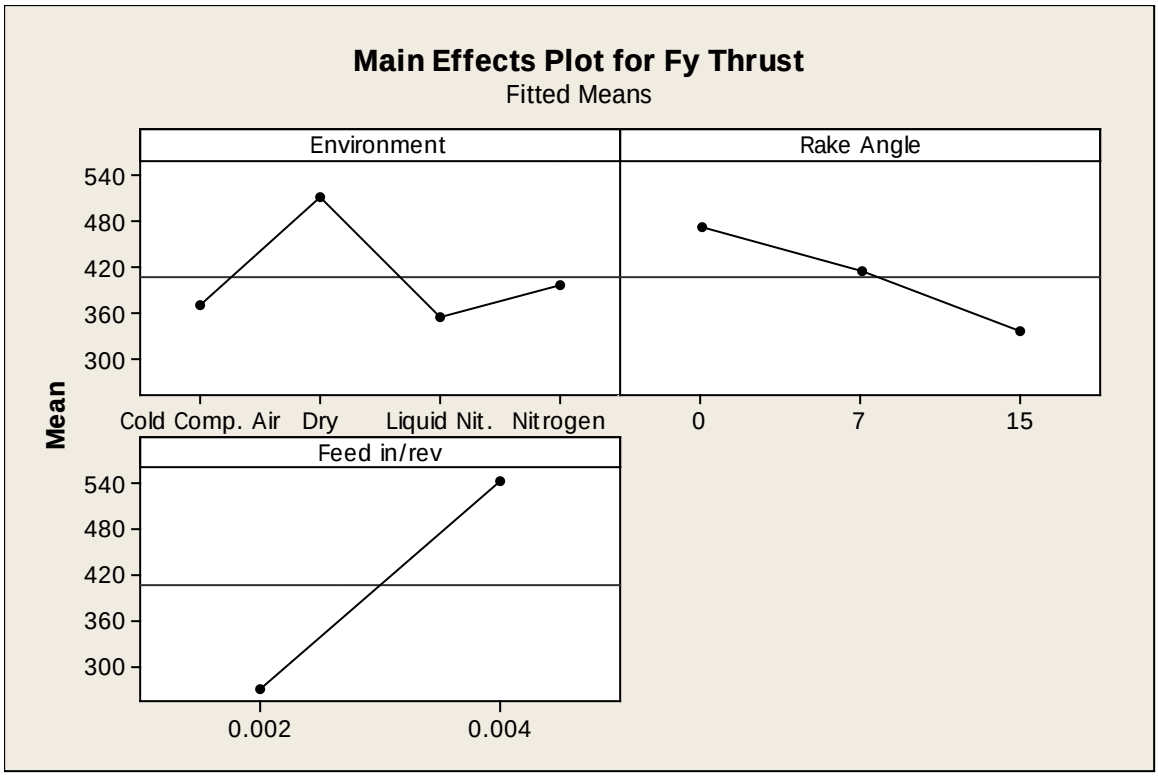
Main Effects Plot for Fy Thrust
Fitted Means
Environment
Rake Angle
Feed in/rev
Mean
540
480
420
360
300
Cold Comp. Air
Dry
Liquid Nit.
Nitrogen
0
7
15
0.002
0.004

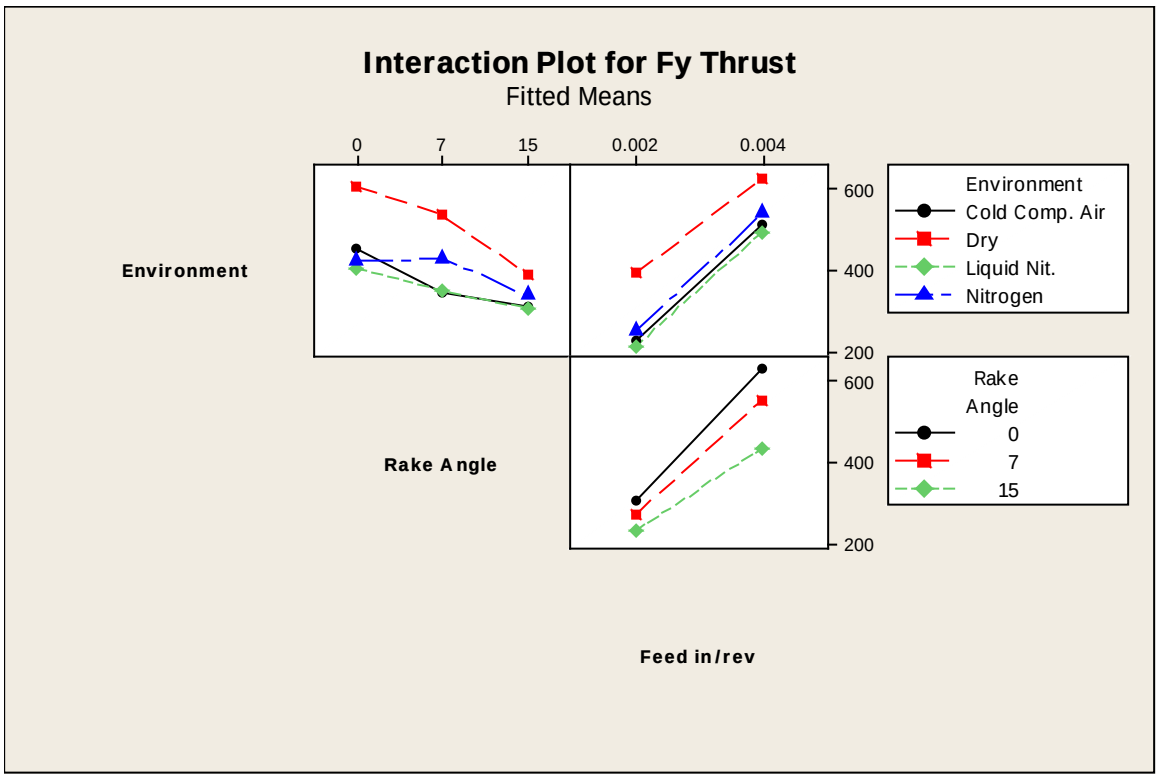
Interaction Plot for Fy Thrust
Fitted Means
Environment
Rake Angle
Feed in/rev
0
7
15
0.002
0.004
600
400
200
Environment
Cold Comp. Air
Dry
Liquid Nit.
Nitrogen
Rake Angle
0
7
15

Analysis of Variance for **Fz Cutting**, using Adjusted SS for Tests

Source	DF	Seq SS	Adj SS	Adj MS	F
Environment	3	127800	127800	42600	237.68
Rake Angle	2	162665	162665	81333	453.78
Feed in/rev	1	3090314	3090314	3090314	17241.73
Environment*Rake Angle	6	14538	14538	2423	13.52
Environment*Feed in/rev	3	46648	46648	15549	86.75
Rake Angle*Feed in/rev	2	30593	30593	15297	85.34
Environment*Rake Angle*Feed in/rev	6	49347	49347	8225	45.89
Error	72	12905	12905	179	
Total	95	3534811			

Source	P
Environment	0.000
Rake Angle	0.000
Feed in/rev	0.000
Environment*Rake Angle	0.000
Environment*Feed in/rev	0.000
Rake Angle*Feed in/rev	0.000
Environment*Rake Angle*Feed in/rev	0.000
Error	
Total	

S = 13.3879 R-Sq = 99.63% R-Sq(adj) = 99.52%

Unusual Observations for Fz Cutting

Obs	Fz Cutting	Fit	SE Fit	Residual	St Resid
49	388.765	413.507	6.694	-24.742	-2.13 R
51	388.832	413.507	6.694	-24.675	-2.13 R
52	467.671	413.507	6.694	54.163	4.67 R
79	787.762	823.198	6.694	-35.437	-3.06 R
81	347.257	371.649	6.694	-24.392	-2.10 R

R denotes an observation with a large standardized residual.

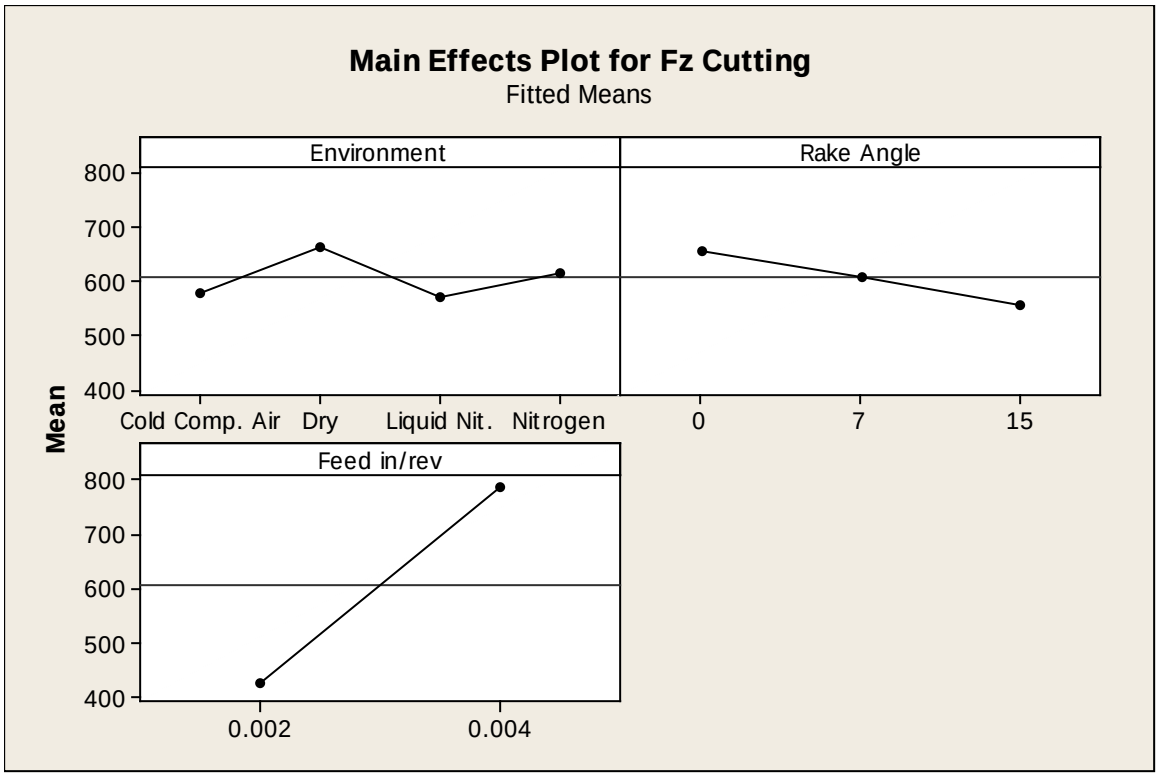
Main Effects Plot for Fz Cutting
Fitted Means
Environment
Rake Angle
Feed in/rev
Mean
800
700
600
500
400
Cold Comp. Air
Dry
Liquid Nit.
Nitrogen
0
7
15
0.002
0.004

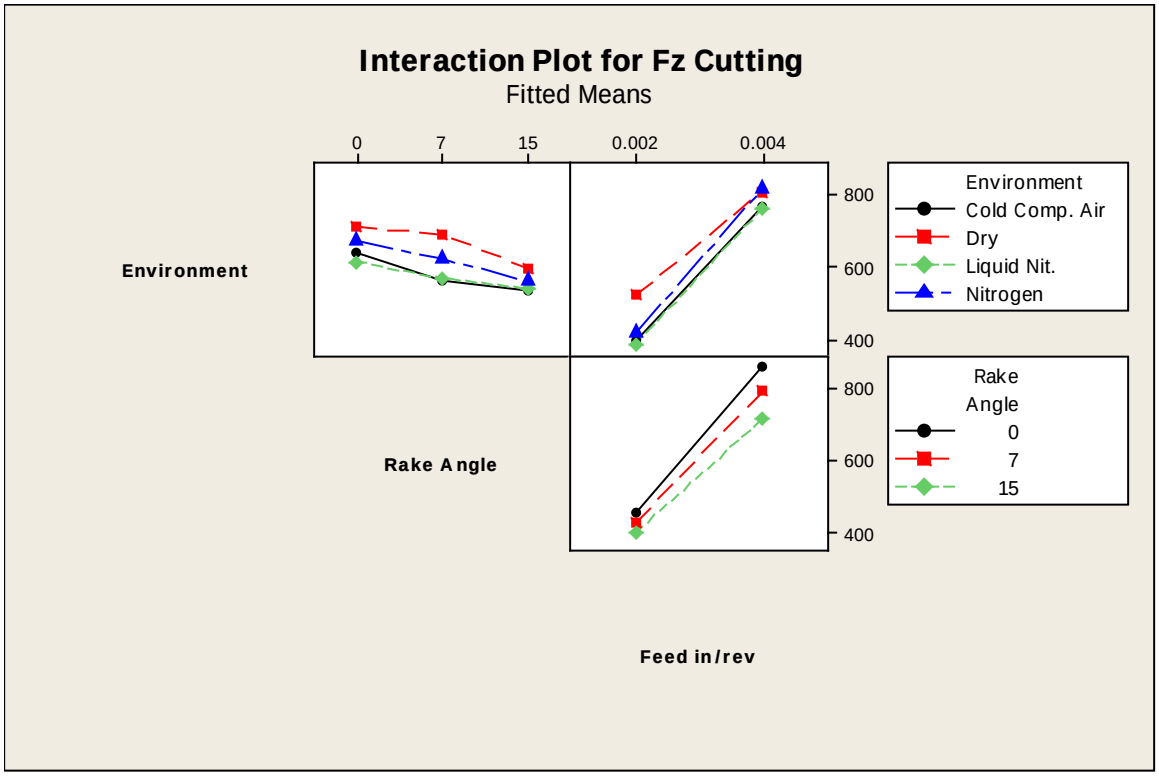
Interaction Plot for Fz Cutting
Fitted Means
Environment
Rake Angle
Feed in/rev
0
7
15
0.002
0.004
800
600
400
Environment
Cold Comp. Air
Dry
Liquid Nit.
Nitrogen
Rake Angle
0
7
15

Analysis of Variance for **Resultant force**, using Adjusted SS for Tests

Source	DF	Seq SS	Adj SS	Adj MS	F
Environment	3	405492	405492	135164	110.78
Rake Angle	2	437943	437943	218971	179.48
Feed in/rev	1	4926337	4926337	4926337	4037.77
Environment*Rake Angle	6	49060	49060	8177	6.70
Environment*Feed in/rev	3	62011	62011	20670	16.94
Rake Angle*Feed in/rev	2	89429	89429	44714	36.65
Environment*Rake Angle*Feed in/rev	6	84030	84030	14005	11.48
Error	72	87845	87845	1220	
Total	95	6142147			

Source	P
Environment	0.000
Rake Angle	0.000
Feed in/rev	0.000
Environment*Rake Angle	0.000
Environment*Feed in/rev	0.000
Rake Angle*Feed in/rev	0.000
Environment*Rake Angle*Feed in/rev	0.000
Error	
Total	

S = 34.9294 R-Sq = 98.57% R-Sq(adj) = 98.11%

Unusual Observations for Resultant

Obs	Resultant	Fit	SE Fit	Residual	St Resid	
52	560.21	482.91	17.46	77.30	2.56	R
54	1213.22	1131.08	17.46	82.14	2.72	R
55	923.76	1131.08	17.46	-207.32	-6.85	R
56	1227.69	1131.08	17.46	96.62	3.19	R
79	945.65	1008.03	17.46	-62.38	-2.06	R

R denotes an observation with a large standardized residual.

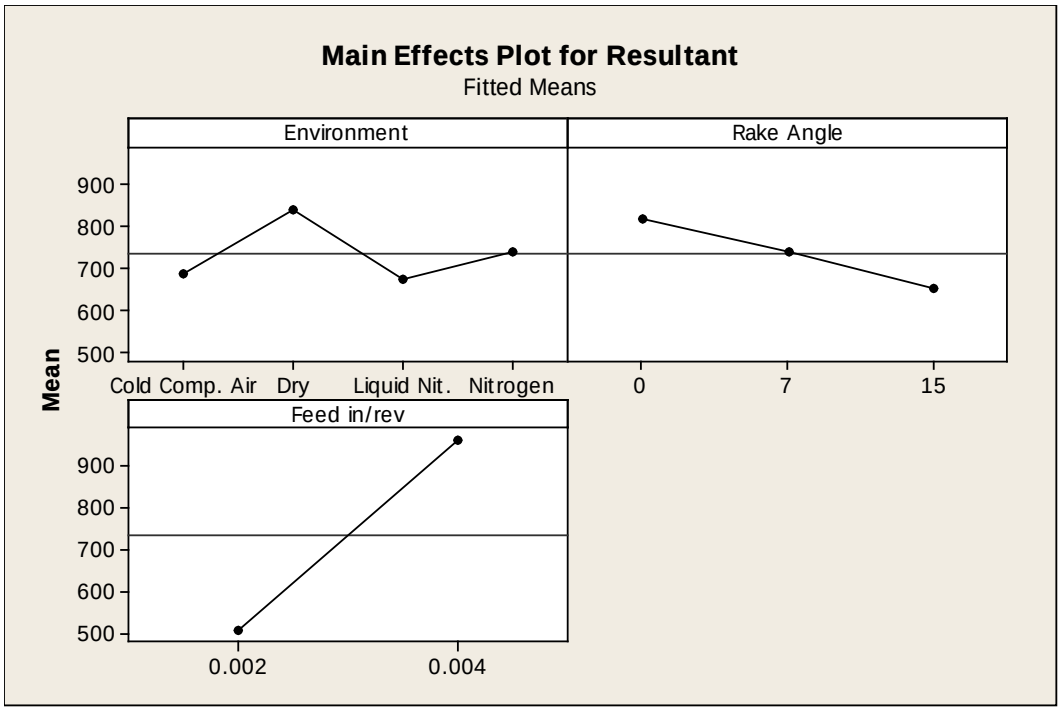
Main Effects Plot for Resultant
Fitted Means
Environment
Rake Angle
Feed in/rev
Mean
900
800
700
600
500
Cold Comp. Air
Dry
Liquid Nit.
Nitrogen
0
7
15
0.002
0.004

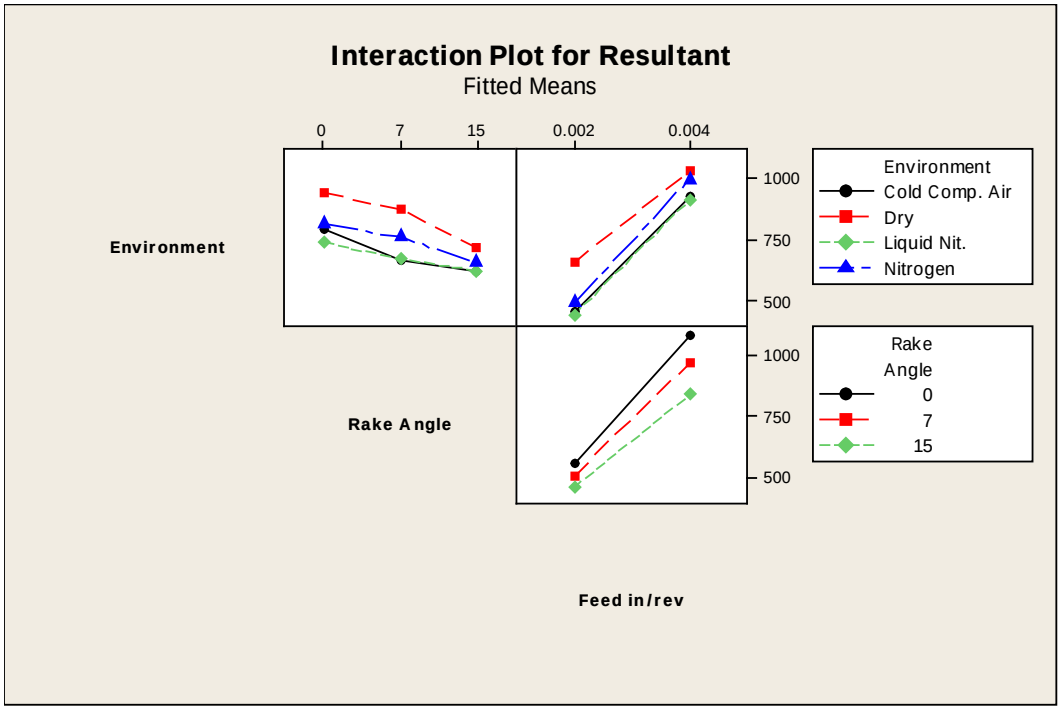
Interaction Plot for Resultant
Fitted Means
Environment
Rake Angle
Feed in/rev
0
7
15
0.002
0.004
1000
750
500
Environment
Cold Comp. Air
Dry
Liquid Nit.
Nitrogen
Rake Angle
0
7
15

Analysis of Variance for **Chip thickness ratio**, using Adjusted SS for Tests

Source	DF	Seq SS	Adj SS	Adj MS	F
Environment	3	0.537200	0.537200	0.179067	2053.66
Rake Angle	2	0.360019	0.360019	0.180009	2064.47
Feed in/rev	1	0.002120	0.002120	0.002120	24.31
Environment*Rake Angle	6	0.064952	0.064952	0.010825	124.15
Environment*Feed in/rev	3	0.019403	0.019403	0.006468	74.17
Rake Angle*Feed in/rev	2	0.008449	0.008449	0.004225	48.45
Environment*Rake Angle*Feed in/rev	6	0.022308	0.022308	0.003718	42.64
Error	72	0.006278	0.006278	0.000087	
Total	95	1.020728			

Source	P
Environment	0.000
Rake Angle	0.000
Feed in/rev	0.000
Environment*Rake Angle	0.000
Environment*Feed in/rev	0.000
Rake Angle*Feed in/rev	0.000
Environment*Rake Angle*Feed in/rev	0.000
Error	
Total	

S = 0.00933776 R-Sq = 99.38% R-Sq(adj) = 99.19%

Unusual Observations for Chip thickness ratio

Obs	Chip thickness ratio	Fit	SE Fit	Residual	St Resid	
22	0.238806	0.263915	0.004669	-0.025109	-3.10	R
23	0.281353	0.263915	0.004669	0.017438	2.16	R
89	0.504197	0.468692	0.004669	0.035506	4.39	R
92	0.436367	0.468692	0.004669	-0.032325	-4.00	R

R denotes an observation with a large standardized residual.

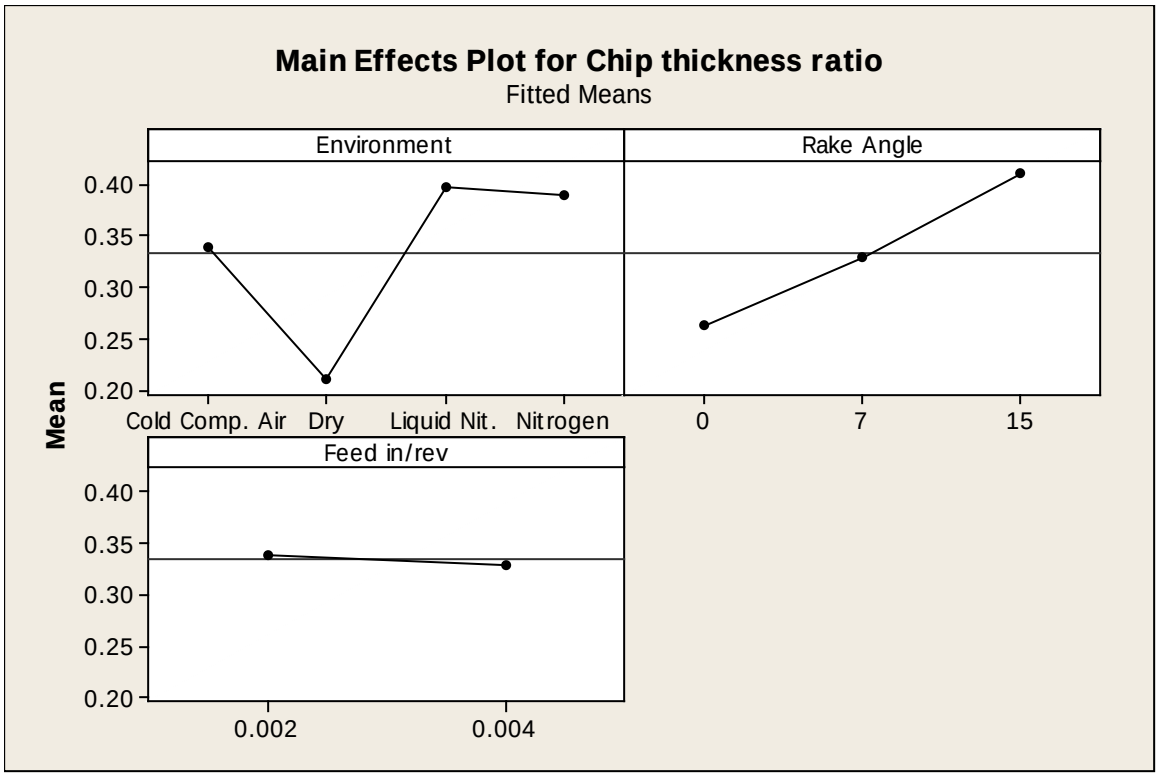
Main Effects Plot for Chip thickness ratio
Fitted Means
Environment
Rake Angle
Feed in/rev
Mean
0.40
0.35
0.30
0.25
0.20
Cold Comp. Air
Dry
Liquid Nit.
Nitrogen
0
7
15
0.002
0.004

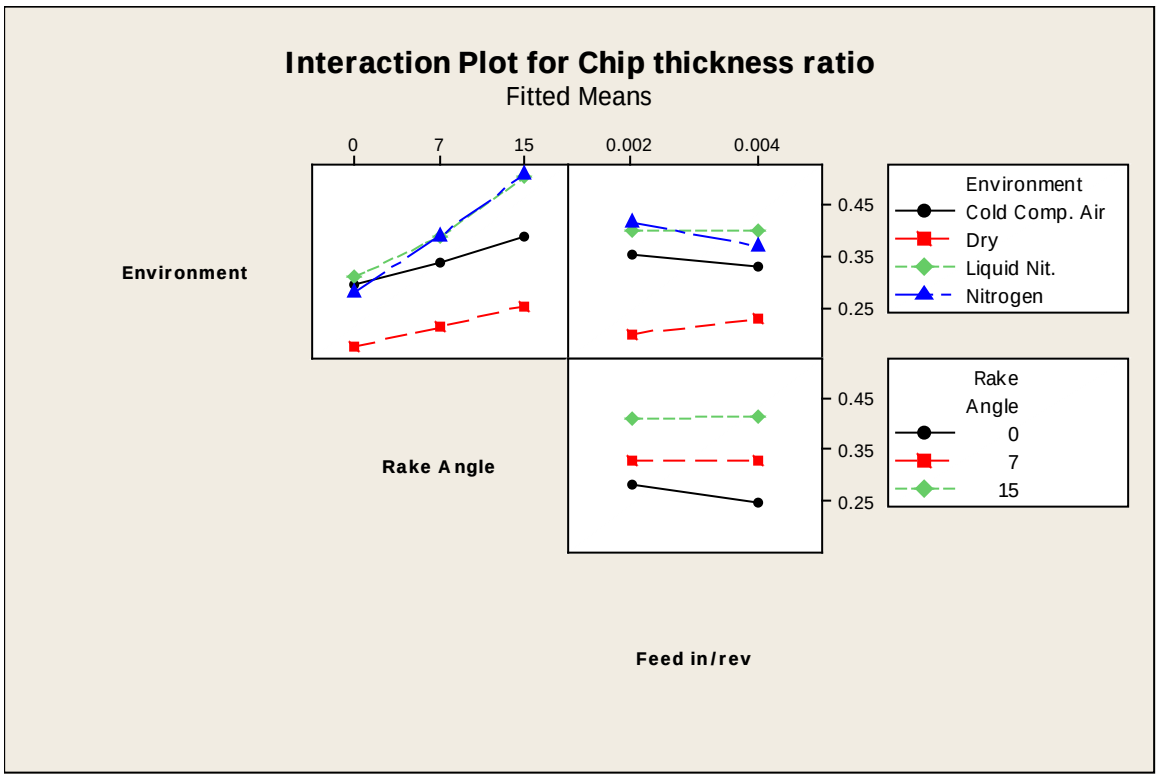
Interaction Plot for Chip thickness ratio
Fitted Means
Environment
Rake Angle
Feed in/rev
0
7
15
0.002
0.004
0.45
0.35
0.25
Environment
Cold Comp. Air
Dry
Liquid Nit.
Nitrogen
Rake Angle
0
7
15

Analysis of Variance for **Phi** degrees, using Adjusted SS for Tests

Source	DF	Seq SS	Adj SS	Adj MS	F
Environment	3	1715.02	1715.02	571.67	2070.32
Rake Angle	2	1377.34	1377.34	688.67	2494.03
Feed in/rev	1	5.15	5.15	5.15	18.64
Environment*Rake Angle	6	231.40	231.40	38.57	139.67
Environment*Feed in/rev	3	59.92	59.92	19.97	72.33
Rake Angle*Feed in/rev	2	24.25	24.25	12.13	43.91
Environment*Rake Angle*Feed in/rev	6	67.97	67.97	11.33	41.03
Error	72	19.88	19.88	0.28	
Total	95	3500.91			

Source	P
Environment	0.000
Rake Angle	0.000
Feed in/rev	0.000
Environment*Rake Angle	0.000
Environment*Feed in/rev	0.000
Rake Angle*Feed in/rev	0.000
Environment*Rake Angle*Feed in/rev	0.000
Error	
Total	

S = 0.525478 R-Sq = 99.43% R-Sq(adj) = 99.25%

Unusual Observations for Phi degrees

Obs	Phi degrees	Fit	SE Fit	Residual	St Resid
22	13.8131	15.3022	0.2627	-1.4892	-3.27 R
23	16.3364	15.3022	0.2627	1.0342	2.27 R
89	29.2536	27.2509	0.2627	2.0027	4.40 R
92	25.4153	27.2509	0.2627	-1.8356	-4.03 R

R denotes an observation with a large standardized residual.

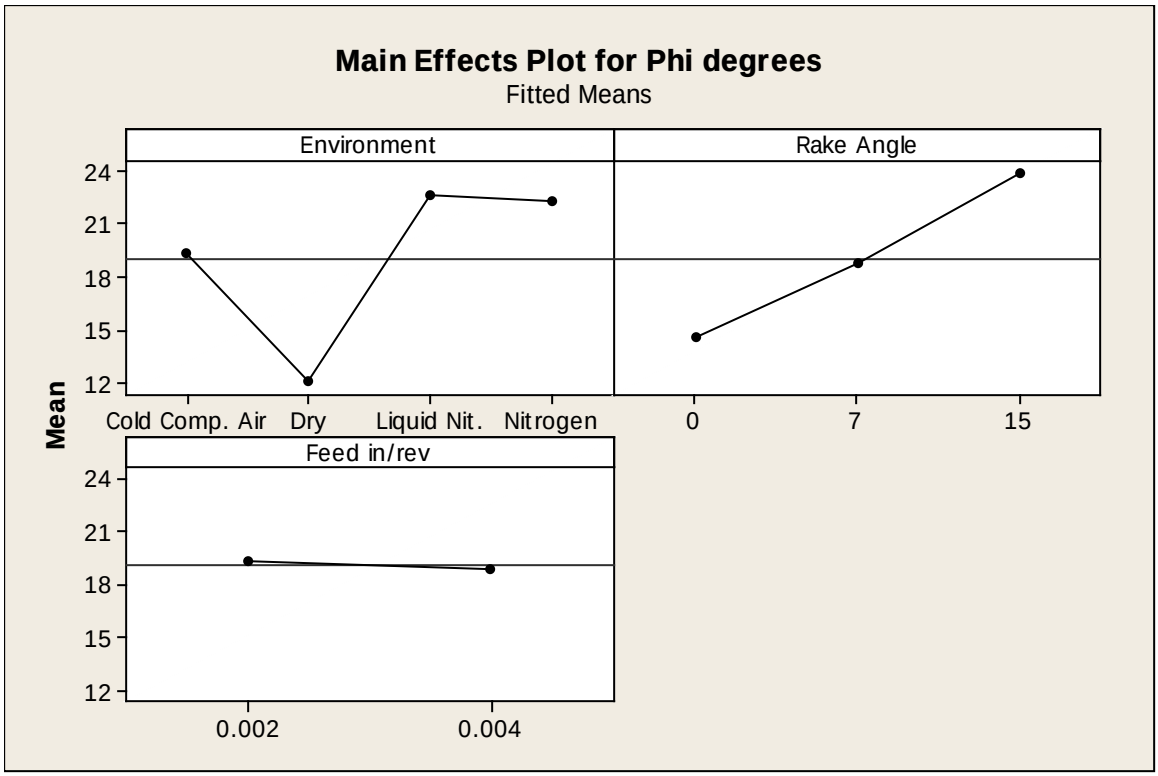
Main Effects Plot for Phi degrees
Fitted Means
Environment
Rake Angle
Feed in/rev
Mean
24
21
18
15
12
Cold Comp. Air
Dry
Liquid Nit.
Nitrogen
0
7
15
0.002
0.004

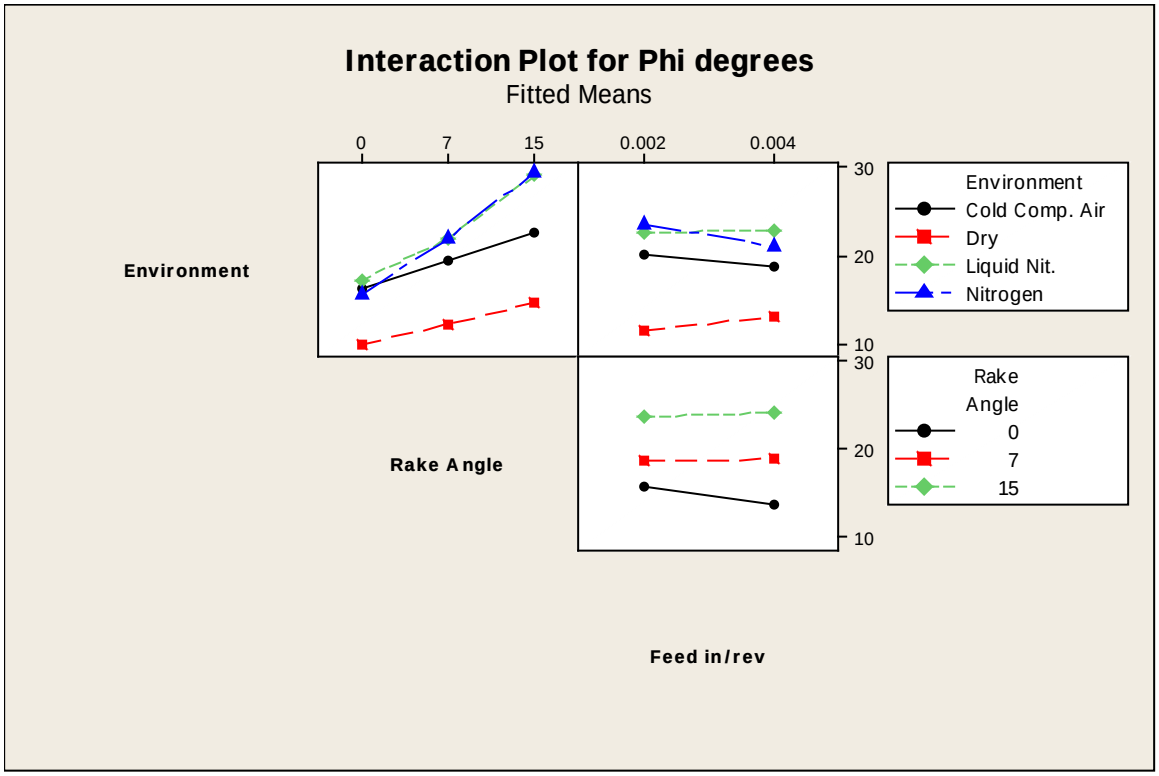
Interaction Plot for Phi degrees
Fitted Means
Environment
Rake Angle
Feed in/rev
0
7
15
0.002
0.004
30
20
10
Environment
Cold Comp. Air
Dry
Liquid Nit.
Nitrogen
Rake Angle
0
7
15

Analysis of Variance for **Psi** degrees, using Adjusted SS for Tests

Source	DF	Seq SS	Adj SS	Adj MS	F
Environment	3	1715.016	1715.016	571.672	2070.32
Rake Angle	2	51.058	51.058	25.529	92.45
Feed in/rev	1	5.147	5.147	5.147	18.64
Environment*Rake Angle	6	231.397	231.397	38.566	139.67
Environment*Feed in/rev	3	59.916	59.916	19.972	72.33
Rake Angle*Feed in/rev	2	24.250	24.250	12.125	43.91
Environment*Rake Angle*Feed in/rev	6	67.969	67.969	11.328	41.03
Error	72	19.881	19.881	0.276	
Total	95	2174.633			

Source	P
Environment	0.000
Rake Angle	0.000
Feed in/rev	0.000
Environment*Rake Angle	0.000
Environment*Feed in/rev	0.000
Rake Angle*Feed in/rev	0.000
Environment*Rake Angle*Feed in/rev	0.000
Error	
Total	

S = 0.525478 R-Sq = 99.09% R-Sq(adj) = 98.79%

Unusual Observations for Psi degrees

Obs	Psi degrees	Fit	SE Fit	Residual	St Resid
22	38.6869	37.1978	0.2627	1.4892	3.27 R
23	36.1636	37.1978	0.2627	-1.0342	-2.27 R
89	23.2464	25.2491	0.2627	-2.0027	-4.40 R
92	27.0847	25.2491	0.2627	1.8356	4.03 R

R denotes an observation with a large standardized residual.

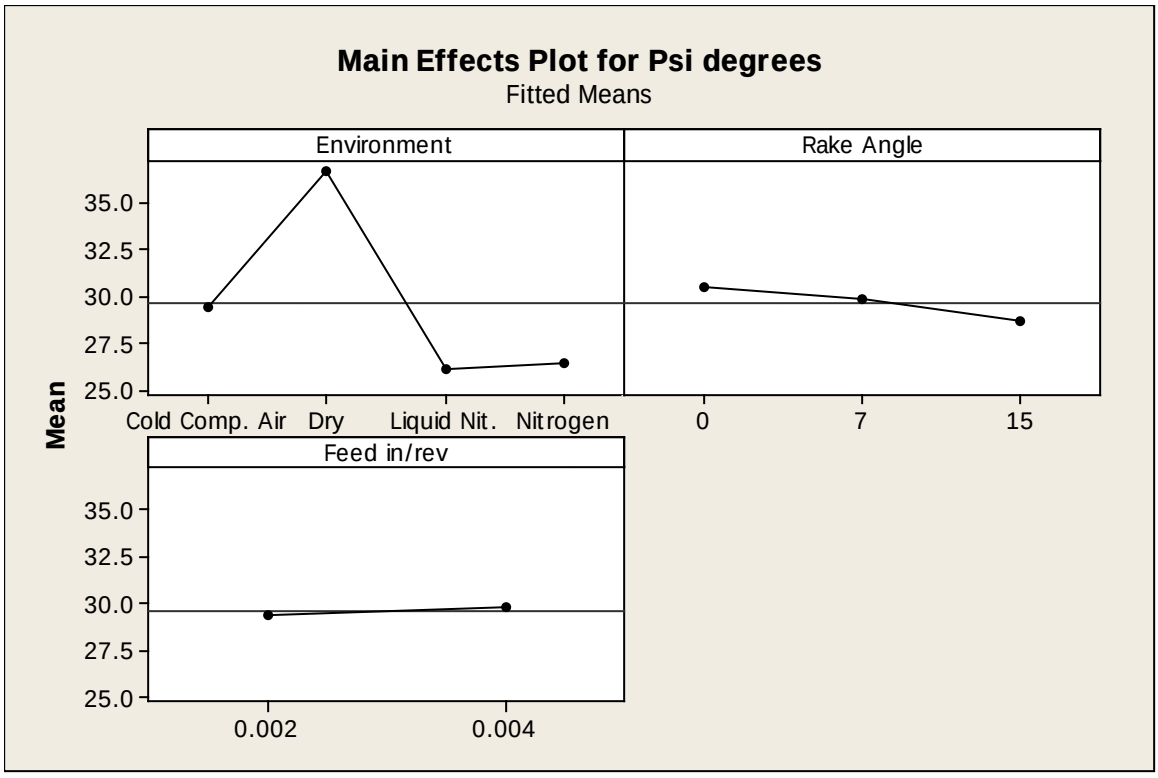
Main Effects Plot for Psi degrees
Fitted Means
Environment
Rake Angle
Feed in/rev
Mean
35.0
32.5
30.0
27.5
25.0
Cold Comp. Air
Dry
Liquid Nit.
Nitrogen
0
7
15
0.002
0.004

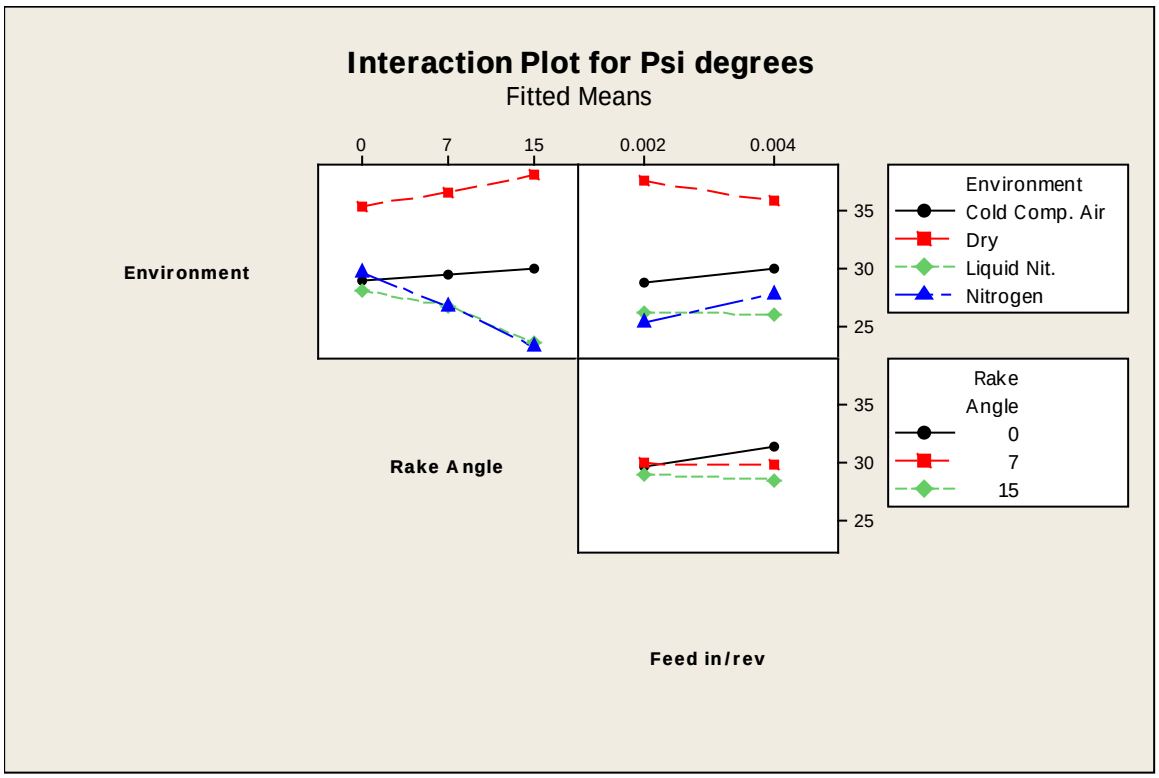
Interaction Plot for Psi degrees
Fitted Means
0
7
15
0.002
0.004
Environment
Rake Angle
Feed in/rev
35
30
25
Environment
Cold Comp. Air
Dry
Liquid Nit.
Nitrogen
Rake Angle
0
7
15

Analysis of Variance for **Friction Force (F)**, using Adjusted SS for Tests

Source	DF	Seq SS	Adj SS	Adj MS	F
Environment	3	408206	408206	136069	25.87
Rake Angle	2	5611	5611	2806	0.53
Feed in/rev	1	2330597	2330597	2330597	443.14
Environment*Rake Angle	6	68180	68180	11363	2.16
Environment*Feed in/rev	3	13812	13812	4604	0.88
Rake Angle*Feed in/rev	2	12103	12103	6052	1.15
Environment*Rake Angle*Feed in/rev	6	35700	35700	5950	1.13
Error	72	378670	378670	5259	
Total	95	3252879			

Source	P
Environment	0.000
Rake Angle	0.589
Feed in/rev	0.000
Environment*Rake Angle	0.057
Environment*Feed in/rev	0.458
Rake Angle*Feed in/rev	0.322
Environment*Rake Angle*Feed in/rev	0.353
Error	
Total	

S = 72.5211 R-Sq = 88.36% R-Sq(adj) = 84.64%

Unusual Observations for Friction Force (F)

Obs	Friction Force (F)	Fit	SE Fit	Residual	St Resid	
53	722.170	592.656	36.261	129.515	2.06	R
54	780.891	592.656	36.261	188.235	3.00	R
55	77.625	592.656	36.261	-515.031	-8.20	R
56	789.937	592.656	36.261	197.281	3.14	R

R denotes an observation with a large standardized residual.

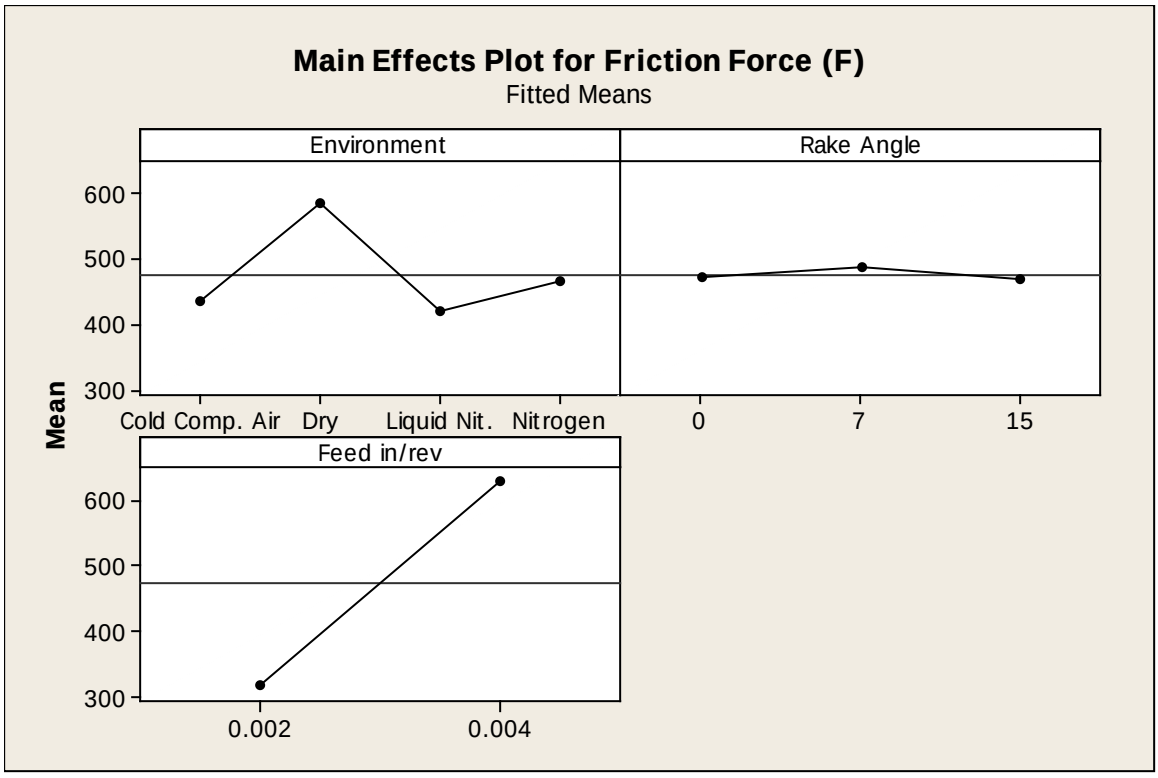
Main Effects Plot for Friction Force (F)
Fitted Means
Environment
Rake Angle
Feed in/rev
Mean
600
500
400
300
Cold Comp. Air
Dry
Liquid Nit.
Nitrogen
0
7
15
0.002
0.004

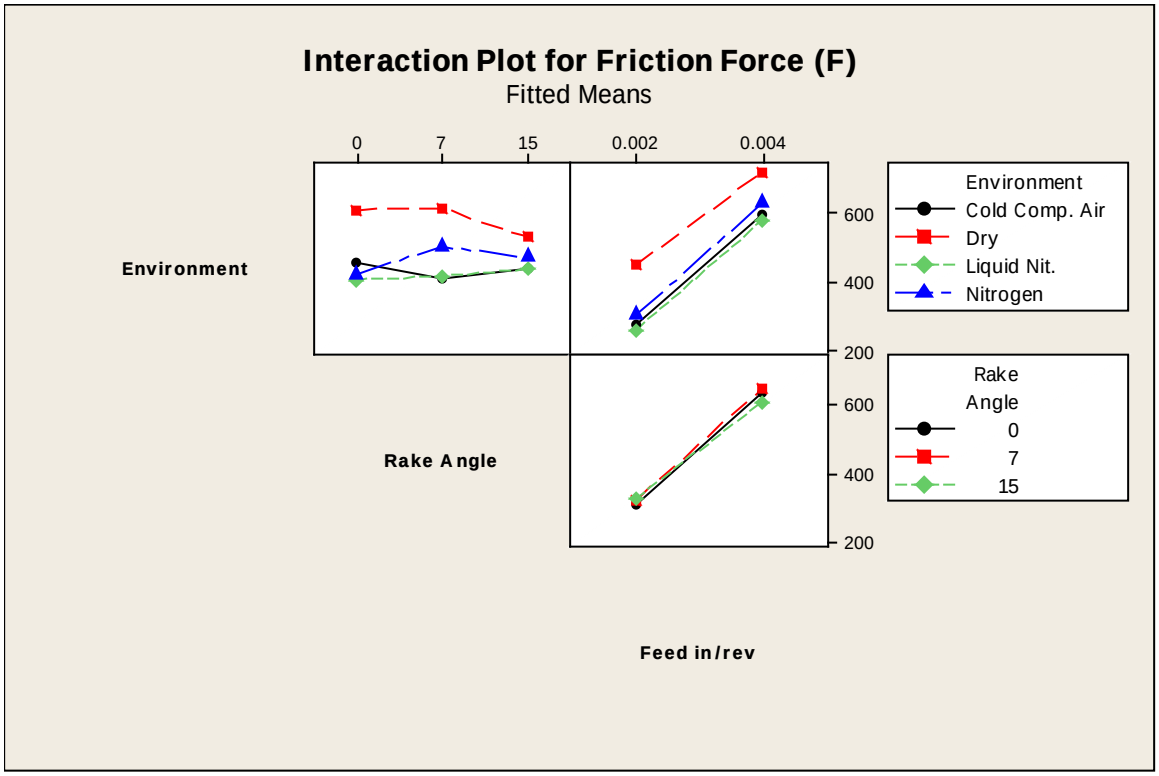
Interaction Plot for Friction Force (F)
Fitted Means
Environment
Rake Angle
Feed in/rev
0
7
15
0.002
0.004
600
400
200
Environment
Cold Comp. Air
Dry
Liquid Nit.
Nitrogen
Rake Angle
0
7
15

Analysis of Variance for **Normal Force (N)**, using Adjusted SS for Tests

Source	DF	Seq SS	Adj SS	Adj MS	F
Environment	3	87031	87031	29010	187.41
Rake Angle	2	681008	681008	340504	2199.71
Feed in/rev	1	2534687	2534687	2534687	16374.50
Environment*Rake Angle	6	14717	14717	2453	15.85
Environment*Feed in/rev	3	46548	46548	15516	100.24
Rake Angle*Feed in/rev	2	91590	91590	45795	295.84
Environment*Rake Angle*Feed in/rev	6	49314	49314	8219	53.10
Error	72	11145	11145	155	
Total	95	3516040			

Source	P
Environment	0.000
Rake Angle	0.000
Feed in/rev	0.000
Environment*Rake Angle	0.000
Environment*Feed in/rev	0.000
Rake Angle*Feed in/rev	0.000
Environment*Rake Angle*Feed in/rev	0.000
Error	
Total	

S = 12.4417 R-Sq = 99.68% R-Sq(adj) = 99.58%

Unusual Observations for Normal Force (N)

Obs	Normal Force (N)	Fit	SE Fit	Residual	St Resid	
49	388.765	413.507	6.221	-24.742	-2.30	R
51	388.832	413.507	6.221	-24.675	-2.29	R
52	467.671	413.507	6.221	54.163	5.03	R
79	787.762	823.198	6.221	-35.437	-3.29	R
81	320.379	343.692	6.221	-23.314	-2.16	R

R denotes an observation with a large standardized residual.

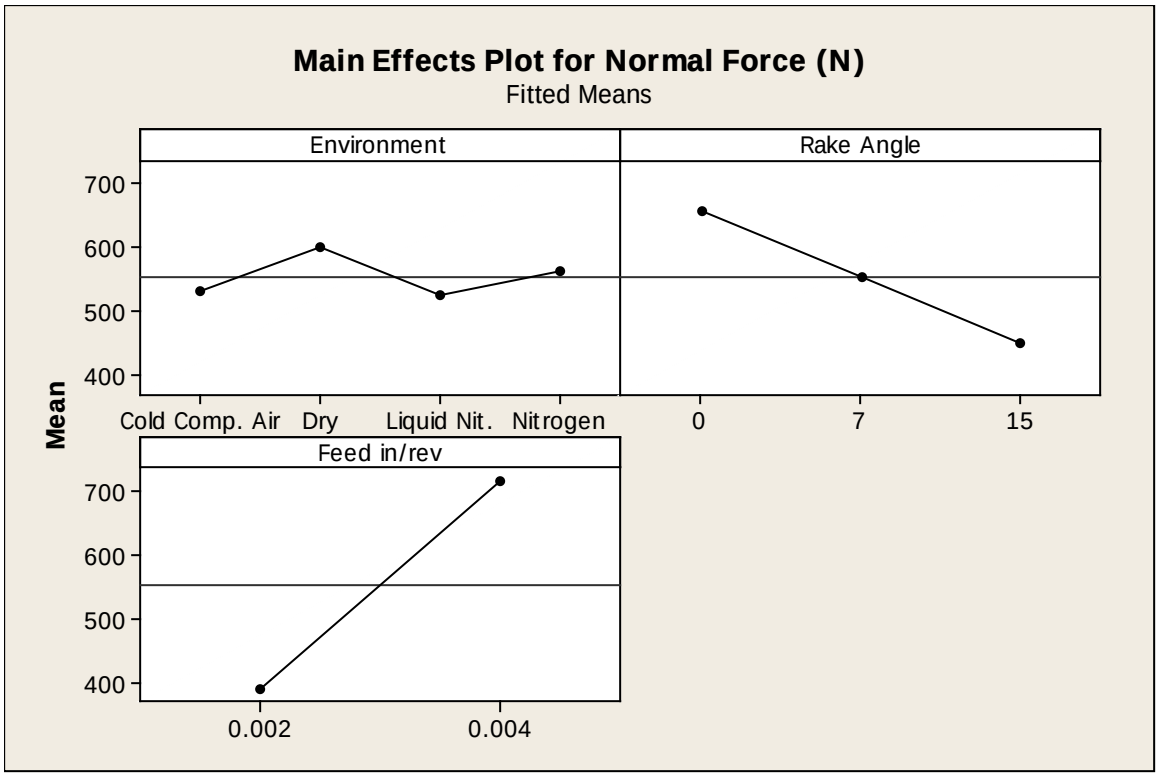
Main Effects Plot for Normal Force (N)
Fitted Means
Environment
Rake Angle
Feed in/rev
Mean
700
600
500
400
Cold Comp. Air
Dry
Liquid Nit.
Nitrogen
0
7
15
0.002
0.004

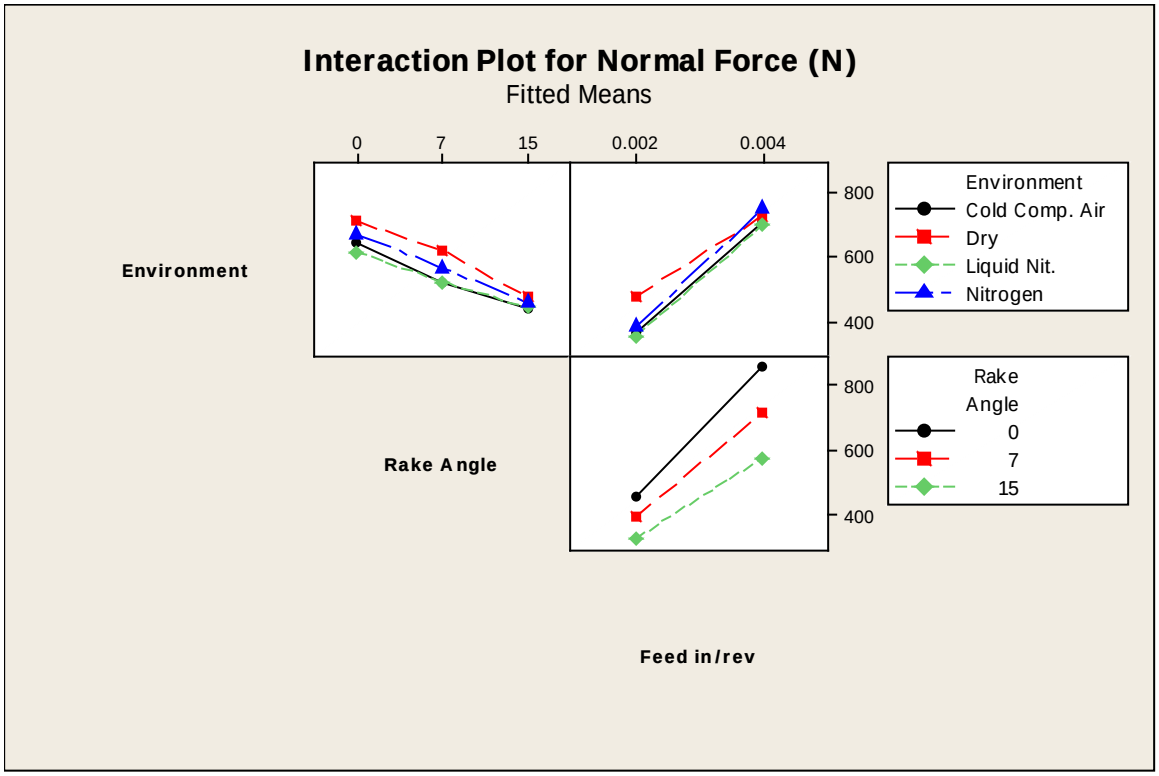
Interaction Plot for Normal Force (N)
Fitted Means
Environment
Rake Angle
Feed in/rev
0
7
15
0.002
0.004
800
600
400
Environment
Cold Comp. Air
Dry
Liquid Nit.
Nitrogen
Rake Angle
0
7
15

Analysis of Variance for **F/N Ratio**, using Adjusted SS for Tests

Source	DF	Seq SS	Adj SS	Adj MS	F
Environment	3	0.52313	0.52313	0.17438	28.62
Rake Angle	2	1.73529	1.73529	0.86764	142.41
Feed in/rev	1	0.14972	0.14972	0.14972	24.57
Environment*Rake Angle	6	0.08066	0.08066	0.01344	2.21
Environment*Feed in/rev	3	0.01525	0.01525	0.00508	0.83
Rake Angle*Feed in/rev	2	0.00933	0.00933	0.00466	0.77
Environment*Rake Angle*Feed in/rev	6	0.02041	0.02041	0.00340	0.56
Error	72	0.43868	0.43868	0.00609	
Total	95	2.97246			

Source	P
Environment	0.000
Rake Angle	0.000
Feed in/rev	0.000
Environment*Rake Angle	0.052
Environment*Feed in/rev	0.480
Rake Angle*Feed in/rev	0.469
Environment*Rake Angle*Feed in/rev	0.762
Error	
Total	

S = 0.0780558 R-Sq = 85.24% R-Sq(adj) = 80.53%

Unusual Observations for F/N Ratio

Obs	F/N Ratio	Fit	SE Fit	Residual	St Resid	
53	0.79594	0.64046	0.03903	0.15548	2.30	R
54	0.84103	0.64046	0.03903	0.20057	2.97	R
55	0.08433	0.64046	0.03903	-0.55613	-8.23	R
56	0.84054	0.64046	0.03903	0.20008	2.96	R

R denotes an observation with a large standardized residual.

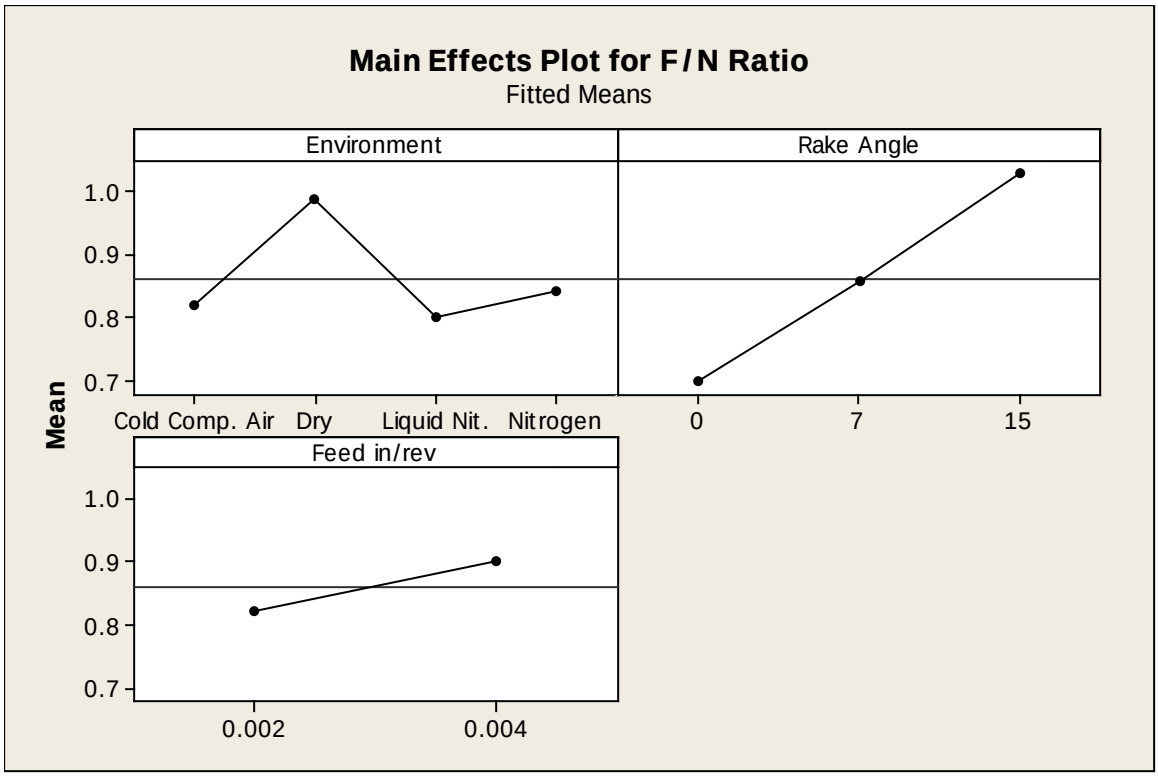
Main Effects Plot for F/N Ratio
Fitted Means
Environment
Rake Angle
Feed in/rev
Mean
1.0
0.9
0.8
0.7
Cold Comp. Air
Dry
Liquid Nit.
Nitrogen
0
7
15
0.002
0.004

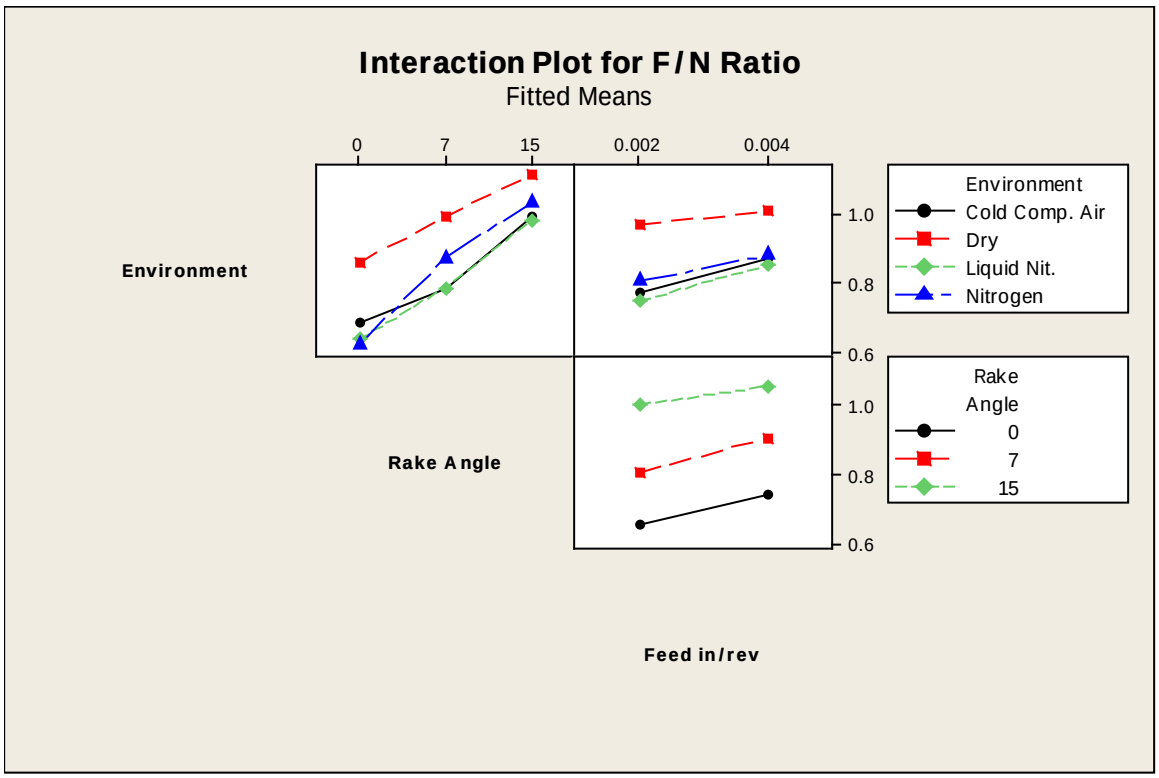
Interaction Plot for F/N Ratio
Fitted Means
0
7
15
0.002
0.004
Environment
Rake Angle
Feed in/rev
1.0
0.8
0.6
Environment
Cold Comp. Air
Dry
Liquid Nit.
Nitrogen
Rake Angle
0
7
15

Analysis of Variance for **Fs (Merchant)**, using Adjusted SS for Tests

Source	DF	Seq SS	Adj SS	Adj MS	F
Environment	3	300534	300534	100178	296.66
Rake Angle	2	364787	364787	182393	540.13
Feed in/rev	1	1563046	1563046	1563046	4628.74
Environment*Rake Angle	6	27797	27797	4633	13.72
Environment*Feed in/rev	3	23752	23752	7917	23.45
Rake Angle*Feed in/rev	2	58400	58400	29200	86.47
Environment*Rake Angle*Feed in/rev	6	61963	61963	10327	30.58
Error	72	24313	24313	338	
Total	95	2424593			

Source	P
Environment	0.000
Rake Angle	0.000
Feed in/rev	0.000
Environment*Rake Angle	0.000
Environment*Feed in/rev	0.000
Rake Angle*Feed in/rev	0.000
Environment*Rake Angle*Feed in/rev	0.000
Error	
Total	

S = 18.3761 R-Sq = 99.00% R-Sq(adj) = 98.68%

Unusual Observations for Fs (Merchant)

Obs	Fs (Merchant)	Fit	SE Fit	Residual	St Resid	
52	353.415	320.212	9.188	33.203	2.09	R
53	711.214	757.726	9.188	-46.512	-2.92	R
54	716.785	757.726	9.188	-40.941	-2.57	R
55	876.356	757.726	9.188	118.631	7.45	R

R denotes an observation with a large standardized residual.

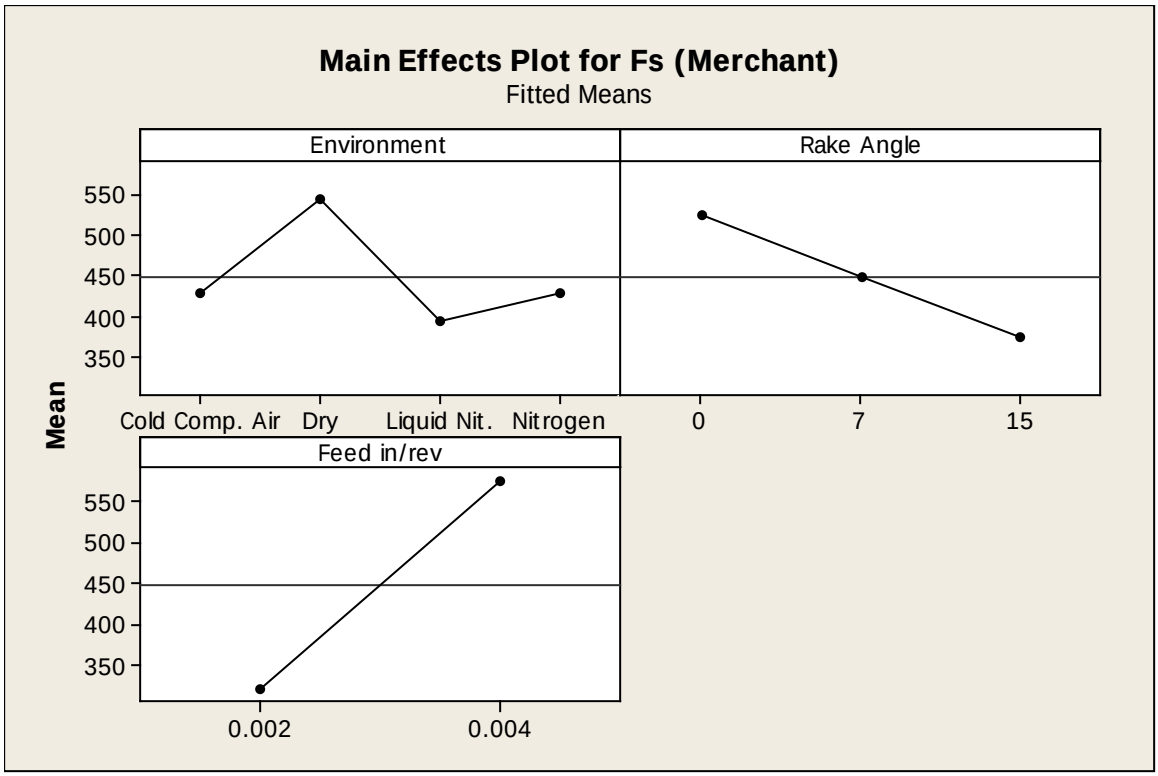
Main Effects Plot for Fs (Merchant)
Fitted Means
Environment
Rake Angle
Feed in/rev
Mean
550
500
450
400
350
Cold Comp. Air
Dry
Liquid Nit.
Nitrogen
0
7
15
0.002
0.004

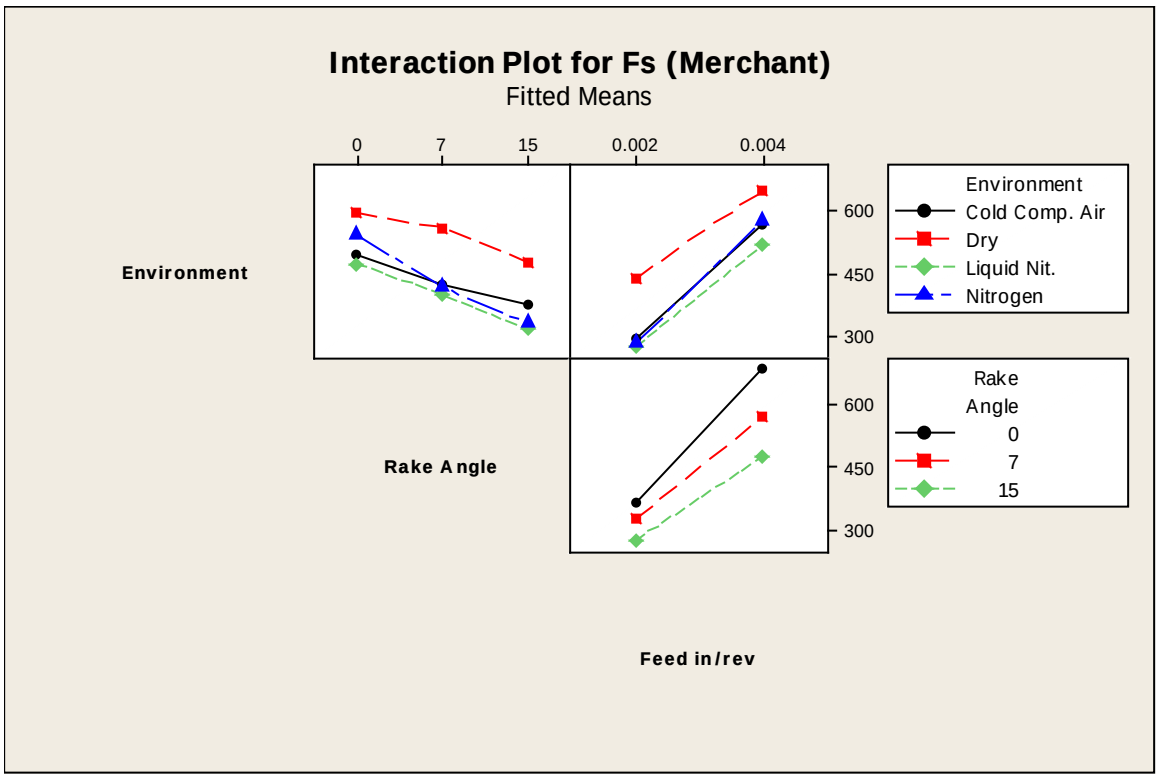
Interaction Plot for Fs (Merchant)
Fitted Means
Environment
Rake Angle
Feed in/rev
0
7
15
0.002
0.004
600
450
300
Environment
Cold Comp. Air
Dry
Liquid Nit.
Nitrogen
Rake Angle
0
7
15

Analysis of Variance for **Fn (Merchant)**, using Adjusted SS for Tests

Source	DF	Seq SS	Adj SS	Adj MS	F
Environment	3	165036	165036	55012	10.74
Rake Angle	2	131310	131310	65655	12.81
Feed in/rev	1	3295811	3295811	3295811	643.16
Environment*Rake Angle	6	119201	119201	19867	3.88
Environment*Feed in/rev	3	35226	35226	11742	2.29
Rake Angle*Feed in/rev	2	34295	34295	17148	3.35
Environment*Rake Angle*Feed in/rev	6	44778	44778	7463	1.46
Error	72	368954	368954	5124	
Total	95	4194612			

Source	P
Environment	0.000
Rake Angle	0.000
Feed in/rev	0.000
Environment*Rake Angle	0.002
Environment*Feed in/rev	0.085
Rake Angle*Feed in/rev	0.041
Environment*Rake Angle*Feed in/rev	0.206
Error	
Total	

S = 71.5847 R-Sq = 91.20% R-Sq(adj) = 88.39%

Unusual Observations for Fn (Merchant)

Obs	Fn (Merchant)	Fit	SE Fit	Residual	St Resid	
54	978.832	794.124	35.792	184.708	2.98	R
55	292.104	794.124	35.792	-502.020	-8.10	R
56	989.623	794.124	35.792	195.499	3.15	R

R denotes an observation with a large standardized residual.

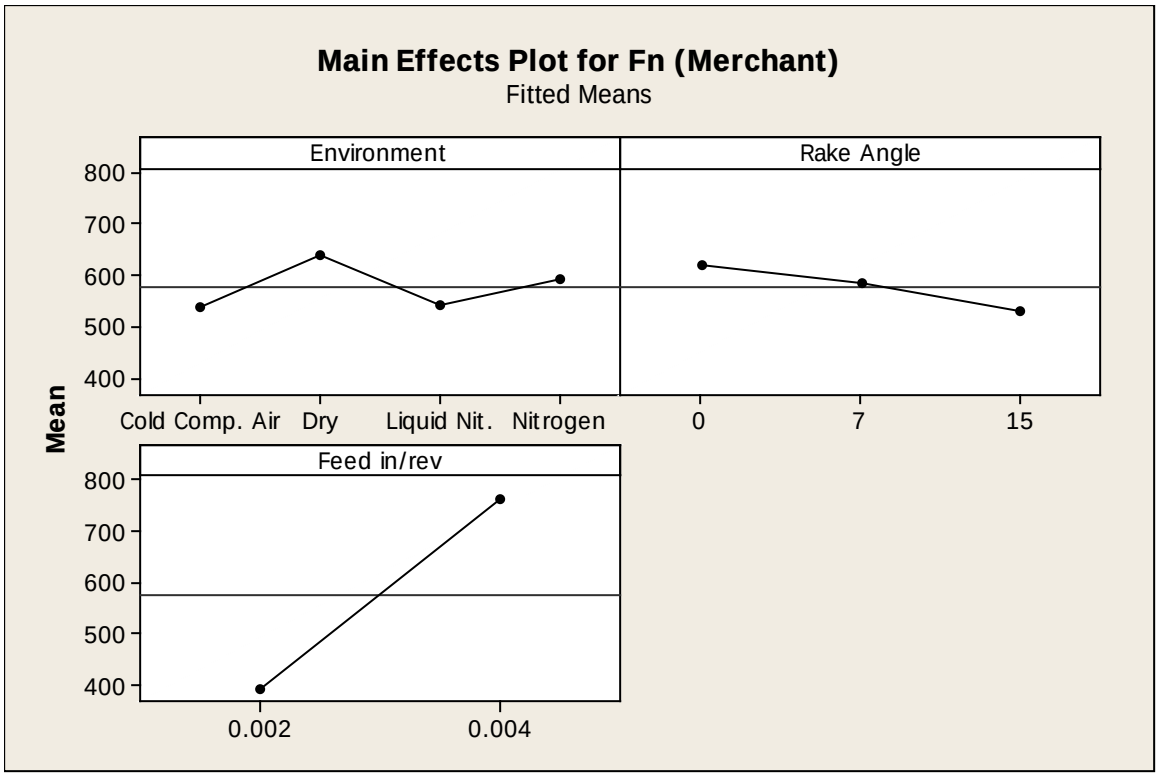
Main Effects Plot for Fn (Merchant)
Fitted Means
Environment
Rake Angle
Feed in/rev
Mean
800
700
600
500
400
Cold Comp. Air
Dry
Liquid Nit.
Nitrogen
0
7
15
0.002
0.004

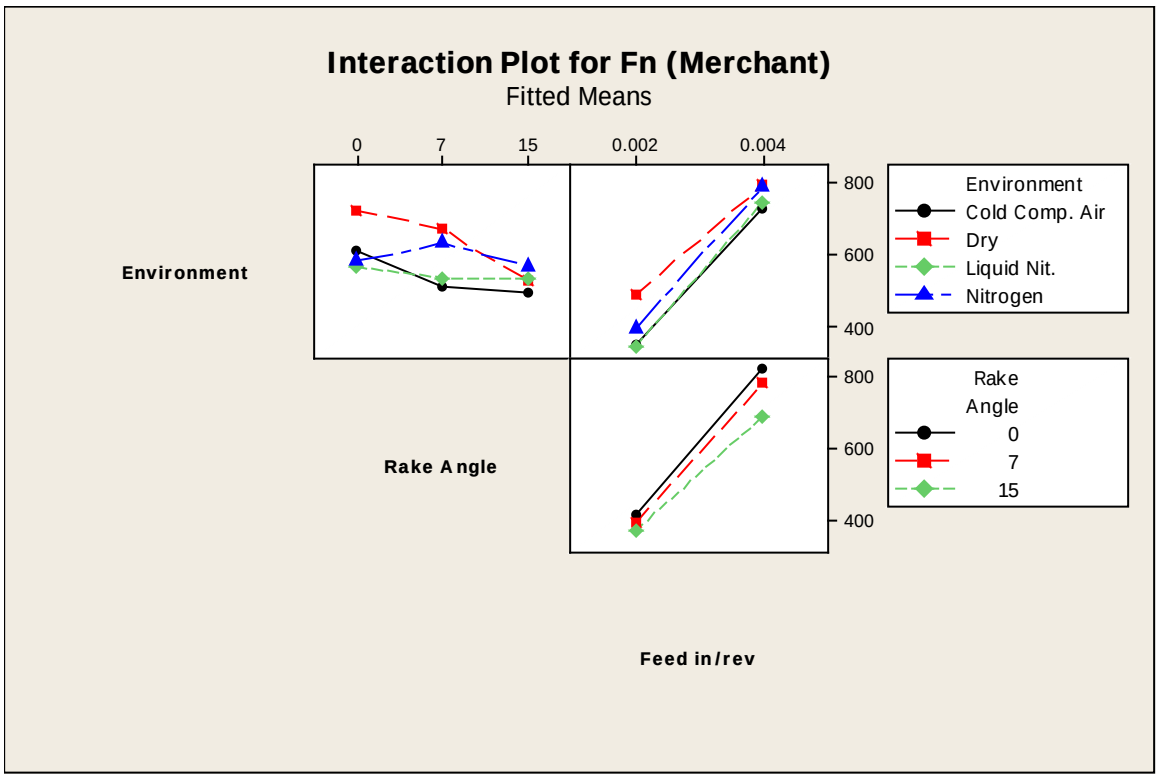
Interaction Plot for Fn (Merchant)
Fitted Means
Environment
Rake Angle
Feed in/rev
0
7
15
0.002
0.004
800
600
400
Environment
Cold Comp. Air
Dry
Liquid Nit.
Nitrogen
Rake Angle
0
7
15

Analysis of Variance for **Fs/Fn (Merchant)**, using Adjusted SS for Tests

Source	DF	Seq SS	Adj SS	Adj MS	F	P
Environment	3	0.17994	0.17994	0.05998	1.12	0.345
Rake Angle	2	0.56640	0.56640	0.28320	5.30	0.007
Feed in/rev	1	0.02911	0.02911	0.02911	0.55	0.463
Environment*Rake Angle	6	0.96677	0.96677	0.16113	3.02	0.011
Environment*Feed in/rev	3	0.20165	0.20165	0.06722	1.26	0.295
Rake Angle*Feed in/rev	2	0.07534	0.07534	0.03767	0.71	0.497
Environment*Rake Angle*Feed in/rev	6	0.24260	0.24260	0.04043	0.76	0.606
Error	72	3.84516	3.84516	0.05341		
Total	95	6.10698				

S = 0.231095 R-Sq = 37.04% R-Sq(adj) = 16.92%

Unusual Observations for Fs/Fn (Merchant)

Obs	Fs/Fn (Merchant)	Fit	SE Fit	Residual	St Resid	
53	0.77649	1.31077	0.11555	-0.53428	-2.67	R
54	0.73229	1.31077	0.11555	-0.57849	-2.89	R
55	3.00015	1.31077	0.11555	1.68938	8.44	R
56	0.73417	1.31077	0.11555	-0.57661	-2.88	R

R denotes an observation with a large standardized residual.

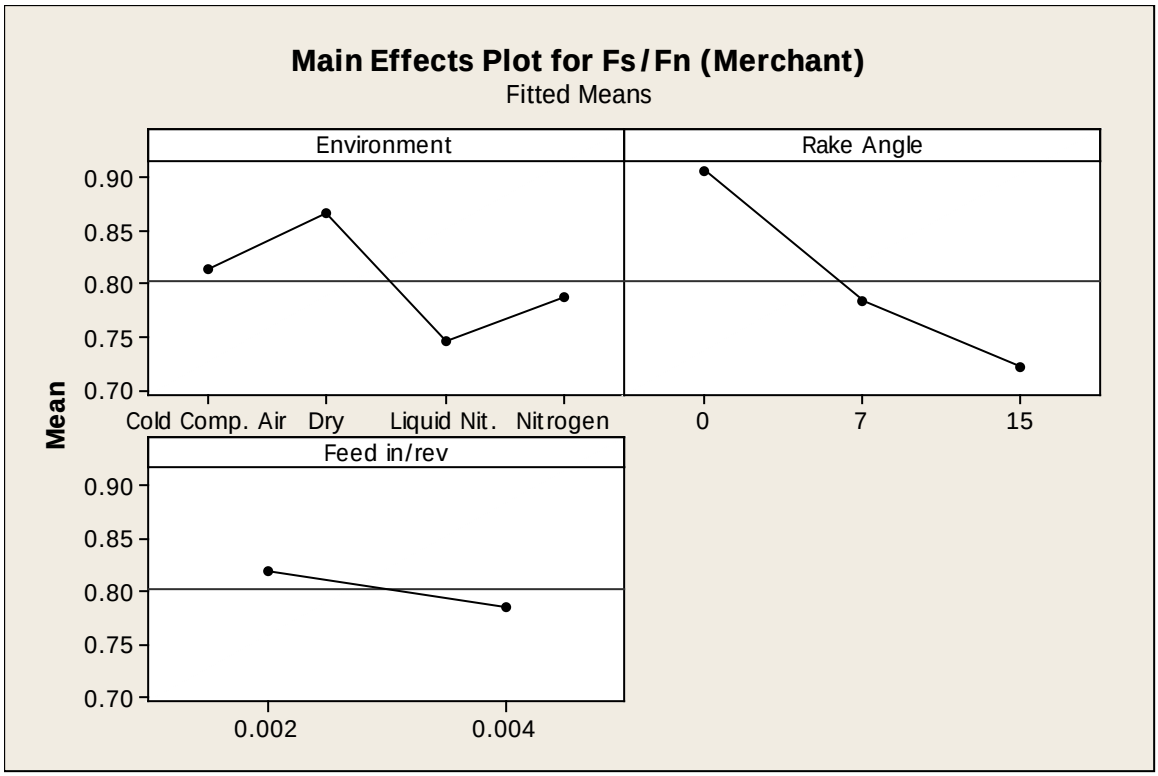
Main Effects Plot for Fs/Fn (Merchant)
Fitted Means
Environment
Rake Angle
Feed in/rev
Mean
0.90
0.85
0.80
0.75
0.70
Cold Comp. Air
Dry
Liquid Nit.
Nitrogen
0
7
15
0.002
0.004

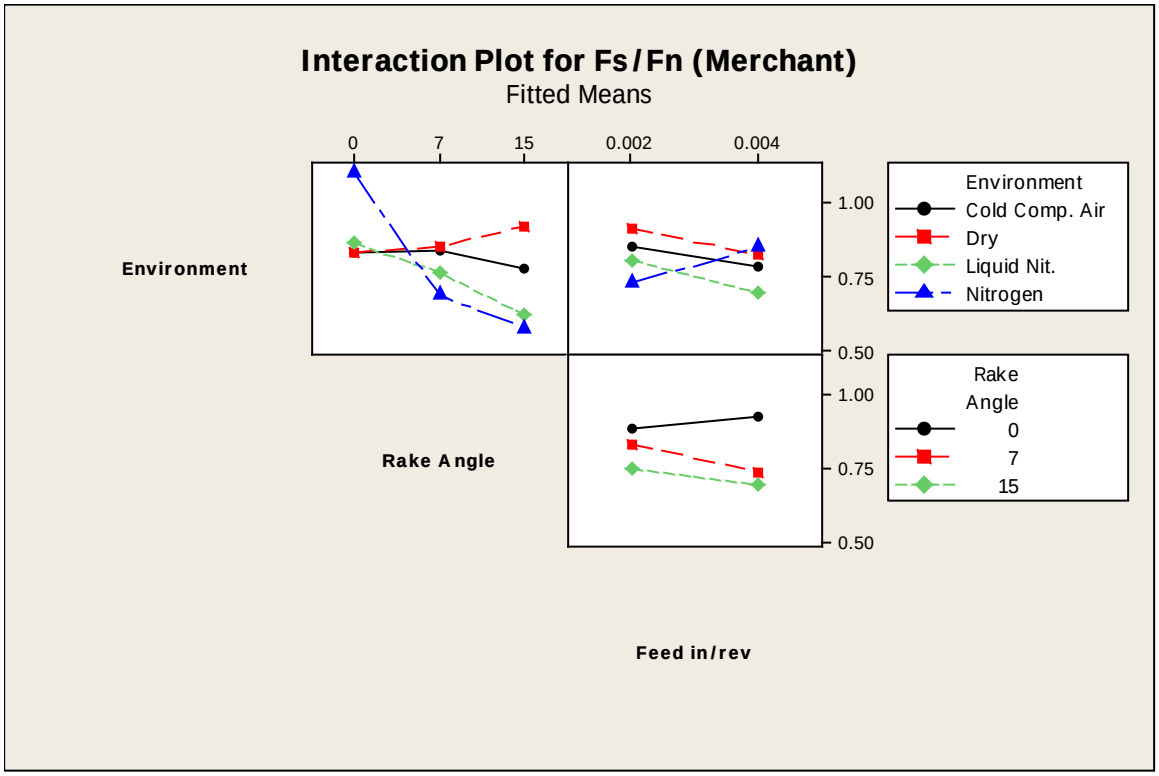
Interaction Plot for Fs/Fn (Merchant)
Fitted Means
Environment
Rake Angle
Feed in/rev
0
7
15
0.002
0.004
1.00
0.75
0.50
Environment
Cold Comp. Air
Dry
Liquid Nit.
Nitrogen
Rake Angle
0
7
15

Analysis of Variance for **Fs (Payton)**, using Adjusted SS for Tests

Source	DF	Seq SS	Adj SS	Adj MS	F	P
Environment	3	50056	50056	16685	6.77	0.000
Rake Angle	2	55577	55577	27789	11.28	0.000
Feed in/rev	1	29733	29733	29733	12.07	0.001
Environment*Rake Angle	6	20250	20250	3375	1.37	0.238
Environment*Feed in/rev	3	5421	5421	1807	0.73	0.535
Rake Angle*Feed in/rev	2	3926	3926	1963	0.80	0.455
Environment*Rake Angle*Feed in/rev	6	10649	10649	1775	0.72	0.634
Error	72	177398	177398	2464		
Total	95	353010				

S = 49.6373 R-Sq = 49.75% R-Sq(adj) = 33.69%

Unusual Observations for Fs (Payton)

Obs	Fs (Payton)	Fit	SE Fit	Residual	St Resid
53	130.922	234.315	24.819	-103.393	-2.41 R
54	104.372	234.315	24.819	-129.943	-3.02 R
55	595.995	234.315	24.819	361.680	8.41 R
56	105.970	234.315	24.819	-128.344	-2.99 R

R denotes an observation with a large standardized residual.

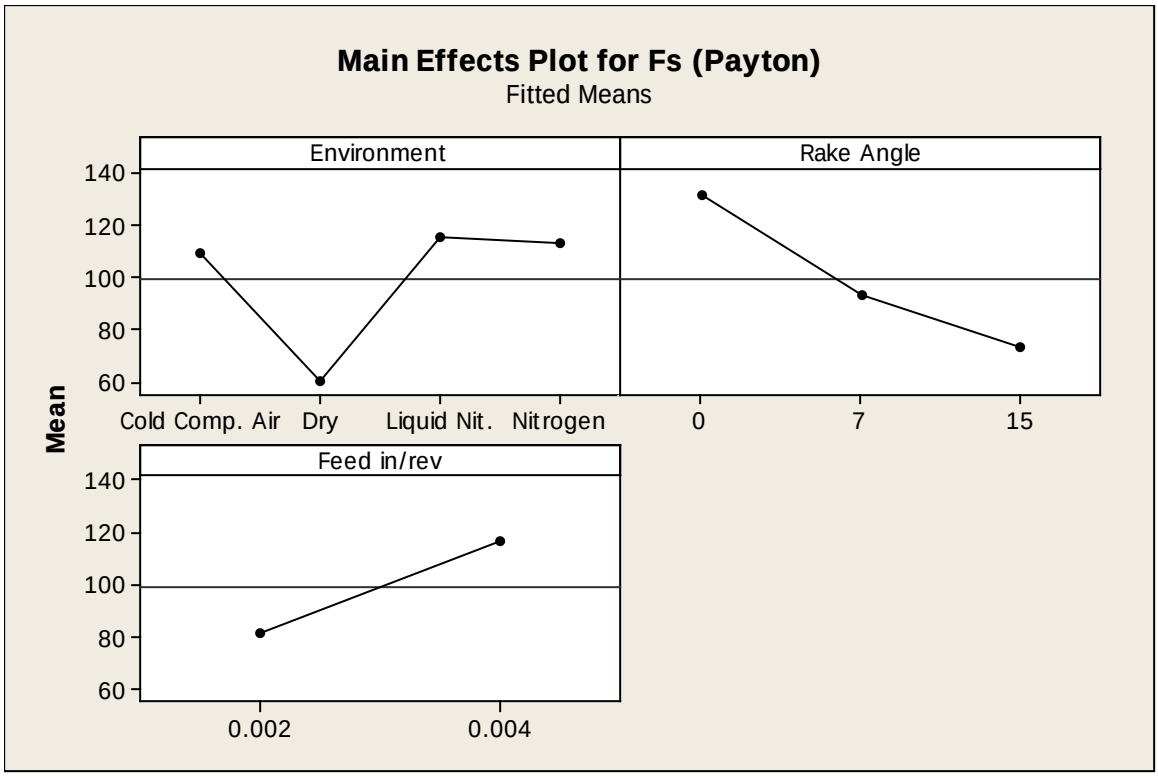
Main Effects Plot for Fs (Payton)
Fitted Means
Environment
Rake Angle
Feed in/rev
Mean
140
120
100
80
60
Cold Comp. Air
Dry
Liquid Nit.
Nitrogen
0
7
15
0.002
0.004

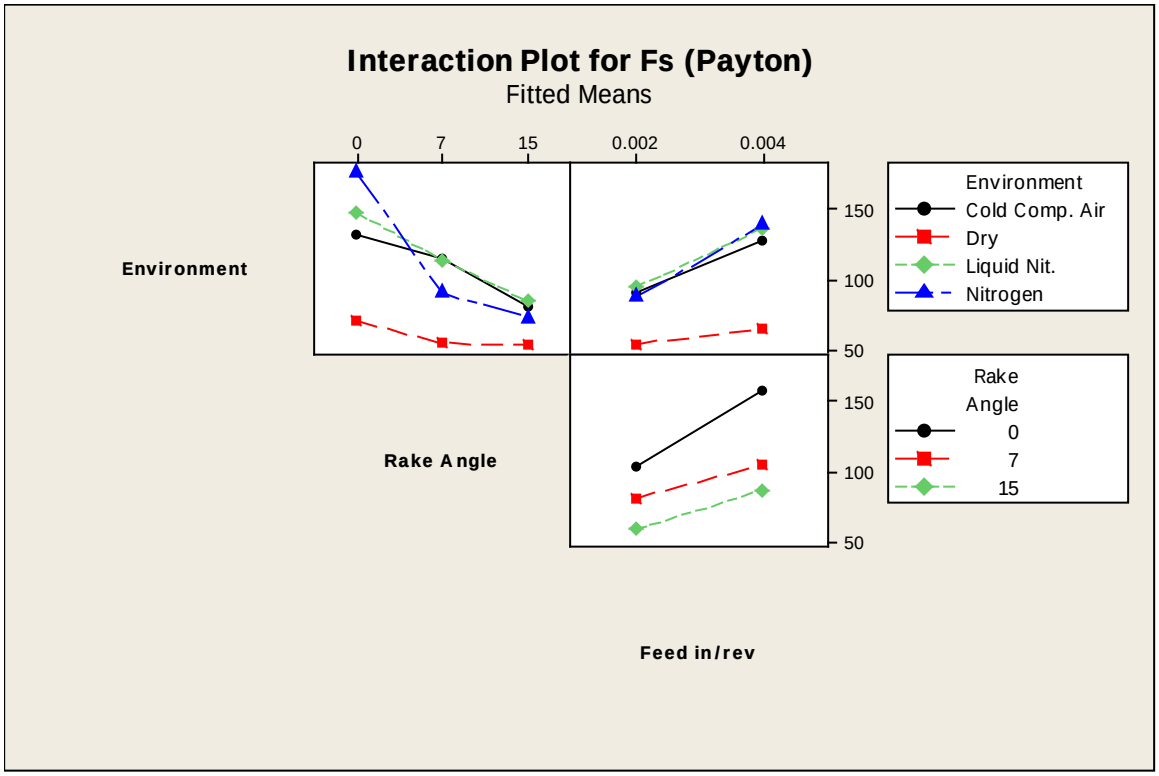
Interaction Plot for Fs (Payton)
Fitted Means
Environment
Rake Angle
Feed in/rev
0
7
15
0.002
0.004
150
100
50
Environment
Cold Comp. Air
Dry
Liquid Nit.
Nitrogen
Rake Angle
0
7
15

Analysis of Variance for **Fn (Payton)**, using Adjusted SS for Tests

Source	DF	Seq SS	Adj SS	Adj MS	F
Environment	3	445482	445482	148494	50.33
Rake Angle	2	375987	375987	187993	63.72
Feed in/rev	1	4855297	4855297	4855297	1645.73
Environment*Rake Angle	6	62345	62345	10391	3.52
Environment*Feed in/rev	3	54245	54245	18082	6.13
Rake Angle*Feed in/rev	2	80022	80022	40011	13.56
Environment*Rake Angle*Feed in/rev	6	75059	75059	12510	4.24
Error	72	212417	212417	2950	
Total	95	6160854			

Source	P
Environment	0.000
Rake Angle	0.000
Feed in/rev	0.000
Environment*Rake Angle	0.004
Environment*Feed in/rev	0.001
Rake Angle*Feed in/rev	0.000
Environment*Rake Angle*Feed in/rev	0.001
Error	
Total	

S = 54.3161 R-Sq = 96.55% R-Sq(adj) = 95.45%

Unusual Observations for Fn (Payton)

Obs	Fn (Payton)	Fit	SE Fit	Residual	St Resid	
54	1208.72	1072.46	27.16	136.26	2.90	R
55	705.77	1072.46	27.16	-366.68	-7.80	R
56	1223.11	1072.46	27.16	150.65	3.20	R

R denotes an observation with a large standardized residual.

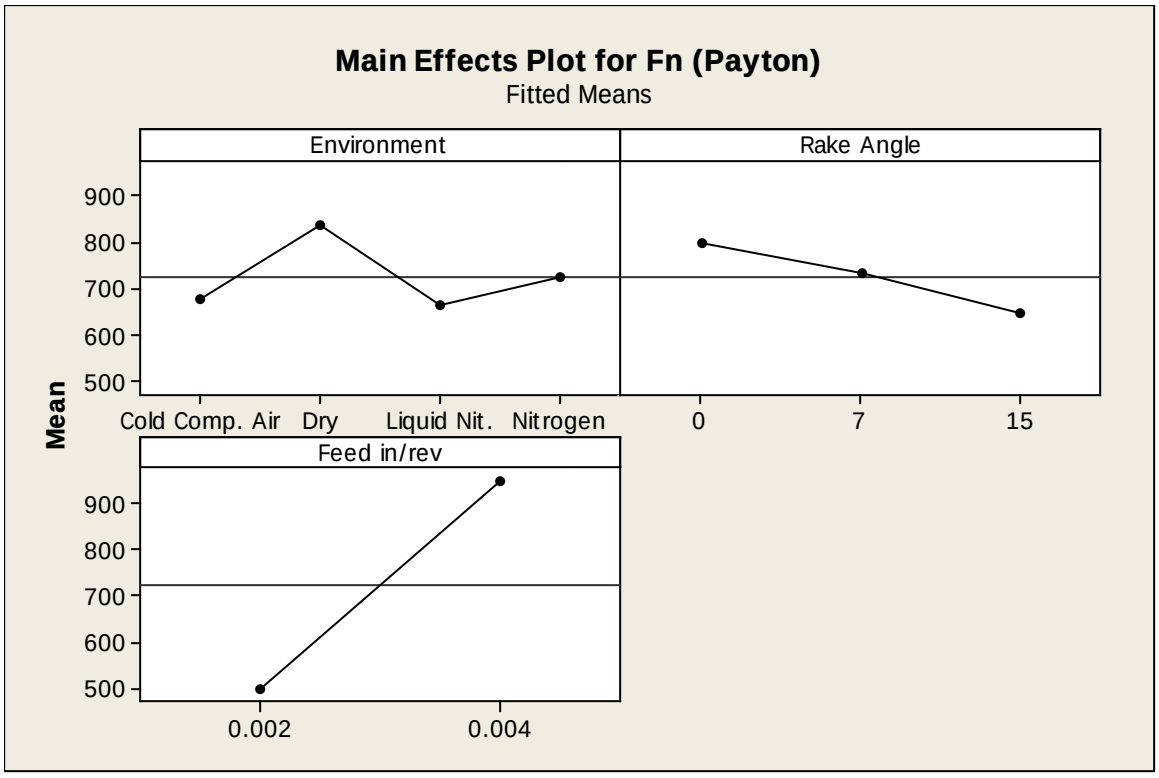
Main Effects Plot for Fn (Payton)
Fitted Means
Environment
Rake Angle
Feed in/rev
Mean
900
800
700
600
500
Cold Comp. Air
Dry
Liquid Nit.
Nitrogen
0
7
15
0.002
0.004

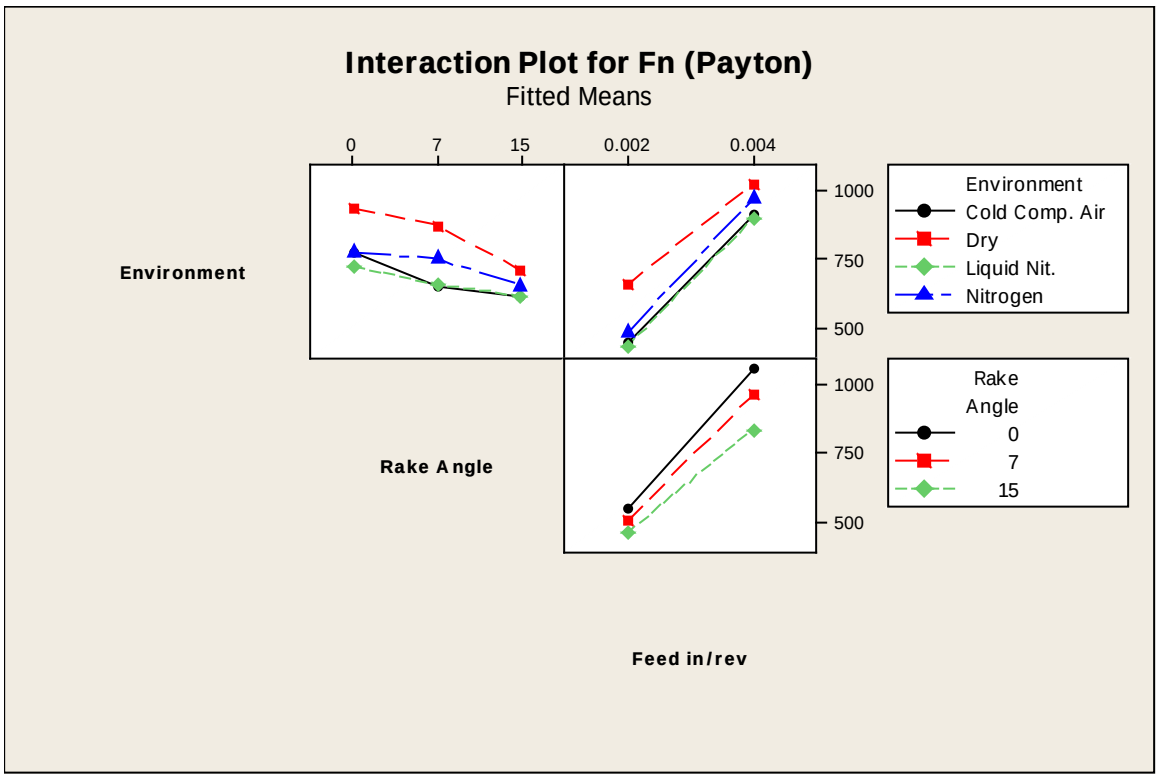
Interaction Plot for Fn (Payton)
Fitted Means
Environment
Rake Angle
Feed in/rev
0
7
15
0.002
0.004
1000
750
500
Environment
Cold Comp. Air
Dry
Liquid Nit.
Nitrogen
Rake Angle
0
7
15

Analysis of Variance for **Fs/Fn (Payton)**, using Adjusted SS for Tests

Source	DF	Seq SS	Adj SS	Adj MS	F
Environment	3	0.190441	0.190441	0.063480	10.60
Rake Angle	2	0.084339	0.084339	0.042170	7.04
Feed in/rev	1	0.046481	0.046481	0.046481	7.76
Environment*Rake Angle	6	0.066748	0.066748	0.011125	1.86
Environment*Feed in/rev	3	0.012310	0.012310	0.004103	0.69
Rake Angle*Feed in/rev	2	0.004445	0.004445	0.002222	0.37
Environment*Rake Angle*Feed in/rev	6	0.020093	0.020093	0.003349	0.56
Error	72	0.431248	0.431248	0.005990	
Total	95	0.856105			

Source	P
Environment	0.000
Rake Angle	0.002
Feed in/rev	0.007
Environment*Rake Angle	0.100
Environment*Feed in/rev	0.564
Rake Angle*Feed in/rev	0.691
Environment*Rake Angle*Feed in/rev	0.761
Error	
Total	

S = 0.0773922 R-Sq = 49.63% R-Sq(adj) = 33.54%

Unusual Observations for Fs/Fn (Payton)

Obs	Fs/Fn (Payton)	Fit	SE Fit	Residual	St Resid
53	0.113625	0.282768	0.038696	-0.169143	-2.52 R
54	0.086349	0.282768	0.038696	-0.196419	-2.93 R
55	0.844457	0.282768	0.038696	0.561689	8.38 R
56	0.086640	0.282768	0.038696	-0.196128	-2.93 R

R denotes an observation with a large standardized residual.

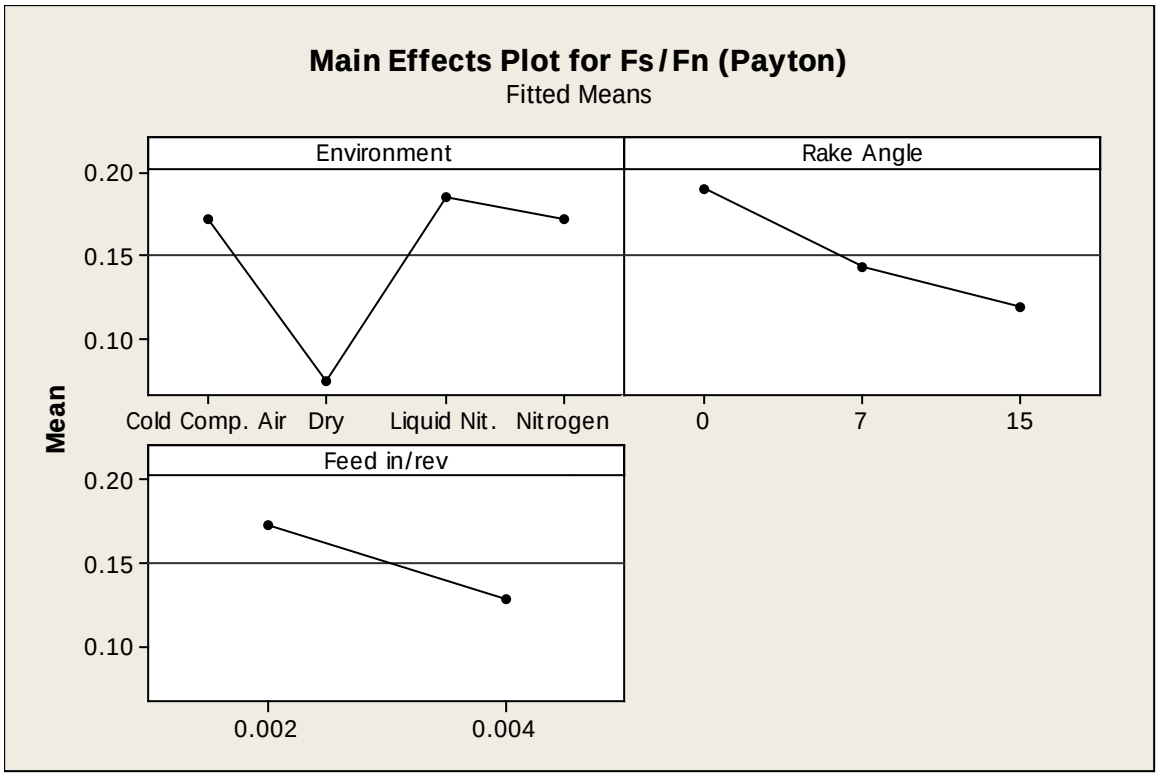
Main Effects Plot for Fs/Fn (Payton)
Fitted Means
Environment
Rake Angle
Feed in/rev
Mean
0.20
0.15
0.10
Cold Comp. Air
Dry
Liquid Nit.
Nitrogen
0
7
15
0.002
0.004

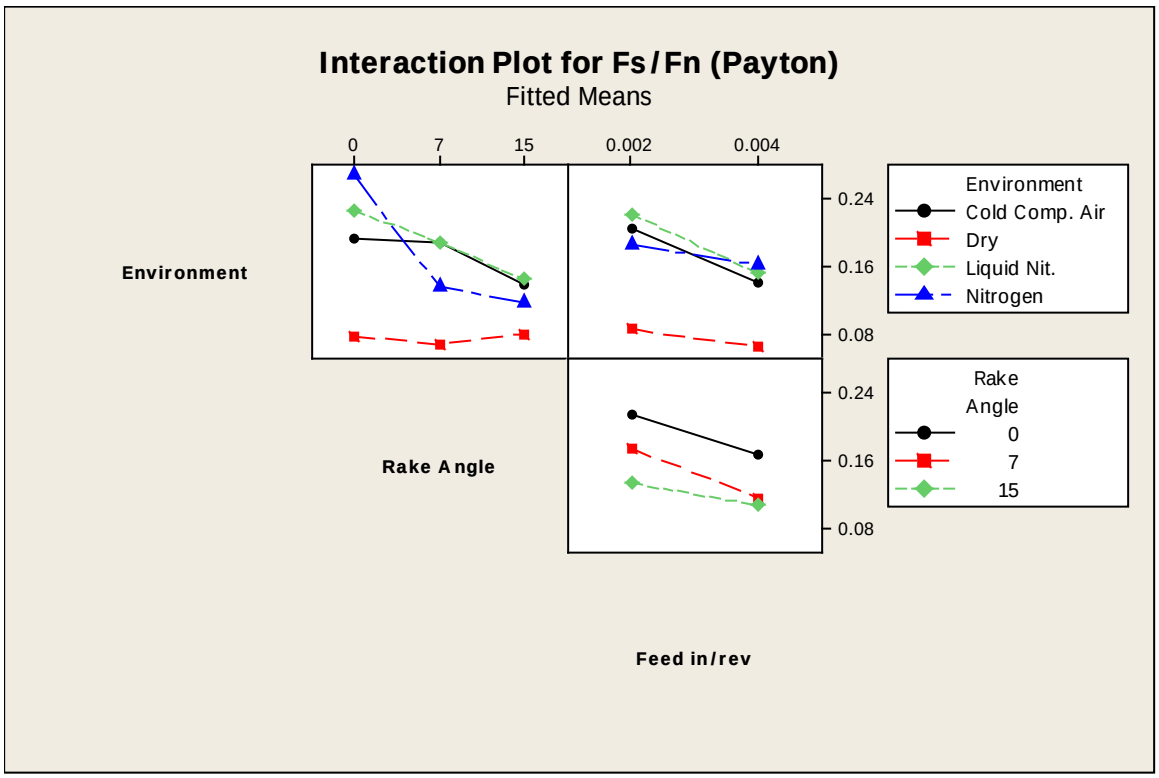
Interaction Plot for Fs/Fn (Payton)
Fitted Means
Environment
Rake Angle
Feed in/rev
0
7
15
0.002
0.004
0.24
0.16
0.08
Environment
Cold Comp. Air
Dry
Liquid Nit.
Nitrogen
Rake Angle
0
7
15

Analysis of Variance for **Beta** (degrees), using Adjusted SS for Tests

Source	DF	Seq SS	Adj SS	Adj MS	F	P
Environment	3	583.89	583.89	194.63	14.96	0.000
Rake Angle	2	2020.23	2020.23	1010.11	77.64	0.000
Feed in/rev	1	160.96	160.96	160.96	12.37	0.001
Environment*Rake Angle	6	165.65	165.65	27.61	2.12	0.061
Environment*Feed in/rev	3	30.19	30.19	10.06	0.77	0.513
Rake Angle*Feed in/rev	2	15.63	15.63	7.82	0.60	0.551
Environment*Rake Angle*Feed in/rev	6	42.30	42.30	7.05	0.54	0.775
Error	72	936.71	936.71	13.01		
Total	95	3955.55				

S = 3.60691   R-Sq = 76.32%   R-Sq(adj) = 68.75%

Unusual Observations for Beta (degrees)

Obs	Beta (degrees)	Fit	SE Fit	Residual	St Resid	
53	38.5176	30.8627	1.8035	7.6548	2.45	R
54	40.0648	30.8627	1.8035	9.2021	2.95	R
55	4.8203	30.8627	1.8035	-26.0424	-8.34	R
56	40.0482	30.8627	1.8035	9.1855	2.94	R

R denotes an observation with a large standardized residual.

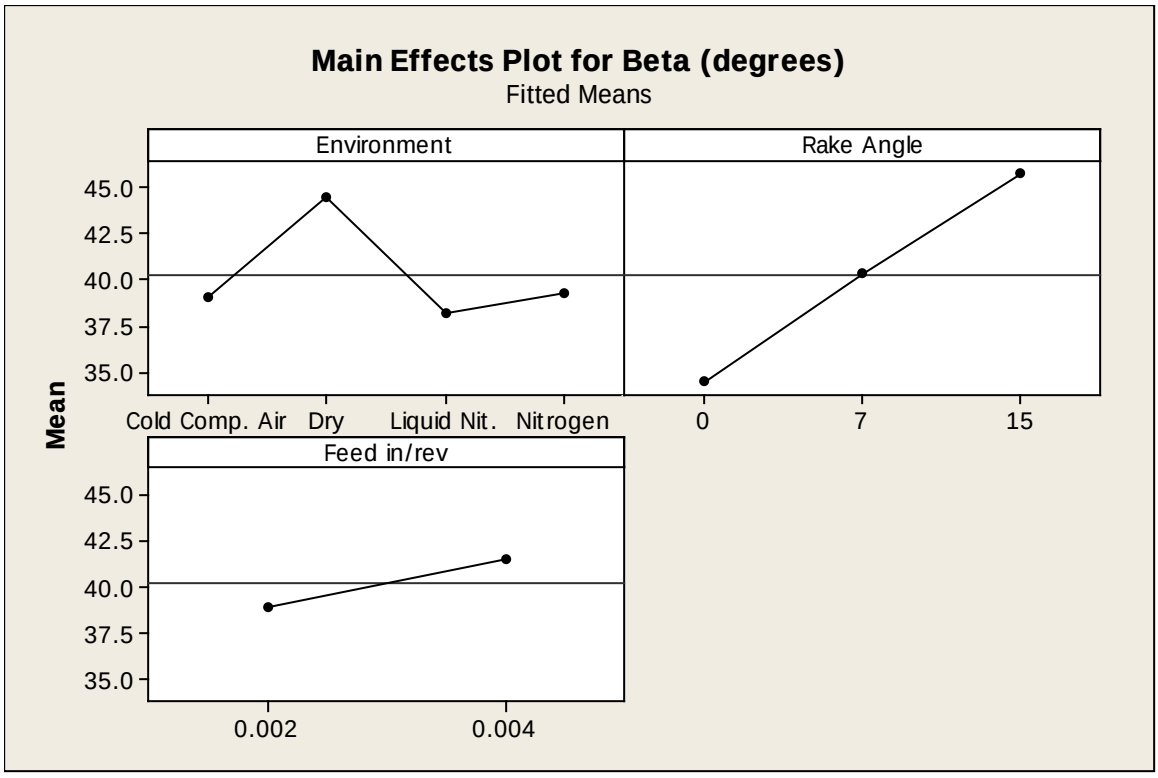
Main Effects Plot for Beta (degrees)
Fitted Means
Environment
Rake Angle
Feed in/rev
Mean
45.0
42.5
40.0
37.5
35.0
Cold Comp. Air
Dry
Liquid Nit.
Nitrogen
0
7
15
0.002
0.004

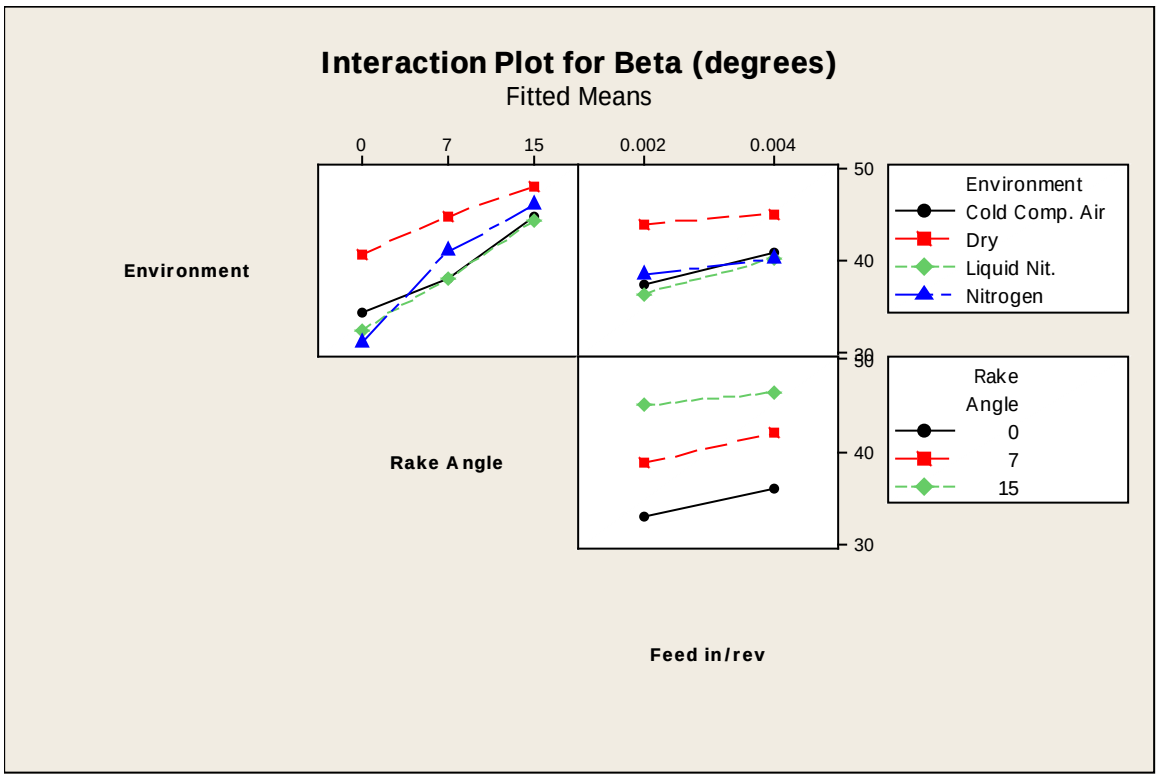
Interaction Plot for Beta (degrees)
Fitted Means
Environment
Rake Angle
Feed in/rev
0
7
15
0.002
0.004
50
40
30
Environment
Cold Comp. Air
Dry
Liquid Nit.
Nitrogen
Rake Angle
0
7
15

Analysis of Variance for **Shear Area**, As, using Adjusted SS for Tests

Source	DF	Seq SS	Adj SS	Adj MS
Environment	3	0.0000085	0.0000085	0.0000028
Rake Angle	2	0.0000052	0.0000052	0.0000026
Feed in/rev	1	0.0000161	0.0000161	0.0000161
Environment*Rake Angle	6	0.0000002	0.0000002	0.0000000
Environment*Feed in/rev	3	0.0000002	0.0000002	0.0000001
Rake Angle*Feed in/rev	2	0.0000011	0.0000011	0.0000005
Environment*Rake Angle*Feed in/rev	6	0.0000001	0.0000001	0.0000000
Error	72	0.0000001	0.0000001	0.0000000
Total	95	0.0000316		

Source	F	P
Environment	2200.78	0.000
Rake Angle	2022.72	0.000
Feed in/rev	12431.54	0.000
Environment*Rake Angle	28.18	0.000
Environment*Feed in/rev	48.58	0.000
Rake Angle*Feed in/rev	416.33	0.000
Environment*Rake Angle*Feed in/rev	17.81	0.000
Error		
Total		

S = 0.0000359798 R-Sq = 99.70% R-Sq(adj) = 99.61%

Unusual Observations for Shear Area, As

Obs	Shear Area, As	Fit	SE Fit	Residual	St Resid	
13	0.002244	0.002130	0.000018	0.000113	3.64	R
16	0.002047	0.002130	0.000018	-0.000083	-2.66	R
21	0.001746	0.001826	0.000018	-0.000080	-2.57	R
22	0.002010	0.001826	0.000018	0.000184	5.91	R
23	0.001707	0.001826	0.000018	-0.000120	-3.84	R

R denotes an observation with a large standardized residual.

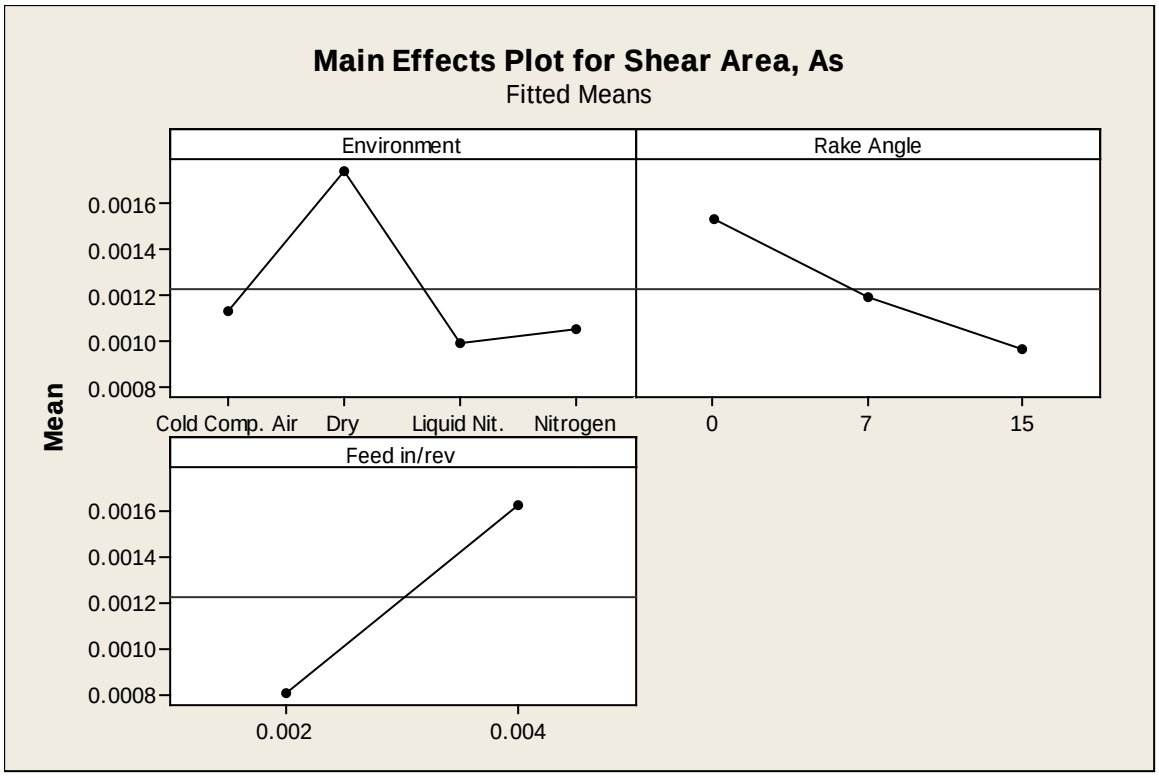
Main Effects Plot for Shear Area, As
Fitted Means
Environment
Rake Angle
Feed in/rev
Mean
0.0016
0.0014
0.0012
0.0010
0.0008
Cold Comp. Air
Dry
Liquid Nit.
Nitrogen
0
7
15
0.002
0.004

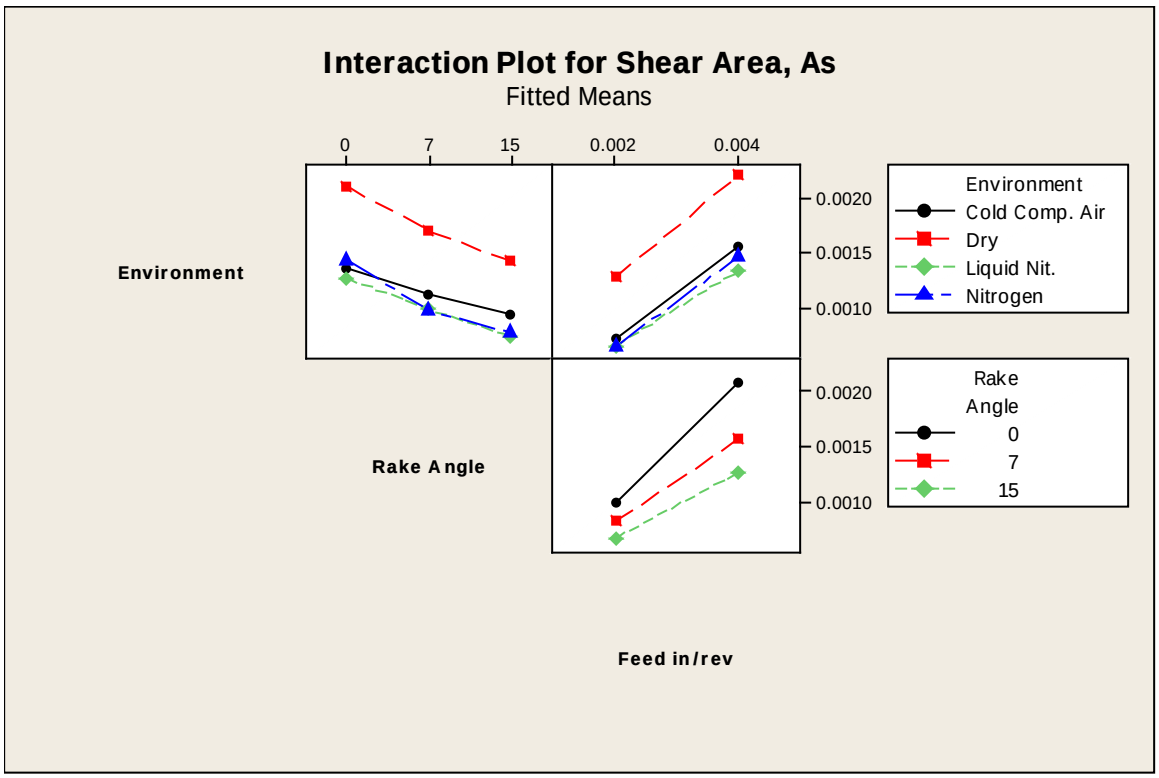
Interaction Plot for Shear Area, As
Fitted Means
0
7
15
0.002
0.004
Environment
Rake Angle
0.0020
0.0015
0.0010
Environment
Cold Comp. Air
Dry
Liquid Nit.
Nitrogen
Rake Angle
0
7
15
Feed in/rev

Analysis of Variance for **Shear Stress, Ts Merchant** (Mpa), using Adjusted SS for
Tests

Source	DF	Seq SS	Adj SS	Adj MS	F	P
Environment	3	344937	344937	114979	249.87	0.000
Rake Angle	2	91892	91892	45946	99.85	0.000
Feed in/rev	1	106235	106235	106235	230.87	0.000
Environment*Rake Angle	6	13613	13613	2269	4.93	0.000
Environment*Feed in/rev	3	1843	1843	614	1.34	0.270
Rake Angle*Feed in/rev	2	1088	1088	544	1.18	0.313
Environment*Rake Angle*Feed in/rev	6	11885	11885	1981	4.30	0.001
Error	72	33131	33131	460		
Total	95	604624				

S = 21.4511 R-Sq = 94.52% R-Sq(adj) = 92.77%

Unusual Observations for Shear Stress, Ts Merchant (Mpa)

Obs	Shear Stress, Ts Merchant (Mpa)	Fit	SE Fit	Residual	St Resid	
22	456.771	500.631	10.726	-43.860	-2.36	R
51	580.177	617.532	10.726	-37.355	-2.01	R
52	685.685	617.532	10.726	68.153	3.67	R
55	666.090	577.886	10.726	88.205	4.75	R
81	590.820	649.154	10.726	-58.334	-3.14	R
82	687.845	649.154	10.726	38.692	2.08	R

R denotes an observation with a large standardized residual.

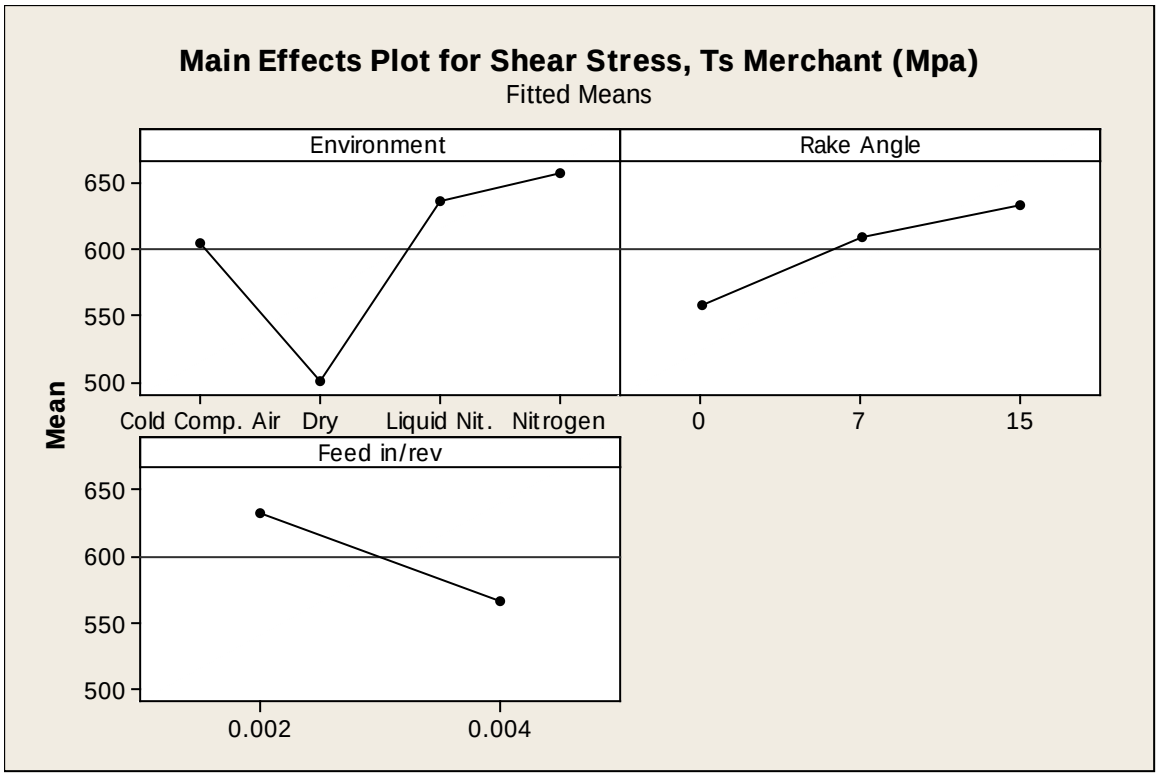
Main Effects Plot for Shear Stress, Ts Merchant (Mpa)
Fitted Means
Environment
Rake Angle
Feed in/rev
Mean
650
600
550
500
Cold Comp. Air
Dry
Liquid Nit.
Nitrogen
0
7
15
0.002
0.004

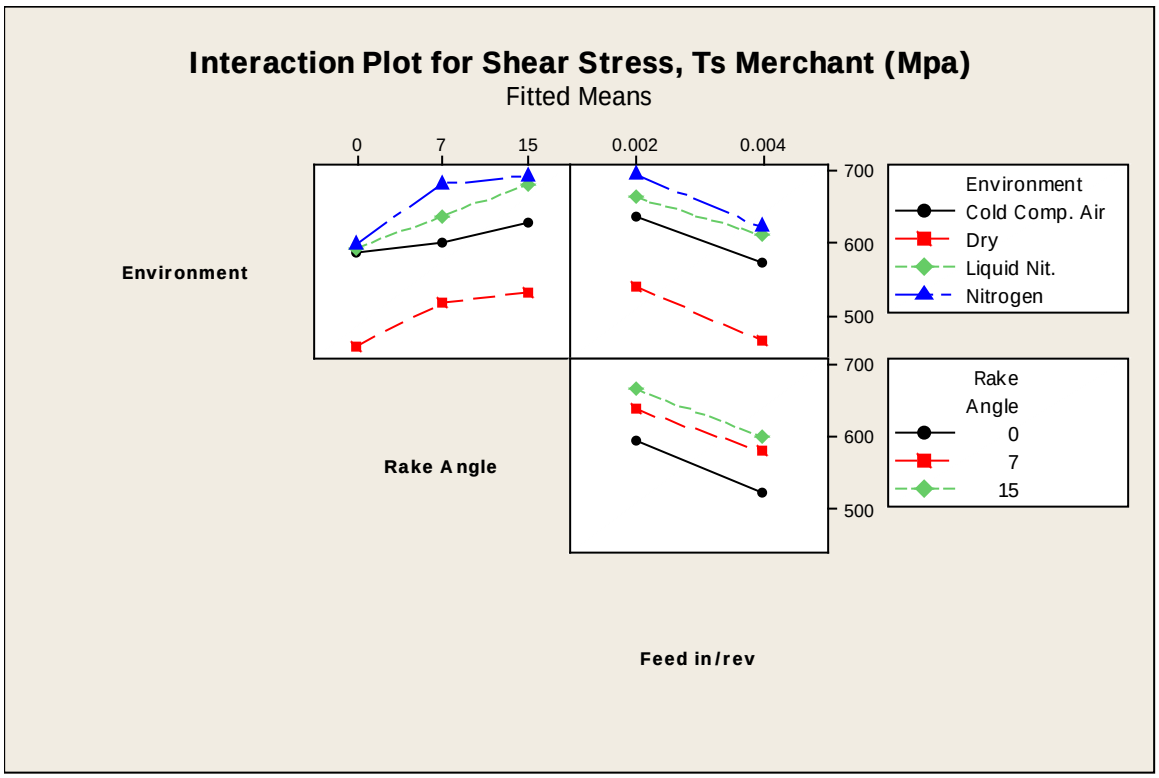
Interaction Plot for Shear Stress, Ts Merchant (Mpa)
Fitted Means
Environment
Rake Angle
Feed in/rev
0
7
15
0.002
0.004
700
600
500
Environment
Cold Comp. Air
Dry
Liquid Nit.
Nitrogen
Rake Angle
0
7
15

Analysis of Variance for **Shear Stress, Ts (Payton)** (Mpa), using Adjusted SS for
Tests

Source	DF	Seq SS	Adj SS	Adj MS	F	P
Environment	3	267439	267439	89146	60.09	0.000
Rake Angle	2	6758	6758	3379	2.28	0.110
Feed in/rev	1	73147	73147	73147	49.31	0.000
Environment*Rake Angle	6	9378	9378	1563	1.05	0.398
Environment*Feed in/rev	3	9536	9536	3179	2.14	0.102
Rake Angle*Feed in/rev	2	3789	3789	1894	1.28	0.285
Environment*Rake Angle*Feed in/rev	6	8463	8463	1411	0.95	0.465
Error	72	106812	106812	1484		
Total	95	485323				

S = 38.5163 R-Sq = 77.99% R-Sq(adj) = 70.96%

Unusual Observations for Shear Stress, Ts (Payton) (Mpa)

Obs	Shear Stress, Ts (Payton) (Mpa)	Fit	SE Fit	Residual	St Resid	
53	99.795	178.396	19.258	-78.601	-2.36	R
54	79.939	178.396	19.258	-98.457	-2.95	R
55	452.997	178.396	19.258	274.601	8.23	R
56	80.853	178.396	19.258	-97.543	-2.92	R

R denotes an observation with a large standardized residual.

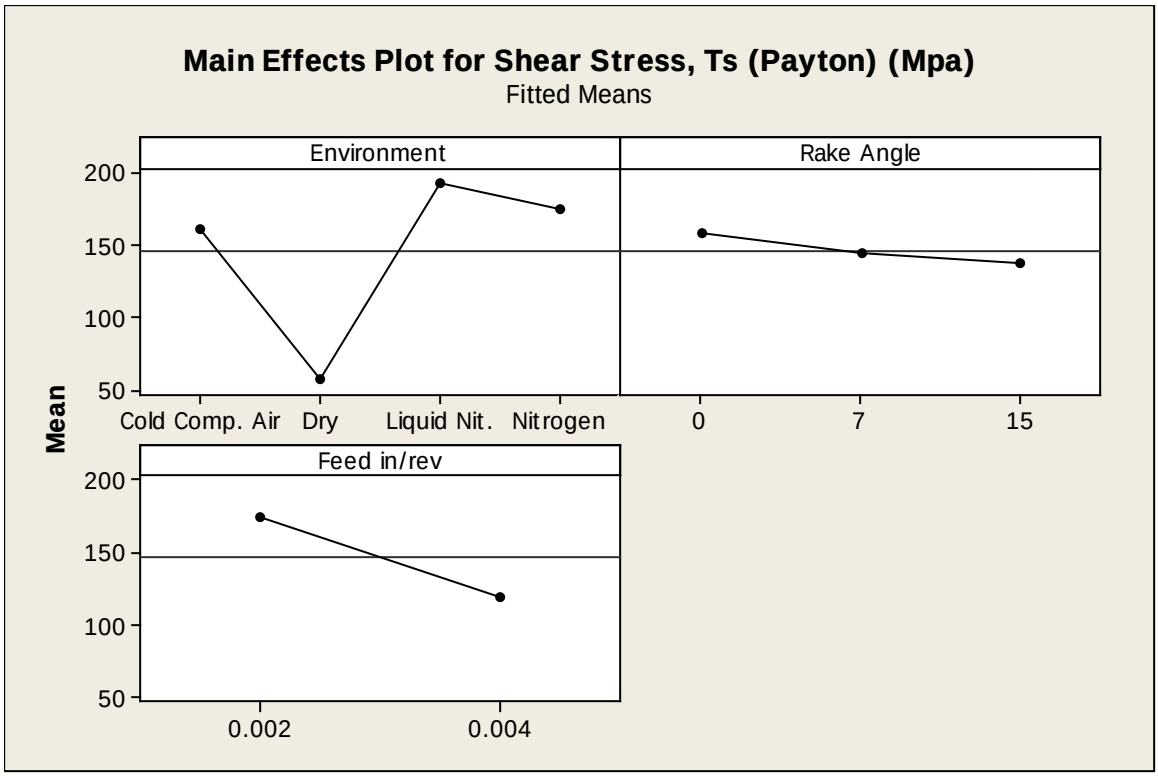
Main Effects Plot for Shear Stress, Ts (Payton) (Mpa)
Fitted Means
Environment
Rake Angle
Feed in/rev
Mean
200
150
100
50
Cold Comp. Air
Dry
Liquid Nit.
Nitrogen
0
7
15
0.002
0.004

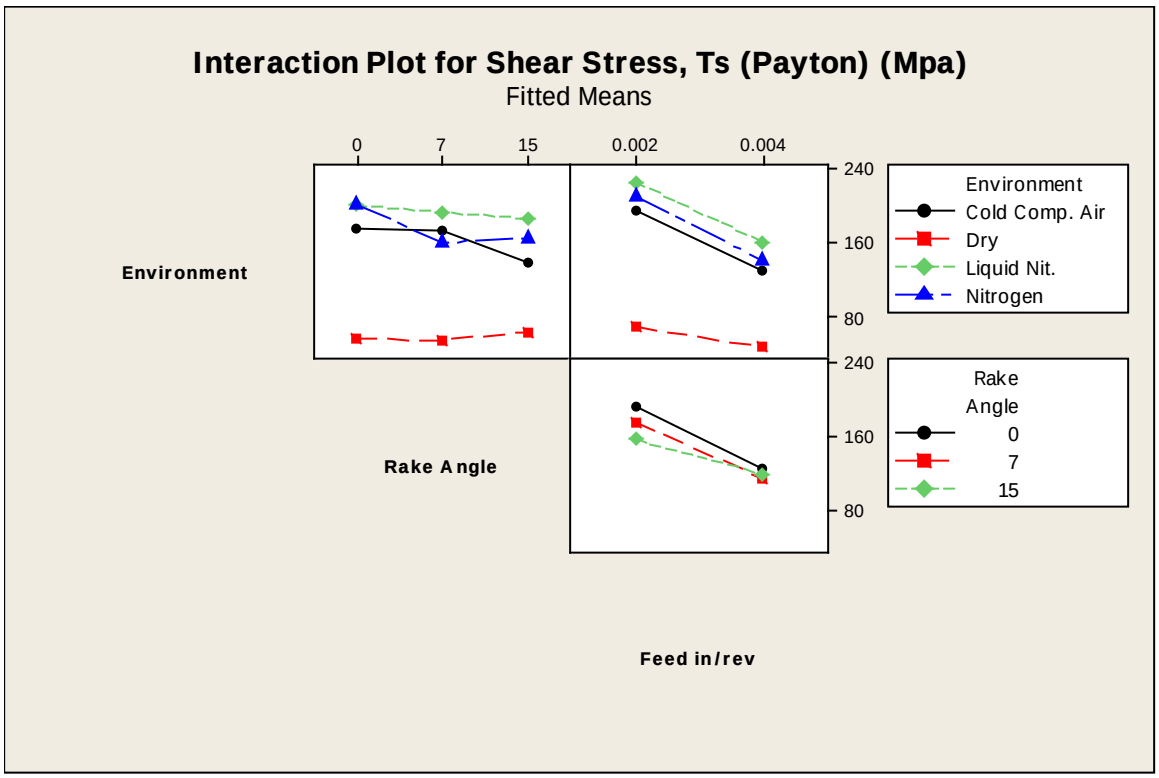
Interaction Plot for Shear Stress, Ts (Payton) (Mpa)
Fitted Means
Environment
Rake Angle
Feed in/rev
0
7
15
0.002
0.004
240
160
80
Environment
Cold Comp. Air
Dry
Liquid Nit.
Nitrogen
Rake Angle
0
7
15

Analysis of Variance for **Friction Co-efficient**, using Adjusted SS for Tests

Source	DF	Seq SS	Adj SS	Adj MS	F
Environment	3	0.177863	0.177863	0.059288	14.96
Rake Angle	2	0.615396	0.615396	0.307698	77.64
Feed in/rev	1	0.049030	0.049030	0.049030	12.37
Environment*Rake Angle	6	0.050459	0.050459	0.008410	2.12
Environment*Feed in/rev	3	0.009195	0.009195	0.003065	0.77
Rake Angle*Feed in/rev	2	0.004762	0.004762	0.002381	0.60
Environment*Rake Angle*Feed in/rev	6	0.012887	0.012887	0.002148	0.54
Error	72	0.285337	0.285337	0.003963	
Total	95	1.204929			

Source	P
Environment	0.000
Rake Angle	0.000
Feed in/rev	0.001
Environment*Rake Angle	0.061
Environment*Feed in/rev	0.513
Rake Angle*Feed in/rev	0.551
Environment*Rake Angle*Feed in/rev	0.775
Error	
Total	

S = 0.0629525 R-Sq = 76.32% R-Sq(adj) = 68.75%

Unusual Observations for Friction Co-efficient

Obs	Friction Co-efficient	Fit	SE Fit	Residual	St Resid	
53	0.672258	0.538656	0.031476	0.133602	2.45	R
54	0.699263	0.538656	0.031476	0.160606	2.95	R
55	0.084131	0.538656	0.031476	-0.454526	-8.34	R
56	0.698974	0.538656	0.031476	0.160318	2.94	R

R denotes an observation with a large standardized residual.

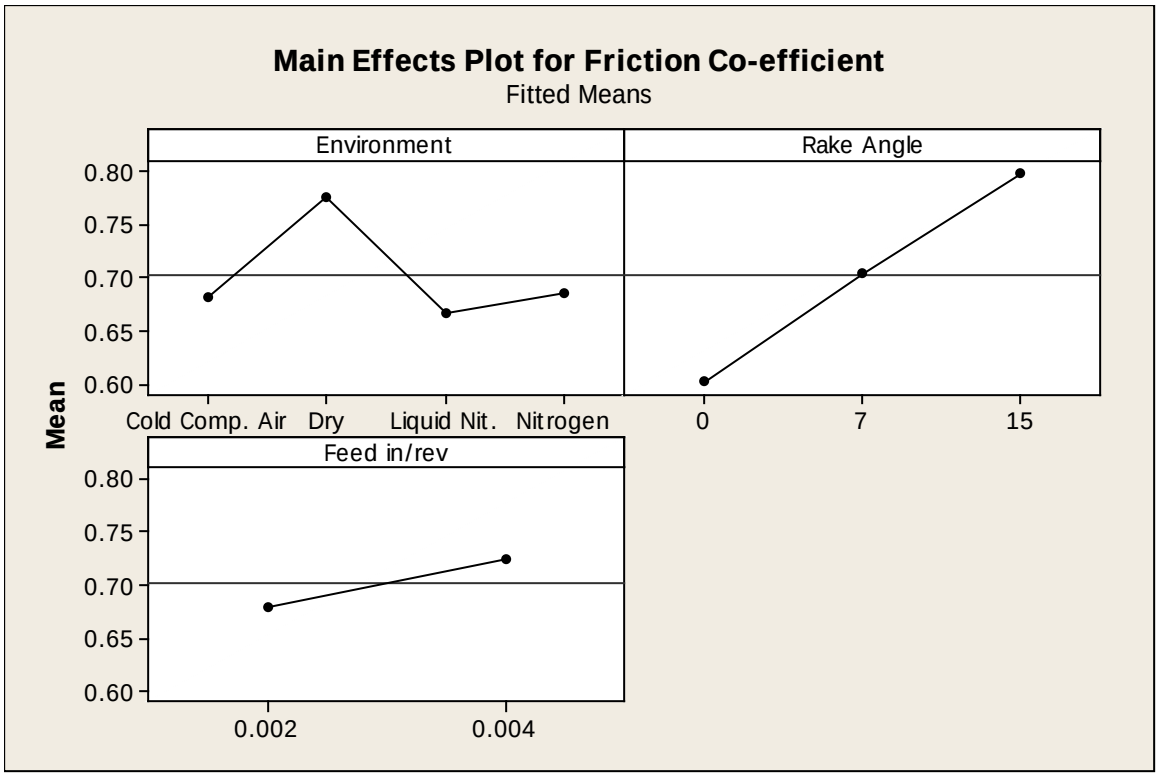
Main Effects Plot for Friction Co-efficient
Fitted Means
Environment
Rake Angle
Feed in/rev
Mean
0.80
0.75
0.70
0.65
0.60
Cold Comp. Air
Dry
Liquid Nit.
Nitrogen
0
7
15
0.002
0.004

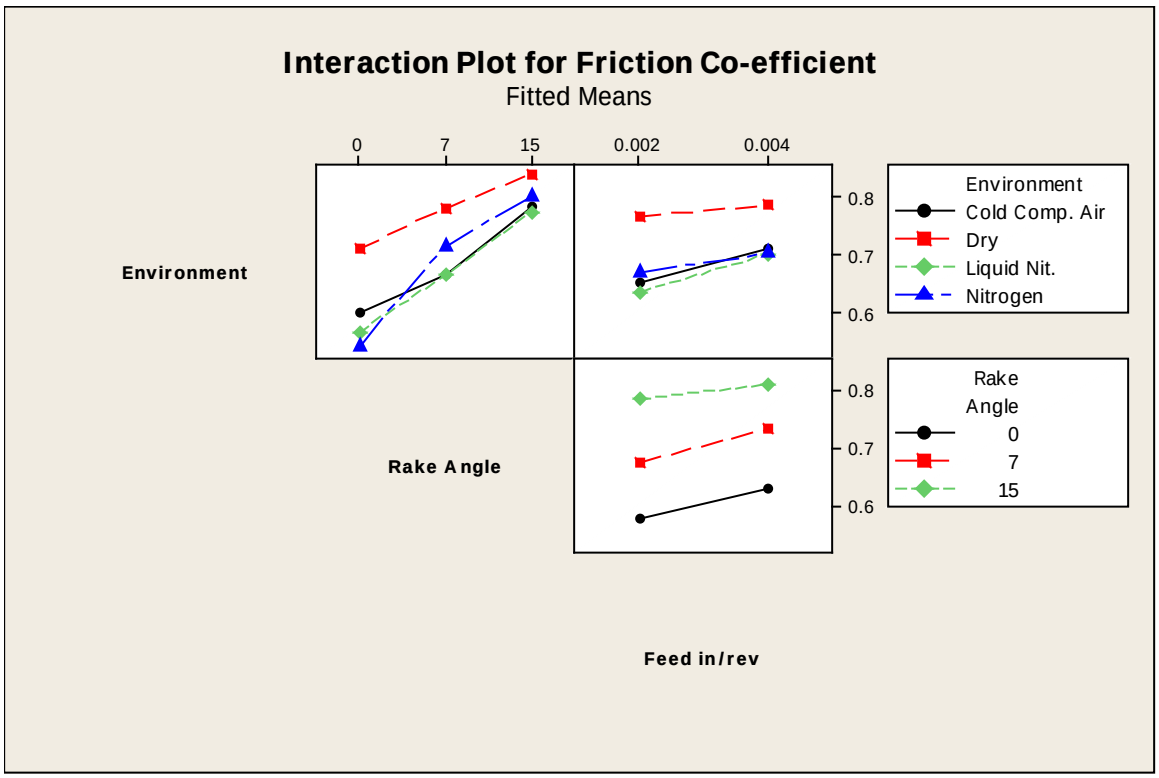
Interaction Plot for Friction Co-efficient
Fitted Means
Environment
Rake Angle
Feed in/rev
0
7
15
0.002
0.004
0.8
0.7
0.6
Environment
Cold Comp. Air
Dry
Liquid Nit.
Nitrogen
Rake Angle
0
7
15

Analysis of Variance for **Normal Stress (Merchant)**, using Adjusted SS for Tests

Source	DF	Seq SS	Adj SS	Adj MS
Environment	3	8.27148E+11	8.27148E+11	2.75716E+11
Rake Angle	2	5.26694E+11	5.26694E+11	2.63347E+11
Feed in/rev	1	6195262377	6195262377	6195262377
Environment*Rake Angle	6	3.52569E+11	3.52569E+11	58761533164
Environment*Feed in/rev	3	43092830644	43092830644	14364276881
Rake Angle*Feed in/rev	2	12003058869	12003058869	6001529435
Environment*Rake Angle*Feed in/rev	6	78315284584	78315284584	13052547431
Error	72	1.34122E+11	1.34122E+11	1862811536
Total	95	1.98014E+12		

Source	F	P
Environment	148.01	0.000
Rake Angle	141.37	0.000
Feed in/rev	3.33	0.072
Environment*Rake Angle	31.54	0.000
Environment*Feed in/rev	7.71	0.000
Rake Angle*Feed in/rev	3.22	0.046
Environment*Rake Angle*Feed in/rev	7.01	0.000
Error		
Total		

S = 43160.3 R-Sq = 93.23% R-Sq(adj) = 91.06%

Unusual Observations for Normal Stress (Merchant)

Obs	Normal Stress (Merchant)	Fit	SE Fit	Residual	St Resid
52	544082	449613	21580	94469	2.53 R
54	483674	391119	21580	92555	2.48 R
55	143238	391119	21580	-247881	-6.63 R
56	487134	391119	21580	96015	2.57 R

R denotes an observation with a large standardized residual.

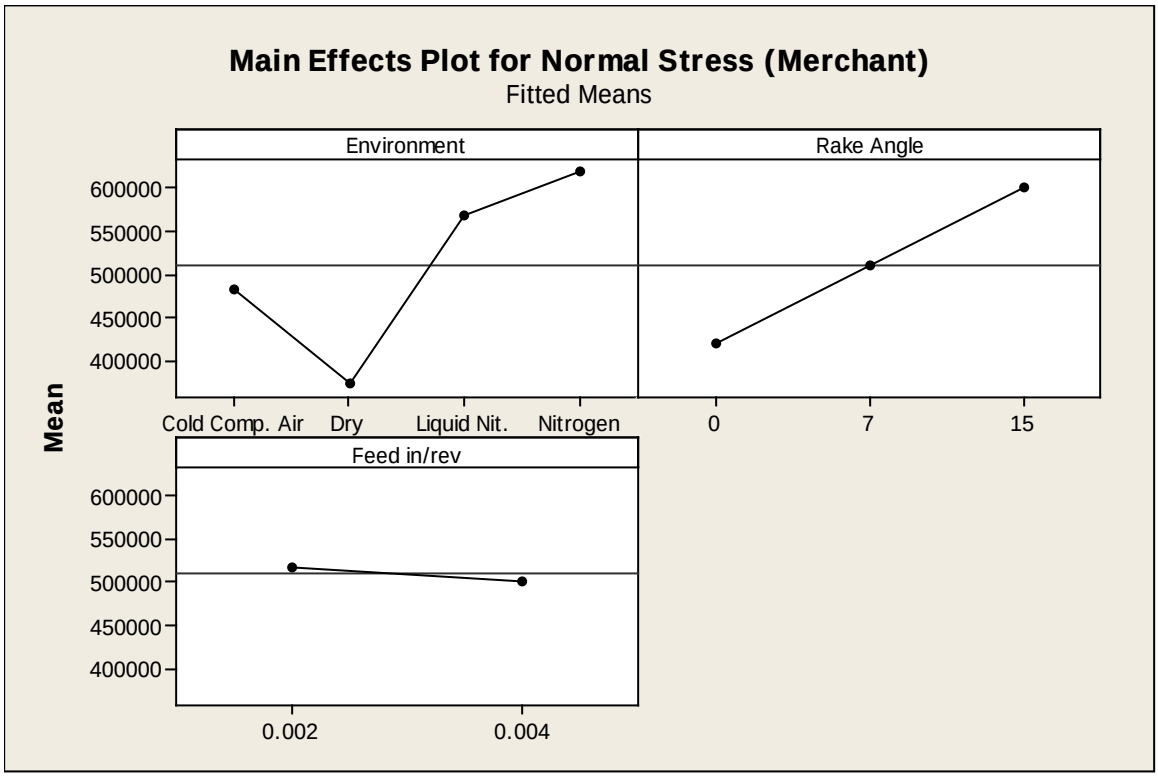
Main Effects Plot for Normal Stress (Merchant)
Fitted Means
Environment
Rake Angle
Feed in/rev
Mean
600000
550000
500000
450000
400000
Cold Comp. Air
Dry
Liquid Nit.
Nitrogen
0
7
15
0.002
0.004

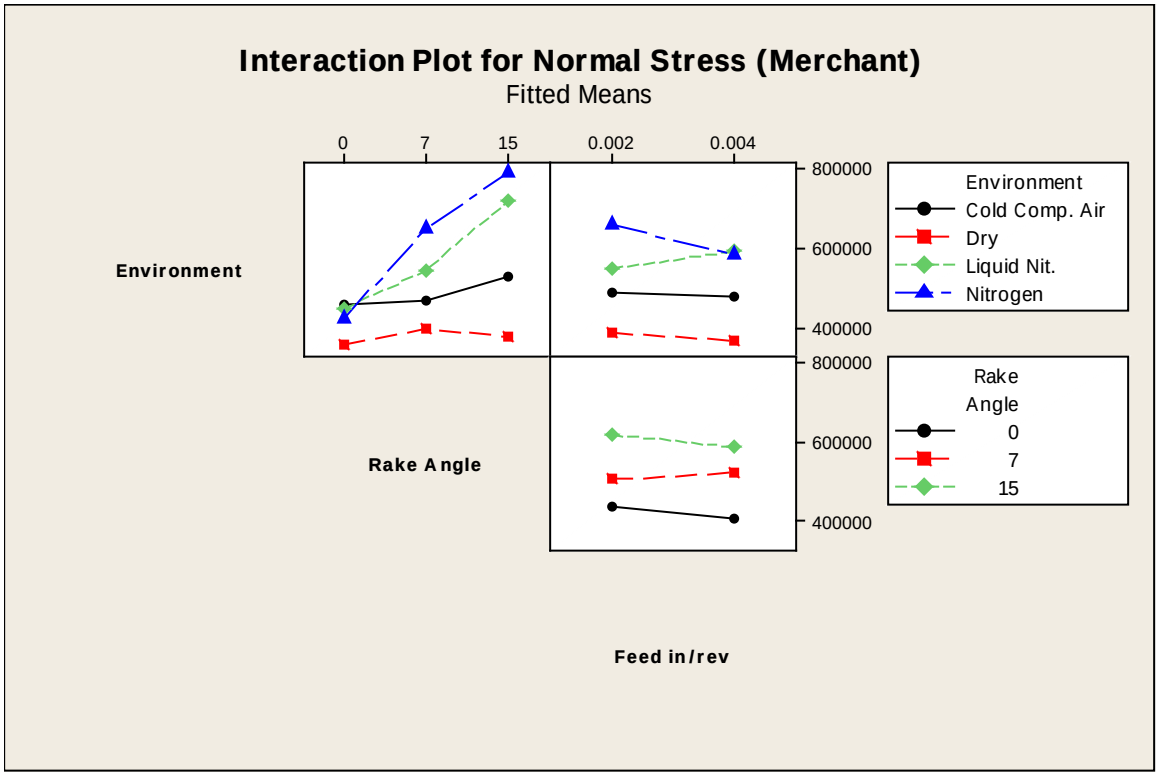
Interaction Plot for Normal Stress (Merchant)
Fitted Means
Environment
Rake Angle
Feed in/rev
0
7
15
0.002
0.004
800000
600000
400000
Environment
Cold Comp. Air
Dry
Liquid Nit.
Nitrogen
Rake Angle
0
7
15

Analysis of Variance for **Shear strain (Merchant)**, using Adjusted SS for Tests

Source	DF	Seq SS	Adj SS	Adj MS	F
Environment	3	70.3490	70.3490	23.4497	3282.20
Rake Angle	2	46.5596	46.5596	23.2798	3258.43
Feed in/rev	1	0.0002	0.0002	0.0002	0.03
Environment*Rake Angle	6	2.1255	2.1255	0.3543	49.58
Environment*Feed in/rev	3	3.8642	3.8642	1.2881	180.29
Rake Angle*Feed in/rev	2	0.7573	0.7573	0.3786	53.00
Environment*Rake Angle*Feed in/rev	6	1.3205	1.3205	0.2201	30.81
Error	72	0.5144	0.5144	0.0071	
Total	95	125.4906			

Source	P
Environment	0.000
Rake Angle	0.000
Feed in/rev	0.860
Environment*Rake Angle	0.000
Environment*Feed in/rev	0.000
Rake Angle*Feed in/rev	0.000
Environment*Rake Angle*Feed in/rev	0.000
Error	
Total	

S = 0.0845251 R-Sq = 99.59% R-Sq(adj) = 99.46%

Unusual Observations for Shear strain (Merchant)

Obs	Shear strain (Merchant)	Fit	SE Fit	Residual	St Resid	
13	4.66010	4.42968	0.04226	0.23042	3.15	R
16	4.26151	4.42968	0.04226	-0.16817	-2.30	R
21	3.51453	3.67571	0.04226	-0.16118	-2.20	R
22	4.04655	3.67571	0.04226	0.37084	5.07	R
23	3.43501	3.67571	0.04226	-0.24070	-3.29	R

R denotes an observation with a large standardized residual.

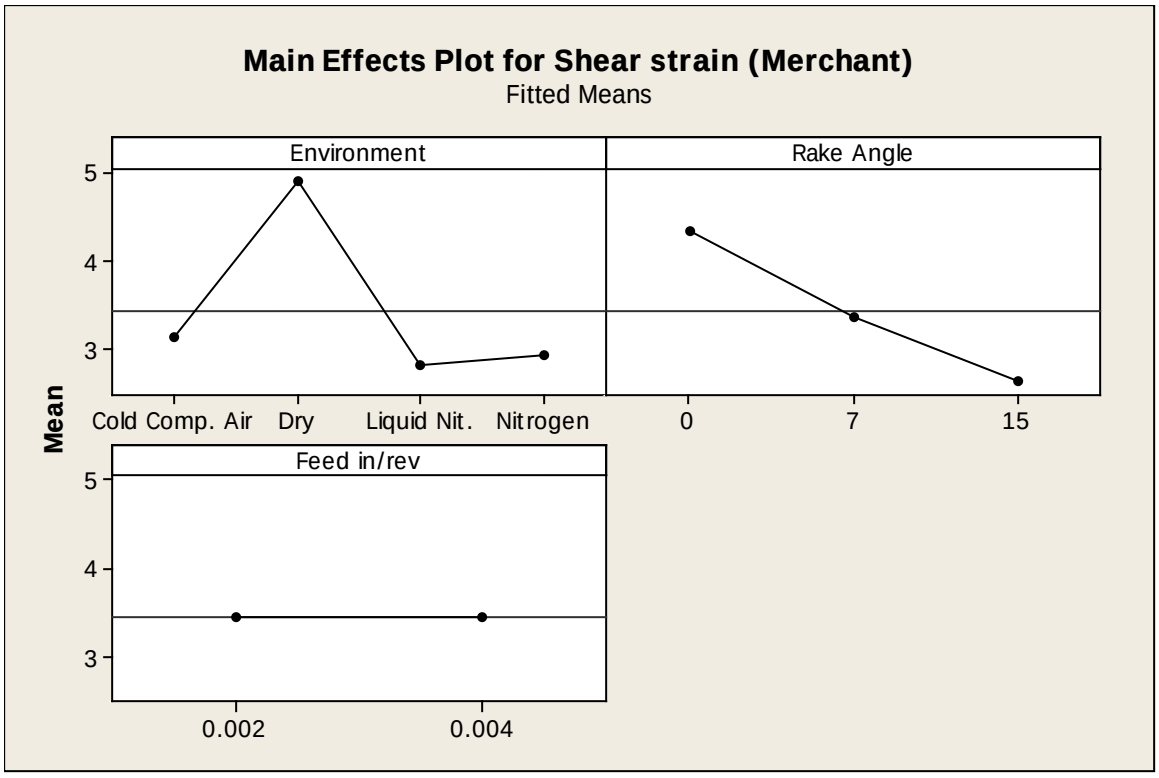
Main Effects Plot for Shear strain (Merchant)
Fitted Means
Environment
Rake Angle
Feed in/rev
Mean
5
4
3
Cold Comp. Air
Dry
Liquid Nit.
Nitrogen
0
7
15
0.002
0.004

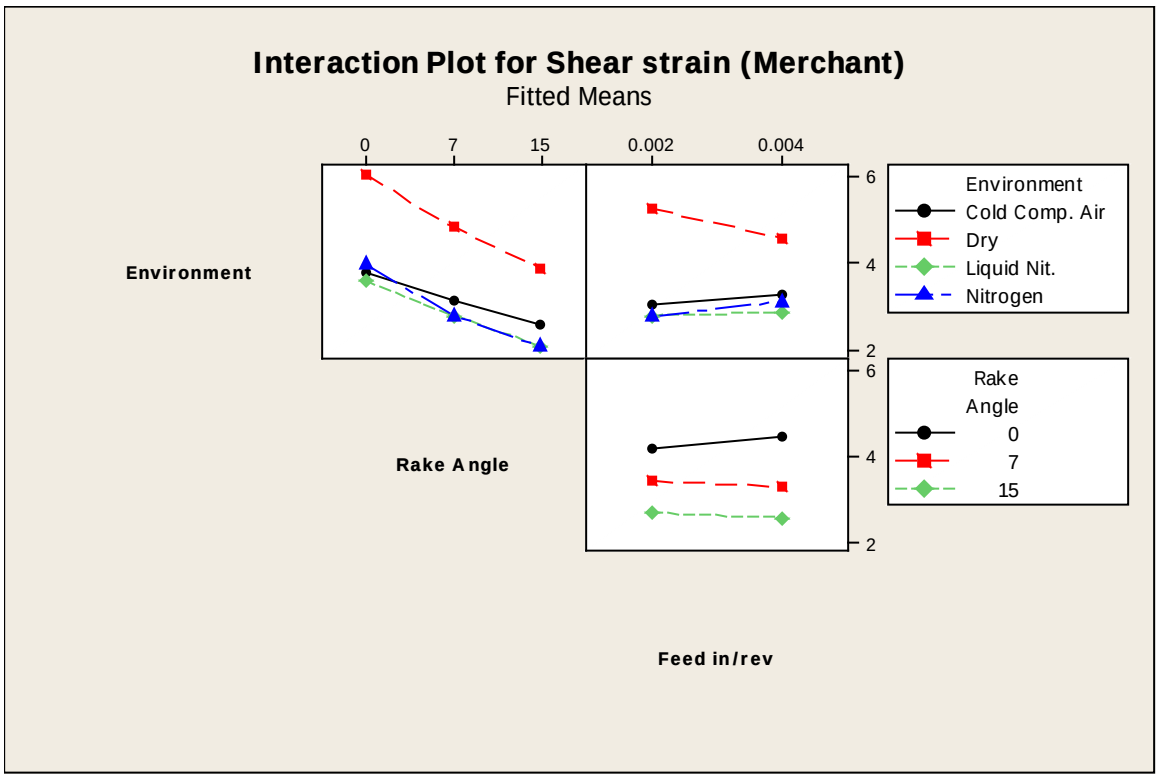
Interaction Plot for Shear strain (Merchant)
Fitted Means
Environment
Rake Angle
Feed in/rev
0
7
15
0.002
0.004
6
4
2
Environment
Cold Comp. Air
Dry
Liquid Nit.
Nitrogen
Rake Angle
0
7
15

Analysis of Variance for **Narmal Stress (Payton)**, using Adjusted SS for Tests

Source	DF	Seq SS	Adj SS	Adj MS
Environment	3	8.56348E+11	8.56348E+11	2.85449E+11
Rake Angle	2	5.26749E+11	5.26749E+11	2.63375E+11
Feed in/rev	1	27163029022	27163029022	27163029022
Environment*Rake Angle	6	2.76508E+11	2.76508E+11	46084632270
Environment*Feed in/rev	3	36719927871	36719927871	12239975957
Rake Angle*Feed in/rev	2	10529038345	10529038345	5264519173
Environment*Rake Angle*Feed in/rev	6	64807176161	64807176161	10801196027
Error	72	1.00406E+11	1.00406E+11	1394522449
Total	95	1.89923E+12		

Source	F	P
Environment	204.69	0.000
Rake Angle	188.86	0.000
Feed in/rev	19.48	0.000
Environment*Rake Angle	33.05	0.000
Environment*Feed in/rev	8.78	0.000
Rake Angle*Feed in/rev	3.78	0.028
Environment*Rake Angle*Feed in/rev	7.75	0.000
Error		
Total		

S = 37343.3 R-Sq = 94.71% R-Sq(adj) = 93.02%

Unusual Observations for Narmal Stress (Payton)

Obs	Narmal Stress (Payton)	Fit	SE Fit	Residual	St Resid	
52	686917	583116	18672	103801	3.21	R
54	597268	528013	18672	69255	2.14	R
55	346087	528013	18672	-181926	-5.63	R
56	602066	528013	18672	74053	2.29	R
92	737918	806482	18672	-68563	-2.12	R

R denotes an observation with a large standardized residual.

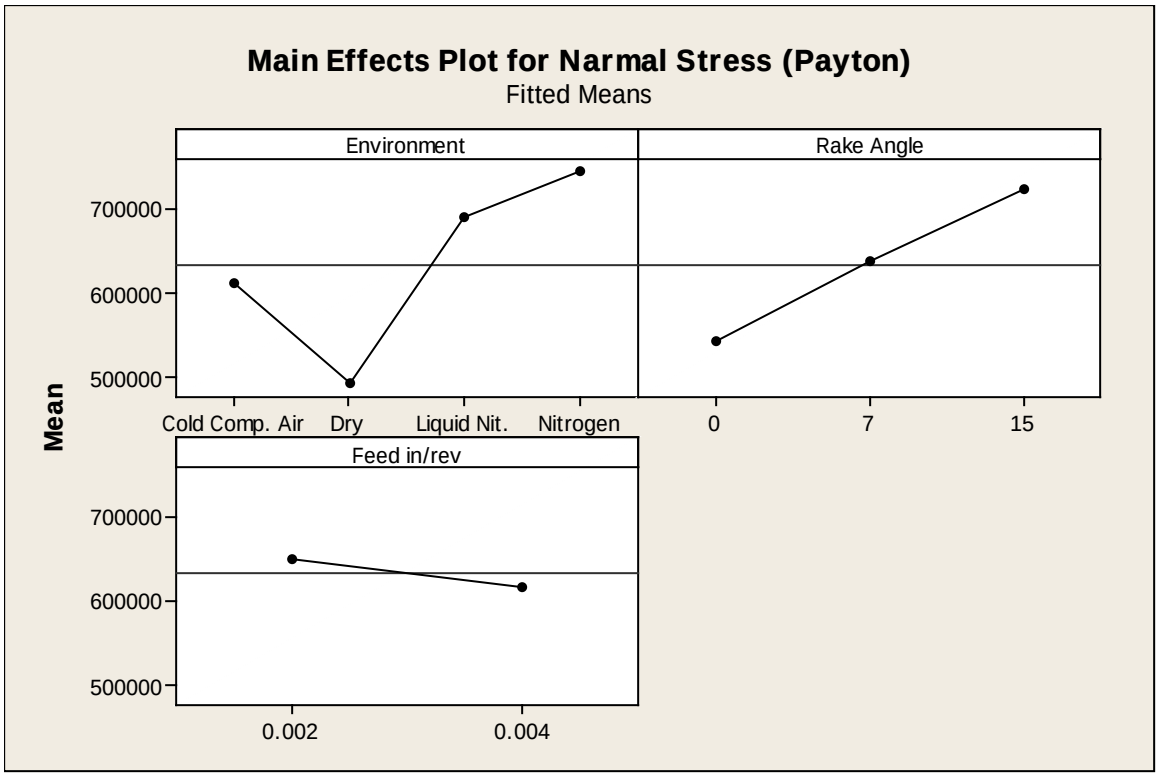
Main Effects Plot for Narmal Stress (Payton)
Fitted Means
Environment
Rake Angle
Feed in/rev
Mean
700000
600000
500000
Cold Comp. Air
Dry
Liquid Nit.
Nitrogen
0
7
15
0.002
0.004

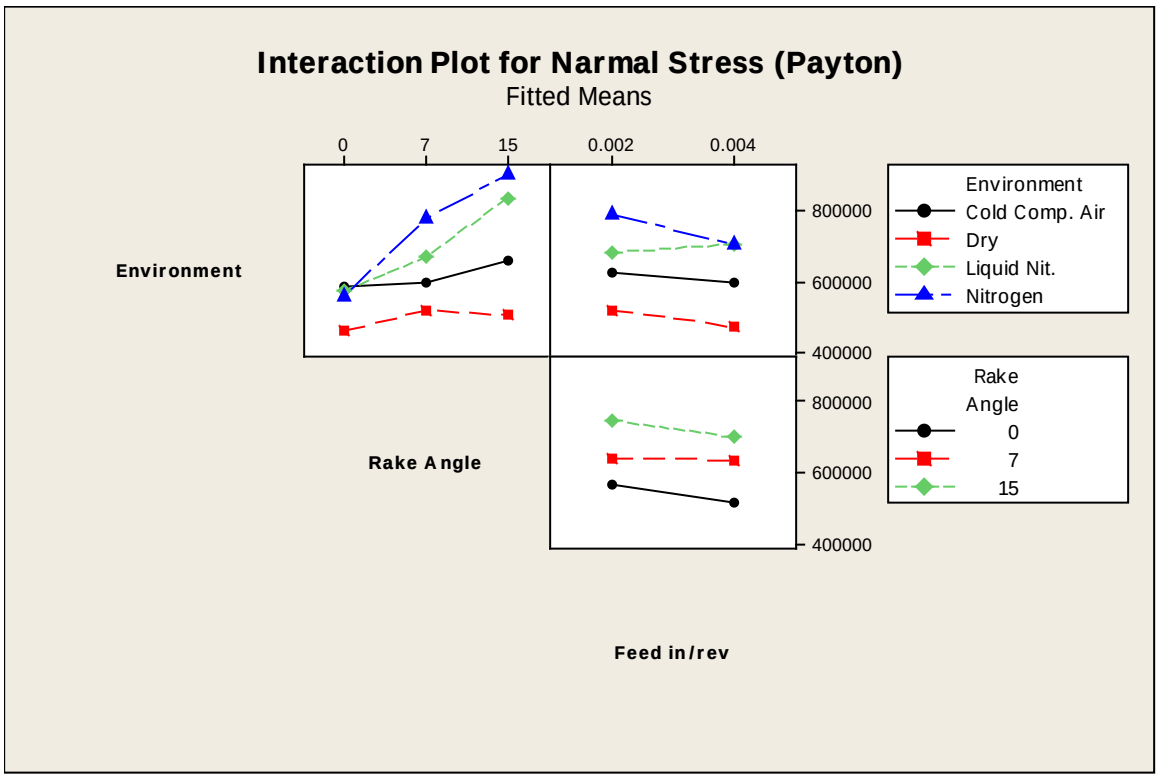
Interaction Plot for Narmal Stress (Payton)
Fitted Means
Environment
Rake Angle
Feed in/rev
0
7
15
0.002
0.004
800000
600000
400000
Environment
Cold Comp. Air
Dry
Liquid Nit.
Nitrogen
Rake Angle
0
7
15

Analysis of Variance for **Shear strain (Payton)**, using Adjusted SS for Tests

Source	DF	Seq SS	Adj SS	Adj MS	F	P
Environment	3	0.00000	0.00000	0.00000	**	
Rake Angle	2	3.46485	3.46485	1.73242	**	
Feed in/rev	1	0.00000	0.00000	0.00000	**	
Environment*Rake Angle	6	0.00000	0.00000	0.00000	**	
Environment*Feed in/rev	3	0.00000	0.00000	0.00000	**	
Rake Angle*Feed in/rev	2	0.00000	0.00000	0.00000	**	
Environment*Rake Angle*Feed in/rev	6	0.00000	0.00000	0.00000	**	
Error	72	0.00000	0.00000	0.00000		
Total	95	3.46485				

** Denominator of F-test is zero.

S = 8.576051E-17 R-Sq = 100.00% R-Sq(adj) = 100.00%

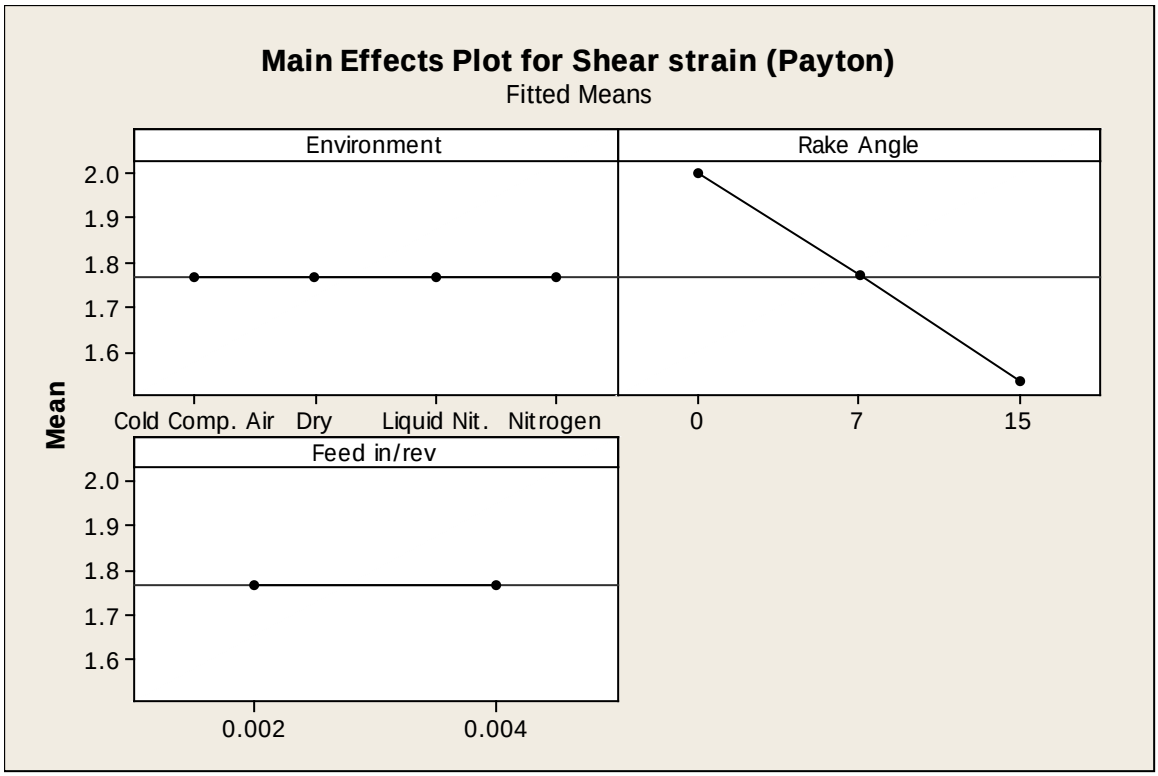
Main Effects Plot for Shear strain (Payton)
Fitted Means
Environment
Rake Angle
Feed in/rev
Mean
2.0
1.9
1.8
1.7
1.6
Cold Comp. Air
Dry
Liquid Nit.
Nitrogen
0
7
15
0.002
0.004

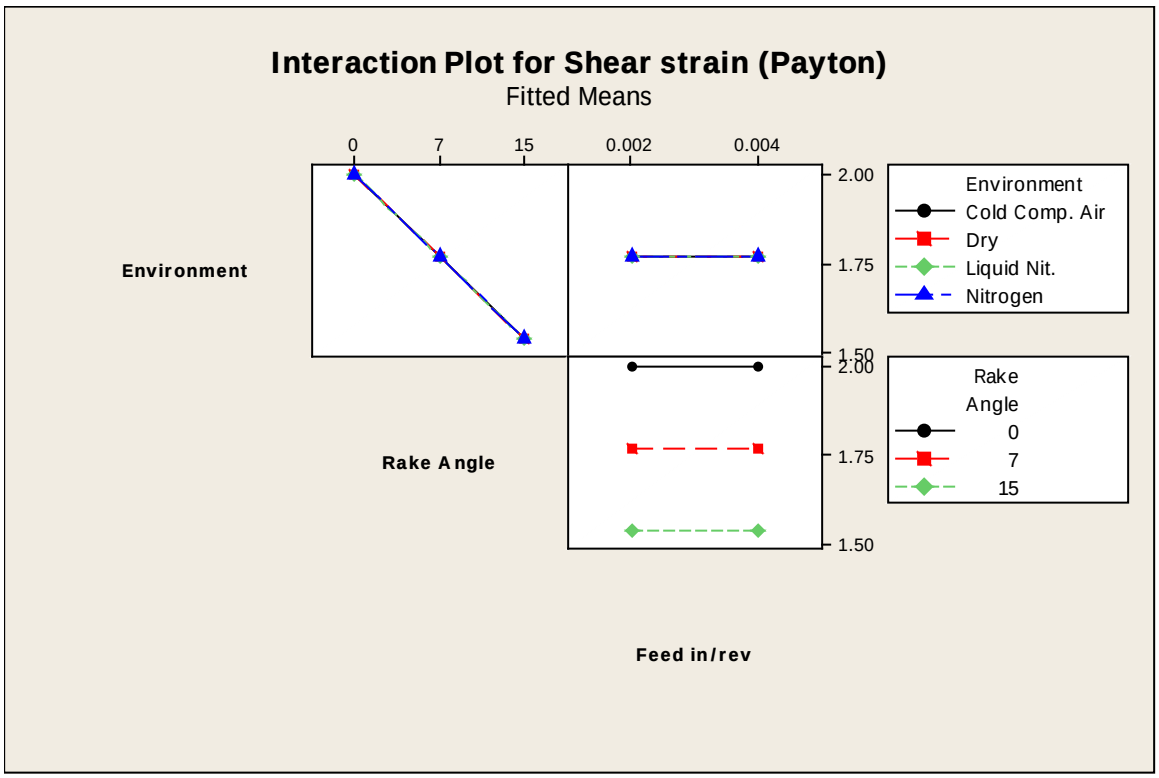
Interaction Plot for Shear strain (Payton)
Fitted Means
Environment
Rake Angle
Feed in/rev
0
7
15
0.002
0.004
2.00
1.75
1.50
Environment
Cold Comp. Air
Dry
Liquid Nit.
Nitrogen
Rake Angle
0
7
15

Analysis of Variance for **Shear Area, As P**, using Adjusted SS for Tests

Source	DF	Seq SS	Adj SS	Adj MS
Environment	3	0.0000163	0.0000163	0.0000054
Rake Angle	2	0.0000133	0.0000133	0.0000066
Feed in/rev	1	0.0000283	0.0000283	0.0000283
Environment*Rake Angle	6	0.0000006	0.0000006	0.0000001
Environment*Feed in/rev	3	0.0000004	0.0000004	0.0000001
Rake Angle*Feed in/rev	2	0.0000026	0.0000026	0.0000013
Environment*Rake Angle*Feed in/rev	6	0.0000003	0.0000003	0.0000000
Error	72	0.0000002	0.0000002	0.0000000
Total	95	0.0000618		

Source	F	P
Environment	2446.52	0.000
Rake Angle	2989.15	0.000
Feed in/rev	12736.92	0.000
Environment*Rake Angle	43.40	0.000
Environment*Feed in/rev	53.92	0.000
Rake Angle*Feed in/rev	582.15	0.000
Environment*Rake Angle*Feed in/rev	19.87	0.000
Error		
Total		

S = 0.0000471029 R-Sq = 99.74% R-Sq(adj) = 99.66%

Unusual Observations for Shear Area, As P

Obs	Shear Area, As P	Fit	SE Fit	Residual	St Resid	
13	0.002983	0.002829	0.000024	0.000154	3.78	R
16	0.002716	0.002829	0.000024	-0.000113	-2.77	R
21	0.002201	0.002302	0.000024	-0.000101	-2.47	R
22	0.002534	0.002302	0.000024	0.000232	5.69	R
23	0.002150	0.002302	0.000024	-0.000151	-3.71	R

R denotes an observation with a large standardized residual.

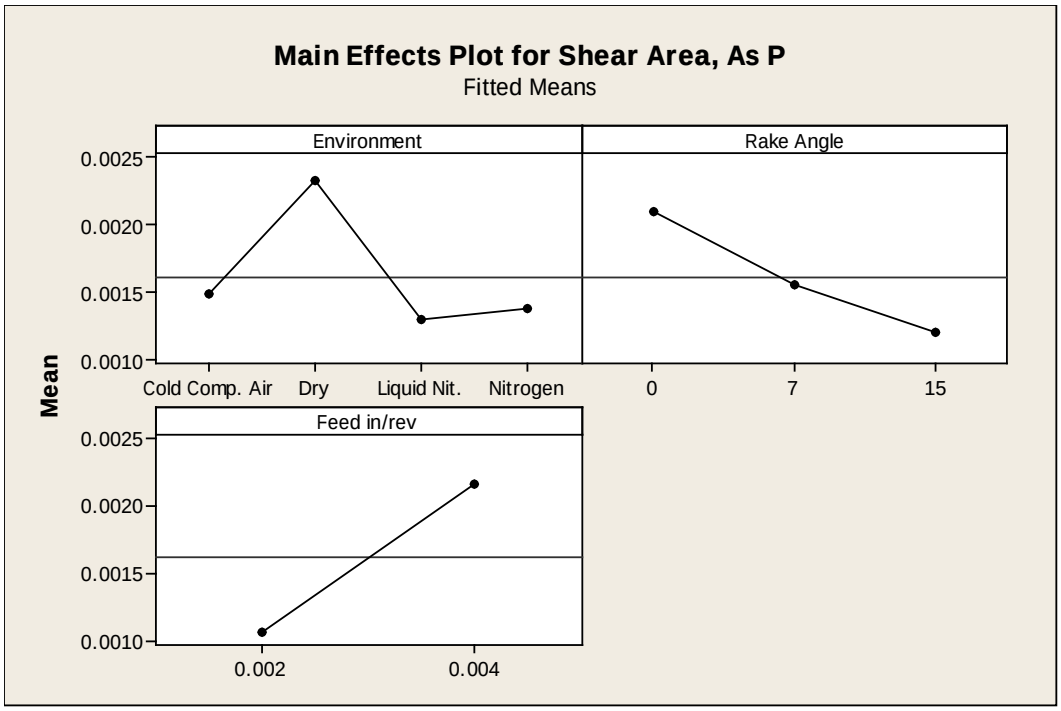
Main Effects Plot for Shear Area, As P
Fitted Means
Environment
Rake Angle
Feed in/rev
Mean
0.0025
0.0020
0.0015
0.0010
Cold Comp. Air
Dry
Liquid Nit.
Nitrogen
0
7
15
0.002
0.004

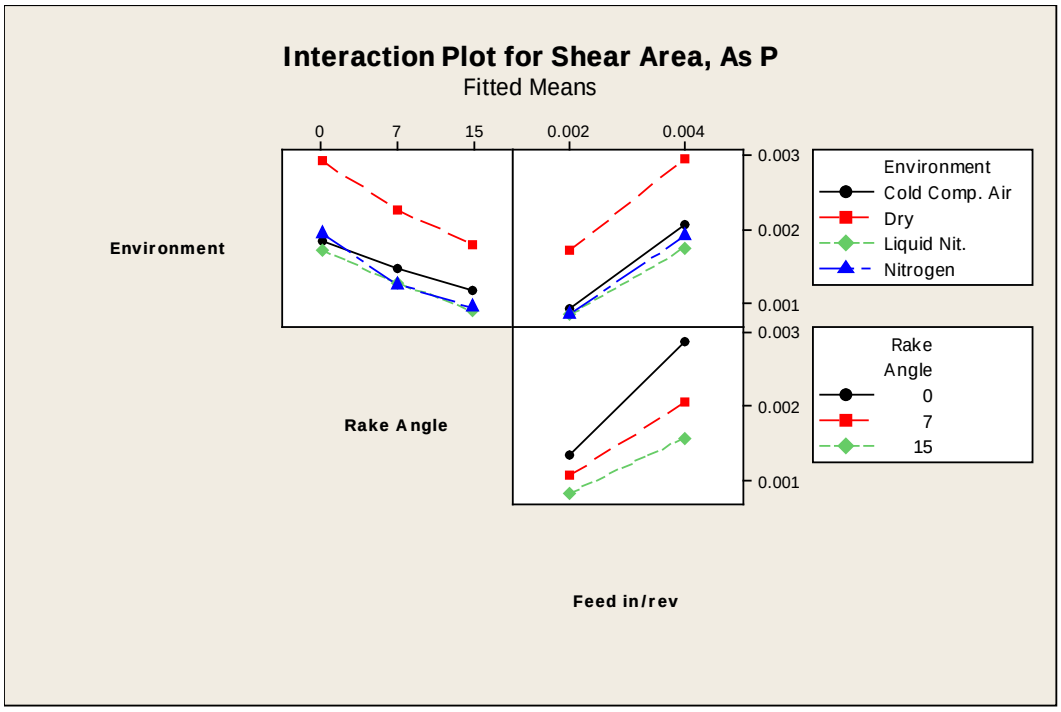
Interaction Plot for Shear Area, As P
Fitted Means
Environment
Rake Angle
Feed in/rev
0
7
15
0.002
0.004
0.003
0.002
0.001
Environment
Cold Comp. Air
Dry
Liquid Nit.
Nitrogen
Rake Angle
0
7
15

Analysis of Variance for **Shear Stress, Ts (Payton) corre**, using Adjusted SS for
Tests

Source	DF	Seq SS	Adj SS	Adj MS	F
Environment	3	163969.4	163969.4	54656.5	68.84
Rake Angle	2	460.5	460.5	230.2	0.29
Feed in/rev	1	44185.6	44185.6	44185.6	55.65
Environment*Rake Angle	6	4534.5	4534.5	755.7	0.95
Environment*Feed in/rev	3	6101.3	6101.3	2033.8	2.56
Rake Angle*Feed in/rev	2	1828.9	1828.9	914.5	1.15
Environment*Rake Angle*Feed in/rev	6	5158.5	5158.5	859.8	1.08
Error	72	57163.8	57163.8	793.9	
Total	95	283402.4			

Source	P
Environment	0.000
Rake Angle	0.749
Feed in/rev	0.000
Environment*Rake Angle	0.464
Environment*Feed in/rev	0.061
Rake Angle*Feed in/rev	0.322
Environment*Rake Angle*Feed in/rev	0.381
Error	
Total	

S = 28.1770 R-Sq = 79.83% R-Sq(adj) = 73.39%

Unusual Observations for Shear Stress, Ts (Payton) corre

Obs	Shear Stress, Ts (Payton) corre	Fit	SE Fit	Residual	St Resid
53	72.618	129.804	14.088	-57.187	-2.34 R
54	58.186	129.804	14.088	-71.618	-2.93 R
55	329.577	129.804	14.088	199.772	8.19 R
56	58.838	129.804	14.088	-70.967	-2.91 R

R denotes an observation with a large standardized residual.

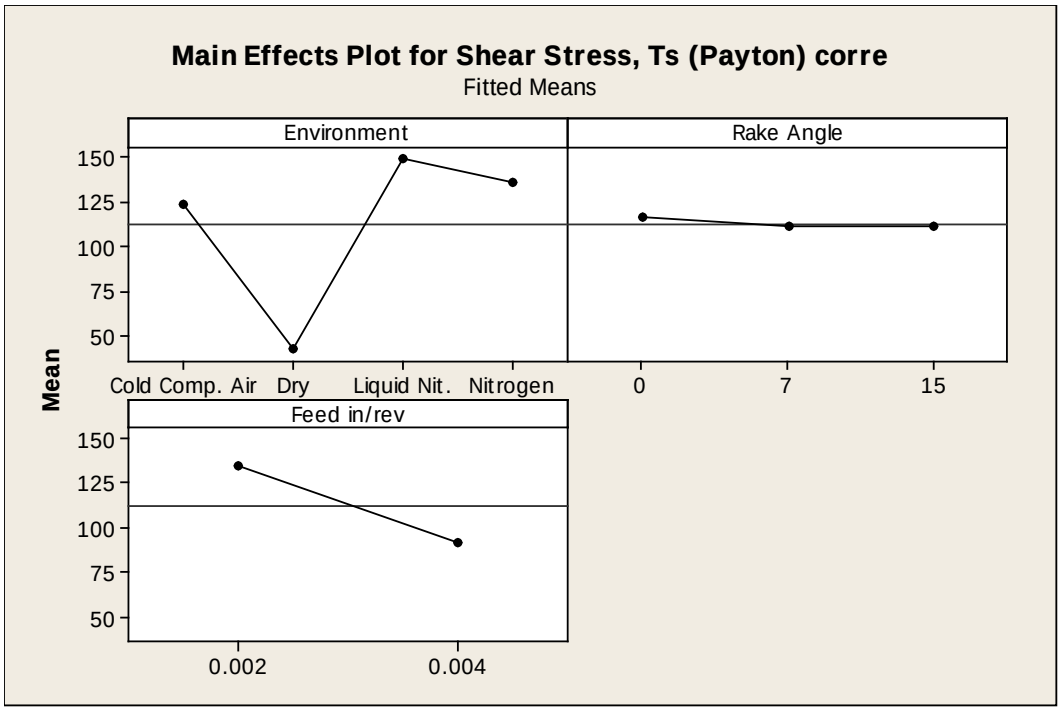
Main Effects Plot for Shear Stress, Ts (Payton) corre
Fitted Means
Environment
Rake Angle
Feed in/rev
Mean
150
125
100
75
50
Cold Comp. Air
Dry
Liquid Nit.
Nitrogen
0
7
15
0.002
0.004

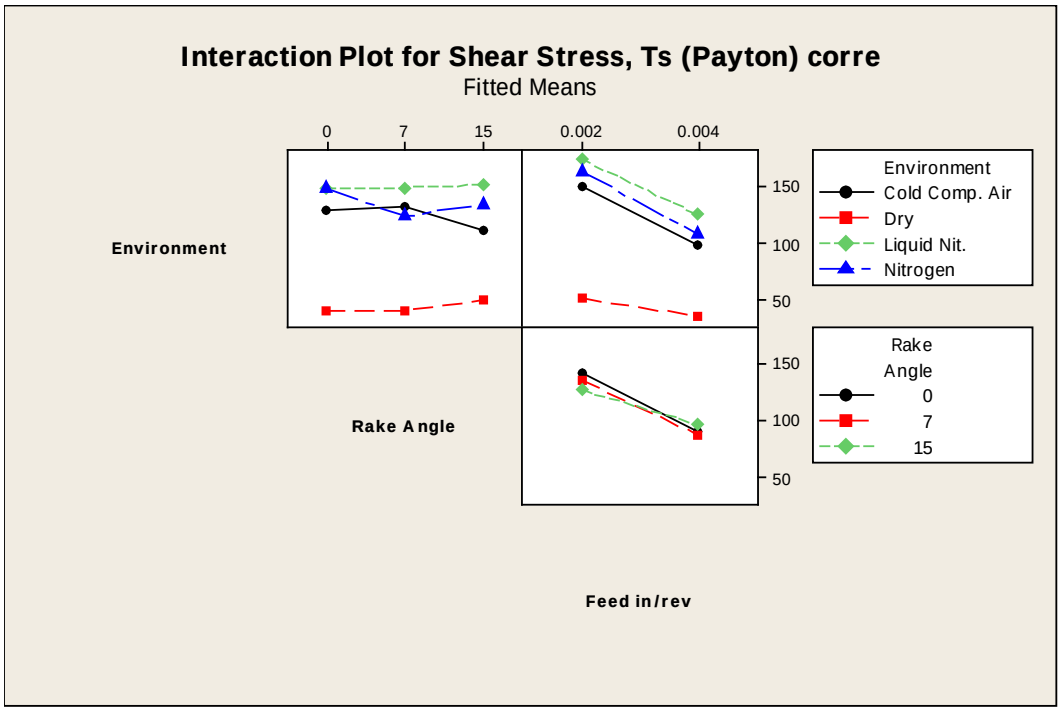
Interaction Plot for Shear Stress, Ts (Payton) corre
Fitted Means
Environment
Rake Angle
Feed in/rev
0
7
15
0.002
0.004
150
100
50
Environment
Cold Comp. Air
Dry
Liquid Nit.
Nitrogen
Rake Angle
0
7
15

Analysis of Variance for **Shear strain new**, using Adjusted SS for Tests

Source	DF	Seq SS	Adj SS	Adj MS	F
Environment	3	4.66764	4.66764	1.55588	1139.32
Rake Angle	2	2.70713	2.70713	1.35356	991.17
Feed in/rev	1	0.03098	0.03098	0.03098	22.69
Environment*Rake Angle	6	1.13194	1.13194	0.18866	138.15
Environment*Feed in/rev	3	0.24737	0.24737	0.08246	60.38
Rake Angle*Feed in/rev	2	0.05767	0.05767	0.02884	21.12
Environment*Rake Angle*Feed in/rev	6	0.45669	0.45669	0.07611	55.74
Error	72	0.09832	0.09832	0.00137	
Total	95	9.39775			

Source	P
Environment	0.000
Rake Angle	0.000
Feed in/rev	0.000
Environment*Rake Angle	0.000
Environment*Feed in/rev	0.000
Rake Angle*Feed in/rev	0.000
Environment*Rake Angle*Feed in/rev	0.000
Error	
Total	

S = 0.0369544 R-Sq = 98.95% R-Sq(adj) = 98.62%

Unusual Observations for Shear strain new

Obs	Shear strain new	Fit	SE Fit	Residual	St Resid	
66	1.57100	1.48274	0.01848	0.08826	2.76	R
68	1.39145	1.48274	0.01848	-0.09128	-2.85	R
89	1.23814	1.07912	0.01848	0.15902	4.97	R
92	0.94261	1.07912	0.01848	-0.13651	-4.27	R
94	1.32809	1.39610	0.01848	-0.06801	-2.13	R

R denotes an observation with a large standardized residual.

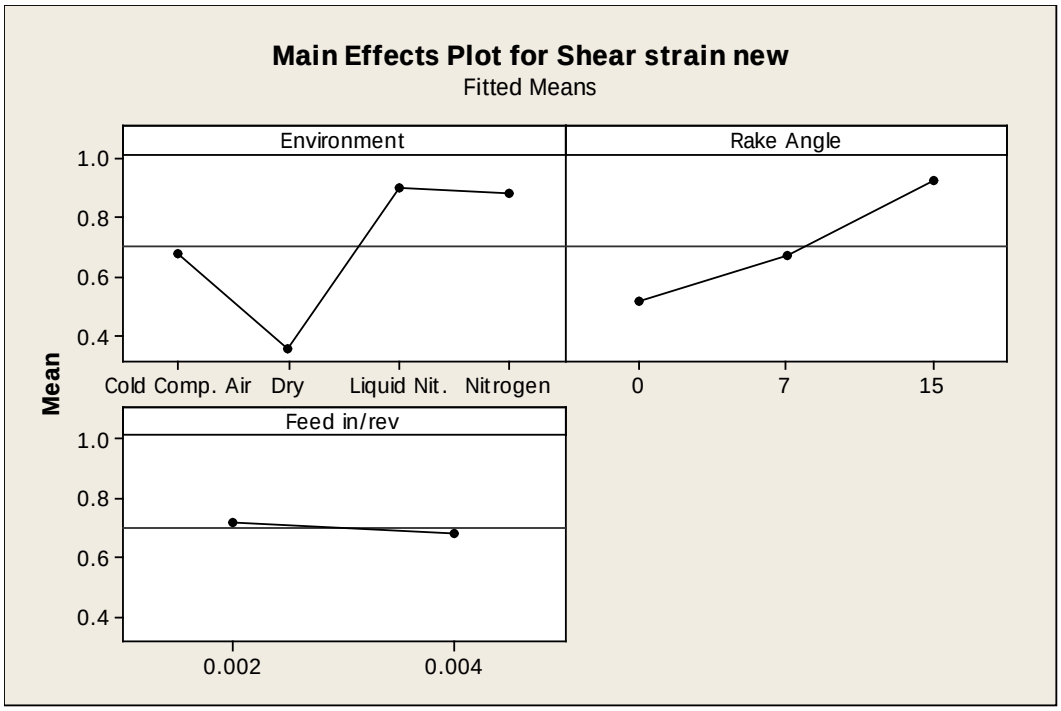
Main Effects Plot for Shear strain new
Fitted Means
Environment
Rake Angle
Feed in/rev
Mean
1.0
0.8
0.6
0.4
Cold Comp. Air
Dry
Liquid Nit.
Nitrogen
0
7
15
0.002
0.004

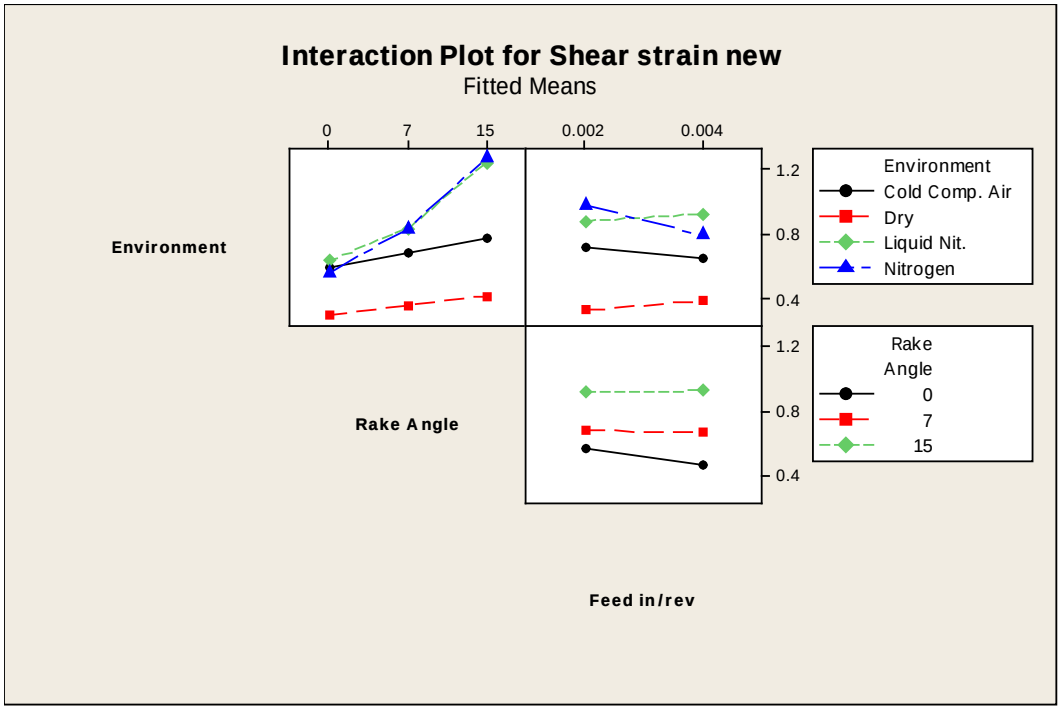
Interaction Plot for Shear strain new
Fitted Means
Environment
Rake Angle
Feed in/rev
0
7
15
0.002
0.004
1.2
0.8
0.4
Environment
Cold Comp. Air
Dry
Liquid Nit.
Nitrogen
Rake Angle
0
7
15

1020 STEEL; UNCOATED CARBIDE

General Linear Model: Fy Thrust, Fz Cutting, ... versus Environment, Rake Angle

Factor	Type	Levels	Values
Environment	fixed	4	Cold Comp. Air, Dry, Liquid Nit., Nitrogen
Rake Angle	fixed	3	0, 7, 15
Feed in/rev	fixed	2	0.002, 0.004

Analysis of Variance for **Fy Thrust**, using Adjusted SS for Tests

Source	DF	Seq SS	Adj SS	Adj MS	F	P
Environment	3	1207769	1207769	402590	106.09	0.000
Rake Angle	2	706070	706070	353035	93.03	0.000
Feed in/rev	1	282527	282527	282527	74.45	0.000
Environment*Rake Angle	6	153454	153454	25576	6.74	0.000
Environment*Feed in/rev	3	169528	169528	56509	14.89	0.000
Rake Angle*Feed in/rev	2	22828	22828	11414	3.01	0.056
Environment*Rake Angle*Feed in/rev	6	285085	285085	47514	12.52	0.000
Error	72	273229	273229	3795		
Total	95	3100488				

S = 61.6023 R-Sq = 91.19% R-Sq(adj) = 88.37%

Unusual Observations for Fy Thrust

Obs	Fy Thrust	Fit	SE Fit	Residual	St Resid
5	466.152	700.569	30.801	-234.417	-4.39 R
6	872.213	700.569	30.801	171.645	3.22 R
8	869.808	700.569	30.801	169.240	3.17 R
17	512.617	391.351	30.801	121.266	2.27 R
57	396.148	241.206	30.801	154.942	2.90 R
76	394.842	268.276	30.801	126.566	2.37 R

R denotes an observation with a large standardized residual.

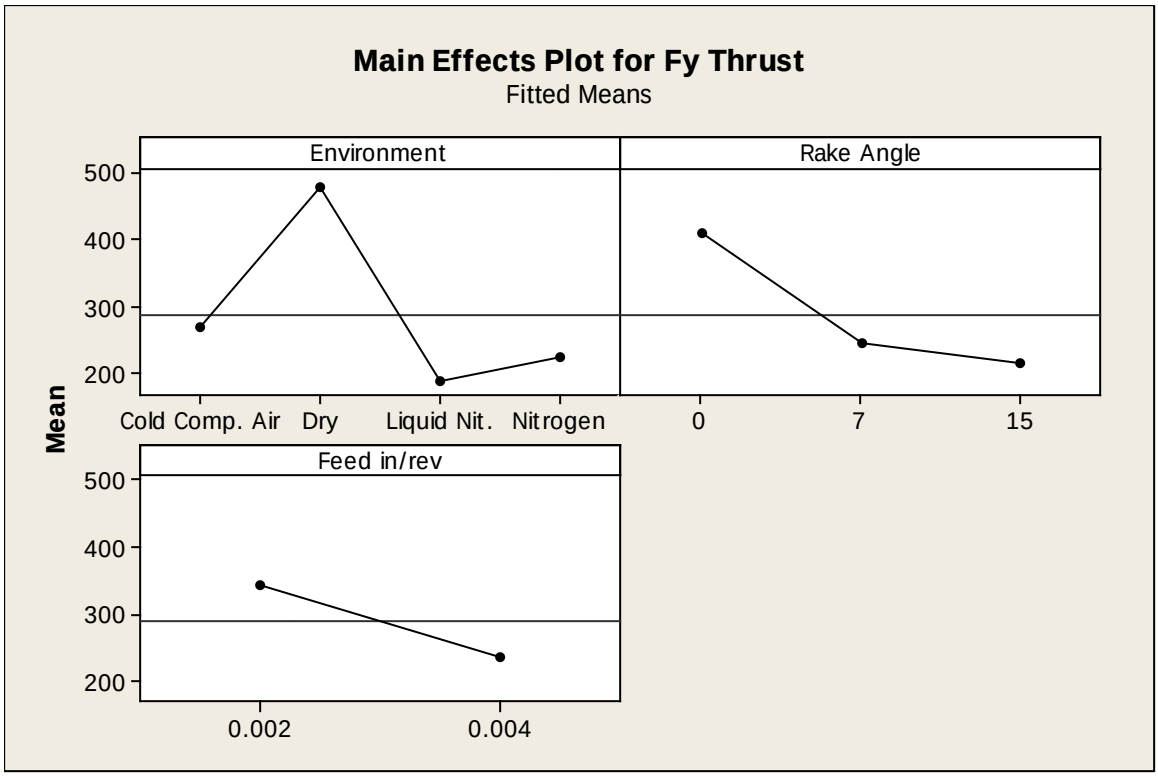
Main Effects Plot for Fy Thrust
Fitted Means
Environment
Rake Angle
Feed in/rev
Mean
500
400
300
200
Cold Comp. Air
Dry
Liquid Nit.
Nitrogen
0
7
15
0.002
0.004

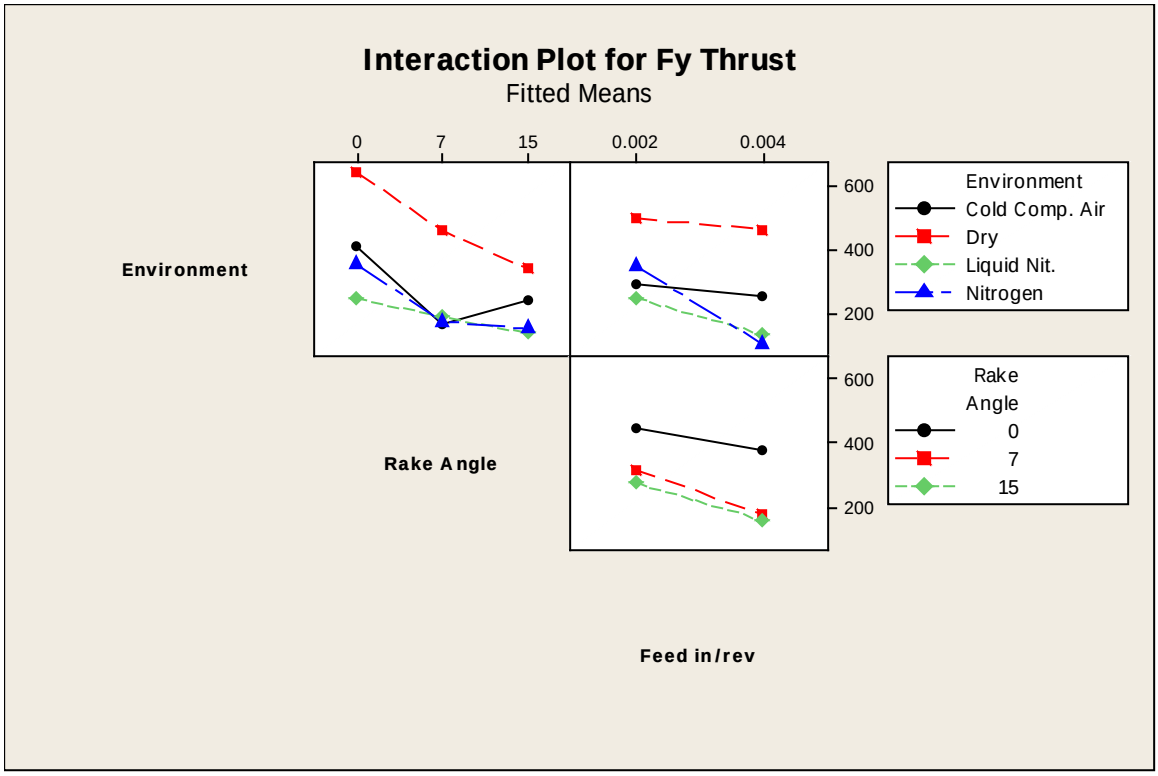
Interaction Plot for Fy Thrust
Fitted Means
Environment
Rake Angle
Feed in/rev
0
7
15
0.002
0.004
600
400
200
Environment
Cold Comp. Air
Dry
Liquid Nit.
Nitrogen
Rake Angle
0
7
15

Analysis of Variance for **Fz Cutting**, using Adjusted SS for Tests

Source	DF	Seq SS	Adj SS	Adj MS	F	P
Environment	3	366676	366676	122225	63.06	0.000
Rake Angle	2	254166	254166	127083	65.57	0.000
Feed in/rev	1	193059	193059	193059	99.61	0.000
Environment*Rake Angle	6	142727	142727	23788	12.27	0.000
Environment*Feed in/rev	3	128588	128588	42863	22.11	0.000
Rake Angle*Feed in/rev	2	63870	63870	31935	16.48	0.000
Environment*Rake Angle*Feed in/rev	6	128584	128584	21431	11.06	0.000
Error	72	139549	139549	1938		
Total	95	1417218				

S = 44.0248 R-Sq = 90.15% R-Sq(adj) = 87.01%

Unusual Observations for Fz Cutting

Obs	Fz Cutting	Fit	SE Fit	Residual	St Resid	
5	656.372	770.586	22.012	-114.214	-3.00	R
6	871.452	770.586	22.012	100.866	2.65	R
7	658.843	770.586	22.012	-111.743	-2.93	R
8	895.677	770.586	22.012	125.091	3.28	R
28	364.375	218.694	22.012	145.681	3.82	R
57	431.403	340.291	22.012	91.112	2.39	R

R denotes an observation with a large standardized residual.

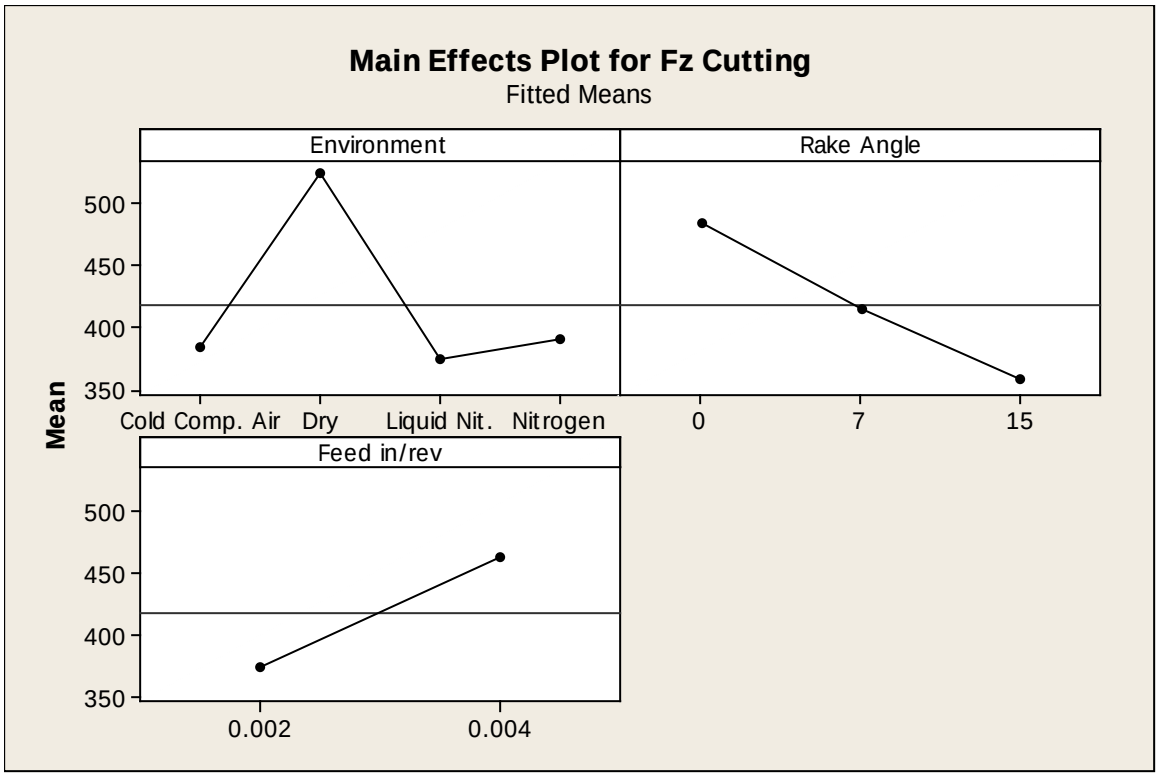
Main Effects Plot for Fz Cutting
Fitted Means
Environment
Rake Angle
Feed in/rev
Mean
500
450
400
350
Cold Comp. Air
Dry
Liquid Nit.
Nitrogen
0
7
15
0.002
0.004

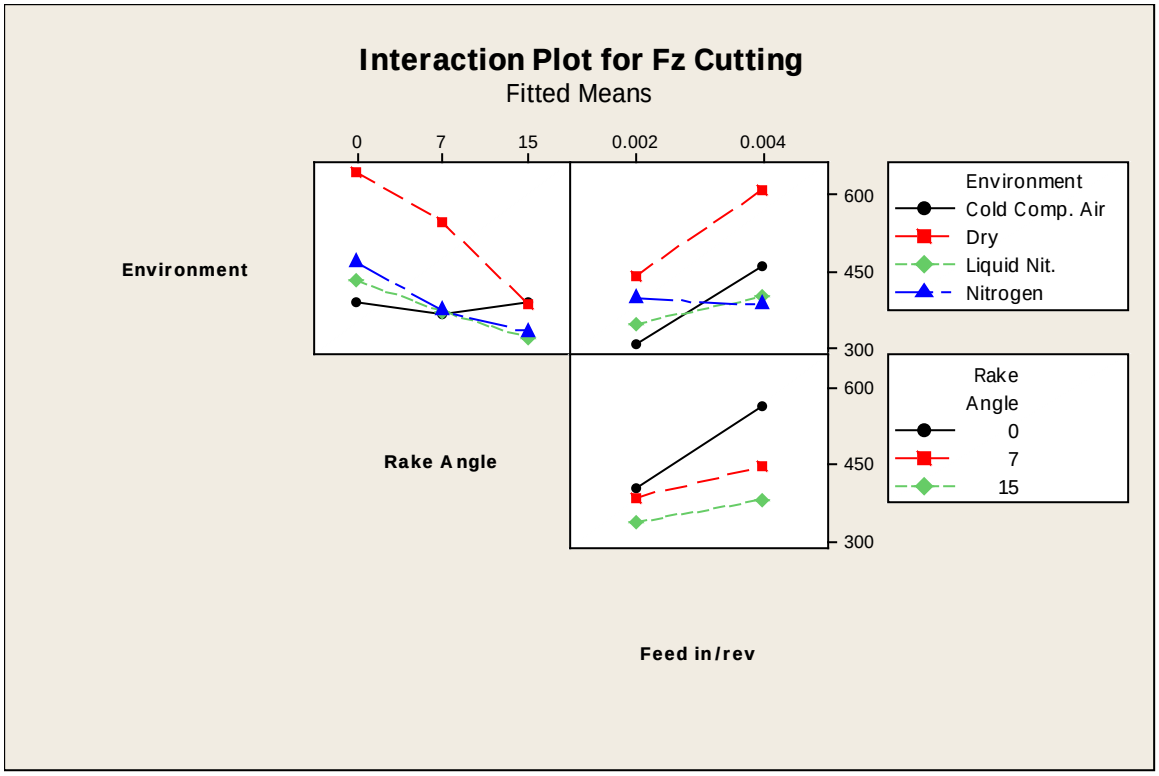
Interaction Plot for Fz Cutting
Fitted Means
Environment
Rake Angle
Feed in/rev
0
7
15
0.002
0.004
600
450
300
Environment
Cold Comp. Air
Dry
Liquid Nit.
Nitrogen
Rake Angle
0
7
15

Analysis of Variance for Resultant, using Adjusted SS for Tests

Source	DF	Seq SS	Adj SS	Adj MS	F	P
Environment	3	1243252	1243252	414417	92.96	0.000
Rake Angle	2	822897	822897	411449	92.30	0.000
Feed in/rev	1	6407	6407	6407	1.44	0.235
Environment*Rake Angle	6	221763	221763	36960	8.29	0.000
Environment*Feed in/rev	3	218630	218630	72877	16.35	0.000
Rake Angle*Feed in/rev	2	60355	60355	30177	6.77	0.002
Environment*Rake Angle*Feed in/rev	6	335784	335784	55964	12.55	0.000
Error	72	320962	320962	4458		
Total	95	3230050				

S = 66.7668   R-Sq = 90.06%   R-Sq(adj) = 86.89%

Unusual Observations for Resultant

Obs	Resultant	Fit	SE Fit	Residual	St Resid	
5	805.06	1043.42	33.38	-238.36	-4.12	R
6	1232.96	1043.42	33.38	189.54	3.28	R
7	887.15	1043.42	33.38	-156.27	-2.70	R
8	1248.52	1043.42	33.38	205.10	3.55	R
57	585.70	418.95	33.38	166.74	2.88	R
76	581.17	448.50	33.38	132.67	2.29	R

R denotes an observation with a large standardized residual.

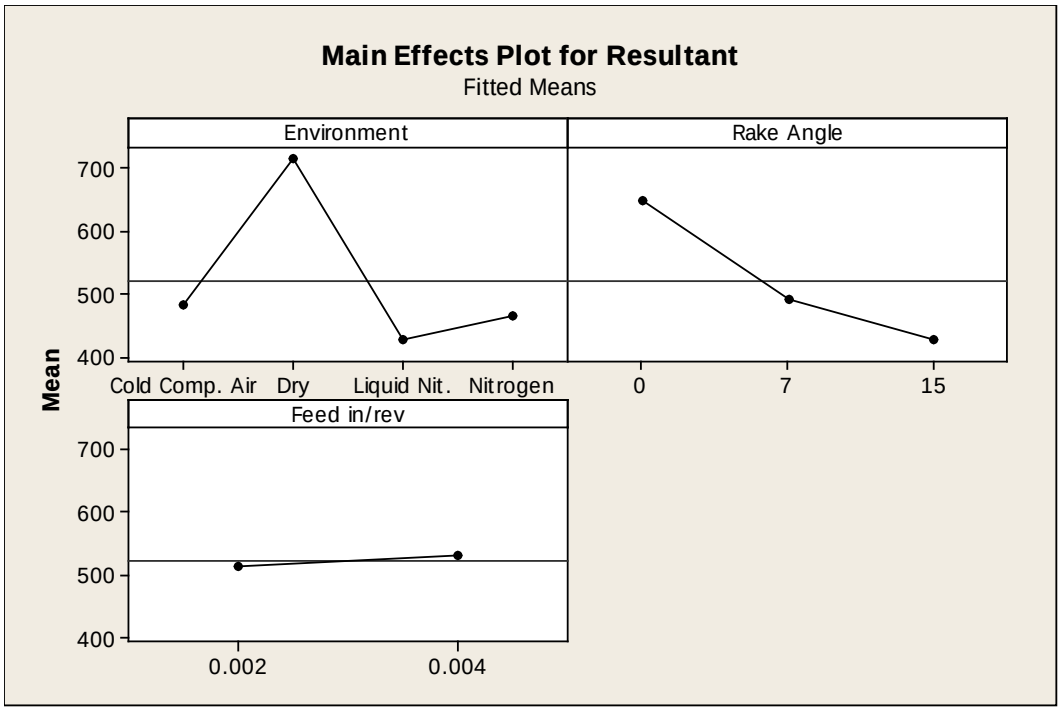
Main Effects Plot for Resultant
Fitted Means
Environment
Rake Angle
Feed in/rev
Mean
700
600
500
400
Cold Comp. Air
Dry
Liquid Nit.
Nitrogen
0
7
15
0.002
0.004

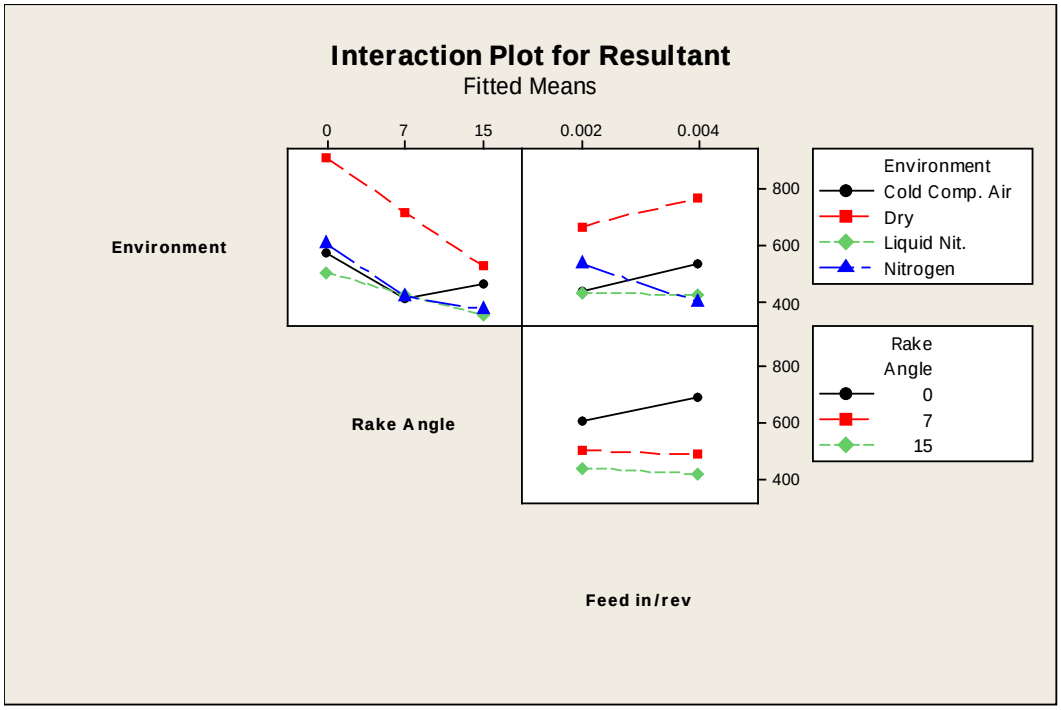
Interaction Plot for Resultant
Fitted Means
Environment
Rake Angle
Feed in/rev
0
7
15
0.002
0.004
800
600
400
Environment
Cold Comp. Air
Dry
Liquid Nit.
Nitrogen
Rake Angle
0
7
15

Analysis of Variance for **Chip thickness ratio**, using Adjusted SS for Tests

Source	DF	Seq SS	Adj SS	Adj MS	F
Environment	3	0.194409	0.194409	0.064803	3587.48
Rake Angle	2	0.111856	0.111856	0.055928	3096.17
Feed in/rev	1	0.022293	0.022293	0.022293	1234.14
Environment*Rake Angle	6	0.294745	0.294745	0.049124	2719.50
Environment*Feed in/rev	3	0.025622	0.025622	0.008541	472.82
Rake Angle*Feed in/rev	2	0.000420	0.000420	0.000210	11.63
Environment*Rake Angle*Feed in/rev	6	0.006868	0.006868	0.001145	63.37
Error	72	0.001301	0.001301	0.000018	
Total	95	0.657516			

Source	P
Environment	0.000
Rake Angle	0.000
Feed in/rev	0.000
Environment*Rake Angle	0.000
Environment*Feed in/rev	0.000
Rake Angle*Feed in/rev	0.000
Environment*Rake Angle*Feed in/rev	0.000
Error	
Total	

S = 0.00425014 R-Sq = 99.80% R-Sq(adj) = 99.74%

Unusual Observations for Chip thickness ratio

Obs	Chip thickness ratio	Fit	SE Fit	Residual	St Resid
18	0.175623	0.186564	0.002125	-0.010940	-2.97 R
19	0.197375	0.186564	0.002125	0.010811	2.94 R
65	0.512821	0.502286	0.002125	0.010535	2.86 R
67	0.487805	0.502286	0.002125	-0.014481	-3.93 R
74	0.290558	0.278959	0.002125	0.011599	3.15 R
76	0.269663	0.278959	0.002125	-0.009296	-2.53 R

R denotes an observation with a large standardized residual.

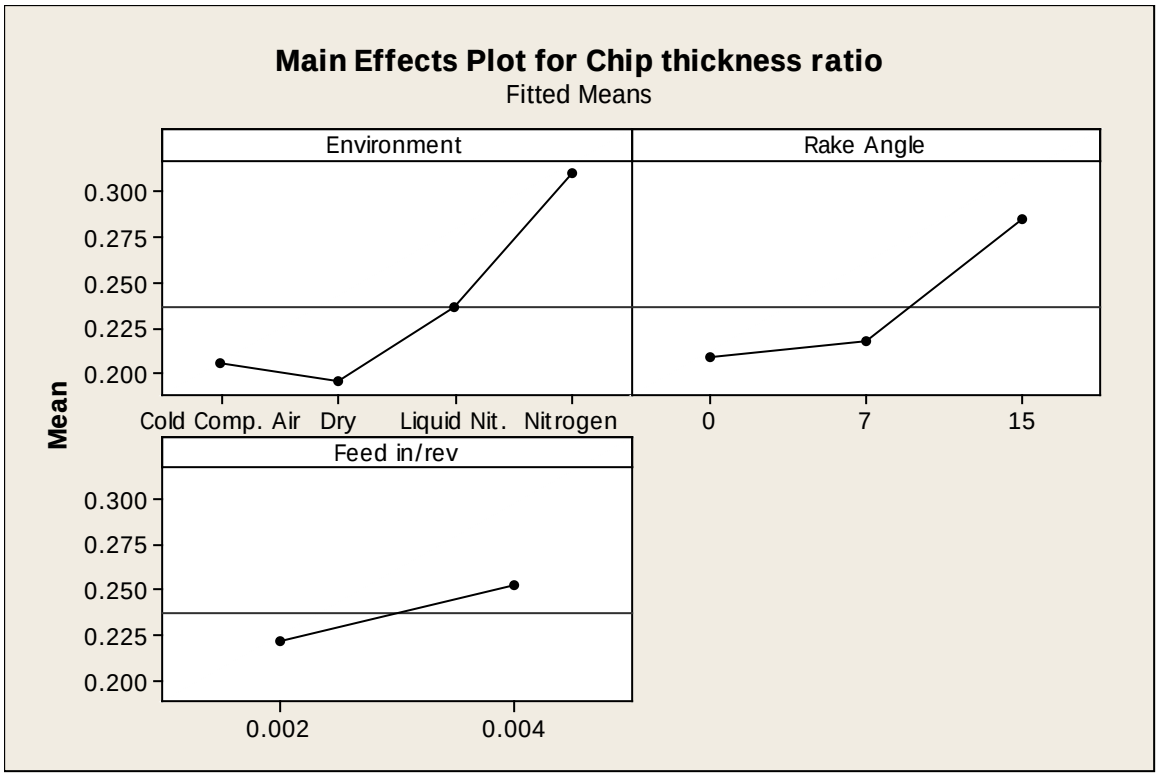
Main Effects Plot for Chip thickness ratio
Fitted Means
Environment
Rake Angle
Feed in/rev
Mean
0.300
0.275
0.250
0.225
0.200
Cold Comp. Air
Dry
Liquid Nit.
Nitrogen
0
7
15
0.002
0.004

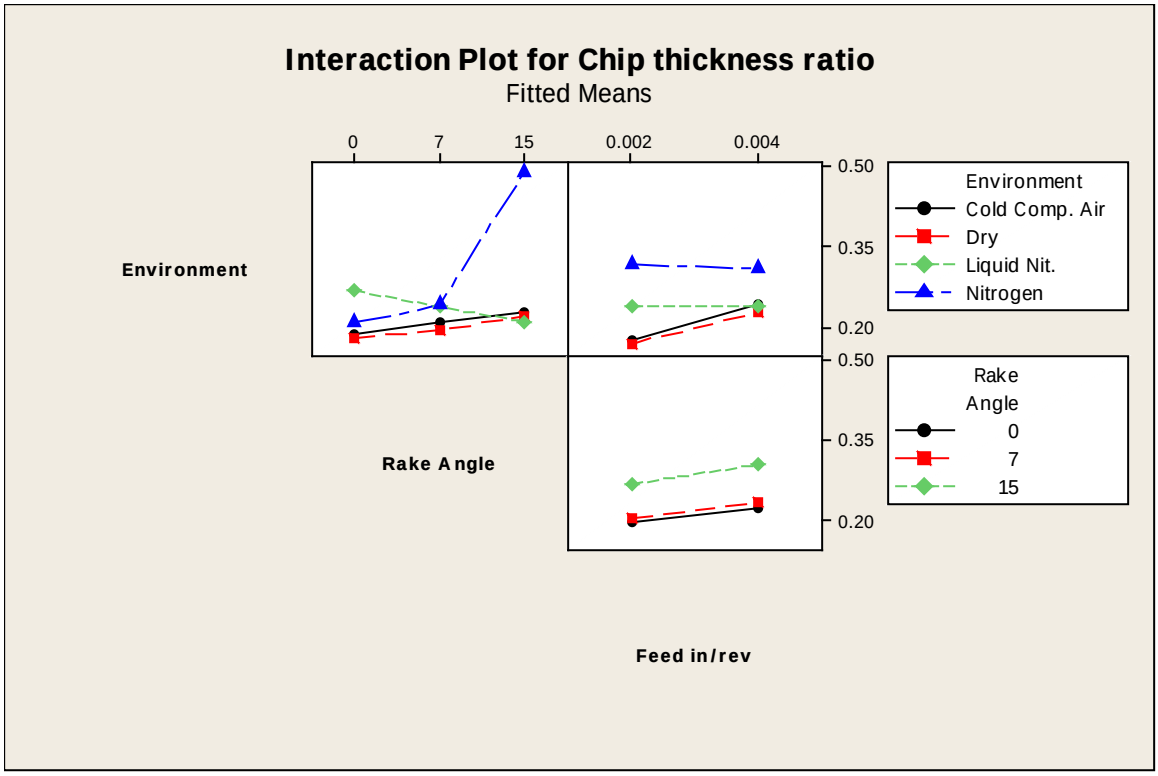
Interaction Plot for Chip thickness ratio
Fitted Means
Environment
Rake Angle
Feed in/rev
0
7
15
0.002
0.004
0.50
0.35
0.20
Environment
Cold Comp. Air
Dry
Liquid Nit.
Nitrogen
Rake Angle
0
7
15

Analysis of Variance for **Phi** degrees, using Adjusted SS for Tests

Source	DF	Seq SS	Adj SS	Adj MS	F
Environment	3	654.536	654.536	218.179	3786.38
Rake Angle	2	415.171	415.171	207.586	3602.54
Feed in/rev	1	74.735	74.735	74.735	1296.98
Environment*Rake Angle	6	994.406	994.406	165.734	2876.24
Environment*Feed in/rev	3	84.221	84.221	28.074	487.21
Rake Angle*Feed in/rev	2	2.073	2.073	1.037	17.99
Environment*Rake Angle*Feed in/rev	6	22.402	22.402	3.734	64.79
Error	72	4.149	4.149	0.058	
Total	95	2251.693			

Source	P
Environment	0.000
Rake Angle	0.000
Feed in/rev	0.000
Environment*Rake Angle	0.000
Environment*Feed in/rev	0.000
Rake Angle*Feed in/rev	0.000
Environment*Rake Angle*Feed in/rev	0.000
Error	
Total	

S = 0.240046 R-Sq = 99.82% R-Sq(adj) = 99.76%

Unusual Observations for Phi degrees

Obs	Phi degrees	Fit	SE Fit	Residual	St Resid	
18	10.0772	10.7223	0.1200	-0.6450	-3.10	R
19	11.3602	10.7223	0.1200	0.6379	3.07	R
65	29.7330	29.1458	0.1200	0.5873	2.82	R
67	28.3365	29.1458	0.1200	-0.8092	-3.89	R
74	16.2017	15.5861	0.1200	0.6156	2.96	R
76	15.0916	15.5861	0.1200	-0.4945	-2.38	R

R denotes an observation with a large standardized residual.

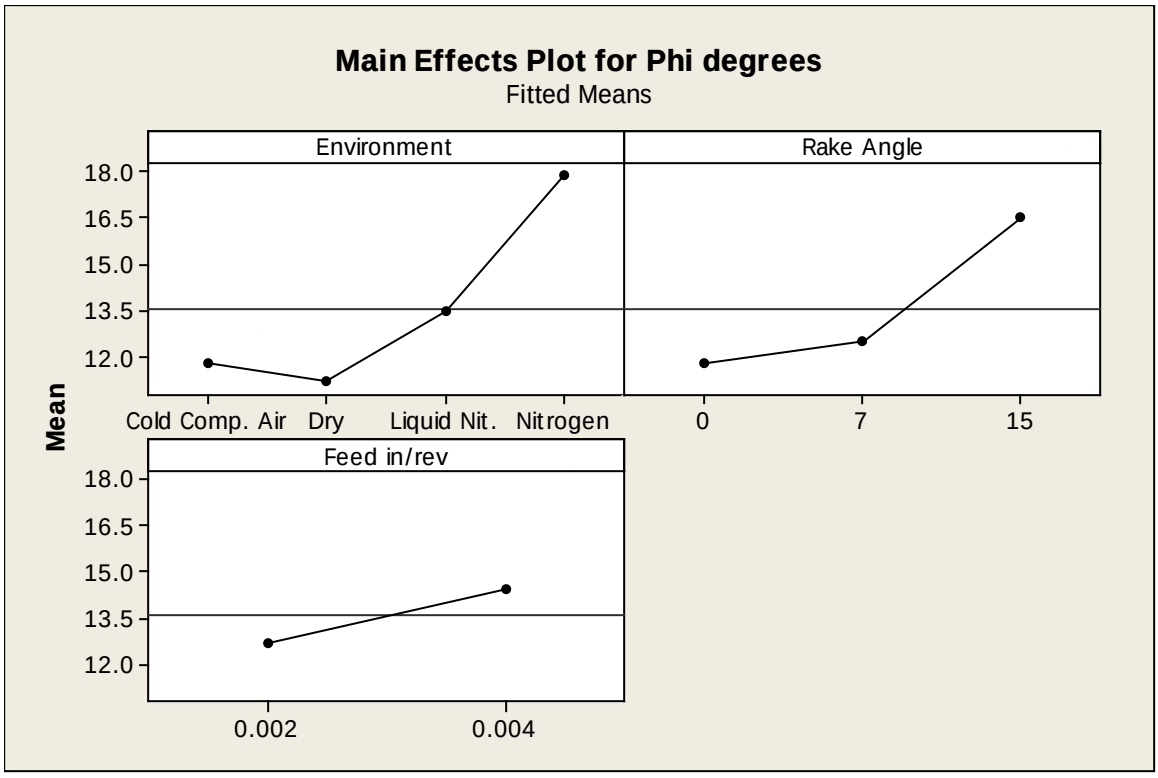
Main Effects Plot for Phi degrees
Fitted Means
Environment
Rake Angle
Feed in/rev
Mean
18.0
16.5
15.0
13.5
12.0
Cold Comp. Air
Dry
Liquid Nit.
Nitrogen
0
7
15
0.002
0.004

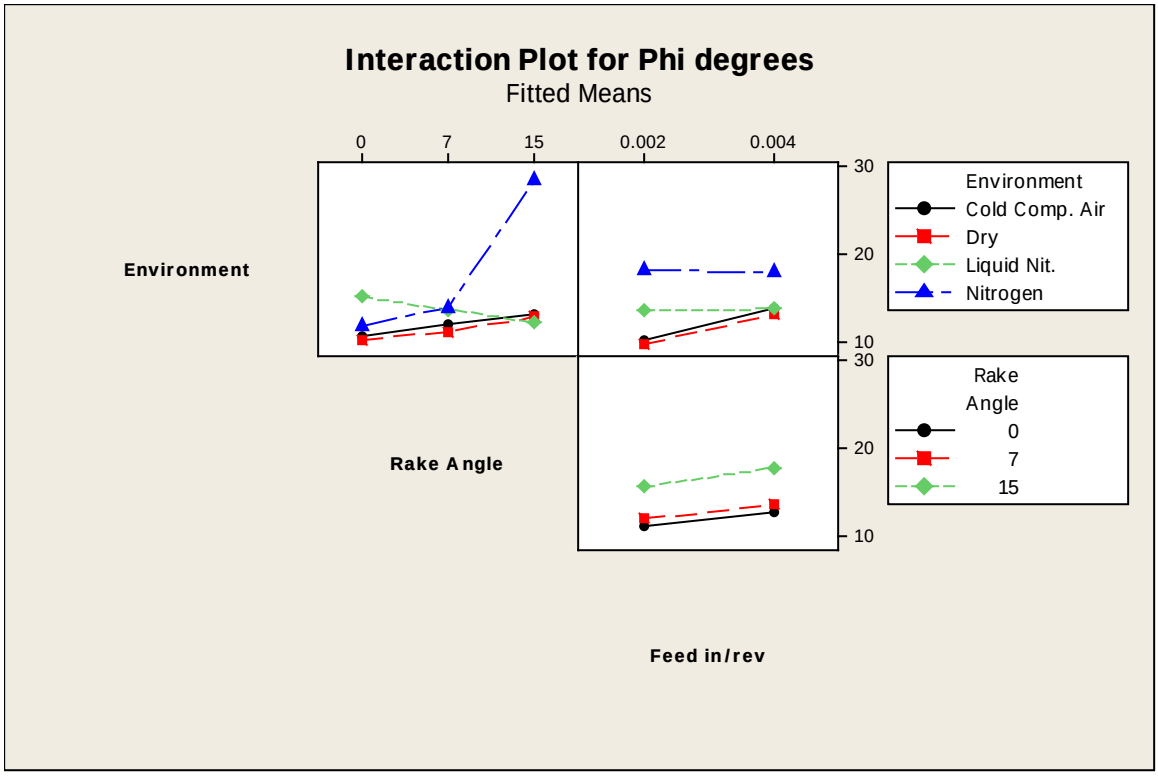
Interaction Plot for Phi degrees
Fitted Means
Environment
Rake Angle
Feed in/rev
0
7
15
0.002
0.004
30
20
10
Environment
Cold Comp. Air
Dry
Liquid Nit.
Nitrogen
Rake Angle
0
7
15

Analysis of Variance for **Psi** degrees, using Adjusted SS for Tests

Source	DF	Seq SS	Adj SS	Adj MS	F
Environment	3	654.536	654.536	218.179	3786.38
Rake Angle	2	161.616	161.616	80.808	1402.38
Feed in/rev	1	74.735	74.735	74.735	1296.98
Environment*Rake Angle	6	994.406	994.406	165.734	2876.24
Environment*Feed in/rev	3	84.221	84.221	28.074	487.21
Rake Angle*Feed in/rev	2	2.073	2.073	1.037	17.99
Environment*Rake Angle*Feed in/rev	6	22.402	22.402	3.734	64.79
Error	72	4.149	4.149	0.058	
Total	95	1998.138			

Source	P
Environment	0.000
Rake Angle	0.000
Feed in/rev	0.000
Environment*Rake Angle	0.000
Environment*Feed in/rev	0.000
Rake Angle*Feed in/rev	0.000
Environment*Rake Angle*Feed in/rev	0.000
Error	
Total	

S = 0.240046 R-Sq = 99.79% R-Sq(adj) = 99.73%

Unusual Observations for Psi degrees

Obs	Psi degrees	Fit	SE Fit	Residual	St Resid	
18	42.4228	41.7777	0.1200	0.6450	3.10	R
19	41.1398	41.7777	0.1200	-0.6379	-3.07	R
65	22.7670	23.3542	0.1200	-0.5873	-2.82	R
67	24.1635	23.3542	0.1200	0.8092	3.89	R
74	28.7983	29.4139	0.1200	-0.6156	-2.96	R
76	29.9084	29.4139	0.1200	0.4945	2.38	R

R denotes an observation with a large standardized residual.

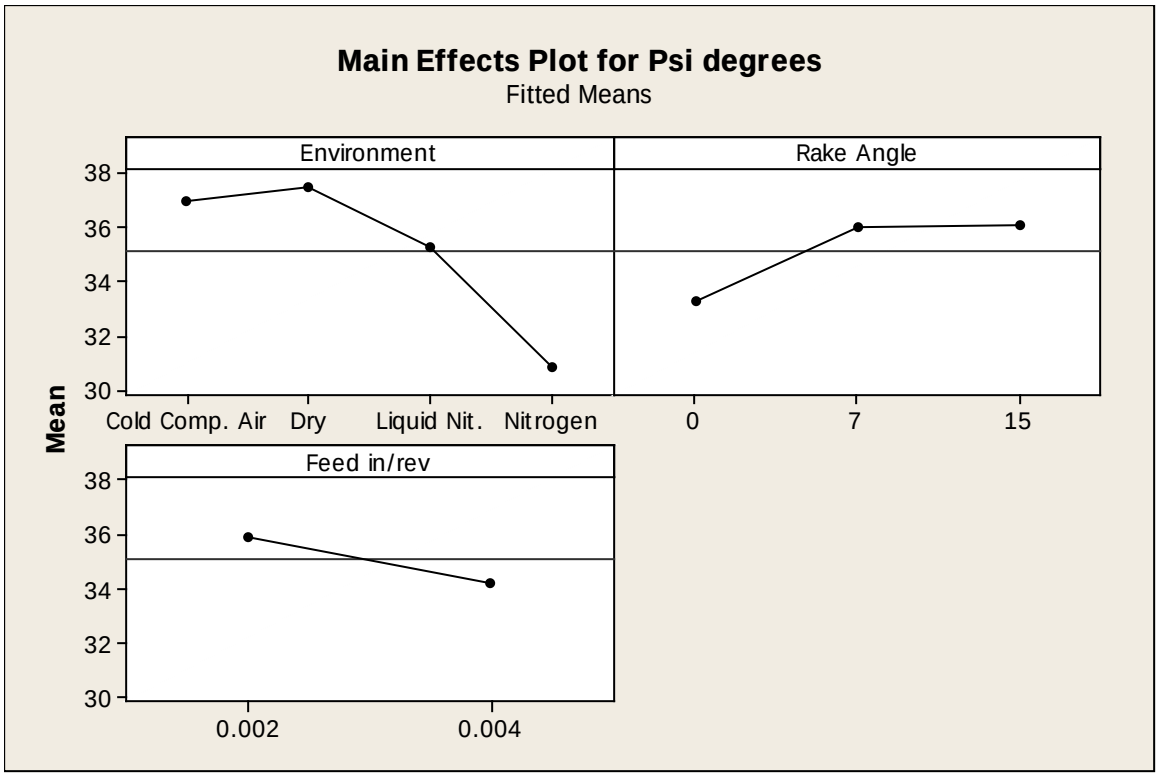
Main Effects Plot for Psi degrees
Fitted Means
Environment
Rake Angle
Feed in/rev
Mean
38
36
34
32
30
Cold Comp. Air
Dry
Liquid Nit.
Nitrogen
0
7
15
0.002
0.004

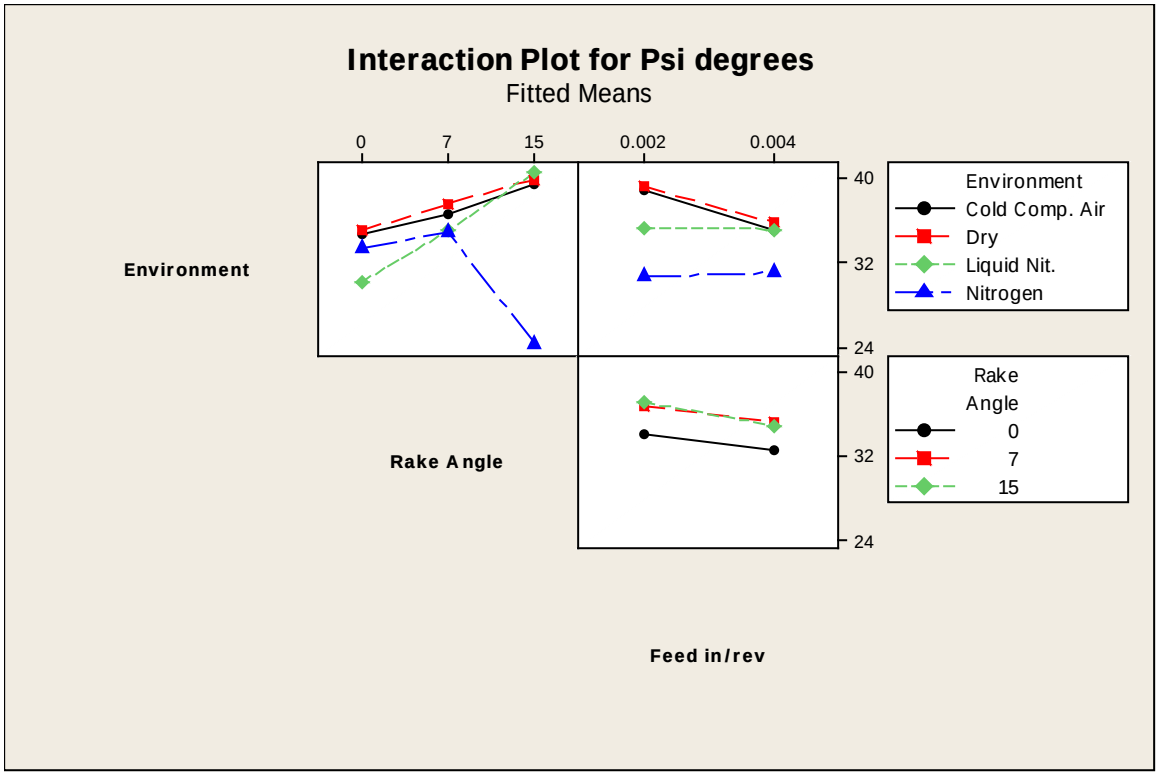
Interaction Plot for Psi degrees
Fitted Means
Environment
Rake Angle
Feed in/rev
0
7
15
0.002
0.004
40
32
24
Environment
Cold Comp. Air
Dry
Liquid Nit.
Nitrogen
Rake Angle
0
7
15

Analysis of Variance for **Friction Force (F)**, using Adjusted SS for Tests

Source	DF	Seq SS	Adj SS	Adj MS	F	P
Environment	3	1290579	1290579	430193	110.06	0.000
Rake Angle	2	274196	274196	137098	35.08	0.000
Feed in/rev	1	241837	241837	241837	61.87	0.000
Environment*Rake Angle	6	162022	162022	27004	6.91	0.000
Environment*Feed in/rev	3	184886	184886	61629	15.77	0.000
Rake Angle*Feed in/rev	2	17368	17368	8684	2.22	0.116
Environment*Rake Angle*Feed in/rev	6	273788	273788	45631	11.67	0.000
Error	72	281415	281415	3909		
Total	95	2726090				

S = 62.5183 R-Sq = 89.68% R-Sq(adj) = 86.38%

Unusual Observations for Friction Force (F)

Obs	Friction Force (F)	Fit	SE Fit	Residual	St Resid	
5	466.152	700.569	31.259	-234.417	-4.33	R
6	872.213	700.569	31.259	171.644	3.17	R
8	869.808	700.569	31.259	169.240	3.13	R
41	264.137	380.340	31.259	-116.203	-2.15	R
57	445.770	280.879	31.259	164.890	3.05	R
76	394.842	268.276	31.259	126.566	2.34	R

R denotes an observation with a large standardized residual.

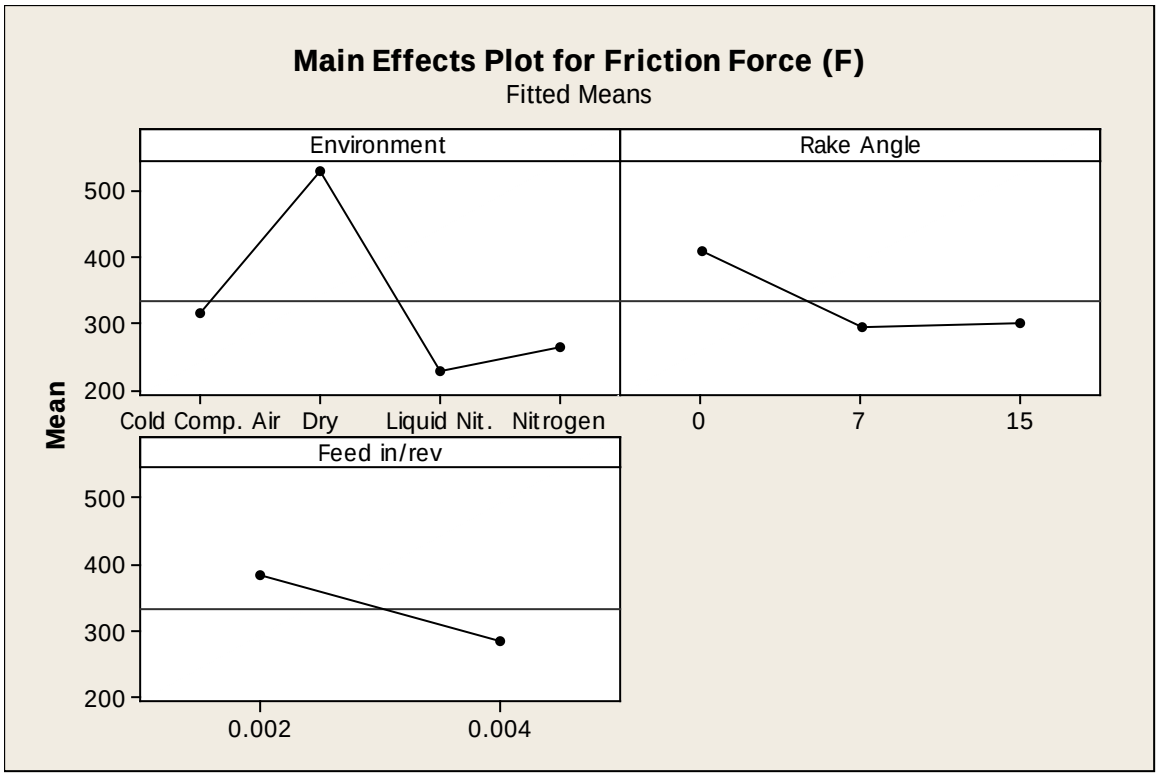
Main Effects Plot for Friction Force (F)
Fitted Means
Environment
Rake Angle
Feed in/rev
Mean
500
400
300
200
Cold Comp. Air
Dry
Liquid Nit.
Nitrogen
0
7
15
0.002
0.004

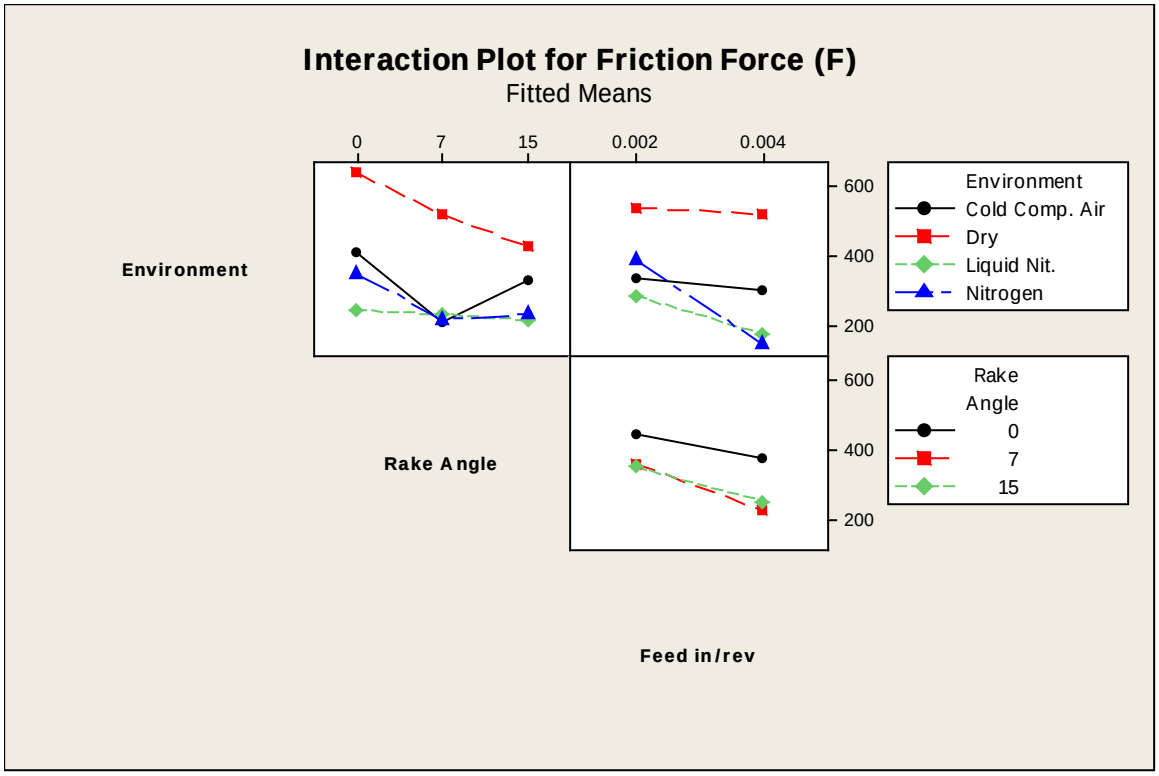
Interaction Plot for Friction Force (F)
Fitted Means
Environment
Rake Angle
Feed in/rev
0
7
15
0.002
0.004
600
400
200
Environment
Cold Comp. Air
Dry
Liquid Nit.
Nitrogen
Rake Angle
0
7
15

Analysis of Variance for **Normal Force (N)**, using Adjusted SS for Tests

Source	DF	Seq SS	Adj SS	Adj MS	F	P
Environment	3	244746	244746	81582	44.72	0.000
Rake Angle	2	599376	599376	299688	164.26	0.000
Feed in/rev	1	263584	263584	263584	144.47	0.000
Environment*Rake Angle	6	173279	173279	28880	15.83	0.000
Environment*Feed in/rev	3	123015	123015	41005	22.47	0.000
Rake Angle*Feed in/rev	2	39494	39494	19747	10.82	0.000
Environment*Rake Angle*Feed in/rev	6	130096	130096	21683	11.88	0.000
Error	72	131363	131363	1824		
Total	95	1704953				

S = 42.7140 R-Sq = 92.30% R-Sq(adj) = 89.83%

Unusual Observations for Normal Force (N)

Obs	Normal Force (N)	Fit	SE Fit	Residual	St Resid	
5	656.372	770.586	21.357	-114.214	-3.09	R
6	871.452	770.586	21.357	100.866	2.73	R
7	658.843	770.586	21.357	-111.743	-3.02	R
8	895.677	770.586	21.357	125.091	3.38	R
17	103.625	205.978	21.357	-102.353	-2.77	R
28	364.375	218.694	21.357	145.681	3.94	R

R denotes an observation with a large standardized residual.

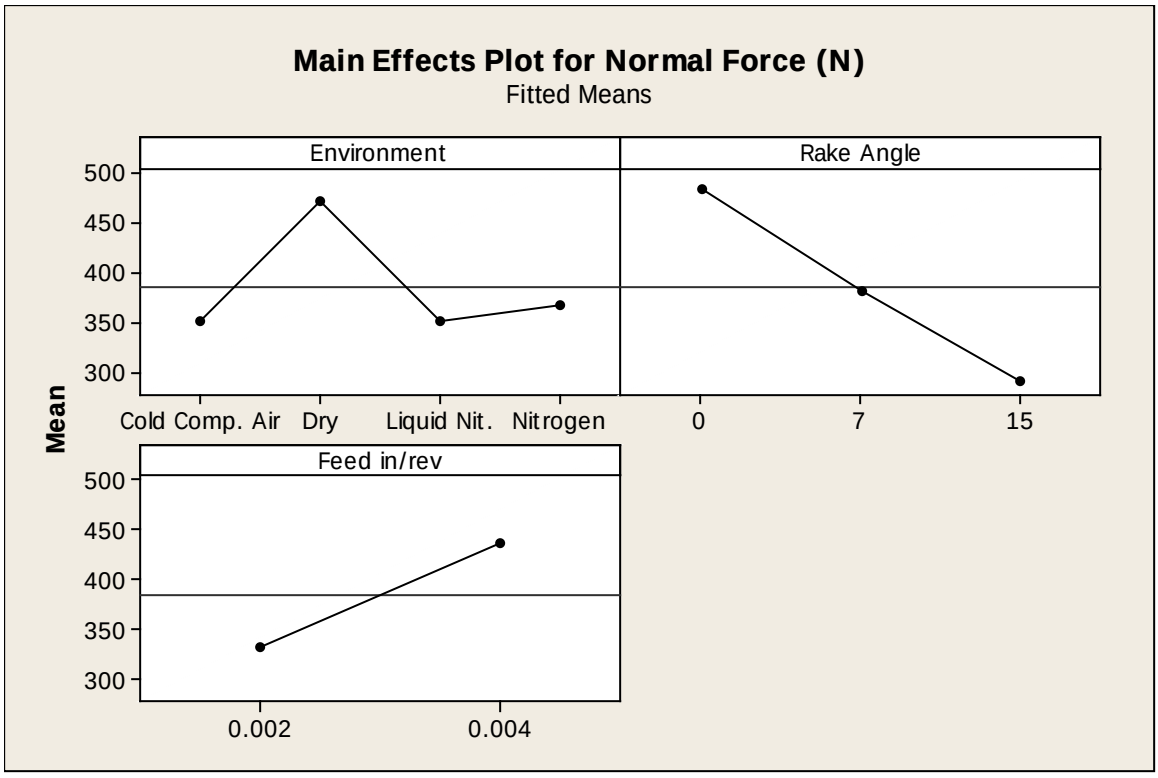
Main Effects Plot for Normal Force (N)
Fitted Means
Environment
Rake Angle
Feed in/rev
Mean
500
450
400
350
300
Cold Comp. Air
Dry
Liquid Nit.
Nitrogen
0
7
15
0.002
0.004

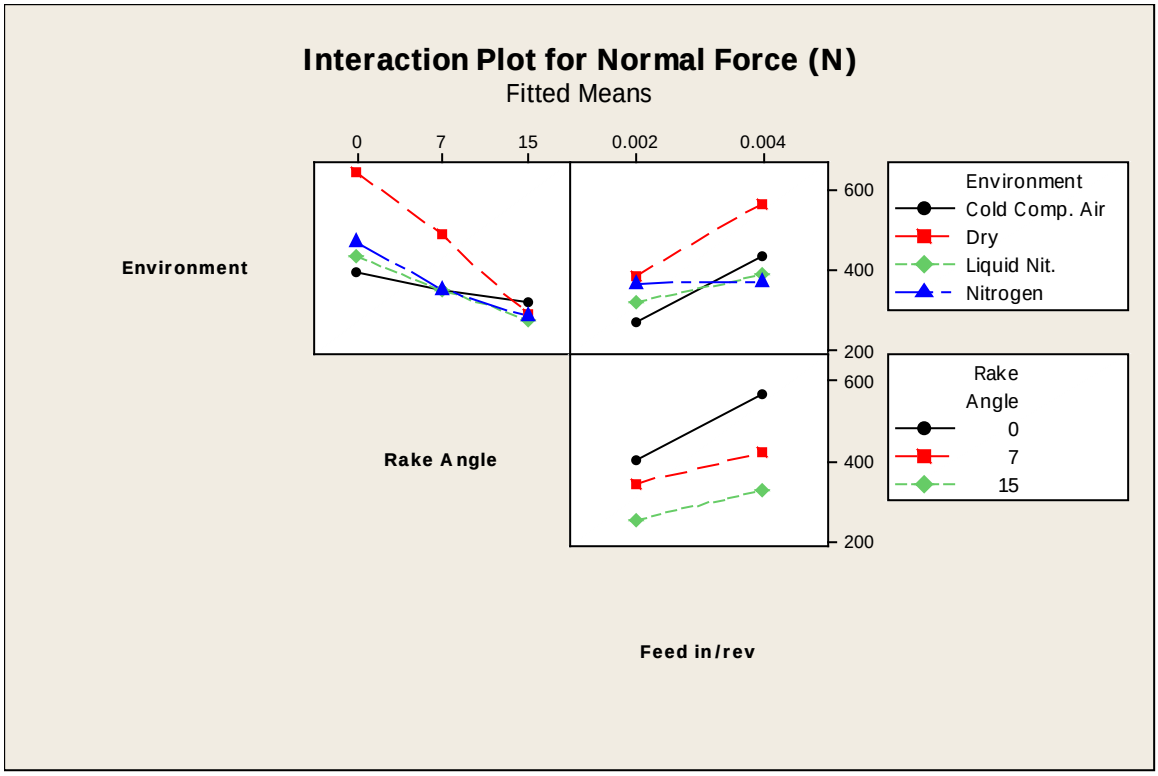
Interaction Plot for Normal Force (N)
Fitted Means
Environment
Rake Angle
Feed in/rev
0
7
15
0.002
0.004
600
400
200
Environment
Cold Comp. Air
Dry
Liquid Nit.
Nitrogen
Rake Angle
0
7
15

Analysis of Variance for **F/N Ratio**, using Adjusted SS for Tests

Source	DF	Seq SS	Adj SS	Adj MS	F	P
Environment	3	6.4765	6.4765	2.1588	13.96	0.000
Rake Angle	2	2.4354	2.4354	1.2177	7.87	0.001
Feed in/rev	1	9.5233	9.5233	9.5233	61.57	0.000
Environment*Rake Angle	6	3.4800	3.4800	0.5800	3.75	0.003
Environment*Feed in/rev	3	0.3634	0.3634	0.1211	0.78	0.507
Rake Angle*Feed in/rev	2	0.3662	0.3662	0.1831	1.18	0.312
Environment*Rake Angle*Feed in/rev	6	2.3529	2.3529	0.3921	2.54	0.028
Error	72	11.1373	11.1373	0.1547		
Total	95	36.1350				

S = 0.393300 R-Sq = 69.18% R-Sq(adj) = 59.33%

Unusual Observations for F/N Ratio

Obs	F/N Ratio	Fit	SE Fit	Residual	St Resid	
17	5.38931	2.70479	0.19665	2.68453	7.88	R
18	1.60870	2.70479	0.19665	-1.09609	-3.22	R
19	1.73753	2.70479	0.19665	-0.96725	-2.84	R
28	1.03542	1.76955	0.19665	-0.73413	-2.16	R

R denotes an observation with a large standardized residual.

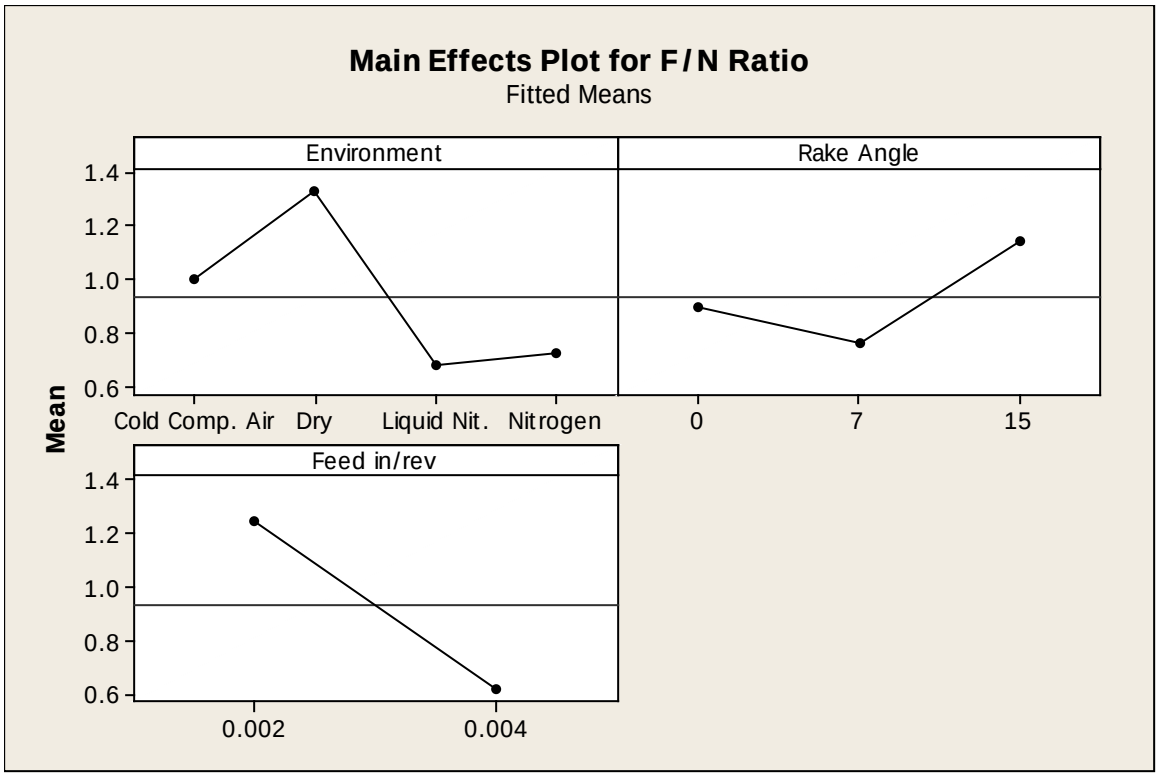
Main Effects Plot for F/N Ratio
Fitted Means
Environment
Rake Angle
Feed in/rev
Mean
1.4
1.2
1.0
0.8
0.6
Cold Comp. Air
Dry
Liquid Nit.
Nitrogen
0
7
15
0.002
0.004

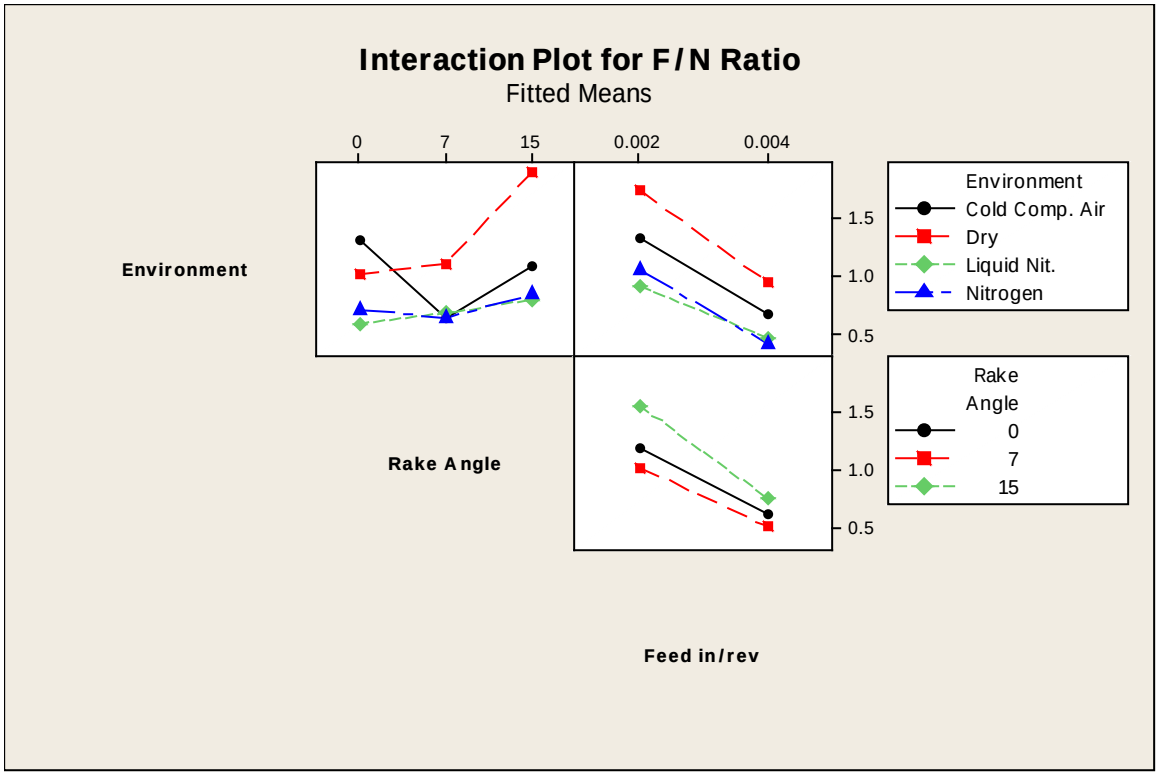
Interaction Plot for F/N Ratio
Fitted Means
Environment
Rake Angle
Feed in/rev
0
7
15
0.002
0.004
1.5
1.0
0.5
Environment
Cold Comp. Air
Dry
Liquid Nit.
Nitrogen
Rake Angle
0
7
15

Analysis of Variance for **Fs (Merchant)**, using Adjusted SS for Tests

Source	DF	Seq SS	Adj SS	Adj MS	F	P
Environment	3	208557	208557	69519	57.79	0.000
Rake Angle	2	191709	191709	95855	79.69	0.000
Feed in/rev	1	244250	244250	244250	203.06	0.000
Environment*Rake Angle	6	137627	137627	22938	19.07	0.000
Environment*Feed in/rev	3	34407	34407	11469	9.53	0.000
Rake Angle*Feed in/rev	2	39971	39971	19985	16.61	0.000
Environment*Rake Angle*Feed in/rev	6	83127	83127	13854	11.52	0.000
Error	72	86606	86606	1203		
Total	95	1026254				

S = 34.6822 R-Sq = 91.56% R-Sq(adj) = 88.87%

Unusual Observations for Fs (Merchant)

Obs	Fs (Merchant)	Fit	SE Fit	Residual	St Resid	
5	548.009	613.292	17.341	-65.283	-2.17	R
6	676.309	613.292	17.341	63.018	2.10	R
7	527.097	613.292	17.341	-86.195	-2.87	R
8	701.752	613.292	17.341	88.460	2.95	R
17	145.121	239.737	17.341	-94.616	-3.15	R
18	310.517	239.737	17.341	70.781	2.36	R
27	97.063	161.378	17.341	-64.315	-2.14	R
28	299.468	161.378	17.341	138.091	4.60	R

R denotes an observation with a large standardized residual.

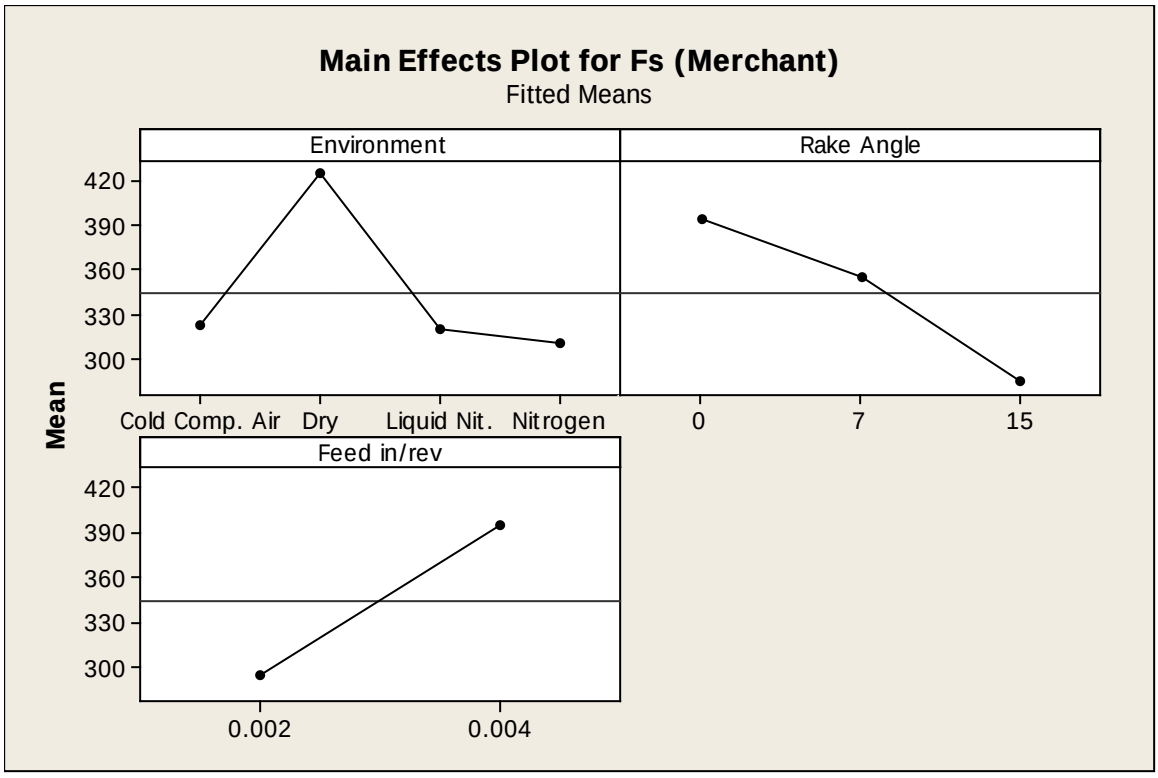
Main Effects Plot for Fs (Merchant)
Fitted Means
Environment
Rake Angle
Feed in/rev
Mean
420
390
360
330
300
Cold Comp. Air
Dry
Liquid Nit.
Nitrogen
0
7
15
0.002
0.004

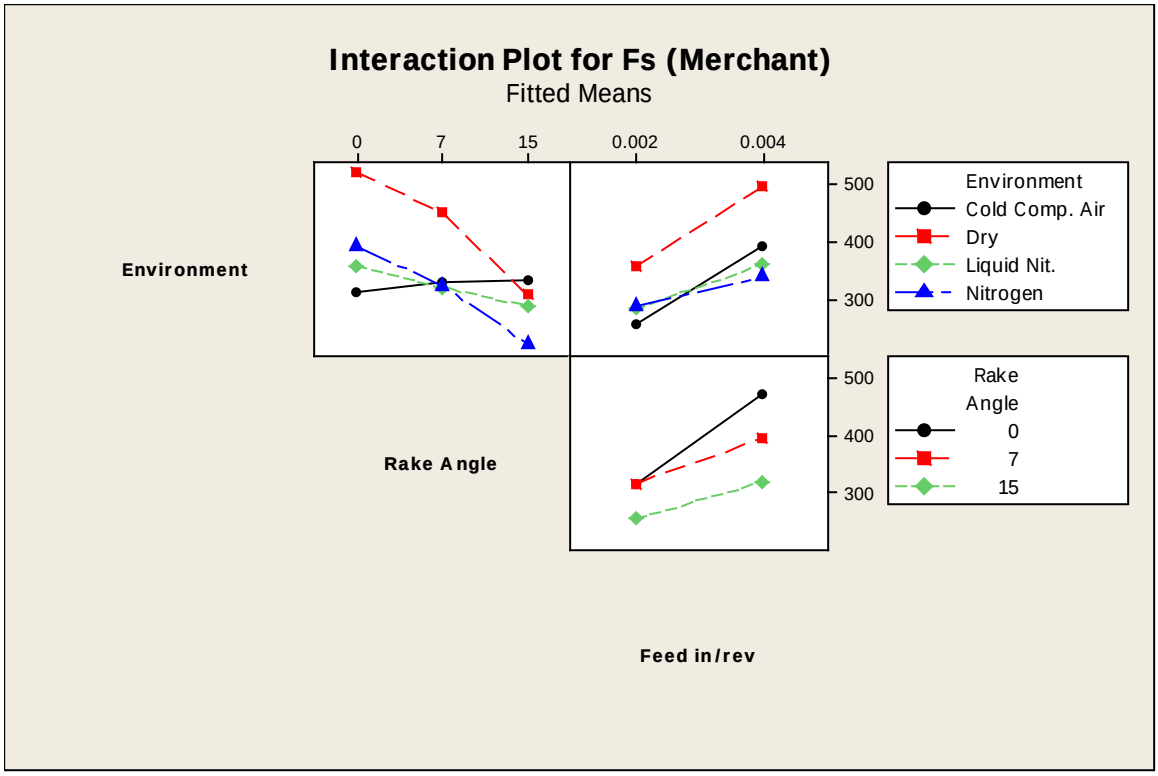
Interaction Plot for Fs (Merchant)
Fitted Means
Environment
Rake Angle
Feed in/rev
0
7
15
0.002
0.004
500
400
300
Environment
Cold Comp. Air
Dry
Liquid Nit.
Nitrogen
Rake Angle
0
7
15

Analysis of Variance for **Fn (Merchant)**, using Adjusted SS for Tests

Source	DF	Seq SS	Adj SS	Adj MS	F	P
Environment	3	1261937	1261937	420646	93.41	0.000
Rake Angle	2	723904	723904	361952	80.38	0.000
Feed in/rev	1	135325	135325	135325	30.05	0.000
Environment*Rake Angle	6	180631	180631	30105	6.69	0.000
Environment*Feed in/rev	3	258671	258671	86224	19.15	0.000
Rake Angle*Feed in/rev	2	35350	35350	17675	3.93	0.024
Environment*Rake Angle*Feed in/rev	6	329843	329843	54974	12.21	0.000
Error	72	324224	324224	4503		
Total	95	3249885				

S = 67.1052 R-Sq = 90.02% R-Sq(adj) = 86.84%

Unusual Observations for Fn (Merchant)

Obs	Fn (Merchant)	Fit	SE Fit	Residual	St Resid	
5	589.75	841.72	33.55	-251.97	-4.34	R
6	1030.92	841.72	33.55	189.19	3.26	R
7	713.58	841.72	33.55	-128.14	-2.20	R
8	1032.64	841.72	33.55	190.92	3.29	R
57	487.39	316.50	33.55	170.89	2.94	R
76	492.25	354.43	33.55	137.83	2.37	R

R denotes an observation with a large standardized residual.

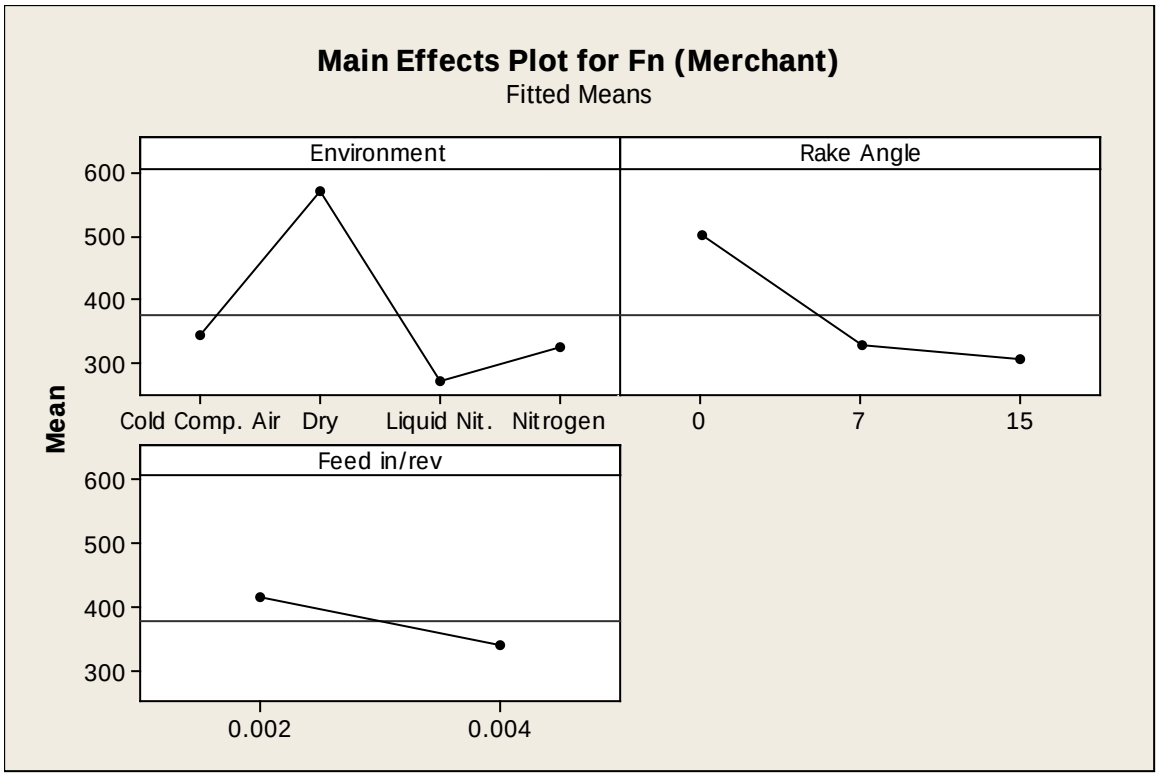
Main Effects Plot for Fn (Merchant)
Fitted Means
Environment
Rake Angle
Feed in/rev
Mean
600
500
400
300
Cold Comp. Air
Dry
Liquid Nit.
Nitrogen
0
7
15
0.002
0.004

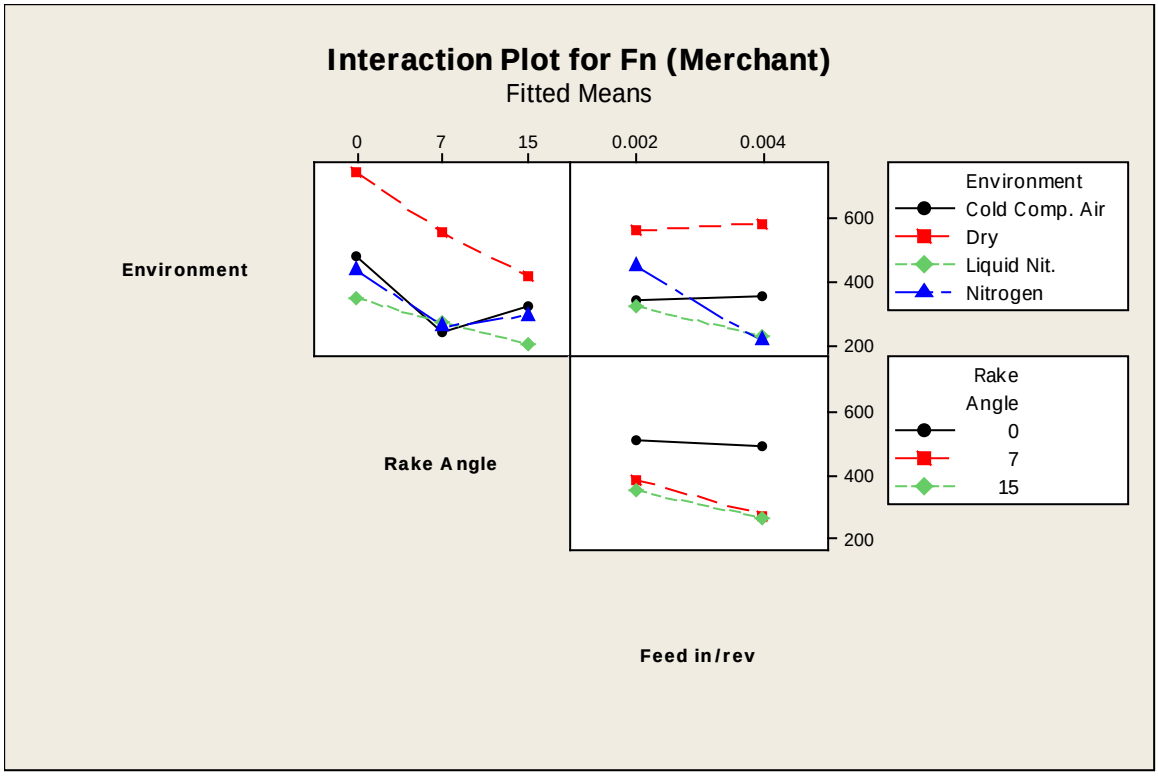
Interaction Plot for Fn (Merchant)
Fitted Means
Environment
Rake Angle
Feed in/rev
0
7
15
0.002
0.004
600
400
200
Environment
Cold Comp. Air
Dry
Liquid Nit.
Nitrogen
Rake Angle
0
7
15

Analysis of Variance for **Fs/Fn (Merchant)**, using Adjusted SS for Tests

Source	DF	Seq SS	Adj SS	Adj MS	F
Environment	3	4.10908	4.10908	1.36969	79.68
Rake Angle	2	2.18564	2.18564	1.09282	63.57
Feed in/rev	1	10.03254	10.03254	10.03254	583.60
Environment*Rake Angle	6	3.33549	3.33549	0.55591	32.34
Environment*Feed in/rev	3	1.82038	1.82038	0.60679	35.30
Rake Angle*Feed in/rev	2	0.31871	0.31871	0.15936	9.27
Environment*Rake Angle*Feed in/rev	6	0.82314	0.82314	0.13719	7.98
Error	72	1.23774	1.23774	0.01719	
Total	95	23.86273			

Source	P
Environment	0.000
Rake Angle	0.000
Feed in/rev	0.000
Environment*Rake Angle	0.000
Environment*Feed in/rev	0.000
Rake Angle*Feed in/rev	0.000
Environment*Rake Angle*Feed in/rev	0.000
Error	
Total	

S = 0.131114 R-Sq = 94.81% R-Sq(adj) = 93.16%

Unusual Observations for Fs/Fn (Merchant)

Obs	Fs/Fn (Merchant)	Fit	SE Fit	Residual	St Resid	
17	0.26427	0.56260	0.06556	-0.29833	-2.63	R
28	0.69544	0.41241	0.06556	0.28303	2.49	R
41	1.13184	0.89768	0.06556	0.23416	2.06	R
55	2.14671	1.88686	0.06556	0.25984	2.29	R
57	0.66640	0.90255	0.06556	-0.23615	-2.08	R
78	1.74534	1.35976	0.06556	0.38557	3.40	R
79	1.03017	1.35976	0.06556	-0.32959	-2.90	R

R denotes an observation with a large standardized residual.

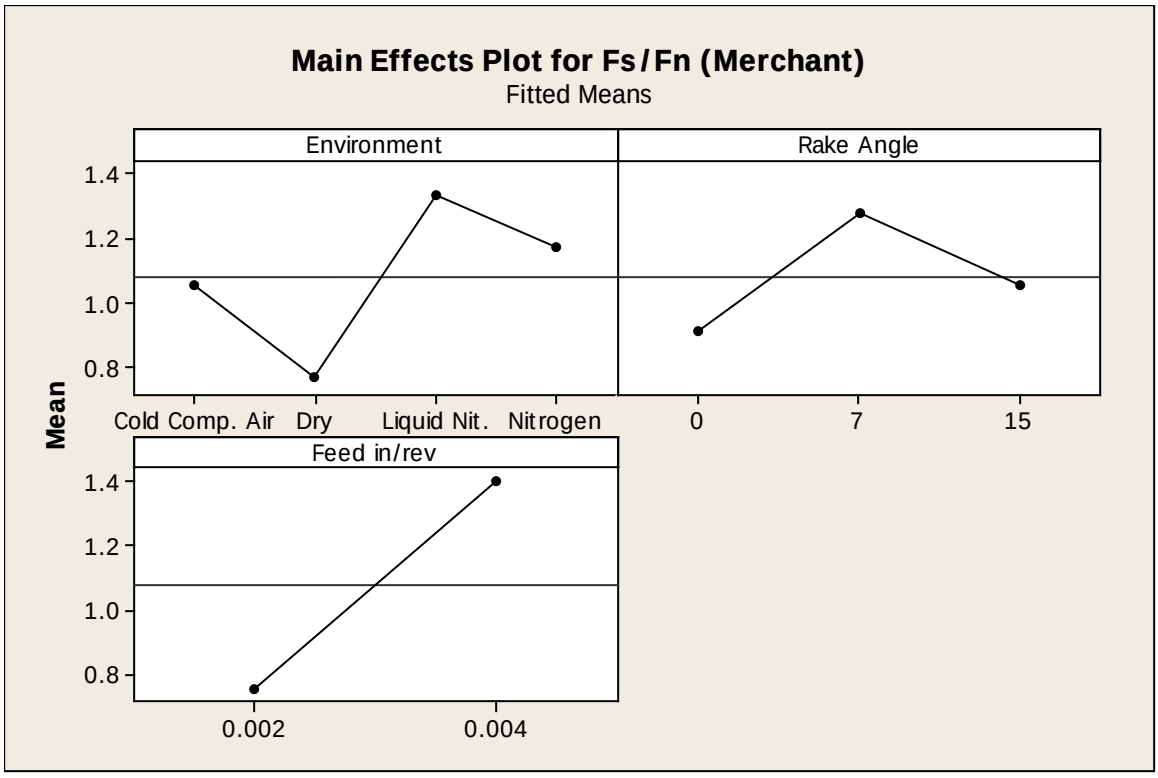
Main Effects Plot for Fs/Fn (Merchant)
Fitted Means
Environment
Rake Angle
Feed in/rev
Mean
1.4
1.2
1.0
0.8
Cold Comp. Air
Dry
Liquid Nit.
Nitrogen
0
7
15
0.002
0.004

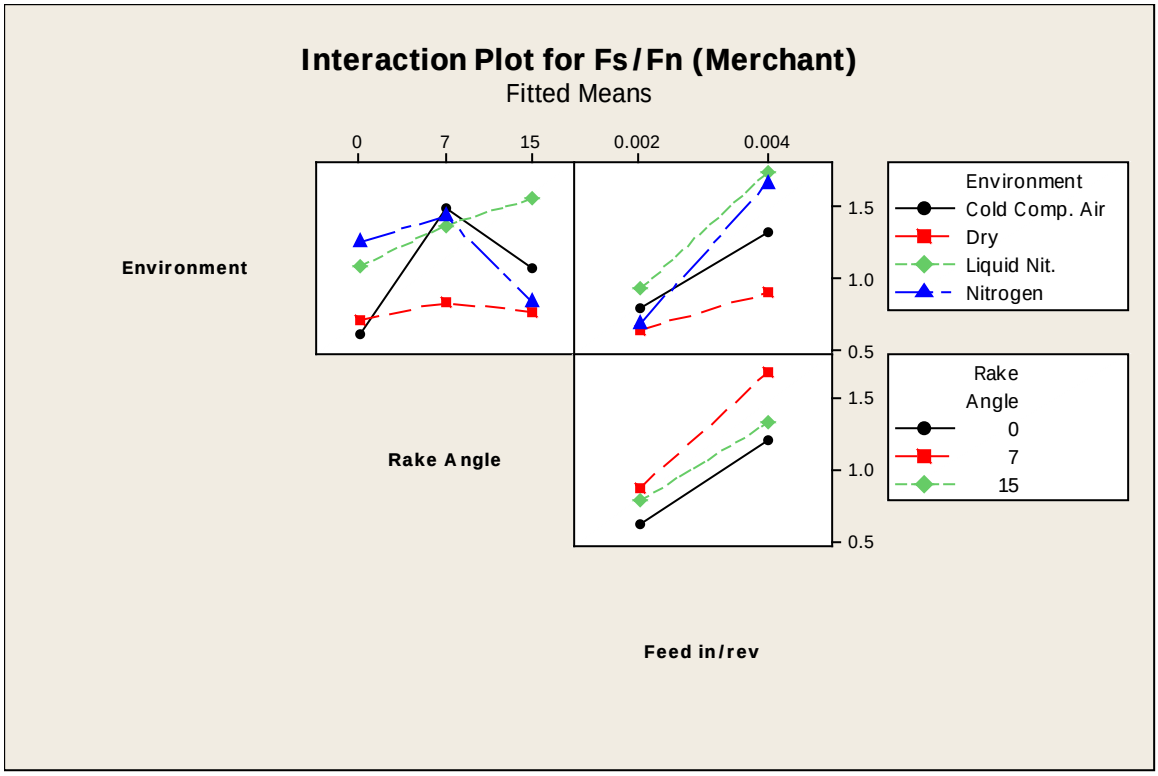
Interaction Plot for Fs/Fn (Merchant)
Fitted Means
Environment
Rake Angle
Feed in/rev
0
7
15
0.002
0.004
1.5
1.0
0.5
Environment
Cold Comp. Air
Dry
Liquid Nit.
Nitrogen
Rake Angle
0
7
15

Analysis of Variance for **Fs (Payton)**, using Adjusted SS for Tests

Source	DF	Seq SS	Adj SS	Adj MS	F	P
Environment	3	183670	183670	61223	61.38	0.000
Rake Angle	2	37800	37800	18900	18.95	0.000
Feed in/rev	1	491091	491091	491091	492.38	0.000
Environment*Rake Angle	6	59484	59484	9914	9.94	0.000
Environment*Feed in/rev	3	6998	6998	2333	2.34	0.081
Rake Angle*Feed in/rev	2	7275	7275	3638	3.65	0.031
Environment*Rake Angle*Feed in/rev	6	29539	29539	4923	4.94	0.000
Error	72	71811	71811	997		
Total	95	887668				

S = 31.5813 R-Sq = 91.91% R-Sq(adj) = 89.33%

Unusual Observations for Fs (Payton)

Obs	Fs (Payton)	Fit	SE Fit	Residual	St Resid	
5	134.506	49.510	15.791	84.996	3.11	R
17	-257.762	-116.829	15.791	-140.932	-5.15	R
18	-50.905	-116.829	15.791	65.925	2.41	R
28	-9.127	-92.329	15.791	83.203	3.04	R
57	-10.841	44.831	15.791	-55.672	-2.04	R

R denotes an observation with a large standardized residual.

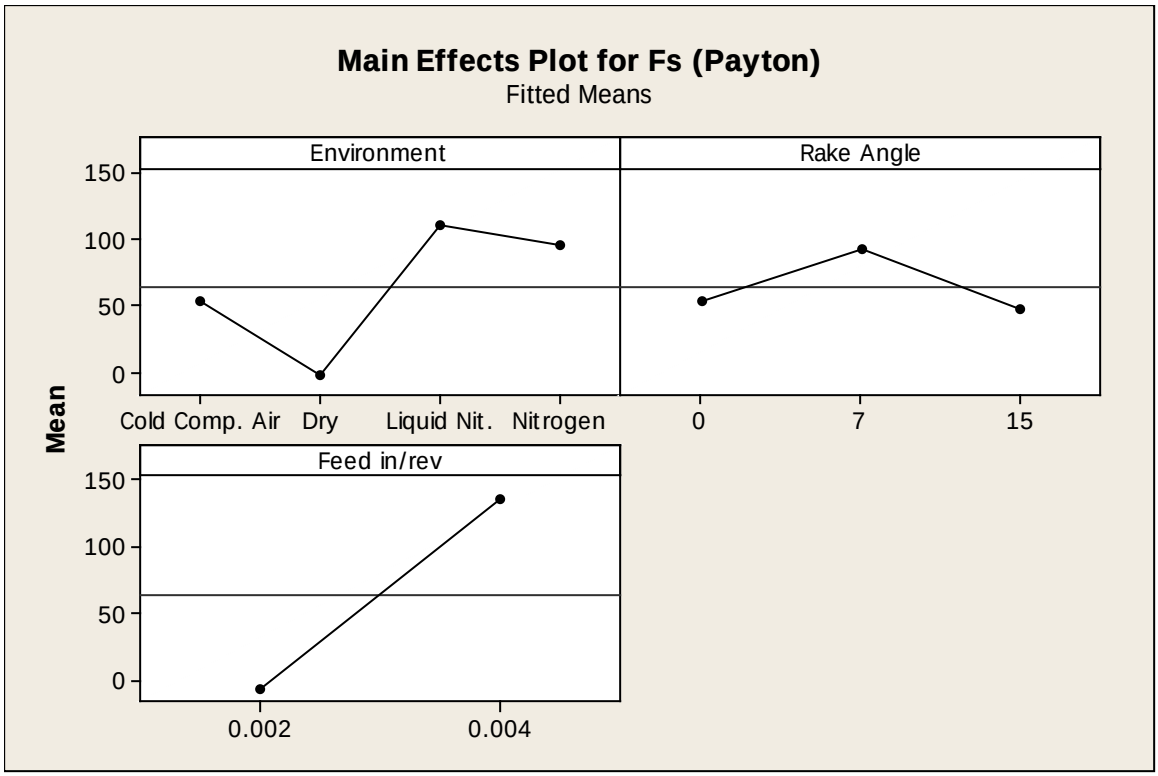
Main Effects Plot for Fs (Payton)
Fitted Means
Environment
Rake Angle
Feed in/rev
Mean
150
100
50
0
Cold Comp. Air
Dry
Liquid Nit.
Nitrogen
0
7
15
0.002
0.004

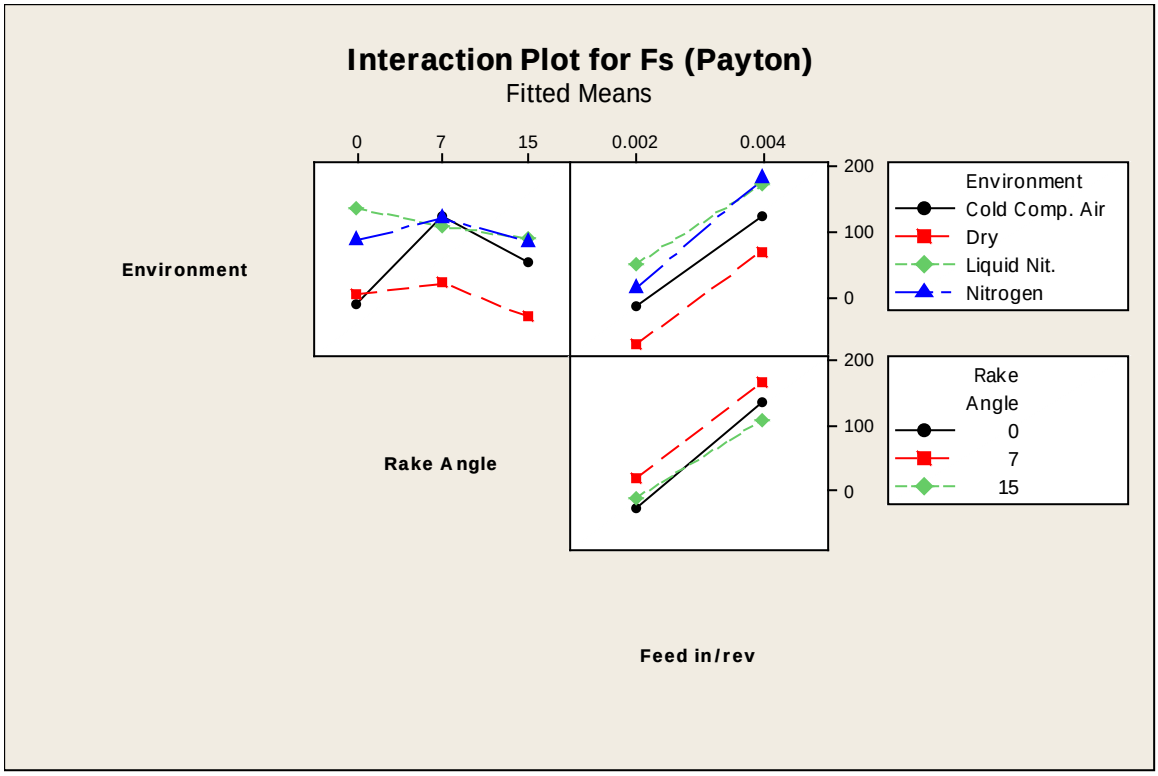
Interaction Plot for Fs (Payton)
Fitted Means
Environment
Rake Angle
Feed in/rev
0
7
15
0.002
0.004
200
100
0
Environment
Cold Comp. Air
Dry
Liquid Nit.
Nitrogen
Rake Angle
0
7
15

Analysis of Variance for **Fn (Payton)**, using Adjusted SS for Tests

Source	DF	Seq SS	Adj SS	Adj MS	F	P
Environment	3	1374775	1374775	458258	96.77	0.000
Rake Angle	2	808574	808574	404287	85.37	0.000
Feed in/rev	1	653	653	653	0.14	0.711
Environment*Rake Angle	6	252697	252697	42116	8.89	0.000
Environment*Feed in/rev	3	296417	296417	98806	20.86	0.000
Rake Angle*Feed in/rev	2	63263	63263	31632	6.68	0.002
Environment*Rake Angle*Feed in/rev	6	378831	378831	63138	13.33	0.000
Error	72	340967	340967	4736		
Total	95	3516176				

S = 68.8160 R-Sq = 90.30% R-Sq(adj) = 87.21%

Unusual Observations for Fn (Payton)

Obs	Fn (Payton)	Fit	SE Fit	Residual	St Resid	
5	793.74	1040.26	34.41	-246.52	-4.14	R
6	1232.96	1040.26	34.41	192.69	3.23	R
7	885.97	1040.26	34.41	-154.30	-2.59	R
8	1248.39	1040.26	34.41	208.12	3.49	R
28	524.43	401.61	34.41	122.82	2.06	R
57	585.60	414.69	34.41	170.91	2.87	R
76	580.74	442.73	34.41	138.01	2.32	R

R denotes an observation with a large standardized residual.

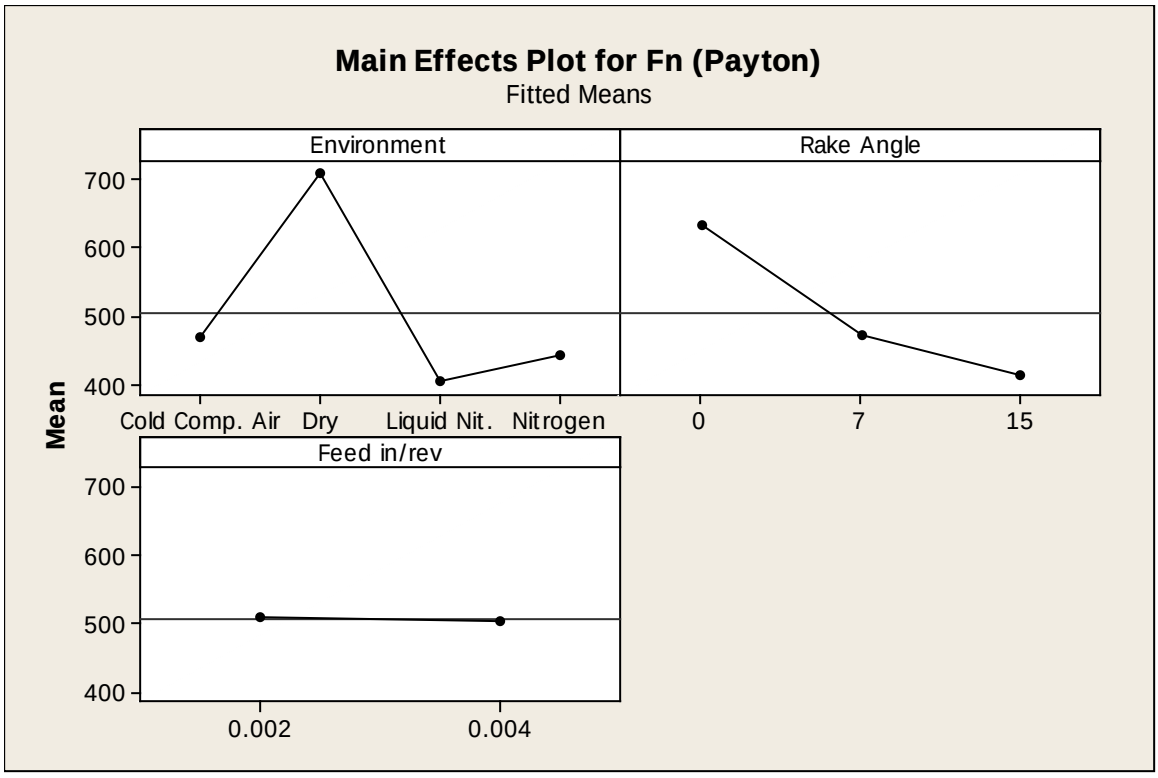
Main Effects Plot for Fn (Payton)
Fitted Means
Environment
Rake Angle
Feed in/rev
Mean
700
600
500
400
Cold Comp. Air
Dry
Liquid Nit.
Nitrogen
0
7
15
0.002
0.004

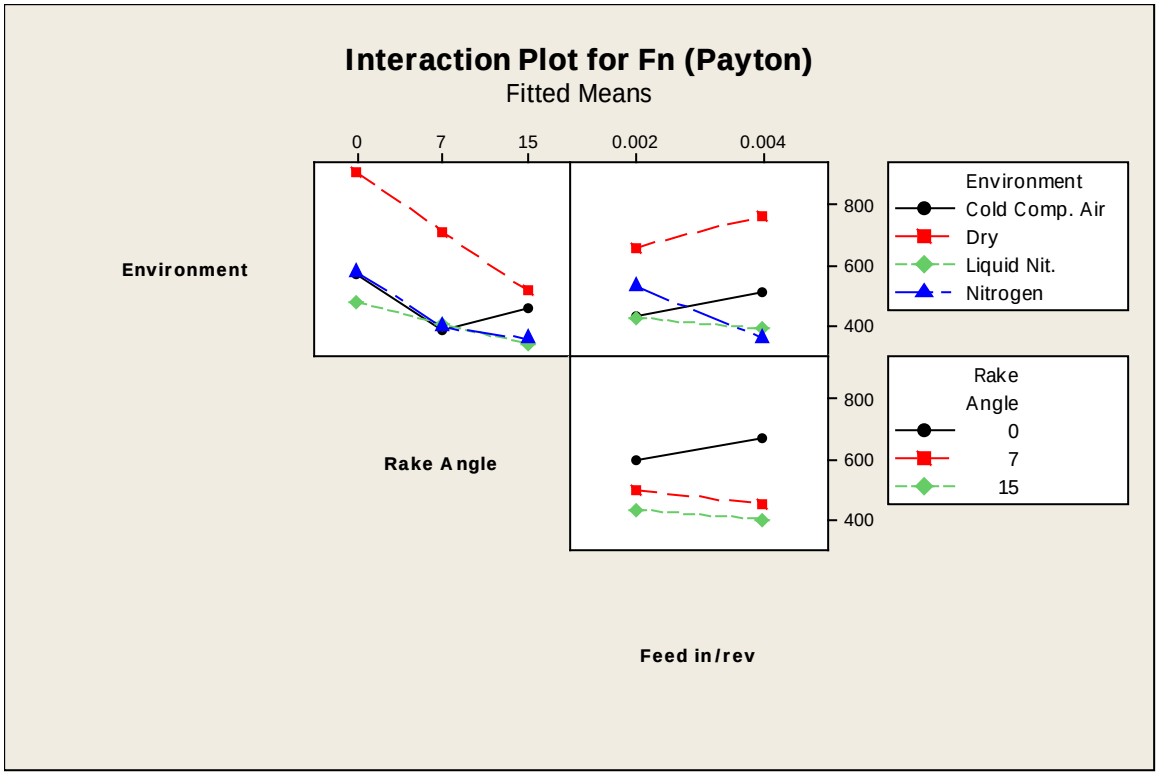
Interaction Plot for Fn (Payton)
Fitted Means
Environment
Rake Angle
Feed in/rev
0
7
15
0.002
0.004
800
600
400
Environment
Cold Comp. Air
Dry
Liquid Nit.
Nitrogen
Rake Angle
0
7
15

Analysis of Variance for **Fs/Fn (Payton)**, using Adjusted SS for Tests

Source	DF	Seq SS	Adj SS	Adj MS	F
Environment	3	1.46889	1.46889	0.48963	88.97
Rake Angle	2	0.29977	0.29977	0.14988	27.23
Feed in/rev	1	2.70283	2.70283	2.70283	491.10
Environment*Rake Angle	6	0.44016	0.44016	0.07336	13.33
Environment*Feed in/rev	3	0.15255	0.15255	0.05085	9.24
Rake Angle*Feed in/rev	2	0.00780	0.00780	0.00390	0.71
Environment*Rake Angle*Feed in/rev	6	0.17000	0.17000	0.02833	5.15
Error	72	0.39626	0.39626	0.00550	
Total	95	5.63827			

Source	P
Environment	0.000
Rake Angle	0.000
Feed in/rev	0.000
Environment*Rake Angle	0.000
Environment*Feed in/rev	0.000
Rake Angle*Feed in/rev	0.496
Environment*Rake Angle*Feed in/rev	0.000
Error	
Total	

S = 0.0741861 R-Sq = 92.97% R-Sq(adj) = 90.73%

Unusual Observations for Fs/Fn (Payton)

Obs	Fs/Fn (Payton)	Fit	SE Fit	Residual	St Resid	
17	-0.509266	-0.237749	0.037093	-0.271516	-4.23	R
18	-0.098651	-0.237749	0.037093	0.139098	2.17	R
28	-0.017403	-0.254992	0.037093	0.237589	3.70	R
57	-0.018513	0.128784	0.037093	-0.147297	-2.29	R
78	0.569110	0.413857	0.037093	0.155253	2.42	R
79	0.270937	0.413857	0.037093	-0.142919	-2.22	R

R denotes an observation with a large standardized residual.

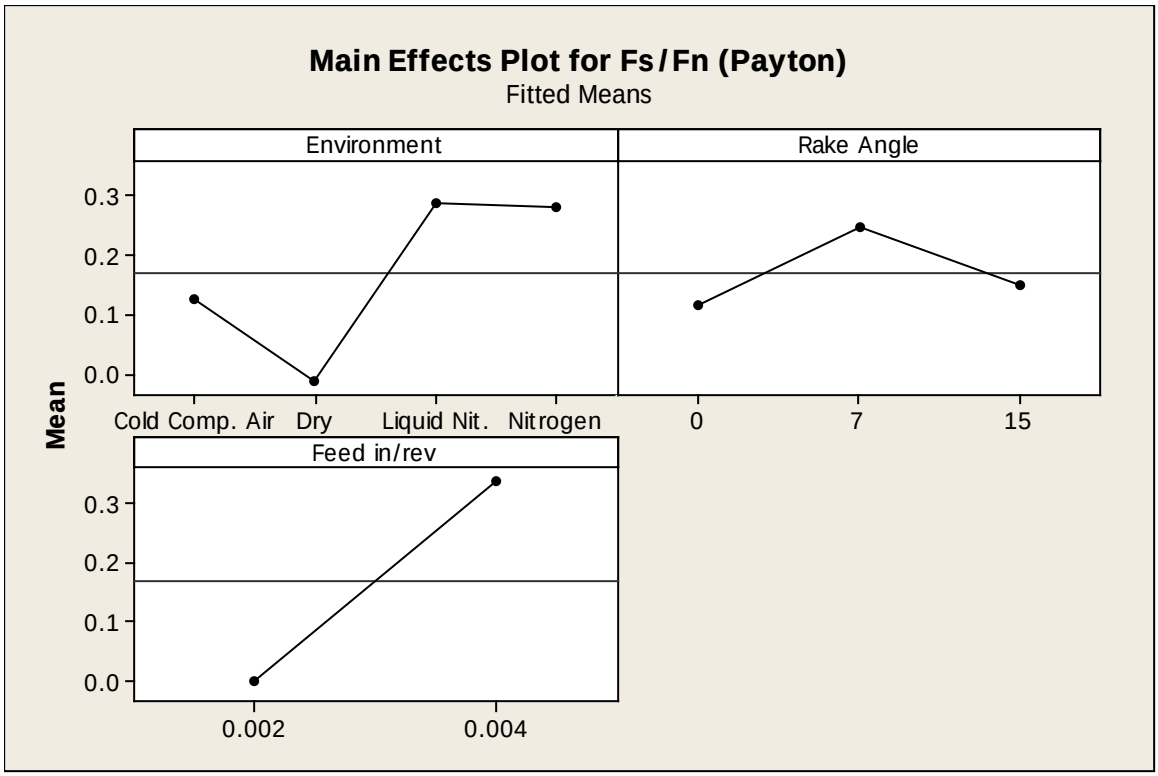
Main Effects Plot for Fs/Fn (Payton)
Fitted Means
Environment
Rake Angle
Feed in/rev
Mean
0.3
0.2
0.1
0.0
Cold Comp. Air
Dry
Liquid Nit.
Nitrogen
0
7
15
0.002
0.004

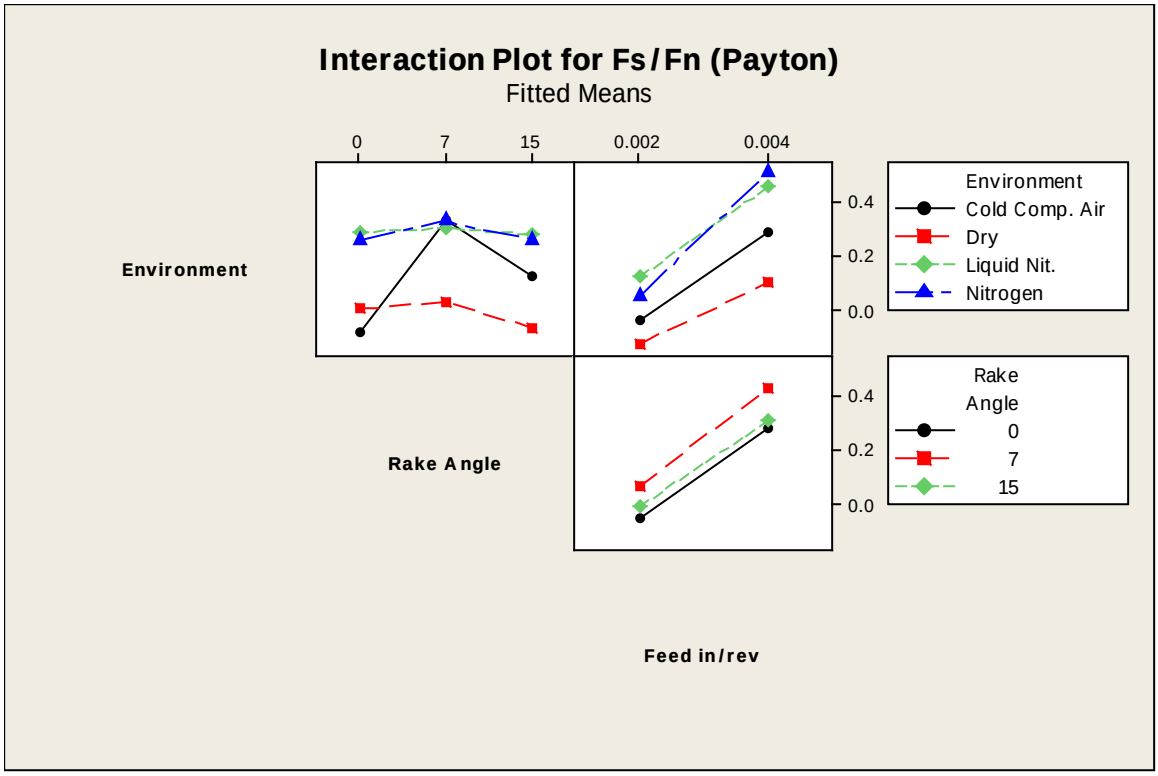
Interaction Plot for Fs/Fn (Payton)
Fitted Means
Environment
Rake Angle
Feed in/rev
0
7
15
0.002
0.004
0.4
0.2
0.0
Environment
Cold Comp. Air
Dry
Liquid Nit.
Nitrogen
Rake Angle
0
7
15

Analysis of Variance for **Beta** (degrees), using Adjusted SS for Tests

Source	DF	Seq SS	Adj SS	Adj MS	F
Environment	3	4219.91	4219.91	1406.64	89.85
Rake Angle	2	1334.33	1334.33	667.16	42.62
Feed in/rev	1	7732.86	7732.86	7732.86	493.94
Environment*Rake Angle	6	1282.43	1282.43	213.74	13.65
Environment*Feed in/rev	3	362.37	362.37	120.79	7.72
Rake Angle*Feed in/rev	2	11.94	11.94	5.97	0.38
Environment*Rake Angle*Feed in/rev	6	477.95	477.95	79.66	5.09
Error	72	1127.19	1127.19	15.66	
Total	95	16548.96			

Source	P
Environment	0.000
Rake Angle	0.000
Feed in/rev	0.000
Environment*Rake Angle	0.000
Environment*Feed in/rev	0.000
Rake Angle*Feed in/rev	0.684
Environment*Rake Angle*Feed in/rev	0.000
Error	
Total	

S = 3.95669 R-Sq = 93.19% R-Sq(adj) = 91.01%

Unusual Observations for Beta (degrees)

Obs	Beta (degrees)	Fit	SE Fit	Residual	St Resid	
17	79.4882	65.5156	1.9783	13.9726	4.08	R
18	58.1341	65.5156	1.9783	-7.3815	-2.15	R
28	45.9970	59.0906	1.9783	-13.0936	-3.82	R
41	45.8536	52.9709	1.9783	-7.1172	-2.08	R
57	49.5606	41.2035	1.9783	8.3571	2.44	R
78	15.3554	22.7166	1.9783	-7.3612	-2.15	R
79	29.8404	22.7166	1.9783	7.1238	2.08	R

R denotes an observation with a large standardized residual.

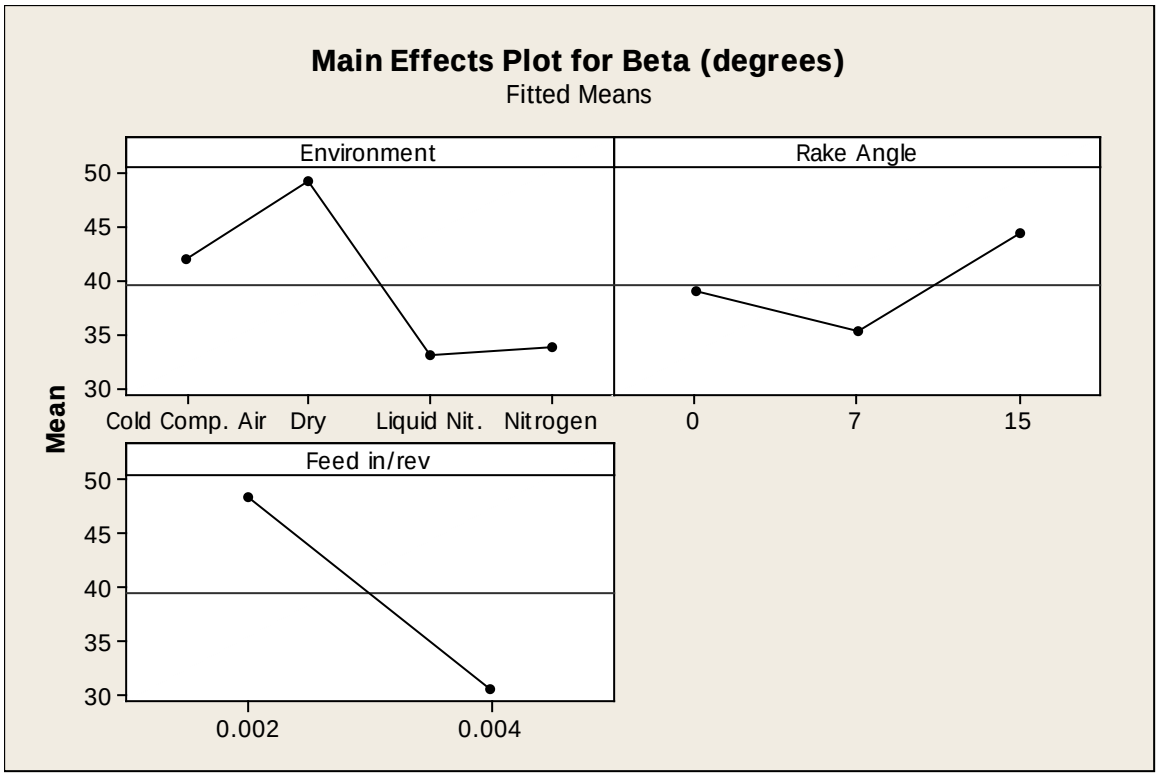
Main Effects Plot for Beta (degrees)
Fitted Means
Environment
Rake Angle
Feed in/rev
Mean
50
45
40
35
30
Cold Comp. Air
Dry
Liquid Nit.
Nitrogen
0
7
15
0.002
0.004

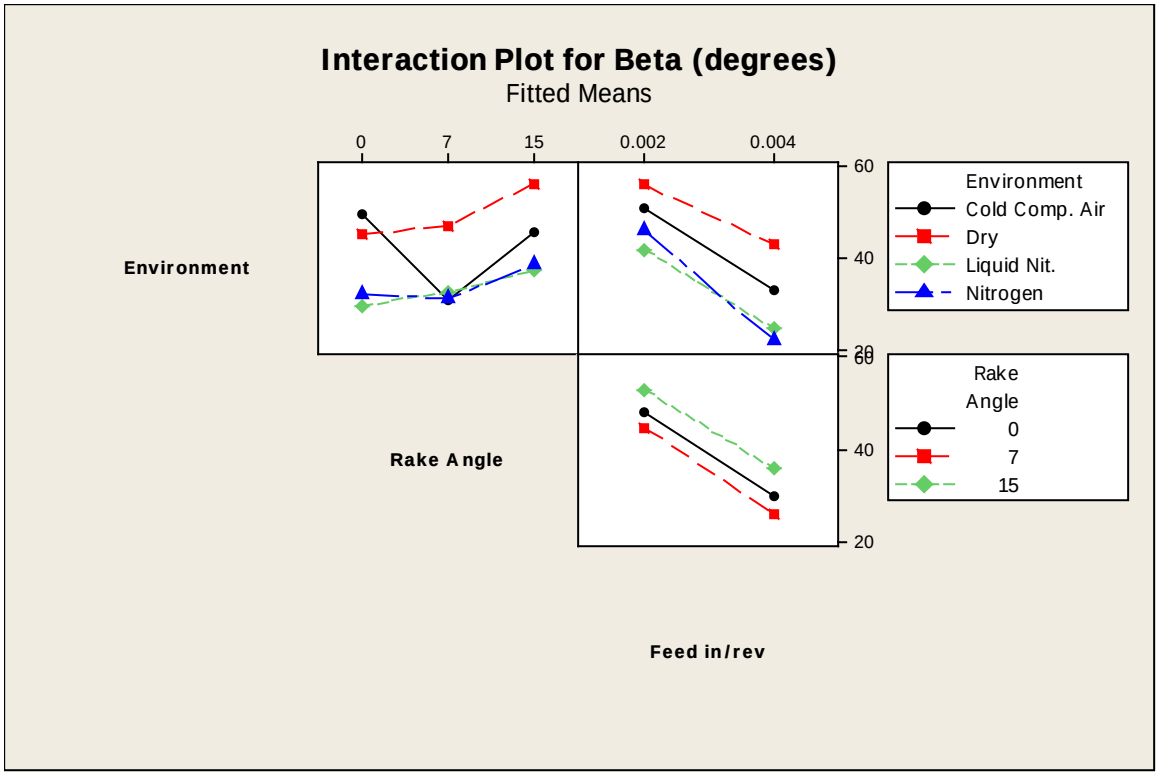
Interaction Plot for Beta (degrees)
Fitted Means
Environment
Rake Angle
Feed in/rev
0
7
15
0.002
0.004
60
40
20
Environment
Cold Comp. Air
Dry
Liquid Nit.
Nitrogen
Rake Angle
0
7
15

Analysis of Variance for **Shear Area**, As, using Adjusted SS for Tests

Source	DF	Seq SS	Adj SS	Adj MS
Environment	3	0.0000030	0.0000030	0.0000010
Rake Angle	2	0.0000023	0.0000023	0.0000012
Feed in/rev	1	0.0000156	0.0000156	0.0000156
Environment*Rake Angle	6	0.0000036	0.0000036	0.0000006
Environment*Feed in/rev	3	0.0000005	0.0000005	0.0000002
Rake Angle*Feed in/rev	2	0.0000003	0.0000003	0.0000002
Environment*Rake Angle*Feed in/rev	6	0.0000002	0.0000002	0.0000000
Error	72	0.0000000	0.0000000	0.0000000
Total	95	0.0000255		

Source	F	P
Environment	1968.87	0.000
Rake Angle	2251.21	0.000
Feed in/rev	30249.00	0.000
Environment*Rake Angle	1173.82	0.000
Environment*Feed in/rev	307.47	0.000
Rake Angle*Feed in/rev	298.67	0.000
Environment*Rake Angle*Feed in/rev	62.75	0.000
Error		
Total		

S = 0.0000226778 R-Sq = 99.86% R-Sq(adj) = 99.81%

Unusual Observations for Shear Area, As

Obs	Shear Area, As	Fit	SE Fit	Residual	St Resid	
9	0.001527	0.001487	0.000011	0.000040	2.05	R
18	0.001372	0.001292	0.000011	0.000079	4.04	R
19	0.001218	0.001292	0.000011	-0.000074	-3.76	R
44	0.001385	0.001331	0.000011	0.000054	2.75	R
89	0.001263	0.001221	0.000011	0.000042	2.14	R

R denotes an observation with a large standardized residual.

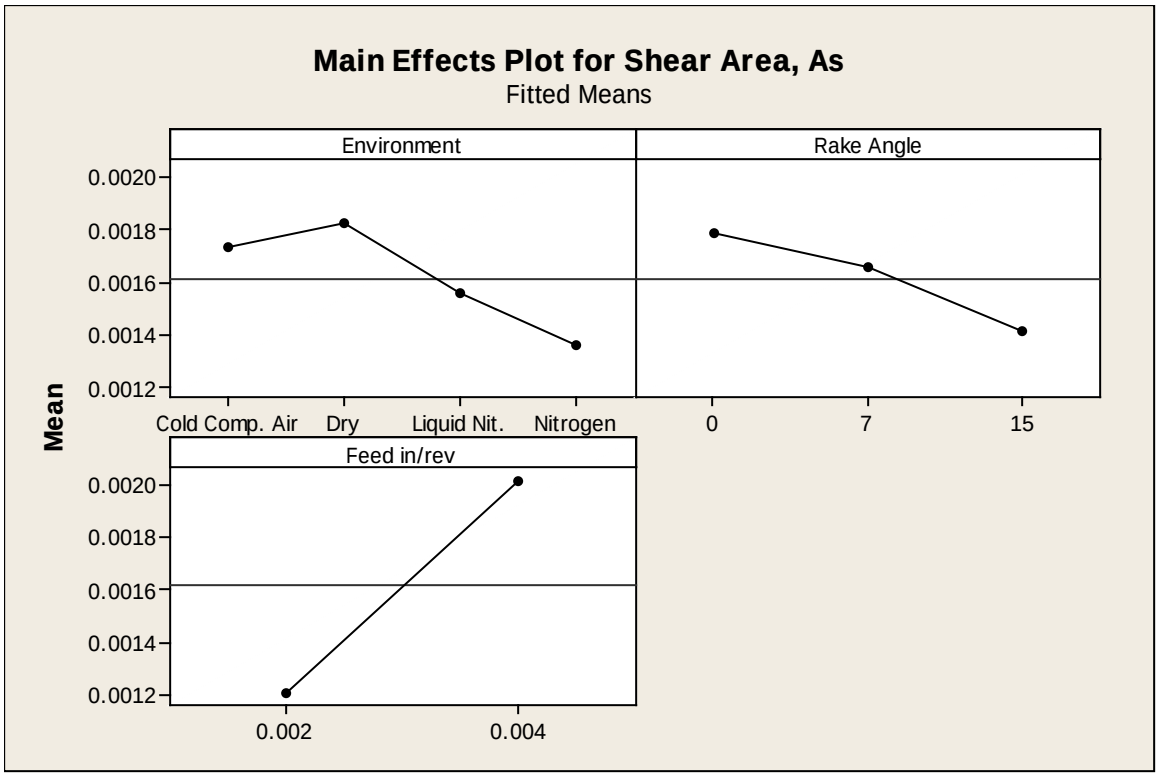
Main Effects Plot for Shear Area, As
Fitted Means
Environment
Rake Angle
Feed in/rev
Mean
0.0020
0.0018
0.0016
0.0014
0.0012
Cold Comp. Air
Dry
Liquid Nit.
Nitrogen
0
7
15
0.002
0.004

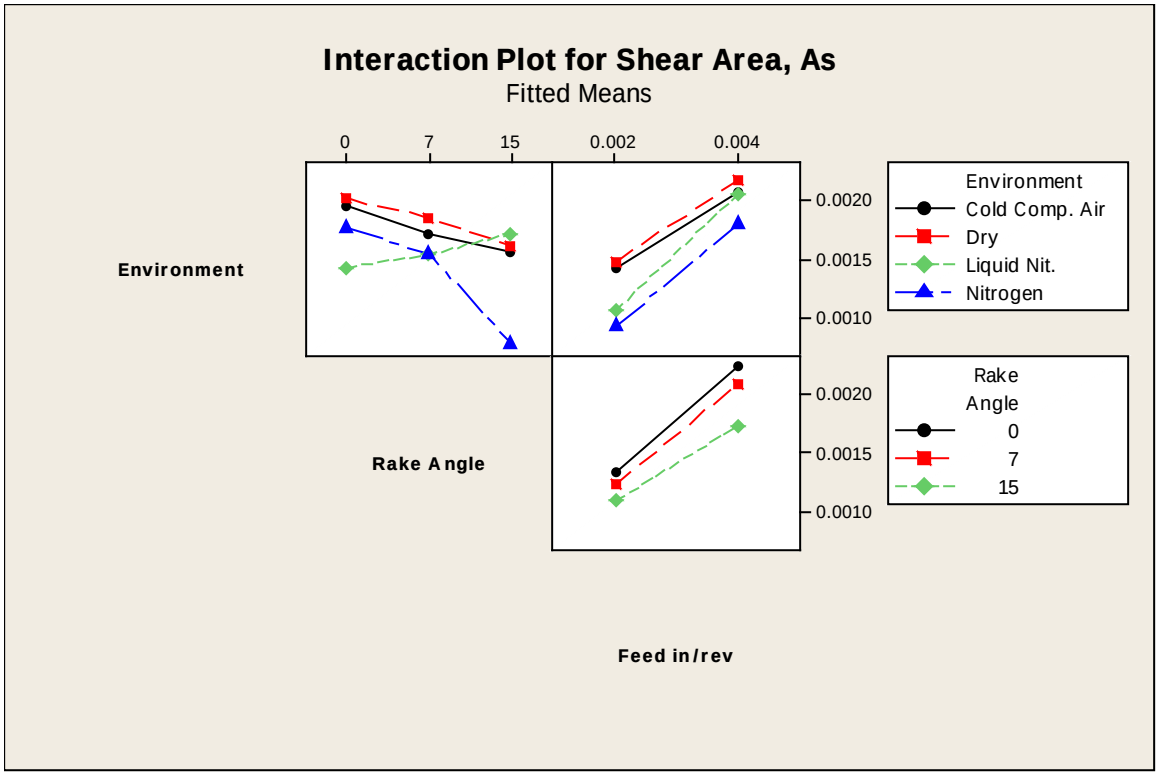
Interaction Plot for Shear Area, As
Fitted Means
Environment
Rake Angle
Feed in/rev
0
7
15
0.002
0.004
0.0020
0.0015
0.0010
Environment
Cold Comp. Air
Dry
Liquid Nit.
Nitrogen
Rake Angle
0
7
15

Analysis of Variance for **Shear Stress, Ts Merchant** (Mpa), using Adjusted SS for
Tests

Source	DF	Seq SS	Adj SS	Adj MS	F	P
Environment	3	153302	153302	51101	42.70	0.000
Rake Angle	2	1420	1420	710	0.59	0.555
Feed in/rev	1	182520	182520	182520	152.53	0.000
Environment*Rake Angle	6	236496	236496	39416	32.94	0.000
Environment*Feed in/rev	3	167870	167870	55957	46.76	0.000
Rake Angle*Feed in/rev	2	14131	14131	7066	5.90	0.004
Environment*Rake Angle*Feed in/rev	6	51816	51816	8636	7.22	0.000
Error	72	86158	86158	1197		
Total	95	893712				

S = 34.5924 R-Sq = 90.36% R-Sq(adj) = 87.28%

Unusual Observations for Shear Stress, Ts Merchant (Mpa)

Obs	Shear Stress, Ts Merchant (Mpa)	Fit	SE Fit	Residual	St Resid	
7	339.518	399.847	17.296	-60.329	-2.01	R
17	174.157	287.545	17.296	-113.388	-3.78	R
18	350.901	287.545	17.296	63.356	2.11	R
19	357.953	287.545	17.296	70.408	2.35	R
27	96.774	163.914	17.296	-67.140	-2.24	R
28	308.775	163.914	17.296	144.861	4.84	R
57	498.936	425.606	17.296	73.330	2.45	R

R denotes an observation with a large standardized residual.

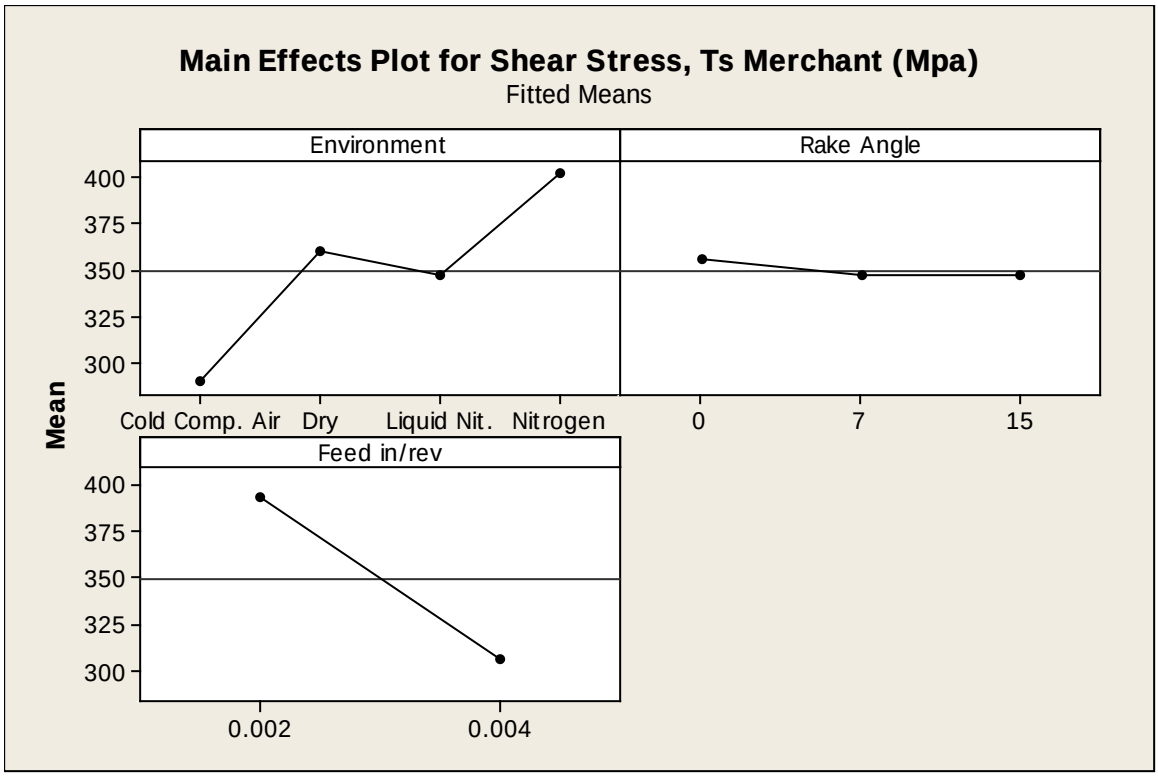
Main Effects Plot for Shear Stress, Ts Merchant (Mpa)
Fitted Means
Environment
Rake Angle
Feed in/rev
Mean
400
375
350
325
300
Cold Comp. Air
Dry
Liquid Nit.
Nitrogen
0
7
15
0.002
0.004

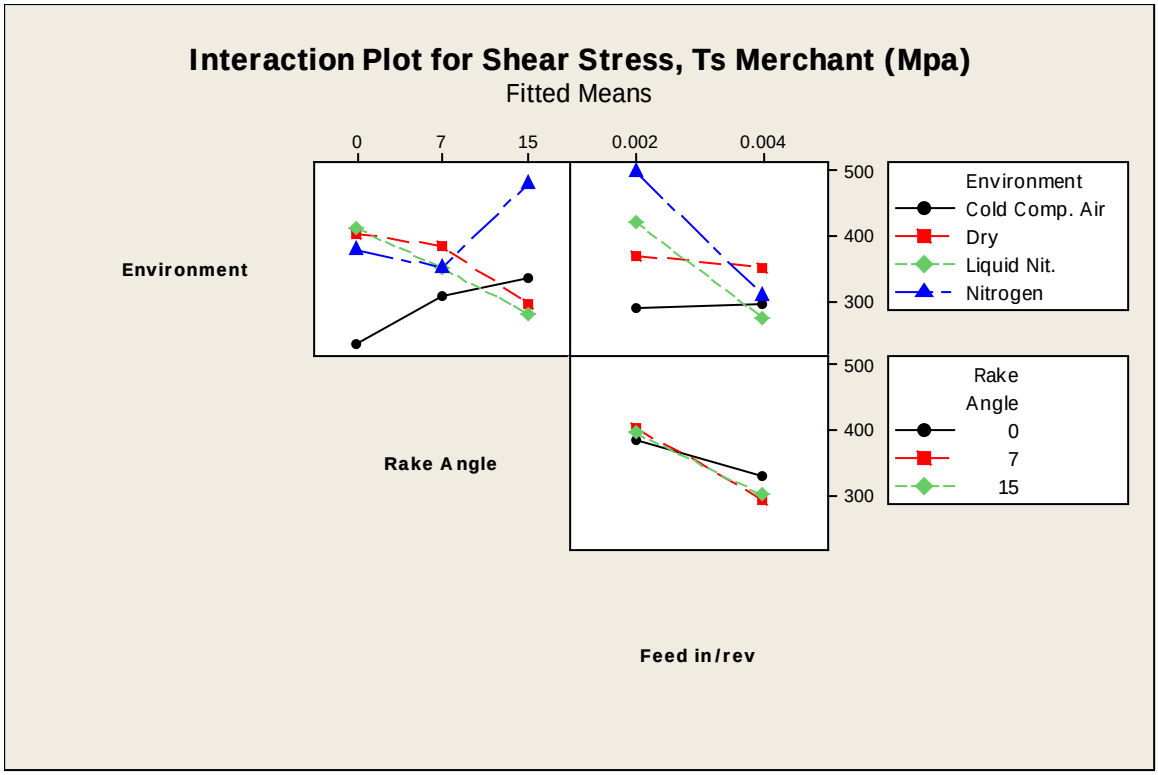
Interaction Plot for Shear Stress, Ts Merchant (Mpa)
Fitted Means
Environment
Rake Angle
Feed in/rev
0
7
15
0.002
0.004
500
400
300
Environment
Cold Comp. Air
Dry
Liquid Nit.
Nitrogen
Rake Angle
0
7
15

Analysis of Variance for **Shear Stress, Ts (Payton)** (Mpa), using Adjusted SS for
Tests

Source	DF	Seq SS	Adj SS	Adj MS	F	P
Environment	3	231394	231394	77131	54.75	0.000
Rake Angle	2	23895	23895	11947	8.48	0.000
Feed in/rev	1	266274	266274	266274	189.00	0.000
Environment*Rake Angle	6	109772	109772	18295	12.99	0.000
Environment*Feed in/rev	3	21529	21529	7176	5.09	0.003
Rake Angle*Feed in/rev	2	2115	2115	1058	0.75	0.476
Environment*Rake Angle*Feed in/rev	6	32353	32353	5392	3.83	0.002
Error	72	101438	101438	1409		
Total	95	788771				

S = 37.5348 R-Sq = 87.14% R-Sq(adj) = 83.03%

Unusual Observations for Shear Stress, Ts (Payton) (Mpa)

Obs	Shear Stress, Ts (Payton) (Mpa)	Fit	SE Fit	Residual	St Resid	
17	-309.335	-140.609	18.767	-168.726	-5.19	R
18	-57.525	-140.609	18.767	83.084	2.56	R
28	-9.410	-92.511	18.767	83.101	2.56	R
57	-16.654	70.914	18.767	-87.567	-2.69	R
68	-3.003	94.730	18.767	-97.733	-3.01	R
76	37.580	110.723	18.767	-73.143	-2.25	R

R denotes an observation with a large standardized residual.

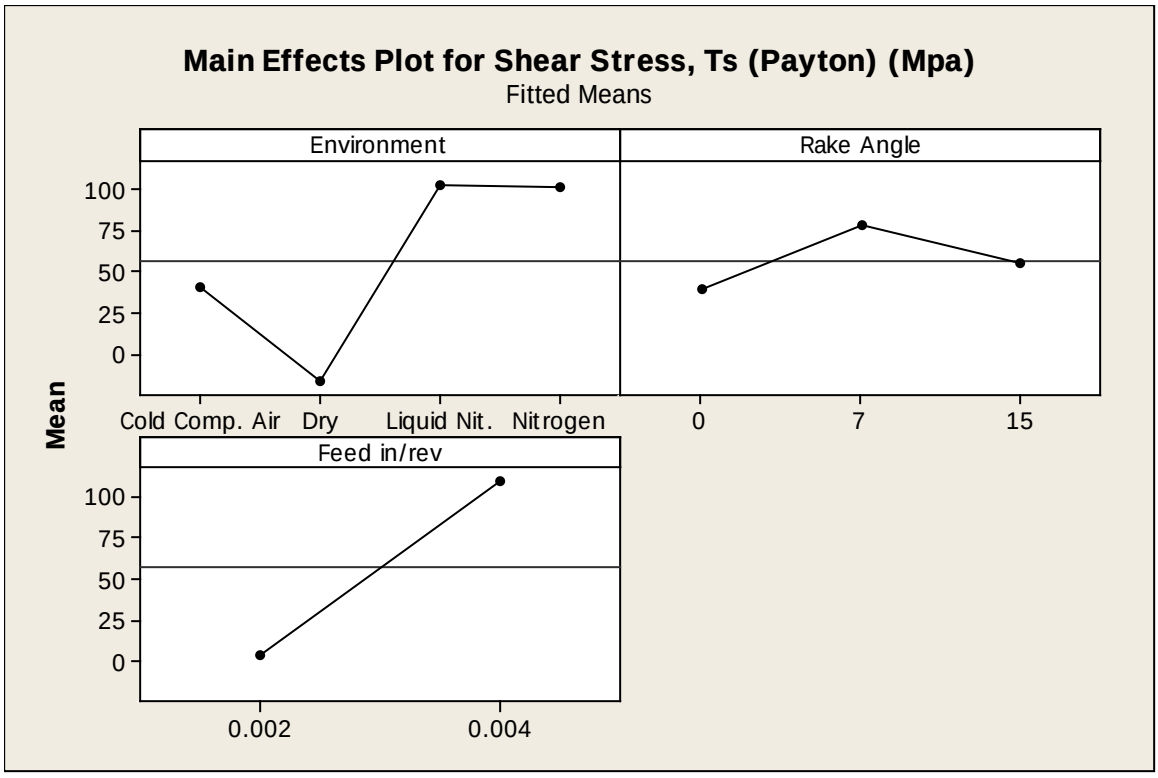
Main Effects Plot for Shear Stress, Ts (Payton) (Mpa)
Fitted Means
Environment
Rake Angle
Feed in/rev
Mean
100
75
50
25
0
Cold Comp. Air
Dry
Liquid Nit.
Nitrogen
0
7
15
0.002
0.004

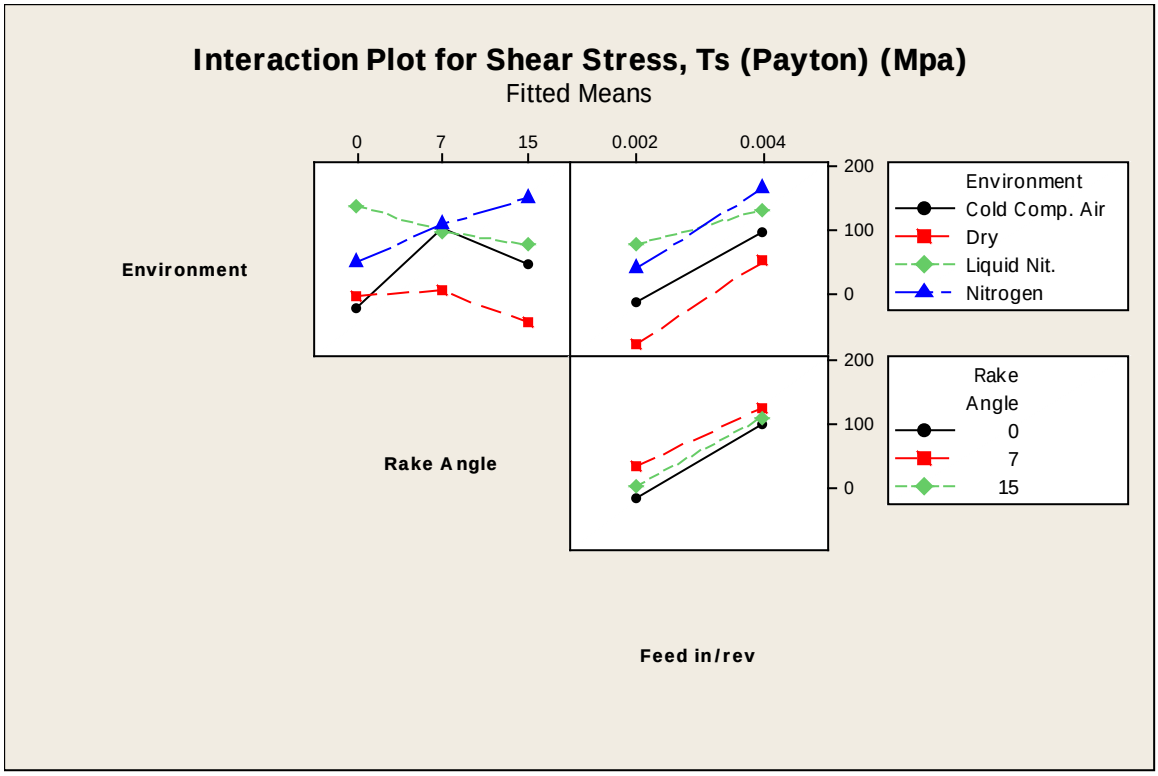
Interaction Plot for Shear Stress, Ts (Payton) (Mpa)
Fitted Means
0
7
15
0.002
0.004
Environment
Rake Angle
Feed in/rev
200
100
0
Environment
Cold Comp. Air
Dry
Liquid Nit.
Nitrogen
Rake Angle
0
7
15

Analysis of Variance for **Friction Co-efficient**, using Adjusted SS for Tests

Source	DF	Seq SS	Adj SS	Adj MS	F
Environment	3	1.28546	1.28546	0.42849	89.85
Rake Angle	2	0.40646	0.40646	0.20323	42.62
Feed in/rev	1	2.35556	2.35556	2.35556	493.94
Environment*Rake Angle	6	0.39065	0.39065	0.06511	13.65
Environment*Feed in/rev	3	0.11038	0.11038	0.03679	7.72
Rake Angle*Feed in/rev	2	0.00364	0.00364	0.00182	0.38
Environment*Rake Angle*Feed in/rev	6	0.14559	0.14559	0.02427	5.09
Error	72	0.34336	0.34336	0.00477	
Total	95	5.04110			

Source	P
Environment	0.000
Rake Angle	0.000
Feed in/rev	0.000
Environment*Rake Angle	0.000
Environment*Feed in/rev	0.000
Rake Angle*Feed in/rev	0.684
Environment*Rake Angle*Feed in/rev	0.000
Error	
Total	

S = 0.0690573 R-Sq = 93.19% R-Sq(adj) = 91.01%

Unusual Observations for Friction Co-efficient

Obs	Friction Co-efficient	Fit	SE Fit	Residual	St Resid	
17	1.38733	1.14346	0.03453	0.24387	4.08	R
18	1.01463	1.14346	0.03453	-0.12883	-2.15	R
28	0.80280	1.03133	0.03453	-0.22853	-3.82	R
41	0.80030	0.92452	0.03453	-0.12422	-2.08	R
57	0.86500	0.71914	0.03453	0.14586	2.44	R
78	0.26800	0.39648	0.03453	-0.12848	-2.15	R
79	0.52081	0.39648	0.03453	0.12433	2.08	R

R denotes an observation with a large standardized residual.

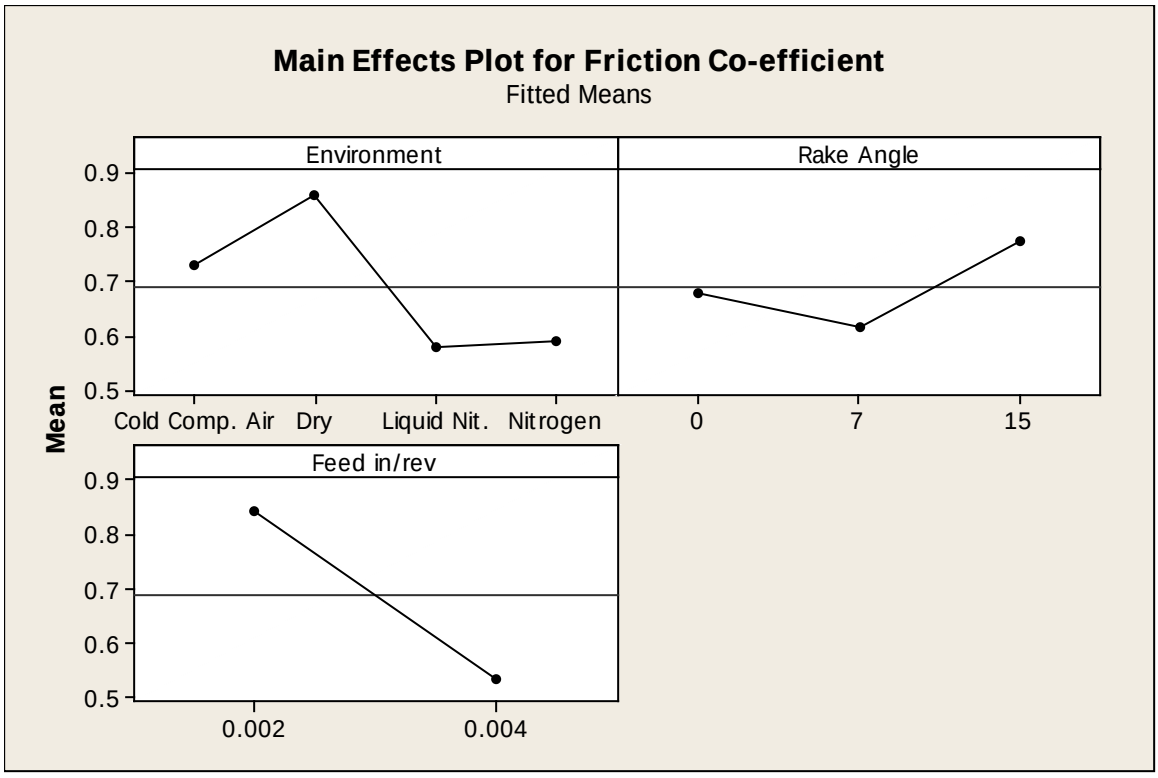
Main Effects Plot for Friction Co-efficient
Fitted Means
Environment
Rake Angle
Feed in/rev
Mean
0.9
0.8
0.7
0.6
0.5
Cold Comp. Air
Dry
Liquid Nit.
Nitrogen
0
7
15
0.002
0.004

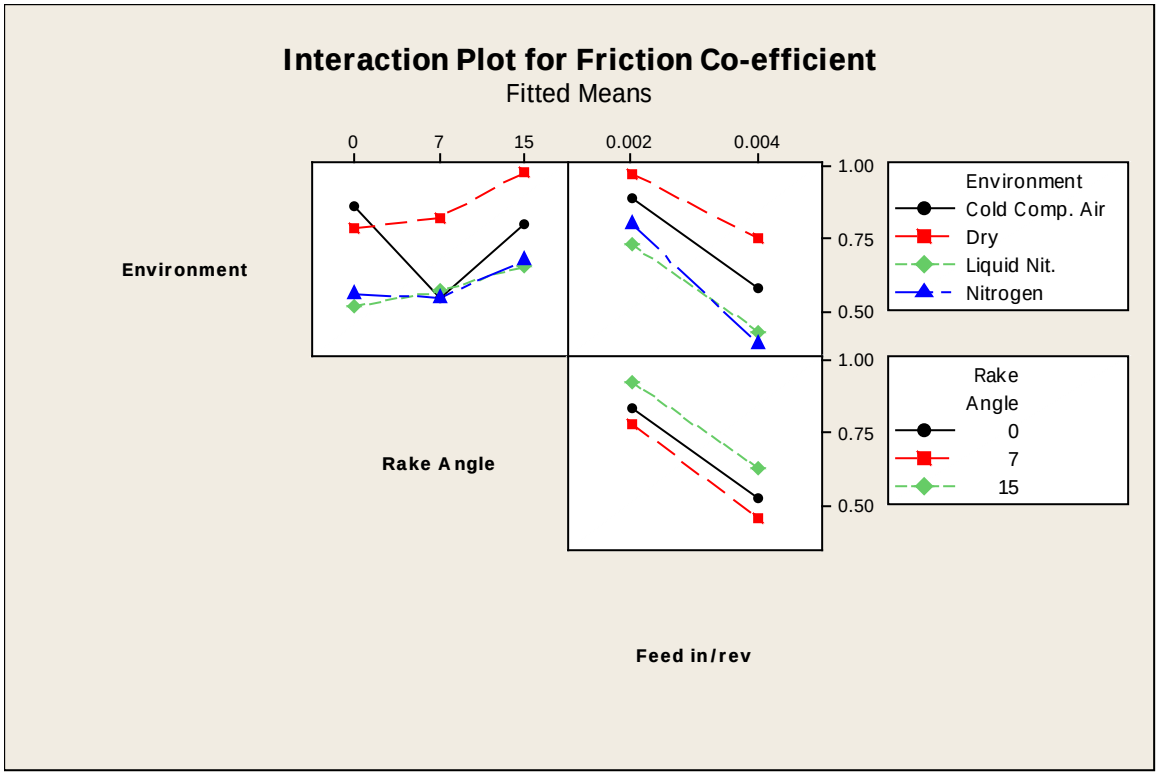
Interaction Plot for Friction Co-efficient
Fitted Means
Environment
Rake Angle
Feed in/rev
0
7
15
0.002
0.004
1.00
0.75
0.50
Environment
Cold Comp. Air
Dry
Liquid Nit.
Nitrogen
Rake Angle
0
7
15

Analysis of Variance for **Normal Stress (Merchant)**, using Adjusted SS for Tests

Source	DF	Seq SS	Adj SS	Adj MS
Environment	3	3.26400E+11	3.26400E+11	1.08800E+11
Rake Angle	2	1.09312E+11	1.09312E+11	54656116720
Feed in/rev	1	9.03005E+11	9.03005E+11	9.03005E+11
Environment*Rake Angle	6	3.25384E+11	3.25384E+11	54230671669
Environment*Feed in/rev	3	3.39665E+11	3.39665E+11	1.13222E+11
Rake Angle*Feed in/rev	2	7546939291	7546939291	3773469645
Environment*Rake Angle*Feed in/rev	6	1.16042E+11	1.16042E+11	19340363452
Error	72	1.82145E+11	1.82145E+11	2529791541
Total	95	2.30950E+12		

Source	F	P
Environment	43.01	0.000
Rake Angle	21.60	0.000
Feed in/rev	356.95	0.000
Environment*Rake Angle	21.44	0.000
Environment*Feed in/rev	44.76	0.000
Rake Angle*Feed in/rev	1.49	0.232
Environment*Rake Angle*Feed in/rev	7.65	0.000
Error		
Total		

S = 50297.0 R-Sq = 92.11% R-Sq(adj) = 89.59%

Unusual Observations for Normal Stress (Merchant)

Obs	Normal Stress (Merchant)	Fit	SE Fit	Residual	St Resid	
5	249554	354010	25149	-104456	-2.40	R
57	483036	318856	25149	164180	3.77	R
66	595339	708039	25149	-112700	-2.59	R
68	880872	708039	25149	172833	3.97	R
76	534019	394870	25149	139149	3.19	R

R denotes an observation with a large standardized residual.

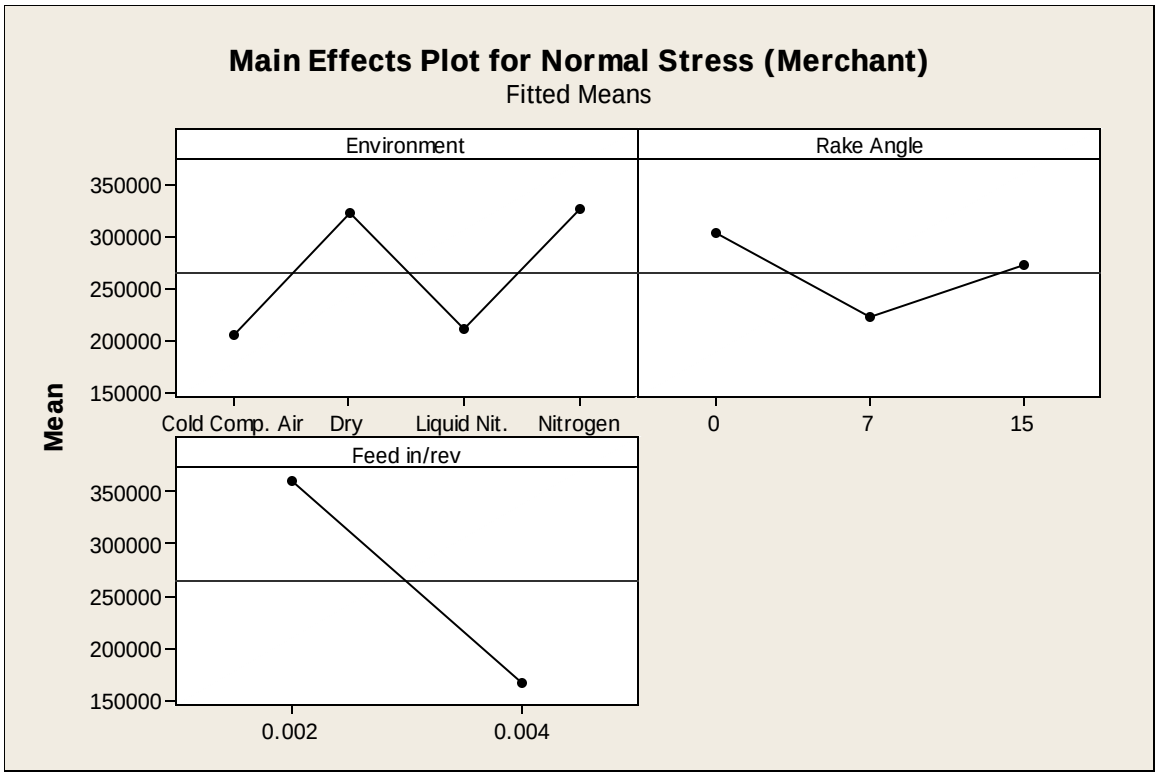
Main Effects Plot for Normal Stress (Merchant)
Fitted Means
Environment
Rake Angle
Feed in/rev
Mean
350000
300000
250000
200000
150000
Cold Comp. Air
Dry
Liquid Nit.
Nitrogen
0
7
15
0.002
0.004

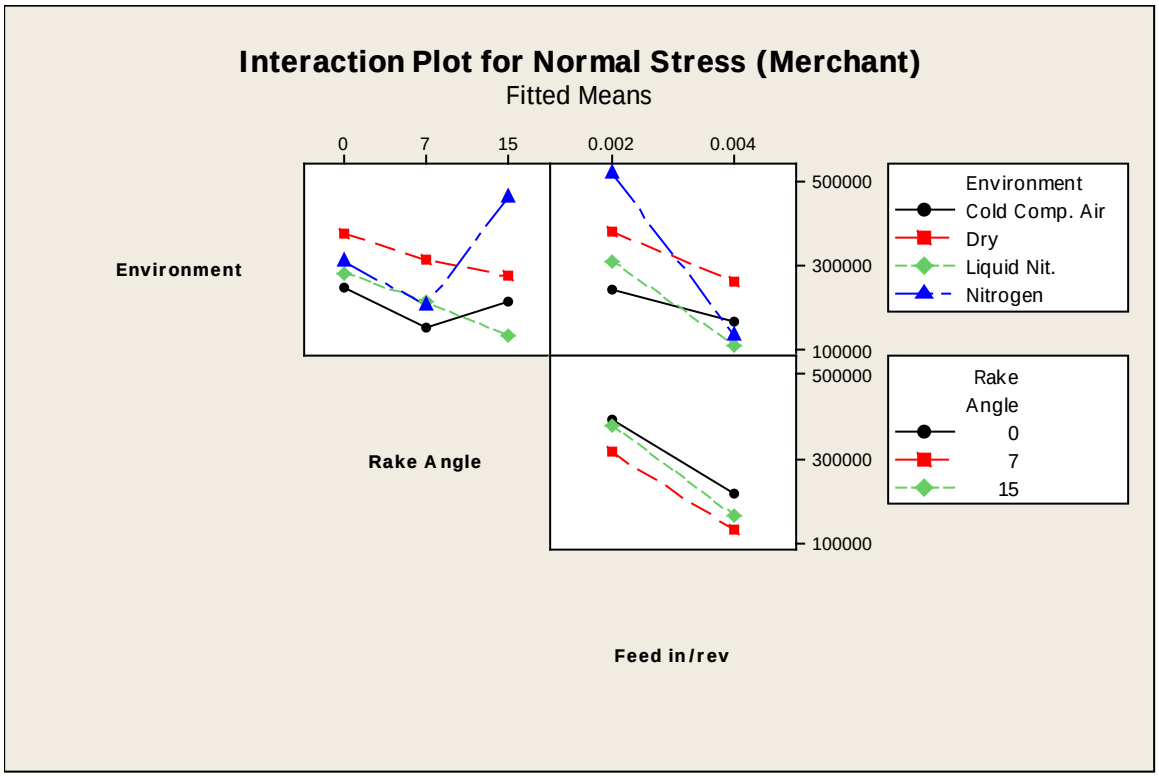
Interaction Plot for Normal Stress (Merchant)
Fitted Means
Environment
Rake Angle
Feed in/rev
0
7
15
0.002
0.004
500000
300000
100000
Environment
Cold Comp. Air
Dry
Liquid Nit.
Nitrogen
Rake Angle
0
7
15

Analysis of Variance for **Shear strain (Merchant)**, using Adjusted SS for Tests

Source	DF	Seq SS	Adj SS	Adj MS	F	P
Environment	3	33.1985	33.1985	11.0662	1595.35	0.000
Rake Angle	2	25.7894	25.7894	12.8947	1858.97	0.000
Feed in/rev	1	16.6020	16.6020	16.6020	2393.43	0.000
Environment*Rake Angle	6	28.6476	28.6476	4.7746	688.33	0.000
Environment*Feed in/rev	3	12.8769	12.8769	4.2923	618.80	0.000
Rake Angle*Feed in/rev	2	0.1562	0.1562	0.0781	11.26	0.000
Environment*Rake Angle*Feed in/rev	6	1.6344	1.6344	0.2724	39.27	0.000
Error	72	0.4994	0.4994	0.0069		
Total	95	119.4045				

S = 0.0832857 R-Sq = 99.58% R-Sq(adj) = 99.45%

Unusual Observations for Shear strain (Merchant)

Obs	Shear strain (Merchant)	Fit	SE Fit	Residual	St Resid	
9	6.31899	6.15333	0.04164	0.16565	2.30	R
18	5.54078	5.21590	0.04164	0.32488	4.50	R
19	4.91367	5.21590	0.04164	-0.30224	-4.19	R
44	5.59699	5.37549	0.04164	0.22150	3.07	R
89	5.09650	4.92490	0.04164	0.17160	2.38	R

R denotes an observation with a large standardized residual.

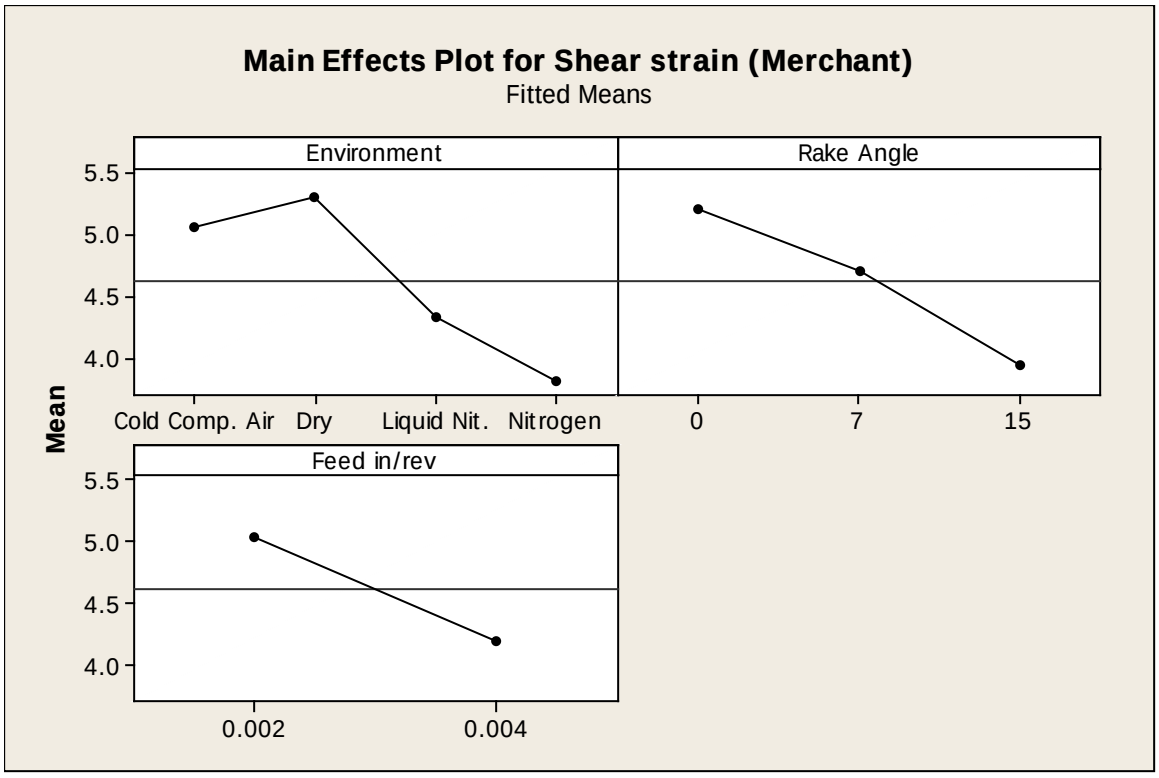
Main Effects Plot for Shear strain (Merchant)
Fitted Means
Environment
Rake Angle
Feed in/rev
Mean
5.5
5.0
4.5
4.0
Cold Comp. Air
Dry
Liquid Nit.
Nitrogen
0
7
15
0.002
0.004

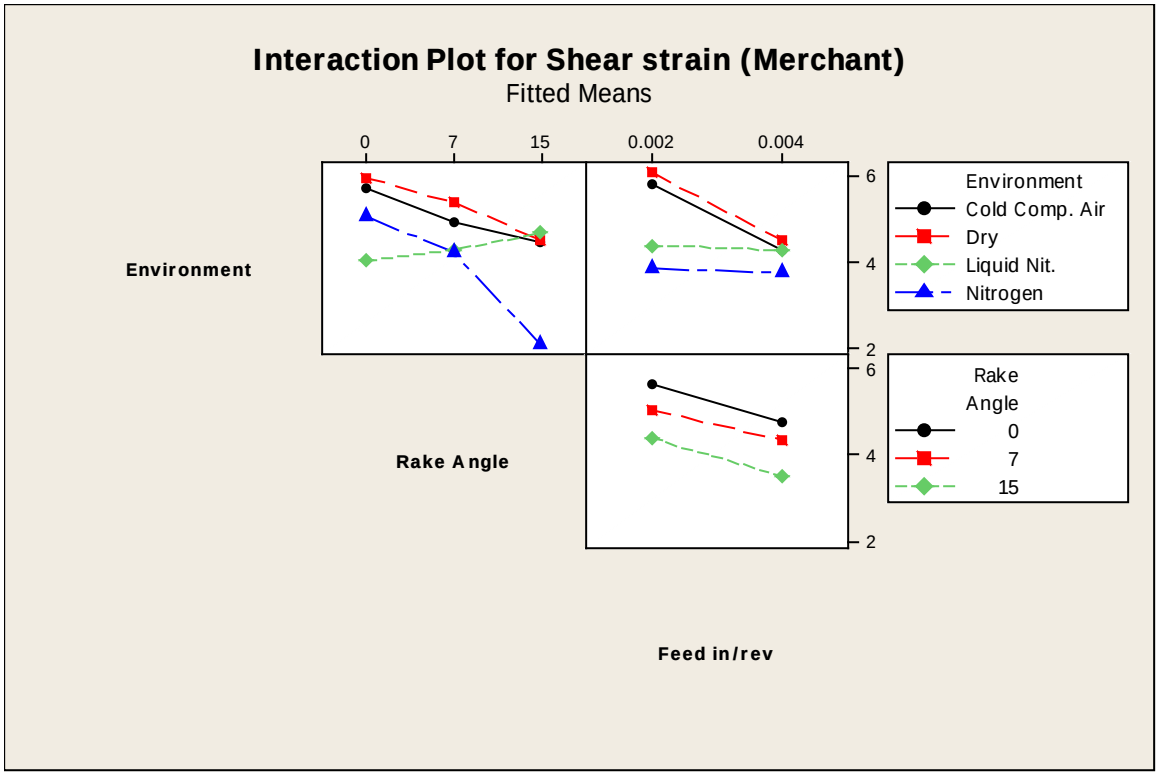
Interaction Plot for Shear strain (Merchant)
Fitted Means
Environment
Rake Angle
Feed in/rev
0
7
15
0.002
0.004
6
4
2
Environment
Cold Comp. Air
Dry
Liquid Nit.
Nitrogen
Rake Angle
0
7
15

Analysis of Variance for **Narmal Stress (Payton)**, using Adjusted SS for Tests

Source	DF	Seq SS	Adj SS	Adj MS
Environment	3	3.35469E+11	3.35469E+11	1.11823E+11
Rake Angle	2	74102330423	74102330423	37051165211
Feed in/rev	1	8.91084E+11	8.91084E+11	8.91084E+11
Environment*Rake Angle	6	3.64797E+11	3.64797E+11	60799478120
Environment*Feed in/rev	3	4.08365E+11	4.08365E+11	1.36122E+11
Rake Angle*Feed in/rev	2	10535323429	10535323429	5267661714
Environment*Rake Angle*Feed in/rev	6	1.23482E+11	1.23482E+11	20580400101
Error	72	1.77908E+11	1.77908E+11	2470947344
Total	95	2.38574E+12		

Source	F	P
Environment	45.26	0.000
Rake Angle	14.99	0.000
Feed in/rev	360.62	0.000
Environment*Rake Angle	24.61	0.000
Environment*Feed in/rev	55.09	0.000
Rake Angle*Feed in/rev	2.13	0.126
Environment*Rake Angle*Feed in/rev	8.33	0.000
Error		
Total		

S = 49708.6 R-Sq = 92.54% R-Sq(adj) = 90.16%

Unusual Observations for Narmal Stress (Payton)

Obs	Narmal Stress (Payton)	Fit	SE Fit	Residual	St Resid	
5	335874	437527	24854	-101653	-2.36	R
8	524770	437527	24854	87243	2.03	R
28	348856	262061	24854	86796	2.02	R
57	580365	418165	24854	162200	3.77	R
66	686014	797675	24854	-111661	-2.59	R
68	959556	797675	24854	161881	3.76	R
76	630011	493682	24854	136329	3.17	R

R denotes an observation with a large standardized residual.

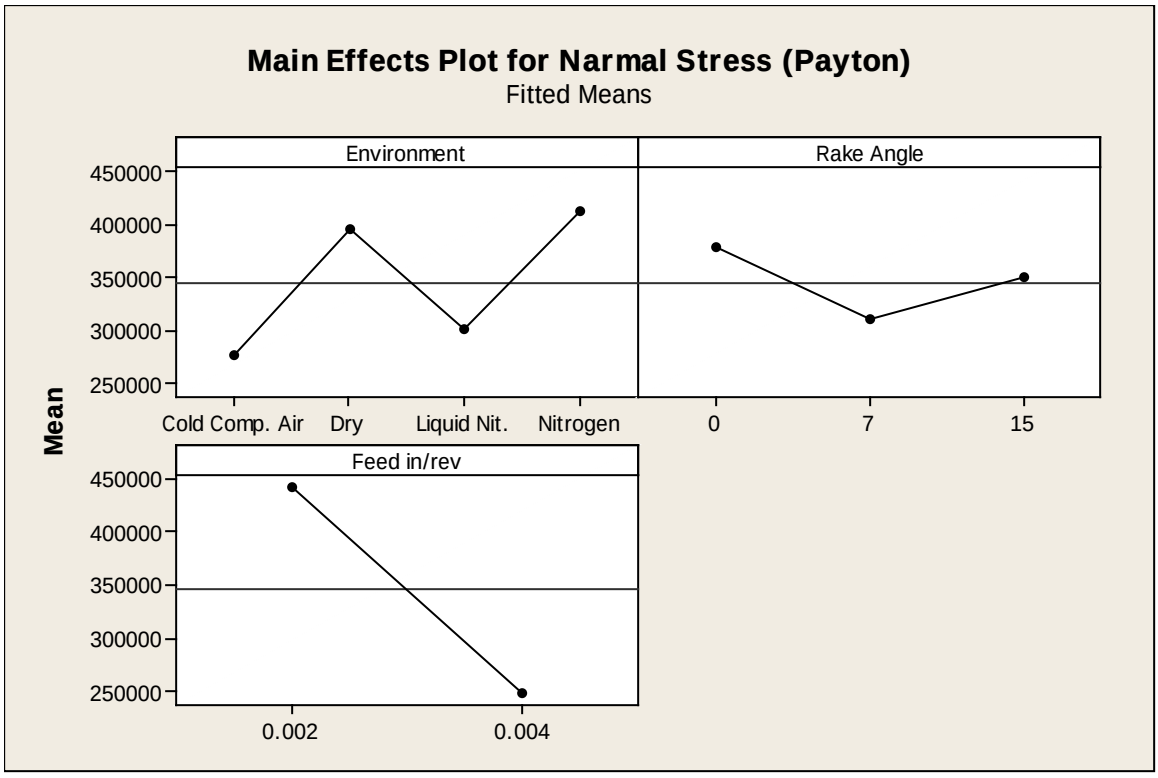
Main Effects Plot for Narmal Stress (Payton)
Fitted Means
Environment
Rake Angle
Feed in/rev
Mean
450000
400000
350000
300000
250000
Cold Comp. Air
Dry
Liquid Nit.
Nitrogen
0
7
15
0.002
0.004

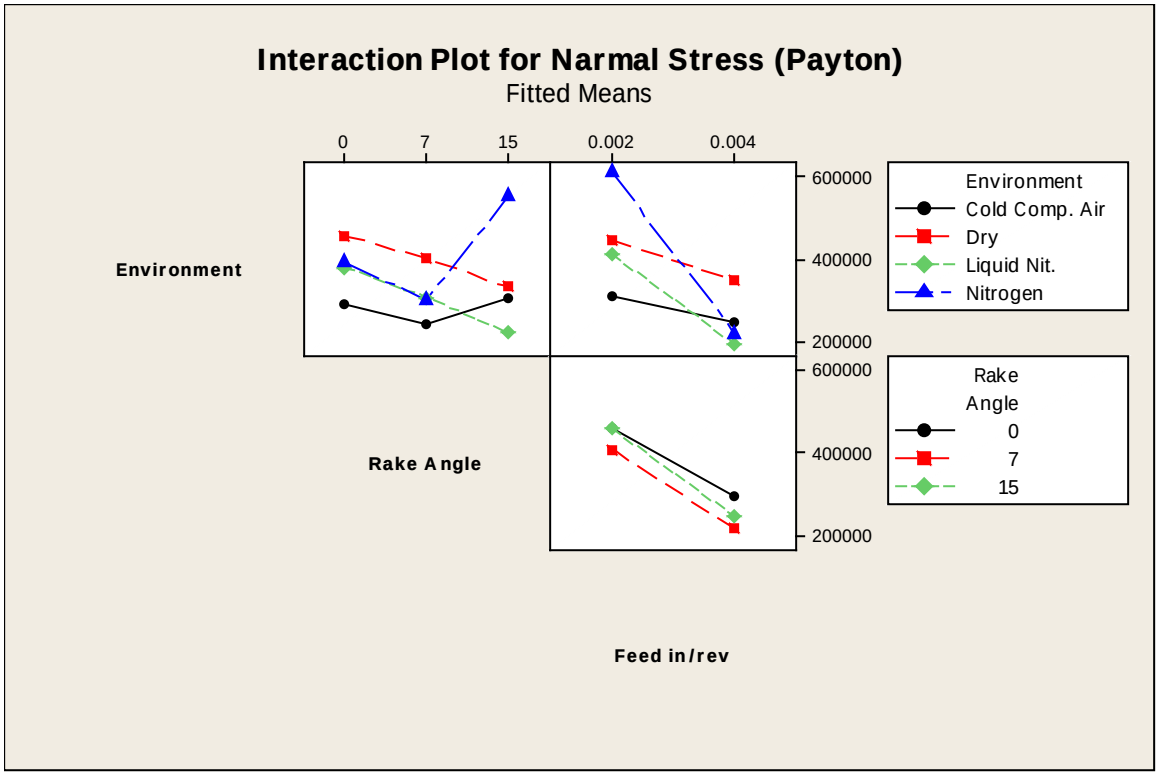
Interaction Plot for Narmal Stress (Payton)
Fitted Means
Environment
Rake Angle
Feed in/rev
0
7
15
0.002
0.004
600000
400000
200000
Environment
Cold Comp. Air
Dry
Liquid Nit.
Nitrogen
Rake Angle
0
7
15

Analysis of Variance for **Shear strain (Payton)**, using Adjusted SS for Tests

Source	DF	Seq SS	Adj SS	Adj MS	F	P
Environment	3	0.00000	0.00000	0.00000	**	
Rake Angle	2	3.46485	3.46485	1.73242	**	
Feed in/rev	1	0.00000	0.00000	0.00000	**	
Environment*Rake Angle	6	0.00000	0.00000	0.00000	**	
Environment*Feed in/rev	3	0.00000	0.00000	0.00000	**	
Rake Angle*Feed in/rev	2	0.00000	0.00000	0.00000	**	
Environment*Rake Angle*Feed in/rev	6	0.00000	0.00000	0.00000	**	
Error	72	0.00000	0.00000	0.00000		
Total	95	3.46485				

** Denominator of F-test is zero.

S = 8.576051E-17 R-Sq = 100.00% R-Sq(adj) = 100.00%

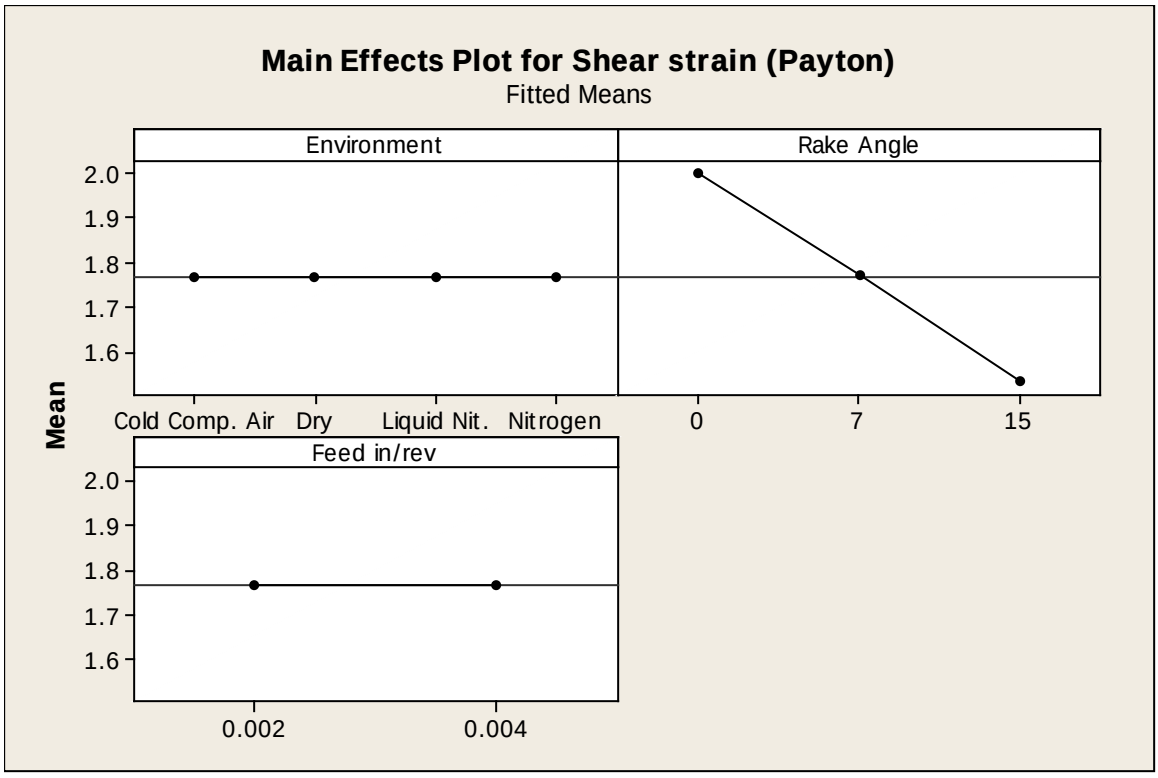
Main Effects Plot for Shear strain (Payton)
Fitted Means
Environment
Rake Angle
Feed in/rev
Mean
2.0
1.9
1.8
1.7
1.6
Cold Comp. Air
Dry
Liquid Nit.
Nitrogen
0
7
15
0.002
0.004

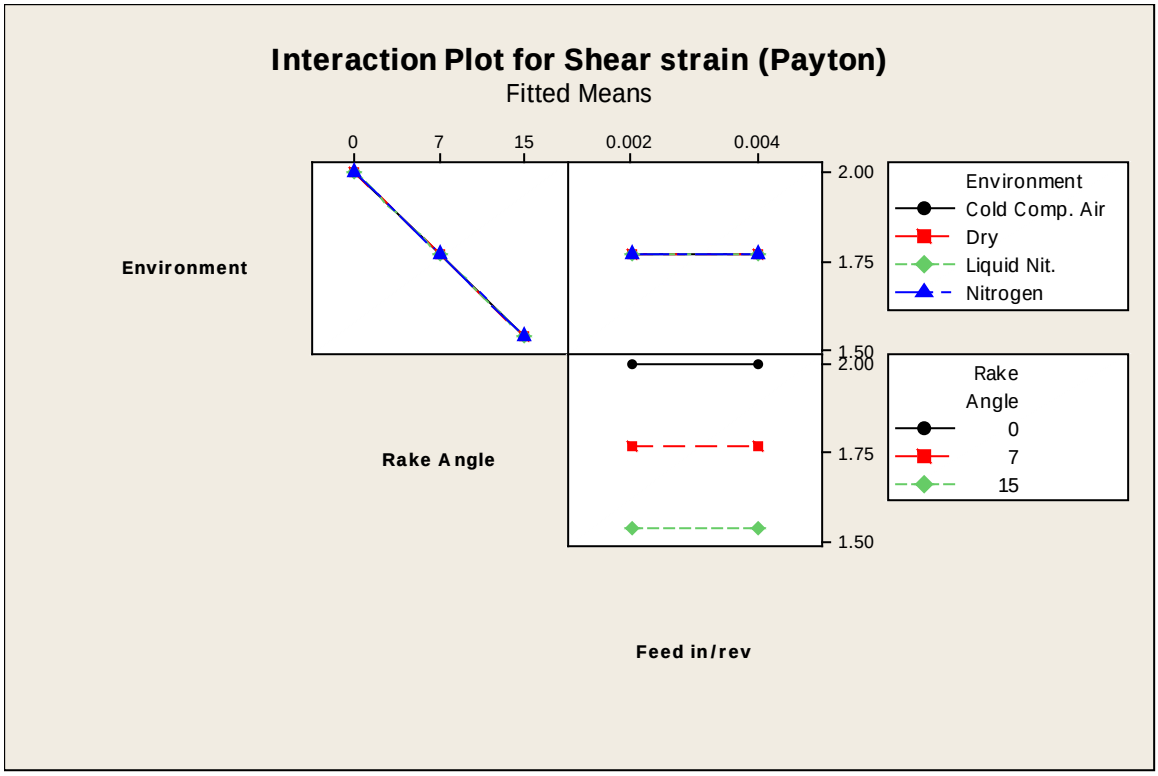
Interaction Plot for Shear strain (Payton)
Fitted Means
Environment
Rake Angle
Feed in/rev
0
7
15
0.002
0.004
2.00
1.75
1.50
Environment
Cold Comp. Air
Dry
Liquid Nit.
Nitrogen
Rake Angle
0
7
15

Analysis of Variance for **Shear Area, As P**, using Adjusted SS for Tests

Source	DF	Seq SS	Adj SS	Adj MS
Environment	3	0.0000055	0.0000055	0.0000018
Rake Angle	2	0.0000080	0.0000080	0.0000040
Feed in/rev	1	0.0000272	0.0000272	0.0000272
Environment*Rake Angle	6	0.0000064	0.0000064	0.0000011
Environment*Feed in/rev	3	0.0000008	0.0000008	0.0000003
Rake Angle*Feed in/rev	2	0.0000008	0.0000008	0.0000004
Environment*Rake Angle*Feed in/rev	6	0.0000003	0.0000003	0.0000001
Error	72	0.0000001	0.0000001	0.0000000
Total	95	0.0000491		

Source	F	P
Environment	2048.05	0.000
Rake Angle	4489.60	0.000
Feed in/rev	30596.57	0.000
Environment*Rake Angle	1192.38	0.000
Environment*Feed in/rev	314.75	0.000
Rake Angle*Feed in/rev	439.83	0.000
Environment*Rake Angle*Feed in/rev	62.76	0.000
Error		
Total		

S = 0.0000298239 R-Sq = 99.87% R-Sq(adj) = 99.83%

Unusual Observations for Shear Area, As P

Obs	Shear Area, As P	Fit	SE Fit	Residual	St Resid	
9	0.002038	0.001983	0.000015	0.000054	2.09	R
18	0.001723	0.001624	0.000015	0.000098	3.80	R
19	0.001533	0.001624	0.000015	-0.000092	-3.55	R
44	0.001739	0.001673	0.000015	0.000067	2.59	R
77	0.002729	0.002674	0.000015	0.000055	2.14	R
89	0.001588	0.001536	0.000015	0.000052	2.02	R

R denotes an observation with a large standardized residual.

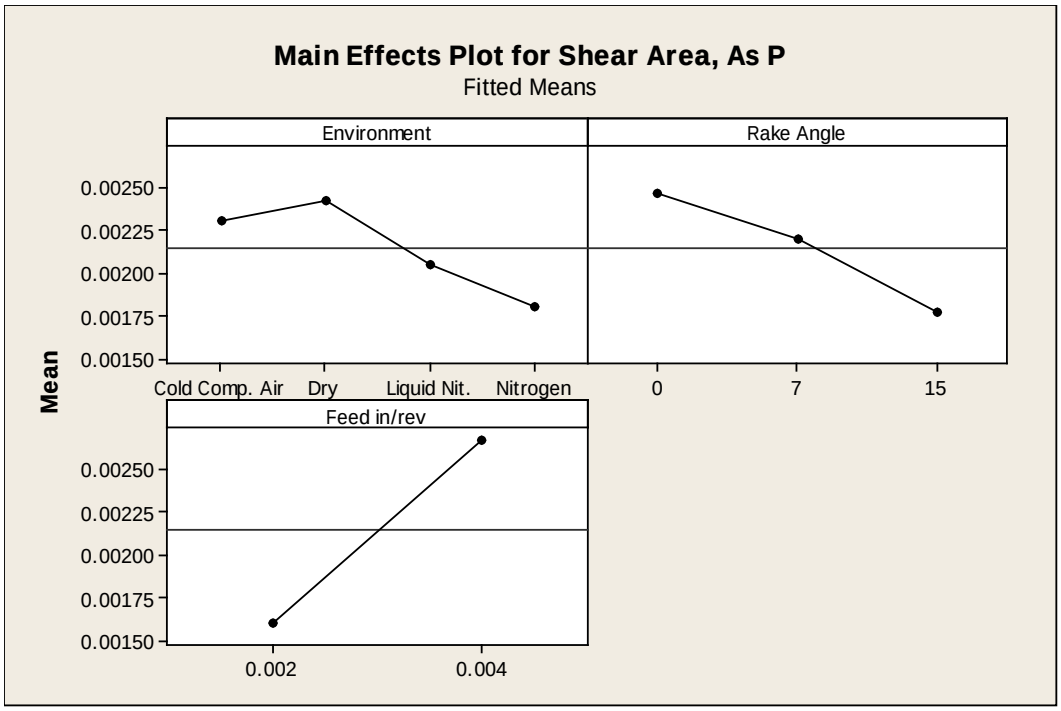
Main Effects Plot for Shear Area, As P
Fitted Means
Environment
Rake Angle
Feed in/rev
Mean
0.00250
0.00225
0.00200
0.00175
0.00150
Cold Comp. Air
Dry
Liquid Nit.
Nitrogen
0
7
15
0.002
0.004

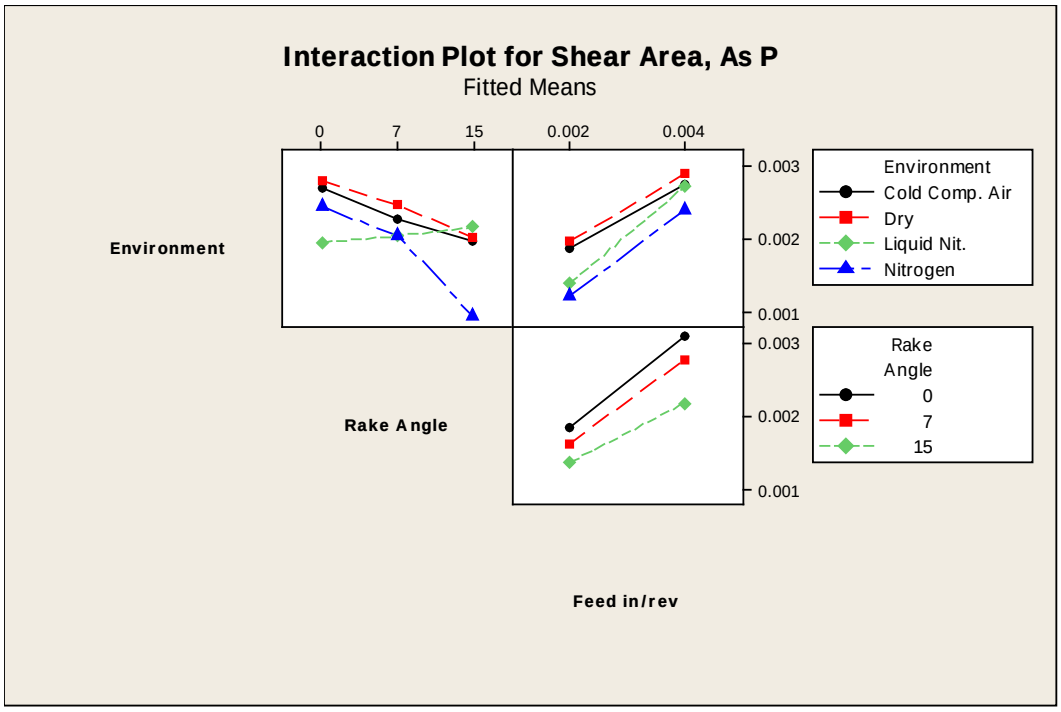
Interaction Plot for Shear Area, As P
Fitted Means
Environment
Rake Angle
Feed in/rev
0
7
15
0.002
0.004
0.003
0.002
0.001
Environment
Cold Comp. Air
Dry
Liquid Nit.
Nitrogen
Rake Angle
0
7
15

Analysis of Variance for **Shear Stress, Ts (Payton) corre**, using Adjusted SS for
Tests

Source	DF	Seq SS	Adj SS	Adj MS	F	P
Environment	3	136657	136657	45552	53.82	0.000
Rake Angle	2	14152	14152	7076	8.36	0.001
Feed in/rev	1	152304	152304	152304	179.94	0.000
Environment*Rake Angle	6	66231	66231	11039	13.04	0.000
Environment*Feed in/rev	3	12629	12629	4210	4.97	0.003
Rake Angle*Feed in/rev	2	1181	1181	591	0.70	0.501
Environment*Rake Angle*Feed in/rev	6	18243	18243	3041	3.59	0.004
Error	72	60942	60942	846		
Total	95	462339				

S = 29.0932 R-Sq = 86.82% R-Sq(adj) = 82.61%

Unusual Observations for Shear Stress, Ts (Payton) corre

Obs	Shear Stress, Ts (Payton) corre	Fit	SE Fit	Residual	St Resid
17	-246.102	-111.862	14.547	-134.240	-5.33 R
18	-45.807	-111.862	14.547	66.055	2.62 R
28	-6.741	-66.217	14.547	59.477	2.36 R
57	-12.560	53.531	14.547	-66.091	-2.62 R
68	-2.456	77.546	14.547	-80.002	-3.18 R
76	27.522	81.335	14.547	-53.813	-2.14 R

R denotes an observation with a large standardized residual.

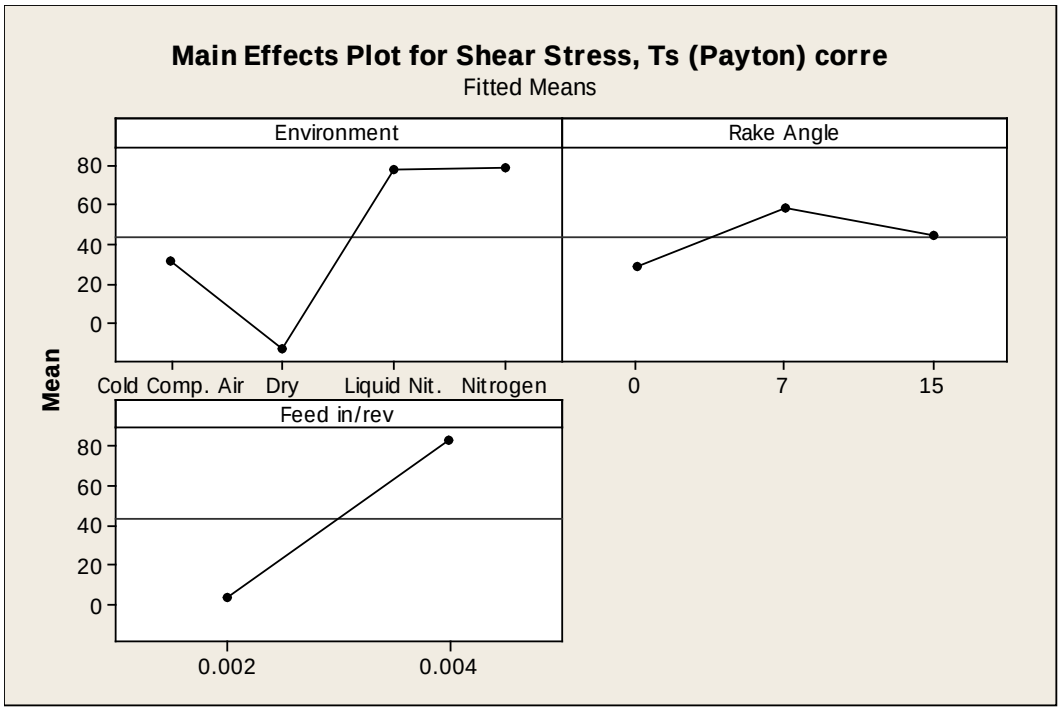
Main Effects Plot for Shear Stress, Ts (Payton) corre
Fitted Means
Environment
Rake Angle
Feed in/rev
Mean
80
60
40
20
0
Cold Comp. Air
Dry
Liquid Nit.
Nitrogen
0
7
15
0.002
0.004

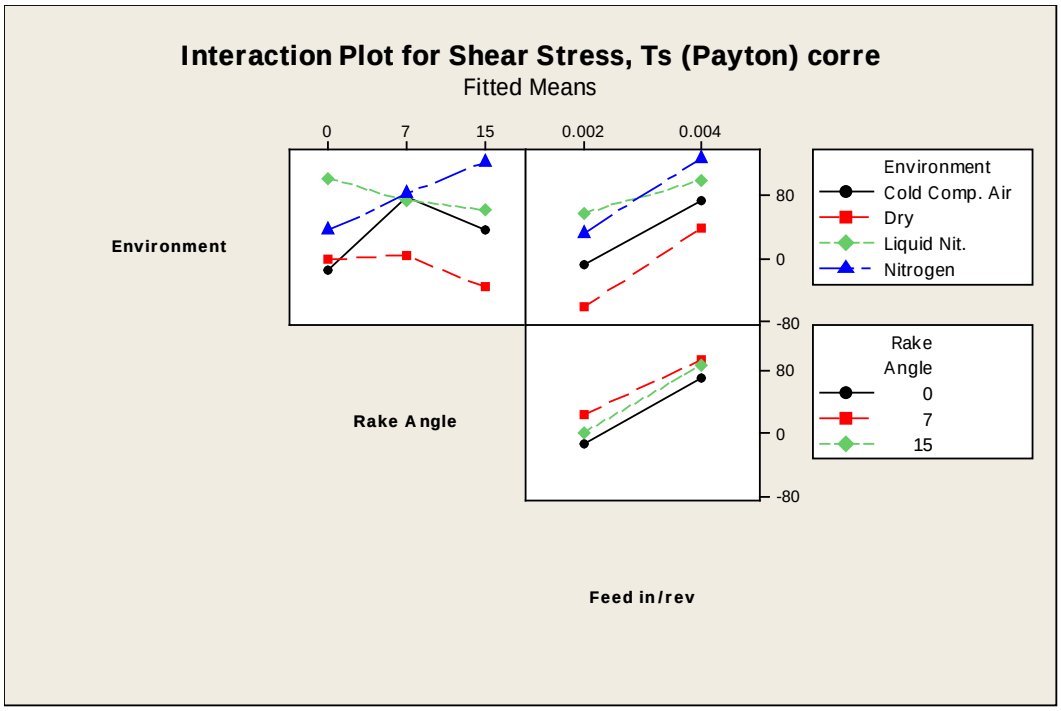
Interaction Plot for Shear Stress, Ts (Payton) corre
Fitted Means
Environment
Rake Angle
Feed in/rev
0
7
15
0.002
0.004
80
0
-80
Environment
Cold Comp. Air
Dry
Liquid Nit.
Nitrogen
Rake Angle
0
7
15

Analysis of Variance for **Shear strain new**, using Adjusted SS for Tests

Source	DF	Seq SS	Adj SS	Adj MS	F
Environment	3	1.59803	1.59803	0.53268	2681.34
Rake Angle	2	0.62996	0.62996	0.31498	1585.52
Feed in/rev	1	0.07263	0.07263	0.07263	365.58
Environment*Rake Angle	6	2.68432	2.68432	0.44739	2252.00
Environment*Feed in/rev	3	0.13878	0.13878	0.04626	232.85
Rake Angle*Feed in/rev	2	0.00012	0.00012	0.00006	0.30
Environment*Rake Angle*Feed in/rev	6	0.05907	0.05907	0.00985	49.56
Error	72	0.01430	0.01430	0.00020	
Total	95	5.19722			

Source	P
Environment	0.000
Rake Angle	0.000
Feed in/rev	0.000
Environment*Rake Angle	0.000
Environment*Feed in/rev	0.000
Rake Angle*Feed in/rev	0.742
Environment*Rake Angle*Feed in/rev	0.000
Error	
Total	

S = 0.0140947 R-Sq = 99.72% R-Sq(adj) = 99.64%

Unusual Observations for Shear strain new

Obs	Shear strain new	Fit	SE Fit	Residual	St Resid	
65	1.28160	1.22960	0.00705	0.05200	4.26	R
66	1.25972	1.22960	0.00705	0.03012	2.47	R
67	1.15955	1.22960	0.00705	-0.07005	-5.74	R
74	0.57920	0.54736	0.00705	0.03184	2.61	R
76	0.52217	0.54736	0.00705	-0.02519	-2.06	R

R denotes an observation with a large standardized residual.

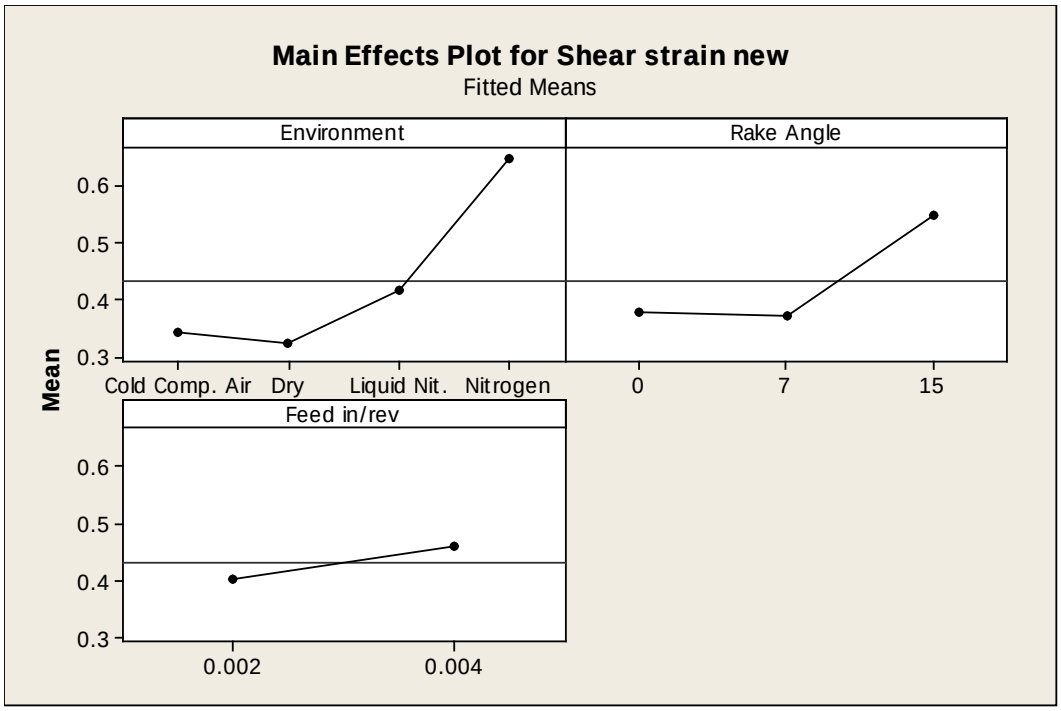
Main Effects Plot for Shear strain new
Fitted Means
Environment
Rake Angle
Feed in/rev
Mean
0.6
0.5
0.4
0.3
Cold Comp. Air
Dry
Liquid Nit.
Nitrogen
0
7
15
0.002
0.004

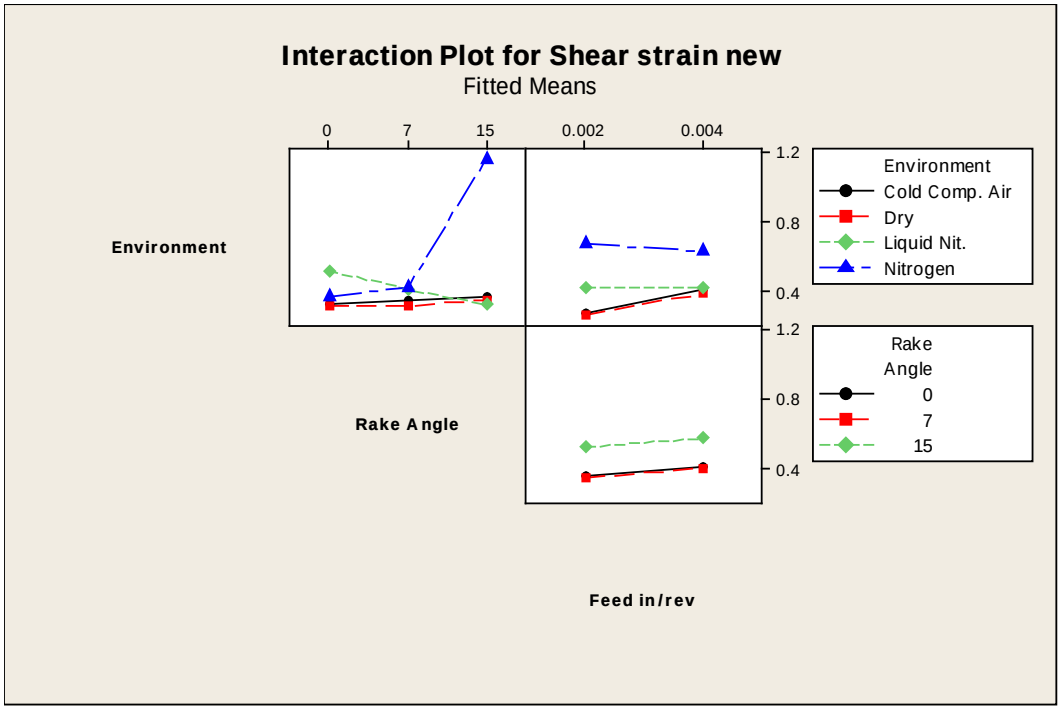
Interaction Plot for Shear strain new
Fitted Means
Environment
Rake Angle
Feed in/rev
0
7
15
0.002
0.004
1.2
0.8
0.4
Environment
Cold Comp. Air
Dry
Liquid Nit.
Nitrogen
Rake Angle
0
7
15

APPENDIX 6

LS Dyna Sample input file

```
$# LS-DYNA Keyword file created by LS-PrePost 3.1 -
02Apr2011(09:25)
$# Created on Jun-26-2011 (21:18:16)
*KEYWORD
*TITLE
$# title

*CONTROL_CONTACT
$#  slsfac    rwpnal    islchk    shlthk    penopt
thkchg     orien    enmass
  1.000000                   1
1
$#  usrstr    usrfrc     nsbcs    interm     xpene
ssthk      ecdt   tiedprj
                                          4.000000
$#   sfric     dfric       edc       vfc        th
th_sf    pen_sf

$#  ignore    frceng   skiprwg    outseg   spotstp
spotdel   spothin

$#    isym    nserod    rwgaps    rwgdth     rwksf
icov    swradf    ithoff
                                         1.000000
$#  shledg


*CONTROL_ENERGY
$#    hgen      rwen    slnten     rylen
         2         2         2         2

*CONTROL_SHELL
$#  wrpang     esort     irnxx    istupd    theory
bwc     miter      proj
 20.000000         1        -1         1         2
2         1
```

```
$# rotascl    intgrd    lamsht    cstyp6    tshell
nfail1    nfail4   psnfail
  1.000000                              1
1         1
$# psstupd    irquad     cntco

*CONTROL_TERMINATION
$#  endtim    endcyc     dtmin    endeng    endmas
 5.0000E-4

*CONTROL_TIMESTEP
$#  dtinit    tssfac      isdo    tslimt     dt2ms
lctm     erode     ms1st
            0.900000
$#  dt2msf   dt2mslc     imscl

*DATABASE_MATSUM
$#      dt    binary      lcur     ioopt
 5.0000E-7                              1

*DATABASE_NODFOR
$#      dt    binary      lcur     ioopt
 1.0000E-7                              1

*DATABASE_BINARY_D3PLOT
$#      dt      lcdt      beam     npltc    psetid
 1.0000E-6
$#   ioopt

*DATABASE_BINARY_D3THDT
$#      dt      lcdt      beam     npltc    psetid
 5.0000E-7

*DATABASE_FORMAT
$#   iform   ibinary

*DATABASE_EXTENT_BINARY
$#   neiph     neips    maxint    strflg    sigflg
epsflg    rltflg    engflg
                                3         1         0
0         0         0
$#  cmpflg    ieverp    beamip     dcomp      shge
stssz    n3thdt   ialemat
                                4         0         0
0         0         0
$# nintsld   pkp_sen      sclp    unused     msscl
therm    intout    nodout
                     1.000000
STRESS    STRESS
```

```
*DATABASE_NODAL_FORCE_GROUP
$#    nsid       cid
         7

*DATABASE_HISTORY_NODE
$#     id1       id2       id3       id4       id5
id6       id7       id8
         1

*BOUNDARY_PRESCRIBED_MOTION_SET
$#    nsid       dof       vad      lcid        sf
vid     death     birth
         1         1         2         1  1.000000
0.000

*BOUNDARY_PRESCRIBED_MOTION_SET
$#    nsid       dof       vad      lcid        sf
vid     death     birth
         2         2         2         2  1.000000
0.000

*BOUNDARY_PRESCRIBED_MOTION_SET
$#    nsid       dof       vad      lcid        sf
vid     death     birth
         3         7         2         3  1.000000
0.000

*BOUNDARY_PRESCRIBED_MOTION_SET
$#    nsid       dof       vad      lcid        sf
vid     death     birth
         4         1         2         4  1.000000
0.000

*BOUNDARY_PRESCRIBED_MOTION_SET
$#    nsid       dof       vad      lcid        sf
vid     death     birth
         5         2         2         5  1.000000
0.000

*BOUNDARY_PRESCRIBED_MOTION_SET
$#    nsid       dof       vad      lcid        sf
vid     death     birth
         6         7         2         6  1.000000
0.000

*BOUNDARY_PRESCRIBED_MOTION_RIGID
$#     pid       dof       vad      lcid        sf
vid     death     birth
         2         1         2         7  1.000000
0.000
```

```
*CONTACT_2D_AUTOMATIC_SINGLE_SURFACE_ID
$#     cid
title
         1
$#    sids      sidm     sfact      freq        fs
fd        dc     membs
         3            1.000000        50  0.300000
0.300000                    6
$#  tbirth    tdeath       sos       som       nds
ndm       cof      init
          1.0000E+20     0.000     0.000

*SET_PART_LIST
$#     sid       da1       da2       da3       da4
solver
         3
$#    pid1      pid2      pid3      pid4      pid5
pid6      pid7      pid8
         1         2

*PART
$# title
Part          1 for Mat         1 and Elem Type         1
$#     pid     secid       mid     eosid      hgid
grav    adpopt      tmid
         1         1         1

*SECTION_SHELL
$#   secid    elform      shrf       nip     propt
qr/irid     icomp     setyp
         1        13  1.000000         4         1
3
$#      t1        t2        t3        t4      nloc
marea      idof    edgset


*MAT_PLASTIC_KINEMATIC
$#     mid        ro         e        pr      sigy
etan      beta
         1 2700.00006.8900E+10  0.330000 2.7000E+8
$#     src       srp        fs        vp
 6000.0000  4.000000  1.150000  1.000000

*PART
$# title
Part          2 for Mat         2 and Elem Type         1
$#     pid     secid       mid     eosid      hgid
grav    adpopt      tmid
         2         1         2
```

```
*MAT_RIGID
$#     mid        ro         e        pr         n
couple         m     alias
         2 3200.0003.0000E+11  0.280000
$#     cmo      con1      con2
  1.000000         7         7
$# lco or a1      a2        a3        v1        v2
v3


*DEFINE_CURVE
$#    lcid      sidr       sfa       sfo      offa
offo    dattyp
         1            1.000000  1.000000
$#               a1                  o1

      5.0000002e-004

*DEFINE_CURVE
$#    lcid      sidr       sfa       sfo      offa
offo    dattyp
         2            1.000000  1.000000
$#               a1                  o1

      5.0000002e-004

*DEFINE_CURVE
$#    lcid      sidr       sfa       sfo      offa
offo    dattyp
         3            1.000000  1.000000
$#               a1                  o1

      5.0000002e-004

*DEFINE_CURVE
$#    lcid      sidr       sfa       sfo      offa
offo    dattyp
         4            1.000000  1.000000
$#               a1                  o1

      5.0000002e-004

*DEFINE_CURVE
$#    lcid      sidr       sfa       sfo      offa
offo    dattyp
         5            1.000000  1.000000
$#               a1                  o1

      5.0000002e-004
```

```
*DEFINE_CURVE
$#    lcid      sidr       sfa       sfo      offa
offo    dattyp
         6            1.000000  1.000000
$#                a1                  o1

      5.0000002e-004



*DEFINE_CURVE
$#    lcid      sidr       sfa       sfo      offa
offo    dattyp
         7            1.000000  1.000000
$#                a1                  o1

      5.0000002e-004          -0.0010500

*SET_NODE_LIST
$#     sid       da1       da2       da3       da4
solver
         1
$#    nid1      nid2      nid3      nid4      nid5
nid6      nid7      nid8
      2212      2232      2233      2234      2235
2236      2237      2238
      2239      2240      2241      2242      2243
2244      2245      2246
      2247      2248      2249      2250      2251
2252      2253      2254
      2255      2256      2257      2258      2259
2260      2261      2262
      2263      2264      2265      2266      2267
2268      2269      2270
```
Contd.

```
*SET_NODE_LIST
$#     sid       da1       da2       da3       da4
solver
         2
$#    nid1      nid2      nid3      nid4      nid5
nid6      nid7      nid8
      2212      2232      2233      2234      2235
2236      2237      2238
      2239      2240      2241      2242      2243
2244      2245      2246
      2247      2248      2249      2250      2251
2252      2253      2254
```

```
      2255      2256      2257      2258      2259
2260      Contd.

*SET_NODE_LIST
$#     sid       da1       da2       da3       da4
solver
         3
$#    nid1      nid2      nid3      nid4      nid5
nid6      nid7      nid8
      2212      2232      2233      2234      2235
2236      2237      2238
      2239      2240      2241      2242      2243
2244      2245      2246
 Contd.



*SET_NODE_LIST
$#     sid       da1       da2       da3       da4
solver
         4
$#    nid1      nid2      nid3      nid4      nid5
nid6      nid7      nid8
        12       212       213       214       215
216       217       218
       219       220       221      2232      2432
2433      2434      2435
      2436      2437      2438      2439      2440
2441      2442      2443
      2444      2445      2446      2447      2448
2449      2450

*SET_NODE_LIST
$#     sid       da1       da2       da3       da4
solver
         5
$#    nid1      nid2      nid3      nid4      nid5
nid6      nid7      nid8
        12       212       213       214       215
216       217       218
       219       220       221      2232      2432
2433      2434      2435
      2436      2437      2438      2439      2440
2441      2442      2443
      2444      2445      2446      2447      2448
2449      2450

*SET_NODE_LIST
$#     sid       da1       da2       da3       da4
solver
```

```
         6
$#    nid1      nid2      nid3      nid4      nid5
nid6      nid7      nid8
        12       212       213       214       215
216       217       218
       219       220       221      2232      2432
2433      2434      2435
      2436      2437      2438      2439      2440
2441      2442      2443
      2444      2445      2446      2447      2448
2449      2450

*SET_NODE_LIST
$#     sid       da1       da2       da3       da4
solver
         7                                        MECH
$#    nid1      nid2      nid3      nid4      nid5
nid6      nid7      nid8
      2212      2232      2233      2234      2235
2236      2237      2238
      2239      2240      2241      2242      2243
2244      2245      2246
      Contd.

*ELEMENT_SHELL
$#   eid     pid      n1      n2      n3      n4      n5
n6      n7      n8
       1       1       1     420     421       3
       2       1     420     419     430     421
       3       1     419     418     439     430
       4       1     418     417     448     439
       5       1     417     416     457     448
       6       1     416     415     466     457
       7       1     415     414     475     466
      ...
      ...
      ...
    6087       2    6318    6273    6272    6324
    6088       2    6323    6274    6273    6318
    6089       2    6322    6275    6274    6323
    6090       2    6319    6276    6275    6322
    6091       2    6321    6277    6276    6319

*NODE
$#   nid               x               y               z
tc      rc
       1       0.0020000  4.8749999e-004
       2       0.0020000  3.6050001e-004
       3       0.0020000  4.4214245e-004
       4       0.0020000  4.1277439e-004
```

```
   5       0.0020000  3.9375920e-004
   6       0.0020000  3.8144726e-004
   7       0.0020000  3.7347554e-004
   8       0.0020000  3.6831404e-004
   9       0.0020000  3.6497205e-004
  10       0.0020000  3.6280820e-004
  11       0.0020000  3.6140715e-004
  ...
   ...
   ...
6346       0.0021769  4.6832458e-004
6347       0.0021032  4.2985147e-004
6348       0.0022402  5.4376246e-004
```